東京帝國大學

地震研究所彙報

第九號

昭和六年

BULLETIN
OF THE
EARTHQUAKE RESEARCH INSTITUTE

TOKYO IMPERIAL UNIVERSITY

Vol. IX.

1931.

目次

第九號

第一冊（昭和六年三月）

頁
1. 關東地方に於ける地殼の垂直變動に就て(英文) 宮部直巳 1
2. 伊豆半島に於ける最近の地震活動に就いて(其一)(英文)…… 那須信治 岸上冬彦 小平孝雄 22
3. 北伊豆大地震の計測學的研究(邦文)…… 今村明恒 36
4. 割れ目の出來方特に雁行性に就いて(邦文)…… 藤原咲平 高山威雄 50
5. 駒ヶ嶽火山の地形變動(邦文)…… 熱海景良 岸上冬彦 80
6. 相模國南西地域の堆積岩の岩石學的研究(一)(英文)…… 津屋弘逵 98
7. 丹後震災地一等水準測量第四回及第五回檢測成果比較(邦文)…… 107
8. 伊豆東海岸に於ける一等水準測量第一回及第二回檢測成果比較(邦文)…… 109
9. 伊豆大震調査概要(邦文)…… 111

第二冊（昭和六年六月）

10. 洋底に傳はる地震波に就て(英文)…… 妹澤克惟 115
11. 嶋弧の曲率に就て(英文)…… 寺田寅彦 144
12. 伊東地方の水準測量の結果に就いて(英文)…… 坪井忠二 151
13. 地震加速度の觀測(豫報)(佛文)…… 石本巳四雄 159

14. 昭和五年十一月廿六日伊豆地震に伴つた音響異常傳播に就いて(英文)…………………… 井上宇胤・杉山友紀 168
15. 昭和五年十一月廿六日伊豆地震に伴ひたる光の現象に就て(邦文)…………………… 武者金吉 177
16. 昭和5年10月17日加賀南西部の强震調査報告(邦文)…………………… 岸上冬彦 216

第三册（昭和六年九月）

17. 地震に伴ふ發光現象に就て(英文)…………………… 寺田寅彦 225
18. 地塊とその運動 第一報 (英文)…………………… 宮部直巳 256
19. 伊豆半島に於ける水準測量の結果に就いて(英文)…………………… 坪井忠二 271
20. 海面大氣壓の擾亂によつて起る地動に就て(英文)…………………… 妹澤克惟・西村源六郎 291
21. 彈性が深さに從つて變る半無限固體上に傳はる一地震波(英文)…………………… 妹澤克惟 310
22. 加速度地震計及び其の記象(佛文)…………………… 石本巳四雄 316
23. 東京灣の出現(英文)…………………… 矢部長克 333
24. 西南日本外帶とフオッサ・マグナとに於ける鮮新期初期末の地殼運動(英文)…………………… 大塚彌之助 340
25. 相模國南西地域の堆積岩の岩石學的研究 (二)(英文)…………………… 津屋弘逵 353
26. 地震觀測報告(英文)…………………… 374

第四册（昭和六年十二月）

27. 地震と雷雨との關係(英文)…………………… 寺田寅彦 387
28. 內部に力核を有する半無限プラスチコ彈性體の變形(英文)…………………… 妹澤克惟 398

29. 地塊とその運動 第二報（關東地震後、房總半島の地殼運動）（英文）…………………………… 宮部直巳 407
30. 昭和二年丹後地震に關聯せる丹後地方の地殼變動に關する研究（第三報）（英文）…………… 坪井忠二 423
31. 丹那隧道內に於ける精密水準測量の結果及び同隧道內に現れた斷層鏡面の運動（英文）…… 高橋龍太郎 435
32. 隧道內及地表に於ける地震動の比較研究（第一）（英文）…………………………………… 那須信治 454
33. 加速度地震計記象より考察せる地震の性質（佛文）…………………………………… 石本巳四雄 473
34. 武田ビルデング振動驗測結果報告（邦文）……… 福富孝治 485
35. 東京市內及近郊に於ける一等水準測量成果（邦文）………………………………………………… 508
36. 地震觀測報告（英文）……………………………………… 509

Contents.

Vol. IX.

Part 1.—March, 1931.

Page

1. N. **Miyabe**, On the Vertical Earth Movement in Kwantô Districts. (in English) 1
2. N. **Nasu**, F. **Kishinouye** and T. **Kodaira**, Recent Seismic Activities in the Idu Peninsula. (Part 1.) (in English) 22
3. A. **Imamura**, Seismometric Study of the Recent Destructive N. Idu Earthquake. (in Japanese) 36
4. S. **Fujiwhara** and T. **Takayama**, On Crack Systems especially those of Echélon Formation. (in Japanese) 50
5. K. **Atsumi** and F. **Kishinouye**, Topographical Changes of the Volcano Komagatake, Hokkaidô, by its Eruption in 1929. (in Japanèse) 80
6. H. **Tsuya**, Petrographic Notes on the Sedimentary Rocks of Southwest Sagami Province. (Part I.) (in English) 98
7. Comparison of the Results of the Fourth and the Fifth Precise Levellings in the Region Disturbed by the Tango Earthquake 1927. (in Japanese) 107
8. Comparison of the Results of the First and Second Precise Levellings on the East Coast Route of the Province of Idu. (in Japanese) 109
9. Outline of Investigations of the Great Idu Earthquake. (in Japanese) 111

Part 2.—June, 1931.

10. **K. Sezawa**, On the Transmission of Seismic Waves on the Bottom Surface of an Ocean. (in English) ………… 115
11. **T. Terada**, On the Curvature of Islands Arc. (in English) ………… 144
12. **C. Tsuboi**, A Note on the Results of the Repeated Precise Levellings across the Itô Earthquake Area. (in English) ………… 151
13. **M. Ishimoto**, Etude préliminaire sur l'accélération des séismes. (en français) ………… 159
14. **W. Inouye** and **T. Sugiyama**, On Sound Phenomena of the Idu Earthquake of Nov. 26th, 1930. (in English) ………… 168
15. **K. Musya**, On the Luminous Phenomenon That Attended the Idu Earthquake, November 26th, 1930. (in Japanese) ………… 177
16. **F. Kishinouye**, Report of the Strong Earthquake in the Southwestern Part of Kaga Province, Oct. 17, 1930. (in Japanese) ………… 216

Part 3.—September, 1931.

17. **T. Terada**, On Luminous Phenomena Accompanying Earthquakes. (in English) ………… 225
18. **N. Miyabe**, Blocks in the Earth's Crust and their Movements. Part I. (in English) ………… 256
19. **C. Tsuboi**, On the Results of Repeated Precise Levellings around Idu Peninsula. (in English) ………… 271
20. **K. Sezawa** and **G. Nishimura**, Movement of the Ground due to Atmospheric Disturbance in a Sea Region. (in English) ………… 291
21. **K. Sezawa**, A kind of Waves transmitted over a Semi-infinite Solid Body of Varying Elasticity. (in English) ………… 310
22. **M. Ishimoto**, Un sismographe accélérométrique et ses enregistrements. (en français) ………… 316
23. **H. Yabe**, Geological Growth of the Tôkyô Bay. (in English) . 333

24. Y. Ôtuka, Early Pliocene Crustal Movement in the Outer Zone of Southwest Japan and in the Naumann's Fossa Magna. (in English) 340
25. H. Tsuya, Petrographic Notes on the Sedimentary Rocks of Southwest Sagami Province. (Part II.). (in English) 353
26. Seismometrical Report. (in English) 374

Part 4.—December, 1931.

27. T. Terada, Earthquake and Thunderstorm. (in English) 387
28. K. Sezawa, The Plastico-Elastic Deformation of a Semi-infinite Solid Body due to an Internal Force. (in English) 398
29. N. Miyabe, Blocks in the Earth's Crust and their Movements. Part II. (Post-Seismic Crustal Movements in Bôsô Peninsula) (in English) 407
30. C. Tsuboi, Investigation on the Deformation of the Earth's Crust in the Tango District Connected with the Tango Earthquake of 1927. (Part 3) (in English) 423
31. R. Takahasi, Results of the Precise Levellings excuted in the Tanna Railway Tunnel and the Movement along the Slickenside that appeared in the Tunnel. (in English) 435
32. N. Nasu, Compartive Studies of Earthquake Motions Aboveground and in a Tunnel. (Part I.) (in English) 454
33. M. Ishimoto, Caractéristiques des ondes séismiques d'aprés les enregistrements accélérométriques. (in français) 473
34. T. Fukutomi, On the Vibration of Takeda Building. (in Japanese) 485
35. The Results of Precise Livellings in Tôkyô and the Environs. (in Japanese) 508
36. Seismometrical Report. (in English) 509

第九號索引

頁
熱海景良、岸上冬彦　(5) 駒ケ嶽火山の地形變動（邦文）……………… 80
藤原咲平、高山威雄　(4) 割れ目の出來方特に雁行性に就いて
（邦文）…………………………………………………………… 50
福富孝治　(34) 武田ビルヂング振動驗測結果報告（邦文）………… 485
今村明恒　(3) 北伊豆大地震の計測學的研究（邦文）……………… 36
井上宇胤、杉山友紀　(14) 昭和五年十一月廿六日伊豆地震に伴つた
音響異常傳播に就いて（英文）……………………………… 168
石本巳四雄　(13) 地震加速度の觀測（豫報）（佛文）……………… 159
石本巳四雄　(22) 加速度地震計及び其の記象（佛文）…………… 316
石本巳四雄　(33) 加速度地震計記象より考察せる地震の性質（佛文） 473
岸上冬彦　(16) 昭和5年10月17日加賀南西部の强震調査報告
（邦文）…………………………………………………………… 216
岸上冬彦、熱海景良；熱海景良、岸上冬彦參照
岸上冬彦、小平孝雄、那須信治；那須信治、岸上冬彦、小平孝雄參照
小平孝雄、那須信治、岸上冬彦；那須信治、岸上冬彦、小平孝雄參照
宮部直巳　(1) 關東地方に於ける地殼の垂直變動に就て（英文）…… 1
宮部直巳　(18) 地塊とその運動　第一報（英文）…………………… 256
宮部直巳　(29) 地塊とその運動　第二報（關東地震後、房總半島の地
殼運動）（英文）……………………………………………… 407
武者金吉　(15) 昭和五年十一月廿六日伊豆地震に伴ひたる光の現象
に就て（邦文）………………………………………………… 177
那須信治　(32) 隧道内及地表に於ける地震動の比較研究（第一）
（英文）…………………………………………………………… 454
那須信治、岸上冬彦、小平孝雄　(2) 伊豆半島に於ける最近の地震
活動に就いて（其一）（英文）……………………………… 22
西村源六郎、妹澤克惟；妹澤克惟、西村源六郎參照
大塚彌之助　(24) 西南日本外帶とフォッサ・マグナとに於ける鮮新
期初期末の地殼運動（英文）………………………………… 340
妹澤克惟　(10) 洋底に傳はる地震波に就て（英文）……………… 115

妹澤克惟 (21) 彈性が深さに從つて變る半無限固體上に傳はる一地震波（英文）………… 310

妹澤克惟 (28) 內部に力核を有する半無限プラスチコ彈性體の變形（英文）………… 398

妹澤克惟、西村源六郎 (20) 海面大氣壓の擾亂によつて起る地動に就て（英文）………… 291

杉山友紀、井上宇胤；井上宇胤、杉山友紀參照

高橋龍太郎 (31) 丹那隧道內に於ける精密水準測量の結果及び同隧道內に現れた斷層面の運動（英文）………… 435

高山威雄、藤原咲平；藤原咲平、高山威雄參照

寺田寅彦 (11) 嶋弧の曲率に就て（英文）………… 144

寺田寅彦 (17) 地震に伴ふ發光現象に就て（英文）………… 225

寺田寅彦 (27) 地震と雷雨との關係（英文）………… 387

坪井忠二 (12) 伊東地方の水準測量の結果に就いて（英文）………… 151

坪井忠二 (19) 伊豆半島に於ける水準測量の結果に就いて（英文） 271

坪井忠二 (30) 昭和二年丹後地震に關聯せる丹後地方の地殼變動に關する研究（第三報）（英文）………… 423

津屋弘逵 (6) 相模國南西地域の堆積岩の岩石學的研究（一）（英文） 98

津屋弘逵 (25) 相模國南西地域の堆積岩の岩石學的研究（二）（英文） 353

矢部長克 (23) 東京灣の出現（英文）………… 333

地震研究所 (7) 丹後震災地一等水準測量第四回及第五回檢測成果比較（邦文）………… 107

地震研究所 (8) 伊豆東海岸に於ける一等水準測量第一回及第二回檢測成果比較（邦文）………… 109

地震研究所 (9) 伊豆大震調查概要（邦文）………… 111

地震研究所 (26) 地震觀測報告（自昭和六年一月至同年三月）（英文）………… 374

地震研究所 (36) 地震觀測報告（自昭和六年四月至同年六月）（英文）………… 509

地震研究所 (35) 東京市內及近郊に於ける一等水準測量成果（邦文） 508

Index to Vol. IX.

Page

Atsumi, K. and Kishinouye, F. (5) Topographical Changes of the Volcano Komagatake, Hokkaidô, by its Eruption in 1929. (in Japanese) 80

Fujiwhara, S. and Takayama, T. (4) On Crack Systems especially those of Echélon Formation. (in Japanese) 50

Fukutomi, T. (34) On the Vibration of Takeda Building. (in Japanese) 485

Imamura, A. (3) Seismometric Study of the Recent Destructive N. Idu Earthquake. (in Japanese) 36

Inouye, W. and Sugiyama, T. (14) On Sound Phenomena of the Idu Earthquake of Nov. 26th, 1930. (in English) 168

Ishimoto, M. (13) Etude préliminaire sur l'accélération des séismes. (en français) 159

Ishimoto, M. (22) Un sismographe accélèrometrique et ses enregistrements. (en français) 316

Ishimoto, M. (33) Caractéristiques des ondes séismiques d'aprés les enregistrements accélérométriques. (en français) 473

Kishinouye, F. (16) Report of the Strong Earthquake in the Southwestern Part of Kaga Province, Oct. 17, 1930. (in Japanese) 216

Kishinouye, F. and Atsumi, K., *See* Atsumi, K. and Kishinouye, F.

Kishinouye, F., Kodaira, T. and Nasu, N., *See* Nasu, N., Kishinouye, F. and Kodaira, T.

Kodaira, T., Nasu, N. and Kishinouye, F., *See* Nasu, N., Kishinouye, F. and Kodaira, T.

Miyabe, N. (1) On the Vertical Earth Movement in Kwantô Districts. (in English) 1

Miyabe, N. (18) Blocks in the Earth's Crust and their Movements. Part I. (in English) 256

Miyabe, N. (29) Blocks in the Earth's Crust and their Movements. Part II. (Post-Seismic Crustal Movements in Bôsô Peninsula) (in English)………… 407

Musya, K. (15) On the Luminous Phenomenon That Attended the Idu Earthquake, November 26th, 1930. (in Japanese)………… 177

Nasu, N. (32) Comparative Studies of Earthquake Motions Above-ground and in a Tunnel. (Part I.) (English)………… 454

Nasu, N., Kishinouye, F. and Kodaira, T. (2) Recent Seismic Activities in the Idu Peninsula. (Part I.) (in English)………… 22

Nishimura, G. and Sezawa, K., *See* Sezawa, K. and Nishimura, G.

Ôtsuka, Y. (24) Early Pliocene Crustal Movement in the Outer Zone of Southwest Japan and in the Naumann's Fossa Magna. (in English)………… 340

Sezawa, K. (10) On the Transmission of Seismic Waves on the Bottom Surface of an Ocean. (in English)………… 115

Sezawa, K. (21) A Kind of Waves transmitted over a Semi-infinite Solid Body of Varying Elasticity. (in English)………… 310

Sezawa, K. (28) The Plastico-Elastic Deformation of a Semi-infinite Solid Body due to an Internal Force. (in English)………… 398

Sezawa, K. and Nishimura, G. (20) Movement of the Ground due to Atmospheric Disturbance in a Sea Region. (in English)………… 291

Sugiyama, T. and Inouye, U., *See* Inouye, U. and Sugiyama, T.

Takahasi, R. (31) Results of the Precise Levellings excuted in the Tanna Railway Tunnel and the Movement along the Slickenside that appeared in the Tunnel. (in English)………… 435

Takayama, T. and Fujiwhara, S., *See* Fujiwhara, S. and Takayama, T.

Terada, T. (11) On the Curvature of Islands Arc. (in English)………… 144

Terada, T. (17) On Luminous Phenomena Accompanying Earthquakes. (in English)………… 225

Terada, T. (27) Earthquake and Thunderstorm. (in English)………… 387

Tsuboi, C. (12) A Note on the Results of the Repeated Precise Levellings across the Itô Earthquake Area. (in English)………… 151

TSUBOI, C. (19) On the Results of Repeated Precise Levellings around Idu Peninsula. (in English) 271

TSUBOI, C. (30) Investigation on the Deformation of the Earth's Crust in the Tango District Connected with the Tango Earthquake of 1927. (Part 3) (in English) 423

TSUYA, H. (6) Petrographic Notes on the Sedimentary Rocks of Southwest Sagami Province. (Part I.) (in English)................... 98

TSUYA, H. (25) Petrographic Notes on the Sedimentary Rocks of Southwest Sagami Province. (Part II) (in English)................. 353

YABE, H. (23) Geological Growth of the Tôkyô Bay. (in English) 333

EARTHQUAKE RESEARCH INSTITUTE. (7) Comparison of the Results of the Fourth and the Fifth Precise Levellings in the Region Disturbed by the Tango Earthquake 1927. (in Japanese)......... 107

EARTHQUAKE RESEARCH INSTITUTE. (8) Comparison of the Results of the First and Second Precise Levellings on the East Coast Route of the Province of Idu. (in Japanese) 109

EARTHQUAKE RESEARCH INSTITUTE. (9) Outline of Investigations of the Great Idu Earthquake. (in Japanese) 111

EARTHQUAKE RESEARCH INSTITUTE. (26) Seismometrical Report. (January 1–March 31, 1931) (in English) 374

EARTHQUAKE RESEARCH INSTITUTE. (36) Seismometrical Report. (April 1–June 30, 1931) (in English) 509

EARTHQUAKE RESEARCH INSTITUTE. (35) The Results of Precise Levellings in Tôkyô and the Environs. (in Japanese) 508

正　誤　表
Errata.

號 Volume	册 Part	頁 Page	行 Line	誤 *for*	正 *read*
VI		98	9	West-Comp.	South-Comp.
„		„	26	West-Comp.	South-Comp.
IX	2	183	27	中郷村々長清水吉彥氏	中郷村前沼津農林學校長、縣史蹟調査委員清水吉彥氏
„	3	317	6	a	a
„	„	320	12	$4\lambda^2 p$	$4\lambda^2 p^2$
„	„	332	2	0·38 dyne	0·19 dyne
„	„	351	20	Honsyû arc	Honsyû arc.
„	„	352	Fig. 7.	Fig. 7.....L in Fig. 6.	Fig. 7.....LM in Fig. 6.
„	„	384	List IV.	Time of occurce	Time of occur
„	„	„	38	22　09　55·3	21　09　55·3
„	4	440	4	$L_n - L_{n-1}$	$L_n - L_{n+1}$
„	„	471	6	otionsm.	motions.
„	„	514	Pl. LIV.	Instrument: No. 7.	Instrument: No. 5.
„	„	514	Pl. LV.	Instrument: No. 7.	Instrument: No. 5.
„	„	490	10	C.G.	C. 9.
„	„	492	Fig. 6.	8·0（縱軸數字の）	0·8
„	„	„	„	4·0（　„　）	0·4
„	„	506	Pl. XLIX.	徵震（第十圖の說明）	微震
„	„	„	Pl. L.	徵震（第十一圖の說明）	微震

be more or less reduced by the process of smoothing the values of the vertical displacements. It may be also considered that those com-

---

1) *Bull. I. E. I. C.*, 11 (1930), No. 4.

2) An abstract is appeared in *Proc. Imp. Acad.*, 6 (1930), 405.

3) T. TERADA and N. MIYABE, *Proc. Imp. Acad.*, 6 (1930), 49.

地震研究部

1. *On the Vertical Earth Movement in Kwantô Districts.*

By **Naomi MIYABE,**

Earthquake Research Institute.

(Read Jan. 20, 1931.—Received Jan. 20, 1931.)

Introduction.

The secondary and tertiary triangulations in Kwantô Districts have been carried out and now completed by the authorities of the Military Land Suvery Department.[1] From the result of these extensive surveys, the vertical displacements of the triangulation points are found which we may assume to have occurred during the time interval of 1889-1925. In the present paper, we tried, in the first place, to discuss the geographical distribution of these vertical displacements.[2] On the other hand, we have already made a preliminary investigation of the horizontal deformation of the earth's crust in the same districts,[3] referring to the result of the primary triangulation which had been completed by the same authorities. In the present paper, the relation between the horizontal divergence and the vertical earth movement will be discussed in the second place.

In the present investigation, however, we leave out the problem whether these displacements of triangulation points represent the true movement of the earth's crust in their neighbourhood or the movement more or less affected by the local disturbances such as the accidental displacements of the triangulation points etc., and simply assume that the displacements of the triangulation points are mainly due to the average crustal movement in their neighbourhood. Even if the components due to other local disturbance existed, their amounts may be more or less reduced by the process of smoothing the values of the vertical displacements. It may be also considered that those components due to the local disturbances, if they exist, are the secondary effect resulting from some irregular local deformation of minor scale, i. e., of less extent than the primary block movement. These minor local disturbances are discussed as the distribution of D (the value that represents the grade of disturbance). It may also be remarked that these vertical displacements include both chronic and acute components, the acute components being the direct effect of the earthquake, as we have already remarked in the previous paper with regard to the horizontal displacements.

---

[1] *Bull. I. E. I. C.,* **11** (1930), No. 4.

[2] An abstract is appeared in *Proc. Imp. Acad.,* **6** (1930), 405.

[3] T. TERADA and N. MIYABE, *Proc. Imp. Acad.,* **6** (1930), 49.

The Process of Smoothing.

To see the general mode of distribution of the vertical movement of the earth's crust, the values of the vertical displacements of the triangulation points are subjected to a process of smoothing which will be described as follows. For this purpose, the topographical maps in 1/50000 scale of Kwantô Districts are taken, and the area of every sheet of these maps are divided into 16 minor meshes of equal areas, so that an unit mesh has the area of $(\Delta\lambda = 15/4') \times (\Delta\varphi = 10/4')$. The values of vertical displacements of triangulation points which fall in a major mesh of the area of $(\Delta\lambda = 15/2') \times (\Delta\varphi = 10/2')$, that is, four adjacent minor meshes, are averaged. This process of smoothing is performed all over the districts where the triangulation points, with their vertical displacements measured, are distributed.

The number of triangulation points which fall in a major mesh is approximately the same for each mesh without much deviation, except for those which are located in the marginal region of the districts. The mean number of the triangulation points in a major mesh amounts to about 10, the triangulation points which are situated on the boundary of the two adjacent meshes being counted twice in both meshes. In the following table, the first column contains the number of triangulation points in a major mesh, the second column the number of the major meshes with the corresponding number of triangulation points therein included and the third column is the percentage of the number of major meshes corresponding to the various number of triangulation points.

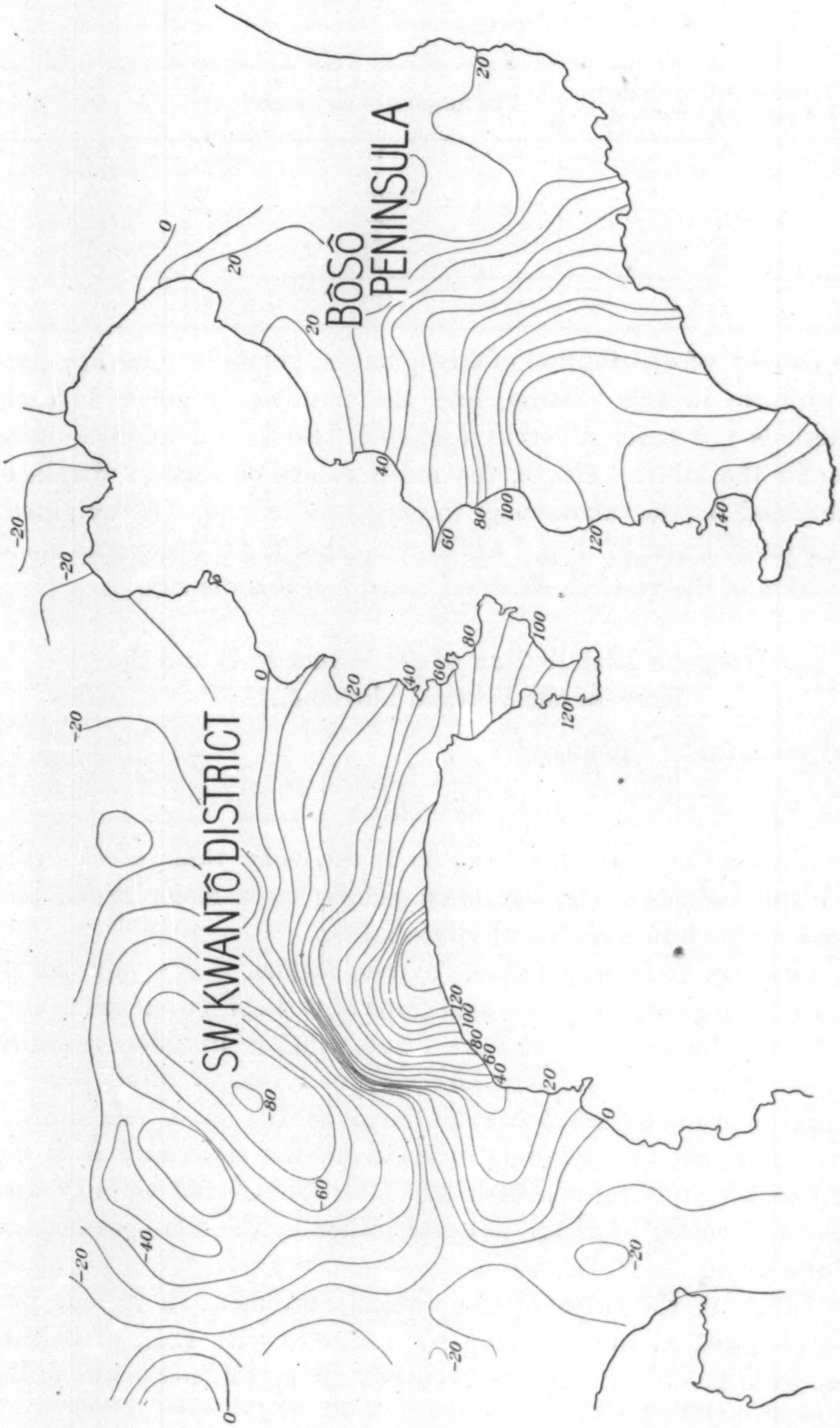
BÔSÔ PENINSULA
SW KWANTÔ DISTRICT
0
20
20
20
40
60
80
100
120
140
-20
-20
0
20
40
60
100
120
-20
20
100
120
80
60
40
20
0
-80
-60
-40
-20
-20
-20
0

Fig. 1. Vertical Earth Movement in Kwantô Districts.

Table I.

The number of triangulation points per major mesh.	The number of major mesh.	%
2 – 5	29	9·8
6 – 7	44	14·9
8 – 9	61	20·6
10 – 11	87	29·5
12 – 13	52	17·6
14 – 15	22	7·5
	295	

The density of distribution of triangulation points is thus approximately uniform in this district, and the number of points in each major mesh is not much different from each other, as mentioned above and seen in the table. Hence, the mean values of vertical displacements obtained in the above may be regarded as equally weighted. Thus the equi-$\overline{\partial h}$ lines[4] of Fig. 1 are drawn, showing the general mode of distribution of the vertical earth movement in this district.

The Irregular Distribution of the Values of *D* and the Slope of the Vertical Movement.

First we consider the quantity

$$D = \overline{\left| \partial h - \overline{\partial h} \right|},$$

where — denotes the mean value, i.e., $\overline{\partial h}$ is the mean value of ∂h's (the vertical displacements of triangulation points) in a major mesh, and $|\ |$ is the usual notation for the absolute value.

The quantity D is determined by two factors. The value of D may turn out large when the general slope of vertical movement is very steep and when the values of ∂h have a wide range of irregular variation in the mesh. In our actual case, however, the values of mean slope of the vertical movement are never so large as the most values of D obtained. The fact that the relation between the slope and D is not expressed in a simple form, which will later be referred to, may also mean that the values of D are not determined by the mere geometrical effect of the slope.

The values of the slope of the vertical movement in various portions are obtained in the following way: circles with radii of 3000m. in actual scale are drawn having their centres at the net-points of the

---

[4] Equi-$\overline{\partial h}$ lines are drawn with the interval of $\overline{\partial h}=10$cm.

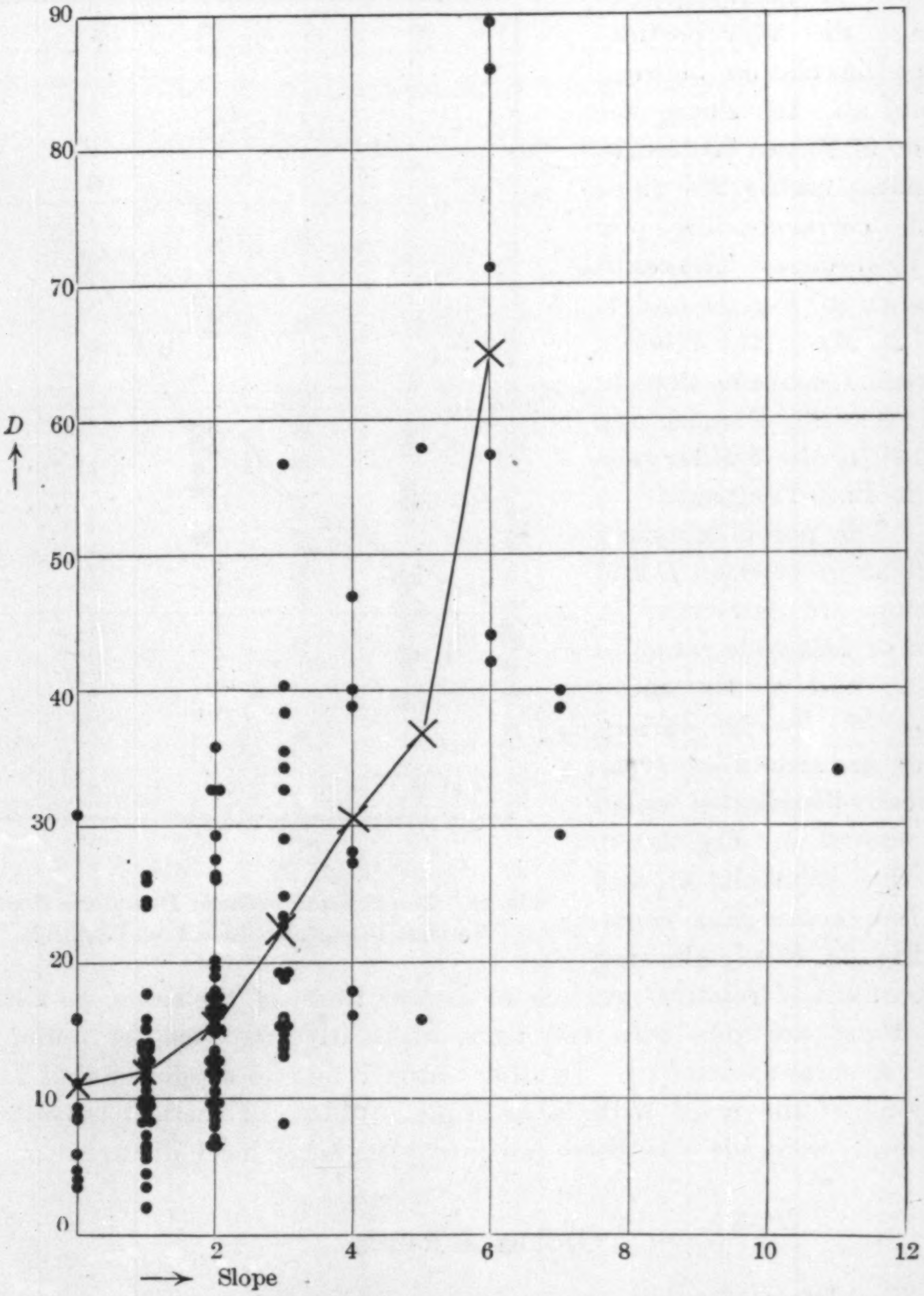

Fig. 2a. The Relation between D and the Slope of Vertical Displacements in SW. Kwantô District.

minor meshes, mentioned in the preceding chapter, and the number of contour lines of the map of Fig. 1 (for this purpose, contour lines are drawn with the interval of $\overline{\delta h} = 5$ cm.) crossing each circular area is

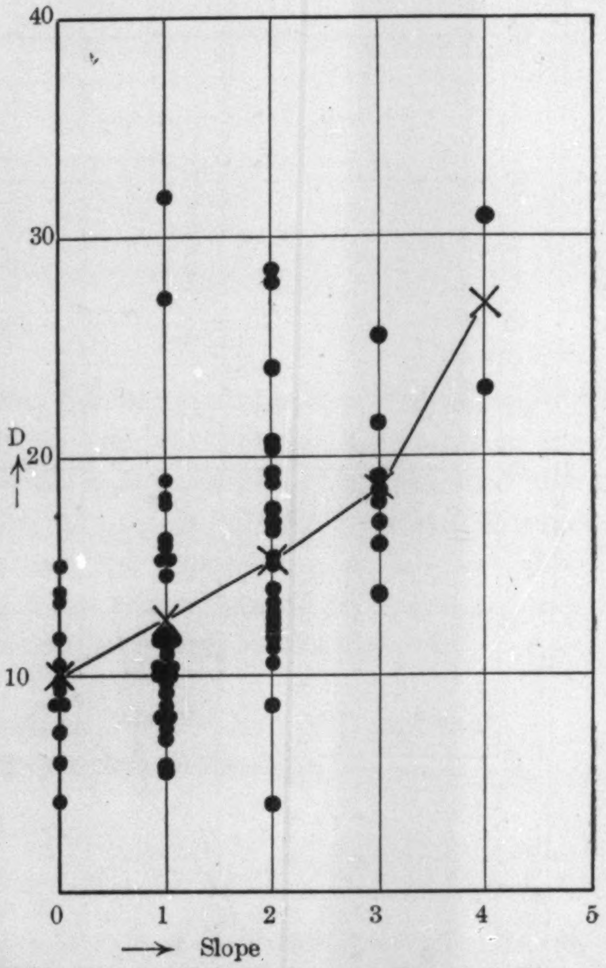

Fig. 2b. The Relation between *D* and the Slope of Vertical Displacements in Bôsô Peninsula.

counted to represent the slope in that very portion. To see the relation between *D* and and the slope, the values of *D* are plotted in ordinates, taking the slope of the corresponding portion in abscissae. The result is shown in Fig. 2a and b. Fig. 2a shows the relation between *D* and the slope in SW. Kwantô District and Fig. 2b is the similar relation in Bôsô Peninsula.

The points showing the relation between *D* and the slope are distributed in more or less wide range in Fig. 2, and yet the mean values of *D*'s for various slopes are somewhat systematically distributed which are shown in Fig. 2a, b, by the symbols × and the line connecting them. In Fig. 3, Pl. 1, showing the portions of relative maxima of *D* and those of the slope, we notice that those portions with two sorts of relative maxima are found to stand in some association. In other words, it may be suggested that some portions of the crust with large angle of slope of vertical movement frequently coincide with those portions with large local disturbance.

Geological Faults.

The deformation of the crust is seen, in the preceding chapter, concentrated in some finite portions. It may be suspected that the geological faults may also be associated in some manner with these portions with large *D* or slope. Under such considerations, the geological faults which are traced in the geological map compiled by Mr. S.

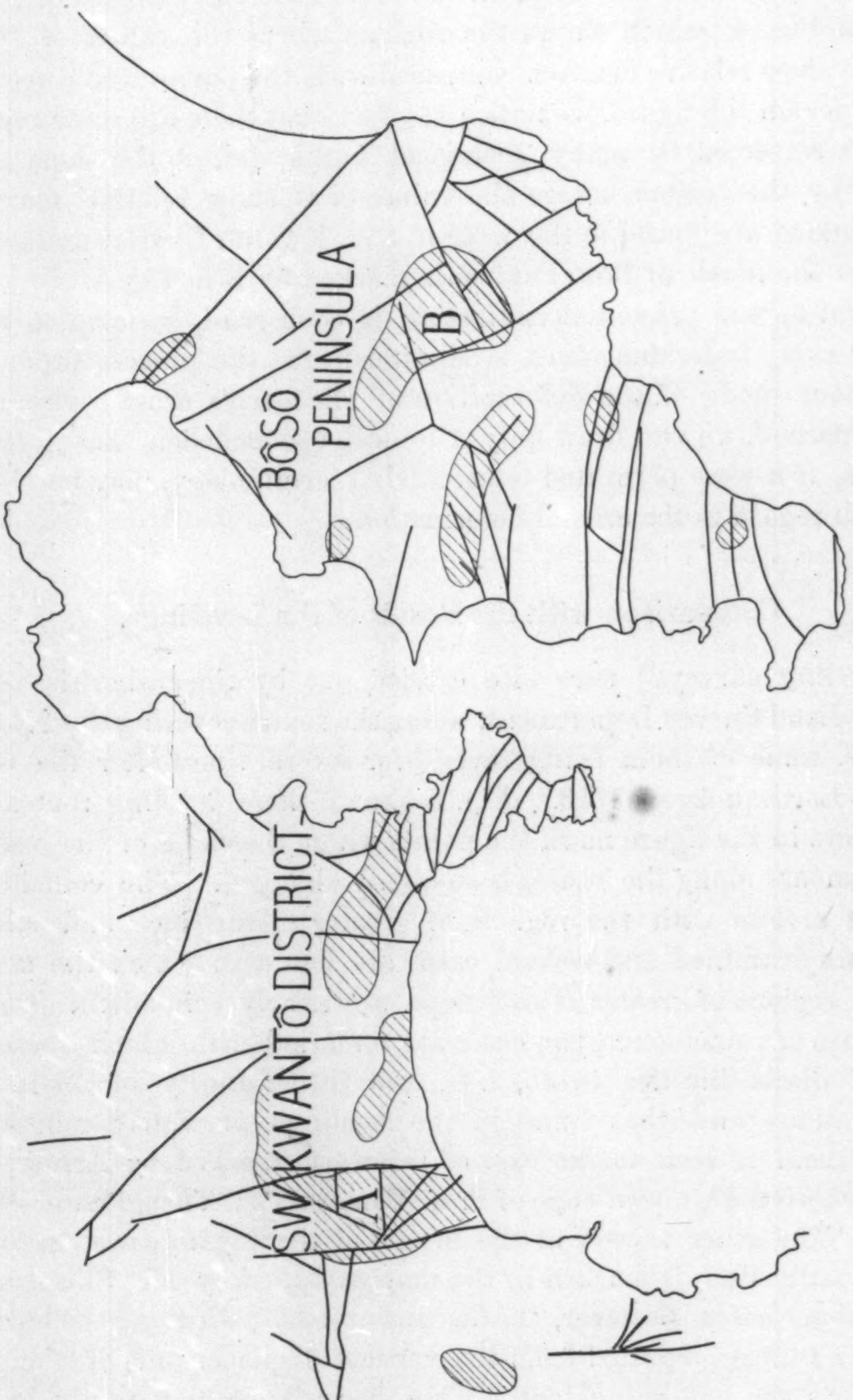
BÔSÔ
PENINSULA
B
SW KWANTÔ DISTRICT
A

Fig. 4. The Distribution of Geological Faults.

Shaded Portions are those where the Values of D and the Slope are greater than the Surrounding Regions. Full Lines are the Geological Faults, due to the Map compiled by Mr. S. Shimizu of Tôhoku University.

Shimizu of Tôhoku University, under Prof. Yabe's guidance, are reproduced in Fig. 4, which shows the regions where the values of D and the slope show relative maxima compared with the surrounding regions. At a glance on the figure, we notice the fact that there are some regions which is traversed by many geological faults and, at the same time, covered by the regions where the values of D show relative maxima. Such regions are found to the west of SW. Kwantô District marked by A and to the north of Bôsô Peninsula marked by B in Fig. 4.

So far as our present investigation is concerned, we cannot know whether every individual fault is significant for the process producing the present mode of the deformation of the earh's crust. From the result obtained, we can draw only a tentative conclusion that a swarm of faults, if it were permitted to use such a terminology, may be significant with regard to the crustal deformation.

Comparison with the Result of the Levelings.

Leveling surveys[5] were also carried out by the authorities of the Military Land Survey Department, along the routes covering the Kwantô Districts, some of them being revised for several times after the Great Kwantô Earthquake of 1923. Fig. 5 shows these leveling routes and the arrows in the figure mark the points where the slope of the vertical displacements along the routes is suddenly changed. The coincidence of these arrows with the regions of greater disturbance and steeper slopes are examined and several cases are found in which the arrows and the regions of greater D and slope are nearly coincident. Out of these cases of coincidence, two cases are remarkable in which these two sorts of discontinuities in δh, i. e., the discontinuity of δh in the triangulations and that found in the levelings, are fairly coincident. One of them is seen to the east of Odawara, marked by Arrow 1 in Fig. 5, where the western edge of Prof. Yamasaki's[6] Yurugi Land Block passes. The other is seen at the mouth of the Sagamigawa, Arrow 2, where a fault line is marked in the map compiled by Mr. Shimizu.

In some cases, however, the discontinuities in δh along the leveling routes and those obtained from the vertical displacements of triangulation points are not coincident. This discordance may partly be due

---

[5] The results of the leveling surveys in this district are published by A. Imamura, *Publ. I. E. I. C.*, 25 (1930), etc.

[6] N. YAMASAKI, *Bull. I. E. I. C.*, 100-B (1925).

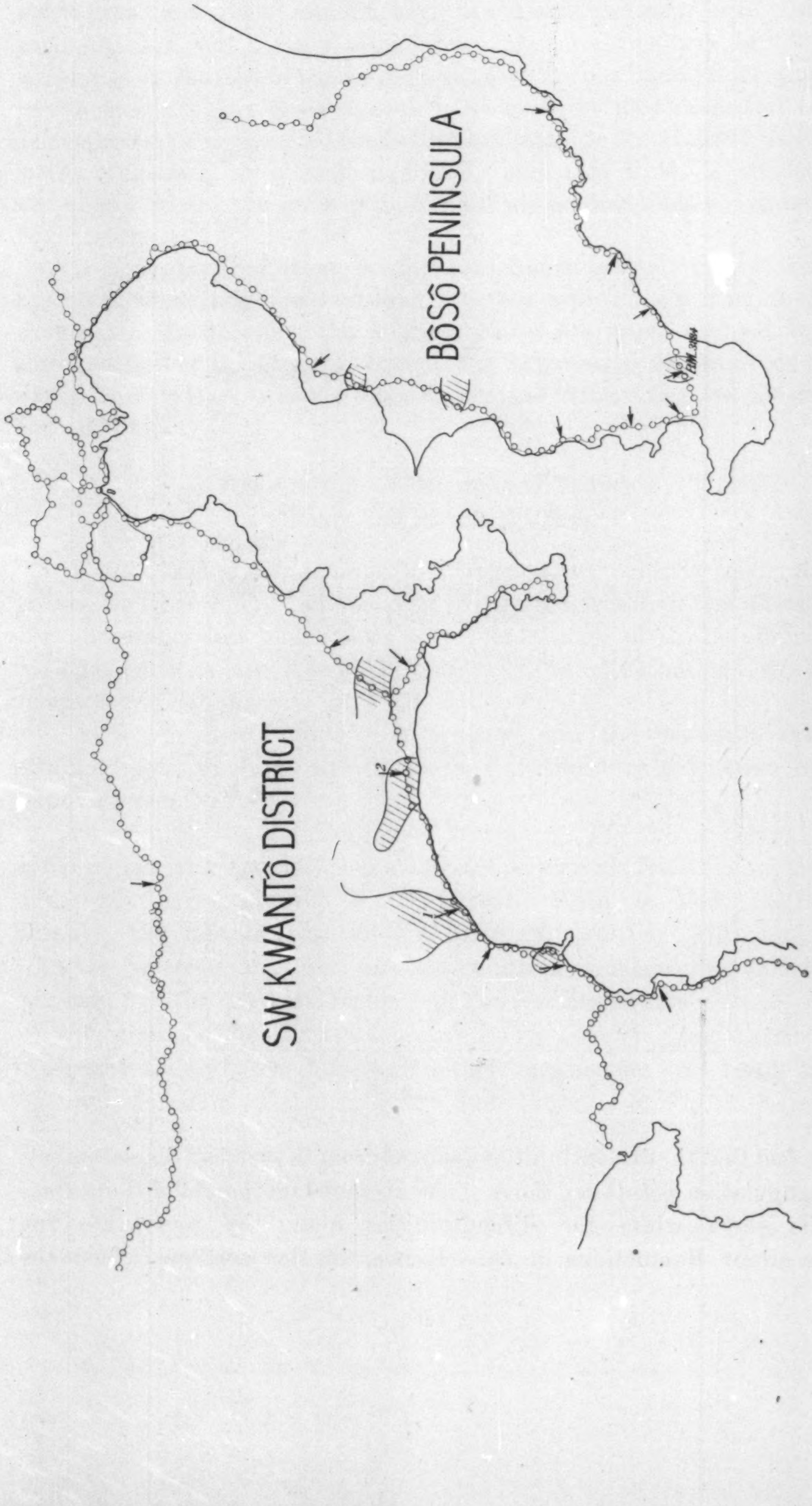
BÔSÔ PENINSULA
SW KWANTÔ DISTRICT

Fig. 5. Leveling Routes.

Arrows are Signs for the Points where the Slope of Vertical Displacements are suddenly changed.
Shaded Portions are the Regions where the Values of *D* and the Slope are greater than the Surrounding Regions.

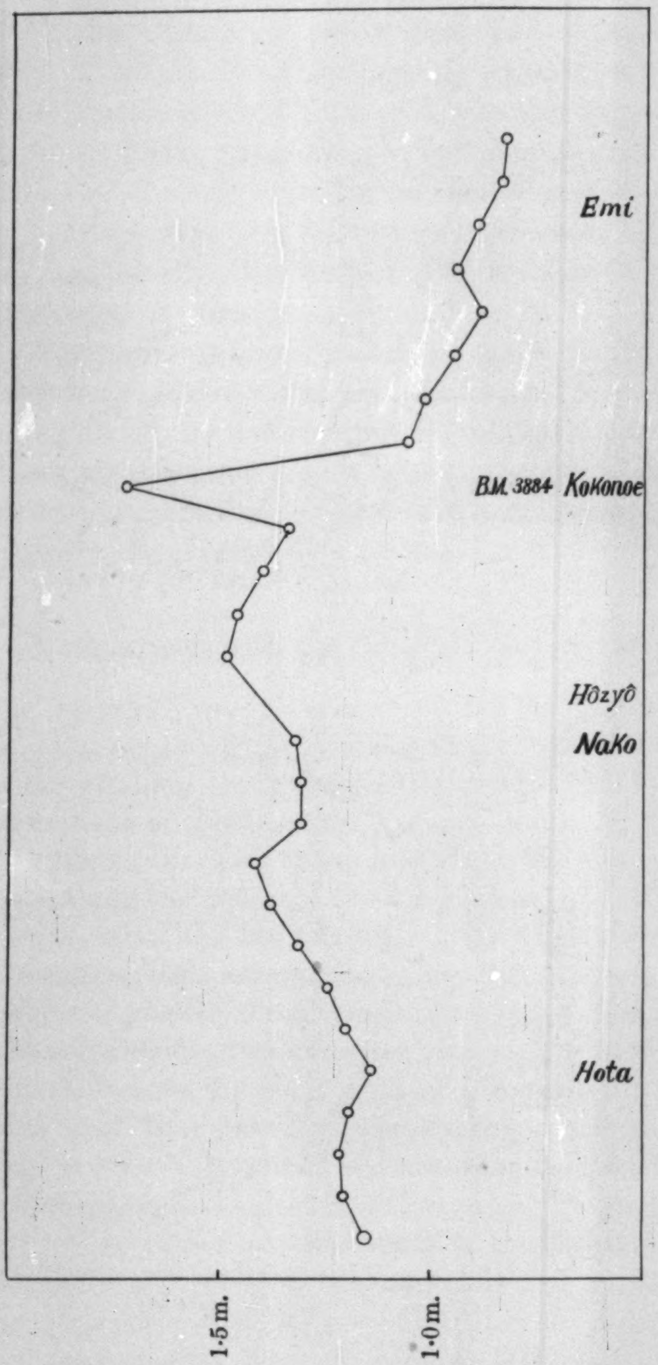

Fig. 6. The Abnormal Upheaval of B. M. 3884.

to the fact that the discontinuities deduced from the vertical displacements of triangulation points are those of the averaged movement of the surface of the earth, while, the discontinuities along the routes are due to the minor fluctuations in δh. Hence, in the portions where the crust was disturbed remarkably, the discontinuities found in the triangulation and those obtained from the levelings are found coincident as in the case of the western edge of Yurugi Land Block and that at the mouth of the Sagamigawa. It should be also remarked that a bench-mark near the SW. End of Bôsô Peninsula, B. M. 3884, is abnormally upheaved, as shown in Fig. 6, and this B. M. is situated in the region where the value of D is relatively greater than the surrounding regions.

We have another cause for the discordance between the two sorts of discontinuities mentioned above. It is a well known fact that the fluctuations in δh along the leveling routes are much affected by the configuration of the routes. Hence, the apparent discontinuities in δh along the routes do not always denote the discontinuities in crustal deformation.7)

Distribution of Divergence, Rotation, Shear and Strain Ellipses.

From the data of horizontal displacements of primary triangulation points, we have calculated the areal divergence, rotation and shear, and also directions and magnitudes of principal axes of strain ellipses in various portions in Kwantô Districts. The distributions of these quantities are shown in Figs. 7–10.

As to the distributions of divergence and the principal axes of strain ellipses, we have already made a preliminary discussion in the paper above cited.8)

Examining the distribution of rotation ζ, Fig. 8, we notice that a zonal region with counter-clockwise rotation extends from the mountainous region lying towards W. of Kwantô Plain to Bôsô Peninsula through the middle part of SW. Kwantô District. This zone lies inserted between northern and the southern regions with clockwise rotation, ζ of the northern region being of less magnitude.

On drawing the contour lines on the map showing the distribution of shear S, the signs are disregarded, their magnitudes only being taken into consideration. Examining the distribution of S, Fig. 9, it may be

---

7) This point will later be discussed in detail.

8) T. Terada and N. Miyabe, *loc. cit.* 3).

In the maps given in the previous paper cited, some errors were found which, though not so serious as to affect the general conclusion, are corrected and shown revised in Figs. 7 and 10 of the present paper.

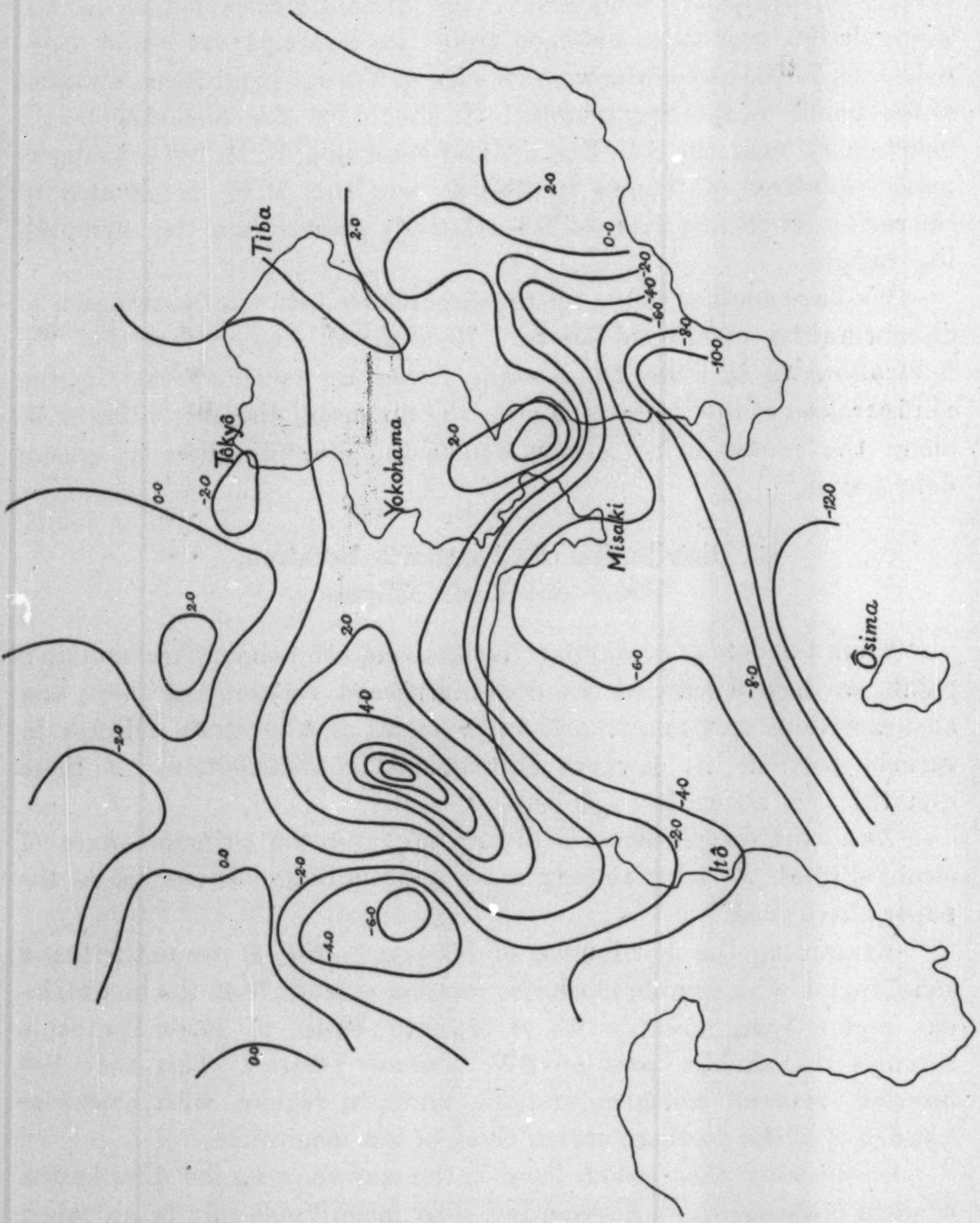
Tiba
Tôkyô
Yokohama
Misaki
Ôsima
Itô
2.0
0.0
-2.0
-4.0
-6.0
-8.0
-10.0
-12.0
4.0

Fig. 7. Distribution of Divergence (10^{-5}).

remarked that the regions with the maximum values of S are found in the west of SW. Kwantô District and in Bôsô Peninsula. The region of maximum S in the west of SW. Kwantô District is approximately coincident with the region of maximum slope and consequently with that of D, which is mentioned in the preceding chapter. It is also seen

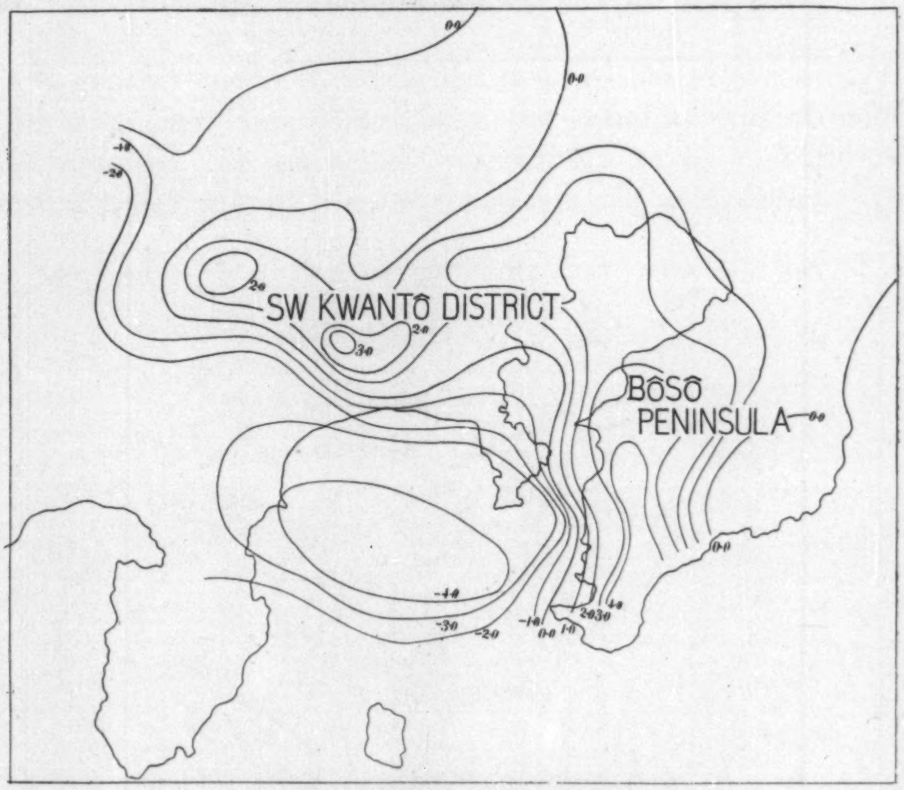
0·0
0·0
-1·0
-2·0
2·0
SW KWANTÔ DISTRICT
2·0
3·0
BÔSÔ PENINSULA
0·0
0·0
-4·0
-3·0
-2·0
-1·0
0·0
1·0
2·0
3·0
4·0

Fig. 8. Distribution of Rotations.
+ ··· Region of Counter-Clockwise Rotation.
− ··· Region of Clockwise Rotation.

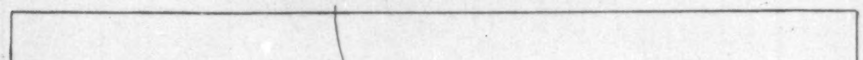
1·0
1·0
3·0
2·0
SW KWANTÔ DISTRICT
5·0
4·0
3·0
2·0
BÔSÔ PENINSULA
1·0
2·0
1·0
3·0
5·0
4·0
4·0
5·0
1·0
2·0
3·0

Fig. 9. Distribution of Shear *S*.

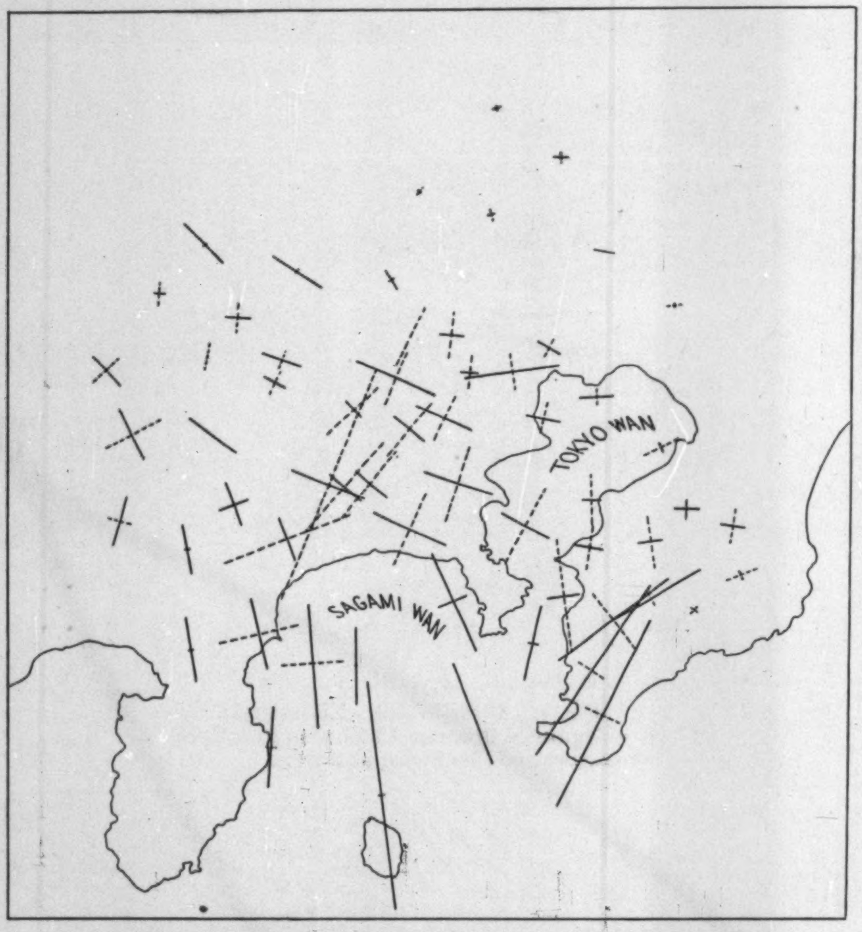

Fig. 10. Distribution of Principal Axes of Strain Ellipses. Full Lines—Contraction, Broken Lines—Elongation. Lengths of Axes denote Approximate Magnitudes.

to be coincident with the western edge of Prof. Yamasaki's Yurugi Land Block.

A region of relative maximum of S is extended in a zonal form over the middle part of Bôsô Peninsula from N. to S. Somewhat similar zonal distributions have been recognized in the distribution of the slope and that of D, but any close coincidence in position of these zones for the slope and D with the region for maximum S is not clearly seen, for the position of the latter cannot be determined with the same accuracy as the former. In this zonal region, however, conspicuous geological faults have not yet been found corresponding to this physical fault.[9]

---

[9] The term "physical fault" is used for the discontinuities found from the data of the geodetic surveys.

The general mode of horizontal deformation of the earth's crust may be more easily appreciated, when the principal axes of elongation and contraction are connected respectively so as to build up the orthogonal trajectories of lines of elongation and contraction. Fig. 11 shows the general features of the system of the orthogonal trajectories of lines of elongation and contraction. We notice in that figure, that there is a region in the neighbourhood of Miura Peninsula which seems to have been instrumental in disturbing the uniform development of the deformation over the districts under consideration.

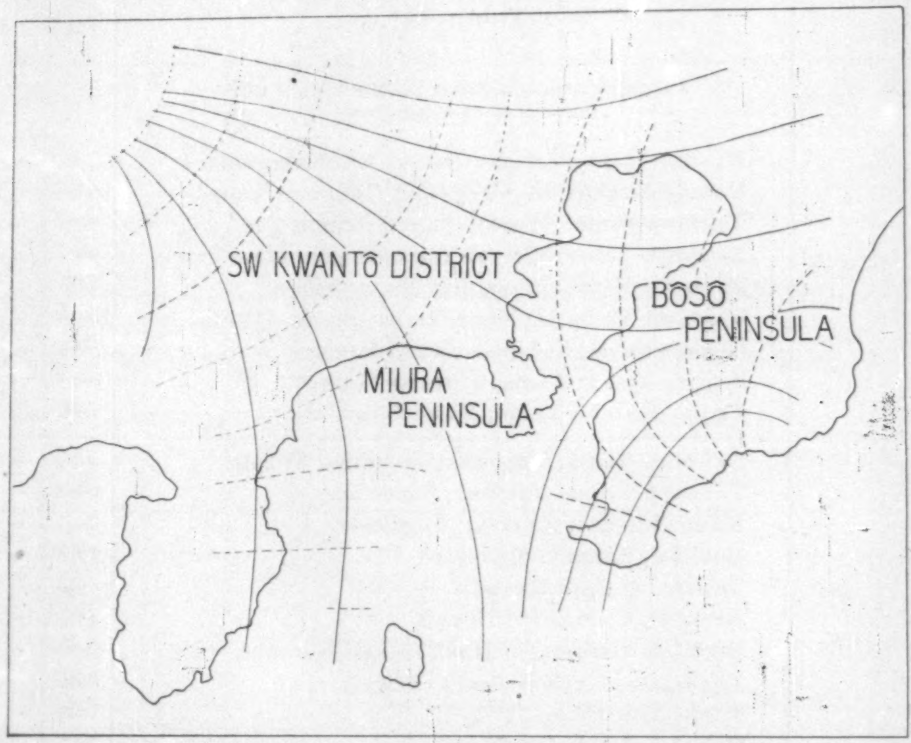

Fig. 11. Lines of Elongation (Broken Lines) and Lines of Contraction (Full Lines).

The Relation between the Vertical Movement and Horizontal Divergence of the Earth's Crust.[10]

As we have mentioned, horizontal divergence Δ for each triangle, the vertices of which are the primary triangulation points, was calculated. The mean vertical movement $\overline{\delta h}$ for each triangle is now calculated from the data of vertical displacements of secondary and tertiary triangulation points which are situated in the corresponding triangle. The table below shows the numerical values of Δ and $\overline{\delta h}$ for each triangle.

---

[10] An abstract is appeared in *Proc. Imp. Acad.*, 6 (1930), 409.

Table II.

No.	Group.	Primary triangulation points which are vertices of triangles.	Δ (10^{-5})	$\overline{\delta h}$ (cm.)
1	A	Misotai-Yama; Asitaka-Yama; Kamurigatake.	− 3·79	− 19·6
2		Kamurigatake; Sengen-Yama; Tanzawa-Yama.	6·06	35·4
3		Tanzawa-yama; Misotai-Yama; Kamurigatake.	− 6·06	− 56·0
4		Tanzawa-Yama; Misotai-Yama; Koganesawa-Yama.	− 4·14	− 46·7
7		Tanzawa-Yama; Simomizo; Segen-Yama.	4·73	27·8
8		Tanzawa-Yama; Tobinoo-Yama; Sengen-Yama.	10·05	40·9
9		Sengen-Yama; Tobinoo-Yama; Zama.	3·14	17·2
10		Sengen-Yama; Zama; Hutako-Yama.	0·14	46·9
11		Zama; Hutako-Yama; Kami-Numabe.	1·92	16·7
5	B	Tanzawa-Yama; Koganasawa-Yama; Takane.	− 0·10	− 39·8
6		Tanzawa-Yama; Takane; Simomizo.	2·86	− 42·3
12		Kami-Numabe; Renkôzi; Nagatuda.	− 0·33	− 20·7
13		Renkôzi; Takane; Simomizo.	− 1·69	− 21·2
14		Takane; Hongô; Renkôzi.	4·33	− 23·7
15		Renkôzi; Tokumaru; Hongô.	1·51	− 34·3
16		Renkôzi; Tokumaru; Hongô Kami-Numabe.	0·83	− 19·3
17		Tokumaru; Kami-Numabe; Tôkyô.	− 3·58	− 16·1
18		Tokumaru; Hôten; Tôkyô.	− 0·65	− 19·1
28		Renkôzi; Simomizo; Nagatuda.	1·62	− 27·3
19	C	Kuranami; Rokudizo; Ôtani.	− 2·91	23·3
20		Ôtani; Rokudizô; Itinomiya.	0·46	13·0
21		Ôtani; Itinomiya; Nonotuka.	2·97	16·0
22		Ôtani; Nonotuka; Mineoka.	0·02	64·0
23		Ôtani; Mineoka; Kanôsan.	− 5·82	102·2
24		Ôtani; Kanôsan; Kuranami.	1·38	57·0
25		Kanôsan; Nokogiri-Yama; Mineoka.	− 4·07	126·6
26		Nokogiri-Yama; Mineoka; Bôtaisan.	−10·21	129·6
27		Mineoka; Bôtaisan; Ôkawa.	−10·10	127·8

In Fig. 12, the relation between Δ and $\overline{\delta h}$ is plotted, taking the values of Δ in ordinates and those of $\overline{\delta h}$ in abscissae. Fig. 13 shows the location of the triangles, the vertices of which are the primary triangulation points. The geographical positions of the triangles represented by the sets of values of Δ and $\overline{\delta h}$ in Fig. 12 may be found by identifying the numbers of the points in Fig. 12 and those of triangles in

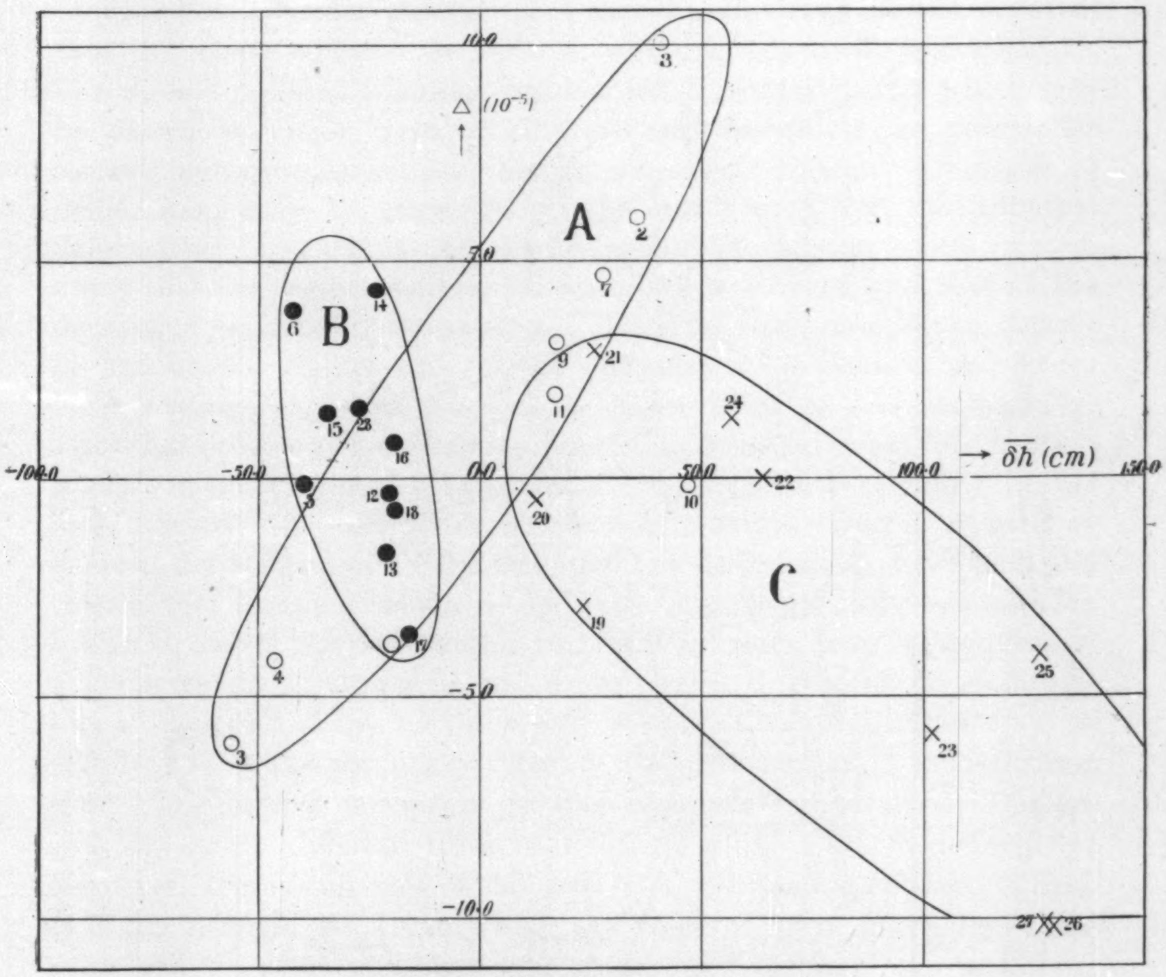

Fig. 12. The Relation between $\varDelta$ and $\overline{\delta h}$.

○··· for Group A

●··· „ „ B

×··· „ „ C

Fig. 13. These plotted points in Fig. 12 may be classified into three groups, A, B and C. The triangles corresponding to the points belonging to Group A are in the southern part and those belonging to Group B are in the northern part of SW. Kwantô District. The triangles corresponding to the points belonging to Group C are situated in Bôsô Peninsula.

For the relation between $\varDelta$ and $\overline{\delta h}$, we will tentatively assume an approximate linear one:

$$\varDelta = \alpha + \beta\overline{\delta h},$$

where α and β are constants.

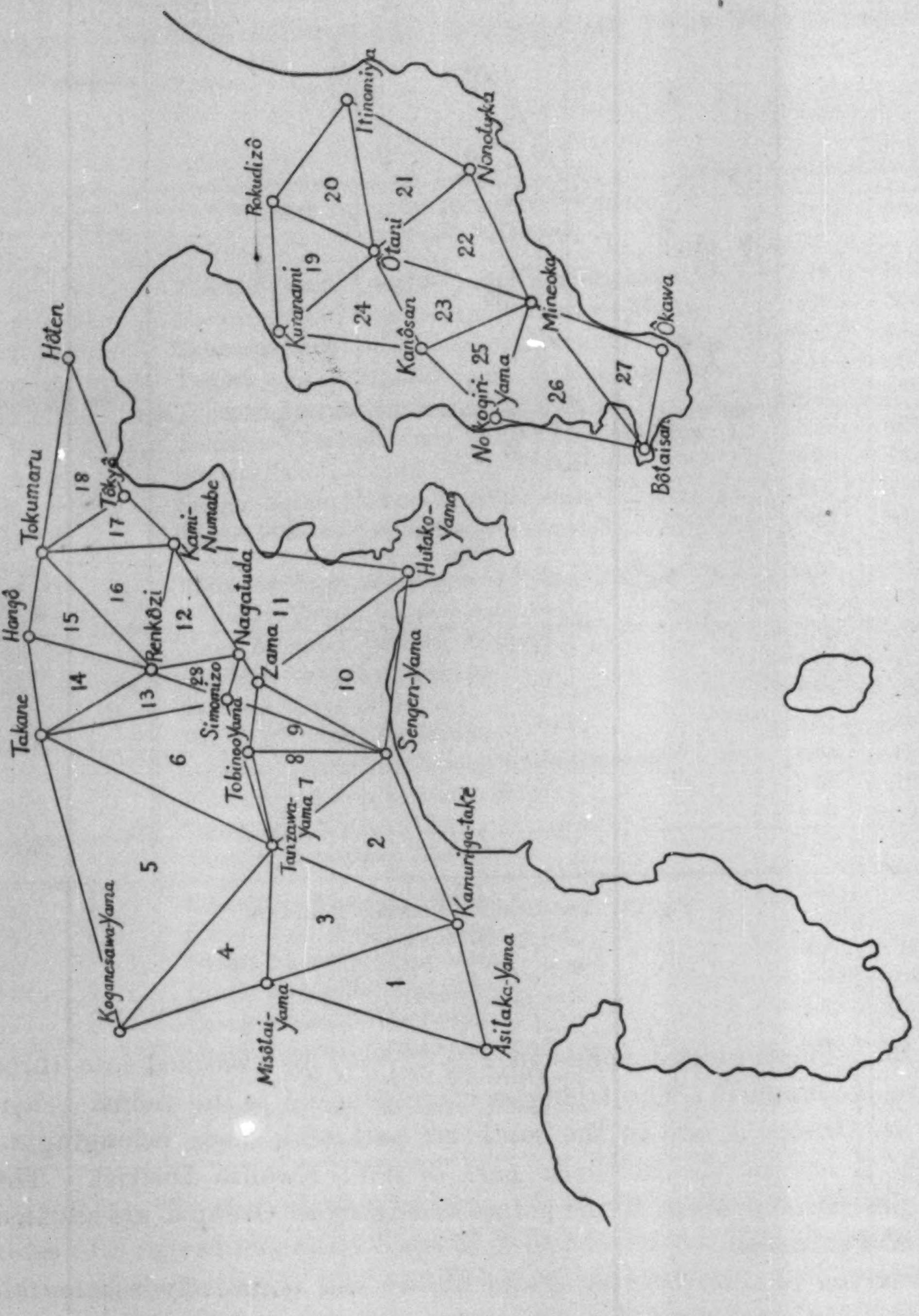
Hôten
Tokumaru
Hongô
Takane
Koganesawa-Yama
Tôkyô
Kami-Numabe
Renkôzi
Nagatuda
Zama
Simomizo
Tobinoo-Yama
Tanzawa-Yama
Misôtai-Yama
Kamuriga-take
Asitaka-Yama
Sengen-Yama
Hutako-Yama
Rokudizô
Itinomiya
Nonotyka
Otani
Kanonami
Kanôsan
Mineoka
Nokogiri-Yama
Ôkawa
Bôtaisan
1
2
3
4
5
6
7
8
9
10
11
12
13
14
15
16
17
18
19
20
21
22
23
24
25
26
27
28

Fig. 13. Primary Triangulation Nets.
(Geographical Distribution of Triangles.)

First we consider the groups A and C. In Group A, the constant β of the above equation is positive, while, in Group C, it is negative. For these simplified relations represented by straight lines which may be drawn as major axes of elliptic areas in which the points for corrresponding groups are distributed, two different processes of deformation may be suggested. The one is such that the principal deformation is a flexure and the horizontal deformation occurs in such a way that the region of upheaval is forced to diverge and that of the depression is forced to to converge. Thus the relation of Group A may be produced. In the case of the deformation of Sakurazima, as we have investigated,[11] this relation is shown more or less remarkably. The other process of deformation is such that the principal deformation consists in the horizontal contraction and the vertical movement. In this case, however, the vertical deformation is possible either in upward or in downward directions. By this mode of deformation, for which the vertical deformation results in an upward movement, the relation for Group C, that is, the deformation in Bôsô Peninsula, may be produced.

The relation between $\varDelta$ and $\overline{\delta h}$ in Group B, that is the deformation of the crust in the northern part of SW. Kwantô District may be mainly due to the secondary effect of the deformation in the southern part. The vertical movement in that region is comparatively smaller and not much different from each other, while $\varDelta$ are varied widely. Moreover, there is an exceptional case, i. e., the relation between $\varDelta$ and $\overline{\delta h}$ of the triangle No. 10, in which the value of $\varDelta$ is much less than what will be calculated from the value of $\overline{\delta h}$ through the equation. This fact will be explained by the assumption that there might be some disturbance preventing the development of the horizontal deformation in this region.

Summary and Conclusion.

In the preceding pages, we have dealt with the vertical movement and its relation with the horizontal deformation of the earth's crust in Kwantô Districts. The results are summarized as follows:

1. Vertical displacements of triangulation points are smoothed so as to see the general mode of the vertical earth movement in this district, from which the mean slope of the vertical displacements is calculated in various places.

---

[11] T. Terada and N. Miyabe, *Proc. Imp. Acad.*, 5 (1929), 322.

2. The quantity $D=\overline{|\delta h-\overline{\delta h}|}$ is calculated for each major mesh. The distribution of this quantity is compared with that of the slope and the coincidence of these two sorts of distributions is discussed.

3. The geological faults are traced and several regions of relative maxima of D and the slope are found to be coincident with those where the geological faults are more densely located.

4. In comparing the distribution of horizontal deformation with that of the vertical one, some regions with maximum horizontal shear are found in the regions of maximum values of D and the slope.

5. The relation between $\varDelta$ (horizontal divergence) and mean vertical displacement $\overline{\delta h}$ is plotted and two different processes of deformation are suggested to serve for the explanation of the simplified relation between $\varDelta$ and $\overline{\delta h}$.

In conclusion, the writer wishes to express his sincere thanks to Professor Torahiko Terada for his kind advices and guidance. The writer's thanks are also due to the authorities of the Military Land Survey Department for placing the valuable data at the writer's disposal.

---

1. 關東地方に於ける地殼の垂直變動に就て

地震研究所　宮部直巳

1923 年の關東地震の後に行はれた三角測量により、關東地方西南部及び房總半島を含む地域に在る二三等三角點の垂直移動が明かにされた。是等の資料により、筆者は、寺田教授指導の下に、この地方の地殼の垂直變動の模樣を調べてみた。

玆に、是等の垂直移動量は、前回の測量との比較によつて算出されたもので、1889-1923 の間に起つた移動であることを考へねばならない。其故この移動量の中には、永年の間の除々なる移動によるものと、地震による急激なる變動によるものとを含む筈である。其等の二つの別々な性質の移動を分析することは困難であるから、此には、その全移動量を其儘取扱つた。

先づ地殼の垂直變動の模樣を見るために、全面積を適當な網目に分ち、各網目内にある三角點の垂直移動量を平均してその網目に相當する面積の部分の垂直移動をあらはす樣にした。かくして第一圖が得られたのである。この圖から各網目内での $D=\overline{|\delta h-\overline{\delta h}|}$ なる量所謂「もめ方」を表はす量、及びそれに相當する場所での傾斜を算出することが出來る。是等の量、即ち D 及び傾斜に就ては、それ等の値の極大値を持つ地域が接近してゐるといふことが知られた。

PENINSULA

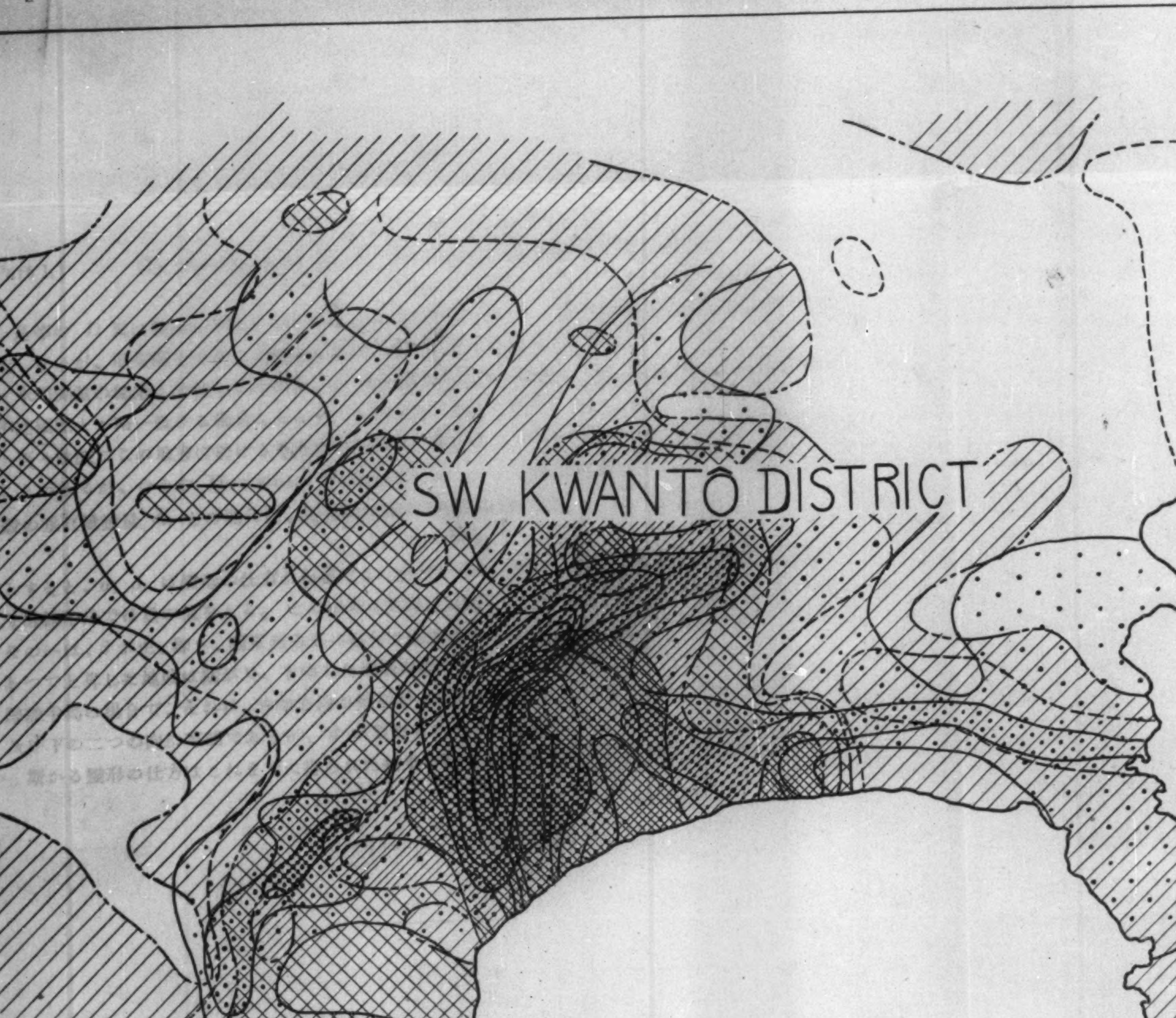
SW KWANTÔ DISTRICT
D
0—10
10—20
20—30
30—40
40—
Slope
0—2
2—4
4—6
6—

Fig. 3. Distribution of *D* and S

（震研彙報、第九號、圖版、宮部）

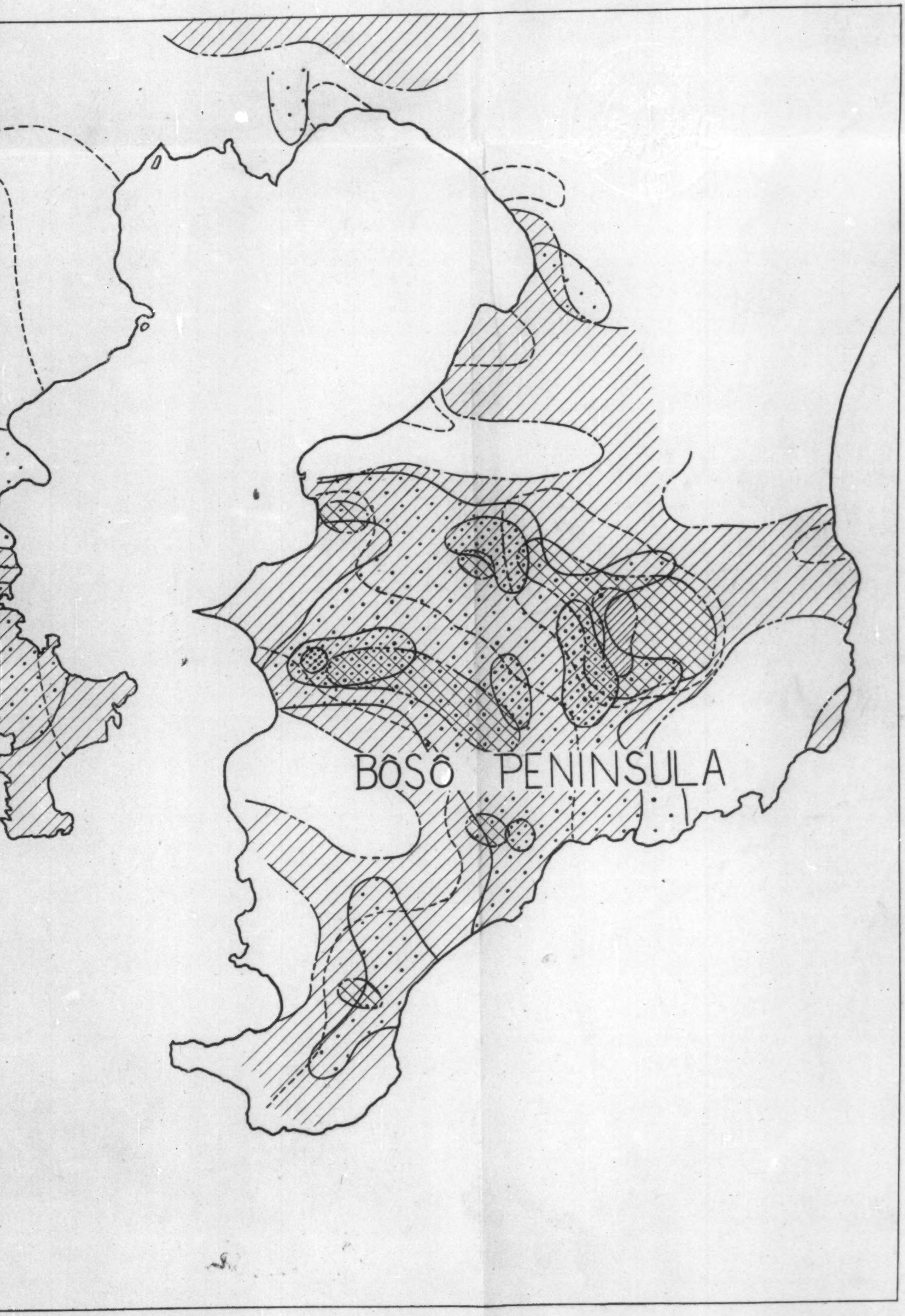
BÔSÔ PENINSULA

d Slope of Vertical Displacements.

是等の D 又は傾斜が周圍に比較して大なる地域は、一つ一つの地質學的斷層とは必ずしも一致しないが、地質圖上で多くの斷層の過つてゐる地域とは略々一致する。

水準測量の結果と比較してみると、D. 及び傾斜の大なる地域と、水準線路に沿ふ水準變化量の不連續點とが略一致する場合も多いが、一致しない場合もある。

吾々は旣にこの地方に於ける水平方向の地殼の變形を、一等三角點の水平移動量から計算したことがあるが、今その Horizontal Divergence Δ と、三角點の垂直移動によつて代表される地殼の垂直變動量 $\overline{\delta h}$ との間には、近以的に簡單な關係が求められる。その關係を假に

$$\Delta = \alpha + \beta\,\overline{\delta h}$$

とすると、α, β, は變形の仕方の相違による恒數である。即ち、關東西南部では β は正の値をとり房總半島では負の値をとる。この簡單な關係に相應して二つの地殼變形の仕方が考へられる。その一は、β が正、即ち、關東西南部の場合に適應するもので、主なる變形は flexure 的のものであつて上昇した地域は擴がり、下降した地域は縮む樣になる。その二は、β が負なる場合、即ち、房總半島の場合で、それは、水平方向の變形が contraction として起り、垂直方向の變形は（上及び下の二つの向に可能であるが、β が負なるために）上昇となる。

斯かる變形の仕方はこれまでに得られた結果の關する範圍內では至當の樣に思はれる。

2. *Recent Seismic Activities in the Idu Peninsula.* (*Part 1.*)

By Nobuji **NASU**, Fuyuhiko **KISHINOUYE** and Takao **KODAIRA**,

Earthquake Research Institute.

(Received Jan. 20, 1931.)

Introduction.

For the benefit of those who may be reading on the subject of the Idu peninsula earthquake for the first time, it should be explained that early last year, 1930, some 9 months before the occurrence of the destructive Idu earthquake which forms the subject of this paper, the town of Itô and vicinity, in the Idu peninsula, with one short period of intermission was, figuratively speaking, bombarded daily for more than two months by showers of earthquakes, the number of sensible ones of which at the end reached the total of more than 4880 shocks. Beginning in February 13, 1930, they increased progressively in both intensity and frequency until the culmination came as the big shock of March 22, at 17h 51m; after which they gradually declined in severity and in numbers, but on May 7 renewed their activities. In August however things had quieted down.

To the amazement of all in the town of Itô, the swarm of earthquake shocks began on November 7, and as on the previous occasion, daily increased in number and severity. On November 25 as many as 690 shocks were recorded at Itô, and on the morning of the 26 came the main destructive shock. It is of interest to note the enormous number of fore-shocks that preceded the principal earthquake.

The purpose of this paper is to consider the relationship that appears to hold between the earthquake swarms that preceded the Itô earthquake of March 22 and the swarms that acted as the prelude to the destructive earthquake of November 26. It will therefore be fitting to begin with a study of the Itô earthquake.

Observations on the Itô Earthquake.

With the object of studying these earthquakes on the spot, a party consisting of members of the Earthquake Research Institute and of the

Seismological Institute of the Tokyo Imperial University had established a network of five temporary seismic stations in and around the disturbed area, and the work of observation started from March 6. Seeing that the main shock–the most important one for our observation occurred sixteen days later, we were not belated as was at first feared. The main object of the seismic survey was to ascertain the foci of these innumerable shocks and their depths.

Unusual Focal Distribution of the Itô Earthquakes. The net results of observations obtained from these five stations are shown in Fig. 1. It will be seen that the foci cluster themselves within a small area in contrast to the after-shocks of the Tango earthquake, which were spread over a comparatively large one. The area embraced by the former could be circumscribed within a circle of radius only 2 kms., whereas in the latter, they embraced a zone roughly 50 kms. long and 15 kms. wide.

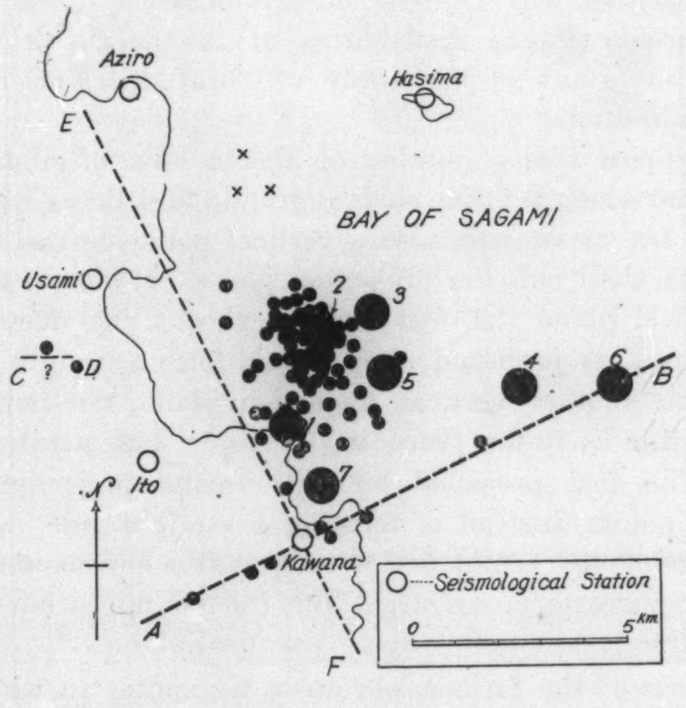

Fig. 1. Distribution of the epicentres of the Itô earthquakes.
Large dots indicate conspicuous earthquakes.
1 : Mar. 22. 2 : May 9. 3 : May 12. 4 : May 14
5 : May 17. 6 : May 26. 7 : June 26.
Small dots; in March. Crosses; in April.

It is of interest to see that besides the foci clustered under Itô Bay, there are some on the line passing near Kawana, extending in an almost N.E. - S.W. direction. A similar line (CD) passing near Usami runs in a east-westerly direction. It will be understood that the foci distributed on these two imaginary lines are nothing more than projections on the surface ground of the foci of earthquakes that have originated along a vertical fault plane. The existence of these planes having been deduced seismometrically, for their geologic significance we must await the verdict of the geologists; but that they are boundaries of crustal blocks there seems hardly room for doubt.

Three-dimensional focal distribution. The method of ascertaining the foci by stereometric projection was first applied to the investigation of the after-shocks of the Tango earthquake. Under Prof. Imamura's direction the same method was employed on this occasion. Briefly stated, it is an investigation of the distribution of the depths of the seismic origins–most important in the study of focal distribution but very difficult of realization.

Let us suppose that a number of shocks have originated along a fault plane that extends to the surface ground and shows itself there as a fault line. Let us suppose also a vertical plane normal to this fault line, which we shall call the projection plane. If now we project on this hypothetical plane the foci of the shocks just mentioned and join the points thus projected, they should form a straight line. Next let us suppose another vertical projection plane, not normal to the surface fault line as in the preceding example, but parallel with the fault line. The foci projected on this second projection plane as a number of points, instead of forming a straight line, will now be scattered without any semblance of order. It is obvious that when the projected epicentres form a straight line, the foci might have originated in a straight line just as well as along a vertical plane.

In the case of the former, obviously no matter in what angle we may project them the projected points will lie on a straight line. In a special case they may project to a single point.

Upon using the foregoing method we generally find that the projected points assume certain orderly forms, while the selection of the proper projection plane is always attended with more or less difficulty; although, if the depths of several shocks are already known, the choice is rendered much less difficult.

In studying the focal distribution of the present earthquake clusters we shall select the principal ones and apply the two methods of stereometrical projection. The first is shown by line EF in Fig. 1 and the second by line AB. These two are hypothetical surface fault lines as previously explained. The distribution of the foci are obtained by projection as follows:

(1). In Fig. 2, the distribution of focal depths as projected on plane EF is viewd from the east. An examination of the figure shows that with the exception of the foci projected on lines AB and CD, practically all the foci are clustered in the form of an inverted cone, densely packed at the top and gradually thinning downwards. The Projected foci as represented by line AB suggest that all the earthquakes there originated along a plane. We further see that they originated from depths greater than 4 kms. It should be added that this so-called hypothetical plane AB was found by a series of precise levellings to be a line of discontinuity between two contiguous crustal blocks. As to line CD there are not enough origins on it to justify any conclusions.

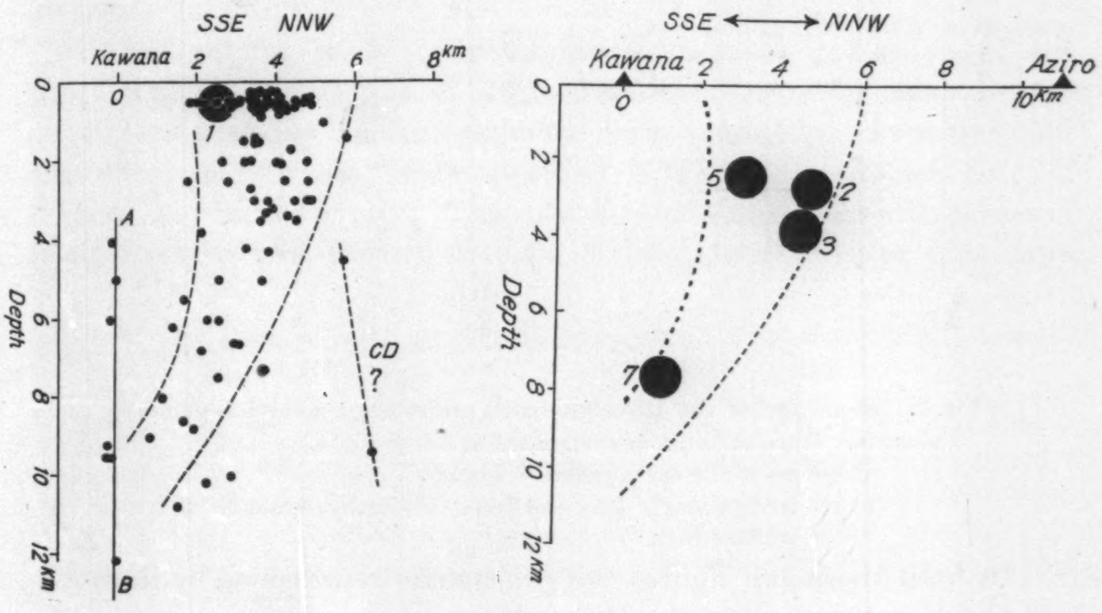

(a) (b)

Fig. 2. Seismic foci of the Itô earthquakes projected on a vertical plane, the surface trace of which is indicated by EF-line in Fig. 1.

(a) relates to the earthquakes of March.

(b) relates to those of May and June. Origins No. 4 and No. 6 in Fig. 1 are omitted here.

(2). Fig. 3 (a) shows the same projection as treated in the preceding paragraph, but viewed from the south. Here the foci are seen grouped together in a more orderly manner, but also densely toward the surface and gradually thinning downwards and ending at a depth of 10 kms.

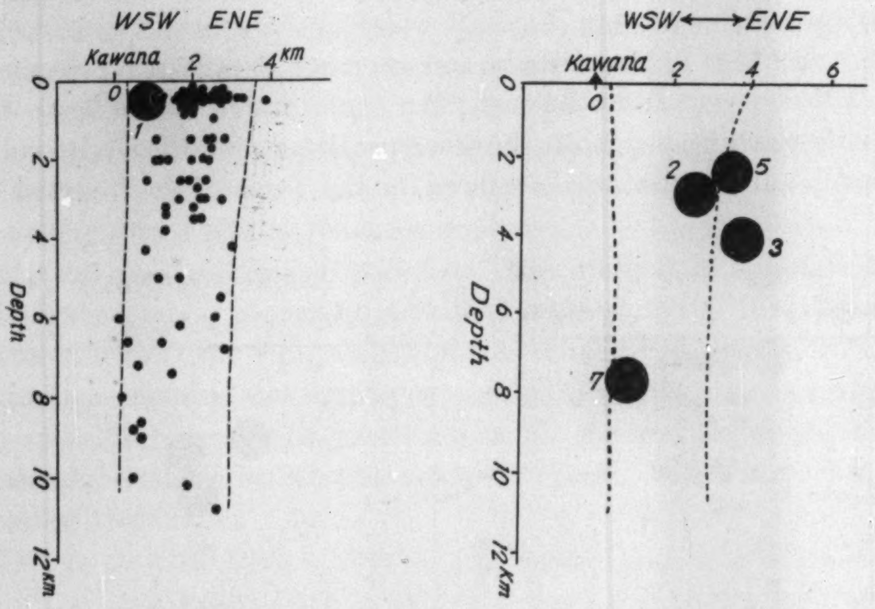

(a) (b)

Fig. 3. Seismic foci of the Itô earthquakes projected on a vertical plane, the surface trace of which is designated as AB of Fig. 1.
(a) relates to the earthquakes of March.
(b) relates to those of May and June. Origins No. 4 and No. 6 are omitted here.

In both these two figures the projections represented by lines AB and CD have been omitted. From these two projections we are led to conclude from the distribution of the majority of the earthquake shocks which harassed Itô and vicinity for nearly two months, that they emanated from a region having the shape of an inverted cone, in structure weaker than the surrounding rock mass. This sets one wondering whether it might not be the *neck* or *vent* leading to an extinct and buried volcanic crater.

The foregoing covers only observations up to the end of March. There was recrudescence of activity in May, when as shown by the method of projection, the foci of the shock-swarm had burst out, so to say, from the eastern side of the 'neck' thus enlarging the neck on that side without however causing any further deformation. Two shocks of importance then followed on June 26, the foci of which were in the neck as seen in Fig. 2(b) and 3(b). Excepting the earthquakes that occurred in the neighbourhood of Mt. Oomuro, there were no more serious disturbances until Nov. 7.

Here a few remarks might be made on the AB line of Fig. 1, the north-eastern end of which touches the 80 m. depression that occurred on the bottom of Sagami Bay at the time of the great 1923 Kwantô earthquake. By producing the line still further it cuts at right angles two great faults in the same sea floor. By producing it still further again it will reach the great trough (100–180m.) that formed on the same sea floor at the time of the earthquake just mentioned. The centre of this great trough lies some 20 kms. north-east of Kawana, one of our seismic stations.

After careful study of observations as made at Tokyo of the great Kwantô earthquake of 1923, Professor Imamura came to the conclusion that the shocks originated from more than one source, and that they were in weak zones running N.W.- S.E. in the sea floor of Sagami Bay and vicinity. The existence of three different sources of seismic origin was detected through certain characteristics that were

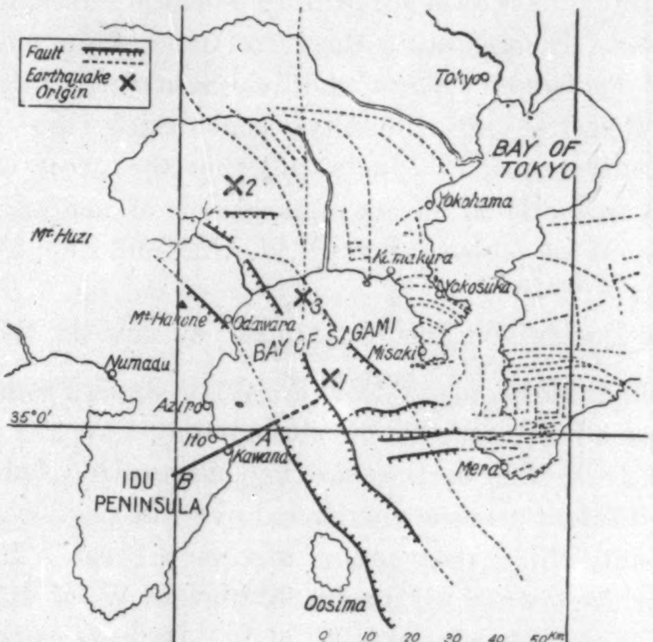
Fault
Earthquake Origin
Tokyo
BAY OF TOKYO
X2
Mt. Huzi
Yokohama
Kamakura
Yokosuka
X3
Mt. Hakone
Odawara
BAY OF SAGAMI
Misaki
X1
Numadu
Aziro
35°0'
Ito
A
Kawana
B
IDU PENINSULA
Mera
Oosima
0 10 20 30 40 50Km
139°0'
140°0'

Fig. 4. Shows the system of faults in and around the Bay of Sagami and the origins of the great Kwantô earthquake of 1923.

exhibited in the seismograms within 10 seconds from the beginning of the earthquakes. The origin first in point of time was in the middle part of Sagami Bay, 75 kms. 35°W. of Tokyo, and indicated by X_1 in Fig.4. The second big shock originated in Mt. Tanzawa (X_2), 72 kms. S. 60°W. of Tokyo, the seismic waves from which reached Tokyo 3 sec. after the arrival of that from the first origin. The third shock originated in Sagami Bay off the coast of Odawara, 67 Kms. S.W. of Tokyo. The seismic waves from this origin reached Tokyo 4½ sec. later than the one last mentioned. As for the other origins, the waves from them were masked to such an extent by the three waves just mentioned that it was impossible to isolate them.

Now the line of weakness AB that appeared with the Itô earthquake, when produced intersects at right angles the line of weakness in Sagami Bay, whence originated the first shock of the great Kwantô earthquake; but it is important to bear in mind that when the latter line was active in 1923, the former (AB) line was inactive or dormant, as was proved by subsequent precise levellings. Now it need hardly be remarked that where lines of weakness in the earth's crust intersect in the manner just stated, it forms a zone of tectonic weakness, thus forming a good vent for the release of pent-up volcanic forces, to say nothing of seismic forces. By assuming the correctness of the magmatic intrusion theory of Professors Ogawa and Ishimoto as the primary cause of earthquakes, there is no difficulty, considering the proximity of notorious volcanic zones, in concluding that the great Kwantô earthquake of 1923 was due to effects of intrusion of magma first into the weak intersections of fault running N.W.–S.E. and line AB.

The Destructive Idu Earthquake of Nov. 26, 1930.

This earthquake occurred Nov. 26 at 4h. 3m. From observations made at Tokyo, Prof. Imamura concluded that, like the great Kwantô earthquake of 1923, this earthquake had a multiple source of origin; namely, four different origins distributed over the northern part of Idu Peninsula, about which destruction was very great. The first origin developed near the town of Ukihashi, 10 kms. N.W. of Itô. The other three sources are situated W. or S.W. of it. Damage caused by seismic waves sent out from the first origin was slight compared with those from the remaining three sources, which were destructive. The foreshocks that kept up for 20 days prior to the main shock of Nov. 26 all came from one (1st) origin, and their number reached the total of 3411 instrumental shocks.

As observed at Itô, the initial motion of these fore-shocks without exception had a N.W. direction, the duration of the preliminary tremors being 1.5 to 2 sec. At Aziro they were E.N.E. and about 1 sec. respectively, while Mr. Kunitomi at Mishima station obtained a direction downward of S.S.E. and 2.5 sec. for the duration of the mean initial motion. From these data the fore-shocks were deduced to have originated near Ukihashi, lying 10 kms. N.W. of Itô. A remarkable fact is that while so many fore-shocks preceded the first big disturbance, the three other forcible earthquakes came independently without any fore-shocks.

The After-shocks. Soon after the destructive earthquake of Nov. 26, two seismographs were installed at Hiyekawa and at Tanna Basin with the object of forming a net of four stations for determining the three dimensional positions of the seismic foci as well as their depths.

Distribution of the After-shocks. As indicated by the small circles in Fig. 5, the after-shocks are clustered near Aziro and distributed along

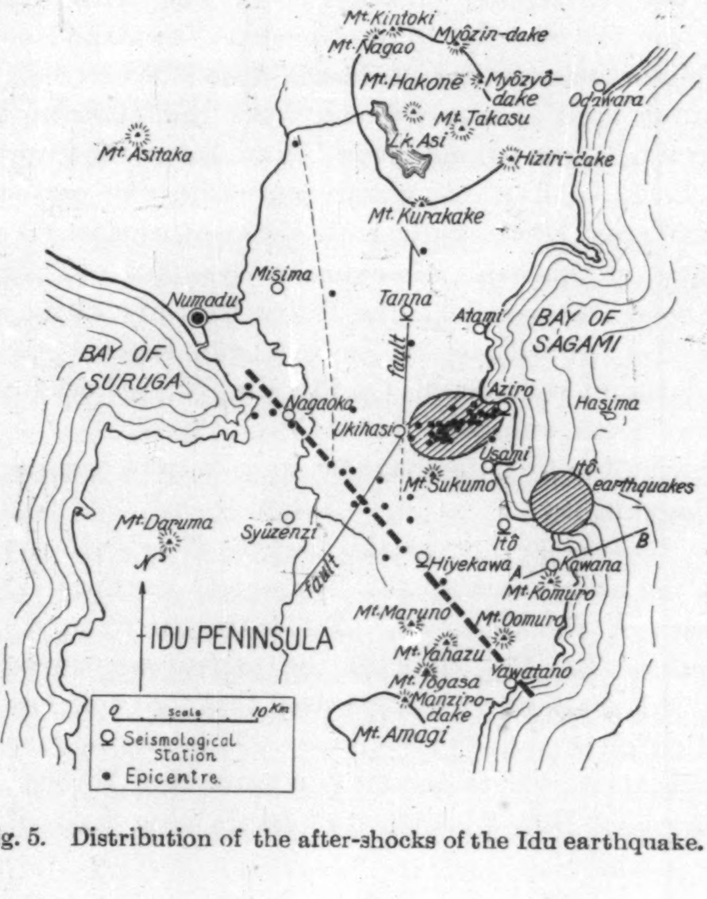
Mt. Kintoki
Mt. Nagao
Myôzin-dake
Mt. Hakone
Myôzyô-dake
Odawara
Mt. Takasu
Lk. Asi
Mt. Asitaka
Hiziri-dake
Mt. Kurakake
Misima
Tanna
Numadu
Atami
BAY OF SAGAMI
BAY OF SURUGA
fault
Aziro
Hasima
Nagaoka
Ukihasi
Usami
Itô earthquakes
Mt. Sukumo
Itô
B
Mt. Daruma
Syûzenzi
Hiyekawa
A
Kawana
Mt. Komuro
fault
N
Mt. Maruno
Mt. Oomuro
IDU PENINSULA
Mt. Yahazu
Yawatano
Mt. Togasa
Manziro-dake
Mt. Amagi
0 Scale 10 Km
○ Seismological Station
● Epicentre.

Fig. 5. Distribution of the after-shocks of the Idu earthquake.

the imaginary line drawn cutting the Peninsula in a N.W. to S.E. direction. Those clustered near Aziro exhibit the same peculiarities as those that clustered themselves near Itô after Feb. 10. This phenomenon may be explained as the continuation of the seismic activities resulting from the migration in a N.W. direction of the seismic centre that was active at Itô 8 kms. distant. The other after-shocks that arranged themselves on the N.W.-S.E. line just mentioned are fresh and independent outbreaks.

The Idu Seismo-tectonic Line. Dr. Ogawa postulates his 'seismo-tectonic' line for any particular region by the intensities of earthquakes that prevail there (judged by the damage wrought) and not by their frequency. That faults should characterize such weak lines hardly needs remarking. As such line in the Idu Peninsula he cites several that run meridionally and also across the Peninsula from N.W. to S.E. Forming on of the last-mentionad lines is the Nagaoka-Yawatano line of weakness as deduced from our investigation of the distribution of after-shocks; a seismo-tectonic line that we have found to exist in reality. On joining the two earthquake clusteres of Itô and Aziro from centre to centre, the line lies parallel to the Nagaoka-Yawatano line of weakness that runs obliquely across the Peninsula from N.W. to S.E.

The Tanna fault is a meridional weak line showing itself for the most part in the Tanna tunnel lying 150 m. below the ground surface of the Tanna Basin, and which was displaced in the earthquake under discussion 240 cms. horizontally with a downthrow of 60 cms. In the neighbourhood of this fault after-shocks were rare. There is another tectonically weak line parallel to the Tanna fault at a distance of 10 kms., which extending upwards, passes between the Hakone mountains and Huzi, both dormant volcanoes. On this line, after-shocks have occurred but not in any great number.

It is interesting to note that after-shocks have occurred also on the bottom of Sagami Bay.

Relation between the Earthquakes and the Tide-level. As will be seen from Fig. 6, the hourly earthquake frequencies at Itô corresponded with certain phases of the tide-level. For instance, upon comparing the frequency curve (See Fig. 6) with the mareogram curve obtained at the Misaki Tide Station, it will be seen that times of low water corresponded with high earthquake frequency. This was the case also with the earthquakes that started to disturb Idu since Nov. 7. (See Fig. 7.) The main big shock of Nov. 26 came two hours after time of lowest tide,

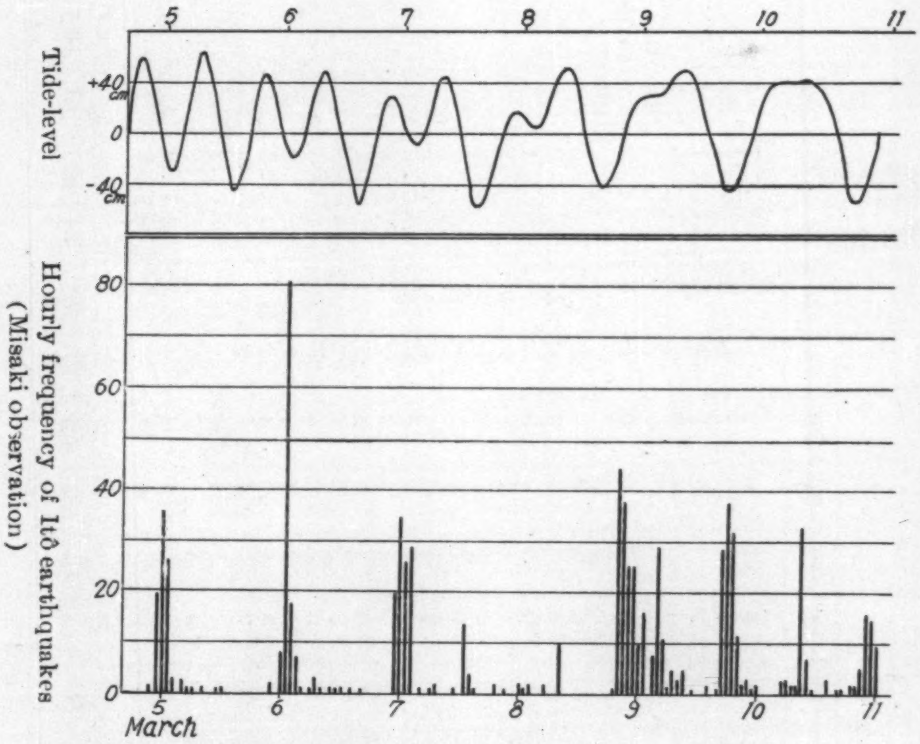

Fig. 6 shows the relation between the tide-level and the hourly frequency of the Itô earthquakes.

when the tidal load was comparatively small. This correspondence, though well-marked during the earlier onsets of the swarms of small shocks, gradually disappeared so that in time the relationship ceased to hold. At all events, the inference is that withdrawals of the tide load during the earlier periods of the earthquake activities were the trigger actions that set in motion the daily earthquake swarms. On the next page is a table of the hourly frequencies of the fore-shocks recorded at Itô.

As to the relation of earthquakes to atmospheric changes, our studies failed to produce any definite results, which is owing probably to our having so far availed ourselves of meteorological data covering Itô only, whereas if data from a few more stations were available some interesting results might have been obtained.

Earthquake swarms as mentioned in the preceding paragraphs are common occurrences before a volcanic eruption. The Idu Peninsula, as is well known, lies on the volcanic line beginning with Mt. Huzi and extending into the Pacific as far as the Sititô group of Islands. In the Peninsula itself are three large dormant volcanoes besides a number of

Table I. Hourly Frequency of the Fore-shocks.

Date / Time	November.																				
	7	8	9	10	11	12	13	14	15	16	17	18	19	20	21	22	23	24	25	26	
h h																					
0—1	0	0	0	0	0	0	1	1	1	2	0	0	0	0	8	1	1	0	1	5	
1—2	0	0	0	0	0	0	1	1	0	2	1	1	0	17	3	3	1	4	1	38	
2—3	0	0	0	0	0	16	0	1	0	0	1	2	1	36	2	3	2	13	1	5	
3—4	0	0	0	0	0	29	0	1	0	0	6	4	?	4	0	0	5	2	0	3	
4—5	0	0	0	0	0	5	4	1	0	0	0	22	?	6	0	1	8	2	3	destructive earthquake	
5—6	0	2	0	0	0	3	33	1	0	0	80	6	0	0	1	3	5	3	5		
6—7	0	0	0	0	0	2	2	0	0	1	27	0	1	2	0	1	21	1	2		
7—8	0	0	0	0	11	3	0	0	0	3	2	0	3	0	2	2	67	2	4		
8—9	0	0	0	0	1	4	1	0	0	17	6	1	0	0	0	4	44	1	2		
9—10	0	1	0	0	4	1	3	0	1	119	2	0	0	1	0	1	33	1	10		
10—11	0	0	0	0	1	0	11	2	2	63	1	0	0	1	11	0	17	0	9		
11—12	0	0	0	0	1	1	9	2	0	28	3	0	0	0	41	1	14	0	3		
12—13	0	0	0	0	0	2	1	3	0	42	3	0	0	1	16	2	10	4	3		
13—14	0	0	0	0	0	1	0	0	0	11	3	2	1	2	3	0	2	1	8		
14—15	0	0	0	0	0	1	1	6	2	7	1	0	1	0	2	5	7	21	127		
15—16	1	0	0	0	1	2	1	?	4	2	6	0	2	0	4	26	0	14	162		
16—17	0	0	0	0	0	4	1	?	14	4	18	0	3	0	4	19	0	4	145		
17—18	0	0	0	0	0	3	1	12	48	4	4	?	4	2	8	1	6	3	76		
18—19	0	0	0	0	0	1	2	2	39	3	1	?	3	40	4	4	3	3	36		
19—20	0	0	0	0	0	12	8	?	?	0	0	?	0	236	7	2	4	1	49		
20—21	0	0	0	0	0	40	79	?	?	0	3	?	1	123	209	3	4	1	12		
21—22	0	0	0	0	0	17	13	0	3	2	3	3	0	71	152	3	2	1	15		
22—23	0	0	1	0	0	1	0	2	1	3	4	0	0	18	98	2	2	2	9		
23—24	0	0	0	0	0	1	1	1	?	6	2	0	1	5	48	0	3	0	7		
Daily Total	1	3	1	0	19	149	173	36	115	319	177	41	21	565	623	87	261	84	690	51	Total 3411

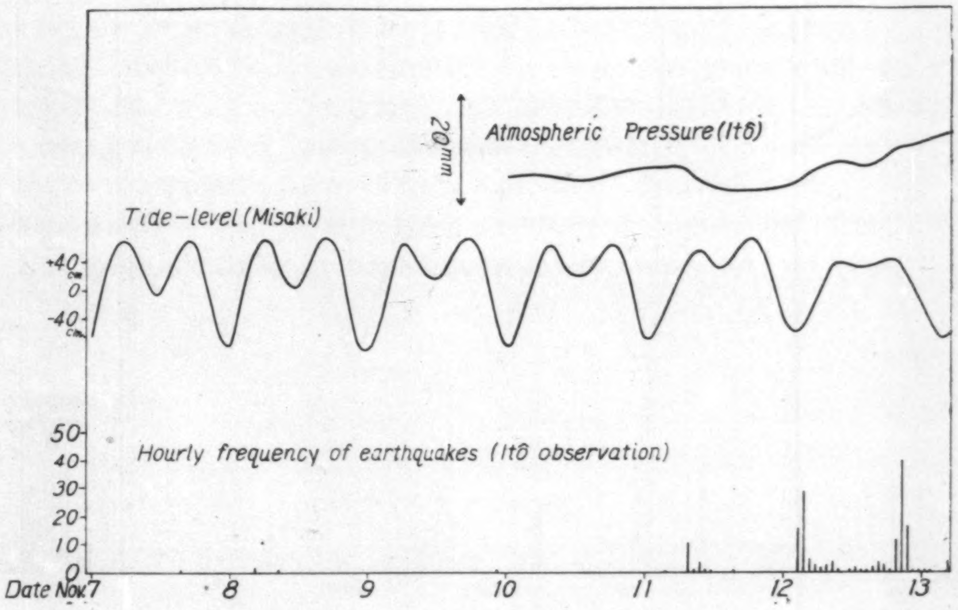
20mm
Atmospheric Pressure (Itô)
Tide-level (Misaki)
+40 cm
0
-40 cm
50
40
30
20
10
0
Hourly frequency of earthquakes (Itô observation)
Date Nov. 7
8
9
10
11
12
13

Fig. 7 (a).

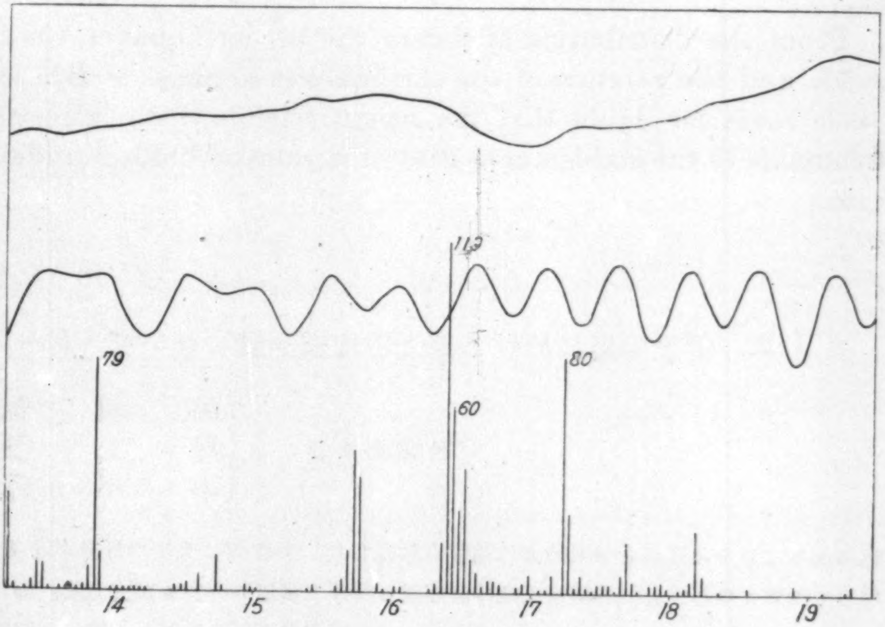
113
79
60
80
14
15
16
17
18
19

Fig. 7 (b)

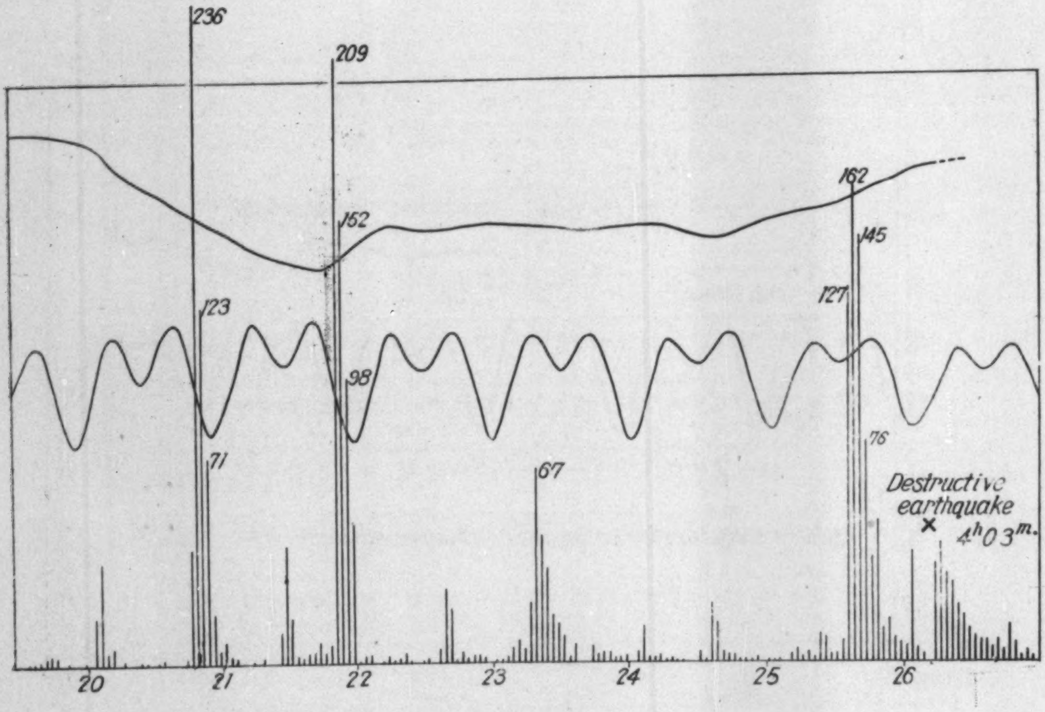

Fig. 7 (c).

minor secondary cones, and Itô itself is not far from what geologists have found to be the remains of an ancient crater a few square kms. in area.

From the distribution of foci of the Itô earthquakes, the swarms of shocks, and the relation of the earthquakes to phase of tide level, there is little room for doubt that the recent seismic disturbances there are attributable to the sudden activities of a volcano hidden under the bay of Itô.

2. 伊豆半島に於ける最近の地震活動に就いて（其一）

地震研究所
那須信治
岸上冬彦
小平孝雄

昭和五年二月十三日から伊東地方に地震が頻發した、筆者等は先年の丹後大地震の餘震觀測に則つて伊東を中心として五箇所に臨時觀測所を設けて震原の分布を調査した。即ち伊東、川奈初島、宇佐美、網代の觀測より震原の分布は一つの漏斗狀をなす範圍と相模灣の陷沒地帶より初まり伊豆半島をほぼ東西に横切る弱線に起つてゐたことが判つた。なほ震原分布研究を進めて關

東大地震の震原と伊東地震の震原とが如何なる位置的關係にあるかといふことにまで言及した。伊東地震は二月より三月末に至る間及五月中は最も活動したが八月に至つて全く平靜になつた。

突然十一月七日より再び網代附近に地震を感じ性質も伊東地震に類似するものであることが判たつが震原位置の測定のために再び觀測點を設置することになり伊東網代に器械を据へ終つたときに伊豆大地震となつた。それより餘震觀測を上の二箇所と丹那、冷川、吉原に於て行ふことゝした。その結果伊豆半島を西北より東南に横切る線にそつて餘震が起つてゐることを知つた。勿論この外にも伊東地震の繼續とも見るべき地震群が網代附近にも盛んに起つてゐた。

大地震の前震に就いて一時間毎の回數の統計をとり三崎に於ける檢潮儀の記錄と比較して矢張り伊東地震の際の如く低潮位のときに地震回數が相當多いことを知つた。

3.　北伊豆大地震の計測學的研究

地震研究所　今村明恒

（昭和六年一月二十日受理）

1. 概　説

昭和五年十一月二十六日北伊豆及び箱根の一角を襲ふた地震は局部的破壞地震の部類に屬し、二五九の人命損失、二一四二の住家、五九五七の非住家潰滅を惹起した。

これから前、一二週間、地震地方には小地震頻りに起り、而もこれが數と强さとに於て次第に勢力を增して來る模樣であつたから、これが單に無害な地震群なるか、將た大地震の前震なるか否かを研究すべき必要を感じ、先づ震原推定に必要な四點觀測をなすべく、那須、岸上兩理學士が出掛けることになつたのは、大震發生に先だつ六日のことであつたけれども、前者は漸く伊東に到達し、後者は網代に器械を据付けたとき、夫の大地震となつたのは遺憾な次第であつた。

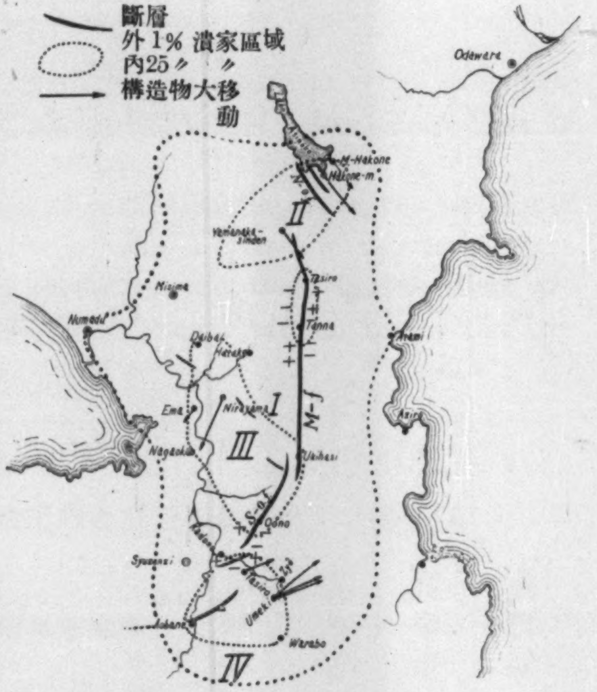
斷層
外 1% 潰家區域
內25 〃 〃
構造物大移動
Odawara
M-Hakone
Hakone-m
II
Yamanaka-sinden
Tasiro
Misima
Numadu
Tanna
Atami
Daiba
I
Ema
Nirayama
M-J
III
Nagaoka
Ukihasi
Asiro
S-O
Ono
Syuzenzi
Warabo
IV

第　一　圖　Fig. 1.

茲に斷つて置きたきは、前震の調査が地震豫知問題の研究に如何程の價値を有するかの點である。凡そ大地震にして小地震を數多く先發せしめる場合は、大地震の全數中一割位である。近年の地震に於ては、安政元年六月十五日伊賀伊勢大和大地震、明治二十九年八月三十一日陸羽大地

震、明治三十八年六月七日伊豆大島强震の數例に過ぎない。而もその小地震發生の經過が、無害な小地震群のそれに類似して居るので、兩者を區別することが頗る困難である。且つ斯様な小地震群發生の例も少くなく、明治三十二年攝津有馬地方鳴動地震、大正四年十一月上總一宮地方地震群、大正九年以來紀伊名草山地方小地震群、近くは昭和五年二月以來數月間伊東地方を脅かした地震群等がこれである。されば地震豫知問題の研究に於て、前震を考慮に入れることは大切ではあるけれども、餘り頼みにならない程のものである。

この際、特に告白して置き度は、今回の地震に關し、予に取りては豫備研究が不十分であつたことである。從來伊豆に於ては大地震が唯一回、承和八年七月五日(西紀八四一年)に起つたのみであつたが、これは正しく、關東地方が歴史年代に於て經驗した三回の非局部性大地震中、第一回弘仁九年(西紀八一八年)大地震の餘震であつたのである。次に大正十二年關東大地震に伴ひ、一時に解放された地震力が複雜な地形變動となつて現はれたけれども、今回の地震地方には、斯様な解放と見做すべき地形變動が起らなかつたことである。地震研究所では昨年三月伊東地震地方に於て十糎程の地盤の膨らみが起りつゝあることを測定し、尋いで十一月に於ては過去七ヶ月間に更に十二糎餘の膨み增加を測定した位であつたから、斯様な地形變動の測定は伊豆地方全體に擴張すべき價値のあつたものである。さうして、場合によりては其處に地盤傾斜の不斷觀測をも實施すべきであつたのであるが、注意が其處に屆かなかつたのは我ながら不覺な次第であつた。

2. 東京に於ける地震計測

今回の地震は東京に於ては比較的に能く觀測せられた。先づ前震或は餘震が、東京では如何なる地動となつて現はれたかを見ることにする。此は今回の大地震の地動を解釋するに、基礎の知識となるものであるからである。

第二版は大地震の前日、卽ち二十五日午後四時六分頃に起つた前震の記象である。此地震は前震及び餘震中で比較的に强いものであつたのである。記象の中、水平の成分は簡單微動計 ($T_0=6$ s, $V=50$, $r=2:1$) から取つたが、上下成分は便宜の爲め、別な地震計 ($T_0=18$ s., $V=7{\cdot}5$, $r\fallingdotseq 2{\cdot}2:1$) から採用した。

此處に此地震を擧げたのは、大地震の記象を分析する場合に於て、これが其基準となるものであるからである。圖版に於て見る通り、記象は實に簡單である。最初の縱波も、13秒後の横波も、略ぼ一回の重な往復振動から成立つて居る。卽ち本地震は一元地震と見ることが出來る。若し今回の伊豆大地震が同様に一元地震であつたならば、其記象と同じ様に、單純な振動から成立つて然るべきである。卽ち故大森博士が得られた様に、地震に大小の相違こそあれ、其記象は互に相似でなければならない筈であるが、實際はさうなつて居ないのである。

第二圖は今回の大地震の震動を分析した結果である。最初の三線は第二版の記象を模寫したものである。第四線は今回の大地震記象の上下成分の模寫である。此原圖（第三版）は前に記した18秒週期の地震計で記錄したものであるが、倍率が7·5倍なる爲め、最初の三つの位相、I II 及び III を記した後、描針が記錄紙の外に飛出した。それで止むを得ず、其以後の部分は二倍强震計及び二分の一大震計によりて之を補ふことにした。併し今回の地震に於ては、徹頭徹尾10秒程度の週期にして且つ他に比べて頗る大なる波動が現はれたから、上記の强震計及び大震計は、動もすれば共鳴の現象を起さんとして居るから、從て眞實の地動が不明瞭となつて居る場合が多い（第三版參照）。それにも拘らず、次の位相IV以下は斯様な器械に依る觀測を採用したのであるから、前の部分に比較して、正確の度合が低いものである。

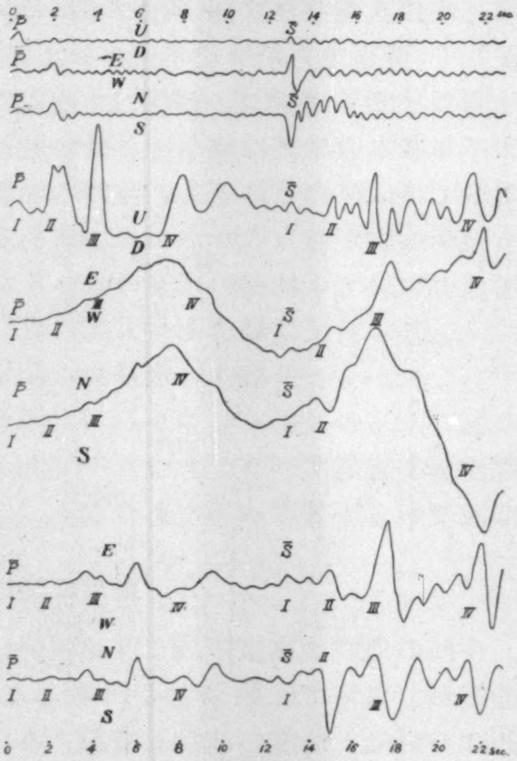

第二圖 Fig. 2.

東京地震記象分析圖

第一—第三線 十一月二十五日
一元地震（倍率二十五）
第四—第八線 十一月二十六日大地震
（倍率第四線二·五 第五、六線二分の一
第七、八線實大）

第二圖の第五、六線は長週期地動計を用ひて得た地動（第四版）の模寫

であつて、記錄された地動の週期最大約 10 s. に比較して、十數倍の週期の振子で得たのであるから、十分に信用を置いて可なる積りである。別に第五、六版に示した樣に東西成分 47 s. 南北成分 36 s. の振子で得られた記象があるけれども、生憎大鼓胴が强震の爲めに不規則な廻轉をなした形跡がある。從つて短波の觀測につき最も大切な週期が不完全に觀測されたのである。但し此記錄は斯く不十分な點を備へて居るけれども、10 秒週期の波動の觀測は比較的に能く出來てゐる。最初から凡そ 30 秒目に、週期 9 s., 二倍振幅 14·7 cm. の波動が見ぇるが、斯く大きな地動が比較的無難に記錄されたことは、吾々の教室に於て最初の例である。

此 10 秒週期の大波動を除去すると、後に殘つた短波が、第七、八線に表はしてある。

以上は今回の大地震の東京で得られた觀測結果を、分析したものであるが、之に用ひた地震計の常數を再錄すれば次の通りである。

第一表　Table I.

地震計 seismograph	(成分) component	倍(縮)率 V	自己振動週期 T_0 (秒)	制動率 r
簡單微動計 tromometer	(東西) E-W	50	6	2·0:1
	(南北) N-S	50	6	1·7:1
	(上下) Vert.	28	5	1·2:1
上下動地震計 Vertical mot. seism.		7·5	18	2·2:1
長週期地動計 long period hor. pend.	(東西) E-W	5·0	133	2·5:1
	(南北) N-S	1·5	155	1·3:1
地動計 horizontal pendulum	(東西) E-W	1·5	47	3·6:1
	(南北) N-S	1·5	36	2·7:1
强震計 strong motion seism.	(東西) E-W	2	9	1·5:1
	(南北) N-S	2	9	1·5:1
	(上下) Vert.	2	3	1·3:1
大震計 large mot. seism.	(東西) E-W	½	9	1·6:1
	(南北) N-S	½	9	1·5:1
	(上下) Vert.	½	4	1·3:1

此等の器械によりて觀測した結果は凡て問題の大地震記象の分析に應用

したのであるが、特に重きを置いたのは、$\bar{\mathrm{P}}$ 波に就いては 18 秒週期の上下動地震計、$\bar{\mathrm{S}}$ 波に就いては 133 秒週期の東西成分長週期地動計が與へた記象であつたことを斷つて置く。

次に分析結果につき、それが最初に示した一元地震と如何に異なるかを吟味し、且つ問題の大地震記象に現はれた各位相が如何なる機構に由つて發生したかを想像して見たい。

先づ 10 秒週期の著しき波動につき、東西竝に南北の成分を組立てゝ見ると、最初は略ぼ北東に動いて居るが、10 幾秒の後、南東に轉じて居る。予はこの波動の發生が、地震の基因たる地塊運動にありと解釋して居るのであるが、果して然らば、この種の波動も、短波と同樣に、震原地方から縱波及び横波の波形によつて傳播するのであらう。但し、波動が如何に大なりとも振動週期大なるが爲めに、人體に與ふる感覺は鈍いが、波長大なるが爲めに能く遠方へ傳達する性質を有して居る。遠方大地震の觀測は卽ち斯樣な長大な波動の存在に依るのであつて、これが到達と共に、その地方に固有な短波も誘起されるのであらう。

今地震記象から、斯樣な長大な波動を除いて見ると、その跡に殘るものは、第二圖底部の二曲線となる。それは 1 秒內外の波動の連續であるが、不思議なことには、それが圖中、上端の一元地震と相似形をなさないことである。悉しく言へば、最初から 1·6 秒間は相似形をなすも、この時突然大なる波動が加はつて居ることが見ゑる。この事は圖中第四曲線上下動地動計記象を第一線に比較して見ると最も明かに了得せられるであらう。$\bar{\mathrm{S}}$ 相に於ても斯樣な特徵が現はれて居る。結局本記象は I II III IV の四元から出發した地震を記錄して居ると見做されるのであつてその各地動は次の通りである。

初動 ($\bar{\mathrm{P}}$)

I 東京時刻 4 時 3 分 6 秒、方位北 47 度東上方、
II 同 7·6 秒 北 51 度東上方、
III 同 9·7 秒 北 39 度東上方、
IV 同 13·5 秒 北 37 度東上方。

主要動 ($\bar{\mathrm{S}}$)

I 全振幅 1·8 粍 週期 1·1 秒、
II 8·9 粍 1·3 秒、
III 14·4 粍 1·7 秒、

IV　12·0 粍　1·0 秒。

以上の外、特に記載すべきは、初期微動繼續時間が概して相等しく、約 13 秒を示して居ること、最大動は最初から凡そ 30 秒目に起り、その全振幅 14.7 粍、週期 9 秒なること、總繼續時間は約 2 時間なりしこと等である。斯様な大地震が地震計によりて斯く完全に記錄せられたのは今回が最初の記錄であらう。

四元の出發點は初動の反方向によりて示されるが、北から數へて II I III IV の順になつて居る。又その大いさに就いては I は最小であつて、震原地方でも破壞作用をなさなかつだであらうが、II III IV は略ぼ同階級の勢力であつて、何れも破壞作用をなしたであらう。試みに、I を單位として大さの比率を作つて見ると、

1 : 5 : 8 : 7

となるのである。これ等は震度分布と比較して極めて興味深い結果が得られるのである。

3. 震度分布

震災地域に於ける震度分布を調べるに最も好都合なるは罹災家屋數の百分率を應用することである。十二月二日調內務省公報に據れば、被害町村中、潰住家數の世帶總數に對する百分率一以上のものは次の通りである。

三島町 3, 北上村 3, 錦田村 11, 中鄉村 15, 函南村 23, 韮山村 41, 江間村 27, 川西村 11, 下狩野村 5, 中狩野村 13, 上大見村 6, 中大見村 8, 下大見村 40, 北狩野村 28, 修善寺町 2, 田中村 4 清水村 3, 深良村 2, 熱海町 1, 箱根町 50, 元箱根村 19, 蘆の湯村 18。

即ちこの表にも見る通り、被害の最も甚しかつた場所が、北から數へて箱根•韮山•大見の三方面に區劃されて居ることが氣附かれる。更にこれを詳細に驗する爲めに、各町村の字別に潰住家數の百分率を取り、その 25 以上の場所を地圖に印して見ると、第三圖に示した通り、上記 3 個の區域が一層明瞭に現はれて來る。

震度大なりし町村に於て、字別を目安とした潰住家百分率は次に示す通りである。

錦田村—谷田（やだ） 9, 中 17, 竹倉 8, 玉澤 0, 川原ヶ谷 13 (元山中 30), 塚原新田 42, 市山新田 37, 三ッ谷新田 11, 笹原新田 30, 山中新田 80。

中鄕村—梅名 8, 中島 22, 大場 56, 多呂 0, 北澤 72, 八反畑（はつたはた） 4, 鶴喰 0, 青木 39, 新谷 4, 玉川 1, 堀之內 0, 平田 4, 杉本 3, 長伏 11, 御園 5, 安久（やすひさ） 63。

函南村—仁田 53, 大土肥 43, 柏谷 69, 畑毛 21, 平井 76, 丹那 41, 畑 40, 輕井澤 55. 田代 50, 桑原 16, 大竹 6, 上澤 38, 間宮 43, 塚本 5, 肥田 18, 日守 1, 新田 24, 奴田湯 40, 大竹鐵道官舎 0, 熱海隧道鹿島細工場 0。

韮山村—韮山 45, 山木 70, 多田 73, 奈古屋 31, 長崎 98, 原木 38, 四日町 66, 寺家 48, 中條 70, 南條 83, 中 72, 內中 90, 土手和田 60。

江間村—南江間 31, 北江間 32。

川西村—長岡 26, 古奈 23, 小坂 9, 天野 32, 長瀨 0, 戶澤 0, 花坂 25, 堋之上 25。

下狩野村—大平 0, 本立野 0, 小立野 7, 日向 5, 加殿 12, 田代 25。

中狩野村—上船原 2, 下船原 1, 青羽根 32, 本柿木 2, 大平柿木 2, 松ヶ瀨 0, 佐野 38, 雲金 68。

上大見村—原保 34, 中原戶 47, 戶倉野 13, 菅引 16, 地藏堂 0, 徭場 0, 貴僧坊 11, 姫之湯 51。

中大見村—城 2, 八幡 25, 梅木 34, 宮上 0, 柳瀨 53, 冷川 19, 德永 7。

下大見村—關野 66, 元村 54, 小川 58, 西 0, 清水 14, 上和田 29, 長者原 14（北狩野村長者原と合算す)。

北狩野村—牧之鄕 3, 柏久保 5, 年川 28, 大野 77, 田原野 26, 浮橋 56, 下畑 73, 長者ヶ原 14（下大見村長者ヶ原と合算す)。

田中村—大仁 2, 吉田 4, 神島 0, 三福 1, 田原 23, 御門 41, 白山堂 17, 守木 50, 宗光寺 0, 田中山 65。

清水村—玉川 1, 新宿 0, 伏見 0, 八幡 0, 長澤 1, 柿田 0, 堂庭 0, 久米田 0, 戶田 0, 畑中 0, 的場 43, 湯川 0, 下德倉 5, 上德倉 20。

此表に於ても氣附かれる通り、斯く推定せられた字別震度分布圖に於ては、其處に往々震度分布の不連續線とも稱すべき特異性が見出されることである。此事は韮山及び大見兩方面の激震區域について特に著明である。試みに一例として大見方面を一瞥して見るならば(第三圖)、潰住家 25% 以上の部落に接して、0% の部落が存在して居ることである。震災地方を視察して居る際、全部落殆んど滅亡の憂目を見て居るのに隣りの部落は、全く無難であつて村民平日の業務を勵み、平和を樂しんで居る狀態など所々に見受けられたのである。

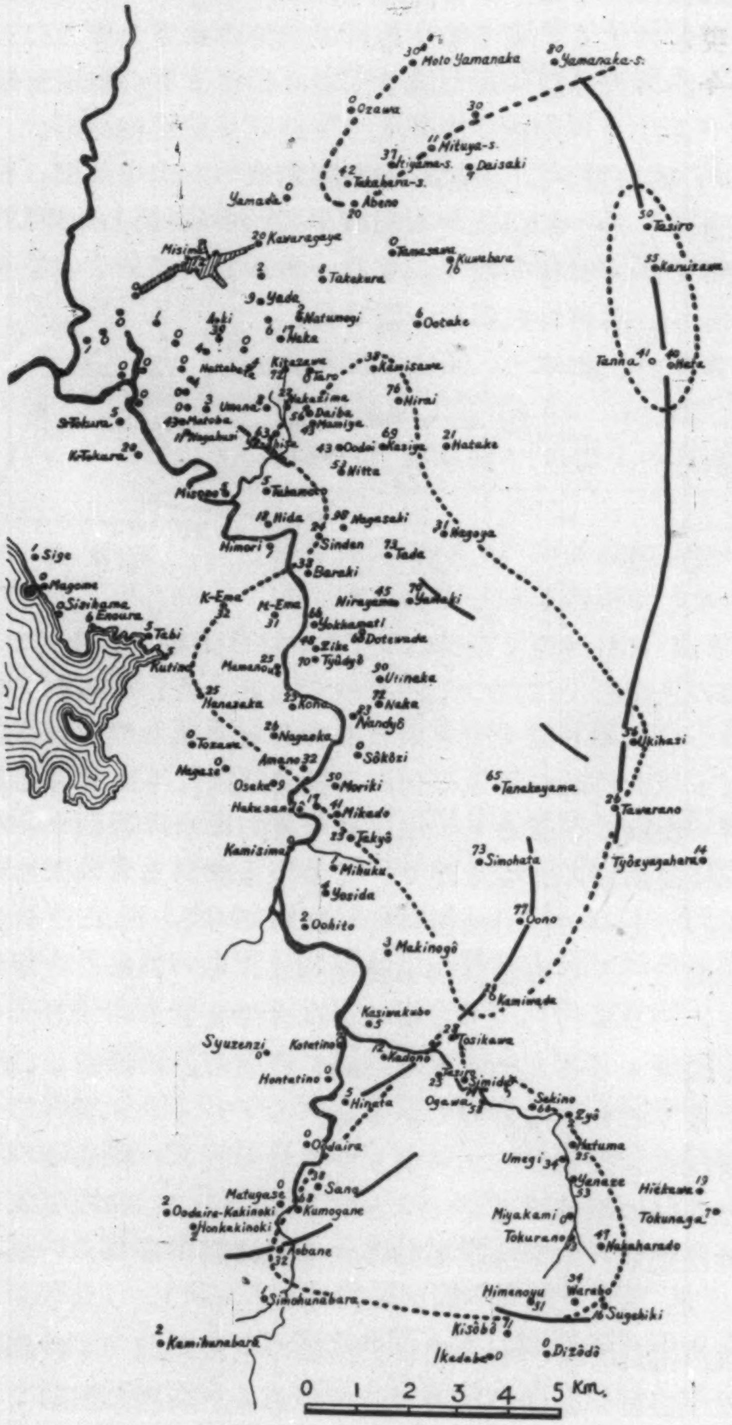
Moto Yamanaka
Yamanaka-S.
Ozawa
Mituya-S.
Kiyama-S.
Daisaki
Takahara-S.
Abeno
Yamada
Kawaragaya
Misima
Tamasawa
Kuwabara
Takakura
Yada
Natumegi
Aoki
Naka
Ootake
Tasiro
Kannizawa
Tanna
Hata
Hattabara
Kitazawa
Taro
Kamisawa
Umena
Nakazima
Daiba
Mamiya
Hirai
S-Tokura
Matoba
Nagakubo
Oodai
Kasiya
Hatake
K-Tokura
Nitta
Misono
Takamoto
Hida
Nagasaki
Nagoya
Himori
Sinden
Tada
Sige
Magome
Baraki
Sisikama
Enoura
K-Ema
M-Ema
Nirayama
Yamaki
Tabi
Yokkamati
Dotewada
Kutina
Zike
Mamano
Tyûdyô
Utinaka
Hanasaka
Kona
Naka
Nandyô
Tozawa
Nagaoka
Ukihasi
Sôkôzi
Amano
Nagase
Osaka
Moriki
Tanakayama
Hakusan
Mikado
Tawarano
Takyô
Kamisima
Simohata
Tyôzyagahara
Mihuku
Yosida
Oono
Oohito
Makinogô
Kamiwada
Kasiwakubo
Syuzenzi
Kotetino
Tosikawa
Kadono
Hontetino
Tasiro
Simida
Hinata
Ogawa
Sakino
Zyô
Oodaira
Hatuma
Umegi
Sana
Yanaze
Hiekawa
Matugase
Oodaira-Kakinoki
Kumogane
Miyakami
Tokunaga
Honkakinoki
Tokurano
Nakaharado
Aobane
Himenoyu
Warabo
Simohunabara
Sugehiki
Kisôbô
Kamihunabara
Ikadaba
Dizôdô
0 1 2 3 4 5 Km.

第三圖 Fig 3.

前記の三區域に於て震度が特に大であつたことは、物體の轉倒及び家屋大移動の現象によりても證明せられる。特に家屋大移動二三尺に及べるものは、今回の大地震に於て數多く現はれた。その數例を擧ぐれば次の通りである。

箱根町—65 糎南東へ。元箱根—40 糎南東へ。山中新田—亞鉛葺、43 糎南東へ。韮山—18 坪瓦葺、70 糎南 30 度西へ（第七版甲圖）。堈之上—2 間に 4 間瓦葺、20 糎南西へ。平井—門 70 糎北微西へ。北狩野村田代—觀音堂、40 糎北 80 度東へ。梅木—5 間に 8 間草葺 62 糎北 70 度東へ。2·5 間に 6 間瓦葺 73 糎北 60 度東へ。4 間に 9 間草葺 63 糎北 75 度東へ。

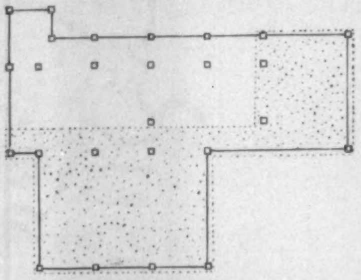

第四圖　點線內混凝土
Fig. 4.

第七版甲は韮山に於て 18 坪の木造家屋が大移動をなした模様を示してゐるが、其平面圖（第四圖）に於て見る通り、14 本の柱は混凝土の上に立ち、12 本の柱は土間の土臺石上に立つて居たのである。若し全部が混凝土の基礎の上に立つて居たならばもつと大きな移動をなしたであらう。

斯の如き家屋大移動の現象は何れも構造堅固な平家建に起るのであつて、構造若し堅固ならざるときは反對の方向に潰れ若しくは傾くのが通常である。今更斷はるまでもなく、この現象は斜なる大振動の反復によりて起るものであつて、大地震に於て經驗せらるべき震度の最大限度を示すものと解すべきである。卽ち構造物は、その斜めなる地動の垂直成分が上方なるとき進行し、下方なるときに停止するのであつて、同様の地動が反復繼續することによりて、同じ方向のみに移動し、隨つて長大なる徑路を畫くことになるのである。

地震が斯様な大振動のみから成立つて居るとき、構造物の木材と、基礎の石材との間の摩擦係數を 0·6 と取るならば大移動の現象を起し得べき限界條件は震度 5 割 1 分、振動の水平面に對する角 31 度となるときである。

一般に震原附近では、右の如き大振動の上に週期 0·1 秒或は 0·2 秒程度の急激な小振動が加はつて居ることがある。斯様な振動はその加速度往々重力の加速度以上にも達することあるべきも、振幅小なる爲め、單獨では構造物の大移動或は倒潰、傾斜を惹起す能力に乏しく、僅に壁體

に龜裂を生ずるか、或は能く結束せられた構造物の小移動(二三寸程度)を惹起すに至ることもある。若し前記の如き急激な小振動が、反復性の斜な大振動と相伴つて起るときは前者が摩擦係數を輕減するに等しき作用をなし、大移動の現象を惹起すべき震度の極限値を小ならしめる傾向がある。併しながら今回の地震に於ける江間小學校々庭魚雷大移動の現象から推測すると、前記の如き摩擦係數減小率は 0·6 に對して最大 0·1 程度に過ぎなかつたものと考へられる。果して然らば構造物の大移動を經驗した地方に於ける震度は、5 割程度なりしと見做して大差ないであらう。

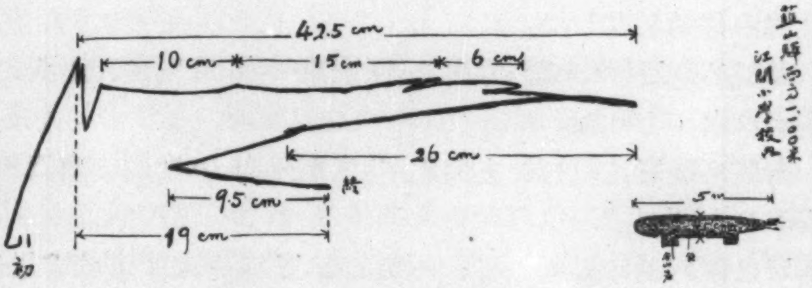

第 五 圖　魚雷面上の地震記象　Fig. 5.

江間小學校々庭にある魚形水雷の面に印せる模様は、最激震地方に於ける地震の天然記象と見做すべきものである(第七版丙圖及第五圖)この魚形水雷は南 5 度東に向け、2 個の安山岩の臺石上に安置してあるが、急激な大振動の爲めに、魚雷が地震計の不動點の役を勤め地動の前記方向に於ける成分を安山岩の一突起點を以て魚雷面の塗料膜上に記したのである。但しその模様が普通の地震記象と異なる點は、曲線が地面上の一點の動いた軌道でなくして、前に記した構造物大移動の軌道を畫いて居ることである。即ち先づ左下方から始めて一往復半の縦波がありしを示し。續いて 4 回 (或は 5 回) の一進一止を繰返して合計 41·5 糎の大移動をなし、更にこれに續いては上下動の位相急變したと見え、逆行の大移動をなして停止して居る。若し接觸面間の摩擦係數を 0·45 とするときは、本現象を起すに足るべき震度の極小限は問題の方向に於ける成分として 3 割 6 分、振動方向と水平面との間の角は 24 度となる。この場處に於ける主要地動の方位は南 30 度西一北 30 度東であつたらうから、前の推測からしてこの場所の震度は少くも 4 割 4 分となる。

以上の意味に於て、本魚雷面の模様は最激震の天然記象としてのみならず、構造物大移動の狀況を如實に記錄した世界唯一のものであらう。

斷層と地震の原因

今回の地震に於て、斷層の講究は尙ほ十分ではないけれども、次のものは先づ確かなものとして良いであらう。

（一） 北斜め斷層（箱根）方向北西—南東。

（二） 縱斷層（丹那）方向南北、丹那盆地では斷層の西側が關係的に南へ240糎の移動をなした。

（三） 南斜め斷層甲（大野）方向北30度東—南30度西、西側の關係的最大橫ずれ南へ100糎。

（四） 南斜め斷層乙（加殿）方向北70度東—南70度西、南側の關係的最大橫ずれ130糎。

以上の斷層は雁行的に竝列して、一個の斷層系をなすものと思はれる。又隆起或は沈下に就ては各斷片の一端に於ける狀況のみが圖に記入してあるが、實際は蝶番の樣な狀態をなし、南斜斷層甲片の西側は南上方へ、乙片の南側は東上方へ向ふものゝ樣である。

地震の原因には、近因あり、遠因あり、專攻者の立場によりて、採用の範圍に遠近深淺の區別があるけれども、地震計測者たる吾人としては、地震及び地形の計測的結果を生ぜしめるに足るべき地震發生の機構を以てその講究の範圍として居る。

斷層の活動は地震の一原因たるに異議はない。併しながら、斷層の活動だけでは說明し難い地震動のあること、最近の計測結果が示す通りである。然るに地塊運動なる立體的動作は地塊の境界に於ては斷層の活動を包含し、地震計測に現はれる各種の地動を說明し得べく、且つその實現が地形測量によりて證明せられるから、吾々の講究範圍に屬する地震發生の機構は具體的の基礎に立脚して居るのである。

今回の地震の主原因は所謂丹那斷層の活動であると速報せられたが、斯く原因を狹く解するとしても、其處に不可解な點が殘されて居る。成程この斷層は他の三斷層片に比較して最も偉大なるに相違ないが、然しながらその規模如何に大なりとしても、それは單に靜的狀態に於て然るのであつて、若し斷層が徐に且つ滑かに起るときの如く、動的條件が地震を起すに不適當な場合もあるのである。事實丹那斷層はこれに近いも

のたる證跡がある。即ち大正十二年關東大地震の場合及び嘉永六年小田原大地震或は安政元年東海道沖大地震の場合に於ても丹那盆地に於ては小規模ながら今回と同様の地裂現象があつたと言はれて居るのである。今回の地震に於ては同じ盆地に於ける震度は2割乃至2割5分であつたらう。1里程正東にある熱海に於ける震度が更に輕かつたことなど、他の斷層片の場合に比較して著しき相違である。

東京の地震計測に現はれた第一元は、三島•沼津•伊東等近所の觀測によりて、第一圖Iの場所。東經139度0分、北緯35度2分たることに大なる誤差はないであらう。

東京地震記象の第一元は右の通りのものとし、又全記象を支配する10秒週期の振動は斷層系の西側地塊が南方へ、隨つて東側の地塊は相對的に北方への運動から起つたと假定するとき、記象上の第二元乃至第四元は多分震度分布上の第二元乃至第四元の何れかに相當すべく考へられる。さうして問題の地塊運動は先づ第一元から始まり、それが斷層系に沿ひ、北と南とへ進行して、順次に箱根元•韮山元•大見元に到着し、其處にそれぞれ破壞作用の急激な振動を惹起し、さうして全部の地塊運動は約10秒間で終つたものであらう。各元に於ける激動が如何なる機構によりて生じたかは、これ亦一個の問題であるけれども、各激震區域に相當する地塊片が斷層發生と共に、斯様な激動を誘起されたものではあるまいかとも考へられる。各區域に於ける激動の立體的方向と相當斷層面喰違の立體的方向とが略ぼ一致すること、及び震度分布が各區域の境界に於て不連續的な傾向を示すことなどによりて、然か想像せられるのであるが、併しこれは全く予一個の說たるに過ぎないのである。

如上の地塊運動を起した歪力は、最初に述べた如く、大正十二年の關東大地震を惹起した歪力と共通なる履歴を有したものであらう。即ち予は今回の地震を以て關東大地震の一餘震（廣義の）と稱へて居るものであるが、伊豆全國に於ける歪が今回の地震によりて如何なる程度まで解放せられるに至つたかは、水準測量及び三角測量の結果によりて始めて解せられるであらう。

3. *Seismometric Study of the Recent Destructive N. Idu Earthquake.*

By **Akitune IMAMURA**,

Earthquake Research Institute.

The destructive earthquake that devastated the northern part of Idu Province, besides causing great damage at the Hakone watering place, occurred in 139°0′ E, 35°2′ N on Nov. 26 at 4 h. 3 m., resulting in a loss of 259 lives and destruction of 2142 dwellings and 5957 houses of other description. Fore-shocks were felt as early as Nov. 11, gradually increasing in number and intensity. Conditions being somewhat threatening, we despatched on the 20th two observers equipped with three seismographs in order to gain some idea as to whether they were harbingers of a large earthquake to come, or whether they were merely a group of harmless shocks. Unfortunately however they reached their destination only on the 25th., so that they were able to observe the great earthquake only at Aziro, and at Ito, where the fourth seismograph was yet running since it had been started 8 months ago. Later, the other instruments were installed at Hiekawa and Tanna, forming altogether a net of four stations.

Of various earthquake phenomena, the outstanding one is the relation between the distributions of faults and seismic intensities (see Fig. 1). Of the number of faults that appeared, four are especially noteworthy. One, which is *meridional* (the pre-existing Tanna fault), underwent a dislocation, as is proved at the Tanna Tunnel which lies some 500 feet below the ground surface of the Tanna basin, with relative horizontal shift of 240 cm., and down-throw of 60 cm. of the west side, though the dislocation is much less apparent on the basin surface. Dislocations along this fault seem to occur fairly easily; similar phenomenon, though on a smaller scale, having been noticed at the time of the 1923 earthquake, and in either or both of the 1853 and the 1854 earthquakes. The second, the Hakone fault, which trends NW–SE, may also be a continuation of the former or, at least, a segment of the Tanna fault-system. The third fault, which begins near Ukihasi obliquely to the meridional fault, and which may be its continuation, is 8 km. long, trending S 30° W–N 30° E with relative southward shift of 100 cm. at maximum. The fourth fault, which may be a continuation of the former, appeared most conspicuously at Kadono, there trending S 70° W–N 70° E,

（震研彙報、第九號、圖版、今村）

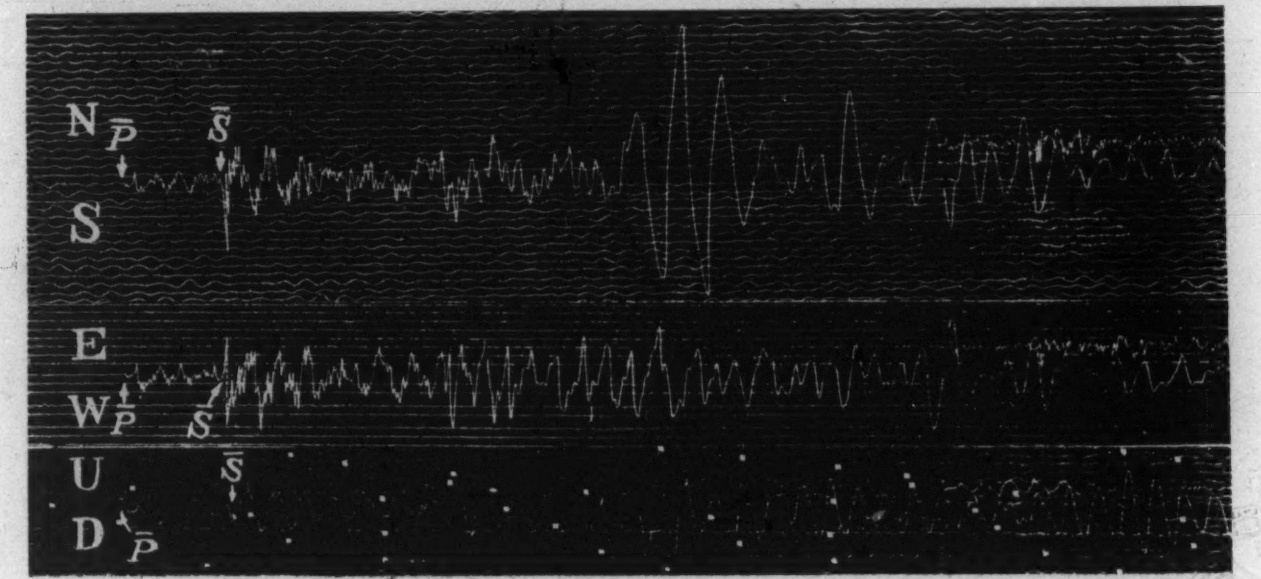

No. 1. Time scale : 1 min.=55 mm.
Magnification : hor. 50, vert. 28.

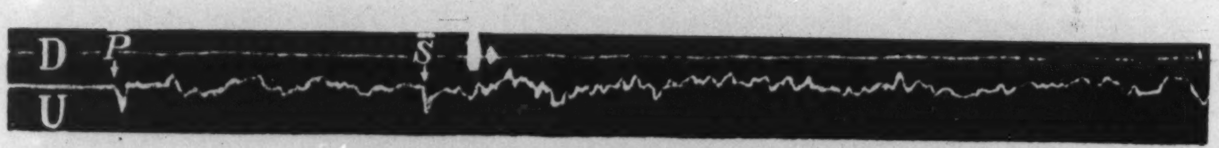

No. 2. Time scale : 1 min.=169 mm. V=37·5.

第六圖　十一月二十五日前震の東京觀測

Fig. 6.

（震研彙報、第九號、圖版、今村）

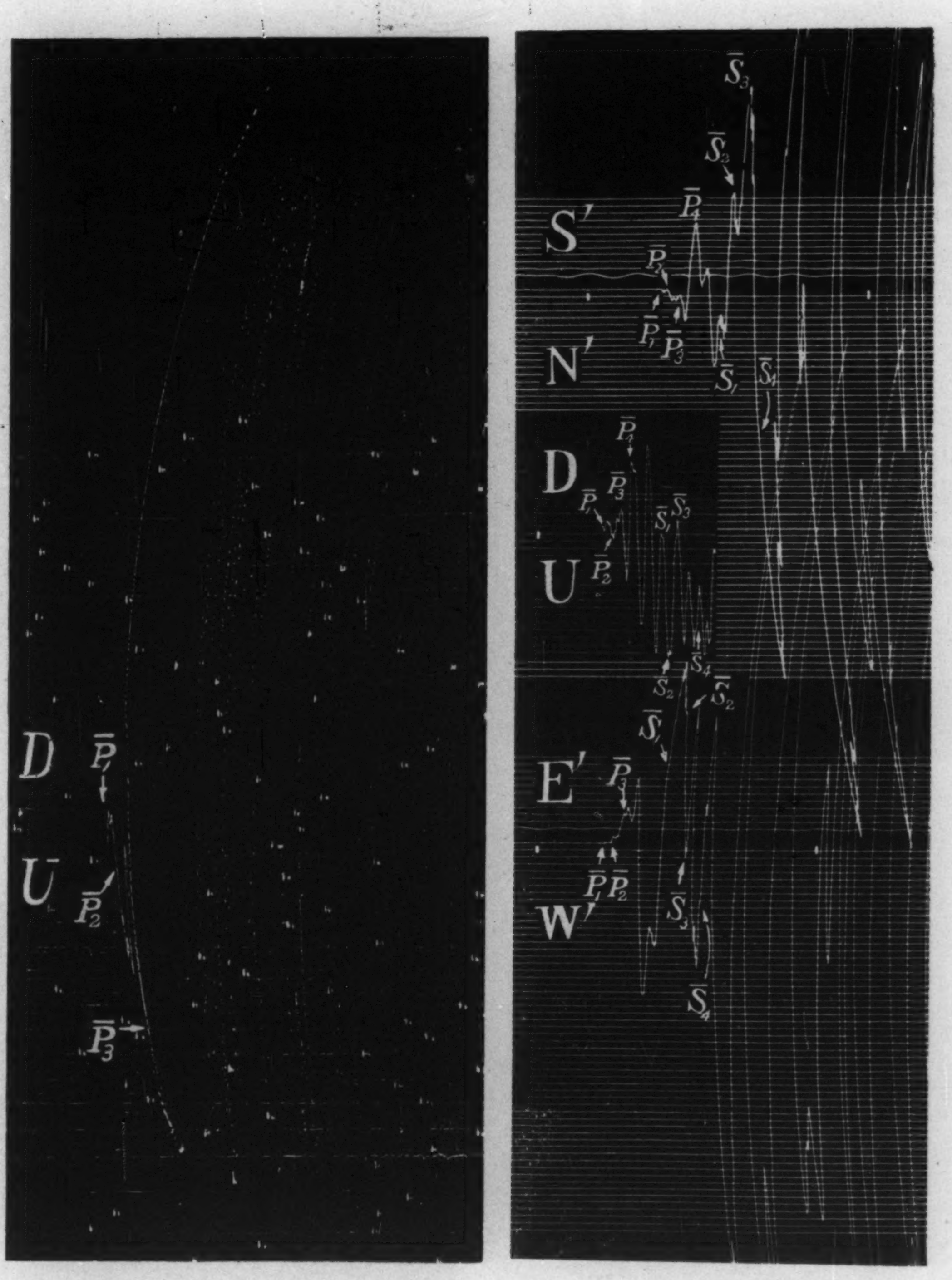

No 1.　Time scale : 1 min. = 35·2 mm.　　No. 2.　Time scale : 1 min. = 40 mm.

第七圖　大地震の東京記象

Fig. 7.

（震研彙報、第九號、圖版、今村）

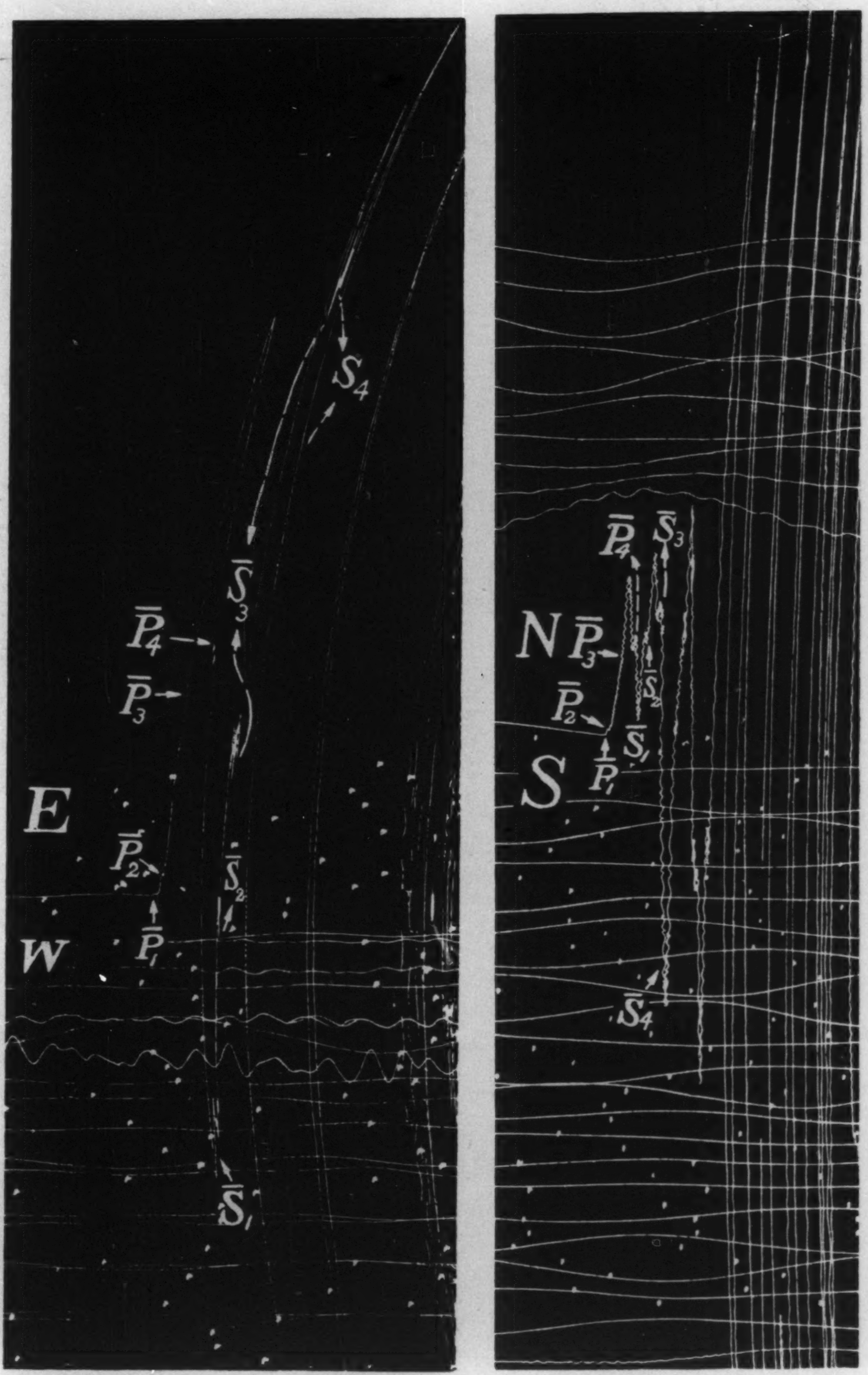

No. 1. Time scale: 1 min. = 30 mm. No. 2. Time scale: 1 min. = 23 mm.

第八圖　大地震の東京記象（長週期地動計）

Fig. 8.

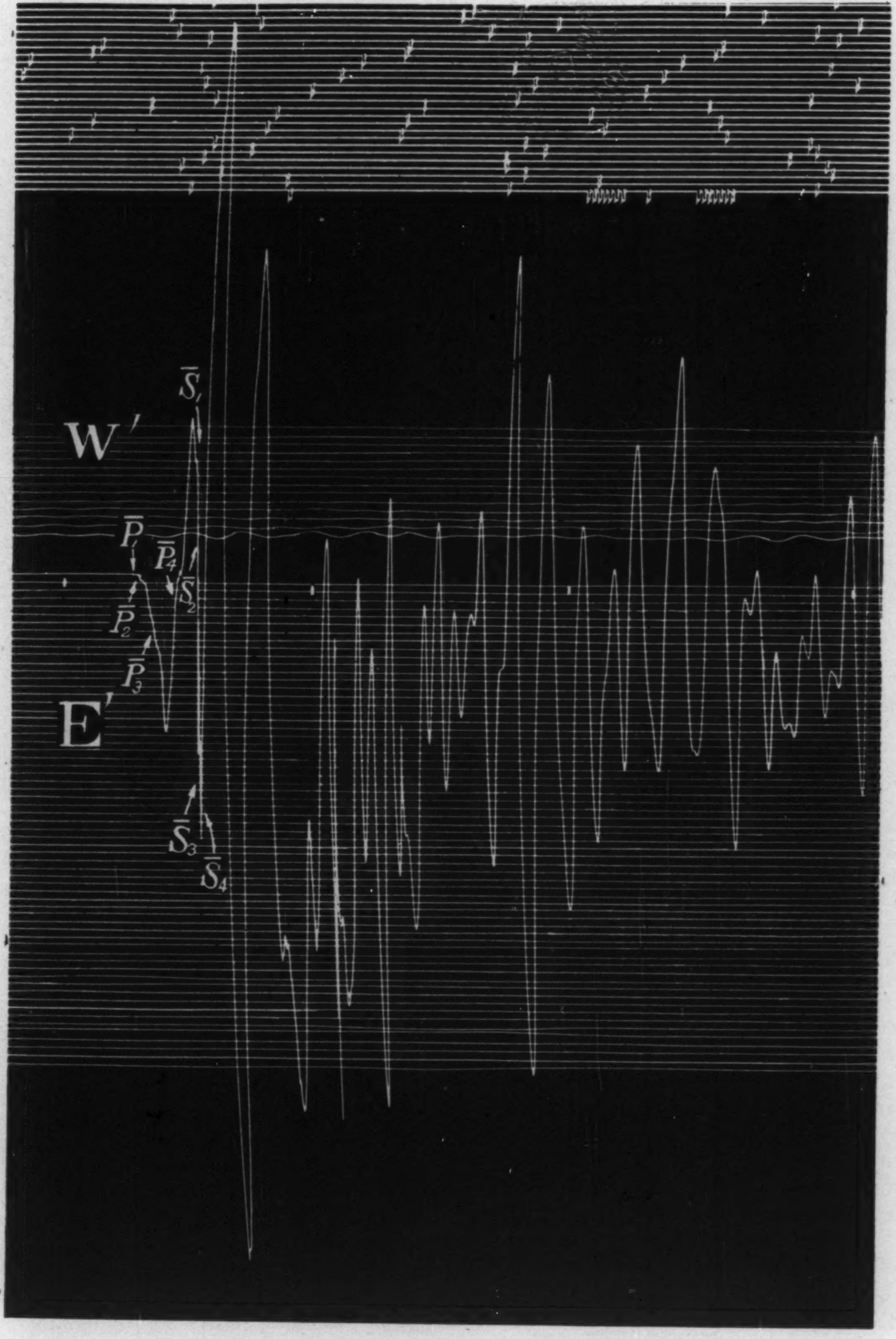

（震研彙報、第九號、圖版、今村）

V=1·5. Time scale: 1 min.=35 mm. E′=N 77° E, W′=S 77° W.

第九圖　大地震東京記象（東西動）

Fig. 9.

（震研彙報、第九號、圖版、今村）

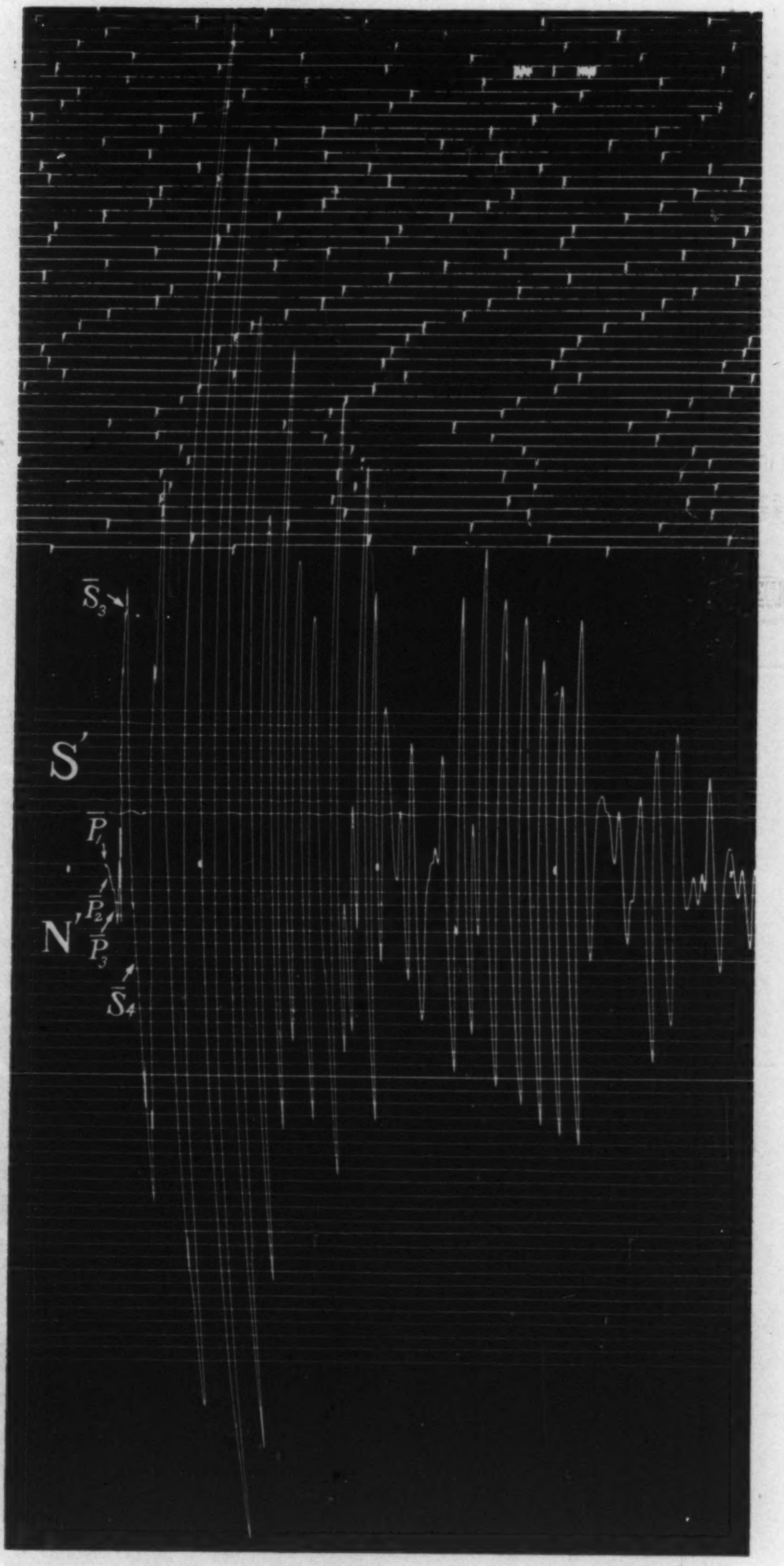

V=1·5.　Time scale: 1 min.=28 mm.　N′=N13° W, S′=S 13° E.

第十圖　大地震東京記象（南北動）

Fig. 10.

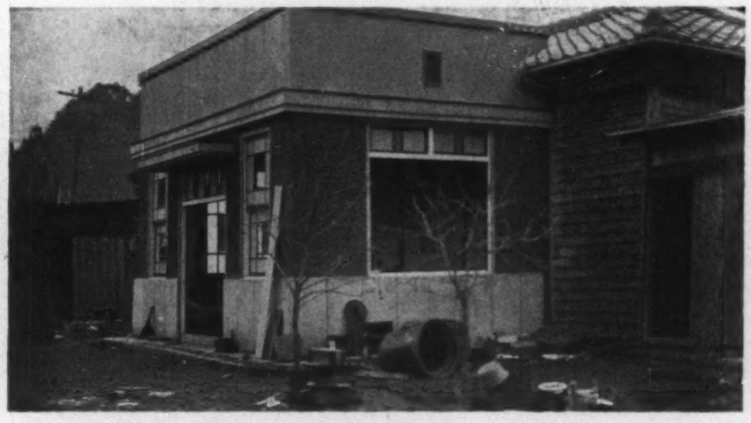

一、韮山、家屋大移動

No. 1. Large displacement at Nirayama.

二、梅木、家屋大移動

No. 2. Large displacement at Umegi.

三、江間、地震の天然記象

No. 3. Natural seismogram obtained at Ema.

（震研彙報、第九號、圖版、今村）

第十一圖 Fig. 11.

with relative southward shift (max. 130 cm.) and upthrow (max. 50 cm.) of the west side. Strangely enough, the maximum seismic intensity was manifested around the Hakone or *north oblique* fault and the two *south oblique* faults, whereas with the *meridional* fault, damages due to earth-shakings were not so great, though structures were thrown down where the ground was crossed by faults or fissures as was experienced at the Tanna basin, etc. How violent was the seismic intensity in the meizoseismal areas is best seen from Figs. 1 and 3; the arrows indicating the direction and extent of large displacements of simple structure, and which serve to indicate the intensity as well as the 3-dimensional direction of the earth-vibration at the respective places. The phenomenon is also illustrated in Pl. VII and Figs. 4 and 5. It may be stated that the earth-shakings that caused so much damages in the seismic area originated mostly along the three oblique faults.

Another characteristic feature was observed in the seismograms obtained at Tokyo as illustrated in Fig. 2, which is the result of analytic study of the diagrams (Pl. II–VI) that have been obtained with seismographs given in Table I. It shows the time of commencement as 4 h. 3 m. 5.7 s., duration of the preliminary tremors as 13.0 sec., period and amplitude of the $\overline{\mathrm{S}}$ phase as 1.1 sec. and 1.8 mm. respectively. Further analysis shows that the earthquake consisted of waves which may be regarded as to have emerged from four different sources as shown in Table II. These sources could be identified with those marked in Fig. 1 as I, II, III and IV.

Another interesting feature is the presence of vibrations of a period of some 10 seconds from the very beginning to the last, and attaining after 30 sec. from the commencement a double amplitude of so much as 14.7 cm. (see Pl. V and VI)—largest amplitude so far perfectly recorded with instruments in Japan. These long waves were propagated to Tokyo first as that of dilatational type and then as that of distortional type, and may be regarded as caused by the bodily movement of the crustal block constituting the seismic region.

The block-movement thus seems to have started somewhere near the middle point of the fault-system, passed, on one hand, quietly over the meridional fault towards the north, and, on the other hand, towards the south, sharp destructive shocks having been emerged from both of the three oblique faults.

4. 割れ目の出來方特に雁行性に就いて

地震研究所 藤原咲平
高山威雄

（昭和六年一月二十日受理）

著者等は大正十二年の關東大震災以來破壞現象に興味を覺へ、二三の研究[1]を發表したが更に初歩の實驗を續け數月に渉つて本所談話會席上に發表した。[2] 以下は其梗概であるが、何回にも作つた原稿である爲に文體用語等の統一が得られて居ない。只是等を整理する時間の餘裕がないが爲に其儘にして發表するのは心苦しい次第である。尙實驗はしても細叙する必要のないものは省略して、只其結果丈を第二章に述べた。又此研究中で一番重點を置いたのは雁行性裂罅の研究で、是は第四章に於て述べた。從て第四章に於ける結論は此雁行性に就いてのみの結論である。總體的結論は第二章に於て述べてある。

第一章 緒論

1. 目的 地震の研究中最も進歩したるは震波論にして最も進歩せざるは破壞の物理ならん。我國は地震國にして從て破壞地震の大なるもの

---

[1] (1)「地形の渦卷と相模灘大地震」氣象集誌 43, 1-6. (2)「相模灘大地震の機巧に於て」驗震時報 1, 161-170. (3)「地渦と地裂線とに就いて」地理敎育 3, 1-11. (4)「火山脈と山體裂線とに就いて」地理學評論 1, 735-758. (5) "Torsional form on the face of the earth," 長岡記念論文集、地球物理學輯報 (1928), (6)「北丹後地震踏査報告」「北丹後地震と割目の實驗」驗震時報 3, 191-209, 125-132. (7) "On the echelon structure of Japanese volcanic ranges and its significance from the vortical point of view," *Gerlands Beiträge*, (1927), 1-14. (8) "On the mechanism of the great Sagami Bay earthquake on Sept. 1, 1923." *Bull. Earthq. Res. Inst.*, 6, 149-176. (9)「地形から地殼の移動從て地殼に働く歪力を判斷することの可能度に就いて」地震研究所彙報 7, 523-530. (10)「北伊豆地震踏査報告及模型實檢」驗震時報 4, 65-73.

[2] (1) 歪み割れの研究、大正十五年七月六日講演。(2) 震源帶相互の活動に就て、昭和二年四月十九日。(3) 緣邊の割目に就て、同年五月十七日、(4) 割目の實驗、同年六月廿一日。(5) 往復的歪力による裂罅の生成、附地震帶相互活動及餘震に關する一考察、三年七月三日。(6) 鍛冶屋澤の山崩に就て、四年三月十九日。(7) 裂罅の一種に就て、同日。(8) 紅海附近の構造に就て、同年七月四日。(9) 切り込みを有する板の撓曲による內力の分布に就て、五年六月十七日。(10) 割れ目の出來方特に雁行性割れ目の出來方に就いて、五年十一月十八日。

あり。故に破壞の物理學的研究は學者間には假令興味少なき問題なりとするも、應用の見地よりすれば打ち捨て置き難きものと思考せらる。

物體破壞に關する研究は從來工學方面に於て材料の强弱の檢定等に於て研究頗る多し、然れ共主として諸種工作物に應用せらるべき方面の研究を、主とするが故に自然吾人の目的に適するもの少なし、吾人の第一の目的は破壞の起りたる後及進行中の形相を見て其破壞を起したる力の加はり方を知らんとするに在り、而して研究の順序としては、知られたる力を加へて種々なる形相の破壞を起らしめ、其間に或種の法則を發見して後是を逆用せんとするに在り。

地球上二大造山帶卽環太平洋及地中海造山帶あるは良く知らるゝ所にして是が我國に關しては或はゼオシンクライン說ありオローゲン說あり。或は大陸よりの側壓を稱へ又は海中よりの傍壓を高潮する等諸說紛々歸する所を知らず要するに地形に依りて其壓力の如何なるかを判斷する知識が正確を缺くに依り、諸說皆空中樓閣の感ある所以なり。

我日本は不幸此環太平洋造山帶に屬し從て地震及火山現象の頻發するを免れず、故に地震火山等の如き地變を豫知せんとせば先づ其大原因たる造山作用を究明するを要す、其爲には空想的研究を捨て、實際に就きて其原動力の發露を探究し其力の本體を捕ふるを要す。然れ共此方針に依るも一朝一夕にして目的を達し得可きには非ず。又一人二人の單なる努力に依りて達せらるゝものにも非ず、吾人は目的と方針とを定め可及的確實なる一步を踏まんと欲す。

2. **方針** 旣に著者等によりて注意せられたる所によれば地球表面に於て或は渦巻式地形の整然たるものあり、1),3)又雁行裂罅の是に伴ふものあり1),3)此種形體は吾人をして其成因の偶然ならざるを思はしむ。然れども此形態たるや幾千幾萬方里の地殼地表の示すものにして、又必ずや幾萬幾億年の營力の下になされたるものなるべし、從て吾人は是を直接實驗に依りて研究するを得ず。是を所謂理論的に誘導せんとするも旣に數學の可能範圍を超越せるを以て其理論たるや只假定と空論に過ぎざるものたる處多し。是に於て吾人の進むべき道の甚限られたるを覺ゆ其一は造山物質の物理的性質を測定する事なり、其二は適當なる寸法と適當な

---

3) (1) "Growth and Decay of Vortical Systems, Appendix II," *Japanese Journal of Astr. & Geophysic*, Vol. I, No. 5, 180. "Vortical Formation on the Face of the Earth, *ditto* Vol III, 103. Also see Prof. Nagaoka's Aniversary Volume. (2) "On the Volcanic Ranges of the Japanese Islands," *Gerl. Beitr.*

る物性を有する材料に依りて小規模の實驗をなす事なり、其三は所謂 principle of similitude 等を用いて測定せられたる岩石の性質と實際の規模を有する形態を小實驗の形態より推斷する事なり。此方法は氣象學地學等に於ては最も信頼し得可き方法の一たるべし。

かくて吾人の第一に知らんと欲するは高溫高壓下に於ける岩石の性質なり、而して此方面の研究は外國に於ては Adams, Goldschmidt, 等吾國に於ては長岡博士、神津博士等の研鑚あり、未だ完了と云ひ難きも駸駸たる進步は吾人の意を强ふするに足るべし。

第二に知らんとするは地殼の成層狀態及岩漿の配置なり。此方面は一方地震波動の檢測よりして、古くは Wiechert 近くは Mohorovicic, Gutenberg 等の研究あり、又 Jefferies, Joly 等の議論もあり、吾國に於ても亦國富氏和達氏松澤氏等の研究あり。尙又無線電波による大氣の檢測の如く電波を利用する地下の檢測は將來に於て希望を繫ぎ得るものなるやも知れず。

第三に知らんとする事は地殼破壞の實狀にして一は地形學的に一は地震學的に進涉すべきものなり此二點に於ては吾國に於ては殊に材料と研究者に富むは世間熟知の事なり。殊に近來我國に於てブロック構造の實情の明になりあるは著しきものなり。

斯くて殘る所は地震の實際破壞又は現狀地形等を示すべき實驗的研究なり、然れ共茲に困難なるは Viscosity 及 Plasticity を有す物質の力學殊に其破壞に於ける基本方程式の確立せざる事なり。又第二は岩石に於て是等諸性質の未だ充分に測定せられざる點なり、よつて吾人は豫め實驗開始に際して寸法、歪力等を決定し難し。依りて止むを得ざる方法として先づ結果に於て地殼及地震に於ける形態と類似したる形態を作り出し置き、將來に於て方程式及常數の明になりたる場合の用に供せんとす。斯くて實驗の結果は尙半途にあるものにして實際の地震に對して結論を得るには困難の場合多きも幸にして實驗の途中破壞に關する一般法則の如きものを得れば、是が應用として地殼に於ける現象を推論するを得べし。

以下に於ては上の趣旨に從ひ物質の變形及破壞に關する實驗及觀察を整理し置き將來の研究に資せんとす。

3. **實驗概論** 實驗としては定量的實驗が望まる可きものなれども初步に於ては先づ定性的に全般の關係を概觀する事も亦必要なり。依りて

本篇に於ては定性的概括的の部分を主とし時々數量的のものを加ふるに過ぎず。

材料としては岩石等を用ゆべき様考ふるは最も自然的なれども小規模に於て模型的に行はるゝ際の彈性、粘性、可捏性(plasticity)は實際造山作用の際に大規模に現はるゝ是等の性質と同一物たり難し、是れは近來氣象學上に於て空氣の粘性として小規模の場合にはmolecular viscosity(分子粘性)を用ゐれども大規模の場合に於ては所謂eddy viscosity(渦亂粘性)が主として働く事と類似し、更に具體的に說明すれば一岩石標本に依りて測定したる彈性粘性、可捏性は分子的のものなれども、實際地殼を形成しある場合は常に縱橫の裂罅を有し、此裂罅を有する大塊に於ける見かけ上の彈性、粘性、可捏性は明に標本の示すものとは異なる、又其裂罅の平均距離數米程度のもの卽所謂joint(節理)の影響する範圍は數十又は數百米以內の現象に於て著しかるべく、更に數十又は數百粁以內の現象に於ては裂罅間の距離數粁程度卽副斷層程度の裂罅に於ける作用を考量したる粘性等ならざる可からず、更に太平洋全局の歪力等を考ふる場合に於ては相當に大なる斷層も粘性係數等の變更の下に割合均一組織の如く見て推論を下し得べし。

かくて大規模のものに於て實際に現はるゝ粘性は標本岩石の分子的粘性と異なるは明なる故に强ひて岩石を以て我等が實驗材料となす必要なく、否寧ろヘルムホルツ等に依りて明なるが如く規模を變じたる模型に於て幾何學的類似ある實驗を試みんとする、同一の材料を用ゐる事は絕對に目的に反し到底相似形を得るに由なきことを知るべし。故に岩石素材の研究も勿論絕對に必要なれども、余等の目的に對しては寧ろ全く別種の材料を用ゐる方妥當なり。併し岩石以外の材料なれば何でも良しと云ふにてはなく。與へられたる寸法に對しては必ず最も適當なる一種の材料ある筈なり、然れども此材料を計算上求むる事は岩石の諸實數不明の場合不可能なるを以て、矢張り實驗上地殼に現はるゝと類似せる形象を呈するが如き材料を索めて實驗する外なし。此意味に於て或時はパテ、或時はパラフィン、或時は麥粉等の如きものをも用ゐたり。

實驗に於ては先づ表面收縮(area-contraction)による裂罅、表面撓曲(surface bending)に依るもの、等に始まり、次第に複雜なる場合に進み、特にshear及rotationの影響に對して尤も注意を加へたり、此理由はshear又rotationが地形等に於て最も重要なりと云ふ考へにては

なく、在來他の力卽側壓又は張力等に依る場合は割合に多く研究せられあれども shear 及 rotation の場合は研究割合に少なきに依るなり。

4. **平等則、對稱則** 概說 總て裂罅を生ずる場合に於ても、他の突然現象の發生の場合と同じく、是を起す爲の力の働きに支配せられ又破壞すべき物質の現狀に支配せられ、是等の支配の及ばざる範圍於ては平等の法則と偶然なる機會とに支配せらる。例へば表面收縮の場合に於ては之を支配する力は從前の結合を維持せんとする分子力と他の物理的條件例へば溫度の降下、乾燥等の爲に分子自身か又は分子間隙の縮少する爲に起る收縮的分子力となり、是等は結晶體に於て素より其方向によりて差あれども等方體に於ては大體四方一樣のものと見做し得べし、方位に關せざる場合に於て、割目が何れの方向に走るべきかは全く不定の問題なれば收縮の爲の張力が分子間の引力に勝りたる瞬間に於て四方一樣に破裂を生ずべきが如きも、如何なる物質とても絕對に對稱、均質、等質なる事は望むべからず、一次、二次、三次、等の近似に於て對稱、等質なりとも更に高次に於て必や不對稱の箇所あるべく、破壞の危急瞬間に於ては普通の場合に問題とならざる高次の小偏差が有力なる役目をなして其方向に破壞を始むるに至るべし、破壞が一度始まれば、其附近は急速に歪力が緩除せらるゝ爲に其附近は破壞に對して安全となれ共、歪力の急激に加はりし場合に於ては其緩除作用の到達遲き部分に於て別の割れ目を生ずべし、かくて現象は高次の小偏差卽世に所謂偶然なるものに支配さるゝも、元來高次の小偏差故其開發の時以外は勢力を逞するを得ず、却つて歪力の傳達の速度と割れ目の發生による是の緩除の速度との關係上生ずる平等の法則によりて支配せらるゝに到るべし、[4]かくて表面收縮の際に生ずる割れ目にありては同時に一點の周に發生したる割れ目は等角又は對稱關係を取る場合多く、既有裂罅を新裂罅が橫斷せんとする場合は直交せんとする傾向を示すべし、又例へば圓壔形撓曲の際には平行裂罅を略等間隔に生ずべし。是等の詳細は後に讓るも要するに割れ目の生ずる際一般に平等性從て對稱性の現はるゝは爭ふ可からざる事實なり。

第二章 結果の大要

順序として實驗を述ぶ可きであるが、其詳細は誠に煩雜讀むに堪へざ

---

4)此關係は既に數學物理學會大正十三年四日年會の席上 "Two forms of expressions of one and the same principle in Nature," なる題下に講演せられたるも印刷せられたるものなし。

るものであるから、先づ以て實驗の結果得られたる知識の梗概を記して了解を便にする。其爲に各種事實を個條書きにし、之に地形等の實例らしきものを附記する。先にも述べたる如く、之を以て實例の地形を說明し盡したりとするものでは固よりない。

1. 內部からの割れ目は緣邊では夫れに直交せむとする性質がある。是は緣邊に於ては夫れに平行な張力又は壓力のみが存在し夫れに直角には應力がないからであるが、一と口に云へば割れ目は對稱的傾向を取る性質があると云ふ事からも說明し得る。

2. 一つの割れ目が既存する割れ目と交らんとする際にも緣邊に於けると同樣で矢張り直交せむとする傾きが有る。

3. 割れ目が幾つも生ずる場合には他に之を束縛する事情のない限り相互に略等間隔を保つ。大きな割れ目は大きい同志、小さいのは小さい同志に大きいのも加へて略等間隔を保つ、平行裂罅にも輻射狀裂罅にも同じ法則が行はれる。日本島弧上にも此種類似の斷層線又は弱線群が略等間隔を保つて居る事は良く知られて居る。

4. 外部からの力で緣邊丈が割れる場合には必しも緣邊と割れ目は直交しない。多くは弧狀をなし、時には弧狀群によりて青海波模樣となる。弧の兩端が緣邊と同一な角度で斜交する。故に一端丈では對稱ではないが、兩端併せて見れば同じく對稱性を現はして居る。此れに類似した形がノルウェイの西の海岸線、カナダの西岸、智利の西岸にも現はれて居る。

5. 內部の一點から數個の割れ目が出發する場合には各割れ目間の角度は略等しくなる傾向が有る。之は (3) の一例であるが、此種の割れ目が數多の點から發して出來るブロックは所謂龜甲型の樣なものをなし易い。ブロックは四角五角六角等になり易い。

6. 底又は周圍で支へられた板が面積の一樣な收縮によりて上記の樣な龜甲型ブロック群を生ずる。但しブロックの形を支配するものは均一な物質では其周圍の形であり不均一な物質では其中に割れ目の核となる可き異質の分布狀況に基づく。收縮が一樣でない場合にも夫れによりてブロックの形及大きさに不規則性が現はれる。

7. 面積收縮が漸增する場合には或極限に於て第一次の裂罅に依る第一次の大ブロックが出來、更に收縮が進めば第二次、第三次と次第に規模を小にする裂罅從てブロック群が出來る。卽裂罅群に於ても親子現象

が伴ふ。

8. 一つの主裂線が先づ生じ其裂線から內部に向つて支裂を發生する場合には支裂は主裂と直交する場合もあるが多くは斜交する。直交する場合は主裂支裂が壓力及張力裂罅の關係の時であり、斜交するは是等に對して剪力裂罅となる場合である。

9. 圓壔形撓曲に依りては平行裂線が出來、圓錐形又は圓頂形撓曲に依りては輻射狀及同心圓弧狀の裂線群が出來る。

10. 面に沿ふて歪力が働く場合に雁行裂罅が出來易い。雁行に就ては主線の右に雁行裂罅の有るものを負とし左りに偏するものを正とする。歪みは主線に沿ふ單純歪力と見て其れに伴ふ廻轉が左まわりを正とし右まわり即時計まはりを負とする。以上の定義の下に雁行裂罅の法則は次の如きものである。負なる張力雁行裂罅と正なる壓力雁行裂罅とは共に主線に沿ふ負の歪みに伴ひ。正なる張力雁行裂罅と負なる壓力雁行裂罅とは共に正の歪みに伴ふ。雁行が火山列又は斷層等に顯著である事は良く知られて居る。

11. 張力裂罅は漸進的に成長し得る。此際外力の方向を轉換すれば一時成長を中止し裂罅は閉口し、更に弱線らしき模樣を現はさず、却つて別處に新裂罅を生じて成長するが、更に外力の方向を變じて復原すれば、今迄眠り居たる裂罅は又成長を始め、一方の裂罅は休止する。餘震の發生に於て地震帶相互活動を示すが如きと似て居る。

12. 單なる剪斷裂罅は漸進的で有り得ない。漸進する場合は雁行をなし、其雁行の各節毎に全部的瞬間的に割れる。特に壓力によつて剪斷の起る場合は雁行性を示す事少なく。全破面が衝動的に瞬時に成生せられる。分割せられたブロックは衝撃を受けて飛躍せむとする。激震は恐らく此種の破壞に依るであらう。

13. 張力に對しての破壞限度は地塊其他多くの物質に於て壓力に對する限度よりも低いから張力裂罅が最も普通に起り、且小規模に起るが、壓力裂罅は稀に起り、且起れば大規模である。要するに壓力は物體の一端に加へられた場合比較的遠方迄傳達せられるが張力は其加へられた附近で裂開を起し易い爲に遠方に傳達する事が少ない。地震等の際で實見せられる雁行は多く張力裂罅であるに反し全局として見た大雁行は壓力裂罅である事、火山列等も多く壓力雁行裂罅をなす事等は、皆此性質から說明出來る。

14. 撓曲に依る破壞に於ては一意的な變位に對しては破壞しない場合に、一旦、力を緩めて逆向きの力を加へれば極めて僅かの變位で破壞する現象がある。物質によりては其程度が異なり或物質では此現象が著しくないものもあるが或物質では力を緩め切らない中に旣に破壞の起る様なものが有る。勿論初めの撓曲は彈性の範圍を遙かに超へ破壞の極限に可なり近付いたものであるが、其引き歸す點と極限との差にも關係する。他種の破壞にも恐らく同様の現象が伴ふで有ろう。

15. 板を其面に沿ふて撓曲した場合又は硝子棒の如きを撓曲して破壞を起した場合に其破壞面が最後の小部分で斜走する場合が多い。直角に起る主たる破壞面は張力裂罅であるが最後の斜走破壞面は壓力の結果起る剪斷面即剪斷力による滑り面である。以上の中表面收縮、撓曲、等に關する實驗の概要は次の第三章に記し (10) の雁行裂罅に關する法則は裂罅(斷層、火山列等も一種の裂罅と見る)の形よりして力の關係を判斷する上に重要であるから少しく綿密に研究する必要を生じた。それに就いては第四章に述べるが如き諸實驗を行ふた。

第三章　表面收縮、撓曲、歪割れ等の實驗

1. **表面收縮に依る皺及裂罅**　この種の事象は常に目擊する處のもので例へば田面沼澤等の乾固する際に現はれる龜裂の現象である。而して其形は所謂龜甲型をなして對稱的に配例するのが常である。然し環境の相違によりて又は物質を異にすることによりて必すしも龜甲型を呈するとは限らない。次に第一圖より第四圖まで實例を示す。

第一圖 (Pl. VIII) は第八圖に示す裝置に亞鉛華粉末を水にて捏り塗り上げたるものを室内に放置し、乾燥して生じた割目である。中央の大割の部分は薄いゴムの膜に乘り。小割の部分は堅固な武力板に乘て居る。厚さは中央が厚く約 1·5 粍にて端は殆ど厚みを有せず、割目を見るに小割の部分の大割に會する所は多くは直角をなす事が認められる。

第二圖 (Pl. IX) は小茶碗の底に墨汁の乾固して生じた割目である。一見放射狀の割目は最も著しくこれに同心圓をなせる如きもの直交し、爲に長方形形狀のもの最も多く現はれて居る。

第三圖 (Pl. IX) はヘットの凝固して生じた模様であり、白線に沿ふ黑線は其割目である。模様及割目の角の鋭くないものゝ例である。

第四圖 (Pl. X) はペイントを小茶碗に入れて放置せるものに生じた表面の皮の皺の模樣である。

2 Conical bending **による皺及裂け目**　第五圖にこの種の一例を示す、圖は厚さ 2–3 粍のパラフインの板を水平に支へ兩面を自由に保ちナイフの刄の方を手にして柄の一端を以て打擊を加へた時生じた割目である。圖には 9 回の結果が出て居る。小斑點は板を作る際自然に生じた模樣にて打擊とは無關係のものである。17 回の實驗の結果は放射狀に射出して居る重なる割目の 3 本ありしもの 7 回 4 本のもの 5 回、2 本のもの 1 回あり、裂線の明瞭を缺くもの 3 回、黑點となりて裂線の射出を見ざるもの 1 回あつた。斯く相違を來した主なる原因は打込の角度及其强さの區々なりしに由る。猶裂線の射出數 3 本あるものに付き其互になす角度を概略測りたる結果は 120° の場合最も多く次に 90° の場合のものも多少見られた。又 4 本の場合には 100° 附近最も多く、次いで 75° のものも多少あつた。

3. Cylindrical bending **による割目**　第六圖 (Pl. X) はこの一例である。圖は道路工事中泥土の地面をローラーにて地均中に生じた割目にて略平行をなして居る。猶この際ローラーに幾分の傾きありて割目の一部に放射狀卽ち conical bending に依ると思はるものも見られた。

4. Plate **の** one directional tension 又は compression **による割目** (圖は印刷せず) 甲圖、乙圖は共に compression に依る例である。此實驗は泥土 (水を加へた) を四ッ切バットに入れ未だ乾固せざる中に二枚の武力板を其表面に乘せ、その間に空地を作り、その部分には寫眞に撮る便宜上亞鉛華粉末を振りかけた。又一方にパラフインの融液を用意し之を一回に表面に流し凝固した後、矢印のある板を矢羽の方向に卽ち他の板に直角に且つ水平に押した場合である。其結果は押板の近くに撓曲を生じその頂上の線に沿ふて割目を生じた、割目には雁行性は認められない。撓曲による皺の傾斜は押板の側は殆ど直角をなし他の側は緩である。

5. Simple shear **による割目**　實驗 1. (圖は印刷せず) カビネ型乾板を縱に約 1 糎の間隔を以て薄いゴム膜にて連結した。この上に麥粉の泥 (水にて捏り) を一樣の厚さに幾重にも塗り重ね室內に置き常溫の下に乾燥した。丙圖 (1) は其形狀及乾割を示す。(2) は矢印の箇所に木片を當て其上部より、數回に亘り次第に力を增して打擊を與へた。爲に A の部分に tension crack (角度は下底のガラス板の椽卽ち中央線

に對し約 40°) を生じた。猶この外に乾割の tension crack の向きに一致して存在せるものが發達した。(3) は更に稍強く 2 回打擊を與へた場合にて硝子緣は多少破損した。爲に既成割目は成長し、又 (B) (C) に新た tension crack を生じた。(4) は打擊の箇所を矢印の所に變へ以前に增して更に 2 回打擊を加へた場合にて硝子板は大破した。勿論既成裂罅は成長し、特に著しく開口した。猶 (D) (E) に tension crack を新生し、又 (X) (Y) (Z) に compression crack らしきものも見られた。

實驗 2. (圖は省く) 1. の場合の硝子板をゴム板 (厚さ約 1·5 粍) に代へ一側の板を台に固定し他の側に打擊を加へずに手にて徐々に力を與へた。試料には同じく麥粉泥を用ひた。始め巾を狹く塗り乾固して後周圍を塗り、後者の乾燥せざる中實驗を行ふた。(2) は約 1 糎押した場合にてゴム板は多少浮き上り、割目は生ま乾きの邊りに slip line に沿ひ slip crack を生じた。猶ほ渦卷樣のものも見へた。この部分の內部には未だ粘性の有る物質の存するに由る。この場合少しく內方に向けて押したにも拘はらず tension crack となりて現はれたることは注意すべき點である。實驗後測りたる試料の厚さは十分乾燥せる部分は 1–1·5 粍。半乾きの部分は 1·5–2·0 粍であつた。

實驗 3. (圖は省く) 2 と同一實驗にて只試料の表面のみ硬くした。それには麥粉泥を一樣の厚さに塗りたるものに火熨をかけて狐色に燒いた(2) は力を加へた場合にて境界線に沿ふて割合に大なる tension crark が數條雁行し、猶ほ割目に直交する數條の皺の狀況を示す。

實驗 4. (圖は省く) 裝置は 2. を使用す。白墨粉末を作り。これをアルコールにて泥となし筆に含ましめてゴム膜上に塗る、厚さは約 0·5 粍。(1) は其表面を示す (2) 力を加へて、中間に tension crack の雁行が現はれ猶 compression による皺が可成の間隔を有して四條位現はれた、(3) に至ては tension crack, compression crack 及皺が可成著しく發達した。

實驗 5. (圖は省く) 4. と同じ但し試料の厚さを 2–3 粍となし一夜室內に放置した。圖の (1) 十分乾燥せざる中に乾割を生じた。(2) (A) (B) (C) (D) 等に tension crack を生じ、且乾割の中之れと同一 sense にあるものも亦發達した。(3) 是等の割目は更に成長し尙ほ compression に依る二條の褶曲を生じその峰に割目を生じた。(4) は (3) の試料を取除き底のゴム板及ゴム膜の皺の模樣を示す。

實驗 6. （圖は省く）(4) (5) に使用した白墨の粉は全く粘性を缺く故にこの粘性を補ふ爲に麥粉を等量に混じて使用した。一夜室内に放置し翌朝時々日向にさらして乾燥す。十分乾燥せざる中に實驗に供す。(1) は表面の模樣を示す、黑色の濃き所程濕氣を多く含む。(2) 兩端に特に著しく tension crack の雁行現はれ又皺曲も相當發達せり。(3) 裂罅及皺曲共に增大す、柔弱なる爲め compression crack は現はれ難し。(4) (3) を更に乾燥して力を與へたるも (3) と殆ど大差なし。

實驗 7. （第七圖 Pl. XI）白墨粉末及麥粉の混合物（割合は 4:6）をアルコールにて薄い泥を作り筆の穗先にてゴム膜面が僅かに隱るゝ程度に塗り乾燥後更に薄く塗り重ね室内に放置乾燥した、最後に 15 分間位更に日光に當て乾割の二三生ずるに及んで室内に取入れ直に實驗に供した。厚さは約 0·5–0·2 粍である。圖の (1) は試料の狀況を示す。左半の薄し黑き部分は未だ十分乾燥せざる處である。

以下の圖は矢羽の方向に順次に力を加へた場合の變化を示す。(2) 先づ tension crack を生じ見事な雁行を呈す、次いで皺が現はれ A の皺の上部には三條の小雁行の tension crack を生ず。(3) 皺の達發著しく其峰は割れて綺麗な compression crack を現はしてゐる、これ等は tension crack と略直交をなす。(4) compression の方特に著しくなる。

實驗 8. （圖は省く）實驗 7 より幾分厚さの厚い場合にして白墨粉、麥粉を約半々にアルコールにて捏ね、ゴム膜上に流し約二十分間室内に置き表面が幾分乾き始めし頃筆先にて表面を均らした。厚さは約 0·6 粍である。(1) 乾割れ、(2) 乾割を基に又は新たに tensiou crack を生ず。(3) 隆起部の皺の頂きには compression crack も見ゆ、(4) compression crack 增々發達す。

實驗 9. （圖は省く）柔軟なるヘットを稍部厚にゴム膜上に塗り其表面に亞鉛華粉を水にて捏ねたるを流し筆先にて表面を平らに均し、室内の通風の良き所にて乾燥した。(1) 乾割を生ず、(2) 皺は下のゴム膜に依るものにて割目は亞鉛華のものである。(3) tension crack 著しくなり又皺に沿ふ割目も出來始めた。(4) 皺に沿ふ割目大となり tension による crack も益々發達す。

實驗 10. （圖は省く）亞鉛華の捏ね物を約 3 粍の厚さに塗り其表面に十分に熔融したるパラフィンを流し込み凝固してより實驗せり、パラフィンの厚さは 0·1〜1 粍である (2)は少しく力を加へた場合にてパラフィ

ンに tension crack を生ず、(3) (4) は既成割目の發達するのみにて新生のものなし。

實驗 11. （圖は省く）實驗裝置を變へ、四ツ切バット中に普通の泥土を以て泥を作り二枚の武力板を 2 糎の間隔にて乘せ濃厚なるワニスの液を其間隙及武力板の上に流し一樣の厚さに行き渡らせ表面に膜の張るを待ちて實驗す、實驗は一方の板を手にて支へ他方をこれに平行に浮かさぬ樣徐々に押した、(1) 表面の模樣。(2) 壓力による皺と張力による割目を生ず。(3) 兩方共發達す。(4) 結局割目は皺に平行せり。以上要するに總て第七圖に示せる所と大同小異の結果を得た、卽雁行に於ては張力罅が先づ生じ壓力皺も生じ壓力罅はずつと後に出來る事がわかつた。

6. Rotational shear **によるもの**實驗裝置の概略は第八圖に示す、A は武力板にて中央を圓形にくり拔き木の臺上に固定す、中に他の B なる武力の圓板を圖の如く取付け H, H なるハンドルにて自由に回轉せしむ、猶任意の位置に止める爲に K のクランプを付す。又 AB の上半の間隙には G なる薄きゴム膜を貼りこの上に試料を塗りハンドルを回して shear を與へるものとす。

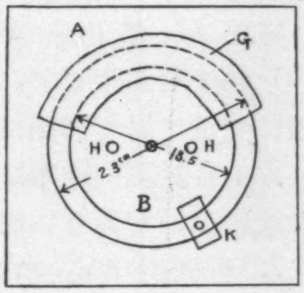

第八圖 弧狀雁行を作る裝置

Fig. 8. Apparatus used in the experiment of shear along a circular arc.
G. thin rubber plate.
H. handles.
B. rotatable metal piece.
A. fixed metal piece.
K. crump.

實驗 1. （圖は省く）亞鉛華、麥粉を等量に（重さにて）混じ水にて捏り、室內にて乾燥す、全面乾き切らず多少の濕氣を殘す中に實驗に供す、厚さは約 1 粍あり、圖の (1) の右左端近くに乾割あり、(2) 矢の方向に回轉す、皺（底のゴム膜に生ずる皺）及 tension crack を生じ、大なる割目は乾割を基に發達せるもの二個所、新たに生ぜるものは一個所にある。小割は主として皺上に群生し、而して大勢に於ては皺に直角に交はる、又皺の峰に沿ふ割目も見へる、(3) (4) 皺の峰に沿ふ割目の發達特に著しく小割はゴム膜の全面に亙りて一樣に配布してゐる。玆に注意すべきは峰線に沿ふ割目は compression crack と同じ sense なれども從來の實驗に於ては compression crack はゴム膜の皺には殆ど支配を受けざる場合が多かつた然るにこの場合に於ては全然ゴム膜上の皺の頂きにのみ生ぜる故に從來の compression crack とは多少趣を異にする事である。

實驗2.（圖は省く）實驗1の濕氣多き場合にてA板とゴム膜の接する線に沿ふて小tension crack雁行して生ぜるのみにて他には余り割目を見ず皺の模樣は實驗1と全く同じ只回轉の向きを異にするのみ。

實驗3（第九圖Pl. XII）實驗2と同じ條件の下に行へるものにて實驗2に於けるが如く、割目は左方に少しく現はれてゐる、皺を横斷するtension crack一面に生ず皺の峰に沿ふcrackは認められない。

實驗4.（圖は省く）試料前者と同じ、戸棚の中に二日間放置し十分乾燥せしむ、厚さは1〜2粍である。(1)は乾割の模樣を示す。(2)乾割を基に割れしものの他にtension crackの雁行列凡そ二列をなして現はる。(3)既成の割目成長せる以外に皺を横切り雁行をなすtension crackの新生あり。又皺の頂に沿ふcompression crackもあり。(4)既成裂罅は凡て發達す皺の數從來の實驗に比し數等少なくゴムノ皺とは關係なきものゝ如し。

實驗5. 第十圖(Pl. XIII)試料にパラフィンを使用す。(1)其表面(2)皺は殆ど生ぜず。割目の數少なきも右端より左端に略中央を殆ど一線にて貫て居り其間に小割目の雁行するものあり。

以上各實驗の結果は前節に於て見た所と大差はない雁行が弧狀に起つた丈の違ひである。尙面積の縮少なした摺曲の著しい發達が起り得る。

7. Diagnonal compressionによるshear crack この實驗裝置の大略は第十一圖に示す。圖に於てXはハンドルにて其回轉の向きによりY（高さ1·5糎の眞鍮角棒）は前後に進退す、即ちYは框の頂點Aを押し込み或はAの頂點を離れる。A C E Gの框は正方形をなし、B.Hは各邊の中央をなし、CDはEDよりも、稍ゝ長く又EDはEFと同長である。是等の邊は同一眞鍮の角材より切り取りたるものにして各邊はボルト及ナットを以て連絡す、始めABCを一邊として使用せる場合にBをナット一ケのみにて締めたれども十分に抑へる事出來ず後にBに添金を渡しB及其兩端の三ヶ所を十分に締めた。（圖には省く）D, F, H,に於ても同樣の事が出來る、又CEG角を一定に保たんとせばEのナットを締めるは勿論この外にEF, EDに適當の間隔を以て板金を渡し即ち三角形を形作りて兩端を各片に締める他の角に於ても同樣（圖には省略）Iは框の支點に過ない、Kは木の臺の縁にて高さ約4糎あり、框以外は凡てこの木の臺に固定してある。

試料には多くはパラフィンの板を使用した、板の大さ及厚さ等には裝

置の大さによりて自ら制限を受くるので手製となした、大さは27糎×27糎にて框に丁度一杯となる程度とし厚さは實驗毎に適當に變へた、板を作るには鑄物の鑄型に倣ひて先づ二枚の硝子板を重ね其間隙は緣に沿ふて挿入せるボール紙の厚さを以て決め、湯口を殘して緣は凡て西洋紙で貼り特に底に當る處は二重三重に丈夫になしてパラフィン融液の逸出を防いだ、パラフィンは可成り一樣に流し込んだ、次に（但しこれには例外もあるが）室內の溫度にて凝固せしめた、この實驗は冬期寒冷の時に行ひし故パラフィンを注ぎ込む時は煖爐の傍にてなした。殆んど、同一操作をなせるにも拘はらずその結果全く同一ではなかつた。同一物に於てすら一樣の厚さのものは得られず多少の厚薄は免かれ得なかつた。特に凝固して後生ずるパラフィン板の模樣に著しい相違があつた。これ等の模樣はパラフィン熔融溫度、硝子板の溫め方、室內の溫度、注ぎ方、冷し方等の諸條件によりて左右されたらしい。

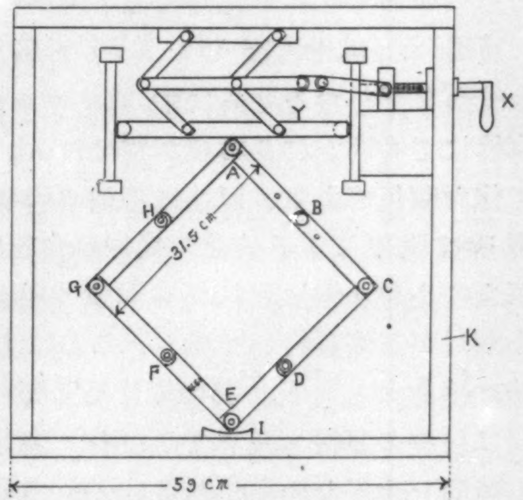

第十一圖　框を押して歪みを與へる裝置

Fig. 11.　Apparatus for producing shear by pushing the frame.

次にこの板を實驗に供するには始め實驗框に半紙一枚にて底を作り、試料の底を持たせ板と框と間隙には別に熔融パラフィンを作りて注ぎ込み其間を埋め同時に板の緣を補强する目的にて幾分高くした。

實驗 1.（第十二圖 Pl. XIV）框の下に紙を貼りて底を作り、これを白墨の粉を敷いた上に乘せパラフィン融液を注ぎ手を以て框を前後左右に搖り動して均一に行き亙らした、この際紙の裏面にパラフィン融が滲みで出大部分の粉を共に凝固した。これ等は後に丁寧に剝取りしも取り盡す事を得ず。寫眞に見ゆる如く黑く點々として殘つてゐる、厚さは約0.5粍にて中程は幾分これよりも厚い、實驗は A, C, E, G の頂角を自由になし他は凡て締めた CG 對角線に直角に A を徐々に押す、始め a に割目を生じ力を增すに連れて成長し、又一方少しく喰違ひて b に新たに割目が生じたこれと殆ど同時に b′ にも現はれ共に成長し b′ は間も

なく成長止み、b のみ急に發達して c に延び b′ と合した、又 a も b に合し、この間三回ぴりぴりと音を發した、最後に a より d なる枝が出た。是等の割目は對角線 C G に沿つて隆起した皺の上に生じたものである結局側壓による撓曲裂罅が出來た。

實驗 2. 第十三圖 (Pl. XV) 實驗 I に同じ只バラフンを注ぐ時、底の紙面を浮したるを異にす、爲にバラフインは底に滴粒となり凝固した、寫眞にても明かに其模様が窺はれる。a はこの滴粒を取り去んとして誤て作た割目である、厚さは裂線の内側は約 1·5 粍外側は 1 粍前後あり。裂線は側壓による撓曲の爲に對角線に沿ふて横に走る可かりしものが、厚さの小なる方にそれて C に於て撓曲裂罅を生じた。始め b の個所に小割目が三條雁行して生じ、これは力を加へても其後餘り發達せずその後は撓曲大となり、其の峯に沿ふ裂線が現はれた。又既成の a の割目には何等の影響も及さなかつた。只最後に AC 邊と臘板との間に少しく隙間を生じたのみである。b, d は剪斷裂罅で、稍〻張力雁行を示して居る。

實驗 3. (圖は省く) 試料バラフイン板厚さ約 3 粍。

(1) は表面を示す數條の縞目は板を作る際にバラフインを幾回にも斷續して注入した結果生じたものである。B, D, F, H を締め G に直角に A を押す、其結果を (2) に示す、割目の大部分は各層の境に沿ふて發達し、甚だしき箇所は遂に剝離した、又中には層理に關係せずに出來た割目もある。

實驗 4. (圖は省く) バラフイン板厚さ約 3·5 粍 A, C, E, G, を緩め他は凡て固定す、A を G C 線に直角に徐々に押した。圖の (1) a, a′ に割目を生じ次いで b, b′ を生じた、又 c に微な割目を認められたがこれは少しの成長をも見なかつた猶數條の皺の如く見ゆる縞は框の底をなす日本紙の歪力を受けて出來た皺で別段上部のバラフイン板の割目には影響を及ぼさなかつた。(2) は一層實驗を進めたる場合にて b は延びて縁に達し直に反射して d を出し d の少しく進みし頃は b′ は發達して e となり又一方 f に新たに割目を生じ g に進んだ、g の e に合する頃は d は縁に達し反射して h を出し、更に f より i の枝が現はれ e は縁に於て反射して j となつた。卽ちこの場合に於ては diagonal cracks 以外 marginal cracks をも合せ生じて居る。

實驗 5 (圖は省く) バラフイン板厚さ約 3 粍、A, C, D, F を緩め他

は全部締める。Aを押しEにて支へる、(1) 實驗前 (2) aに割目現はれ瞬時にして、他の縁に達す、殆ど同時にa′にも現はれしがこれは成長せず。猶加力中にbの割目が出來た、其後はAの頂角の處碎けて浮き上りしのみにて他には割目を見ず、猶十數條の略平行してゐる模樣は底の紙の皺である。

實驗 6 (圖は省く) 十分に乾燥せざる粘土板、A, Cを緩め (他を固定す、Aを押す、a, a′は最初よりありし割目、始めbの處高まり頂きが割れ次にcの處が高まりcには雁行する小割目を生ず、即ち二條の大なる皺を生じ其頂きに割目を見た場合である。

8. **Marginal crack.** 實驗裝置及試料のパラフイン板の製法等は7.に同じ。

實驗 1. (第十四圖 Pl. XVI) パラフイン板厚さ2·5粍〜3粍、A, C, E, Gの角を凡て緩め、Aを押す、(1) 實驗前、(2) 少し押した場合、先づaの割目を生じ、次いでbの枝を出しbが縁に達して反射しc′と延びる頃は既にcの枝が出てゐる。(3) より進めた場合にてcよりeの枝を出し又cは延びてdとなりdの處で更に小さい枝を出してゐる。この實驗に於て割目はc′を除く外は凡て山の峯に生じた、猶ほ割目の枝は本の割目の中間より出てゐることも一の特長である。又marginal crackの通有性とも見らるべき事は割目が良き對稱をなして順次に發達する事である。(3) (圖は省く) 數條平行せる皺狀のものは前にも屢々説明せる框の底紙の皺である。猶ほ力を加ふるに峯は高くなりfは幾分内側に彎曲して他の側に達したるのみにて他に大した變化を見ず。

實驗 2. (圖は省く) パラフイン板厚さ3粍前後Aを押す、aに割目を生じ急に延びる、次いでb, cと新たに割目が出來た。以後は縁が碎けて浮上るのみにて他の個所に新たに割目を見なかつた。

實驗 3. (圖は省く) 實驗2と同じ條件にて繰返せしものである。割目はa, b, cの順に生ず、板の模樣はパラフイン板を作る時凝固する際生じたるものである。

9. **其他の實驗**　以上の外歪力を往復的に施した實驗、夫れに關聯して居る場合の破壞等の實驗も試みたが、詳細の説明は煩はしいから茲では省く事にする。又撓曲による割れ目の最後に於ける斜走は今尙實驗解析中の部分があるので他の機會に讓る。又豫め弱線を有するブロックの破壞に就ても他の機會に於て報告する事にする。

第四章　捩れを伴ふ側壓の實驗

本章に述ぶる處のものは物理學的精密實驗の手段に依らずに極めて簡單なる裝置の下に試みたる數種の實驗の概況及其結果である。

1. **裝置**　試料としては麥粉を次に記す操作に依りて壓縮して作つたものを使用した。先づ麥粉を三四日間日光の直射する通風の宜しき屋上にさらし時折り混ぜ返して十分乾燥せしめたるものを桝にて枠型の中に計り取り1·2糎の厚さとなし表面を輕く均齊し1·3糎の厚さを有する眞鍮板を蓋に乘せ壓縮機にかけ略〻一様の速度（約操作の始めより終りまで10秒）を以て所定の全壓力約15000瓩に至るまで壓縮を續けその後は約15分間機械を止め放置した。この間に壓力計の指針は多くの場合15000瓩より14000〜13000瓩まで低下した。蓋板の大さは15·7×12·0糎^{2}なる故に約80瓩糎^{2}の壓力を以て壓縮したことになる。麥粉は壓縮の結果約6粍（半減）厚さを減少し脆弱なる板狀（厚さ6〜6·5粍）となりその四周は枠椽の影響を蒙り幾分軟弱となり實驗試料としては硬度に均齊を缺く爲めそれ等の部分を取除き内部の良好なる部分を選び使用した。併し時には堅さ及厚さに於て幾分不均一なるものを用ひたる場合

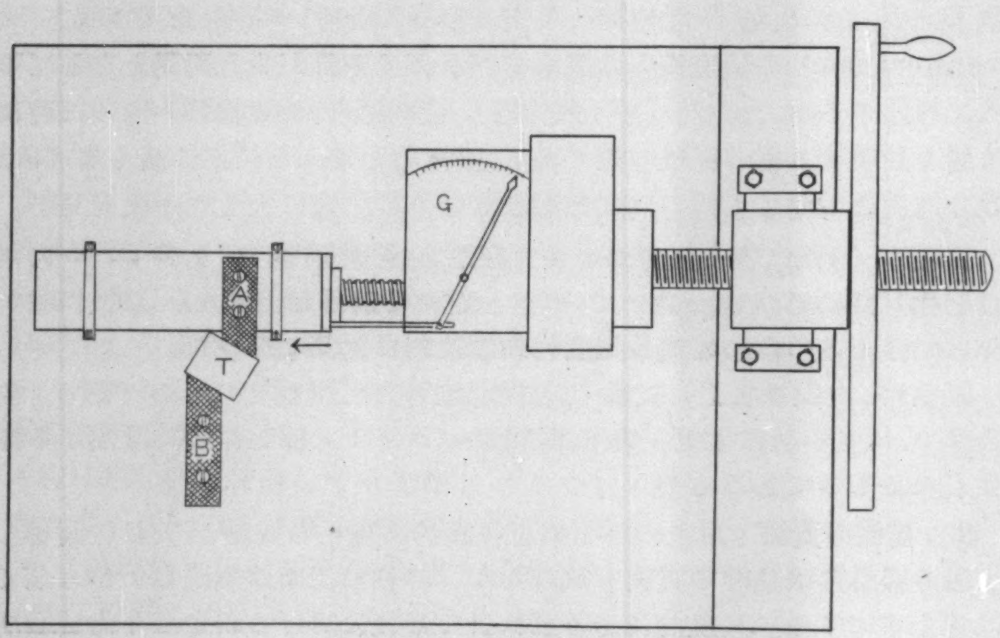

第十五圖　實驗裝置略圖（平面圖）

Fig. 15.　Apparatus used in the experiment of the oblique compression

もあるが其等は凡て不良の結果を與へた。試料片を作る際は十分の注意を拂ひ一定の巾に且其兩側面（金屬の押し板、及受板に當る面）が表裏の二面に直交する樣に仕上げた。それには先づ水平なる臺上に所要の巾を有する木の臺（巾 39 粍）を置きその上に幾分の餘裕を持して切取た試料を乘せ定規の一邊を水面の臺に當てこれに直角の邊を以て木臺の側面に觸れるまで注意して削磨した。

第十五圖は實驗裝置の略圖（平面圖）で、T は試料 A は押板, B は受板である。受板は木ネジを以て臺上に取付けてある。A はハンドルの回轉に從ふて矢印の方向に進行する。A, B の表面の高さは試料面上より 4–5 粍高く出て居る、AB の板は眞鍮製にて試料片を啣へる面は細な目のヤスリにて平らに仕上げてある。押板を壓す軸のネジ山のピッチは 2 粍であるが測力計 G の縮みのある爲め一回轉に 2 粍の進みはない。

2. **實驗方法** は第十六圖に示す如く A, B の位置を夫々變更して試みた。ハンドルは手廻にし一回轉 7–8 秒の割合にて極めて徐々に斷續して回轉し割目を生じて實驗に一段落を遂げたる場合は急速にハンドルを逆轉し力を緩めた。併し割目の生長の緩かに現るる場合は一時、力を止め、その模樣のスケッチを取り、更に力を加へて其の後の經過を見た場合もある。

實驗は押板の試料にかゝる力の向きを (I) (II) (III) の三種に類別し、その各々に付いて押板と受板との距離の關係を 1), 2), 3) 種に (III) の場合は 4) まで變へて試みた、それ等力のかゝる關係は第十六圖に示す。

以下に記載せる割目の觀察は主として其表面に現はれたる狀況に基き數種の型式に分類し記せるものである。

3. **實驗** (I) 30 度の角度より力を作用したる場合 (I) の 1) (第十六圖)、十七圖 a, 二十三圖 b Pl. XXII 第一表)

實驗回數 24 回。これ等の結果を見るに一見支離滅裂の觀を呈すれども尙ほ仔細に觀察する時は第十七圖 a の如く割目を a, b, c, d, e, f, g なる七種の型式に分類整理することを得。e, f は各々楔狀をなし殆ど例外なく多少の差こそあれ表面を押上げて居る。24 回の實驗中 a 型のみ現はれたる場合は 9 回、b 型のみの場合は 1 回 ab 共に現はれたる場合は 6 回ある。而して ab 共にある場合は必ず e か又は f を伴ふて居る。斯く試料片によりて發生せる割目の型式の數に相違を來したるは作用せし

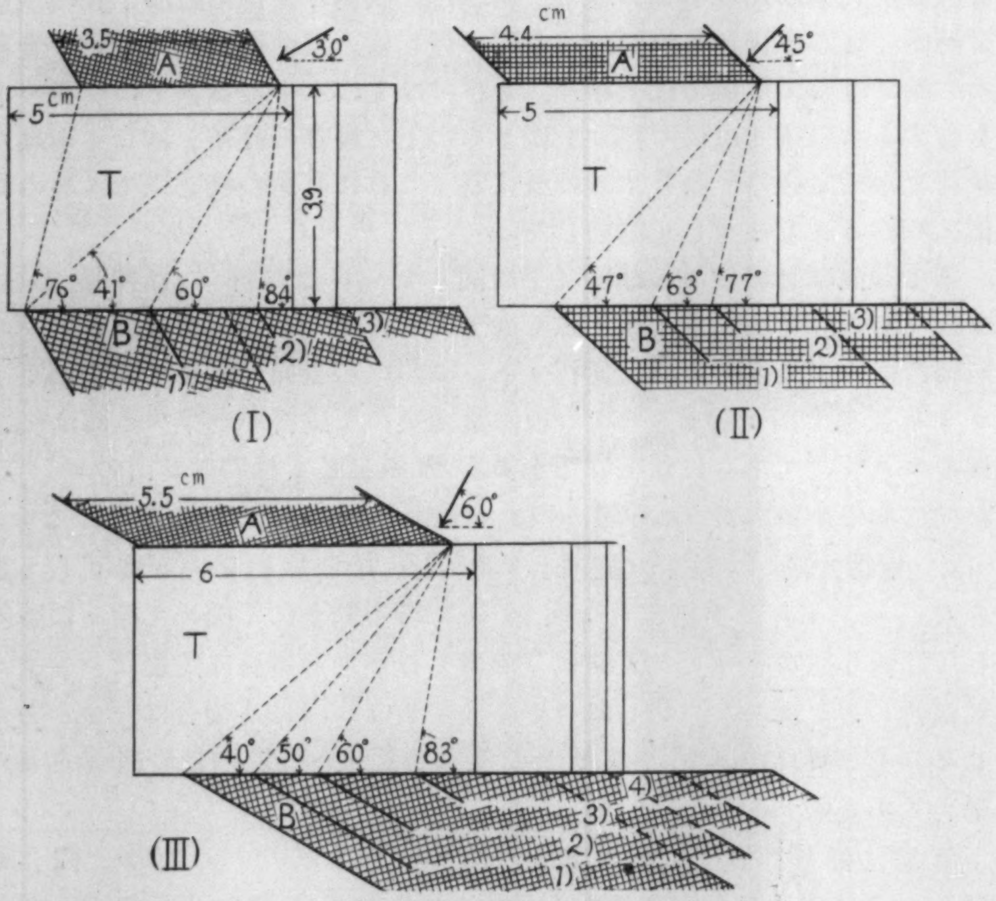
3.5
A
30°
5 cm
T
39
76°
41°
60°
84°
B
1)
2)
3)
(I)
4.4 cm
A
45°
5
T
47°
63°
77°
B
1)
2)
3)
(II)
5.5 cm
A
60°
6
T
40°
50°
60°
83°
B
1)
2)
3)
4)
(III)

第十六圖 壓力關係圖

Fig. 16. Classes and varieties of the experiments of the oblique compression.

めたる力の强さに大小ありしことも一の原因であらう。第十七圖には割目の種類の代表的のものの實例を示す。圖の上圖は平面圖にて A は押板 B は受板である。下圖は受板を取外しその側より見たる見取圖である。圖の (1) に於て e' は楔狀をなし e の下に押込みたるものにて a なる割目を誘發して居る。圖の矢印の方向は力の向きを示す。

測力計の讀み取は 1–5 瓩である。

(I) の 2) (第十六圖、十七圖 b、十八圖、Pl. XVII 二十三圖 a Pl. XXI 第一表)

實驗回數 13 回。a, b, c, d, e, f の六型式を生ず、第十七圖に代表的のものを示す。13 回中十七圖 b 圖の (2) に屬するもの 5 回。(2) に屬するもの 5 回、(4) に屬するもの 5 回、以上の中 2 回は割目の成長不十分なる爲め (2) (4) 兩者に算入してある。

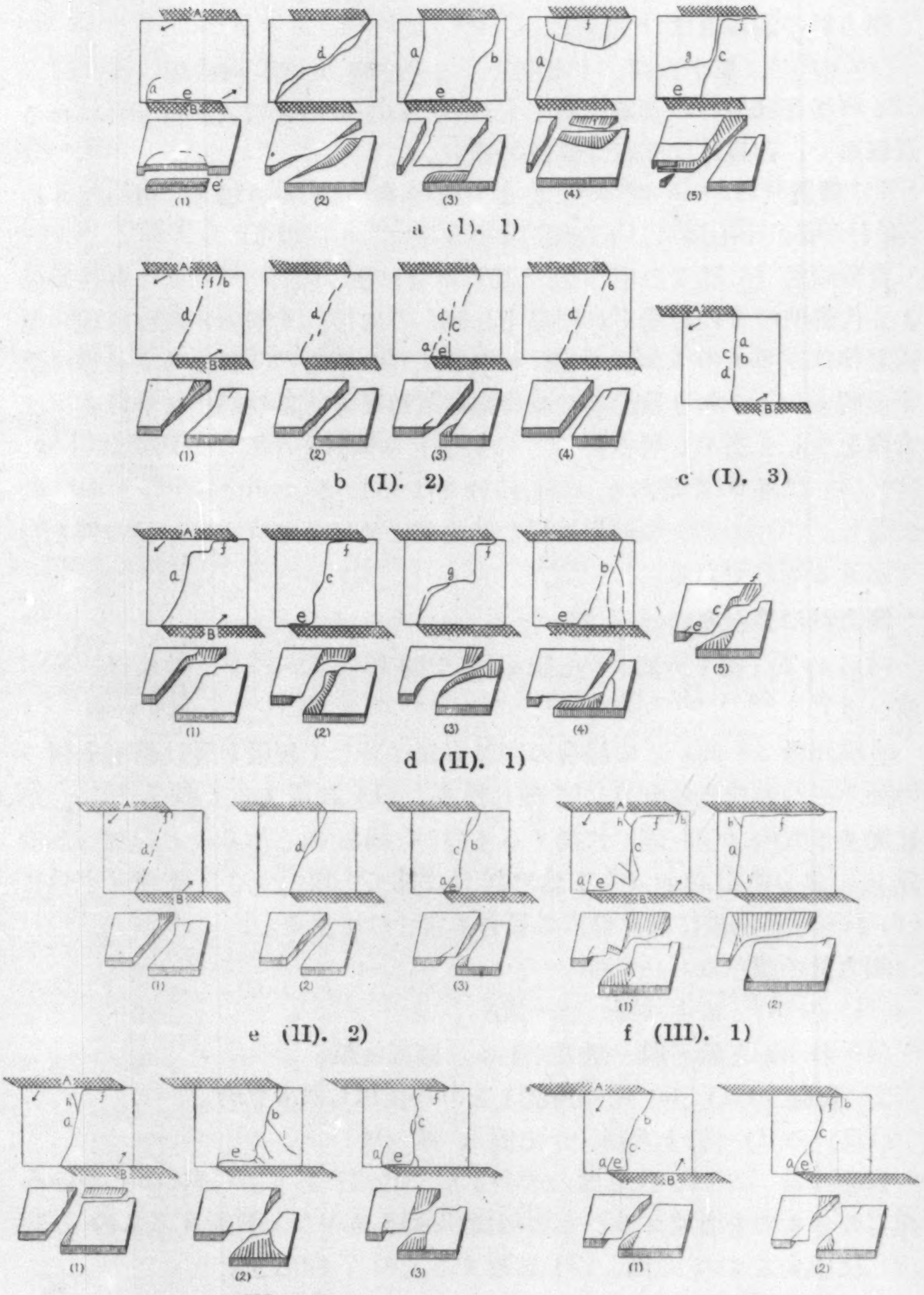
a (I). 1)

b (I). 2)

c (I). 3)

d (II). 1)

e (II). 2)

f (III). 1)

g (III). 2)

h (III). 3)

第十七圖　偏れる側壓によりて生じたる割目説明圖

Fig. 17. Diagrammatic explanation of cracks produced by skew compression.

測力計の讀み取は 1 瓩以內。

(I) の 3) (第十六圖、十七圖 c、二十三圖 a、第一表)

この場合は何れの實驗に於ても a, b, e, d 等の諸型式が重り合ひたる直線形で、割目には雁行性は認め難い。

4. **實驗** (II) 45 度の角度より力の作用したる場合 (II) の 1) (第十六圖、十七圖 d、十九圖 Pl. XVIII 二十三圖 a)

實驗回數 16 回この中 2 回は試料不良に依り除外し 14 回の實驗結果より代表的のものを擧ぐれば第十七圖d の如し。(e 型のみ現はれ他の型式を伴はざるもの 1 回及 f 型、a 型を生じたるもの 1 回あり、是等は第十七圖 a (1) の如き狀況なる故に圖に省略せり) 圖の (1) に於ける f は表面を少しく高めて居る。(2) に類似せる割目を生じたる回數は 4 回、(3) (4) は各々 2 回あり。(3) に於ては g なる compression crack 特に著し。(5) は (2) の部類に屬し其內部に於ける割れ方の一種の例として示せるものである。

測力計の讀み取は 4–7 瓩。

(II) の 2) (第十六圖、十七圖 e、二十圖 Pl. XIX 二十三圖 a、Pl. XXI 第一表)

實驗回數 16 回。この場合の割れ方には著しく制限を受け第十七圖 e の如く三つの代表的割目に整理し得る。(1) に屬するもの 7 回。(2) に屬するもの 5 回 (3) に屬するもの 4 回あり。然るに力の加へ方の程度に多少の相違ありたる爲め割目は總て一樣の大さに發達せず爲に (1) か (3) か明瞭に別け得ざる場合も含まれて居る。

測力計の讀み取 1—2 瓩

(II) の 3) (第十六圖、第一表)

(I) の 3) と殆ど同一型式である。圖は省略、

5. **實驗** (III) 60 度の角度より力の作用したる場合。

(III) の 1) (第十六圖、十七圖 f、第一表)

實驗回數 15 回、代表的のものを擧ぐれば三あり。(圖には e 型のみ生じたるものを省略する、この例は 2 回あり) (1) に屬するもの 7 回 (2) に屬するもの 4 回、(3) に屬するもの 2 回あり。

測力計の讀み取 5–6 瓩

(III) の 2) (第十六圖、十七圖 g、二十三圖 a Pl. XXI 第一表)

實驗回數 15回。代表的のもの三あり。第十七圖 g の (1) に屬するも

の 7回、(2) に屬するもの 4回、(3) に屬するもの 4回。

測力計の讀み取 3–6 瓩。

(III) の 3) (十六圖、十七圖 h、二十一圖 Pl. XX 二十三圖 a Pl. XXI 第一表)

實驗回數 13 回、代表的のもの三あり 十七圖 h の (1) に屬するせの 6 回 (2) に屬するもの同じく6回 (3) に屬するもの 1 回 (第十七圖 f、(2) に類似なる故に圖は省略す。)

測力計の讀み取 3–5 瓩

(III) の 4) (第十六圖、第一表)

(I) の 3) の場合と殆ど同一型式である。

以上を概括したものが次表である。

第 一 表 Table I.

實驗種別壓力の方向と邊のなす角度	(I) 30°			(II) 45°			(III) 60°			
細別	1	2	3	1	2	3	1	2	3	4
押し受け金屬片端の距離粍	4·5	2·3	0·4	3·6	1·9	0·8	4·7	3·5	2·3	0·4
實驗回數	24	13	20	14	16	8	15	15	13	4
裂罅種類	裂罅發現回數									
a	17	12	20	7	12	8	9	13	12	4
b	8	9	20	8	15	8	8	13	12	4
c	5	4	20	7	7	8	13	13	11	4
d	2	7	20	2	10	8			6	4
e	6			9	2		12	9	2	
f	5			9	1		13	9	1	
g	2			2			1			
h	1				2		4	5	2	
i					1		4	3	3	

6. **ゴム板の實驗** 麥粉の板の實驗に於ては極めて微少なる變位にて既に破壞を來すので其變形よりして雁行の分布狀態を、從て如何なる機巧の下に割目を生じて居るかを analysis するには困難である。この爲に

手元にありし消しゴムを試みに使用した。大さは 6×3·8×1·2 糎^3（厚さは 1·2 糎までに削り取つたものである）にて殆ど麥粉の實驗の場合の試料片の大さと同形である。只厚さに於て前者よりも約二倍の厚みを有する。表面の變位量を知る爲めに 2 粍の間隔を以て方眼を畫き前裝置の下に同様の實驗を繰返し試みた。但變位量を明らかに知る必要上前者の場合に比し遙に多くの壓縮を加へた。

同一乾板に實驗前後の形を重ね撮り。(第二十四圖 Pl. XXII に (I) の 2) の例を示す。analysis には第一の點と第三の點を用ひた)。

原板を幻燈にてケント紙上に擴大し各點の變位量 x, y をルーペにて讀み取り analysis を施した。この際 X 軸としては方眼横線中最も直線に近きもの一本を選び、他は之に準據した。

7· 應力の解析 寫眞原板の大さは實物の 1·4 倍にて、擴大圖の原版よりの倍率は 8·7 倍擴大圖の實物よりの倍率は 12·2 倍である。斯く高倍率なる事及重寫なる事によりて擴大された變位量 x, y の讀み取りに當りて 0·1 粍の誤差は免れ難い處である。それで變位量を曲線に畫き突飛なる點の現れたる場合はその前後の點より ±0·1 粍以內の補正を施した。猶ほこの補正のみにては十分の結果は得られなかつたので更に smooth をなした。それには其點の weight を 2 となし其周圍 8 點の weight を 1 と取り卽ち其點の値の 2 倍に周圍 8 點の値を加算し其十分一の値を以て其點の値と見做して analysis を施した。而して算出したるものは次の量に就いてである。

先づ divergence $\varDelta$, shear s を求め

$$\varDelta = \frac{\partial u}{\partial x} + \frac{\partial v}{\partial y},$$

$$2s = \frac{\partial u}{\partial y} + \frac{\partial v}{\partial x}.$$

次に strain ellipse の主軸方向の伸縮 γ 及其軸の方位角 θ を求めた。

$$\gamma_1 = \varDelta + \sqrt{(2s)^2 + (a_1 - b_2)^2},$$

$$\gamma_2 = \varDelta - \sqrt{(2s)^2 + (a_1 - b_2)^2},$$

$$tg\,\theta_1 = \frac{\gamma\,xx - \gamma_1}{2s},$$

$$tg\,\theta_2 = \frac{\gamma\,xx - \gamma_2}{2s}.$$

勿論 θ_1 と θ_2 とは一直角の差がある。θ_1 及 θ_2 を別々に計算して比較するに誤差は總て 1 度以下である。茲に

$$a_1 = \frac{\partial u}{\partial x},$$

$$b_2 = \frac{\partial v}{\partial y},$$

$$\gamma_{xx} = 2\frac{\partial u}{\partial x}.$$

次に stress diffierence に相當する主軸伸縮の差 λ 卽

$$\lambda = \gamma_1 - \gamma_2 = 2\sqrt{(2s)^2 + (a_1 - b_2)^2}$$

を求めた。

8. **解析の結果** 此如き計算を主要點 220–400 點に就いて試み之を圖示す(第十八圖 Pl. XVII 第二十一圖 Pl. XX)。には stress diffierence の等しき點を實線にて $-\gamma$ 卽ち contraction を點線にて $+\gamma$ 卽ち elongation を破線にて示してある。又方向は θ_2 の方向を實線で示してある、卽ち con-traction の方向である。此如き圖を作るには非常に勞力を要する故に總ての實驗に對して試みるを得ず、只 (I) の 2) (II) の 1) (II) の 2) (III) の 3) のみに對して製作した。比較の爲に各其割目の標準的のものを赤にて記入した但し斜線を施せるものと實線のものとは同種實驗に屬する二つの別の實驗の結果である。第二十三圖 a Pl. XXI には是等割目の寫眞を示す。

9. **各種裂罅の本性** 以上記する所よりして明瞭となつた事は割れ目 d は專ら剪力による剪斷裂罅で其歪みは割れ目の面內にあるもので、主として金屬片 A 及 B を連ねる線上に於ける剪應力の最大なる帶に沿ふて起つたものである。a, b は矢張り剪斷裂罅であるが金屬片 A 及 B の直接の稜角作用に依るものである、尤も其延長には c 同樣張力による部分もある。c は主として張力裂罅である。前後に壓迫せられて左右に擴がらんとする力の爲に起る。

e, f は A, B の重なりの深き場合、及壓する力の角度が面に對して立つて居る場合卽 I よりも III に於て、2 よりも 1 に於て多く起り 3 又は 4 の場合は殆んど起らない。是は壓力による剪斷裂罅で其壓縮應力は裂罅面にはなく、罅裂と直角な水平面內に存する。其裂面はつまり垂直と約 45° をなし壓力を受ける側面の水平稜と平行な線卽裂線を含む斜面であ

る。只金屬片 AB と試料片との接觸の關係より其接部に近く現はれるが、g の如く全く同じ種類ではあるが中央部に現はれる事も稀にはある。

hei とは c に伴ふ斜裂で多分壓力による剪斷裂罅が緣邊に近く本裂線に 45° をなした垂直面內現はれるものであろう。

かくて表に示した各割れ目の發現回數の分布も明に說明せられる。何となれば圖の第十八、二十と十九、二十一との比較で判る樣に押し方によりて壓縮力が顯著となり剪斷力の顯著でない場合と、之に反對の場合とが觀取せられ、前者に於て e, f c, g の如きが多く後者に d が多いので知られる。

偖雁行は主に d に伴ふて起る事は著しい事實で雁行が歪力に伴ふ現象で有る事を示す。かくて第十八圖及第二十圖に見るに雁行裂線の主軸は最大剪力帶と一致して居るが、個々の割れ目は其點の主應力 (principal stress) の方向と一致し此例に於ては其中壓縮方向と一致して居る。之れは卽此方向と直角なる張力によりて生じたものなる事を示す。卽雁行は剪斷應力の最大帶又は最大線の方向と主應力の方向とが一致せざる時に起るものなる事を知り得た。是れが今回の實驗での一番の收獲である。

此實事より以前に提示した雁行の法則緒言中の (10) に述べたものは必然的のものとして說明し得る。

10. 雁行法則の說明 任意の一點の附近の應力の狀況が第二十二圖に示すが如く大體一方から壓力が加はり之と直角に張力が働きある場合を考へる。壓力の方向は大體 OY に平行であり O を去るに從て次第に少しづゝ變はる、張力は同樣に大體 OX に平行であるとする。裂罅の主軸が第一象限又は第三象限に起つた場合を考へる。其線を OA とする。此線上に張力列罅が出來るとすれば其等は總て OX に直

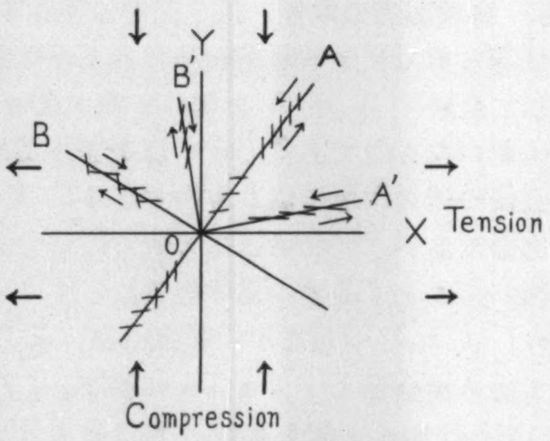

第二十二圖 雁行性說明圖

Fig. 22. Explanation of the law of echélon formation.

角 OY に平行であるから雁行の向きは主軸 OA に對して左りに偏よる卽是は正の雁行と名づけたものである。此場合 OA に沿ふ單純歪力は圖に示す如く其廻轉は左り廻りであり、之を同じく正の歪みと名づけた、かくて正の張力雁行裂罅は正の歪みと伴ふ、もし又 OA 上に壓力雁行裂罅が出來るとすれば是等は OX に平行であり雁行は負となる。卽負の壓力雁行裂罅は正の歪と伴ふ。同樣に第二及第四象限に就て考へるに此象限では張力裂罅は負の雁行を作るが歪みは OB に沿ふて負である。壓力裂罅は正の雁行を作る、かくて必然的に

> 正の張力裂罅、負の壓力裂罅は正の歪みと伴ひ、負の張力裂罅と正の壓力裂罅とは負の歪みと伴ふ可きものである。

事が證明せられた。

11. **注意事項**　以上の關係は極めて微妙な點迄實現せられる第十八圖での雁行は大勢に於て三段の正の雁行で勿論法則に一致して居るが更に其中央の一本が其れ自身に雁行小裂罅より成つて居るが、其上端に於て雁行が正となり下端に於ては負となつて居る。一見甚奇怪なるが如くであるが、是を併記した主應力の方向と比較するに、正しく上端では雁行主軸は主應力方向の左り卽第二象限に出て居る。卽此部では歪みの方向が負であるから當然雁行も負となる可きで、下端は之に反して主應力の方向の右に主軸が向いて居るから歪みの向きが正で從て雁行も正となる。

雁行の方向と主軸の方向とのなす角の大小はかくて主應力の方向と最大應力帶の軸の方向とのなす角の大小を示すものである。後者の角が零なる時卽主應力方向と最大應力帶の方向とが一致した場合は雁行は起らない。

雁行の間隔は物質と加へられた外力の程度とに關するものであるが此點は尙研究を要する。以上雁行の法則はかくて極めて一般性を有するものであるから、模型に於ても又實地に於ても總ての場合に於て嚴重に支配力あるものである。

德田博士の論文にある部分的直線移動によりて起る二列の雁行及先端の橫裂又は皺は全く以上の說明を各部に加へれば完全に說明し得る。

以上で本論を終るが尙多少注意を要するは割れ目の出來る時間的關係である。A, B が深く合はせある場合には殆んど何等の前兆なく破壞が突然に只急激に起るが、AB の合せ方の淺く、又力の方向が斜な場合に

は割れ目は多くは試料の中程より稍々下方に先づ開口を見次第に上方及下方に伸びるを見た、殆んど總ての場合に雁行を現はした。卽是等は結局d種又はc種の割れ目にあつた、尤も稀には緣部より始まつたものもあつたが是は押し金受け金の稜角の作用が主なものであつた。此緩に起る式のものに於ても最後に切斷なされる時には矢張り相當の衝擊は起つた。是等は大地震の際の豫震の有無と考へ合せて興味ある現象で有る。

（昭和六年一月廿日）

---

4. *On Crack Systems especially those of Echélon Formation.*

By **Sakuhei FUJIWHARA and Takeo TAKAYAMA,**

Earthquake Research Institute.

There are crack systems appearing on plates. They are:—

(1) Parallel cracks with nearly equal intervals or the multiples or regular fractions. Such cracks are produced by the homogeneous cylindrical bending of a homogeneous plate. When homogeneity either of stress or of material is missed, so far the deviation from the law of equal intervals arises.

(2) Radial cracks with nearly equal angular intervals are produced by the homogeneous conical bending of a homogeneous plate. The law on the equality of the angular intervals is nearly the same as in the case (1).

(3) Concentric circular cracks are produced by the conical or domelike bending of a plate.

(4) Regular poligonal cracks are produced by the homogeneous isotropic contraction of area of a homegeneous plate, when supported at the basal plain surface of the plate. The elementally poligon can be square rectangle, pentagon, hexagon etc. or their mixtures according to the condition at the base or at the boundary.

(5) Cracks in echélon formation are produced when a shearing stress is applied on a plate. Heterogeneity of stress and of material is favourable to the production of echélons.

Several experiments are made for all the above systems of cracks. Those of (1) to (4) are too simple and need not to give any further explanation in detail.[5]

---

[5] Lectures were given on these before the meeting of the Earthquake Research Institute, Tokyo, but the labour of printing them in foreign language is saved. See text in Japanese, also see "On the mechanism of great Kwantô earthquake etc," *Journ. Met. Soc., Jap.*, 1924 Jan. Also see Leith, "Stractural Geology. Joints in Relation to Causal Stresses."

The crack system of echélon formation is most commonly appears in the natural phenomena such as the faults or cracks in the case of a destructive earthquake. Never the less its mechanism of formation is rather obscure. In the present note the method and the results of experiments on the echélon crack formation and allied phenomena are given.

The apparatus used for the experiments is shown in Fig. 15. T is the test piece which is of dimension 6·0, 3·9, 0·6 cm^3 and made of wheat powder compressed under pressure of 80 kg per 1 cm^2 of the surface. The test piece is compressed on from its side obliquely as is shown in Fig. 15 and also in Fig. 16 in which 3 modes of experiments with 3 or 4 varieties each are also shown. Thick arrows show the directions of the pressure which is applied partially on the side of the test piece along the shaded parts which imply the brass pieces in contact with and pushing the test piece. The relative position of the ends A, B of the two opposite brass pieces is important to give characteristic forms to the crack of the wheat plate. The cracks thus produced are classified into 10 groups, which are shown in Plate XVII and XVIII and also diagrammatically in Fig. 17. The number of experiments of each variety and the frequency of the appeared cracks are shown in the next table.

Experiment	(I)			(II)			(III)			
Inclination of pressure direction from the edge of the test piece	30°			45°			60°			
Variety	1	2	3	1	2	3	1	2	3	4
Distance in cm. of the ends AB of the brass pieces	4·5	2·3	0·4	3·6	1·9	0·8	4·7	3·5	2·3	0·4
Number of experiments	24	13	20	14	16	8	15	15	13	4
Frequency of the appearance of each crack										
a	17	12	20	7	12	8	9	13	12	4
b	8	9	20	8	15	8	8	13	12	4
c	5	4	20	7	7	8	13	13	11	4
d	2	7	20	2	10	8			6	4
e	6			9	2		12	9	2	
f	5			9	1		13	9	1	
g	2			2			1			
h	1				2		4	5	2	
i					1		4	3	3	

In order to know the stress distribution, a plate of india rubber nearly of the same size with the wheat plate was compressed under the same condition with the same apparatus. Square net had been drawn on the surface of the plate previous to the experiment and the deformation of the net was photographed at 3 stages in the course of the compression as shown in Plate XVIII, Fig. 24. The component displacements u, v of every point of the net were read off and from which the divergence Δ, simple shear S, rotation R etc. were reckoned.

$$\Delta = \frac{\partial u}{\partial x} + \frac{\partial v}{\partial y}, \quad 2S = \frac{\partial u}{\partial y} + \frac{\partial v}{\partial x}, \quad 2R = \frac{\partial u}{\partial y} - \frac{\partial v}{\partial x},$$

$$\gamma_1 = \Delta + \sqrt{(2S)^2 + (a_1 - b_2)^2}, \quad \gamma_2 = \Delta - \sqrt{(2S)^2 + (a_1 - b_2)^2},$$

$$\tan\theta_1 = \frac{2a_1 - \gamma_1}{2S}, \quad \tan\theta_2 = \frac{2a_1 - \gamma_2}{2S}, \quad \lambda = \gamma_1 - \gamma_2,$$

where

$$a_1 = \frac{\partial u}{\partial x} \quad \text{and} \quad b_2 = \frac{\partial v}{\partial y}.$$

The principal strains γ_1 and γ_2, their direction θ and the strain difference or the total shear λ were calculated for every point of the net. These values were entered in charts and isopleths of γ_1, γ_2, and λ are drawn together with the direction θ. They are shown for selected cases in Fig. 18, 19, 20 and 21. The cracks actually produced are also entered additionally in the chart.

By examining these charts we can easily see that the cracks a and b are products due to shearing stress at the ends A and B of the metal pieces. c are the tension cracks due to the lateral elongation. d is the shear crack along the line connecting the two end points A and B, e and f are products due to the compression against which the breaking limit of shearing stress is first reached along the lateral oblique surface inclined to the vertical with an angle of 45° or about. g is the same as e and f but appeared in the central part instead of at the bordering parts. h and i are secondary cracks of the main crack c making angles of 45° or about with this, having the surface of fracture in vertical planes. They are also the shear products due to the compression and favourably appear in the bordering parts.

Echélon formation is seen mostly in cracks d, a and b, sometimes with h and i and obviously related with shearing stress which acts in the plane in which the cracks appear. It does not occur in e and f though they are of shear products, because the plane in which e and f appear is the plane of compression for e and f but is not that of shear. Hence we can sometimes see the echélon on the vertical section of the test piece perpendicular to e and f, along which shearing stress is acting. We can see the zone of maximum shear and maximum elongation just in the position of d crack in Fig. 18, 19 and 20. But the direction of the each small crack which composes the crack d in echélon formation coinsides well with the direction of principal strain at that part. This shows that the elementary crack of echélon in this case is evidently the tension crack opening normal to the principal tensile stress at that part, or the same thing, along the principal compression.

（震研彙報、第九號、圖版、藤原、高山）

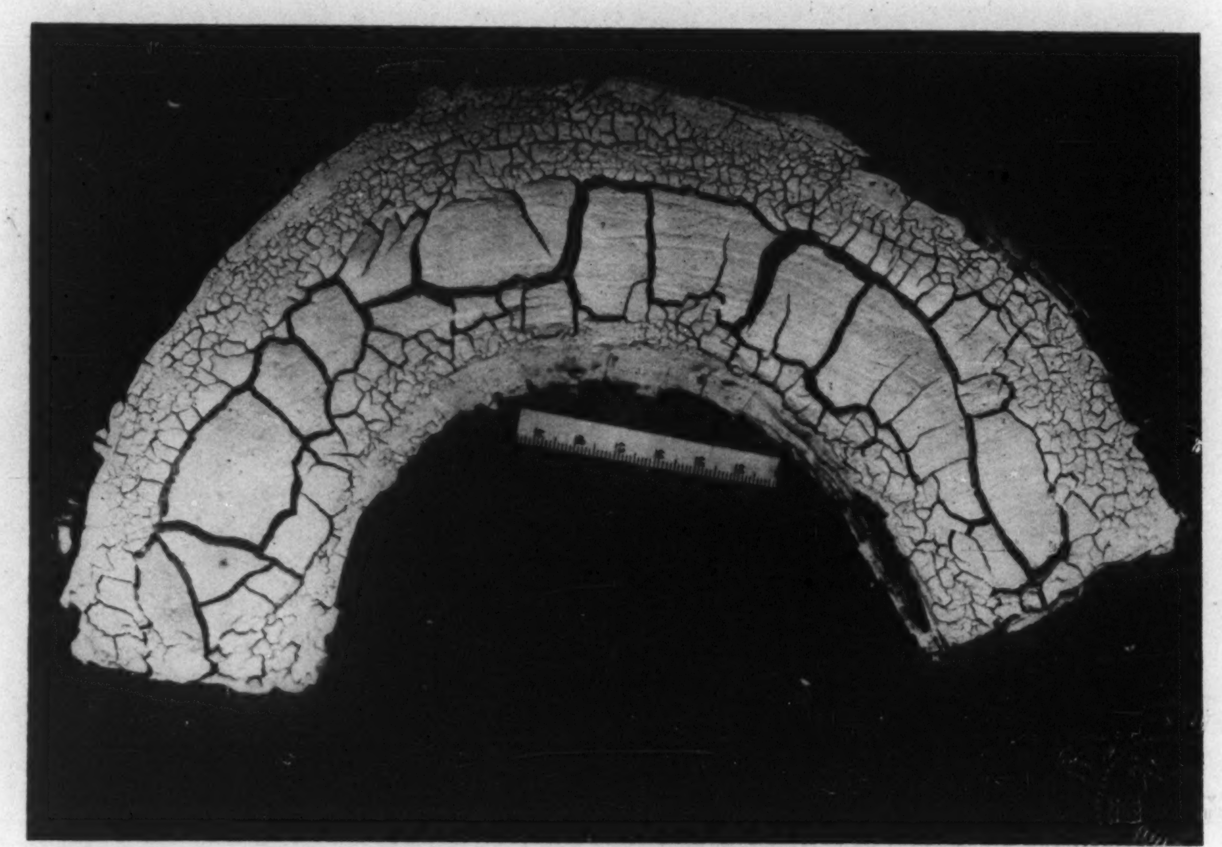

第一圖　面積收縮裂罅

Fig. 1. Cracks due to surface contraction. Tendency of the normal intersect of cracks is seen. Localized and variable dimensions of elementary cracks are seen.

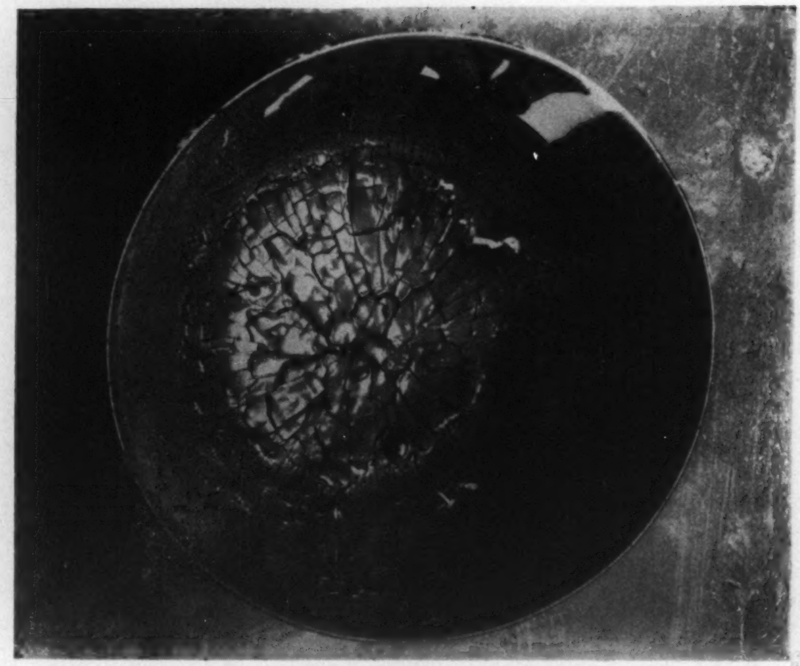

第二圖　墨汁の乾固して生じた割目

Fig. 2. Cracks due to surface contraction. Radial cracks produced first. Transverse one then developed perpendicular to the former.

（震研彙報、第九號、圖版、藤原、高山）

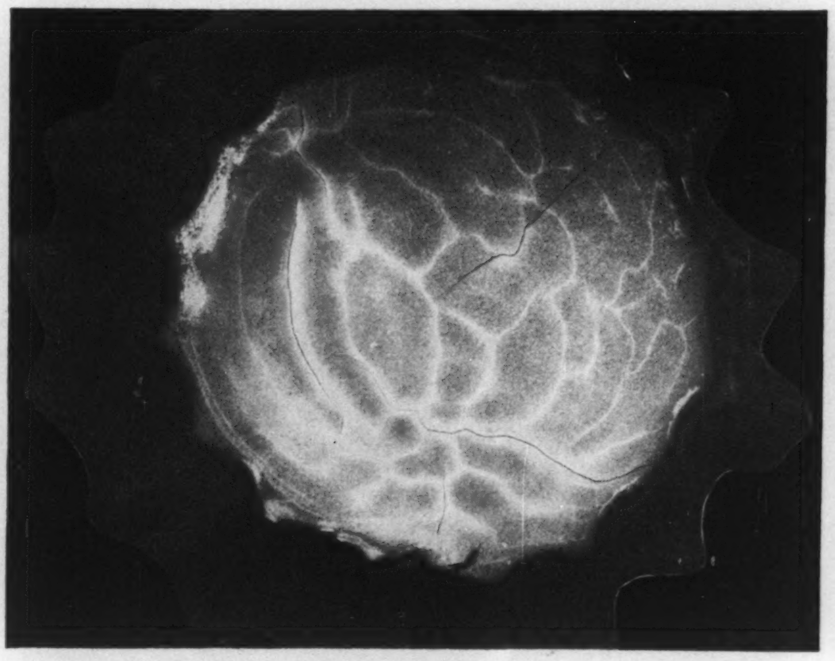

第三圖　ヘットの凝固して生じた割目

Fig. 3. Cracks due to the heterogeneous contraction of the material. White lines the seat of heterogeneity; dark lines on or crossing them are cracks.

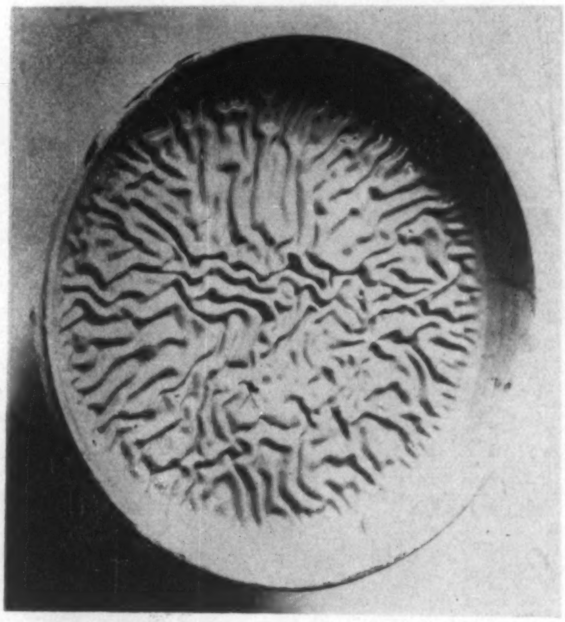

第四圖　ペーントの表面凝固して生じた皺

Fig. 4. Folds on the skin due to the contraction of the internal material.

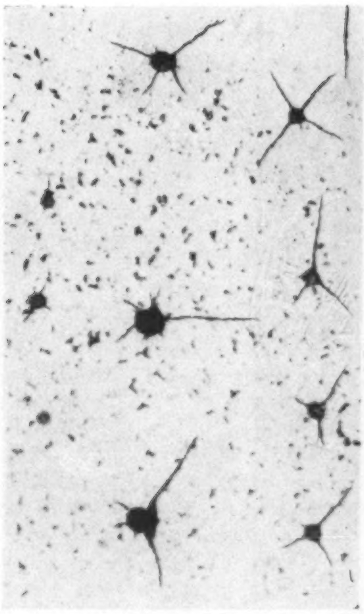

第五圖　パラフィンの板に打撃を加へたる場合の割目

Fig. 5. Cracks due to conical bending produced on paraffin plate by the impact of a pointed metal.

（震研彙報、第九號、圖版、藤原、高山）

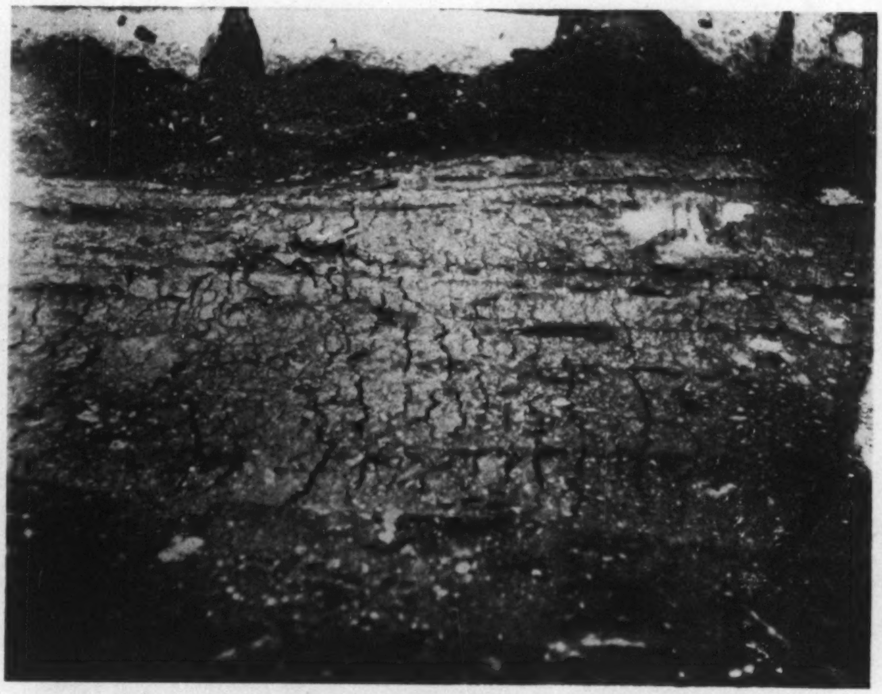

第六圖　道路工事中のローラーによつて生じた地面の平行な割目

Fig. 6. Parallel cracks due to cylindrical bending of a rough surface.

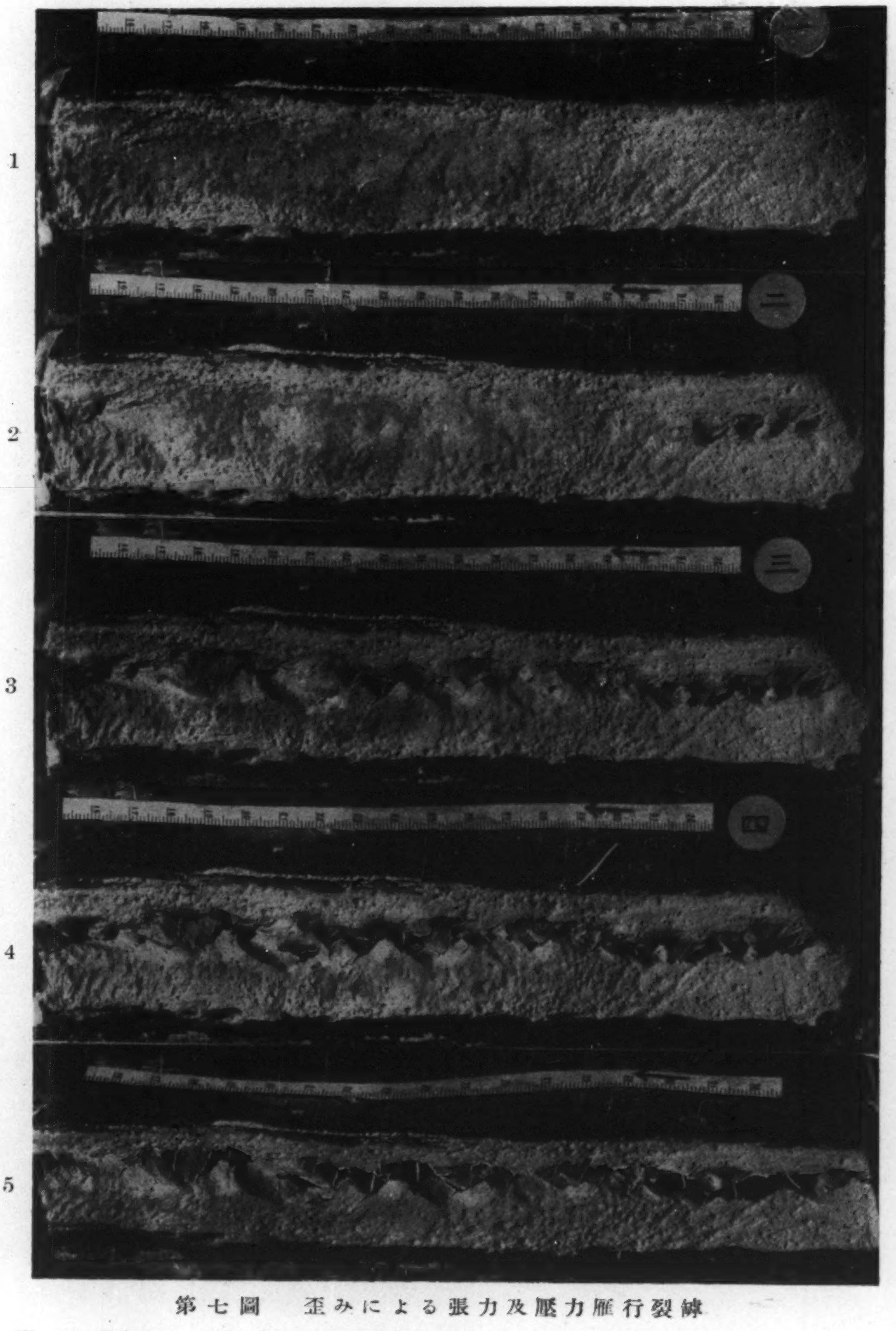

（震研彙報、第九號、圖版、藤原、高山）

第七圖　歪みによる張力及壓力雁行裂罅

Fig. 7. Cracks and creases in echélon produced by shearing process. // tensoin cracks; \\ creases and cracks by compression. Tension cracks appear always first see 2, then compression creases see, 3, then compression cracks see 4. 5 is the same as 4 but seen obliquely in order to show elevation along creases.

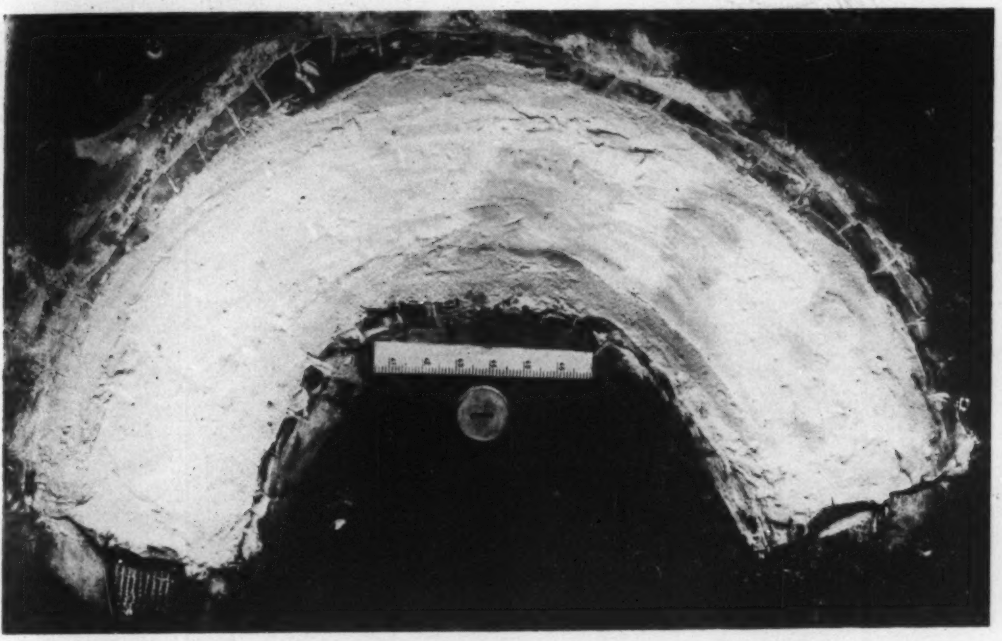

1. Before the experiment.

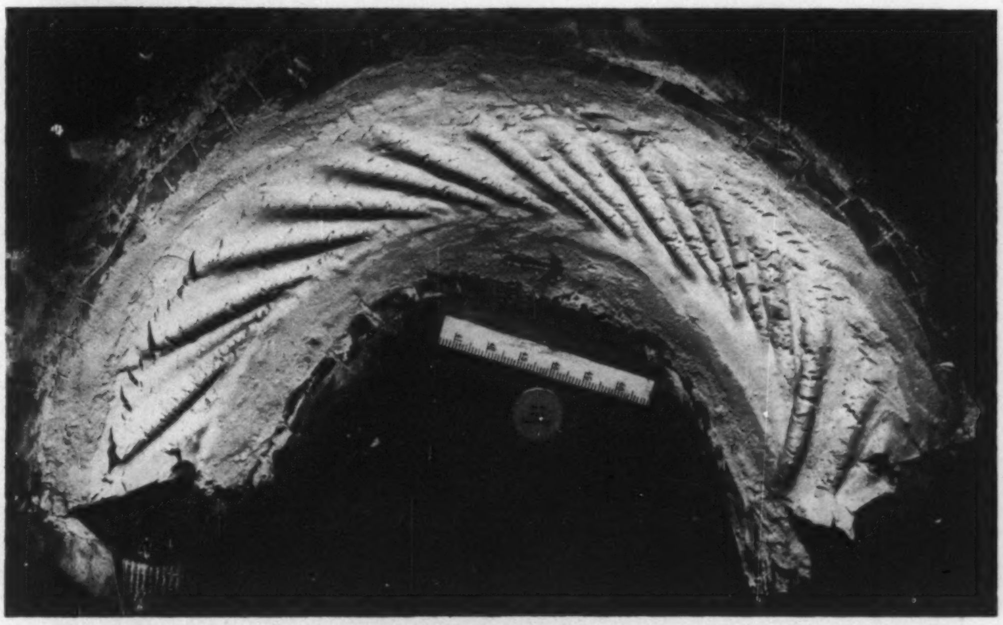

2. After rotation.

第九圖　麥粉と亞鉛華粉の混合物の回轉による弧狀雁行褶曲及裂罅、褶曲は壓縮により、裂罅は張開によりて生ず、方向は直交

Fig. 9. Folds and cracks due to shear along an arc. Folds can be thus produced without any sensible alteration of the surface area. Cracks are perpendicular to the creases.

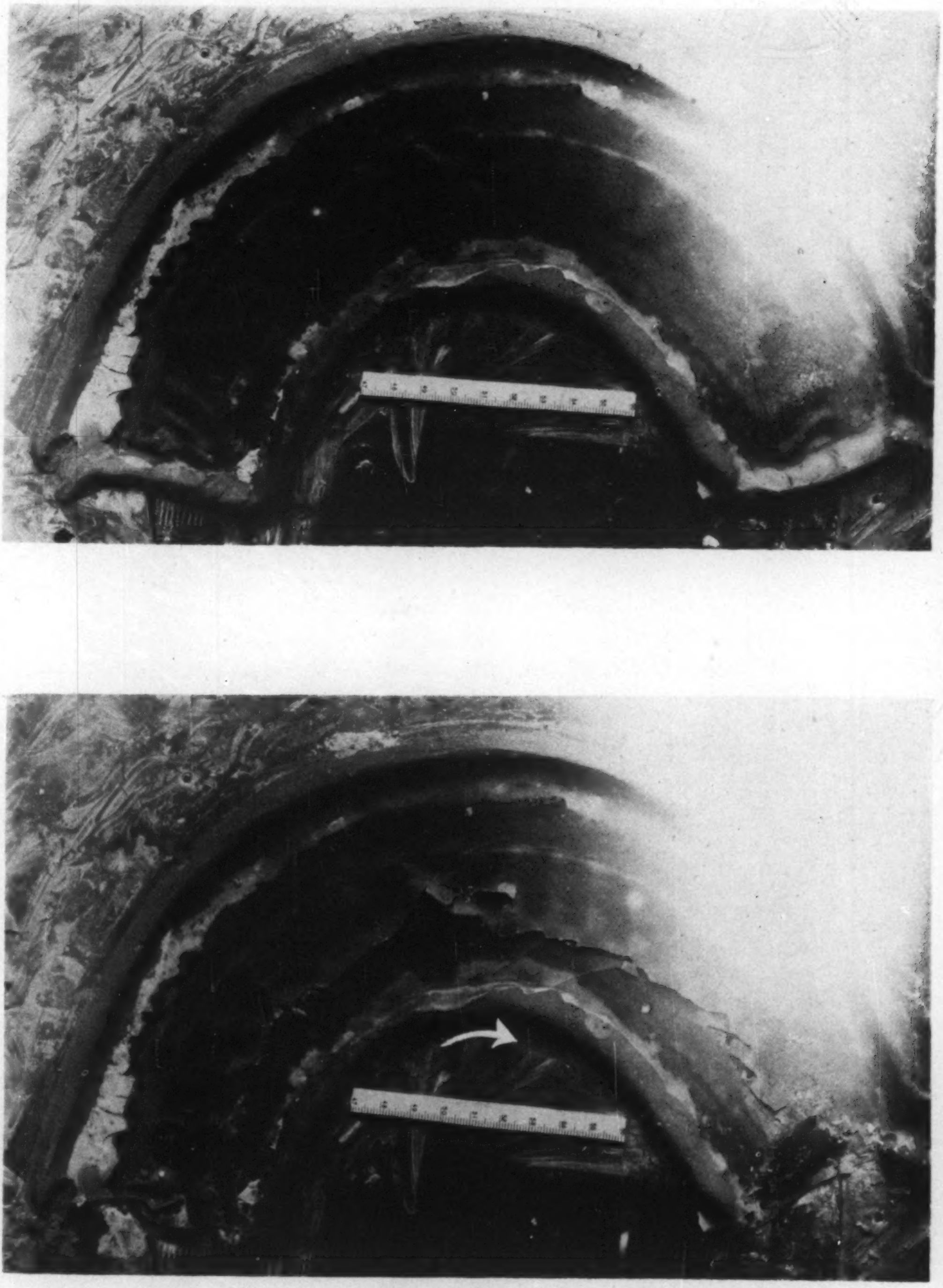

第十圖　パラピン板の回轉による純粹剪斷裂罅(中央より左)及雁行裂罅(中央より右)

Fig. 10. Tension cracks in echélon and a genuine shear crack produced on a paraffine plate by simple shear along a circular arc.

(震研彙報、第九號、圖版、藤原、高山)

（震研彙報、第九號、圖版、藤原、高山）

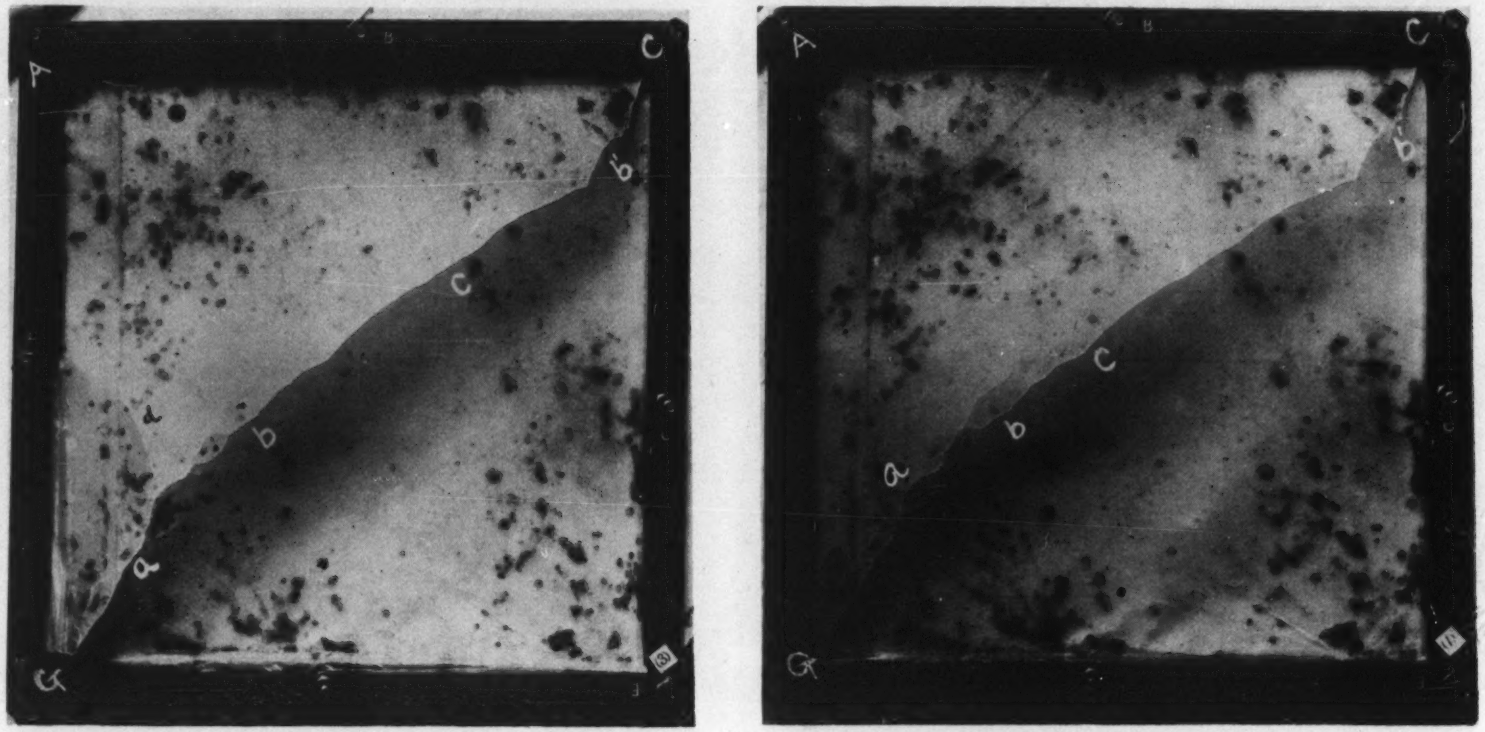

2. After compression. 3. Further compression.

第十二圖　對角線上の壓縮による撓曲裂罅

Fig. 12. Bending crack a, b, c, d′ produced on paraffin plate by diagonal compression along A E, the joints A, C, E, G being free.

（震研彙報、第九號、圖版、藤原、高山）

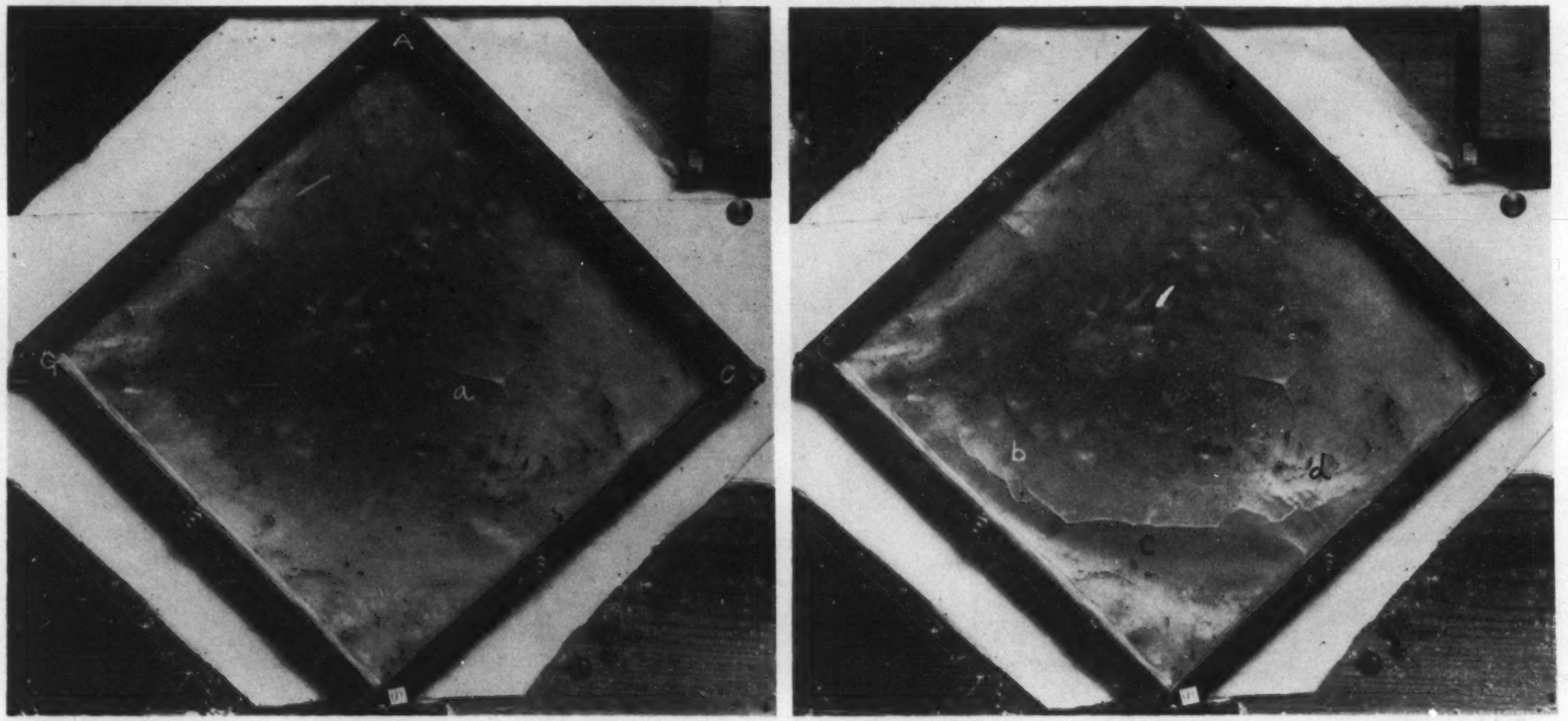

1. Before the experiment. 2. After the experiment.

第十三圖　對角線の方向に加へたる壓力による剪斷裂罅 b と撓曲裂罅 c.

Fig. 13. Compressive bending crack c and shear cracks b and d produced on paraffin plate by diagonal compression of the frame along AE. Joints of the frame at A, C, E and G are free.

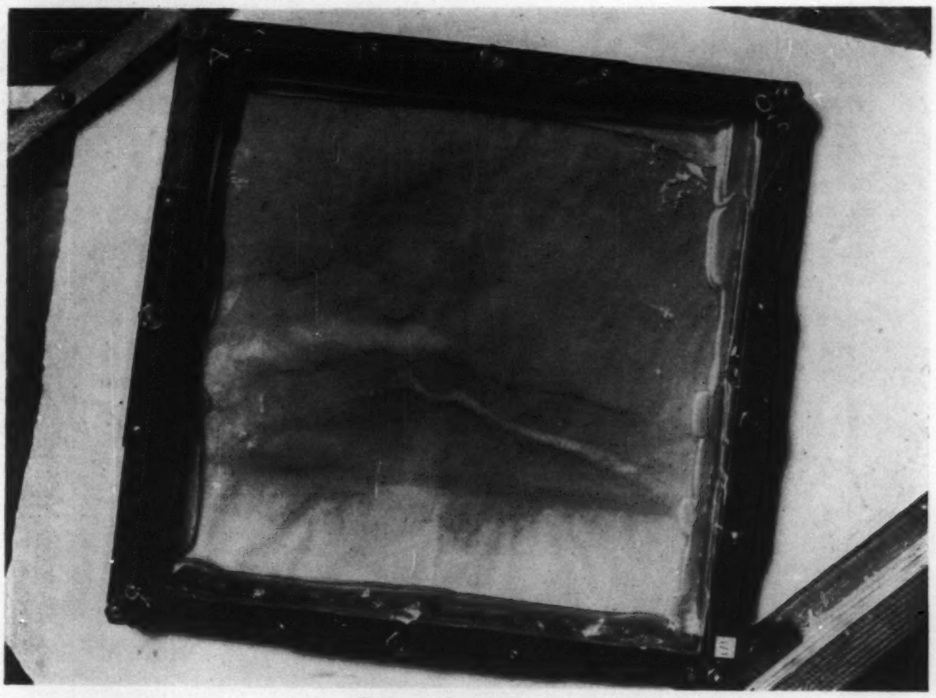

1. Before the experiment.

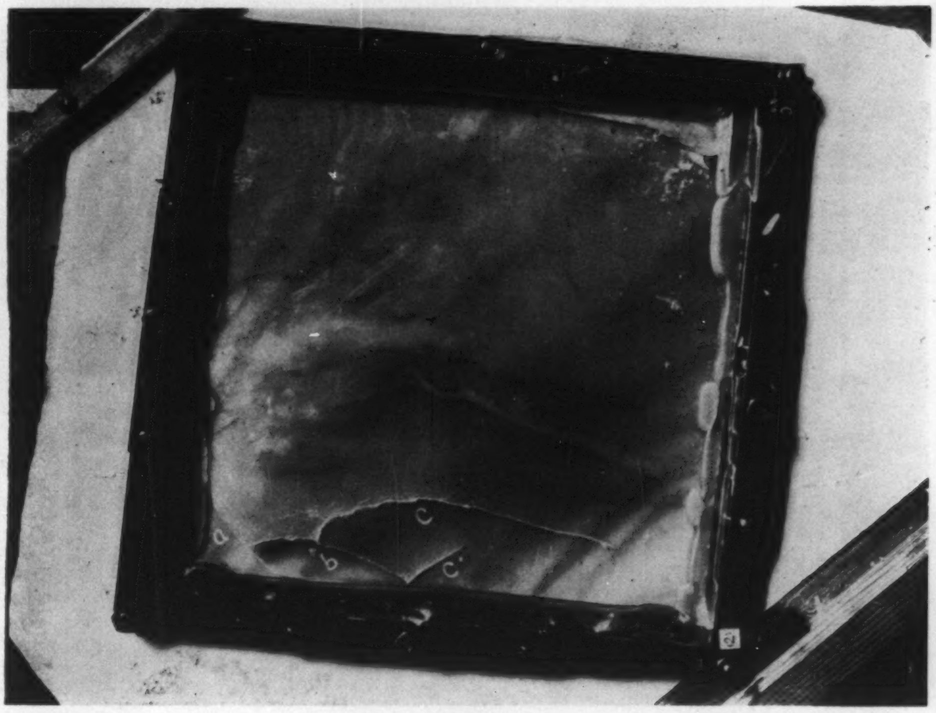

2. After the experiment.

（震研彙報、第九號、圖版、藤原、高山）

第十四圖　パラフインの板の緣邊の割目青海波模樣ワレ目外側より進入する場合

Fig. 14. Marginal arcuate cracks b, c, c' produced on paraffine plate by diagonal compression along AE, the joints at A, C, E and G being free.

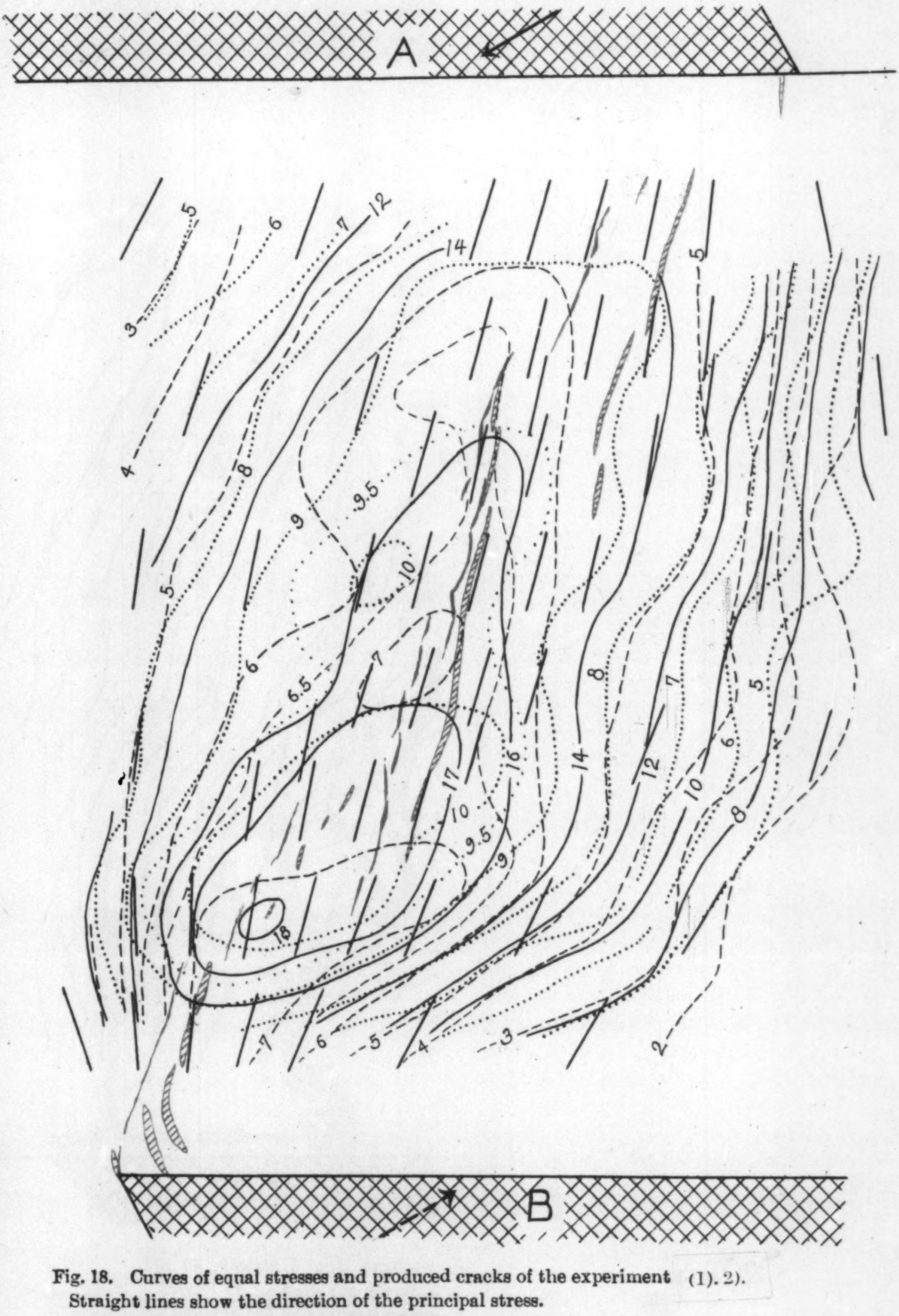
A
5
6
7
12
14
3
5
4
8
9
9.5
10
5
6
6.5
7
8
7
5
6
14
12
10
8
16
17
10
9.5
9
18
7
6
5
4
3
2
B

Fig. 18. Curves of equal stresses and produced cracks of the experiment (1). 2).
Straight lines show the direction of the principal stress.
Curves in full line show the equal total shear.
Curves in broken line show the equal principal compressive stress.
Curves in dots show the equal principal tensile stress.
Lines in red are the cracks produced. Full and Shade indicate the results of two different experiments belonging to the same class and same variety.

（震研彙報、第九號、圖版、藤原、高山）

（震研彙報、第九號、圖版、藤原、高山）

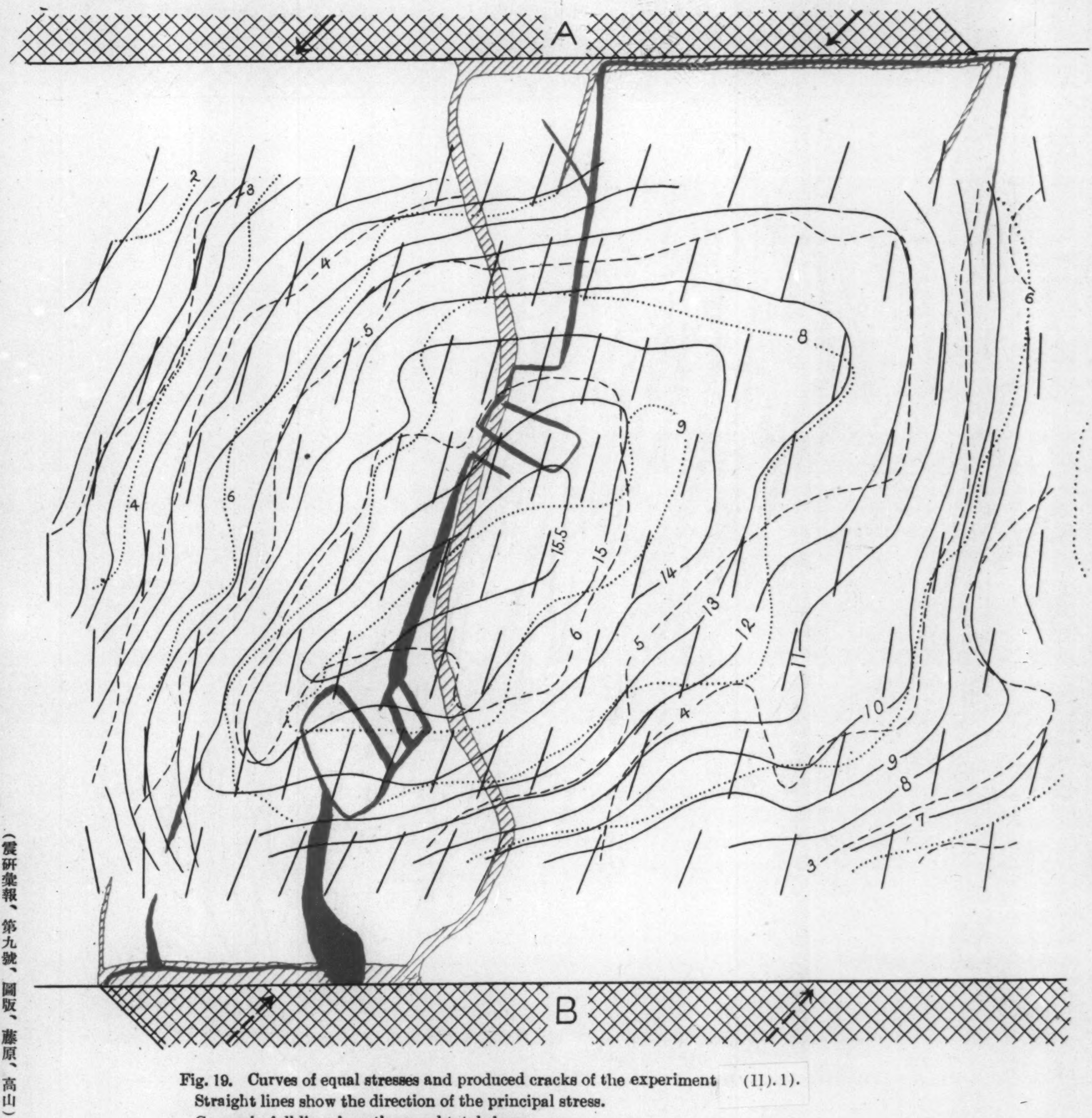

Fig. 19. Curves of equal stresses and produced cracks of the experiment (II). 1).
Straight lines show the direction of the principal stress.
Curves in full line show the equal total shear.
Curves in broken line show the equal principal compressive stress.
Curves in dot show the equal principal tensile stress.
Lines in red are the cracks produced. Full and Shade indicate the results of two different experiments belonging to the same class and same variety.

（震研彙報、第九號、圖版、藤原、高山）

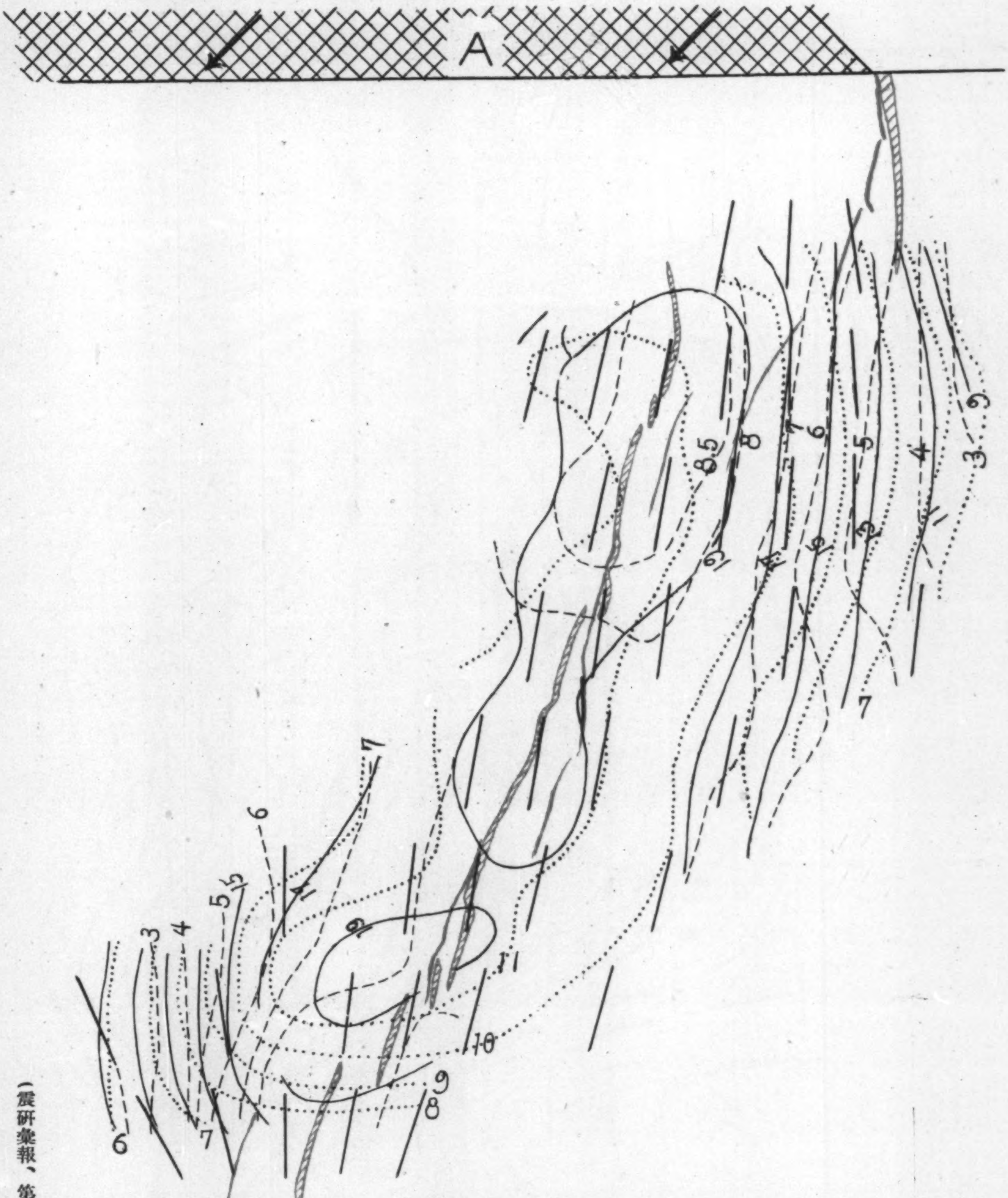

Fig. 20. Curves of equal stresses and produced cracks of the experiment (II). 2).
Straight lines show the direction of the principal stress.
Curves in full line show the equal total shear.
Curves in broken line show the equal principal compressive stress.
Curves in dot show the equal principal tensile stress.
Lines in red are the cracks produced. Full and Shade indicate the results of two different experiments belonging to the same class and same variety.

（震研彙報、第九號、圖版、藤原、高山）

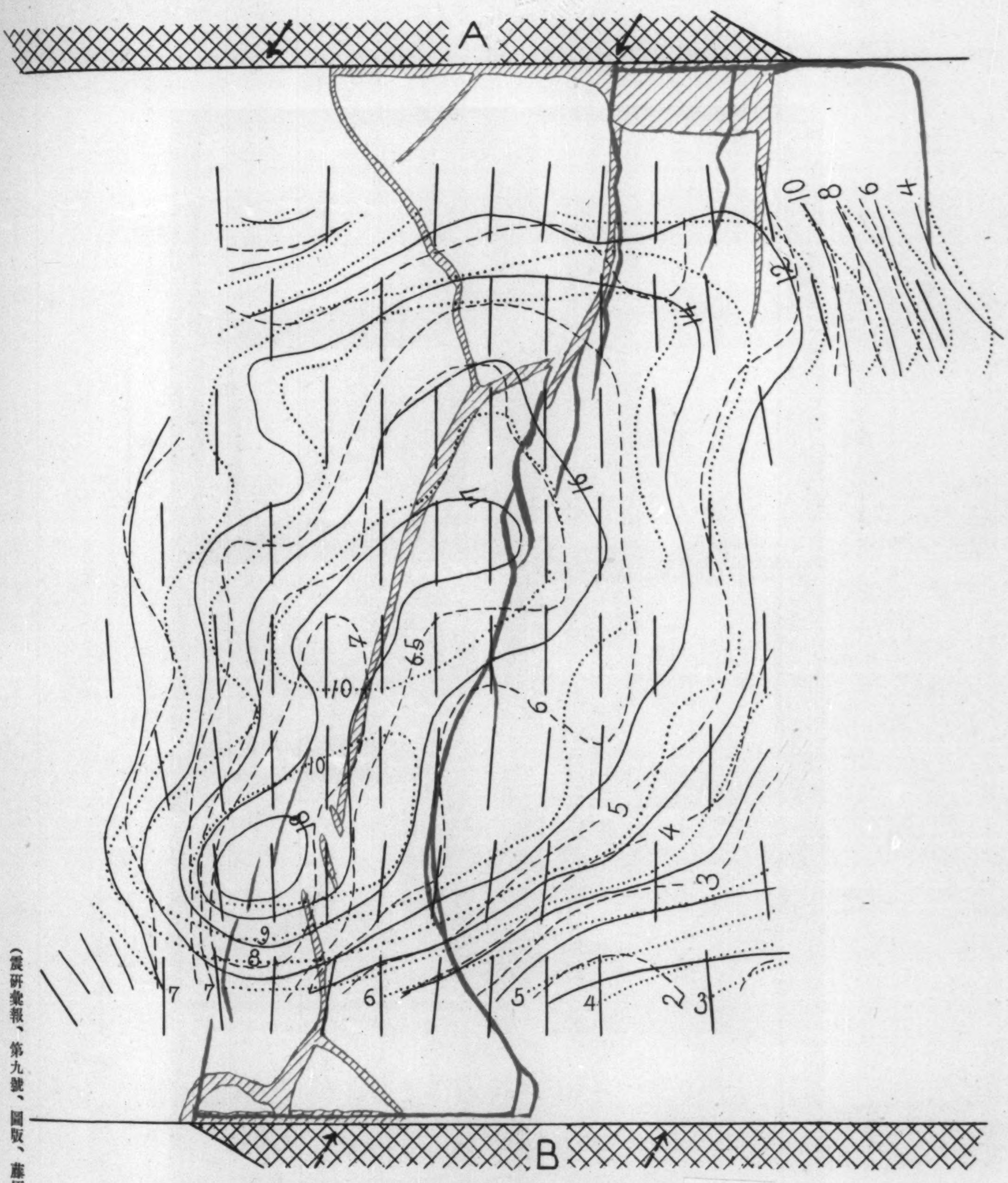

Fig. 21. Curves of equal stresses and produced cracks of the experiment (III).3).
Straight lines show the direction of the principal stress.
Curves in full line show the equal total shear.
Curves in broken line show the equal principal compressive stress.
Curves in dot show the equal principal tensile stress.
Lines in red are the cracks produced. Full and Shade indicate the results of two different experiments belonging to the same class and same variety.

（震研彙報、第九號、圖版、藤原、高山）

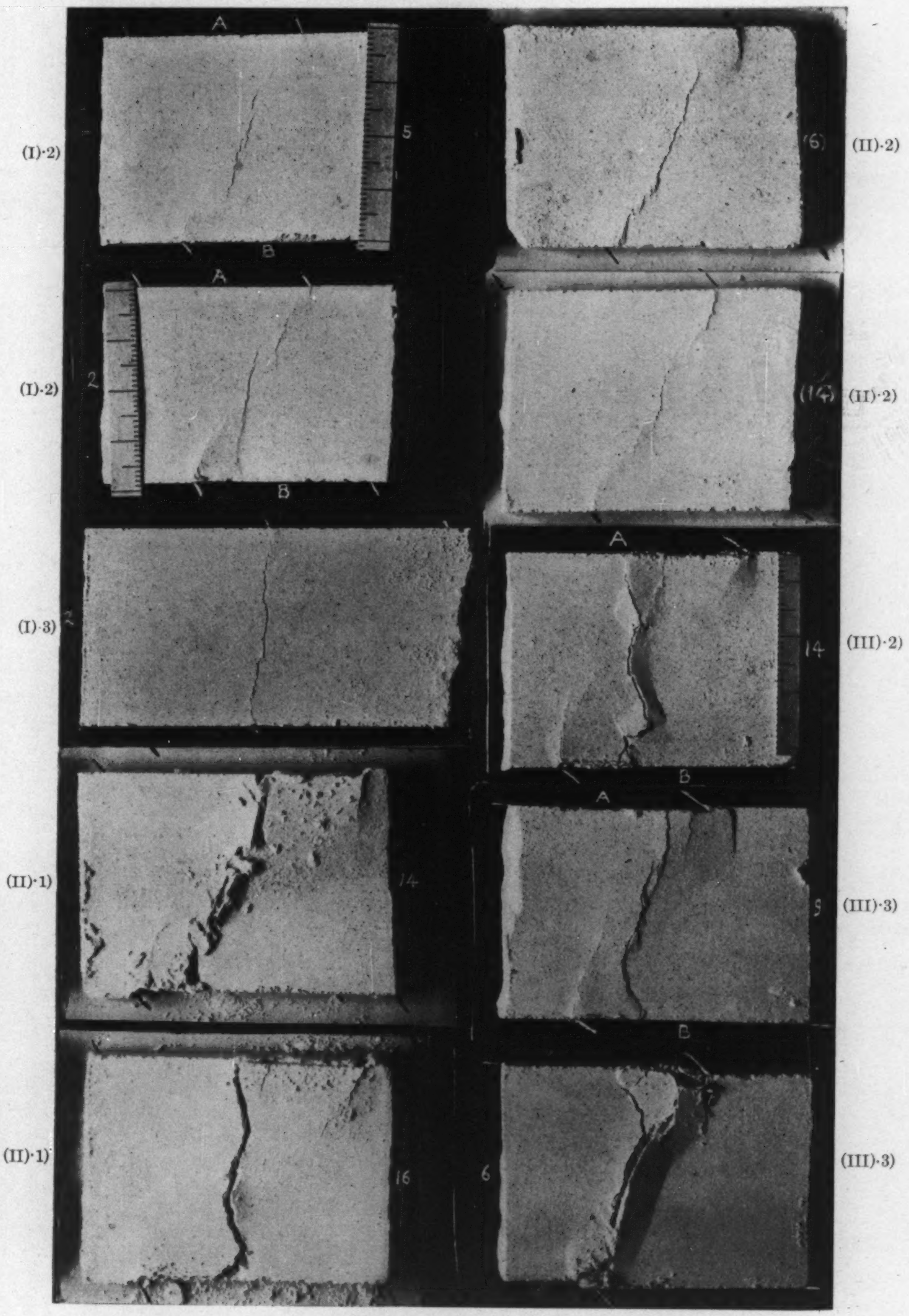
(I)-2
A
B
5
(II)-2
(6)
(I)-2
A
B
2
(II)-2
(14)
(I)-3
2
(III)-2
A
B
14
(II)-1
14
(III)-3
A
B
9
(II)-1
16
(III)-3
6

第二十三圖 a、表粉枚を前後兩側より斜に押して生じたる種々の割目

Fig. 23 a. Cracks produced.

（震研彙報、第九號、圖版、藤原、高山）

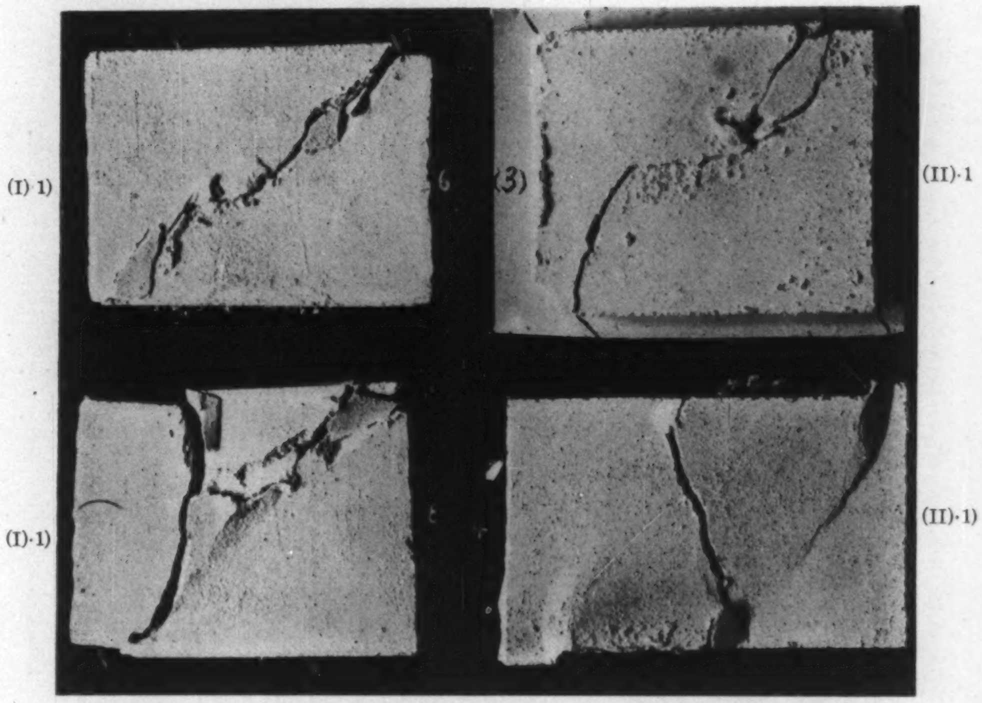

第二十三圖 b、表粉の板を前後より斜に押して生じたる種々の割れ目

Fig. 23 b. Cracks produced.

(震研彙報、第九號、圖版、藤原、高山)

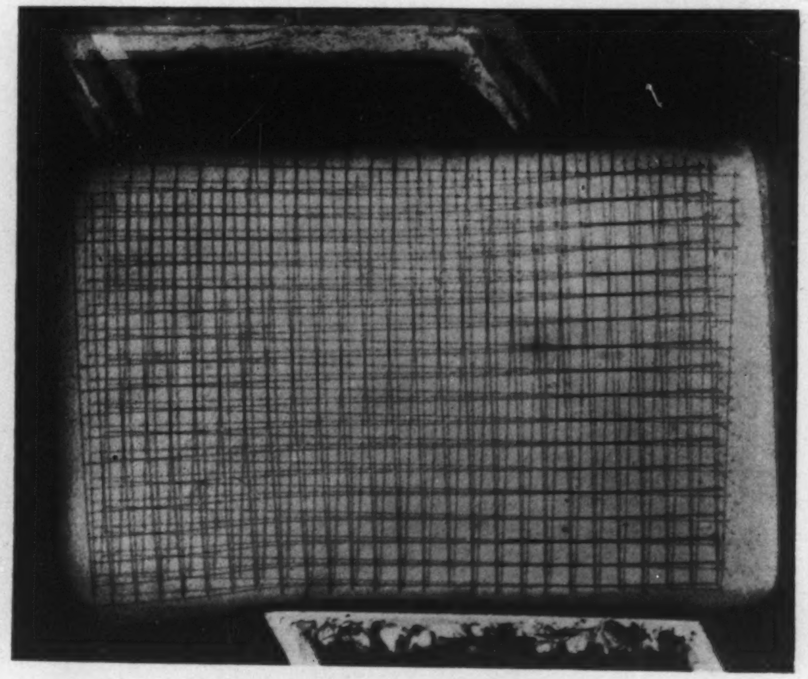

第二十四圖 ゴム板を歪めた狀況

Fig. 24. Strain experiment.

Thus an interesting fact is found that the fracture must proceed along the zone of maximum stress, but individual fissures take place in the direction of the principal stresses at individual points in the zone. Thus *the actual fracture thus caused inevitably becomes an echélon formation along the zone of the maximum stress with elementary cracks in the direction of the principal stress.*

The sense of echélon was defined as positive when elementary cracks deviate to the left of the direction of the zone of fracture and negative when deviate to the right. The sense of echélon, therefore, depends on the relation between the directions of the line or zone or perhaps better word, ridge of maximum stress and of the principal stress. Suppose that the directions of the principal stress are nearly parallel for all points in the area concerned as shown in Fig. 22 in which the compression and tension are shown by arrows. Suppose that the maximum zone of str ss runs in any direction between OX and OY say OA. The sense of shear along OA is positive. If the elementary cracks are tension cracks then they are nearly parallel to OY and hence the positive echélon of tension cracks must be formed along OA along which the sense of shear is positive i.e. the rotation is anticlockwise. The compression cracks are always normal to the tension cracks. They are parallel to OX in Fig. 22. Hence a negative echélon of the compression cracks must be formed accompanied by a positive shear along the main line of fissure. If, however, the line of the maximum stress runs along any direction between OY and O (−X) say OB then the sense of shear along the line is negative. And just as proved above, it can be easily shown that the negative echélon of tension cracks and the positive echélon of compression cracks are inevitably accompanied by the negative shear along the line of fracture. *Thus the law on the sense of echélon formation formerly raised*⁶⁾ *is now affirmed.*

When the break occurs parraliel to OY or OX then no echélon occurs but a continuous crack or parallel irregular cracks. Which of tension or compression cracks will appear in an actual case depends only on the property of the material concerned. When the material is weaker against the tesile stress than against the compressive or shearing stress then the tension cracks are prodused. When, however, the material is weaker against the shearing stress than against the tensile stress then the compression echélon is favourably formed, because in nearly all materials shearing fracture is produced by the compression. In some cases both the tension and compression cracks can be produced simultaneously. In such cases they form a zig-zag crack along the zone of the maximum stress. A tension crack has naturally opening while a compression crack is closed and shows evidence of slip such as dislocation of the two sides of the crack. Hence by a close examination of the crack, we can determine the sense of stress applied on the material as already pointed out by the present authors from the practical point of view.

---

6) S. Fujiwhara, *Gerlands Beitr.*, **16** (1927), 1–14.

5. 駒ヶ嶽火山の地形變動

陸地測量部　熱海景良
地震研究所　岸上冬彦

（昭和五年十月二十一日發表――昭和六年一月二十日受理）

緒言

昭和四年六月十七日、北海道駒ヶ嶽の大噴火によつて噴火口並びに其周圍に著しい地形の變化が生じたので、陸地測量部に於ては其の測量標卽三角點と水準點の損害の實狀と地形の變動の概要を知つて、復舊測量を行ふ時の資料を得るため、本年七月十八日から約二十日間此の火山の調査を行ふことになり、熱海が此作業に從事することを命ぜられた。先づ火山四周の調査を終へて、火口附近の調査に從事するの時機に、恰も地震研究所の用務を帶びて駒ヶ嶽に出張した岸上と會したので、共に八月一日から同月四日迄、四日間に亙つて、火口附近の調査を實施した。天候は霧多く、眞に視通を許した晴天は八月四日の一日に過ぎなかつたが、此間實施をした作業は、豫め七月下旬火山の北麓に準備して置いた三角測量に引續いて、火口附近の三角測量を行ひ、同時に地形測板測量、寫眞撮影及一般の地形偵察等を最も迅速な方法を以て實施したので、短時日の爲めに作業の不完全、觀察の不行屆は免れない。

1. 噴火口の三角測量

楕圓形火口の輪廓の一部をなして居る砂原岳と隅田盛には噴火前陸地測量部の三角點が存在して居たが、爆發の結果砂原岳の方は轉落したらしく其の姿を見せず、隅田盛の方は噴出物の爲め地表下十數米に埋沒して終つた。駒ヶ嶽の最高峰 1140 米の獨立標高點は、爆發後何等變化がないとの報告が多いが、其峰を見るに鋸齒狀の尖峰は甚しく尖銳度を増して一部は缺壞して散飛した樣子があるので、現在の最高峰が果して舊來の獨立標高點であるかどうか疑問の餘地がある。結局噴火口附近の測量をするとして基準點を此等に求めることが出來ない狀況にあつた。勿論此等が現存して居たとしても、爆發の影響によつて三角點の位置は十

分移動したであらうから、夫れ等を不動として出發することは出來ないとしても、他の不動三角點から三角測量に依つて其の點の移動を算出することが出來たとすれば、精密測量上は勿論地形變動の機構を知るに於て其利益は頗る大であつたらうと考へる。

短時日に火口附近の測量をするため、可成近く完全に殘つて居る三角點を探し、之れを砂原岳の北麓に見出した。「茅野」「紋兵衛砂原」の二個の三等三角點がこれである。火口の東西南の三方面の山腹は岩屑や浮石流のために大部の三角點が埋沒されてゐるために基準點を得ることが出來なかつた。此の二個の三角點は殆ど損害を蒙つて居ない外觀を有するので、其の距離、方位、標高を噴火前後に變化しないものと假定し、舊來の測量成果の値を其儘採用し此二點から砂原岳上に二點を撰んで測角し、紋兵衛砂原三角點を坐標原點として計算により砂原岳上の二點の坐標を計算し、此の二點を以て火口附近迅速測量の據點とした。此の二點の距離は約450米であつて、此の兩點からは噴火口の外輪をなせる駒ヶ嶽尖峰、隅田盛竝各鞍部を視る事が出來る上に、火口內の重要點は殆ど瞰制することを得る。此れだけの測量は豫め七月下旬に約三日を要して終了してあつた。

火口內の三角測量は砂原岳上此二點を基線として第一圖に示す樣に三角網を擴張し、測角をしたのである。卽砂原岳三角點位置と同峰の西端點なる基線西端點に器械を置いて基礎三角點茅野、紋兵衛砂原を測角した上、同點の外、隅田盛(三角點名馬脊越)と火口附近の最高所に一點併せて四點を以て測站として主要の三角網を編成し、此等の諸點から噴火口附近の重要點に目標を置き、或は天然目標を撰んで三角測量を行つたのである、其の測量網の編成は第一圖に示してある。

測量は用ひた器械は「カール、ツアイス」會社製の轉鏡經緯儀第二號型で水平垂直測角十二秒讀のもの、精度は測量部三等三角測量用の「カールバンベルヒ」經緯儀には及ばないが、測角數を增加すれば略此れに近い精度を得るものであることが過去の試驗に依つて確められてゐるものであつた。三角點の標識としては新設點は大抵白赤の大きな測量用旗を竿桿に卷いて樹てゝ鐵線で四方に張り其旗の頂部の高さを地面から一米位にして其上に之れを撤去しないでも器械が設置し得る樣にして、觀測點と目標點との一致に依つて偏心計算の面倒を避けるやうにした。

○三角測量の結果

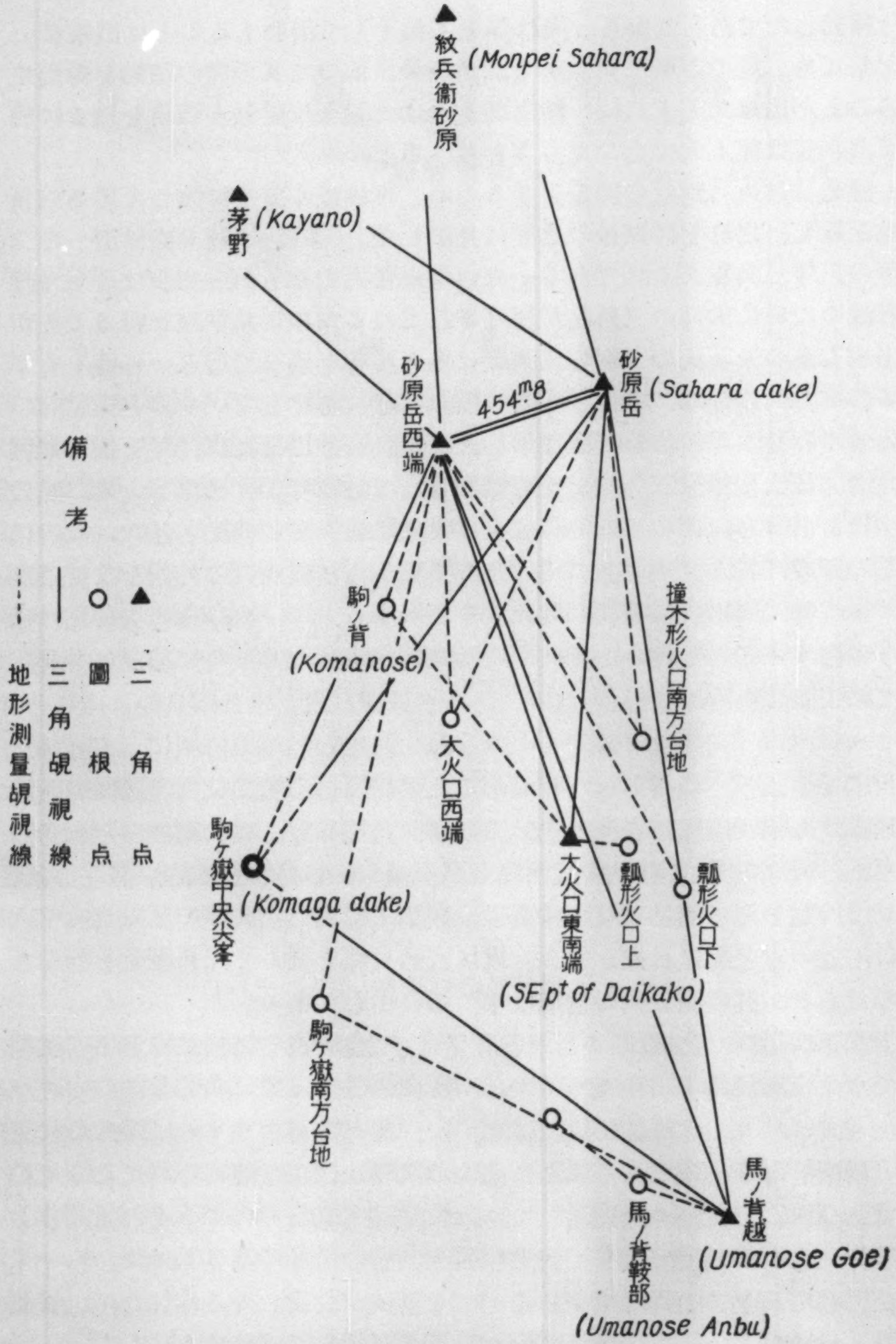
紋兵衛砂原
(Monpei Sahara)
茅野
(Kayano)
砂原岳西端
454.m8
砂原岳
(Sahara dake)
備考
▲ 三角点
○ 圖根点
三角覘視線
地形測量覘視線
駒ノ背
(Komanose)
大火口西端
撞木形火口南方台地
駒ヶ獄中央尖峯
(Komaga dake)
大火口東南端
瓢形火口上
瓢形火口下
(SE pt of Daikako)
駒ヶ獄南方台地
馬ノ背越
(Umanose Goe)
馬ノ背鞍部
(Umanose Anbu)

第一圖 駒ヶ嶽噴火口附近三角網及圖根網圖

Fig. 1. Triangulation and maping net about crater of Komagatake Volcano.

砂原岳、隅田盛は舊三角點の存在したと想像せられる其の峰の最高部を新設點とした。又駒ヶ嶽の尖峰は現在の中央最高峰を測定し、尚點檢のために其南北にある尖峰をも測定をした、此等の結果其の舊點との位置の比較をすると次の表に示す通りであつて、勿論之れは舊三角點とは連絡のないものであるから土地の移動を示すものではないが、これに依つて色々の事實が推定されることは後に述べることによつて了解されるであらう。

新舊位置の比較表

三角點名 ＼ 坐標		坐標			標高	
	標	X	Y	比較	H	比較
砂原岳 (Saharadake)	新 New	m −324101·97	m −129308·20	m $X+3{\cdot}37$ $Y+1{\cdot}42$	m 1114·60	「−」 m 0·51
	舊 Old	−324105·34	−129309·62		1115·11	
馬脊越 (Umanosegoe)	新 New	−326231·94	−129036·70	$X+0{\cdot}56$ $Y-32{\cdot}94$	893·10	「＋」 m 12·65
	舊 Old	−326232·50	−129003·76		880·45	
駒ヶ嶽 (Komagatake)	新 New	−325301·57	−130272·74	$X+52{\cdot}23$ $Y-2{\cdot}88$	1135·52	「−」 m 4·58
	舊 Old	−325249·34	−130269·86		1140·10	

備考　舊新坐標 XY は測量部に於て設定した北部原點 $\left(\begin{array}{l}B=45^\circ\,00'\,00''\\L=142^\circ\,15'\,17,''\,2085\end{array}\right)$ に基く平面直角坐標で X は子線に沿うて居る

Comparison of new and old geographical positions of triangulation points.

2. 地形測量

上述の三角點を基準點として三角測量の施行と同時に測板上に二萬分の一の地形測圖を行つた。其圖根網の編成は第一圖の中に點線を以て示した通りである。之れに使用した器械類は前掲經緯儀によつて一部の水平角の測定と大部の圖根點の垂直角の測定を行ひ、「ベネニブ」と稱する輕易な小型經緯儀を以て地物の間接高程測量を行ひ,鋼鐵二十米卷尺、短距離用レンジフアインダーを用ひて直接の距離測量、道線距離測量を行ひ、最も主なものとして測斜儀と測板とを以て上の各種の方法で得た結

果を圖根の根幹としつゝ細部の測圖を行つた。測圖の主眼點は地貌の變化に置き、地物例へば龜裂の如きは或部分省略されてゐる。

○地形測量の結果

地形測量の爲めに設けた圖根點の中で稍精度の良好なものを次に掲げる。これ等は三角點の標高と共に噴火口の附近の地形、標高の變化が生ずる場合の參考となるであらう。

點名	標高 m
砂原岳西端點	1122·34
大火口東南端	941·04
同　西端	930·45
撞木形火口南方臺地（ナマコ山）	939·42
瓢形火口上	935·21
同　下	896·78
馬の脊鞍部	880·07

地形測量の迅速な方法としては、豫め從來噴火前の地形圖を所要の梯尺に伸寫して其上に修正測圖をなすのにあるが、此の場合に準備の餘裕が得られなかつたので現地で新しく測圖したものを歸京後伸寫した舊地形圖と比較して變動を研究した。第二圖は噴火前の五萬分の一駒ヶ嶽地形圖を二萬分の一に伸寫したもので、第三圖は現地測量の圖、第四圖は舊地形圖の伸寫要圖の上に新しい噴火口の輪廓を記入して位置の變化を示したものである。

3. 寫眞測量

普通の寫眞機械を用ひて寫眞測量の初歩原理を應用し噴火口附近一部の製圖を行ふことが出來た。第五圖は砂原岳西端と砂原岳三角點の二點から噴火口の内大火口附近を異つた二個のカビネ型寫眞機を以て撮影し此れを處理して交會法により一萬分の一の梯尺を以て表はした結果であつて、測量部の鈴木猶吉測量師の手になつたものである。水平曲線の精度には餘り信用は出來ないが火口の輪廓や龜裂の狀態は甚だ良く表現されてゐる。同一の器械を用ひて少許の距離を隔てゝ同一の目標に對しコンバーゼントするやうに撮影することが出來たならばステレォの現示に依つて水平曲線の描畫が更に良好に容易になされたであらう。

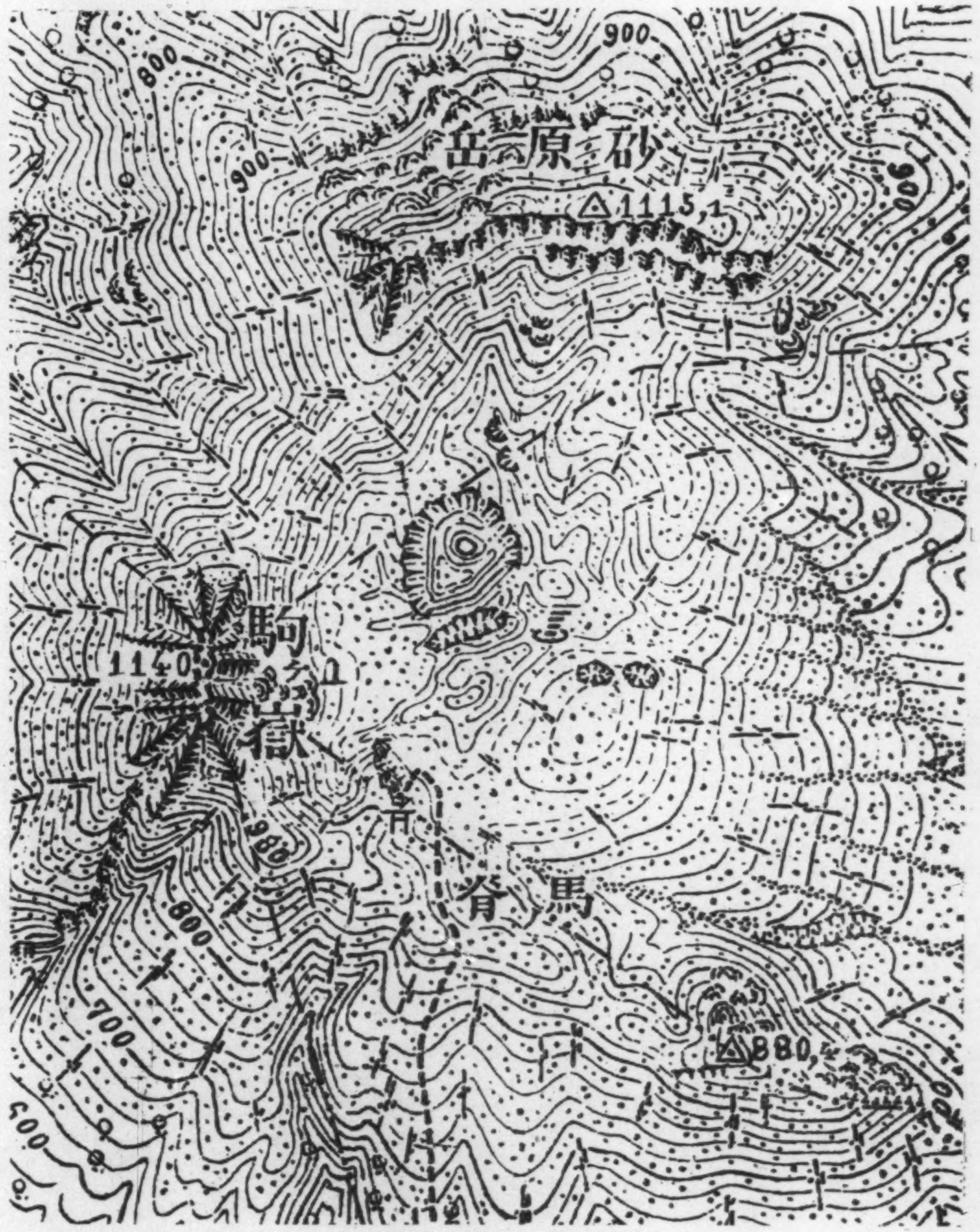
砂原岳
1115,1
駒ケ嶽
1140
馬脊
880
900
800
700
600

第二圖　噴火前ニ於ケル駒ケ嶽頂上部ノ地形

Fig. 2. Topography of the Volcano Komagatake before the recent eruption.

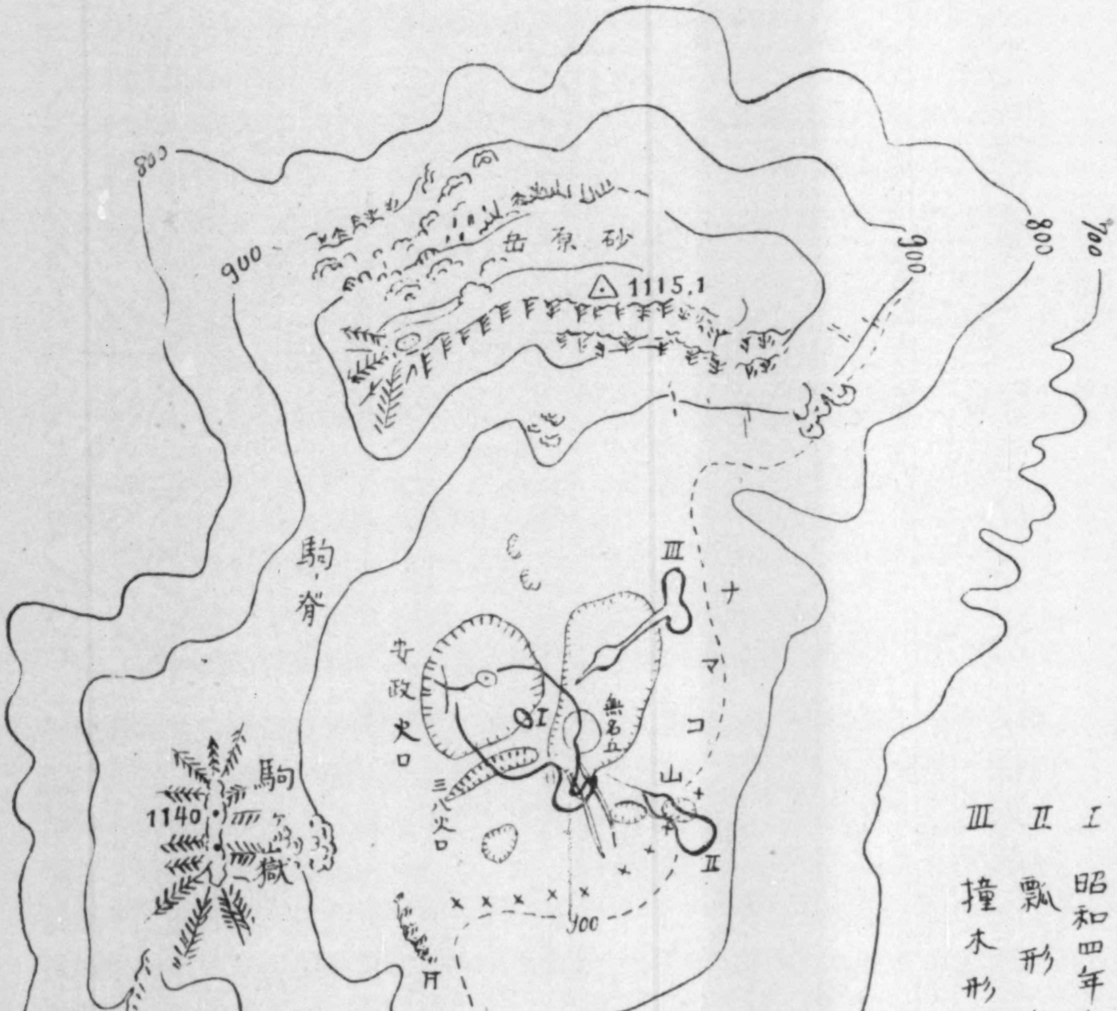
砂原岳
1115.1
駒ヶ嶽
1140
駒脊
馬脊
安政火口
三八火口
無名丘
ナマコ山
隅田盛
880.4
900
800
700
I
II
III
I 昭和四年大火口
II 瓢形火口
III 撞木形火口
前噴火口
× 噴氣孔

第四圖 駒ケ嶽噴火口變化圖

Fig. 4. Sketch-map showing the change of the craters of Komagatake.

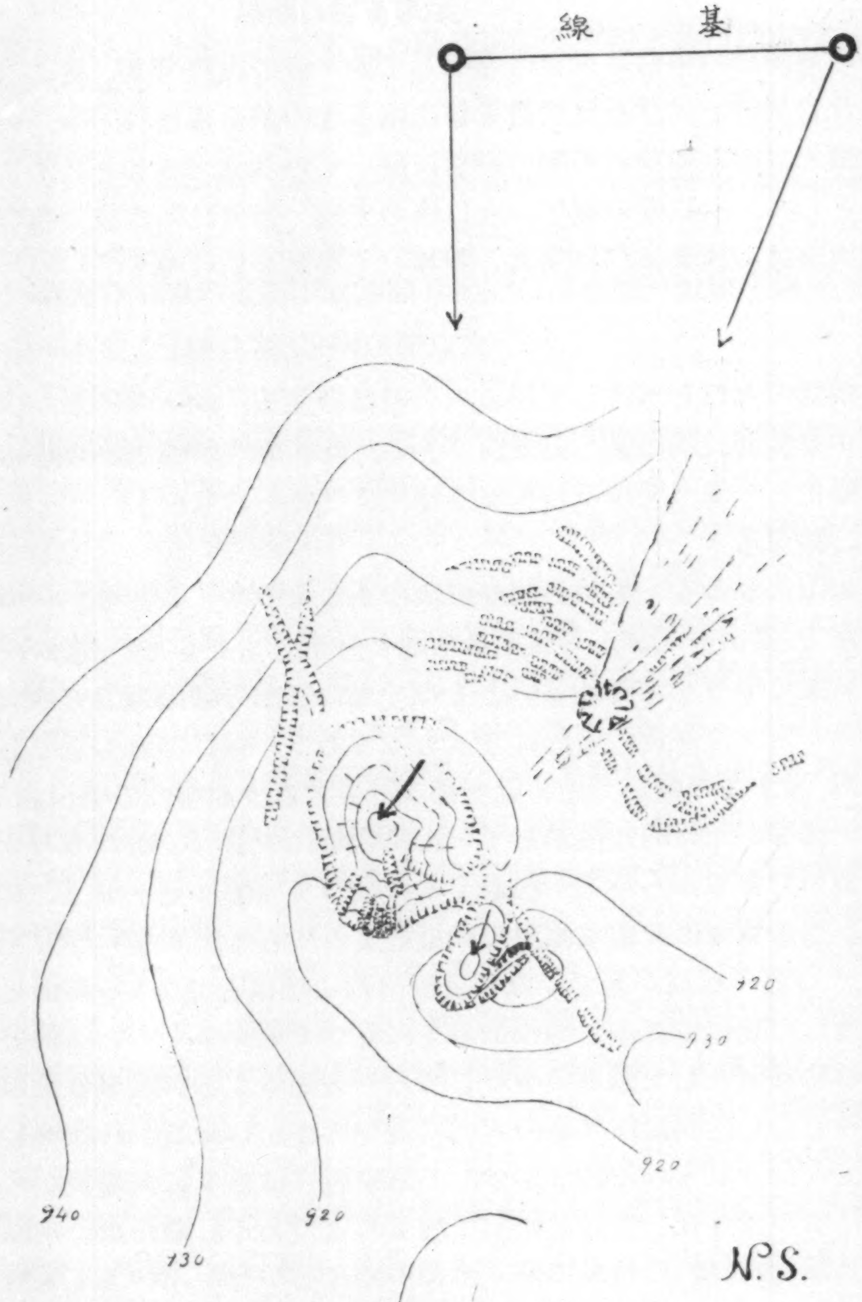
基線
940
930
920
920
930
920
N.S.

1 : 10000

第五圖 駒ヶ嶽大火口附近寫眞測量圖

Fig. 5. Map by the photographic surveys of the great craters of Komagatake.

4. 地形變動の狀態

地形變動の中には火口に遠隔して駒ヶ嶽の山腹·裾野、更に遠方迄落下した岩屑併びに浮石流の被覆等に依るものがあるけれども、此處には單に噴火口附近の狹い範圍の變動に就いてのみ述べることにする。其の順序として、火口壁の變化、火口底の充塡、新火口の生成、龜裂について逐次前述の成果並びに寫眞と對照して要點をあげやう。

（イ） 火口壁の變化（第六圖）

楕圓形火口を形成して居る火口壁は砂原岳、駒ノ脊鞍部、駒ヶ嶽鞍部、馬ノ脊鞍部、隅田盛、海鼠山である。此れ等は新噴出物の堆積による地の變化と一部の缺壞の外大なる變化は認められない。

○砂原岳

此山に登ること前後三回登攀口の主なものは二つある。一つは砂原岳の東方、圓山の北側から砂原岳東端を目指して登るもの、他の一つは目下の狀況で辛うじて許さるべきもので火口底から砂原岳中央の內斜面を三角點の西又は東側の鞍部に登るものである。何れの道も急であるが後者は四、五十度の傾斜で崖に近い樣な部分もあり崩壞性の噴出岩屑、浮石流の一部等が一時的に固結して居て降雨毎に少量づゝ崩れ落ちる如き自然傾斜面であるから時期が經過するに從つて登攀は益々困難となるであらう。然し舊時は此處は絕望で到底近よることも出來ない部分であつたのが、火口底の標高が高まつたのと噴出物の堆積とでかゝる斜面となつたのは著しい變化である。砂原岳の上に登つて氣がつくことは頂上が楕圓火口の北側壁として弧形の辛うじて人一人通ることが出來る位の甚だ狹い脊稜をなし內斜面は其峯の大部に亙つて多かれ少なかれ缺壞を生じ或は懸崖の削り取られた部分が多く、且中腹には處々に大龜裂が火口緣の方向に沿つて存在し白煙を出して居ることである。砂原岳三角點は新設の三角點（假目標）の位置の南3米餘の處にあつたが此れは丁度缺壞轉落した內斜面の部分に相當するから缺壞の幅は此の部位に於て2米餘はあつたかと思はれる。峯の高さの變化は少しく低められたに過ぎないけれども現在の地表は新噴出物に依つて若干被覆せられて居るから內斜面の破壞と共に處に依り一、二米は低められたと見ることが出來よう。浮石流の現出狀態に就いては後に論ずることゝして內斜面の缺壞の理由を想像するに內斜面近くで行はれたと考へられる小規模の爆發、浮石流の

衝突跳躍、山體の震動、噴出及落下岩屑の衝突等を擧げることが出來ようが其内最初のものは後に述べる駒ヶ嶽の缺壞の原因と共に理由の主なるものと考へられる。

○駒ノ脊鞍部

從來の高さに比して大差はないが數米を增加したのは押出澤浮石流の通路になつたこと其他の原因に依つて、若干の削り取りを受けて低められし以上に噴火口一帶の標高の增加卽ち岩屑及浮石流の被覆に依つて高められたのであらう。

○駒ヶ嶽尖峯(第八圖)

内外側は噴出物に被はれた爲め中腹迄は自然傾斜面を示し麓にあつた色々の奇巖等は其姿を沒して居るが頂は益々鋸齒狀に尖銳の度を加へた。現在其峯に三個の著明な尖峯がある。就中中央のものは一番高い。そして諸報告を綜合して見るに獨立標高點には何等異狀なしとの事であるが、測量部地形圖の獨立標高點は此の中央尖峯と北側の尖峯との間にあつて今は噴火の爲め轉落して姿を沒して終つたと言ふ結果を測量に依つて得たのである。卽ち現在の中央最高峯の北52米の處に以前には高さはこれよりも4·60糎高き最高峯が存在したと見做し得るのである。此事は噴火前に實物を見てゐない我等には不思議に思はれることであるが然し測量の結果が之れを示すのみならず又新舊の駒ヶ嶽の寫眞を對照して見れば成程と首肯出來る。そして此の峯の缺壞崩落は砂原岳内斜面の夫れと同じく震動のみならず内斜面附近に行はれた一部の爆裂に起因するものではあるまいか。宮部氏は地震研究所彙報第八號第二冊に於て現在駒ヶ嶽内斜面大龜裂中にある噴氣口を指摘して大火口と地中に於て連絡あるものとして居られるが、噴火の途中に於て斯かるものと同じ機構の更に大なる噴氣口が駒ヶ嶽の内斜面に開かれて尖銳の頂部を爆飛せしめたのであるまいか。兎に角駒ヶ嶽の斜面から火口底にかけて又其他附近一帶に散亂して居る熔岩破片(大なるもの中徑五、六米あり)が駒ヶ嶽尖峯の熔岩質と同じであることは注意を要する。

○馬ノ脊鞍部

此の鞍部は噴出物によつて著しく被覆せられ、舊標高825米なるに對し約50乃至60米を增加した、其の標高の增加は特に火口底の標高增加の原因に關する考察に重要な資料を提供するであらう。

○隅田盛

馬脊越三角點のある山は外觀著しく變化した、卽ち內側の安山岩懸崖が姿を沒したのみならず一般に標高を增加し頂部に於ては 13 米程度であつて現在の最高部卽ち三角測量の假目標を設けた點は舊三角點の西約 33 米に移つてゐる。この峯の移動の理由は容易に考へられることが出來る。卽ち元の三角點の東側は急な斜面である爲に噴出物が積つてもずり落され三角點の西側は緩斜面で鞍部に迄連絡して居るため此方面に堆積したものは落下が少量であつたものであらう。

○海鼠山

噴火前迄は噴火口の東壁をなした丘陵であつたが火口內の充塡のために著明であつた其形を失つて終つて現在ではこれに代はる東側の火口壁は存在しない形である、海鼠山の上に積まれた厚さは所により 60 乃至 100 米である。

（ロ） 火口底の充塡、新火口の生成

噴火前に於ける楕圓形火口底は噴火口上面に於ても駒ヶ嶽尖峯より低きこと實に約320米であつて然も此れに安政、三八其他の諸火口が不規則に配列されて低き火口底に複雜なる地貌を表はして居たのであるが、今度の噴火によつて底部全體が標高を增加し中央にフクラミを有する單純なる地形の火口底を現出した、其の最高部は大火口の東南端で目下941米、舊の値 820 米に對し 120 米の增加である。噴火前の諸火口に對する新火口の關係位置は第四圖に表はれてゐる。

○昭和四年大火口

昭和四年の爆裂口の中最大なものは其中心が安政火口の中心に較べて東南に約100米移動して恰も舊の安政火口、明治三十八年火口と海鼠山との間に陷凹して舊火口跡と目せられて居た無名丘を含む凹地の三者に跨る位置に生成せられてゐる、昭和四年の大火口とこれを呼ぶことにする其形狀は主要部は大體圓形であるが東側に連接して二個の裂罅狀火口があり、主要部と此れとの連接點には擂鉢形の爆裂小火口がある。主要部の中徑約 230 米深さ 50 米餘、底は北西から南東に長さ約 30 米に亘り其間に小高い部分がある、此の底に向つて北側の斜面は急峻であるが南側斜面はこれに比してはるかに緩であつて要心をすれば底近く迄降りることが出來るであらう。此大火口底の小高い部分の南側を除く他の周圍部分からは雨の後、曇天には白色の蒸氣を音なく噴出してゐるが八月

四日の如き快晴の日等は漸次發煙が終熄して底の狀態が良く見えた（第九圖參照）。

主要部の東側の裂罅狀火口は略南北の方向に走り長さ約120米幅30乃至40米深さ20米乃至25米である、兩壁は急で噴出物を露出し兩側壁からは白色の瓦斯を混じた蒸氣を出してゐるが活動は全くないと云つても良い。此裂罅に隣つて更に幅20米弱、深さ10米强の短小な裂罅が東北の方向に延びて居る。此二つの裂罅の間の障壁は幅も狹く側面も急で良く其の形が保たれて居ることに驚くのである。最後の裂罅の東側壁の上が駒ヶ嶽噴火口內の最高部である。

○瓢形火口（第十一圖）

大火口の主要部の東端、裂罅狀火口の起部から北西から南東方向に走つて居る斷片的の龜裂を傳つて行くと其の盡きる所に恰も龜裂線の方向に軸を有し噴火口を東方鹿部村方向に曝露して二つの火口を併べた瓢形の噴火口がある。全長は約200米で二個の小火口の狹窄部は幅30米深さ20米餘、大火口に近い方の火口は稍小であるが、反對側の瓢の底の膨らみに當る火口は中徑約80米內外、內斜面の傾斜30乃至40度、深さ30米であつて其の形狀は誠に美しい摺鉢形である。瓢形火口は遠方鹿部や其西方の山々から遠望すると雨の後等殊に白煙を發散してゐるのが良く見得るが其發煙の主な位置は瓢底の火口にあらずしてむしろ大火口に近い方の火口であるらしく見える、と云ふのは八月四日晴天の夕方近く此火口を調査した所、東の火口の底に水溜りがあるのを發見した（圖にも表はれてゐる）。又煙の出るのを隅田盛から見たときの觀察では一見全體から出て居る樣に見えるが良く注意すると大火口に近い方から出て風のために東の火口に煙がなびいて恰も兩火口から出る樣に見えるらしいことが知れた。要するに此火口は昨年噴火の後には盛に噴煙をあげてゐたが現在では左程活動が旺盛とは云はれない。むしろ次の撞木形火口の方が活動力があると見られた。一般に大火口に就いて述べた樣にどの火口でも四日間の調査中は各火口共殆ど活動らしい活動をしてゐないで其の一部の噴氣口から白色の蒸汽を發散して居たが、これとても四日の如く晴天且氣壓の高い日には全く熄むで陽炎の如き熱氣が其代りに昇つて居る程度に過ぎなかつた。若し噴氣口の位置を明瞭に知るためには雨後の霧なきときが觀察最も容易であらう。

○繭形火口

海鼠山頂上部に該當する所に略繭形をした二火口が相接して略南北方向に並んでゐる。其の中央部から大火口に向つて大龜裂が數條になつて走つてゐて大火口に少しく寄つた中央部に小さい火口がある。此等の集つた形が撞木に似た所から商工省赤木氏は撞木形火口と名付けて居られる。繭形火口の北部のものは中徑約 40 米、深 20 米弱、南部のものは中徑約 50 米、深約 25 米で四日の夕方に近く觀察した所に依ると南部火口の底部に近い岩塊の間から白煙を出し又底から約 5 米の高さの西側壁には眞赤な熔岩が見えた、此時他の大火口や瓢形火口には此等の現象は現れて居なかつた。

此れ等のことから此の繭形火口は他の火口よりも現在のところ活動力が最も旺盛であるかの如くに思はれた。繭形火口の西側の中央部から大火口の方向には非常に大きな龜裂否龜裂と云ふよりは炸裂と云ふ方が適當であらうが、これが數條交錯しながら走つて居て略中央から大火口寄りの處に極めて小さい噴火口がある。底も淺く活動も止むで居るが此等炸裂の數條は噴氣が可なり旺盛である。

（ハ） 龜裂（第五圖及第六圖）

火口附近の龜裂は大火口や其他の火口を中心にして大體放射狀及圓周狀に配列して居るが、更にこれを詳細に調べるならば注意すべきことが多い。先づ第一に大火口と他の二火口とが大なる龜裂を以て連結せられて居ることで、これは大火口や中心から他の二火口に向つて正しく放射狀である。そして瓢形火口の方は此の放射線上に其二火口の軸線が一致して居るに比し、繭形火口では放射線に對して二火口の軸線は直交に近い。瓢形火口への龜裂は階段狀に並んで其の大さも極めて小さく活動は殆どしないが繭形火口の方の龜裂は前述の樣に大龜裂で小火口さへ含み現在尙活氣を呈してゐる。其噴氣狀態は雨後特に烈しく一般に噴火口の發煙に先だつて發煙し、又晴天となつて火口の噴煙止むや之れに遲れて發煙を熄むる樣である。此等の龜裂への接近は目下と雖も危險である。圓周狀の龜裂を見るに其數は頗る多い。特に大火口の北東の部分繭形火口と大火口との間のものは相當に活動を續けて居て、龜裂の集團の有樣を第五圖の寫眞測圖に依つて見ると大火口に近い部分は其の圓周狀の方向に從つて居るが、放射狀の龜裂を橫切つて東側の方に來ると曲り方を反對に變へて繭形火口の南側の周圍に沿つて生じて居る。此は此火口が活動

の旺盛なることに關連してゐるのであらう。

龜裂の成因は噴出物の冷却に伴ひ地形に從つて發生し又助長せられるだけでなく、火口の活働に支配せられるものであらうし、又龜裂の生ずる部分を見るのに他の部位に比較して噴氣活動の特に旺盛なることからして龜裂附近の噴出物中に龜裂を生ぜしむるに足るエネルギーを存し、これが地形や他の火口の活動力等と關連して發生せしめるものではあるまいか。此作用が旺盛なときには龜裂はむしろ炸裂となり、更に進んでは爆裂口の發生に迄及ぶ。繭形火口から大火口への炸裂や龜裂は斯くして出來たのではあるまいか。而て此のエネルギーを供給する源は次に述べる噴火口相互の關係に依つて説明せられるであらう。

龜裂發生に對する以上の考へ方は駒ヶ嶽東斜面や砂原岳南側斜面、馬ノ背鞍部、隅田盛頂上部又浮石流の中の方々に存在する大龜裂や小噴火口を見ても確からしく思はれる。

5. 噴火口の生成に就いて

現在の火口底の標高の増加が100米以上にも及んでゐることに就いては前述の通りであるが、斯かる大なる標高の變化を説明するのに噴出物の堆積に依るは困難であるとして舊火口底の地盤上昇説がある。卽ち噴火に際して舊火口底は現在の位置近く迄上昇し新噴出物は此れを薄く被覆するに過ぎずとするものである。然し此説は馬ノ脊の鞍部が標高60米を増加したことも同樣の作用を以て説明しなければならない。噴火口の作られた大體の範圍は三火口を含む程度の面積であつて、これに比して馬ノ脊の鞍部は甚しく遠方にあるのみならず、火口と鞍部との中間では昔の形狀に殆ど相似たる谷地が入込んで居る。隆起作用が此谷地に何等の變化を與へることなしに馬ノ背に迄及ぶことは一寸考へられない。又此の考へ方は餘りに噴出物の量殊に浮石流の量を輕く見過ぎて居ると思はれる。馬ノ背鞍部堆積の厚さは矢張現在の變化量だけあつたとして可いと考へる。果して然らば火口附近に於て100米内外の堆積あるは別に不思議でもなく當然とすべきであらう。舊火口底の隆起等が極めて少しく起つた時には地表の一部は爆發して火道が空中へ衝き抜けたのであるまいか。筆者等は噴火口底は噴出岩屑及浮石流の充塡に依つて標高を高く増加したと云ふ見地の下に噴火口生成の觀察をして見たい。

噴火口三個を見て感ずることは此れが爆裂口として甚だ形が整つて居

ることである。大火口の主要部は擂鉢形、其隣りの二つの裂罅狀火口は誠に狹い壁で兩者が境されて居りながら其缺壞は少ない。又瓢形火口と云ひ繭形火口と云ひ二個の噴火口が並んで美しく形を保つてゐる。此等は何としても初期爆發當時の姿ではない。岩屑が多量に拋出し浮石流が噴出したら此等は當然形が崩れて終ふべきであらう。此等の火口の生成は寧ろ最も旺盛に爆發が續けられた六月十七日午後六時後の所產ではあるまいか。卽ち浮石流發生の後ではなからうか。浮石流及岩屑の堆積に依つて夫れ迄に出來てゐた(勿論中心は大火口附近ではあらうが)火口を埋沒することに依つて更に地下の壓力を高め其の極遂に地表近くに三個の火口相連絡しつゝ爆發を行つたのではあるまいか。火口相互は龜裂を以て結ばれ此の龜裂に活動力の現存すること等、此の考へ方を助ける樣に思はれる。此の考へ方は餘りに想像に過ぎる樣ではあるが少くも現存の火口が噴火當初の所產では無いと云ふことは考へられる。

6. **浮石流に就いて**(第十一圖、第十二圖)

浮石流の發生の狀態に就いても色々說がある。問題は砂原岳と駒ヶ嶽を越えて其一部が流下したことに起因して拋出說、溢出說、其他諸說に分れるのであるが之れを餘りに巧妙な機構を假設して說明せずとも平凡に單純な考へ方で說明が可能に思はれる。卽ち浮石流の實體は其の流下の狀態からして半固半液の狀態であることは確實に認められ其の溫度も數百度に保たれたことも事實であらう。然らば噴火口を出て來た際には地下の壓力と熱とで沸騰狀態を以て火口內一體に充滿し、時の火口內の地形の狀態に從つて或時はクルミ坂に、或時は押出澤に、或時は馬ノ背を越えて大沼方面に流下の緖を見出したであらう。卽ち溢出したであらう。然し其の火口內に充滿する中にも下からの大噴火の壓力は半固半液の浮石塊を空中へ噴上げ恰も沸騰せる熱湯の如きものもあつたのであらう。砂原岳や駒ヶ嶽を越えた浮石流は此の類ではなかつたらうか。以上の樣に考へれば拋出說と溢出說とは同時に起つたとして予盾は來さないと思ふ。

浮石流の山腹を流下する速さは每秒數米に達し物凄い勢であつたとの事であるが高溫の熱灰が液體の如き作用をなして浮石を浮かせて走つたと認められて居る。七月三十一日大雨の日クルミ坂に於て地隙の中に雨を避けてゐたところ異樣な音に驚いて飛出すと上流から物凄い岩石流が

襲來して來て一瞬の間に憩つてゐた地隙を山の如き岩石流で埋め地隙の幅も深さも見る見る中に倍加されて流れ行くのに驚いた。其進む有様は丁度現在浮石流の跡を尋ねたときに見た姿其儘でたつた(第十二圖)。これから想像しても浮石流は多分水の働きをする熱灰流に乘つて走つたものと考へられる。筆者の見た岩石流の速度は途中の障碍物があるに從つて一進一止であつて速い時は秒速 5 米にも達した(クルミ坂は緩斜面である)。そして障碍物に當ると岩石流は流下を休止する。泥水が其の下を通つて岩塊を浮かすときには流れ出す岩塊は非常な大きな體積となつて方々に流れ山を生成する。水の上に浮いた大きな山が抵抗に打勝つて物凄い音を發して一擧に流下する有様は實に恐しい様である。之を見て多分かゝる有様で浮石流も流れたことであらうと想像して見た。

---

5. *Topographical Changes of the Volcano Komagatake, Hokkaidô, by its Eruption in 1929.*

By Keiryô ATUMI and Fuyuhiko KISHINOUYE.

The Volcano Komagatake, Hokkaidô, erupted on June 17, 1929, and topographical changes generated at that time have been reported by many observers. The writers surveyed the changes for several days in July and August, 1930. The results they obtained are shown on accompanying maps, and some descriptions are given below.

1. Trigonometrical Survey. In the neighbourhood of the volcano, many trigonometrical points are buried or removed by volcanic ejecta or pumice-flows. Only two points of the third order, *Kayano* and *Monbe-sahara* which lie at the northern foot of the volcano have not been changed. Then, assuming that the two points had not changed their positions, a base-line about 450 m. long was derived by trigonometrical survey on Saharadake, a ridge on the north-side of the caldera. The instrument used for the survey was Zeiss' repeating theodolite No. II, and numerical results obtained are shown in Table.

2. Photographical Survey. From the both ends of the base-line on Saharadake, the craters were photographed with two cameras of different types, their focal lengths are 17 cm. and 18 cm. respectively. And map shown in fig. 5 was drawn from photographs taken by authors. On the map, the shape of craters and fissures are shown distinctly, but contour lines are drawn not well in comparison with that of topographical survey.

3. Topographical Changes near the Caldera. Topographical changes of some places will be stated below in detail.

Saharadake. The inner wall of Saharadake which had been a vertical cliff before the eruption, was destroyed at the eastern half. The trigonometrical point temporarily settled by the writers was 3 m. north of the old one as shown in the Table, and from this result the destroyed breadth of the wall seems to be at least 2 m. The height is supposed to be lowered by more than 1 m., though the summit is now covered with ashes and pumice-stones.

The peak of Komagatake. The peak is covered with volcanic ejecta on both in and outsides of the caldera, and it is said that the shape of the peak has not been changed. But after the survey it was observed that, 52 m. north of the present highest point, there had been a point 4.60 m. higher than it. The change is also recognized by comparing both photographs of the peak taken before and after the eruption.

Umanose. This saddle point was thickly covered with ejecta, and its heights is increased about 50 m.

Sumidamori. The inside cliff of andesite which was seen before the eruption is covered with ejecta, and now it can not be recognised. The present highest point is 33 m. west of the trigonometrical point settled before, and is 13 m. higher than it.

Namakoyama. Namakoyama was a hill consisting eastern wall of the caldera before the eruption, but now it is entirely covered with ejecta from 60 m. to 100 m. thick, and there is no trace of it.

Craters. On the inside of the caldera ejecta accumulated as deep as 100 m., and the maximum 120 m. The positions of the craters were changed as shown in fig. 4.

The largest crater is round in shape, and at its eastern side two crevice-shaped craters are connected. The radius of the round crater is about 230 m., and its depth from its margin is about 50 m. At its bottom there is a narrow and low hill 30 m. long in NW-SE direction, and usually white smoke is rising noiselessly around the hill except its southern side.

About 500 m. SE far from the round crater, there is a crater, which has issued much smoke with roaring sounds from the southeastern crater-bottom in the summer of 1929. But on August 4. 1930, there was seen only a small pool of water. (Hisagogata Crater in Fig. 10.)

At the northern part of the caldera, there are two craters connected each other in NS direction. In the evening of August 4. 1930, the writers saw red heated lava in a crevice of western wall of the crater, and this crater seemed most active at that time.

Fissures. Many radial and concentric fissures are seen around the craters, and most of them are blowing smokes since the eruption. When the writers were near the caldera, a group of fissures running northeast from the main round crater were most violently issuing volcanic steam. Observing activities of these fissures, the writers thought that the origin of the fissures of this volcano will depend upon its activities, and when it becomes more vigorous, fissures may grow into a crater.

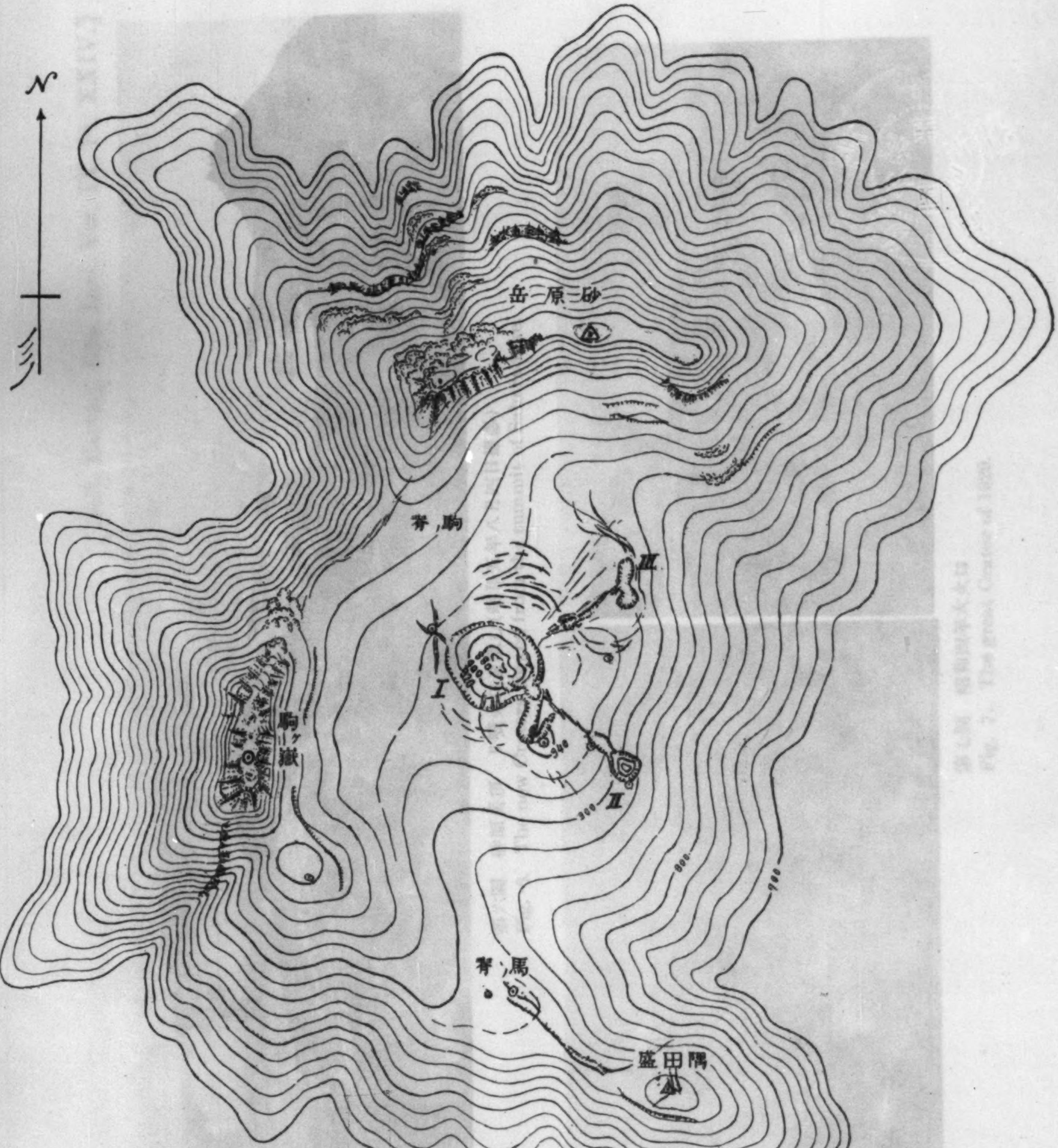
N
砂原岳
駒脊
駒ケ嶽
I
II
III
馬脊
隅田盛

（震研彙報、第九號、圖版、熱海、岸上）

第三圖　爆發後ノ駒ケ嶽噴火口ノ圖本圖中龜裂ヘ一部ノミヲ表ハセリ

Fig. 3. Map showing the top of Komagatake Volcano after the eruption.

$\frac{1}{20000}$

I 昭和四年大火口

II 瓢形火口

III 撞木形火口

3. Topographical Changes near the Caldera. Topographical changes of some places will be stated below in detail.

Sabaedake. The inner wall of Sabaedake which had been a vertical cliff before the eruption, was destroyed at the eastern half. The [illegible] point [illegible] by the writers was 8 m. north of the old one as shown in the [illegible] and [illegible] the destroyed [illegible] of the [illegible] supposed to be [illegible] by [illegible] the [illegible] covered with ashes and pumice.

The peak of [illegible]. [illegible] with volcanic ejecta on [illegible] the shape of the peak [illegible] changed. [illegible] it was observed that, 60 m. [illegible] of the [illegible] there had been a point [illegible] m. higher than [illegible]. The change [illegible] by comparing both photographs of the peak taken before [illegible] the eruption.

[illegible]. This saddle point was [illegible] with ejecta, and its height is increased about 30 m.

[illegible]. The inside cliff of [illegible] before the eruption is covered with ejecta, and now it can not be recognized. The present highest point is [illegible] m. west of the trigonometrical point [illegible] before, and is 13 m. higher than it.

[illegible]. [illegible] a hill consisting [illegible] wall of the caldera before the eruption, but now it is entirely covered with ejecta from 60 m. to 100 m. thick, [illegible] of it.

Craters. On the [illegible] at 100 m. and the maximum [illegible]. The positions of the [illegible] were changed as shown in [illegible].

The largest crater is [illegible] shape, and at its eastern [illegible] crevice-shaped [illegible] connected. The radius of the [illegible] is about [illegible] m. and its depth from its margin is about 50 m. [illegible] there is a narrow and low hill 20 m. long in NW-SE direction and [illegible] white smoke is rising noiselessly around the hill except its [illegible] side.

About [illegible] m. SE far from the round crater, there is a crater which has issued [illegible] smoke with roaring sounds from the [illegible] crater-bottom in the summer of 1929. But on August [illegible], there was seen only a small pool of water. ([illegible] Crater in Fig. [illegible].)

At the northern part of the caldera, there are two craters connected each other in NE direction. At the evening of August [illegible], the writers saw red-heated lava in a crevice of western wall of the crater and this crater seemed most active at that time.

Fissures. Many radial and concentric fissures are seen around the craters and most of them are blowing smokes since the eruption. When the writers were near the caldera, a group of fissures running northeast from the main round crater were most violently issuing volcanic steam. Observing [illegible] of these fissures, the writers thought that the origin of the fissures of this volcano will depend upon its activities, and when it becomes more vigorous, fissures may grow into a crater.

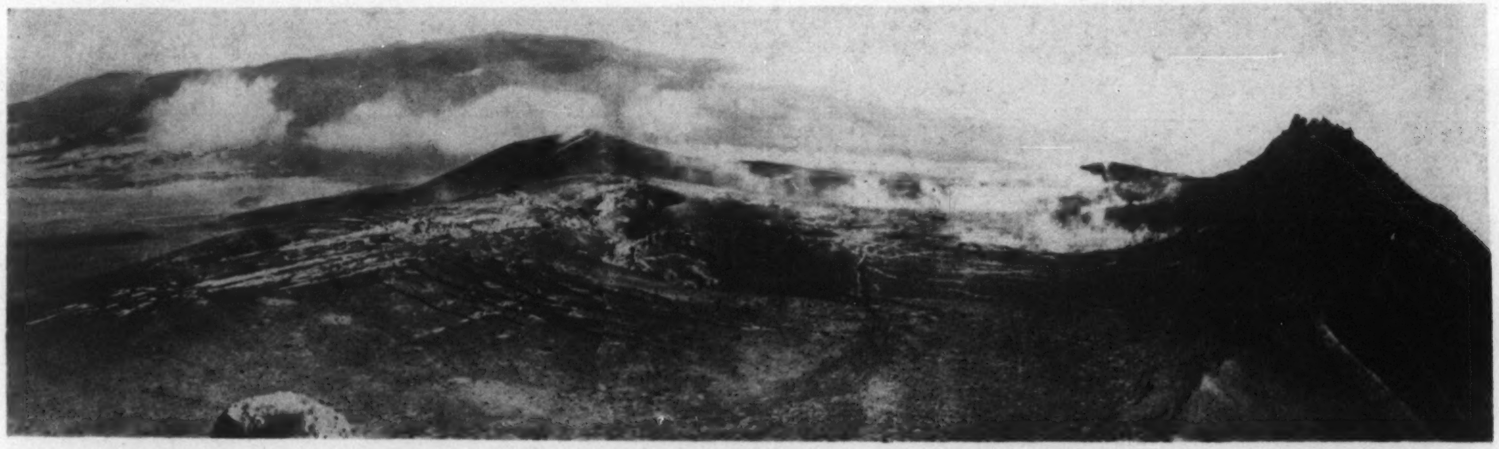

第六圖　砂原岳頂　り噴火口を望む（昭和五年八月四日撮影）
Fig. 6. The new Craters viewed from the summit of Saharadake.

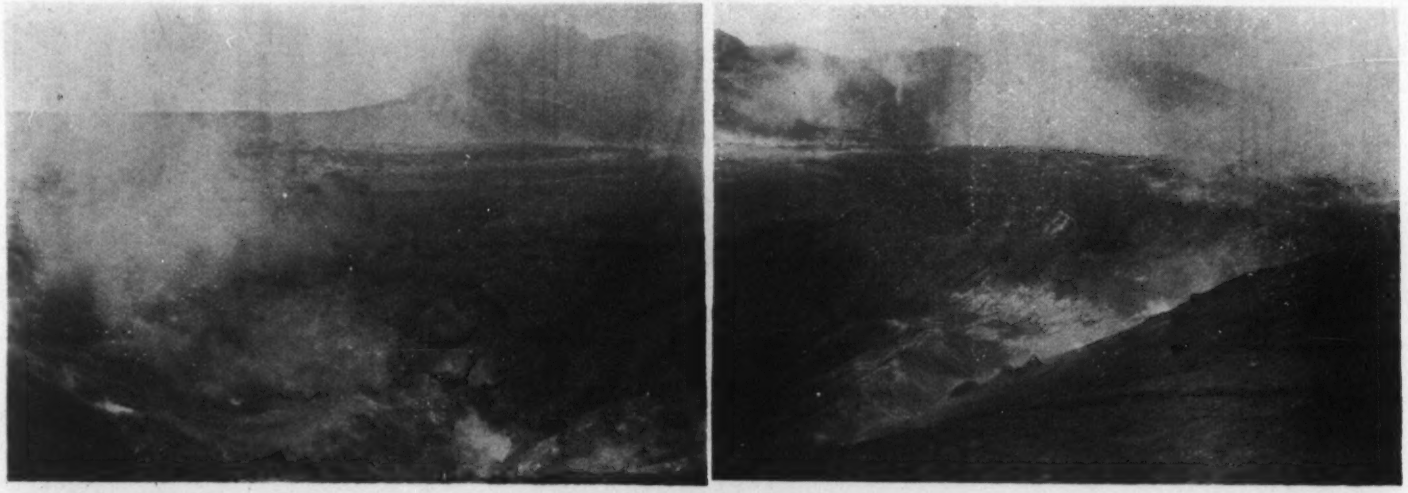

第七圖　昭和四年大火口
Fig. 7. The great Crater of 1929.

（震研彙報、第九號、圖版、熱海、岸上）

(震研彙報、第九號、圖版、熱海、岸上)

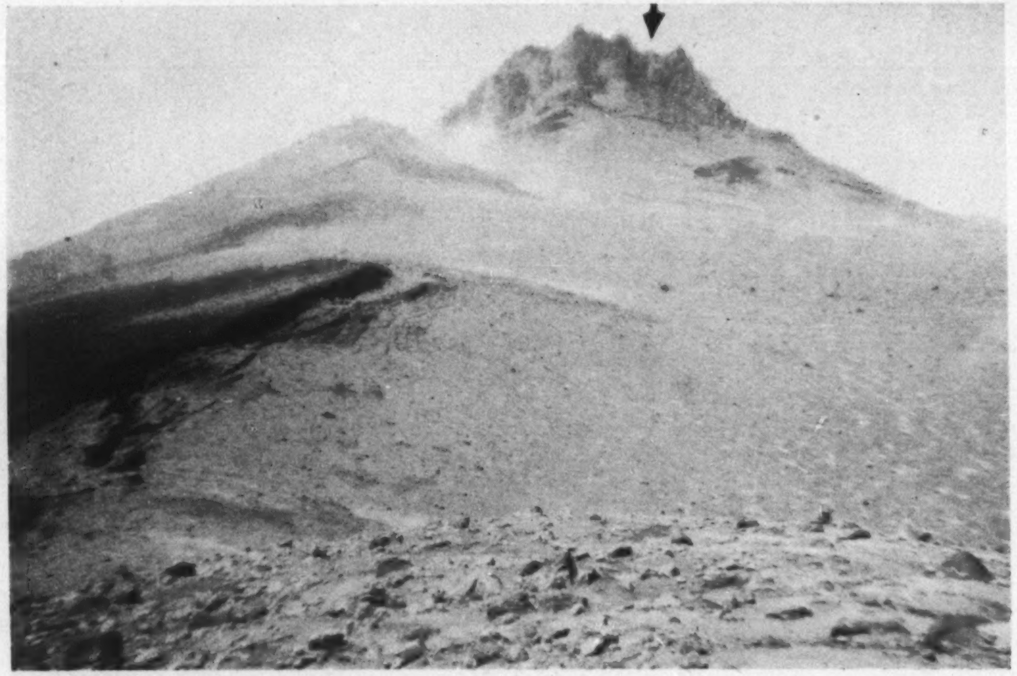

第八圖　隅田盛より駒ヶ嶽を望む(↓印は缺壞せる獨立標高點の位置を示す)

Fig. 8. Komagatake. (Arrow shows the position of the lost peak.)

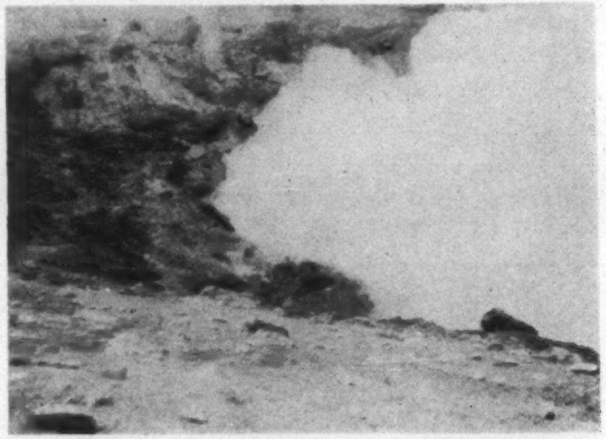

第九圖(其一)　昭和四年大火口底部(噴煙旺盛の時)
(昭和五年八月一日正午頃、曇天)

Fig. 9 (1). The bottom of the Great Carter of 1929.
(About noon, Aug. 1, 1930, cloudy.)

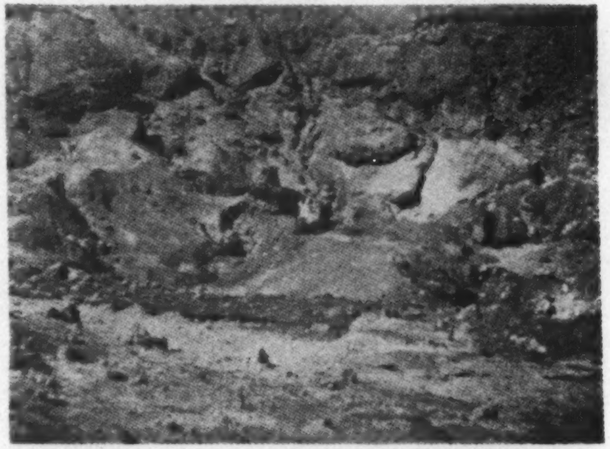

第九圖(其二)　昭和四年大火口底部(噴煙なき時)
(昭和五年八月四日午後四時頃、快晴)

Fig. 9 (2). The bottom of the Great Crater of 1929.
(About 4:00 p.m. Aug. 4, 1930, fine.)

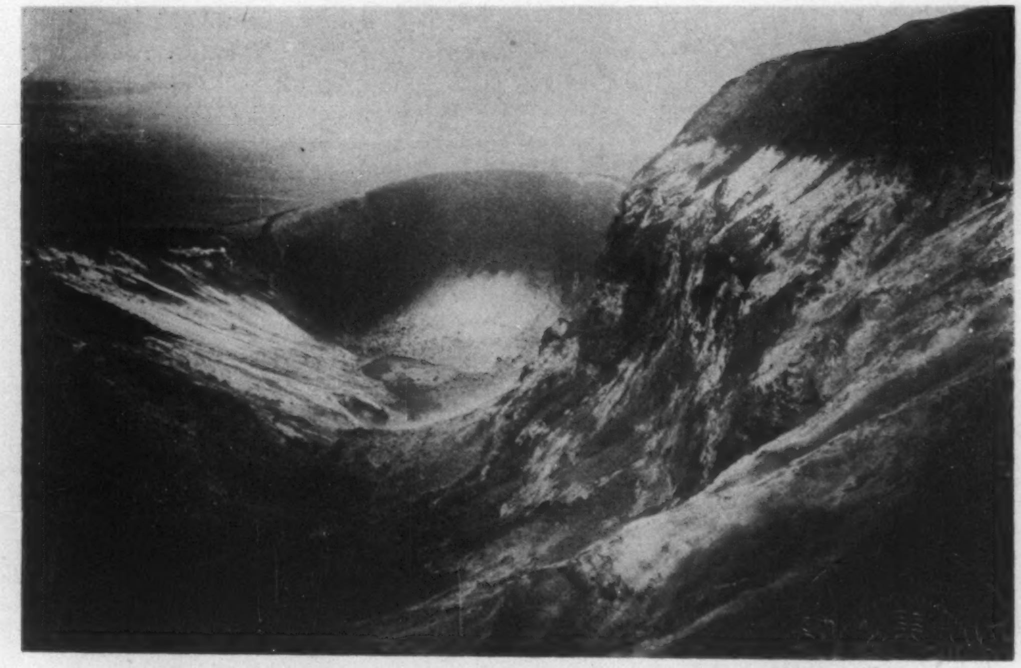

第十圖　瓢形火口を其の口頭部より望む（八月四日午後六時）
Fig. 10. Hisagogata Crater. (6:00 p.m. Aug. 4, 1930.)

（震研彙報、第九號、圖版、熱海、岸上）

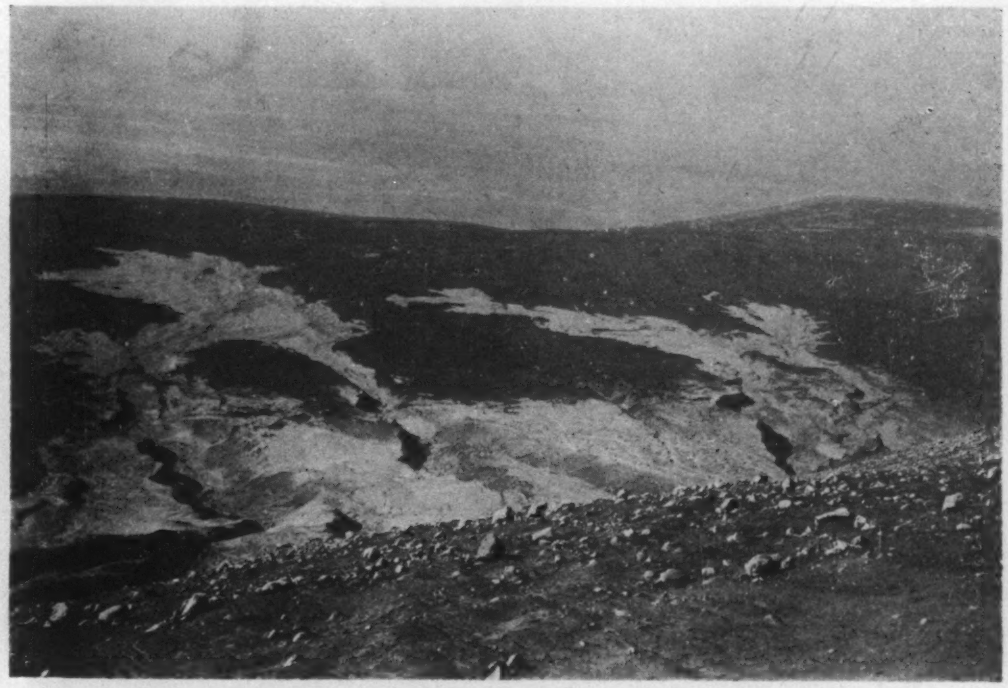

第十一圖　砂原岳より砂原方面に流れたる浮石流を望む
Fig. 11. The Pumice-flows on the north side of Saharadake.

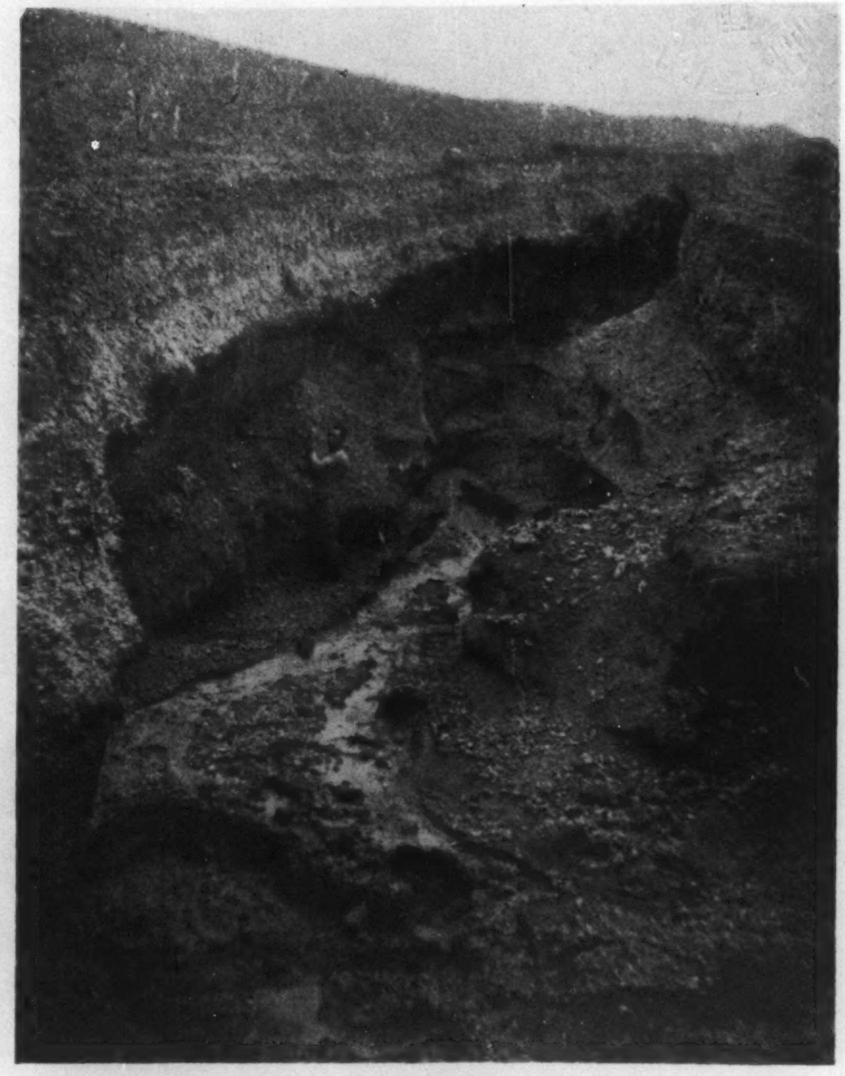

第十二圖　水流によつて生じた溝梁(昭和五年八月一日留場の北方にて)
Fig. 12. Gully formed by rain water on the pumicc-flow.

Pumice-flow. To this day pumice-stones are occationally carried down the mountain-slope by rain. A photograph of a gully made by rain on the pumice-flow is shown in fig. 12.

Many authors disscussed on the origin of pumice-flows. Some of them think that pumice-stones were thrown from the crater over the summits of Saharadake and Komagatake, and fell down the sides of the volcano after much piled on the outside of the caldera. The writers think that the above two origins would be existed at the time of the eruption.

---

6. *Petrographic Notes on the Sedimentary Rocks of Southwest Sagami Province. (Part I.)*

By Hiromichi TSUYA,

Earthquake Research Institute.

(Read Jan. 20, 1931.—Received Jan. 20, 1931.)

Introduction.

The Cainozoic formations so widely distributed in the Kwantô district include various sedimentary rocks formed by accumulations of detritus and of fragmental material of volcanic origin. They exhibit great variety of composition and lithic characters, and are divided stratigraphically into various groups. Although no less important; contrasted with the igneous rocks, they have not received the attention they deserve from petrologists. Microscopic study of these sedimentary rocks may reveal many subdivisions, each exhibiting characteristics due to the physiographic conditions under which they were deposited, as well as to the sources whence they were derived. By recognizing these two conditions it should be possible to determine what physiographic changes, if any, have occurred, and what kind of volcanic products were ejected in the Kwantô district in geologically recent time, a determination important for detecting recent crustal movements and volcanic activities that have played their part in the district.

From the petrogenic standpoint a detailed determination of the rock-minerals composing the volcanic sediments is particularly desirable, in that it may furnish a clue to the genetic relation of these sediments to the materials that went to form the volcanoes, and from which material these sediments are derived.

This paper is a preliminary contribution to the petrography of the sedimentary rocks of the Kwantô district, particularly those of the southwestern part of Sagami Province.

Petrography of the Sedimentary Rocks of Enosima, Sagami.

Enosima is an island, about 0·25 sq. km. in area, lying near Kamakura on the northern shore of Sagami Bay, and well-known for its beautiful scenery. Geologically, the island is of Cainozoic formation which, according to the late Y. Ozawa, may be divided as follows:

Pliocene....Miura series
  Lower group: Massive tufaceous sandstone and tuff-breccia.
  Upper group: Tufaceous sandstone and agglomerate-tuff.
Pleistocene....Loam bed with gravel bed at its base.
Holocene....Valley gravels.

The more important petrographical types in these formations will be described below.

1. *Tufaceous sandstone and tuff-breccia.* (The lower group of the Miura series of Enosima.)

Except in the northeastern part of the island, these rocks are well exposed on the sea-cliffs. The bedding plane strikes N.W.–S.E. and dips 30–40° N.E. The bedding is generally due to alternation of coarse and fine material. The lower beds exposed in the western part of the island are characterised by distinct stratification of alternated layers of tufaceous sandstone and tuff-breccia; while in the eastern part of the island, where the higher beds are unstratified, the tufaceous sandstone presents a massive appearance.

Megascopic Characters.- The tufaceous sandstone is generally light gray. The sand-grains in it are subangular, but often well rounded, and show considerable variation in color, and include a variety of isolated crystals and rock-fragments. There is more or less of a gradation between the fine and coarse tufaceous sandstone and between the coarse tufaceous sandstone and tuff-breccia, some few fragments in which exceed 1 cm. in diameter. The tuff-breccia contains lenticular rock-fragments of various texture—porphyritic, scoriaceous, pumiceous, and glassy—cemented with sandy material.

Microscopic Characters.—Microscopically, the tufaceous sandstone is characterized by its numerous angular constituents (Fig. 1), of which the following are most abundant:—

(1) Numerous fractured and euhedral plagioclase-crystals. They are not zonally built, being identified as andesine $Ab_{60}An_{40}$—$Ab_{65}An_{35}$, with $n_{1D} = 1{\cdot}547$ (3)–$1{\cdot}544$ (7).
(2) Isolated crystals of augite ($n_{1D} = 1{\cdot}698$) and hypersthene.
(3) Rock-fragments of pyroxene-andesite exhibiting various crystallinity and textures.
(4) Glass-pieces.

In addition to the foregoing, the tufaceous sandstone contains a few fragments of a granitic rock and a silicified rock, besides orthoclase, quartz, and hornblende.

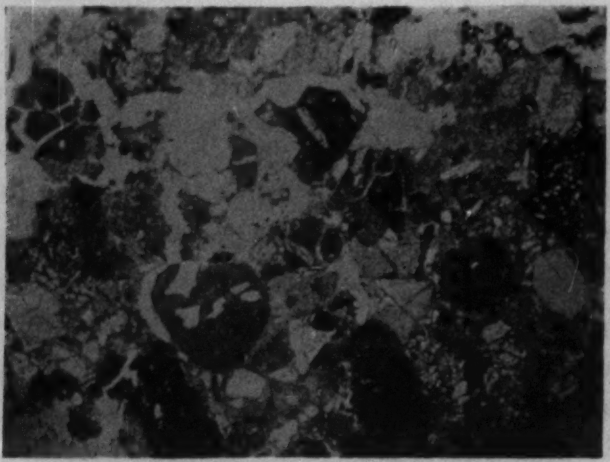

Fig. 1. Microphotograph of tufaceous sandstone. ×10.

Except in its coarser grain and brecciated structure, the tuff-breccia (Fig. 2) is practically similar, microscopically, to the tufaceous sandstone already described.

Fig. 2. Microphotograph of tuff-breccia. ×10.

2. *Agglomerate-tuff.* (The upper group of the Miura series of Enosima.)

This rests unconformably on the massive tufaceous sandstone described in the preceeding section. At the northeastern coast of the island, the unconformable relation of the two groups—lower and upper—is clearly apparent on the wave-cut platform that rises about one meter above sea level, and which was pushed up at the time of the great Kwantô earthquake in 1923. Here there is a decided difference in the physical characters of the two groups; the lower is massive, while the basal breccia of the upper group contains angular fragments of the tufaceous sandstone of the lower group, being overlain by well-bedded agglomerate-tuff. The bedding plane of the upper group strikes N. 60°W. on the western, and E.-W. on the eastern part of the northeastern section of the island. Passing close to the boundary of the two groups, is a distinct strike-fault. Near the boundary, the lower beds of the upper group dip steeply, 70–80° to the north; while higher up the dip becomes gentler, it being 20–30° about 100 m. from the base.

Megascopic Characters.—The tuff is dark gray. It consists of angular rock-fragments which rarely exceed 3 cm. in diameter, besides well-defined crystals of plagioclase (5–1 mm. in diameter) and pyroxene (1 mm. in length), together with a fine tufaceous matrix. Occasionally, the agglomerate-tuff grades into fine tuff showing distinct bedding.

Microscopic Characters.—Microscopically, the agglomerate-tuff contains numerous angular rock-fragments, of which the following are most abundant:—

(1) Andesite scoriae.
(2) Fragments of basaltic rock.
(3) Fragments of propylitic rock.

A few fragments of quartz-gabbro are also seen.

In thin section the andesite scoria (Fig. 3) shows a few phenocrysts

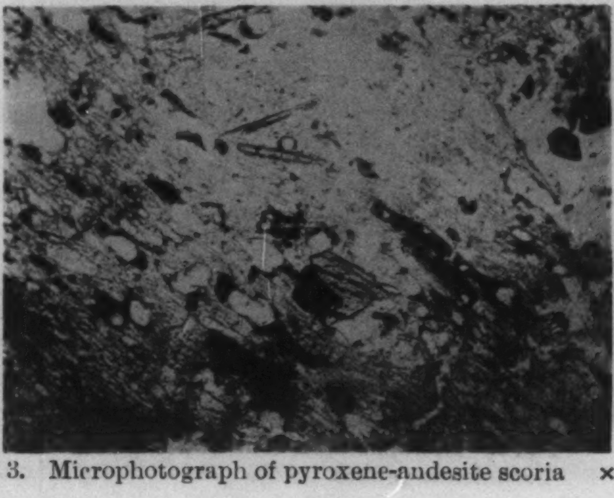

Fig. 3. Microphotograph of pyroxene-andesite scoria ×40.

of plagioclase, augite, and hypersthene. The plagioclase-phenocryst is 0·5 mm. by 0·1 mm. Faint zoning of less and more calcic plagioclases is exhibited. $n_{1D} = 1{\cdot}565$. Accordingly, the plagioclase-phenocryst was identified as labradorite $Ab_{30}An_{70}$. The augite-phenocryst, $n_{1D} = 1{\cdot}694$, and hypersthene are about 0·2 mm. in length. The groundmass is brown glass with $n_D = 1{\cdot}542$.

The basaltic rock has numerous phenocrysts of plagioclase and hypersthene. The plagioclase-phenocryst varies in diameter from 7 mm. to 0·5 mm. It is euhedral, and twinned according to the Carlsbad and albite laws. Zoning of less and more calcic plagioclases is absent. The plagioclase-phenocryst was identified as anorthite Ab_5An_{95}, with $n_{1D} = 1{\cdot}578(4)$, $n_{2D} = 1{\cdot}585(6)$. The hypersthene is euhedral, and about 1 mm. in length, but it is completely altered to bastite. The groundmass is hypocrystalline, consisting of lath-shaped plagioclase-microlites, minute grains of augite, and isometric magnetite with more or less of a glass base.

The propylitic rock contains numerous spots of chlorite, up to 2 mm. in diameter. The plagioclase-phenocrysts have been replaced by chlorite and quartz. The groundmass is of pilotaxitic texture, consisting of plagioclase-prismoids (0·1 mm. in length), pyroxene, and iron ores. The plagioclase in the groundmass was identified as andesine $Ab_{70}An_{30}$, with $n_{1D} = 1{\cdot}546$. The pyroxene in the groundmass has altered to chlorite. A small amount of quartz, probably secondary, is observed in the groundmass.

The quartz-gabbro (Fig. 4) consists of plagioclase, augite, hornblende, biotite, and quartz. The accessory minerals are apatite and magnetite.

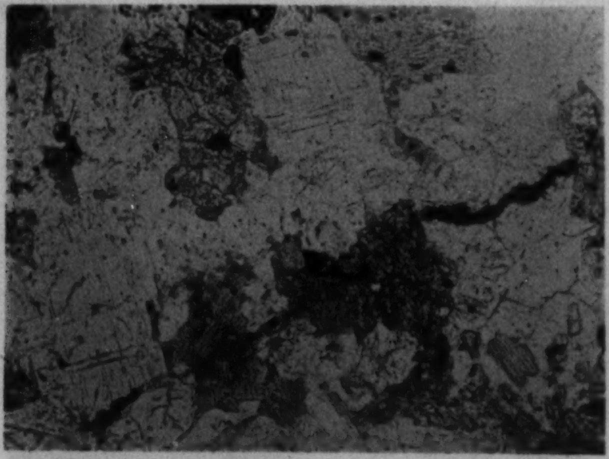

Fig. 4. Microphotograph of biotite-quartz-hornblende-gabbro. ×30.

Plagioclase is subhedral and twinned according to the Carlsbad, albite, and (rarely) pericline laws. Very faint zoning of less and more calcic plagioclases is exhibited. The plagioclase was identified as bytownite $Ab_{15}An_{85}$, with $n_{1D} = 1{\cdot}573$. Biotite occurs in small quantity, filling the interstices of other minerals.

The agglomerate-tuff contains numerous isolated crystals, of which anorthite-crystals (Ab_5An_{95}) are most abundant. These isolated crystals are probably derived from the andesite or the basaltic rock, abundant fragments of which are found in the agglomerate-tuff.

3. Loam. (The Pleistocene deposit of Enosima.)

Resting on the erosion-surface of the foundation built up of rocks of the Miura series is the so-called loam bed, the total thickness of which is about 20 m.

Megascopic Characters.—Megascopically, the loam is light brown and somewhat tufaceous. In fineness of grain, the materials composing the loam are intermediate between sand and clay.

Upon close examination however the size of the grains in the loam, barring those in the basal gravels, is found to increase in coarseness with height; the individual grains being more angular in the coarser than in the finer part of the loam.

The loam is composed of a brown earthy substance, with isolated crystals of plagioclase, pyroxene, and magnetite. The brown earthy substance forms the bulk of the loam. The plagioclase-crystal is glassy, 0·3–1·0 mm. in diameter, and can be detected with the naked eye. There are also numerous plagioclase-crystals, 0·5 mm. in diameter, in the upper horizon of the loam bed, which are largely decomposed. Pyroxene-crystals occur as stout prismoids, 1 mm. in length, or as irregular fragments, 0·1–0·5 mm. in diameter. Magnetite occurs as round grains, 0·1 mm. in diameter, and is strongly magnetic.

Microscopic Characters.—Under the microscope, most of the grains composing the loam are subangular; but many are well-rounded, particularly those in the lower horizon of the loam bed. (Fig. 5) Minerals seen under the microscope are plagioclase, augite, hypersthene, and magnetite. There are two kinds of plagioclase. One was identified as anorthite Ab_5An_{95}, with $n_{1D} = 1{\cdot}576\,(8)$, $n_{2D} = 1{\cdot}584\,(6)$, and the other as labradorite $Ab_{30}An_{70}$, with $n_{1D} = 1{\cdot}565\,(5)$, $n_{2D} = 1{\cdot}569\,(4)$. The anorthite-crystals, which are quite fresh, are plentiful in the lower horizon of the loam bed but scarce in the upper, where labradorite-crystals predominate, and which, megascopically, are found to have decomposed to a white earthy substance.

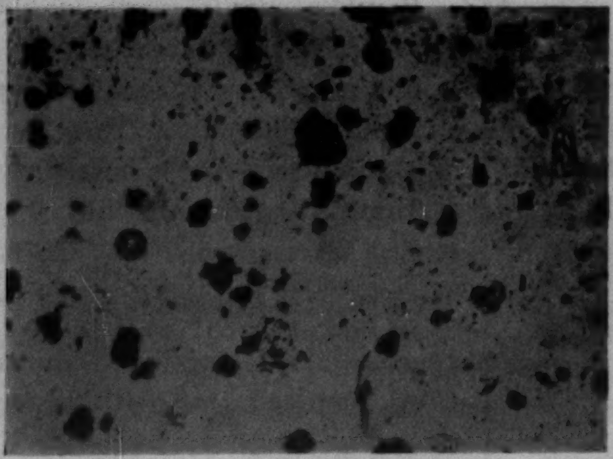

Fig. 5. Microphotograph of loam. × 40.

The augite-crystals are found throughout the loam bed. In the lower horizon they are microscopic while in the upper they occur as stout prismoids, about 1 mm. in length, and can be seen with the naked eye. The megascopic crystal of augite is: $n_{1D} = 1{\cdot}692$. The hypersthene-crystals are fewer.

The brown earthy substance of which the greater part of the loam is composed, is microscopically yellowish and flocculent. It becomes reddish by ignition, the reddening being probably due to oxidation of the iron ore contained in it. It does not effervesce in dilute hydrochloric acid, showing absence of carbonate of lime. Rarely, it contains small fragments of colorless or colored minerals, though none of them have been optically determined. Its refractive index is not uniform, varying from $n_D = 1{\cdot}535$ to $n_D = 1{\cdot}545$. In the refractive index the brown earthy substance resembles volcanic glass, but it does not show the vitroclastic structure characteristic of vitric tuff which consists practically of volcanic glass shards.

Summary.

In the foregoing pages are given the petrographic descriptions of the rocks of Enosima.

The rocks of the Miura series, which form the foundation of Enosima, are largely composed of fragmental volcanic material, probably laid down under water, including agglomerate-tuff, tuff-breccia, and tufaceous sandstone, together with lithic tuff and crystal tuff. This volcanic material might have been derived from near-by sources as products of volcanic eruptions. The tufaceous sandstone may be detrital tuff, but its ingredients occur as angular fragments, showing that at no stage of their history have they been subjected to considerable attrition.

The two groups of the Miura series possess the respective petrographic characteristics of their ingredients. The lower group is represented by tuff-breccia and tufaceous sandstone, together with lithic tuff and crystal tuff. These rocks consist principally of isolated crystals of plagioclase and pyroxene, and rock-fragments of pyroxene-andesite containing plagioclase-phenocrysts, which have been identified as andesine $Ab_{60}An_{40}$—$Ab_{65}An_{35}$. The upper group is represented by agglomerate-tuff, consisting principally of isolated crystals of anorthite and pyroxene, and rock-fragments of pyroxene-andesite scoriae containing plagioclase-phenocrysts identified as labradorite $Ab_{30}An_{70}$. It is also remarkable that the rocks of the lower group contain subordinately not only isolated crystals of orthoclase, quartz, and hornblende, but also fragments of a granitic rock and a silicified rock; while the rocks of the upper contain fragments of basic rocks such as hypersthene-basalt, quartz-gabbro, and propylite.

The difference in the ingredients of the lower and upper groups of the Miura series would seem to indicate changes in the physiographic condition of the terranes in which the Miura series is developed, and also changes in volcanic activities by which the pyroclastic rocks in the two groups of the Miura series were produced. This petrographic boundary corresponds with the structural unconformity between the lower and upper groups. But it may be said that, on the whole, the volcanic activity in the period of the Miura series is represented by extrusion of pyroxene-andesite.

The loam of Enosima consists of a brown earthy substance and isolated crystals of anorthite, augite, hypersthene, and magnetite. The brown earthy substance occurs as irregular particles containing minute grains of iron ore, but none are found to have been derived from pieces of volcanic glass. It is considered to be fine-grained material—clay—derived from the disintegration of pre-existing rocks.

Under the microscope, most of the crystal grains in the loam are subangular, but many, particularly those in the lower horizon of the loam bed, are distinctly rounded, indicating considerable attrition.

In considering the origin of the loam bed the prime requisite is to know whether aeolian or aqueous agencies have acted in the deposition of the loam. Although the grains composing the loam of Enosima are much rounded, there is no definite evidence on the condition of their deposition, whether aeolian or aqueous. Further study is needed to decide this question.

---

6. 相模國南西地域の堆積岩の岩石學的研究(一)

地震研究所 津屋弘逵

關東地方には所謂關東ローム層を初めとして種々の新生代地層が廣く分布してゐる。かゝる地層を構成する岩石の岩石學的研究が關東地方全般に亙つて系統的に行はれると、その岩石の本源が推定され、最近地質時代に於ける關東地方の地理的輪廻が明かにされるのみならず、かゝる地層に多量に含まれてゐる火山噴出物と隣接地方に現存する火山の岩石或は火成岩體との成因的關係の有無が確められる。尙、岩石學的方法によつてこの地方の地層の對比が可能である。

昭和五年十一月二十六日の伊豆地震の震域地方特に箱根、熱海諸火山の地質構造と地質的位置とを明かにするにはこれらの火山の基底地層の地質を確かにしなければならぬのであるが、同地方に於ては普通の層序學的方法による地層の對比が可成り困難と考へられる。夫故に隣接する相模國南西地域の地層を構成する岩石(特にその中の火山物質)がこの地方の既知の層序に從ひ如何に變移するかを知り、それを標準として伊豆地方の地層を岩石學的方法によつて對比しやうと企てゝゐる。

かゝる目的のために先づ相模江ノ島を構成する地層の岩石を檢べた。江ノ島は所謂三浦層及び關東ローム層より成る。江ノ島の三浦層は凝灰岩、凝灰角礫岩、凝灰質砂岩より成る下部層と集塊凝灰岩より成る上部層とに不整合及び斷層によつて區分されてゐる。この兩層は岩石學的に著しい相違を示してゐる。卽、その中に含まれてゐる斜長石の成分より見て、下部層の岩石が主として中性の安山岩の碎片を材料とするに反して、上部層の岩石は主として基性の安山岩のスコリアを材料としてゐる。且、前者は往々正長石、石英、角閃石及び花崗岩、珪化岩片等を含み、後者は灰長石及び玄武岩、變朽安山岩、石英斑糲岩片等を含む。江ノ島のローム層は上述の三浦層を不整合に蔽ひ、斜長石、輝石、磁鐵鑛等の結晶と淡褐色粘土狀物質とより成る。この中、斜長石と輝石との光學性質を檢べた結果、該層の下部と上部とに於て含まれてゐる結晶の分量のみならず光學性質が一樣でないことが判明した。

江ノ島の地層を構成する物質の本源、堆積條件等を確定するには尙廣範圍に亙る岩石學的研究を俟たねばならぬ。

7.　丹後震災地一等水準測量第四回及第五回檢測成果比較

丹後震災地に於て彙報第三號に揭げたる線路の一部に沿ひ一等水準測量第五回檢測が本所の委囑により陸地測量部により行はれたり。其成果を曩に彙報第七號第三冊に記載せし第四回のものと比較し別紙要圖に圖示して參考に供す。

第四回竝に第五回檢測作業の期間は次の如し。

第四回　昭和四年八月七日より同年十月十日迄。
第五回　昭和五年七月十七日より同年九月二十一日迄。

今回の測量は帝國學士院學術研究費より經費の補助を受けて之を行へり。此機會を以て帝國學士院に對し深厚なる謝意を表す。

（昭和六年一月十日　所長）

---

7. *Comparison of the Results of the Fourth and the Fifth Precise Levellings in the Region Disturbed by the Tango Earthquake 1927.*

The precise levelling for the fifth time in the Tango district along a part of the route shown in Vol. III had been entrusted, as in previous cases, to the Land Survey Department. The result of comparison of the present data with those of the fourth levelling (see the Bulletin Vol. VII, Part 3) is summarised in the synoptic map reproduced in the accompanying plate.

The time and duration of the field work for the two levellings were as follows:—

The fourth levelling: August 7—October 10, 1929.
The fifth levelling: July 17—September 21, 1930.

(Jan. 10th., 1931. The Director.)

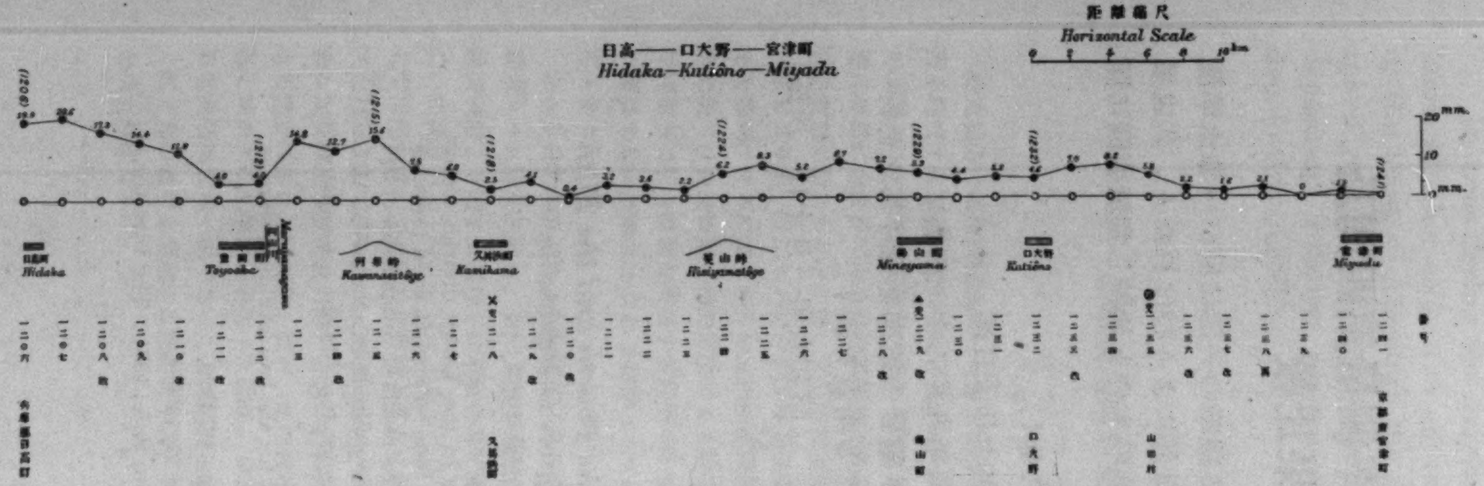

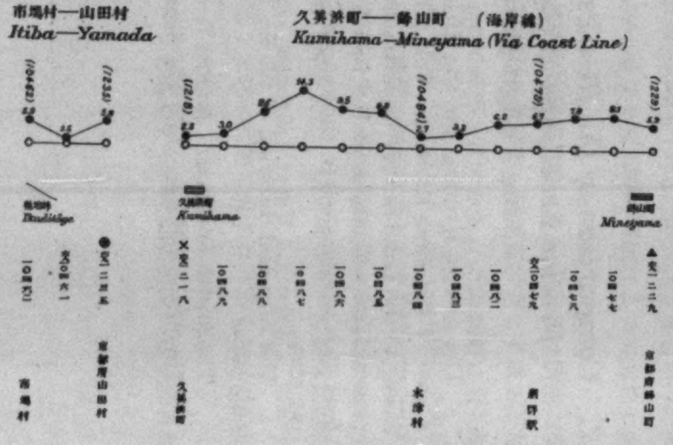

説　　明

1. 曲線ハ第五回觀測値ヲ第四回觀測値＝比較セル變動量ヲ示スモノナリ。
2. 變動量ノ基準ハ宮津町所在一等水準點第一二四一號ヲ不動ト見做シタルモノナリ。
3. —○— 昭和四年自八月七日至十月十日觀測値。
   —●— 昭和五年自七月十七日至九月二十一日觀測値。
   改、再字ヲ附シタルハ昭和二年七月改埋、再設後觀測シタルモノ。
4. ⊙▲× 等ノ記號ヲ附シタルハ分岐相互點ヲ示ス。

EXPLANATION.

1. The broken lines show the profile of the vertical displacements obtained by comparing the results of the fifth levelling with those of the fourth.
2. B.M. No. 1241 at Miyadu is assumed to be stationary in the above comparison.
3. —○—: The fourth levelling: August 7—October 10, 1929.
   —●—: The fifth levelling: July 17—September 21, 1930.
   改, 再: Bench marks replaced in July, 1927.
4. ⊙▲×: Junctions of routes.

丹後震災地一等水準測量第四回及第五回檢測成果比較要圖

Comparison of the Results of the Fourth and Fifth Precise Levellings in the Region Disturbed by the Tango Earthquake 1927.

8. 伊豆東海岸に於ける一等水準測量第一囘及第二囘檢測成果比較

曩に彙報第八號第三冊に於て豫告せし通り陸地測量部に委囑し伊豆東海岸に於ける水準線路の一部に沿て第二囘の水準測量を行へり。其成果を第一囘檢測（前掲彙報參照）のものと比較して求め得たる土地高低變化は附圖に掲ぐるが如し。

第一囘竝に第二囘檢測作業の期間は次の如し。

第一囘　昭和五年三月十五日より同年四月十四日迄。
第二囘　昭和五年十一月十日より同年十二月四日迄。

今囘の測量に於て特記すべきは作業中に昭和五年十一月二十六日の伊豆大震が發生せし事實なりとす。圖に示すが如く先原（9339號）八幡野（9341號）間の區分に於ては一方向の測量は實に地震發生の前日に於て施行せられ他方向の測量は發生直後に於て行はれたり。此兩方向の檢測の閉塞差は圖に特記して參考に資す。

此機會を以て陸地測量部員が例の如く本所の爲め此の困難なる事業を遂行せられたる事を感謝し殊に今囘は作業の央に於て大震災に遭遇されたるに關らず測量を繼續せられ以て有益なる資料を提供せられたる事に對し深厚なる敬意を表す。

（昭和六年一月十日　所長）

---

8. *Comparison of the Results of the First and Second Precise Levellings on the East Coast Route of the Province of Idu.*

As was described in our previous issue (Vol. VIII, Part 3), the second precise levelling along the east coast of the Province of Idu was carried out by the Land Survey Department at our request. The result of comparison of the present data with the previous ones (loc. cit.) is embodied in the synoptic map reproduced in the accompanying plate.

The time and duration of the field work for the two levellings were as follows:—

The first levelling: March 15—April 14, 1930.
The second levelling: November 10—December 4, 1930.

It is worthy of attention that, while the survey was being carried out, a great earthquake occurred on the northern part of the province on the 26th. of November, last. Indeed, the survey on two sections (namely, between the bench marks Nos. 9339–9341) was done in one direction on the day previous to the occurrence of the earthquake, and the same in the contrary direction just after it. The closing errors are shown in the plate.

(Jan. 10th., 1921. The Director.)

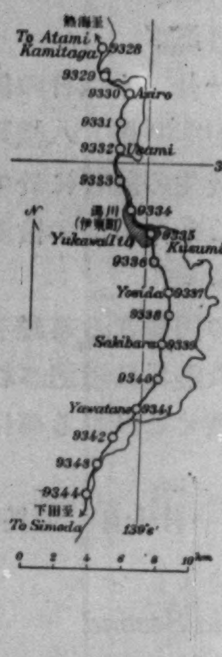
熱海至
To Atami
Kamitaga
9328
9329
9330
Aziro
9331
9332
Usami
35°0'
9333
湯川 (伊東町)
9334
Yukawa
9335
Kusumi
9336
Yosida
9337
9338
Sakibara
9339
9340
Yawatano
9341
9342
9343
9344
下田至
To Simoda
139°0'
N
0 2 4 6 8 10 km.

線 路 圖
(數字ハ水準點番號ヲ示ス)
Map of route.
(Figures show the numbers of bench marks.)

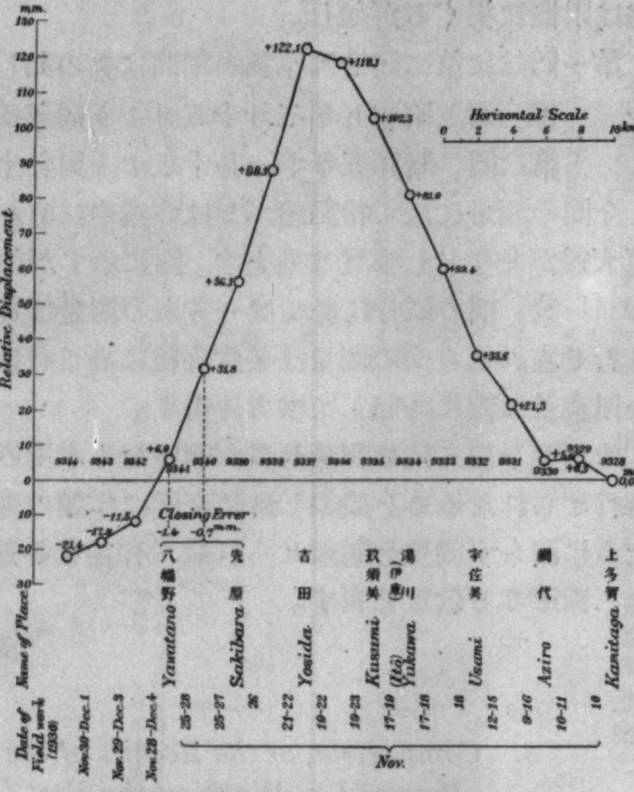

水準觀測斷面圖 (上多賀ヲ不動點ト假定ス)
Profile showing relative vertical displacement.
(No. 9328 is assumed to be stationary.)

伊豆東海岸地方一等水準測量第一回及第二回檢測成果比較要圖

Comparison of the Results of the First and Second Precise Levellings on the East Coast Route of the Province of Idu.

9. 伊豆大震調査概要

昭和五年十一月二十六日の伊豆大震に關し本所は其發生以前及以後に於て次記の如き調査を完了し又は之れに從事しつつある。既に其二三のものは彙報第八號第三冊以降に報告せられてゐる。其他は調査終了次第本彙報に報告する筈である。

（イ） 地震計測

昭和五年二月伊豆伊東地方に地震が頻發するに及び兼任所員今村教授指導の下に地震敎室那須信治及當研究所の岸上冬彥兩氏により三月六日より網代、宇佐美、伊東、川奈、初島ノ五個所に於て地震觀測を開始し七月上旬迄之を繼續してゐた。伊東地方の地震が一時稍鎭靜したので伊東外の地震計を一時取り外したが大震發生の直前に再び地震が續發するに及び觀測を再始するの必要を認め十一月二十五日に前記の那須、岸上の兩氏は地震計を携へて伊豆に赴き岸上氏は網代に於て那須氏は伊東に於て觀測を開始し其翌朝大震に遭遇した。現今は上記の伊東、網代二個所の外尙冷川、吉原、小山の各地に於て地震觀測が爲されてゐる。尙丹那に於ては地表及其直下の隧道內に各一個づつの不銹鋼製の全然同一型の地震計を据附けて地表及地中の振動の比較研究を爲してゐる。

（ロ） 地殼傾斜計測

大震發生前に於ては昭和五年三月中旬より伊東及川奈に石本式熔融水晶製傾斜計を据附け十月下旬迄石本、高橋兩所員により觀測が繼續せられた。其結果は既に前號に報告してある。止むを得ざる事情から大地震の直前に觀測を中絕した事は甚だ遺憾とするところである。大地震發生後五日目より丹那隧道內に於て西側に三揃東側に一揃を据附けて觀測をしてゐる。

（ハ） 隧道內の精密水準測量

水管式水準器による丹那隧道內全長に涉る水準測量は高橋所員により地震發生後直ちに準備に着手せられ既に昨年十二月二十五日より計測が實施せられてゐる。

(ニ) 丹那斷層兩側の相互移動測定

丹那隧道内に顯れた辷り鏡面には「ダイヤルゲージ」を取附け辷り面の相互移動が計測せられつつある。此計測は昨年十二月二十日から高橋所員の手により開始せられた。

尙之れと同時に地表に於ける斷層兩側の相互移動を計測する爲め丹那盆地の一地點に自記微動計を取附くる事は坪井所員の手により計畫されつつあり。今月下旬より測定に着手し得る見込である。

(ホ) 丹那盆地に於ける水準及三角測量

丹那盆地に於ける地殼變動を見出す目的を以て該地に多數の水準點及三角點を設置し坪井所員により時々檢測が繰返へされつつある。

(ヘ) 地質調査

大震發生前に於ては伊東を中心とせる伊豆東海岸地方地質調査が昨年四月津屋所員によりて行はれ其報告は彙報第八號第四册に掲載されてゐる。

大震直後より今日尙引續き津屋、大塚兩所員により震災地方の地質調査が行はれてゐる。

(ト) 建築物調査

地震直後齊田所員及所長により震災地の建物の調査が行はれた。

(チ) 伊東地方水準測量

昨年中に於て伊豆東海岸地方の水準測量が二回施行せられ其成果は彙報第八號第三册及本號に掲載してある。伊豆國全體に渉る測量は現今陸地測量部の手により行はれてゐるから本所は之れを計畫せぬ。

(リ) 三角測量

伊豆國全體に渉る二等三角測量を二等點十七點に對して行ふ外尙該地及四圍にある一等點十二點に對し一等三角測量を施行して土地の水平移動を見出す計畫である。此作業は陸地測量部に委囑した。同部に於て近々之れに着手する筈である。

(ヌ) 光現象調査

今回の大震には光現象殊に著しかりし爲め寺田所員及武者囑託により之れに關する研究及調査が行はれてゐる。其研究の一部は既に帝國學士院記事第六卷第十號に報告せられてゐる。

（昭和六年一月二十日　所長）

9. *Outline of Investigations of the Great Idu Earthquake.*

Our investigations of the Idu Earthquake of November 26, 1930, previous to and after its occurrence, are as described below. Some of them have already been reported in our Bulletin Vol. VIII, Parts 3 and 4; others will be reported as soon as the investigations are completed.

(a) Seismometry.

As swarms of earthquakes occurred near Itô in the province of Idu since February, 1930, Mr. Nasu and Mr. Kishinouye started seismometrical observation from March 6, under the supervision of Professor Imamura, at five places comprising Aziro, Usami, Itô, Kawana and Hasima and continued the observation until early in July. The occurrence of earthquakes in the Itô district having become less frequent the observation was temporarily discontinued, except that in Itô. Owing to the fresh occurrence of swarms of earthquakes, however, the necessity of re-opening the observation was realised, just before the outbreak of the great earthquake. Accordingly the above mentioned gentlemen were again despatched to Idu on November 25 and one of them began observations at Itô, and the other at Aziro and the next morning they encountered the great earthquake. At present, the seismometrical observation is being carried out at Hiyekawa, Yosiwara and Koyama, besides at Itô and Aziro. Moreover at Tanna two seismometers made of stainless steel and of exactly the same type are placed, one on the ground surface and the other in the tunnel directly below it, and the comparative study of the after shocks on the crustal surface and in the interior of the crust is being done.

(b) Measurement of the Tilting of the Crust.

Previous to the occurrence of the great earthquake the Ishimoto tiltmeters made of fused silica were set in Itô and Kawana, and Mr. Ishimoto and Mr. Takahasi continued the observation from the middle of March 1930 until last October. This result has already been reported in the last issue. It is very regrettable that the observation was discontinued just before the great earthquake, owing to unavoidable circumstances. From the fifth day after the occurrence of the great earthquake three sets of the instruments were placed on the western side of the interior of the Tanna Tunnel and one set on the eastern side, and the observation is still being carried on.

(c) Precise Levelling in the Tunnel.

The levelling along the whole length of the bored portion of the Tanna Tunnel with water tube levels was contemplated directly after the occurrence of the earthquake by Mr. Takahasi and the measurement was carried out from the 25th. of last December.

(d) Measurement of the Relative Movement of Both Sides of the Tanna Fault.

To the slickenside appearing in the Tanna Tunnel, dial gauges have been fitted, and the mutual movement of the sliding surfaces is under observation. This measurement was started by Mr. Takahasi from

December 20, 1930. At the same time, in order to measure the relative movement of both sides of the fault on the surface of the ground, the setting of self-recording micrometers at the Tanna Basin is now under preparation by Mr. Tsuboi; the measurement is expected to be started towards the end of this month.

(e) Levelling and Triangulation in the Tanna Basin.

In order to investigate the movement of the crust, numerous bench marks and triangulation points have been set and Mr. Tsuboi is repeating the survey.

(f) Geological Investigations.

Previous to the occurrence of the great earthquake, the geological investigation of the eastern district of Idu with Itô as the center was carried out by Mr. Tsuya in April, 1930, and the report was published in the Bulletin Vol. VIII, Part 4. The geological investigation of the whole province of Idu is now being carried on by Mr. Tsuya and Mr. Otsuka.

(g) Investigation of Buildings in the Disturbed Area.

The investigation of buildings in the devastated area was carried out by Mr. Saita and the Director, just after the great earthquake.

(h) Levelling of the Itô District.

The precise levelling along the eastern coast line crossing Itô was done twice last year, and the results are published in Vol. VIII, Part 3 and in the present issue.

The survey over the whole province of Idu being at present carried on by the Land Survey Department, this Institute does not take further steps.

(i) Triangulation.

The secondary triangulation over the whole province of Idu will be carried out for 17 secondary points, and further the primary triangulation will be executed for 12 primary points in this district and surroundings. This work having been entrusted to the Land Survey Department, they will begin the work immediately.

(j) Luminous Phenomena.

An investigation into luminous phenomena accompanying earthquakes, which were particularly remarkable on the occasion of the great Idu earthquake is being done by Mr. Terada and Mr. Musha. A preliminary report was published in the Proceedings of the Imperial Academy Vol. VI (1930), No. 10.

(January 20th., 1931. The Director.)

10. On the Transmission of Seismic Waves on the Bottom Surface of an Ocean.

By **Katsutada SEZAWA**,

Earthquake Research Institute.

(Read March 17, 1931.—Received March 20, 1931.)

I. Introduction.

The object of this paper is to find the effect of an ocean water upon the two-dimensional transmission of Rayleigh-type waves on the bottom surface of that ocean, and especially to know the nature of the dispersion of an arbitrary wave progressing outwards from an epicentre. Even though Bromwich[1] and Stoneley[2] treated of similar problems, yet their cases are relatively particular. Bromwich studied so long ago as 1898 the influence of gravity of water on a one-dimensional propagation of elastic waves of harmonic type of an infinite extent, while Stoneley gave recently a like problem in which the compressibility of water is taken into account. As these authors appeared to aim at the formulation of the velocity equation of the waves, their treatments did not involve any result as to the behaviour of arbitrary waves, or as to the transmission of waves on a two-dimensional surface of the bottom of the ocean, or even as to the propagation of annular waves on the same surface; all of these have hitherto been left unknown. The investigation of these unknown cases will give us some clue to the dispersive phenomena of the seismic waves at the bottom surface of an ocean, rather than to enable us to understand the nature of the movement of the earth's solid due to a regular train of harmonic waves. There are moreover several data[3] of seismic observations concerning surface waves transmitted through a long distance along the bottom of the ocean; and, by comparing these data with results of the mathematical analysis, a good deal of obscurity which attaches to the distant earthquakes may perhaps be cleared.

---

[1] T. J. I'A. BROMWICH, *Proc. Math. Soc.*, London, **30** (1898), 98–120.

[2] R. STONELEY, *M.N.R.A.S. Geophys. Suppl.*, **1** (1926), 349–356.

[3] B. GUTENBERG, *Handb. d. Geophys.*, **4** (1930), 254–255.

II. Motion of a Semi-infinite Elastic Body.

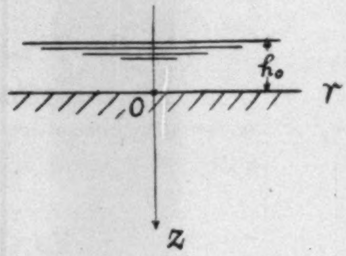

Let the axis of z is directed downwards from the surface of the body, the senses of r, θ being horizontal. Let u, v, w be the components of the displacement in radial, azimuthal and vertical directions, and ρ, λ, μ, the density and Lamé's elastic constants. The equations of motion of the body in cylindrical co-ordinates are expressed by

$$\left.\begin{aligned}
\rho\frac{\partial^2 u}{\partial t^2} &= (\lambda+2\mu)\frac{\partial\Delta}{\partial r}-\frac{2\mu}{r}\frac{\partial\varpi_z}{\partial\theta}+2\mu\frac{\partial\varpi_\theta}{\partial z},\\
\rho\frac{\partial^2 v}{\partial t^2} &= (\lambda+2\mu)\frac{1}{r}\frac{\partial\Delta}{\partial\theta}-2\mu\frac{\partial\varpi_r}{\partial z}+2\mu\frac{\partial\varpi_z}{\partial r},\\
\rho\frac{\partial^2 w}{\partial t^2} &= (\lambda+2\mu)\frac{\partial\Delta}{\partial z}-2\mu\frac{1}{r}\frac{\partial}{\partial r}(r\varpi_\theta)+2\mu\frac{1}{r}\frac{\partial\varpi_r}{\partial\theta}+\rho g,
\end{aligned}\right\}\quad\cdots\cdots\cdots(1)$$

where

$$\left.\begin{aligned}
\Delta &= \frac{1}{r}\frac{\partial(ru)}{\partial r}+\frac{1}{r}\frac{\partial v}{\partial\theta}+\frac{\partial w}{\partial z}, & 2\varpi_r &= \frac{1}{r}\frac{\partial w}{\partial\theta}-\frac{\partial v}{\partial z},\\
2\varpi_\theta &= \frac{\partial u}{\partial z}-\frac{\partial w}{\partial r}, & 2\varpi_z &= \frac{1}{r}\left(\frac{\partial(rv)}{\partial r}-\frac{\partial u}{\partial\theta}\right).
\end{aligned}\right\}\quad\cdots\cdots(2)$$

If we eliminate u, v, w in (1) by means of (2), we get

$$\left.\begin{aligned}
\rho\frac{\partial^2\Delta}{\partial t^2} &= (\lambda+2\mu)\left[\frac{\partial^2\Delta}{\partial r^2}+\frac{1}{r}\frac{\partial\Delta}{\partial r}+\frac{1}{r^2}\frac{\partial^2\Delta}{\partial\theta^2}+\frac{\partial^2\Delta}{\partial z^2}\right],\\
\rho\frac{\partial^2\varpi_r}{\partial t^2} &= \mu\left[\frac{\partial^2\varpi_r}{\partial r^2}+\frac{3}{r}\frac{\partial\varpi_r}{\partial r}+\frac{\varpi_r}{r^2}+\frac{1}{r^2}\frac{\partial^2\varpi_r}{\partial\theta^2}+\frac{\partial^2\varpi_r}{\partial z^2}+\frac{2}{r}\frac{\partial\varpi_z}{\partial z}\right],\\
\rho\frac{\partial^2\varpi_\theta}{\partial t^2} &= \mu\left[\frac{\partial^2\varpi_\theta}{\partial r^2}+\frac{1}{r}\frac{\partial\varpi_\theta}{\partial r}-\frac{\varpi_\theta}{r^2}+\frac{1}{r^2}\frac{\partial^2\varpi_\theta}{\partial\theta^2}+\frac{\partial^2\varpi_\theta}{\partial z^2}+\frac{2}{r^2}\frac{\partial\varpi_r}{\partial\theta}\right],\\
\rho\frac{\partial^2\varpi_z}{\partial t^2} &= \mu\left[\frac{\partial^2\varpi_z}{\partial r^2}+\frac{1}{r}\frac{\partial\varpi_z}{\partial r}+\frac{1}{r^2}\frac{\partial^2\varpi_z}{\partial\theta^2}+\frac{\partial^2\varpi_z}{\partial z^2}\right].
\end{aligned}\right\}\quad(3)$$

As it is difficult to solve the original equations in (1), we shall investigate the equations in (3). From the first and the last equations in (3), we obtain the solutions of the forms :-

$$\left.\begin{aligned} \Delta &= A_m H_m^{(2)}(kr)\, e^{-\alpha z+int} \begin{matrix}\cos\\ \sin\end{matrix}\Big\}\, m\theta, \\ 2\varpi_z &= B_m H_m^{(2)}(kr)\, e^{-\beta z+int} \begin{matrix}\sin\\ -\cos\end{matrix}\Big\}\, m\theta, \end{aligned}\right\} \quad \cdots\cdots\cdots\cdots\cdots\cdots\cdots\cdots(4)$$

where

$$k^2 = \alpha^2+h^2 = \beta^2+j^2, \quad h^2 = \frac{\rho n^2}{\lambda+2\mu}, \quad j^2 = \frac{\rho n^2}{\mu}.$$

Substituting the solution in the second of (4) in the second of the equations (3), and finding the particular and the complementary solutions, we get

$$2\varpi_r = \left\{ C_m \frac{H_m^{(2)}(kr)}{r} - \frac{\beta}{k^2} B_m \frac{\partial H_m^{(2)}(kr)}{\partial r} \right\} e^{-\beta z+int} \begin{matrix}\sin\\ -\cos\end{matrix}\Big\}\, m\theta. \quad \cdots\cdots(5)$$

Substituting this in the third of (3), and, proceeding as before, we find

$$2\varpi_\theta = \left\{ \frac{C_m}{m} \frac{\partial H_m^{(2)}(kr)}{\partial r} - \frac{\beta_m}{k^2} B_m \frac{H_m^{(2)}(kr)}{r} \right\} e^{-\beta z+int} \begin{matrix}\sin\\ \cos\end{matrix}\Big\}\, m\theta. \quad \cdots(6)$$

Displacement answering to Δ in (4) and satisfying $\varpi_r=\varpi_\theta=\varpi_z=0$ in (2), is expressed by

$$\left.\begin{aligned} u_1 &= -A_m \frac{1}{h^2} \frac{\partial H_m^{(2)}(kr)}{\partial r}\, e^{-\alpha z+int} \begin{matrix}\cos\\ \sin\end{matrix}\Big\}\, m\theta, \\ v_1 &= A_m \frac{m}{h^2} \frac{H_m^{(2)}(kr)}{r}\, e^{-\alpha z+int} \begin{matrix}\sin\\ -\cos\end{matrix}\Big\}\, m\theta, \\ w_1 &= A_m \frac{\alpha}{h^2} H_m^{(2)}(kr)\, e^{-\alpha z+int} \begin{matrix}\cos\\ \sin\end{matrix}\Big\}\, m\theta. \end{aligned}\right\} \quad \cdots\cdots\cdots\cdots\cdots(7)$$

Displacement answering to ϖ_z in (4) besides the second terms of the right-hand sides of ϖ_r and ϖ_θ, both given in (5) and (6), under the condition that $\Delta = 0$ in (2), is expressed by

$$\left.\begin{aligned} u_2 &= B_m \frac{m}{k^2} \frac{H_m^{(2)}(kr)}{r}\, e^{-\beta z+int} \begin{matrix}\cos\\ \sin\end{matrix}\Big\}\, m\theta, \\ v_2 &= -B_m \frac{1}{k^2} \frac{\partial H_m^{(2)}(kr)}{\partial r}\, e^{-\beta z+int} \begin{matrix}\sin\\ -\cos\end{matrix}\Big\}\, m\theta, \\ w_2 &= 0. \end{aligned}\right\} \quad \cdots\cdots\cdots\cdots\cdots(8)$$

Displacement derived from the values of the first terms of the right-hand sides of the expressions of ϖ_r and ϖ_θ, both given in (5) and (6), and fulfilling the conditions $\Delta = \varpi_z = 0$ in (2), is written by

$$\left.\begin{aligned} u_3 &= C_m \frac{\beta}{mj^2} \frac{\partial H_m^{(2)}(kr)}{\partial r} e^{-\beta z + int} \left.\begin{matrix}\cos\\ \sin\end{matrix}\right\} m\theta, \\ v_3 &= -C_m \frac{\beta}{j^2} \frac{H_m^{(2)}(kr)}{r} e^{-\beta z + int} \left.\begin{matrix}\sin\\ -\cos\end{matrix}\right\} m\theta, \\ w_3 &= -C_m \frac{k^2}{mj^2} H_m^{(2)}(kr)\, e^{-\beta z + int} \left.\begin{matrix}\cos\\ \sin\end{matrix}\right\} m\theta. \end{aligned}\right\} \quad \cdots\cdots\cdots\cdots\cdots(9)$$

Of these three components of the displacement, namely (u_1, v_1, w_1), (u_2, v_2, w_2) and (u_3, v_3, w_3), the first and the third are available to obtain Rayleigh-type waves, and the second is useful to get Love-type waves. In the present case the former set of combination will be considered. The latter set will perhaps be employed in some future occasion.

III. Motion of the Superficial Water.

Let u', v', w' be the components of the displacement of the superficial water in r, θ, z directions, ρ_0' the density of water in an undisturbed state, p_1 the charge of the pressure in a disturbed state, and μ' the viscosity of the water. The equations of motion of the water in Eulerean system are then expressed by

$$\left.\begin{aligned} \rho_0' \frac{\partial^2 u'}{\partial t^2} &= -\frac{\partial p_1}{\partial r} + \mu' \frac{\partial}{\partial t} \left\{ \frac{\partial^2 u'}{\partial r^2} + \frac{1}{r} \frac{\partial u'}{\partial r} \right. \\ &\qquad \left. - \frac{u'}{r^2} + \frac{1}{r^2} \frac{\partial^2 u'}{\partial \theta^2} + \frac{\partial^2 u'}{\partial z^2} - \frac{2}{r^2} \frac{\partial v'}{\partial \theta} \right\}, \\ \rho_0' \frac{\partial^2 v'}{\partial t^2} &= -\frac{1}{r} \frac{\partial p_1}{\partial \theta} + \mu' \frac{\partial}{\partial t} \left\{ \frac{\partial^2 v'}{\partial r^2} + \frac{1}{r} \frac{\partial v'}{\partial r} \right. \\ &\qquad \left. - \frac{v'}{r^2} + \frac{1}{r^2} \frac{\partial^2 v'}{\partial \theta^2} + \frac{\partial^2 v'}{\partial z^2} + \frac{2}{r} \frac{\partial u'}{\partial \theta} \right\}, \\ \rho_0' \frac{\partial^2 w'}{\partial t^2} &= -\frac{\partial p_1}{\partial z} + \mu' \frac{\partial}{\partial t} \left\{ \frac{\partial^2 w'}{\partial r^2} + \frac{1}{r} \frac{\partial^2 w'}{\partial r} \right. \\ &\qquad \left. + \frac{1}{r^2} \frac{\partial^2 w'}{\partial \theta^2} + \frac{\partial^2 w'}{\partial z^2} \right\} + \rho' g. \end{aligned}\right\} \cdots(10)$$

The actual density ρ' and the similar pressure p are denoted by

$$\rho' = \rho_0' + \rho_1', \qquad p = p_0 + p_1, \quad \cdots\cdots\cdots\cdots\cdots\cdots\cdots\cdots(11)$$

where ρ_1' is the change of the density due to the disturbance and p_0 the statical pressure. The equation of continuity of a compressible fluid is written by

$$\frac{D\rho'}{Dt}+\rho_0'\frac{\partial}{\partial t}\left\{\frac{1}{r}\frac{\partial(ru')}{\partial r}+\frac{1}{r}\frac{\partial v'}{\partial\theta}+\frac{\partial w'}{\partial z}\right\}=0, \quad\cdots\cdots\cdots\cdots(12)$$

where D/Dt denotes a differentiation following the motion of the fluid. Again, the change of pressure and that of density are related in a form:

$$\frac{Dp}{Dt}=c^2\frac{D\rho'}{Dt}, \quad\cdots\cdots\cdots\cdots\cdots\cdots\cdots\cdots\cdots\cdots(13)$$

in which $c^2=\dfrac{\varkappa}{\rho_0'}=\left(\dfrac{dp}{d\rho'}\right)_{\rho'=\rho_0'}=\dfrac{\gamma p_0}{\rho_0'}$ in adiabatic law. ($\varkappa=2{\cdot}045\times10^{10}$ dyne per sq. cm for water at 15°C.)

From (11), (12), (13), we get

$$\frac{\partial p'}{\partial t}+\rho_0' c^2\left\{\frac{1}{r}\frac{\partial(ru')}{\partial r}+\frac{1}{r}\frac{\partial v'}{\partial\theta}+\frac{\partial w'}{\partial z}\right\}+\rho_0' g\frac{\partial w'}{\partial t}=0, \quad\cdots(14)$$

in which use is made of

$$\frac{Dp}{Dt}\doteqdot\frac{\partial p}{\partial t}+\frac{\partial p}{\partial(z+w')}\frac{\partial(z+w')}{\partial t}=\frac{\partial p_1}{\partial t}+\frac{\partial p_0}{\partial z}\frac{\partial w'}{\partial t}. \quad\cdots\cdots\cdots(15)$$

Eliminating p_1, ρ_0' between (10), (12), (14), we obtain

$$\left.\begin{aligned}
\rho_0'\frac{\partial^3 u'}{\partial t^3}&=\frac{\partial}{\partial r}\left[\rho_0' c^2\frac{\partial}{\partial t}\left\{\frac{1}{r}\frac{\partial(ru')}{\partial r}+\frac{1}{r}\frac{\partial v'}{\partial\theta}+\frac{\partial w'}{\partial z}\right\}+\rho_0' g\frac{\partial w'}{\partial t}\right]\\
&\quad+\mu'\frac{\partial^2}{\partial t^2}\left[\frac{\partial^2 u'}{\partial r^2}+\frac{1}{r}\frac{\partial u'}{\partial r}-\frac{u'}{r^2}+\frac{1}{r^2}\frac{\partial^2 u'}{\partial\theta^2}+\frac{\partial^2 u'}{\partial z^2}-\frac{2}{r^2}\frac{\partial v'}{\partial\theta}\right],\\
\rho_0'\frac{\partial^3 v'}{\partial t^3}&=\frac{1}{r}\frac{\partial}{\partial\theta}\left[\rho_0' c^2\frac{\partial}{\partial t}\left\{\frac{1}{r}\frac{\partial(ru')}{\partial r}+\frac{1}{r}\frac{\partial v'}{\partial\theta}+\frac{\partial w'}{\partial z}\right\}+\rho_0' g\frac{\partial w'}{\partial t}\right]\\
&\quad+\mu'\frac{\partial^2}{\partial t^2}\left[\frac{\partial^2 v'}{\partial r^2}+\frac{1}{r}\frac{\partial v'}{\partial r}-\frac{v'}{r^2}+\frac{1}{r^2}\frac{\partial^2 v'}{\partial\theta^2}+\frac{\partial^2 v'}{\partial z^2}+\frac{2}{r^2}\frac{\partial u'}{\partial\theta}\right],\\
\rho_0'\frac{\partial^3 w'}{\partial t^3}&=\frac{\partial}{\partial z}\left[\rho_0' c^2\frac{\partial}{\partial t}\left\{\frac{1}{r}\frac{\partial(ru')}{\partial r}+\frac{1}{r}\frac{\partial v'}{\partial\theta}+\frac{\partial w'}{\partial z}\right\}+\rho_0' g\frac{\partial w'}{\partial t}\right]\\
&\quad+\mu'\frac{\partial^2}{\partial t^2}\left[\frac{\partial^2 w'}{\partial r^2}+\frac{1}{r}\frac{\partial w'}{\partial r}+\frac{1}{r^2}\frac{\partial^2 w'}{\partial\theta^2}+\frac{\partial^2 w'}{\partial z^2}\right].
\end{aligned}\right\}\quad(16)$$

These may be satisfied by a function ϕ which is connected with u', v', w' in the forms:

$$\frac{\partial u'}{\partial t} = -\frac{\partial \phi}{\partial r}, \quad \frac{\partial v'}{\partial t} = -\frac{1}{r}\frac{\partial \phi}{\partial \theta}, \quad \frac{\partial w'}{\partial z} = -\frac{\partial \phi}{\partial z}, \cdots\cdots\cdots(17)$$

provided

$$\frac{\partial^2 \phi}{\partial t^2} = \left(c^2 + \nu\frac{\partial}{\partial t}\right)\left\{\frac{\partial^2 \phi}{\partial r^2} + \frac{1}{r}\frac{\partial \phi}{\partial r} + \frac{1}{r^2}\frac{\partial^2 \phi}{\partial \theta^2} + \frac{\partial^2 \phi}{\partial z^2}\right\} + g\frac{\partial \phi}{\partial z}, \cdots(18)$$

where $\nu = \mu'/\rho_0'$.

Now, putting

$$\phi = \varPhi H_m^{(2)}(kr)\left.\begin{matrix}\cos\\ \sin\end{matrix}\right\} m\theta \quad \cdots\cdots\cdots\cdots\cdots\cdots\cdots\cdots\cdots(19)$$

in (18), and solving the resulting equation, we get

$$\phi = H_m^{(2)}(kr)\left.\begin{matrix}\cos\\ \sin\end{matrix}\right\} m\theta \; e^{-\frac{gz}{2c^2}}\left[D_m \cosh k_1 z + E_m \sinh k_1 z\right] e^{-\frac{\nu k^2 t}{2}} e^{in_1 t}, \cdots(20)$$

where

$$k_1^2 = \frac{g^2}{4c^4} - k^2\left(\frac{c_1^2}{c^2} - 1\right), \quad n_1^2 = k^2 c_1^2 - \frac{(\nu k^2)^2}{4}, \cdots\cdots\cdots\cdots\cdots(21)$$

in which $c_1^2 = n^2/k^2$.

The values of ν at 10°C is nearly 0·0131, while $k = 2{\cdot}09 \times 10^{-5}\,\mathrm{cm}^{-1}$ for waves of 3 km length and $k = 2{\cdot}09 \times 10^{-6}\,\mathrm{cm}^{-1}$ for waves of 30 km length, so that we have $e^{-\frac{\nu k^2 t}{2}} = e^{-2\cdot86\times10^{-9}}$ and $e^{-\frac{\nu k^2 t}{2}} = e^{-2\cdot86\times10^{-11}}$ for respective waves at the time $t = 100$ sec. Again, if we assume that the velocity of the waves is of the order 3 km per sec, then $k^2 c_1^2 = 39{\cdot}4\,\mathrm{sec}^{-2}$ for 3 km wave length, and $k^2 c_1^2 = 0{\cdot}394\,\mathrm{sec}^{-1}$ for 30 km wave length; and hence $n_1^2 = k^2 c_1^2 - \dfrac{(\nu k^2)^2}{4} = (39{\cdot}4 - 2{\cdot}86 \times 10^{-12})\,\mathrm{sec}^{-2} \doteqdot n^2$ and $n_1^2 = (0{\cdot}394 - 2{\cdot}86 \times 10^{-14})\,\mathrm{sec}^{-2} = n^2$ in respective cases. We may thus write $e^{-\frac{\nu k^2 t}{2}} = 1$ and $e^{in_1 t} = e^{int}$ without any sensible error in all practical problems.

Lastly, we may note that $e^{-\frac{gz}{2c^2}}$ may also be taken to be unity, but $\cosh k_1 z$ cannot be replaced by $\cosh kz$. Because, if we take $z = -1$ km and -10 km, we obtain $e^{-\frac{gz}{2c^2}} = e^{2\cdot40\times10^{-3}}$ and $e^{-\frac{gz}{2c^2}} = e^{2\cdot40\times10^{-2}}$ for respective cases, both of the exponentials being thus very near unity; while $\cosh k_1 z \doteqdot \cosh\sqrt{1-\frac{c_1^2}{c^2}}\, kz = \cos 1{\cdot}84\, kz$, which is obviously different from $\cosh kz$. This fact was also pointed out by Stoneley.[4)]

We may therefore write the expression of ϕ in the following form:

$$\phi = [D_m \cosh k_1 z + E_m \sinh k_1 z]\; H_m^{(2)}(kr) \left.\begin{matrix}\cos\\ \sin\end{matrix}\right\} m\theta\, e^{int}, \quad \cdots\cdots(22)$$

where $k_1^2 = -k^2\left(\frac{c_1^2}{c^2}-1\right)$. The values of the corresponding components of the displacement is written by

$$\left.\begin{aligned} u_1' &= \frac{i}{n}[D_m \cosh k_1 z + E_m \sinh k_1 z]\frac{\partial H_m^{(2)}(kr)}{\partial r} \left.\begin{matrix}\cos\\ \sin\end{matrix}\right\} m\theta\, e^{int}, \\ v' &= -\frac{im}{n}[D_m \cosh k_1 z + E_m \sinh k_1 z]\frac{H_m^{(2)}(kr)}{r} \left.\begin{matrix}\sin\\ -\cos\end{matrix}\right\} m\theta\, e^{int}, \\ w' &= \frac{ik_1}{n}[D_m \sinh k_1 z + E_m \cosh k_1 z]\, H_m^{(2)}(kr) \left.\begin{matrix}\cos\\ \sin\end{matrix}\right\} m\theta\, e^{int}. \end{aligned}\right\} \cdots\cdots(23)$$

These expressions are obtained from the relation in (17) without difficulty.

IV. Boundary Conditions.

As there is no water pressure at the free surface of the ocean, we must have

$$z = -h_0; \qquad p = 0, \qquad (\text{or} = \text{constant},) \quad \cdots\cdots\cdots\cdots\cdots(24)$$

where h_0 is the depth of the ocean.

The theorem of Bernoulli concerning the pressure distribution of fluid in wave motion is such that

$$\frac{p}{\rho'} = \frac{\partial\phi}{\partial t} + gw'. \cdots\cdots\cdots\cdots\cdots\cdots\cdots\cdots\cdots\cdots(25)$$

We know, however, that

$$\frac{\partial w'}{\partial t} = -\frac{\partial\phi}{\partial z}.$$

Substituting this in (25), the condition (24) may be replaced by

---

[4)] R. Stoneley, *loc. cit.*

$$z=-h_0\,; \qquad \frac{\partial^2\phi}{\partial t^2}=g\frac{\partial\phi}{\partial z}. \quad\cdots\cdots\cdots\cdots\cdots\cdots\cdots\cdots(26)$$

Hence, from (22) and this equation, we get

$$(gk_1\cosh k_1h_0-n^2\sinh k_1h_0)\,E_m=(gk_1\sinh k_1h_0-n^2\cosh k_1h_0)D_m. \cdots(27)$$

When the depth of the water is relatively small, we have approximately

$$(gk_1-n^2k_1h_0)E_m=(gk_1^2h_0-n^2)D_m. \quad\cdots\cdots\cdots\cdots\cdots\cdots(27')$$

The boundary conditions at the bottom of the ocean are such that

i. The displocement of the solid and that of the water are continuous in all components.

ii. The normal and shearing stresses are also continuous.

Since the viscosity of water, as we have seen in the last chapter, gives little effect on the motion of the seismic waves, it is evident that the tangential stresses of the water are practically zero at the bottom surface, and therefore the shearing stresses of the solid at that surface should be taken to be zero. The tangential displacements of the solid and of the water may accordingly be discontinuous at the same boundary. The vertical displacements and the similar stresses must be continuous on account of the reason that the active forces except the viscosity of the water act in this direction and also that the material points should be continuous in the normal sense of the contacting boundary.

From the condition that the component of the displacement in the normal direction is continuous, we have

$$z=0\,; \qquad w=w', \quad\cdots\cdots\cdots\cdots\cdots\cdots\cdots\cdots\cdots(28)$$

where $w=w_1+w_3$. Substituting from (7), (9), (23), we get

$$k_1E_m=-in\left(\frac{\alpha}{h^2}A_m-\frac{k^2}{j^2}\frac{C_m}{m}\right). \quad\cdots\cdots\cdots\cdots\cdots\cdots(29)$$

From the conditions of the tangential stresses, we have

$$z=0; \qquad \left.\begin{aligned}&\frac{\partial w}{\partial r}+\frac{\partial u}{\partial z}=0,\\ &\frac{1}{r}\frac{\partial w}{\partial\theta}+\frac{\partial v}{\partial z}=0,\end{aligned}\right\} \cdots\cdots\cdots\cdots\cdots\cdots\cdots(30)$$

in which $u=u_1+u_3,\ v=v_1+v_3,\ w=w_1+w_3$. Substituting from (7), (9) in (30), we obtain

$$\frac{C_m}{m}\Big/ A_m = \frac{2\mathfrak{j}^2\sqrt{k^2-h^2}}{h^2(2k^2-\mathfrak{j}^2)} \cdots\cdots\cdots\cdots\cdots\cdots\cdots\cdots\cdots\cdots (31)$$

From the condition of the normal stress, we get

$$\lambda\varDelta + 2\mu\frac{\partial w}{\partial z} - g(\rho-\rho')w + \rho'\frac{\partial\phi}{\partial t} = 0. \quad \cdots\cdots\cdots\cdots\cdots (32)$$

Substituting from (4), (7), (9), (22), we obtain

$$\left(2-\frac{\mathfrak{j}^2}{k^2}\right)^2 - \frac{4\alpha\beta}{k^2} - \frac{g\rho\mathfrak{j}^2\alpha}{\mu k^4} + \frac{\rho'\mathfrak{j}^2\alpha}{\mu k^4}\left\{g + n^2\frac{g-n^2h_0}{gk_1{}^2h_0-n^2}\right\} = 0. \quad \cdots (33)$$

V. Velocity- and Displacement-Equations.

The Equation (33) may be written in the form:

$$\left(2-\frac{\mathfrak{j}^2}{k^2}\right)^2 - \frac{4\alpha\beta}{k^2} - \frac{g\rho}{\mu k}\,\frac{\mathfrak{j}^2\alpha}{k^3} + \frac{\rho'\mathfrak{j}^2\alpha}{\mu k^4}\left\{\frac{\dfrac{g^2k_1{}^2h_0}{n^2}-n^2h_0}{\dfrac{gk_1{}^2h_0}{n^2}-1}\right\} = 0. \quad \cdots\cdots (33')$$

When $\dfrac{gk_1{}^2h_0}{n^2}$, which is very small in the ordinary case of the ocean, is omitted, we have

$$\left(2-\frac{\mathfrak{j}^2}{k^2}\right)^2 - \frac{4\alpha\beta}{k^2} - \frac{g\rho}{\mu k}\,\frac{\mathfrak{j}^2\alpha}{k^3} + \frac{\rho'}{\rho}(\alpha h_0)\frac{\mathfrak{j}^4}{k^4} = 0. \quad \cdots\cdots\cdots\cdots (34)$$

If $\dfrac{gk_1{}^2h_0}{n^2}$ is not omitted, we obtain, neglecting squares of small quantities,

$$\left(2-\frac{\mathfrak{j}^2}{k^2}\right)^2 - \frac{4\alpha\beta}{k^2} - \frac{g\rho}{\mu k}\,\frac{\mathfrak{j}^2\alpha}{k^3} + \frac{\rho'}{\rho}(\alpha h_0)\frac{\mathfrak{j}^4}{k^4}\left\{1 - \frac{g^2k^2\rho^2}{\mu^2\mathfrak{j}^4}\right.$$

$$\left. + \frac{g^2\rho}{\mu\mathfrak{j}^2c^2} + \frac{k_0gk^2\rho}{\mu\mathfrak{j}^2} - \frac{h_0g}{c^2}\right\} = 0. \quad \cdots\cdots (35)$$

If we write $\dfrac{\mathfrak{j}^2}{k^2} = j'^2$, $\dfrac{h^2}{k^2} = h'^2$, we have

$$(2-j'^2)^2 - 4\sqrt{(1-k'^2)(1-j'^2)} - \left(\frac{g\rho}{\mu k}\right)j'^2\sqrt{1-h'^2} + \left(\frac{\rho'h_0k}{\rho}\right)j'^4\sqrt{1-h'^2}$$

$$- \frac{\rho\rho'h_0g^2}{\mu^2k}\sqrt{1-h'^2} + \frac{\rho'h_0g^2j'^2}{\mu kc^2}\sqrt{1-h'^2} + \frac{\rho'h_0{}^2gk}{\mu}j'^2\sqrt{1-h'^2}$$

$$- \frac{\rho'h_0gk}{\rho c^2}j'^4\sqrt{1-h'^2} = 0. \quad \cdots\cdots (35')$$

This is the equation to determine the velocity of waves propagated in two dimensions on the bottom surface of an ocean. Now it is exceedingly difficult to solve the equation (34) or (35), so that the following approximation has been made. As $j'^2 = \dfrac{\rho n^2}{\mu k^2} = \left(\dfrac{\rho}{\mu}\right) \times$ (velocity)^2, we may write

$$j'^2 = \xi_0 + \delta\xi, \quad \cdots\cdots\cdots\cdots\cdots\cdots\cdots\cdots\cdots\cdots\cdots\cdots(36)$$

under the assumption that the velocity of propagation of the waves of the present case is not much different from that of Rayleigh-waves on the free surface of a semi-infinite body. In (36), $\xi_0 \times (\mu/\rho)$ is the square of the velocity, V_0, of the ordinary Rayleigh-waves, and $\delta\xi \times (\mu/\rho)$ is the deviation of the square of the velocity, V, of the waves on the bottom surface of an ocean, from that of the ordinary Rayleigh-waves. In the case, in which the solid is incompressible ($h'=0$) and also $\dfrac{gk_1^2h_0}{n^2}$ is very small, we obtain

$$2\delta\xi\left[\frac{1}{\sqrt{1-\xi_0}} - (2-\xi_0)\right] - \left(\frac{\rho g}{\mu k}\right)\xi_0 + \left(\frac{\rho'}{\rho}h_0 k\right)\xi_0^2 = 0. \quad \cdots\cdots(37)$$

The value of ξ_0 in the case of $h' = 0$ is 0·91262 and $V_0 = \sqrt{\dfrac{\mu\xi_0}{\rho}}$, $V = \sqrt{\dfrac{\mu(\xi_0+\delta\xi)}{\rho}}$. Hence

$$\frac{V-V_0}{V_0} \doteqdot \frac{1}{2}\,\frac{\delta\xi}{\xi_0} \doteqdot 0{\cdot}109\frac{g\rho}{\mu k} - 0{\cdot}0994\frac{\rho'}{\rho}h_0 k. \cdots\cdots \cdots\cdots(38)$$

To get the order of the numerical value of this expression, we put $\mu/\rho = 3{\cdot}14^2\mathrm{km}^2/\mathrm{sec}^2$, $k = 2{\cdot}09\times10^{-6}\,\mathrm{cm}^{-1}$, (nearly 10 sec. period.), $g = 980$ dyne, $h_0 = 2\mathrm{km}$, $\rho'/\rho = 0{\cdot}4$, $\rho' = 1$. Then we have

$$\frac{V-V_0}{V_0} = 0{\cdot}00129 - 0{\cdot}0166.$$

In the case of a solid whose Poisson's ratio is 1/4, we have

$h'^2 = \frac{1}{3} j'^2$ and the equation similar to (37) is expressed by

$$\delta \doteq (2-\xi_0)\left[\frac{4}{3}\frac{1}{\sqrt{(1-\xi_0)\left(1-\frac{\xi_0}{3}\right)}}-2\right]-\left(\frac{g\rho}{\mu k}\right)\xi_0\sqrt{1-\frac{\xi_0}{3}}$$

$$+\left(\frac{\rho'}{\rho}h_0 k\right)\xi_0^{\,2}\sqrt{1-\frac{\xi_0}{3}} = 0. \quad \cdots\cdots\cdots\cdots(39)$$

The value of ξ_0 in the case $h'^2 = \frac{1}{3} j'^2$ is approximately 0·8453. Therefore

$$\frac{V-V_0}{V_0} = 0{\cdot}183\frac{g\rho}{\mu k} - 0{\cdot}155\frac{\rho'}{\rho}h_0 k. \quad \cdots\cdots\cdots\cdots\cdots\cdots(40)$$

Generally, we can write the velocity equation in the form:

$$V = V_0 + \frac{c_1}{k} - c_2 k, \quad \cdots\cdots\cdots\cdots\cdots\cdots\cdots\cdots\cdots\cdots(41)$$

where $c_1 = 0{\cdot}109\frac{g\rho}{\mu}V_0$ and $c_2 = 0{\cdot}0994\frac{\rho'}{\rho}h_0 V_0$ for an incompressible solid and $c_1 = 0{\cdot}183\frac{g\rho}{\mu}V_0$ and $c_2 = 0{\cdot}155\frac{\rho}{\rho'}h_0 V_0$ for a material whose Poisson's ratio is 1/4. For a material whose Poisson's ratio is between $\frac{1}{2}$ and $\frac{1}{4}$, the respective values of c_1 and c_2 are intemediate between their two particular values written above.

The expressions of the displacement of the bottom of the ocean is now written by

$$\left.\begin{aligned} u &= A_m\frac{(2k^2-j^2-2\alpha\beta)}{\alpha j^2}\frac{\partial H_m^{(2)}(kr)}{\partial r}\left.\begin{matrix}\cos\\ \sin\end{matrix}\right\}m\theta\, e^{i(V_0k+c_1-c_2k^2)t}, \\ v &= -A_m\frac{m(2k^2-j^2-2\alpha\beta)}{\alpha j^2}\frac{H_m^{(2)}(kr)}{r}\left.\begin{matrix}\sin\\ -\cos\end{matrix}\right\}m\theta\, e^{i(V_0k+c_1-c_2k^2)t}, \\ w &= A_m H_m^{(2)}(kr)\left.\begin{matrix}\cos\\ \sin\end{matrix}\right\}m\theta\, e^{i(V_0k+c_1-c_2k^2)t}, \end{aligned}\right\} \cdots\cdots\cdots(42)$$

and the motion of the water particle is expressed by (23), where D_m and E_m are to be determined from (27), (29), (31).

From these expressions it may be seen that the azimuthal component of the displacement of the solid as well as that of the water become quiescent as the distance from the epicentre increases. The ratio of the vertical and the horizontal components of the displacement of the solid is not much different from that of the ordinary Rayleigh-waves. It is certain, however, that the ratio of the horizontal and the vertical components of the displacement of the bottom surface at a certain distance from the epicentre is more or less altered from that of Rayleigh-waves propagated on the free surface of a semi-infinite body. When the material is incompressible, the ratio of both components of the displacement of the ordinary Rayleigh-waves is

$$\frac{u_{\text{max.}}}{w_{\text{max.}}} = \frac{2-\xi_0-2\sqrt{1-\xi_0}}{\xi_0}\left(= 0{\cdot}543\right); \cdots\cdots\cdots\cdots (43)$$

while that of the waves propagated on the ocean bottom is

$$\frac{u_{\text{max.}}}{w_{\text{max}}} = \frac{2-\xi_0-2\sqrt{1-\xi_0}}{\xi_0}+\left(\frac{2-\xi_0}{\sqrt{1-\xi_0}}-2\right)\delta\xi$$

$$\left(= 0{\cdot}543+0{\cdot}403\frac{g\rho}{\mu k}-0{\cdot}367\frac{\rho'}{\rho}h_0 k\right). \cdots\cdots (44)$$

If we take $\mu/\rho = 3{\cdot}14^2\,\text{km}^2/\text{sec}^2$, $k = 2{\cdot}09\times 10^{-6}\text{cm}^{-1}$, $g = 980$ dyne, $h_0 = 2\,\text{km}$, $\rho'/\rho = 0.4$, $\rho' = 1$; we get from (44)

$$\frac{u_{\text{max.}}}{w_{\text{max.}}} = 0{\cdot}543+0{\cdot}00477-0{\cdot}0614,$$

so that we find that the change of the ratio of the amplitudes in some cases is not so small. From the equation (44), we may conclude that the ratio of the horizontal component of the displacement to the vertical component becomes large for long waves and the ratio becomes small for short waves.

Lastly, it may be seen from (23) and (27′) that the motion of the water particle on the free surface is mainly of a vertical type. This nature is quite different from that of the ordinary long water waves, and may perhaps be due to the fact that the displacement of the water caused by the movement of the ocean bed is chiefly in the sense of the vertical but not of the horizontal.

VI. Transmission of Arbitrary Waves.

We may now proceed to study the transmission of arbitrary waves on the two-dimensional surface of the bottom of an ocean. The equation of harmonic vibrations of the bottom surface of the ocean similar to (42) is written directly in the forms:

$$\left.\begin{aligned}
u &= A_m\frac{(2k^2-j^2-2\alpha\beta)}{\alpha j^2}\,\frac{\partial J_m(kr)}{\partial r}\begin{matrix}\cos\\ \sin\end{matrix}\Big\}\, m\theta\,\begin{matrix}\cos\\ \sin\end{matrix}\Big\}(V_0k+c_1-c_2k^2)t,\\
v &= -A_m\frac{m(2k^2-j^2-2\alpha\beta)}{\alpha j^2}\,\frac{J_m(kr)}{r}\begin{matrix}\sin\\ -\cos\end{matrix}\Big\}\, m\theta\,\begin{matrix}\cos\\ \sin\end{matrix}\Big\}(V_0k+c_1-c_2k^2)t,\\
w &= A_m J_m(kr)\begin{matrix}\cos\\ \sin\end{matrix}\Big\}\, m\theta\,\begin{matrix}\cos\\ \sin\end{matrix}\Big\}(V_0k+c_1-c_2k^2)t.
\end{aligned}\right\}\text{(45)}$$

When the initial disturbance is of the forms:

$$t=0,\ z=0;\ w=f(r)\cos m\theta,\ \frac{\partial w}{\partial t}=\varphi(r)\cos q(\theta+\varepsilon);\ \cdots\cdots\text{(46)}$$

we have the general expressions of the displacement as follows:

$$\left.\begin{aligned}
u &= \cos m\theta\int_0^\infty F(k)\frac{(2k^2-j^2-2\alpha\beta)}{\alpha j^2}\,\frac{\partial J_m(kr)}{\partial r}\cos(V_0k+c_1-c_2k^2)t\,kdk\\
&\quad+\cos q(\theta+\varepsilon)\int_0^\infty \Phi(k)\frac{(2k^2-j^2-2\alpha\beta)}{\alpha j^2}\,\frac{\partial J_m(kr)}{\partial r}\,\frac{\sin(V_0k+c_1-c_2k^2)t}{V_0k+c_1-c_2k^2}kdk,\\
v &= -m\sin m\theta\int_0^\infty F(k)\frac{(2k^2-j^2-2\alpha\beta)}{\alpha j^2}\,\frac{J_m(kr)}{r}\cos(V_0k+c_1-c_2k^2)t\,kdk\\
&\quad-q\sin q(\theta+\varepsilon)\int_0^\infty \Phi(k)\frac{(2k^2-j^2-2\alpha\beta)}{\alpha j^2}\,\frac{J_m(kr)}{r}\,\frac{\sin(V_0k+c_1-c_2k^2)t}{V_0k+c_1-c_2k^2}kdk,\\
w &= \cos m\theta\int_0^\infty F(k)J_m(kr)\cos(V_0k+c_1-c_2k^2)t\,kdk\\
&\qquad\qquad+\cos q(\theta+\varepsilon)\int_0^\infty \Phi(k)J_m(kr)\frac{\sin(V_0t+c_1-c_2k^2)}{V_0k+c_1-c_2k^2}kdk;
\end{aligned}\right\}\text{(47)}$$

provided

$$F(k)=\int_0^\infty f(\sigma)J_m(k\sigma)\sigma d\sigma,\qquad \Phi(k)=\int_0^\infty \varphi(\sigma)J_m(k\sigma)\sigma d\sigma.\ \cdots\cdots\cdots\cdots\text{(48)}$$

If we put particularly

$$\left.\begin{aligned} f(r) &= A\frac{r}{a}e^{-\frac{r^2}{a^2}}, \quad \varphi(r)=0, \quad [m>1] \\ f(r) &= A\,e^{-\frac{r^2}{a^2}}, \quad \varphi(r)=0, \quad [m=0] \end{aligned}\right\} \cdots\cdots\cdots\cdots(49)$$

we obtain

$$F(k)=\frac{A}{a}\int_0^\infty e^{-\frac{\sigma^2}{a^2}}J_m(k\sigma)\sigma^2d\sigma=\frac{A}{a}\sum_{q=0}^{\infty}\frac{(-1)^q\left(\frac{k}{2}\right)^{m+2q}}{q!\,\Gamma(m+q+1)}\frac{\Gamma\left(\frac{m}{2}+\frac{3}{2}+q\right)}{\left(\frac{2}{a}\right)^{m+2q+3}},$$

$$[m>2] \quad \cdots(50)$$[5]

$$F(k)=\frac{A}{a}\int_0^\infty e^{\frac{\sigma^2}{a^2}}J_1(k\sigma)\sigma^2d\sigma = A\frac{a^3}{4}k\,e^{-\frac{a^2k^2}{4}}, \qquad [m=1] \quad \cdots(51)$$

$$F(k)=A\int_0^\infty e^{-\frac{\sigma^2}{a^2}}J_0(k\sigma)\sigma d\sigma = A\frac{a^2}{2}e^{-\frac{a^2k^2}{4}}; \qquad [m=0] \quad \cdots(52)$$

so that we find the expression of w as follows:

$$w=\frac{A\cos m\theta}{a}\sum_{q=0}^{\infty}\frac{(-1)^q\Gamma\left(\frac{m}{2}+q+\frac{3}{2}\right)}{q!\,2^{m+2q}\Gamma(m+q+1)}\left(\frac{a}{2}\right)^{m+2q+3}$$

$$\times\int_0^\infty J_m(kr)\cos(V_0k+c_1-c_2k^2)t\,k^{m+2q+1}dk, \qquad [m>2]\cdots(53)$$

$$w=\frac{Aa^3}{4}\cos\theta\int_0^\infty e^{-\frac{a^2k^2}{4}}J_1(kr)\cos(V_0k+c_1-c_2k^2)t\;k^2dk, \qquad [m=1]\cdots(54)$$

$$w=\frac{Aa^2}{2}\int_0^\infty e^{-\frac{a^2k^2}{2}}J_0(kr)\cos(V_0k+c_1-c_2k^2)t\,kdk; \qquad [m=0]\cdots(55)$$

the expressions of u and v can be similarly written.

In (53), (54), (55), the asymptotic expansions of $J_m(kr)$ may be taken for a relatively large value of kr. We shall employ such expansions hereafter, because of the reason that we are to investigate the behaviour of waves in transmission through a certain epicentral distance. For the evaluation of the integrals contained in (53), (54), (55), we have introduced the idea of stationary points of an oscillating function due to Debye[6] and Lord Kelvin[7]. The integrals in (53), (54), (55) may be of the forms:

---

[5] G. N. WATSON, *Theory of Bessel Functions* (Cambridge, 1922), 394.

$$\frac{1}{2}\sqrt{\frac{1}{2\pi r}}\int_0^\infty\Big[e^{i\left\{\left(c_1t-\frac{2m+1}{4}\pi\right)+(V_0t+r)k-c_2tk^2\right\}}$$

$$+e^{-i\left\{\left(c_1t-\frac{2m+1}{4}\pi\right)+(V_0t+r)k-c_2tk^2\right\}}$$

$$+e^{i\left\{\left(c_1t+\frac{2m+1}{4}\pi\right)+(V_0t-r)k-c_2tk^2\right\}}$$

$$+e^{-i\left\{\left(c_1t+\frac{2m+1}{4}\pi\right)+(V_0t-r)k-c_2tk^2\right\}}\Big]k^{m+2q+\frac{1}{2}}dk,\quad [m>2]\quad (56)$$

$$\frac{1}{2}\sqrt{\frac{1}{2\pi r}}\int_0^\infty e^{-\frac{a^2k^2}{4}}\Big[e^{i\left\{\left(c_1t-\frac{3}{4}\pi\right)+(V_0t+r)k-c_2tk^2\right\}}$$

$$+e^{-i\left\{\left(c_1t-\frac{3}{4}\pi\right)+(V_0t+r\,k-c_2tk^2\right\}}$$

$$+e^{i\left\{\left(c_1t+\frac{3}{4}\pi\right)+(V_0t-r)k-c_2tk^2\right\}}$$

$$+e^{-i\left\{\left(c_1t+\frac{3}{4}\pi\right)+(V_0t-r)k-c_2tk^2\right\}}\Big]k^{\frac{3}{2}}dk,\qquad [m=1]\quad (57)$$

$$\frac{1}{2}\sqrt{\frac{1}{2\pi r}}\int_0^\infty e^{-\frac{a^2k^2}{4}}\Big[e^{i\left\{\left(c_1t-\frac{\pi}{4}\right)+(V_0t+r)k-c_2tk^2\right\}}$$

$$+e^{-i\left\{\left(c_1t-\frac{\pi}{4}\right)+(V_0t+r)k-c_2tk^2\right\}}$$

$$+e^{i\left\{\left(c_1t+\frac{\pi}{4}\right)+(V_0t-r)k-c_2tk^2\right\}}$$

$$+e^{-i\left\{\left(c_1t+\frac{\pi}{4}\right)+(V_0t-r)k-c_2tk^2\right\}}\Big]k^{\frac{1}{2}}dk.\qquad [m=0]\quad (58)$$

Now, we have to equate the derivative of the factor { } in the index of each exponential of these integrals to zero as follows:

$$\frac{d}{dk}\Big\{\qquad\qquad\Big\}\equiv 0,\cdots\cdots\cdots\cdots\cdots\cdots\cdots\cdots\cdots(59)$$

---

6) P. Debye, *Math. Ann.*, **67**, 535.

7) W. Thomson, *Proc. Roy. Soc.*, **42** (1887), 80.

the solution of this equation being named k_1. We get, for the first and the second terms of each integrand of (56), (57), (58),

$$k_1 = \frac{V_0 t + r}{2c_2 t}\,; \quad \cdots\cdots\cdots\cdots(60)$$

and, for the third and the fourth terms of the same integrand,

$$k_1 = \frac{V_0 t - r}{2c_2 t}. \quad \cdots\cdots\cdots\cdots(60')$$

In (60) and (60′) k_1 should be positive, because of the fact that k_1 must lie within the range of integration, namely between zero and infinity in the present case. Hence we must have

$$V_0 t > r. \qquad [t > 0,\ r > 0] \quad \cdots\cdots\cdots\cdots(61)$$

We have also to find the value of

$$\frac{d^2}{dk^2}\left\{ \qquad \right\}, \quad \cdots\cdots\cdots\cdots(62)$$

its value being

$$\mp 2c_2 t. \quad \cdots\cdots\cdots\cdots(63)$$

In this the upper sign is taken for the first and the third terms of each integrand, and the lower sign for the second and the fourth terms of the same integrand.

Thus, by the criterion of Kelvin and Debye, we obtain the integrals of (56), (57), (58) in the forms:

$$\frac{1}{\sqrt{2c_2 t r}}\left[\left\{\frac{V_0 t - r}{2c_2 t}\right\}^{m+2q+\frac{1}{2}} \cos\left\{c_1 t + \frac{2m+1}{4}\pi + \frac{(V_0 t - r)^2}{4c_2 t} - \frac{\pi}{4}\right\}\right.$$
$$\left. + \left\{\frac{V_0 t + r}{2c_2 t}\right\}^{m+2q+\frac{1}{2}} \cos\left\{c_1 t - \frac{2m+1}{4}\pi + \frac{(V_0 t + r)^2}{4c_2 t} - \frac{\pi}{4}\right\}\right],$$
$$[V_0 t > r;\quad m > 2] \quad \cdots\cdots\cdots(64)$$

$$\frac{1}{\sqrt{2c_2 t r}}\left[\left\{\frac{V_0 t - r}{2c_2 t}\right\}^{\frac{3}{2}} e^{-\frac{a^2}{4}\left(\frac{V_0 t - r}{2c_2 t}\right)^2} \cos\left\{c_1 t + \pi + \frac{(V_0 t - r)^2}{4c_2 t}\right\}\right.$$
$$\left. + \left\{\frac{V_0 t + r}{2c_2 t}\right\}^{\frac{3}{2}} e^{-\frac{a^2}{4}\left(\frac{V_0 t + r}{2c_2 t}\right)^2} \cos\left\{c_1 t - \pi + \frac{(V_0 t + r)^2}{4c_2 t}\right\}\right],$$
$$[V_0 t > r;\quad m = 1] \quad \cdots\cdots\cdots(65)$$

and similar expression when $m = 0$.

The expressions of w then become

$$w = \frac{A \cos m\theta}{\sqrt{c_2 tr}} \sum_{q=0}^{\infty} \frac{(-1)^q a^{m+2q+2}}{2^{3m+6q+4}\, q!} \frac{\Gamma\left(\frac{m}{2}+q+\frac{3}{2}\right)}{\Gamma(m+q+1)} \left[\left(\frac{V_0 t - r}{c_2 t}\right)^{m+2q+\frac{1}{2}} \cos\left\{c_1 t + \frac{m\pi}{2} + \frac{(V_0 t - r)^2}{4c_2 t}\right\} + \left(\frac{V_0 t + r}{c_2 t}\right)^{m+2q+\frac{1}{2}} \cos\left\{c_1 t - \frac{m+1}{2}\pi + \frac{(V_0 t + r)^2}{4c_2 t}\right\}\right]$$

$$[V_0 t > r; \quad m > 2] \cdots\cdots\cdots(66)$$

$$w = \frac{Aa^3}{16} \frac{\cos\theta}{\sqrt{c_2 tr}} \left[\left(\frac{V_0 t - r}{c_2 t}\right)^{\frac{3}{2}} e^{-\frac{a^2}{4}\left(\frac{V_0 t - r}{2c_2 t}\right)^2} \cos\left\{c_1 t + \frac{(V_0 t - r)^2}{4c_2 t} + \pi\right\} + \left(\frac{V_0 t + r}{c_2 t}\right)^{\frac{3}{2}} e^{-\frac{a^2}{4}\left(\frac{V_0 t + r}{2c_2 t}\right)^2} \cos\left\{c_1 t + \frac{(V_0 t + r)^2}{4c_2 t} - \pi\right\}\right],$$

$$[V_0 t > r; \quad m = 1] \cdots\cdots\cdots(67)$$

$$w = \frac{Aa^2}{4} \frac{1}{\sqrt{c_2 tr}} \left[\sqrt{\frac{V_0 t - r}{c_2 t}}\, e^{-\frac{a^2}{4}\left(\frac{V_0 t - r}{2c_2 t}\right)^2} \cos\left\{c_1 t + \frac{(V_0 t - r)^2}{4c_2 t}\right\} + \sqrt{\frac{V_0 t + r}{c_2 t}}\, e^{-\frac{a^2}{4}\left(\frac{V_0 t + r}{2c_2 t}\right)^2} \cos\left\{c_1 t + \frac{(V_0 t + r)^2}{4c_2 t} - \frac{\pi}{2}\right\}\right].$$

$$[V_0 t > r; \quad m = 0] \cdots\cdots\cdots(68)$$

When $V_0 t < r$, the integrals in (56), (57), (58) disappear owing to the cancelling nature of the fluctuating functions of the integrands. Hence we may write

$$w = 0. \qquad [V_0 t < r] \cdots\cdots\cdots\cdots\cdots\cdots\cdots\cdots(69)$$

Though the expressions of u and v may be obtained in similar manners as that employed in the evaluation of w, I have omitted the investigation of such components for the sake of simplicity.

A few examples of the space distribution of the displacements of the case in which $\frac{c_1 a}{V_0} = \frac{0{\cdot}001}{3}$ and $\frac{c_2}{V_0 a} = 0{\cdot}06$ are shown in Figs. 1, 2, 3, 4. Fig. 1 gives the case, $m = 0$, $\frac{V_0 t}{a} = 7{\cdot}5$, while Fig. 2 the case, $m=0$, $\frac{V_0 t}{a} = 15$. Both of these cases belong to the waves due the initial disturbance of the type:

$$t = 0, \quad z = 0: \quad f(r) = A\,e^{-\frac{r^2}{a^2}}; \quad \text{.........................(70)}$$

but correspond to different stages of the transmission of the disturbance. Figs. 3 and 4, both belonging to the kind, $m = 1$, give the cases, $\frac{V_0 t}{a} = 7{\cdot}5$ and $\frac{Vt}{a} = 15$ respectively. The original disturbance is of the type:

$$t = 0, \quad z = 0: \quad f(r)\cos\theta = A\frac{r}{a}\,e^{-\frac{r^2}{a^2}}\cos\theta. \quad \text{............(71)}$$

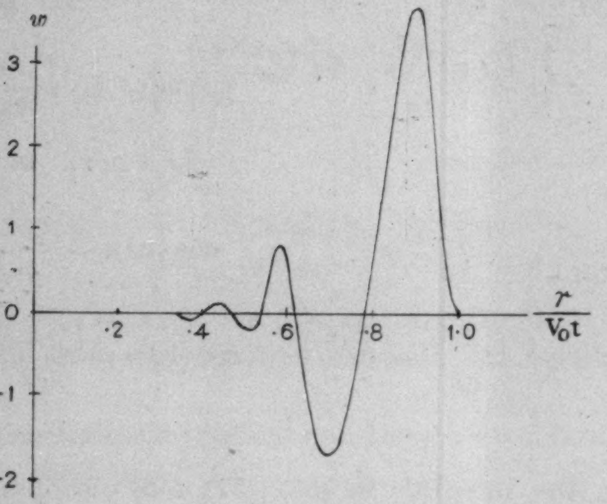

Fig. 1. $m = 0, \quad \frac{V_0 t}{a} = 7{\cdot}5.$

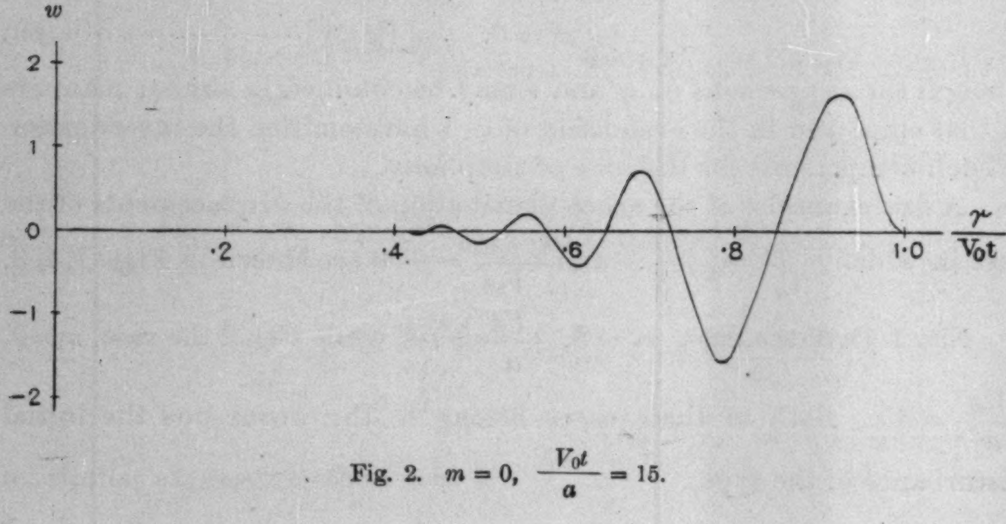

Fig. 2. $m = 0, \quad \frac{V_0 t}{a} = 15.$

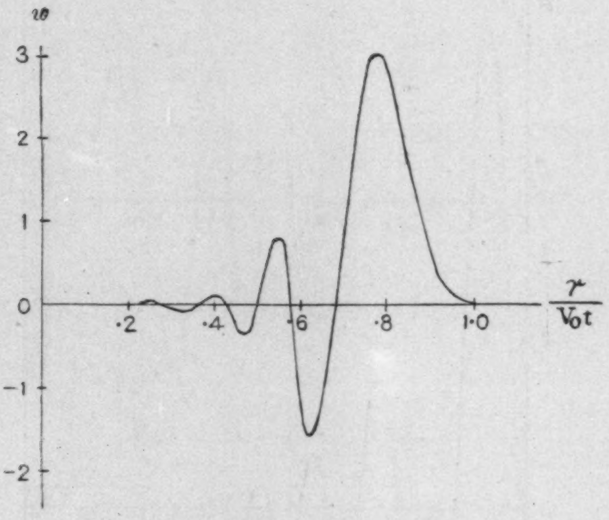

Fig. 3. $m = 1, \quad \frac{V_0 t}{a} = 7{\cdot}5.$

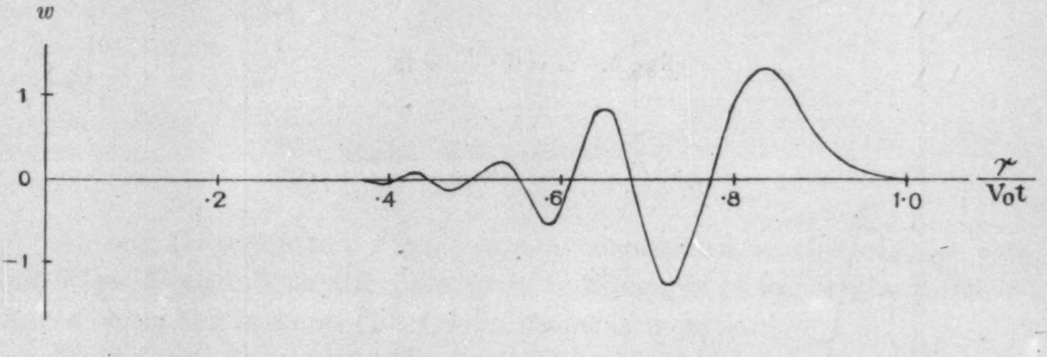

Fig. 4. $m = 1, \quad \frac{V_0 t}{a} = 15.$

Similar examples of the time variation of the displacement at some distances from the epicentre are shown in Figs. 5, 6, 7, 8; the values of $\frac{c_1 a}{V_0}$ and $\frac{c_2}{V_0 a}$ being taken to be the same as those of the last examples.

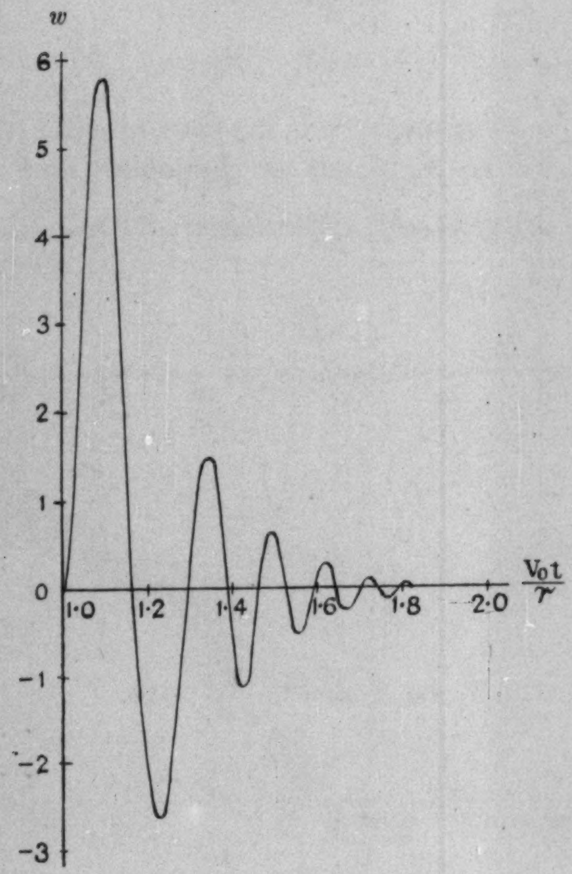

Fig. 5. $m = 0, \quad \frac{r}{a} = 15.$

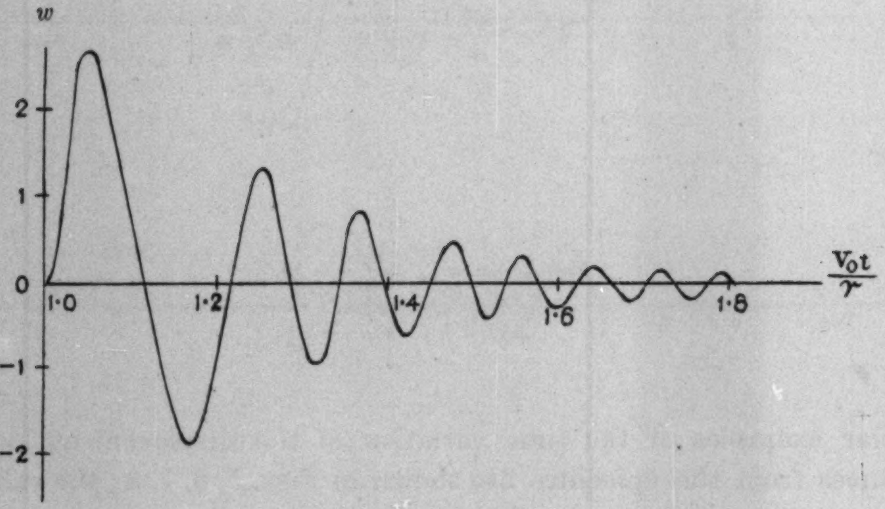

Fig. 6. $m = 0, \quad \frac{r}{a} = 30.$

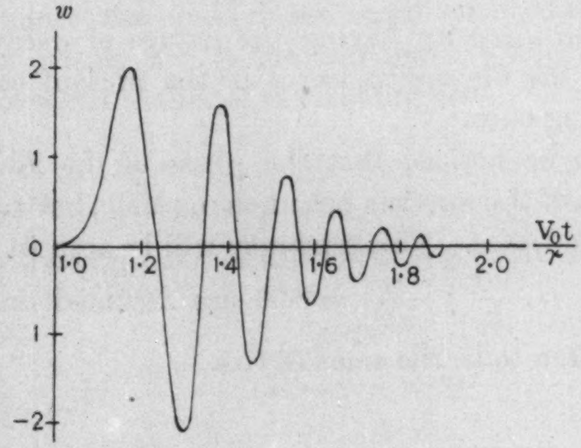

Fig. 7. $m = 1,\quad \frac{r}{a} = 15.$

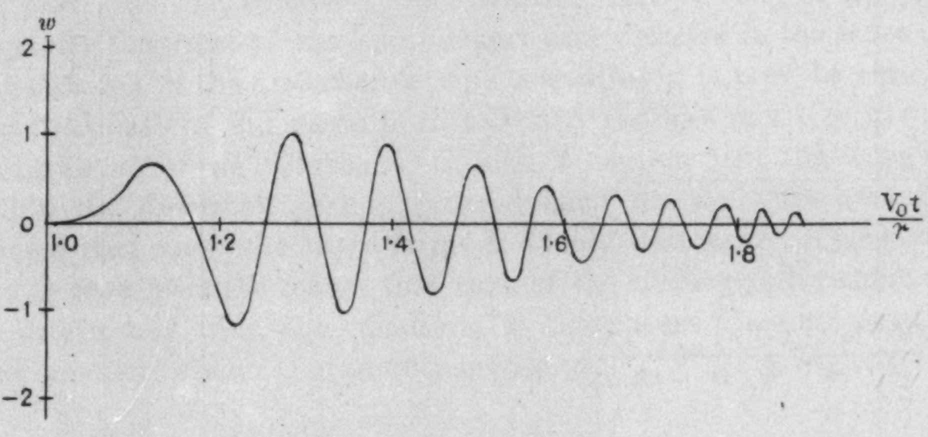

Fig. 8. $m = 1,\quad \frac{r}{a} = 30.$

Among these figures, Figs. 5 and 6 correspond to the case $m = 0$ and Figs. 7 and 8 to the case $m = 1$, the types of the original disturbances being the same as (70), (71) in respective cases.

From these figures and the preceding equations, it may be seen that the transmitted waves are more and more dispersed as the distance from the epicentre increases, and the leading part of the dispersed waves is propagated with the definite velocity of the ordinary Rayleigh-waves. It appears, moreover, that in spite of the concentrated type of the original disturbance, the propagated waves are of harmonic types, with gradually decreasing periods and amplitudes. This fact is in good accordance with some of seimic records. The wave length of the oscillatory part becomes larger and the form of the displacement is more and more flattened as the waves proceed. We have not introduced any element like solid viscosity having the nature of decaying the waves; yet we find that the dispersive waves of the present case indicate the feature of diffusing ones.

It is also to be noticed that the phase of the leading part of the disturbed portion of the waves is not unchangeable, but varies during the progression of the waves. This tendency will be seen in Fig. 9. In this case, $m=0,\ \frac{c_1 a}{V_0}=\frac{0{\cdot}1}{3};\ \frac{c_2}{aV_0}=0{\cdot}06$ are assumed and the original disturbance is taken to be the same as (70).

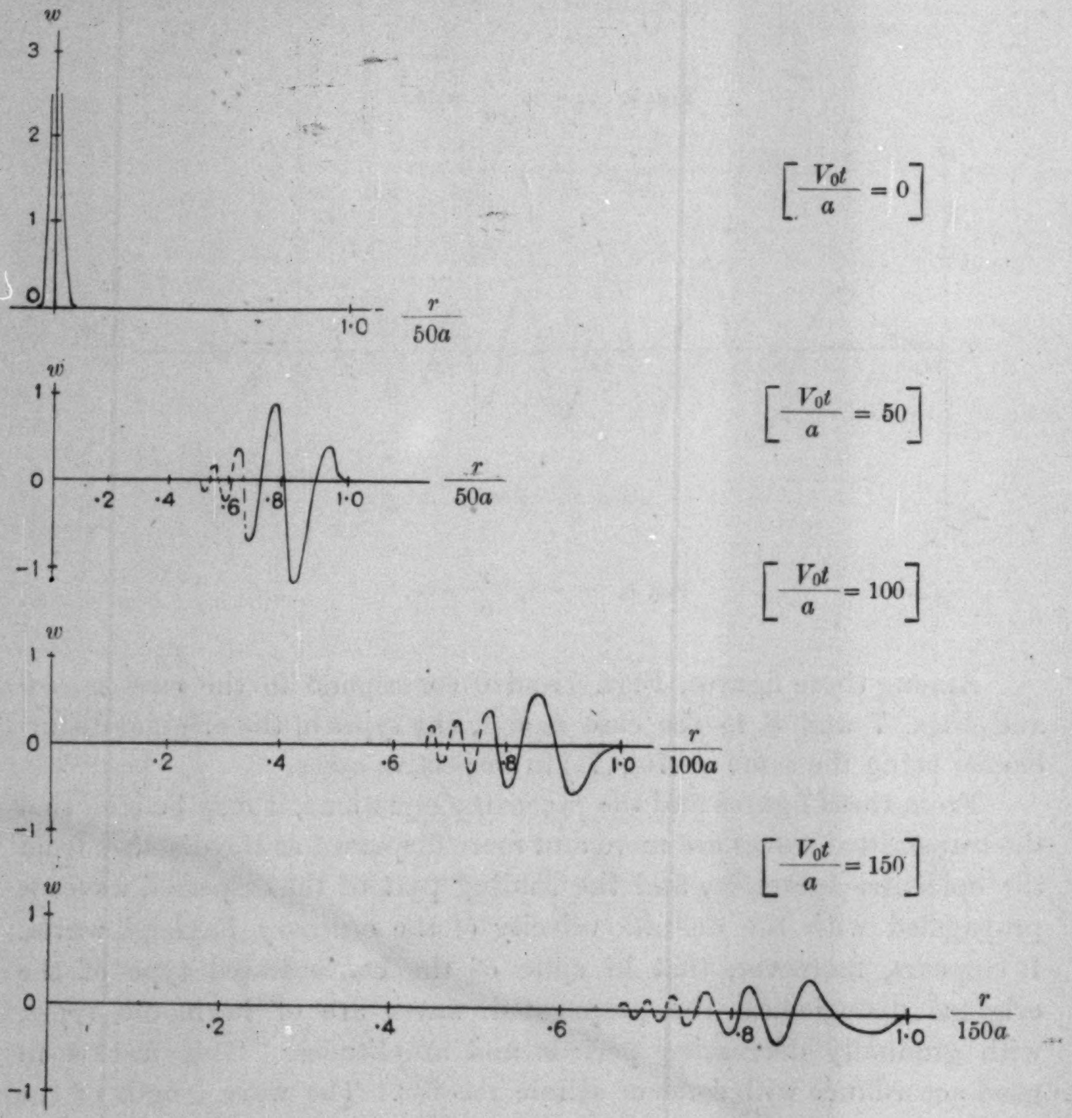

Fig. 9. $m=0,\ \frac{c_1 a}{V_0}=\frac{0{\cdot}1}{3},\ \frac{c_2}{aV_0}=0{\cdot}06,$

The variation of the phase in the neighbourhood of the leading part of the waves is mainly due to the fact that the velocity of the phase of the waves is not equal to that of the leading part. Consider

$$\left.\begin{matrix}\cos\\ \sin\end{matrix}\right\}\left\{c_1 t+\frac{(V_0 t-r)^2}{4c_2 t}\right\}. \quad\cdots\cdots\cdots\cdots\cdots\cdots(72)$$

Differentiating the argument of this harmonic function with respect to t, we find

$$\frac{\partial r}{\partial t}=V_0+\frac{2c_1c_2t}{(V_0-r)}-\frac{V_0t-r}{2t}. \quad\cdots\cdots\cdots\cdots\cdots\cdots(73)$$

In this equation $\frac{\partial r}{\partial t}$ is the phase velocity, while V_0 that of the leading part. We may thus easily find that the phase velocity in many cases is greater than that of the leading part and directed in the sense of the transmission of the disturbance; and accordingly it may be concluded that the phase of the waves in this vicinity changes in the course of the transmission of the disturbance in such a manner that the wave forms within the disturbed portion proceed from the tail part towards the leading part where the wave forms suddenly disappear. This fact may also be seen from the reason that each of the nodal points, which are to be determined from the equation (72), disappears discontinuously one after another, when t is grudually increased.

VII. Group and Phase Velocities.

It is not without importance to remark here that both of the group and the phase velocities are variable with respect to the wave length and the time. We can write from (41) the expression of the group velocity U such that

$$\begin{aligned}U&=\frac{d(Vk)}{dk}\\ &=\frac{d(V_0k+c_1-c_2k^2)}{dk}\\ &=V_0-2c_2k. \quad\cdots\cdots\cdots\cdots\cdots\cdots(74)\end{aligned}$$

The maximum group velocity is evidently V_0, which is the same as the velocity of propagation of Rayleigh-waves. This maximum occurs when the length of the elementary waves is infinitely long. The other group velocities are all less than V_0. Thus, we find why the wave length in the neighbourhood of this part is relatively long. The reason that the length of the disturbed portion is more and more prolonged as the waves are transmitted, is also understood. Nextly, the phase velocity, as it may be seen from the equation (73), is also variable with respect to r and t. In the immediate neighbourhood of the point, $r = V_0t$, it becomes exceedingly large. This, however, only occurs at the very point of $r = V_0t$ and at a point very near to this the velocity is not so high, so that there needs a certain interval of time before the phase of the leading part changes its sign.

When we examine the forms of the equations (66), (67), (68), we shall find that c_2 plays an important part in the action of flattening the wave forms and of the elongation of the wave length, while c_1 is most effective in changing the phases of the leading part of the disturbed portion of the waves. We know that c_1 and c_2 are connected with the gravity force of the solid and the superposition of the water respectivety, so that it may be concluded that the gravity mainly changes the phase of the waves and the superposed water the form of waves.

VIII. Undispersive Waves.

Lastly, we may add a few remarks on the propagation of Rayleigh-waves on the surface of a simple semi-infinite solid body. In this case the solution can be obtained by putting $c_1 = c_2 = 0$ in (53), (54), (55). If we take only the cases $m = 0$ and $m = 1$, we get, by means of the formula,

$$\left.\begin{aligned} \int_0^\infty J_0(kr)\sin kV_0t\,dk &= \frac{1}{\sqrt{(Vt)^2-r^2}}, & [Vt > r] \\ ,, \quad &= 0, & [Vt < r] \end{aligned}\right\}^{8)} \cdots\cdots(75)$$

the solutions of the forms:

$$\left.\begin{aligned} w &= -\frac{Aa^2}{2}\left[\frac{(Vt)}{\{(Vt)^2-r^2\}^{\frac{3}{2}}} + \frac{a(Vt)\{6(Vt)^2+5r^2\}}{4\{(Vt)^2-r\}^{\frac{7}{2}}} + \cdots\cdots\right], \\ & \qquad\qquad\qquad\qquad [m = 0;\quad Vt > r] \\ ,, &= 0, \qquad\qquad\qquad\qquad [m = 0;\quad Vt < r] \end{aligned}\right\} \cdots\cdots(76)$$

---

8) H. LAMB, *Proc. Math. Soc.*, London [2], **7** (1907), 122; S. SANO, *Bull. Centr. Met. Obs.*, Japan, **2** (1913), 13.

and

$$\left.\begin{aligned} w &= \frac{Aa^3}{4}\cos\theta\left[\frac{3(Vt)r}{\{(Vt)^2-r^2\}^{\frac{5}{2}}}+\frac{a^2(Vt)r\{52(Vt)^2+25r^2\}}{4\{(Vt)^2-r^2\}^{\frac{9}{2}}}+\cdots\cdots\right\}, \\ &\qquad\qquad\qquad\qquad\qquad\qquad [m=1;\quad Vt>r] \\ ,, &= 0. \qquad\qquad\qquad\qquad\qquad\quad [m=1;\quad Vt<r] \end{aligned}\right\}\quad(77)$$

The results for which $m = 0$ and $m = 1$ are shown in Figs. 10, 11, 12, 13. It may be seen that no fluctuating phenemenon happens, but

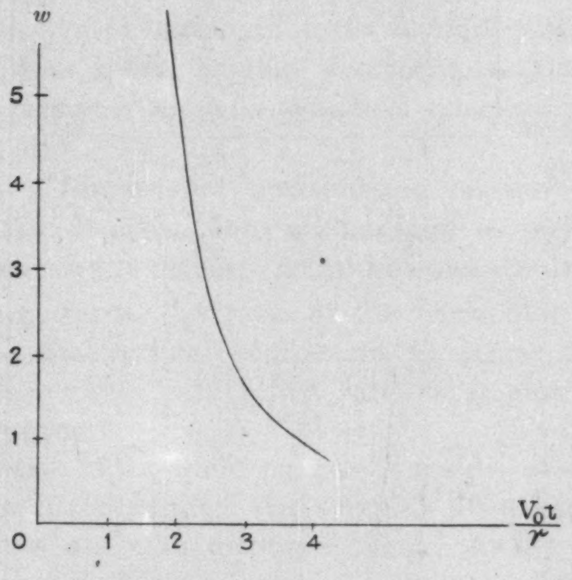

Fig. 10. $m = 0, \quad \frac{r}{a} = 2.$

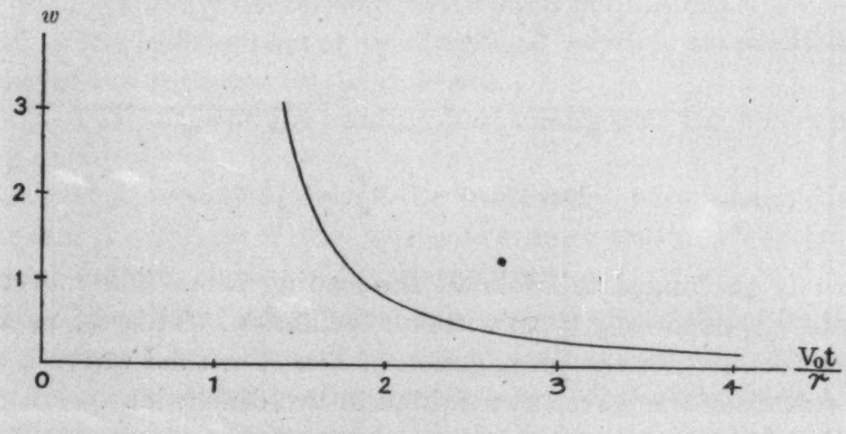

Fig. 11. $m = 0, \quad \frac{r}{a} = 5.$

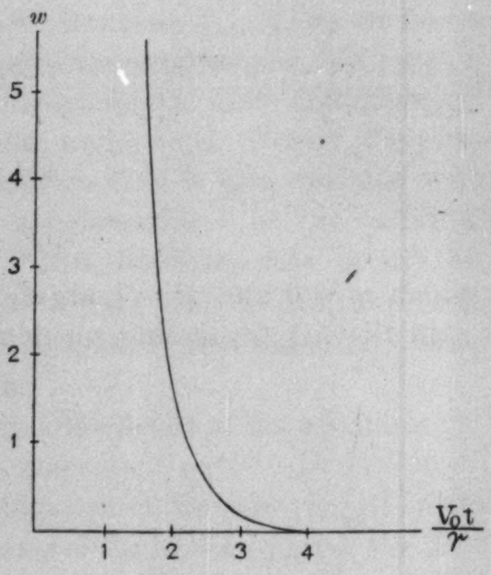

Fig. 12. $m = 1, \quad \frac{r}{a} = 2.$

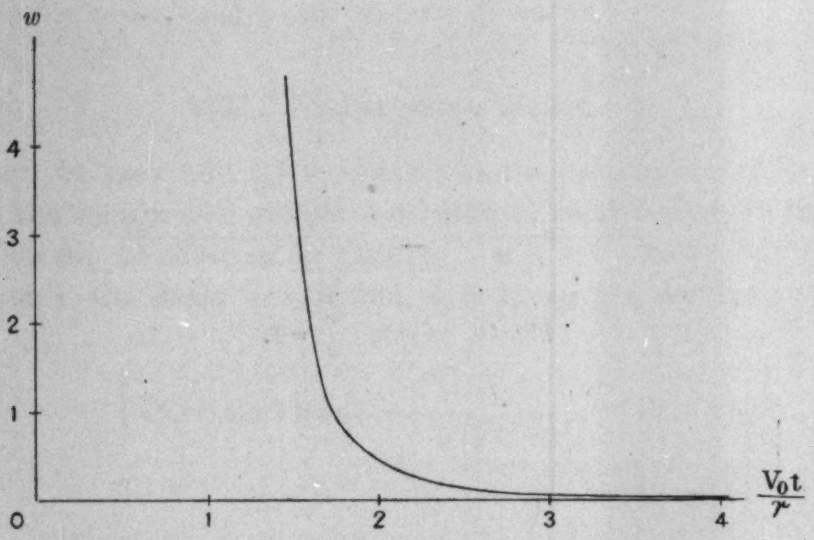

Fig. 13. $m = 1, \quad \frac{r}{a} = 5$

an infinitely prolonged tail follows the leading part. The movement is of a gradually subsiding type without oscillation. This is, as already noticed by Lamb[9] for the propagation of sound or tidal waves, a characteristic feature of the waves transmitted in two dimensions.

---

[9] H. LAMB, *Proc. Math. Soc.*, London, 35 (1902), 141.

XI. Summary.

We may now complete this paper with a brief summary.

1. The viscosity of water gives no influence upon the transmission of Rayleigh-type waves on the bottom surface of an ocean.

2. The compressibility of water is effective only on the movement of the superposed water, but not on the motion of the ground.

3. The pressure of the water in the sense of forming surface water waves is of a great importance in connection with the transmission of the seismic waves.

4. The velocity of harmonic waves changes with the wave length, and this velocity is quick or slow according as the wave length is long or short. There is no definite critical velocity for harmonic waves of an infinite extent.

5. In a two-dimensional transmission of waves, the azimuthal component of the displacements of the solid as well as of the water becomes quiescent as the distance from the epicentre is increased.

6. For long waves, the ratio of the horizontal component of the displacement to the vertical component is larger than that of the ordinary Rayleigh-waves, while this ratio is smaller than that of the latter for short waves.

7. The motion of the water particle is mainly of a vertical type.

8. However concentrated the original disturbance may be, the transmitted waves are of a dispersed form. As the distance from the epicentre is increased, this tendency becomes more distinct.

9. The dispersed waves are apparently of an oscillatory type, having a tail with gradually decreasing periods and amplitudes.

10. The leading part of the dispersed waves is propagated with the velocity of the ordinary Rayleigh-waves.

11. The phase of the leading part changes as the waves proceed to a long distance.

12. The wave lengths of the oscillatory part become larger and larger and the forms of the waves are more and more flattened in the course of the progression of the disturbance.

13. The disturbed portion has various group velocities depending upon the harmonic elements involved in that portion. The maximum of the group velocities is the same as that of Rayleigh-waves, and this maximum velocity corresponds with the harmonic element of an infinitely long wave length.

14. The phase velocity is also variable for different parts of the disturbed waves.
15. When the effects of gravity and of water are omitted, the transmitted waves due to a concentrated disturbance is of a gradually subsiding type without oscillation.

In conclusion I must express my sincerest thank to Dr. G. Nishimura who has assisted me in preparing this paper. All of the numerical calculations, of which the result is shown in Figs. 1–13, have, indeed, been carried out by him in his accomplished mathematical ability.

10. 洋底に傳はる地震波に就て

地震研究所 妹澤克雄

此論文の目的は地震波が洋底に於て二次元的に波動する場合の諸現象を數學的に研究する事にある。調和波が一次元的に傳播する場合に其波動速度を求める事は既に一二の學者によつて手をつけられて居るけれども、それ以外の事は未だ誰も注目して居らぬ樣に見える。二次元的の場合、殊に勝手な震動が發生した場合に其が傳播して行く模樣を研究して見ると、種々の不思議な事柄が見出されるのである。其等を取纒めて箇條書きとし、且つ計算中に得た特別な結果を附加へて見ると大體次の如くなる。

1. 水の粘性は洋底を傳はるレーリー型地震波に對して殆ど影響を與へぬものである。
2. 水の壓縮性は地震と共に動く水の運動には非常に影響を與へるけれども、土地それ自身の震動にはあまり異常を起さぬものと考へられる。
3. 水の重力的壓力は地震の波動に非常に關係がある。
4. 洋底を傳播する地震波が調和型である場合に、其速度は波長によつて異なり、長波の場合には速に、短波の場合には遲くなる。而して其波動速度の局限などといふものは見當らぬ。
5. 二次元的傳播に於て波動方向に直角な向の振動は、土地の震動に就ても水の動きに就ても、振動部が震源から遠かるに從て非常に速に減少する事がわかる。
6. 波長が長い場合には波動方向に平行な向の振幅と其に直角な鉛直方向の向の振幅との比が普通のレーリー波の場合の其比よりも大なる事がわかり、又波長が短い時は其が逆になる事が知られる。
7. 水の振動は鉛直方向が一番大である。
8. 源點の震動が如何に集中性のものであつても、傳播する波は分散性を有し、震源から距離が遠くなるに從て波動部分が一層分散して行くものである。
9. 分散した波は割合に規則正しい繰替しの振動性を有し、振動形の後の部位程、振幅は小さく、振動週期は短くなるのである。

10. 振動の初動部は水のない場合の純粋のレーリー波の速度で傳播する。

11. 初動部の位相は地震波が遠方へ進むに從て漸次變つて行く事がわかる。

12. 分散波動の波長は地震波が遠方へ進むに從て次第に長くなり、振幅の形狀は次第に低く平たくなる。

13. 擾亂部分は種々の群波速度を有し、其最大極限の速度はレーリー波の速度に等しい。此等の群波速度は擾亂部分中にある調和的の波素に因るのであつて、其最大極限の速度は無限に長い波長の波素によるものと考へられる。

14. 位相波の速度は擾亂部分の種々の場所によつて夫々違つて居る樣に思はれる。

15. 重力と水との影響を除いて考へると、波動は初動部から振動する事なく漸次衰へる形狀をなす事がわかる。

此研究に當て種々の數學的考究事項に遭遇した。それを適當に解決したのではあるけれども、猶數多の計算上の困難があつた。しかしこの計算的困難は幸にも西村學士の助力によつて殆ど切拔ける事が出來た事を附記して置く。

11. *On the Curvature of Islands Arc.*

By Torahiko **TERADA**,

Earthquake Research Institute.

(Read March 17, 1931.—Rec. March 19, 1931.)

A few years ago, the present author communicated before the Meeting of the Colloquium of our Institute a short note regarding a supposed relation between the radius of curvature, ρ, of islands arc and its latitude, φ, pointing out that there seems to exist a statistical tendency of a positive correlation between these two quantities.

The subject was recently resumed for a further investigation extending its scope a little more. The result will be briefly reported in the following.

The method of investigation is very simple. In the case of a large arc extending to several ten degrees, a globe of 19-inch diameter was taken and by means of a divider the approximate radius of curvature was estimated and the geographical coordinates, φ_0, λ_0, of its centre of curvature read off. For the shorter arcs Justus Perth's Maps were chiefly used. The latitude of the middle point of the arc, φ_m, was also noted down.

In some cases the arcs are very nearly circular but in many cases not so. In the latter cases there is a margin of arbitrariness in the choice of the circular arc which we assume as best conforming with the islands arc in question. Recently, Dr. Kumagai[1] of Kyoto Imperial University wrote an interesting paper on a method of determining the curvature of nearly circular arc, applying his method to the case of Japan Arc. As, however, the present paper deals with a very rough approximation for a large number of arcs, the simplest method above mentioned was preferred.

On the other hand, the narrow curved strip of land such as the part of Central America extending from Costa Rica to Panama was divided into two nearly circular segments and the respective curvatures were determined.

---

[1] N. KUMAGAI, *Jap. J. Astr. Geophys.*, (1930), 1.

Mountain-ranges were also treated in the similar manner for comparison. In the case of a long extended range, the curvature varies continuously from a positive maximum to the next negative maximum, passing zero value between these two maxima. As, however, we take here the curvature as a measure of the degree of disturbance in the surface features of the earth, it will suffice that we take the maximum curvatures from among the continuously varying train of values, just in the same sense as we measure the intensity of a train of waves as the function of its maximum amplitudes.

In the case of Central-American Arcs the comparison with islands arcs may appear less objectionable than in the case of mountain-ranges. The discussions may, however, be at first suspended and we may proceed to a mere phenomenological comparison.

The results are tabulated in the following:

Table I.

Grp.	Arcs	Abbrev. in Fig.	Centre of Curv.		Centre of Arc. φ_m°	Rad. of Curv. ρ km.
			φ_0°	λ_0°		
Pacific	Aleutian	Aleut.	62·0 N	179·2 E	51·7 N	1180
	Kurile	Kur.	57·7	127·4	47·0	1960
	Honsyû and Hokkaidô*	Hons.-Hok.	42·4	130·2	37·8	930
	Honsyû*	Hons.	41·0	131·5	35·9	800
	Loochoo	Looch.	31·8	121·3	26·3	860
	Marianna	Mar.	17·4	141·6	16·7	690
W. Indies	Cuba, western 3/4	Cub.	18·5	81·7 W	22·5	500
	Windward Is.	Wind.	14·2	64·2	14·0	360
	Costa Rica and W. half of Panama	Cost. Pan.	11·3	81·3	8·5	320
	Panama, eastern 2/3	Pan.	7·7	79·3	9·3	170
Atlantic	Cerigo, Kreta, Karpathos, Rhodos	Kr. Rh.	36·7	25·5 E	35·2	280
	Canaries Is.	Can.	30·0	15·8 W	28·0	240
	Cap Verde Is.	C. Verd.	16·4	24·6	15·3	180
Indian	Luzon, C. Bolinao-Palawan	Luz. Par.	13·8	114·0 E	11·7	660
	Camarines, Samar, E. Mindanao	Cam. Sam.	8·2	119·0	11·0	760
	Andaman, Nicobar	And. Nic.	11·0	100·0	10·5	830
	Sangi, Celebes	Sang. Cer.	3·5	122·5	11·0	340
	Halmahera, C. Bisoa-Tg. Libobo	Halm.	0·8	129·7	0·7	230
	Ceram, Selaroe	Cer. Sel.	5·9 S	129·3	4·5 S	170
	Java, Sumatra	Jav. Sum.	13·0 N	119·0	7·5	2400
	Seychelles, Mauritius	Sey. Maur.	12·9 S	52·7	12·9	1100

* For these two arcs, φ_0 and λ_0 are taken from Kumagai's paper cited.

Table II.

Grp.	Mountain-Ranges	Abbrev. in Fig.	Centre of Curv.		Centre of Arc.	Radius ρ km.
			φ_0°	λ_0°	φ_m°	
Asia	Stanowoi, northern arc.	Stan.	68 N	152 E	62 N	760
	Ural I, between polar circle and 60°N	Ur. I	61	75	63	850
	Ural II, between polar circle and 52°N	Ur. II	58	82	59	1280
	Tannu-ola	Tan.-ol.	49	94	51	280
	Sichota-alin	Sich.-al.	51	121	47	1250
	Altai	Altai	56	102	46	1250
	Altyn, Mus-tag-ata to Tokkus.	Altyn	42	81	36	400
	Alla-tag to Hindukush	Hind.	43	65	35	860
	Himalaya, Kashmir to Bhutan	Him.	39	89	29	1400
Europe and Mediterranean	Erg-Riesen Gebirge	Erz.-Ries	49	15	51	220
	Tatra to E. end of Karpath	Tatr.-Karp.	45	20	49	470
	Jura	Jur.	45	9	47	280
	E. parts of Karpath and Transsilv. Alps.	Karp.-Trans.	46	25	46	90
	Coltic Alps	Colt.	45	9	46	180
	Ligurian Alps	Lig.	43	9	45	140
	Sicily, Calabria	Sic. Cal.	39	14	38	180
	Lesser Atlas	L. Atl.	36	4W	35	150
N. & S. Am.	S. Nevada to S. part of Cascade	Nev.-Casc.	43	110W	40	1000
	Tolima to Misti	Tol. Mist.	4 S	15	7 S	1500
	Misti to Azufre	Mist. Azuf.	23	78	20	1000

These results are also plotted in the annexed figures, Fig. 1 and 2 taking the latitudes φ_m of the middle point of the arcs and the radii of curvature ρ for the abscissae and ordinates respectively. Another figure was also constructed taking the latitude φ_0 of the centre of curvature as abscissa. The qualitative character of the result is, however, not essentially modified by this substitution.

A rather remarkable fact will be observed at the first glance of Fig. 1, namely, the area of the figure may be divided into three regions by means of the two lines I and II such that in each of these regions are grouped those arcs which are situated in a certain coherent portion of the earth's surface. Firstly, the Pacific Group lies in the middle section intercepted between the lines I and II. Also the Group including the West Indies and Central America lies on the same section, though clustered nearer to the origin of coordinates than the Pacific Group.

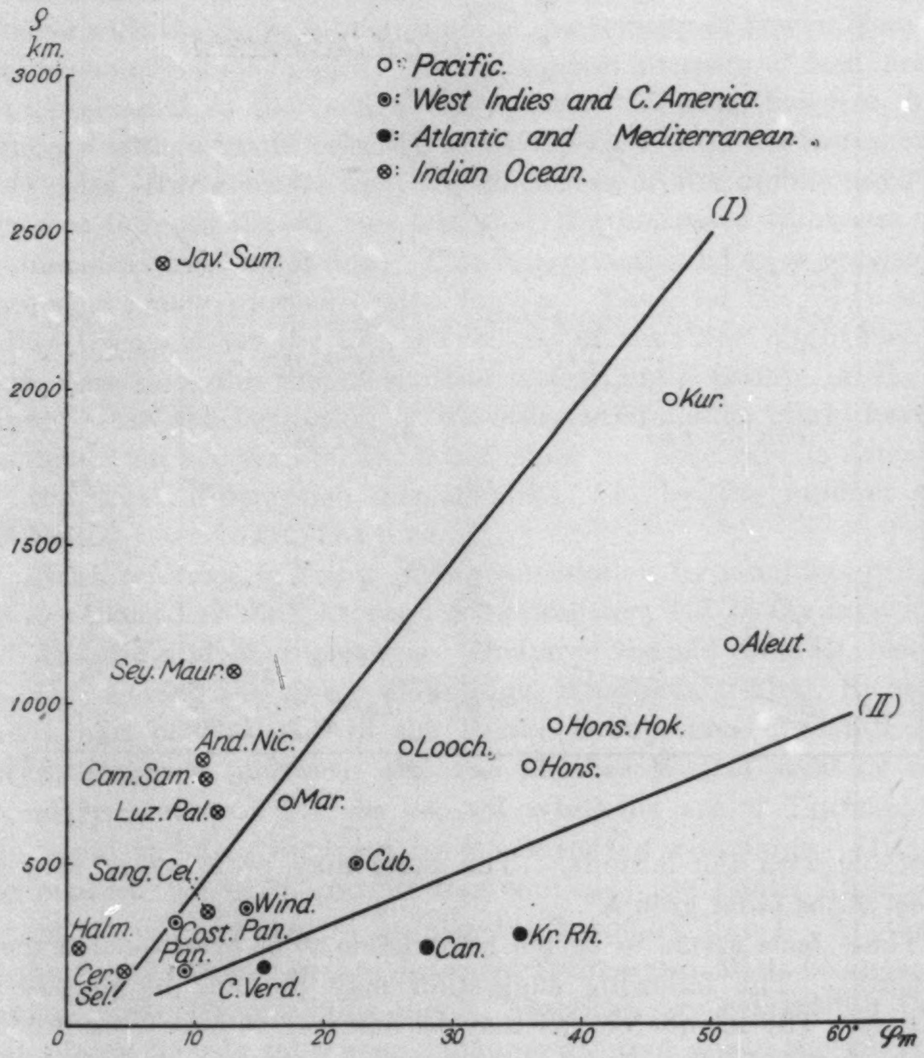

Fig. 1.

This is interesting, as the West Indies is usually cited as belonging to the Pacific type in morphological and petrological characters. Secondly, the Atlantic Group comprising Mediterranean arcs, lies entirely below the line II. Thirdly, the Indian Ocean Group comprising as far as Luzon is mostly above the line I.

Next, referring to the middle section containing the Pacific and the West Indies Groups, we may say that the radius of curvature increases

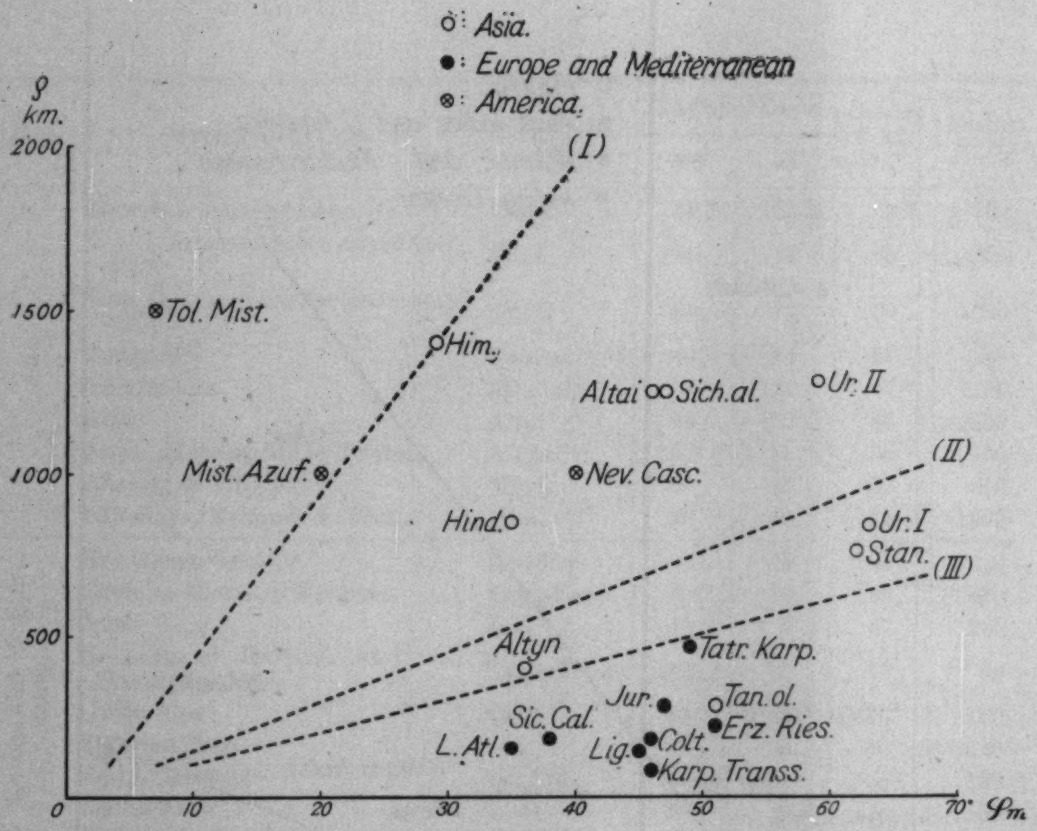

Fig. 2.

statistically with the latitude. The same may probably be said with respect to the other groups[2].

These facts seems to be too remarkable to be overlooked as merely accidental. The following suggestion may perhaps be proposed as plausible. The islands chains may be assumed to have been produced from less curved strips of sial mass by some non-uniform motion of the underlying sima mass. The space variation or fluctuation in the displacement due to this flow, of which the second space derivative is the essential factor for determining the average curvature, will generally increase with the average magnitude of the velocity of flow. Hence, the fact above noticed may signify that the general intensity of flow increases as we proceed from the pole to the equator. This is, however, just in harmony with what is believed to be the case from the arguments on other sides, if we consider that the thickness of the mobile sima layer increases towards the equator and that the increased thickness means the increased freedom of flow. This interpretation taken as provisionally granted, we may proceed a step further. Thus, for the *least disturbed*[3] Indian Ocean either the average velocity of sima flow might have been much less than for the most disturbed Atlantic Group, or the time elapsed since the beginning of the differential motion might have been less for the former than for the latter, since the curvature is determined by the total differential displacement, i.e. by the product of the differential velocity into the time.

---

[2] The irregularity in ρ-φ relation may in some measure be explained by taking the depth of the sea on the concave side of the arc into consideration, especially in the case of the Pacific Group. Thus, the relatively large values of ρ for the Kurile and Loochoo Arcs may be associated with the relative shallowness of the Okhotsk and China Seas respectively, compared with the Bering and Japan Seas. The exceptionally large ρ for Java-Sumatra arc allows the same explanation. An attempt was also made to find some correlation between ρ and the azimuth of the chord of the arc, but no apparent relation could be found.

On the other hand, it seems rather significant that the Marianna approaches the Indian Group and Sangi-Celebes instrudes upon Pacific Group.

Next, referring to Fig. 2 giving ρ-φ relation for mountain-ranges we will see that all of the European mountain-arcs fall in the same zone as the Atlantic and Mediterranean Groups of islands arcs, i.e. below the line II. Among the Asian mountains, Hindukush, Altai, Sichota-alin and a part of Ural fall in the Pacific Group, i.e. between I and II. Altyn, Stanowoi (northern arc) and another part of Ural lie on the boundary zone near the the line, II, while the arc of Tannu-ola alone falls amid the area occupied by the European mountains. Himalayan arc between Kashmir and Bhutan and also the South American arc between Misti and Azufre lie near the boundary line I. Another part of the South American arc between Tolima and Misti belongs to the Indian Ocean Group, while the N. American arc comprising Cascade and Sierra Nevada falls near Japanese Honsyû arc in the midst of the Pacific Group. The distribution may appear quite fortuitous, but if we consider the general statistical tendency we may notice a decided contrast between the European and Asian mountains. It is interesting to observe that in the case of mountain-ranges the line of demarcation between the Asian and European Groups may be drawn much lower than II, somewhere in the position as indicated by III in Fig. 2. S. and N. American taken as a whole may be said to be *less disturbed* than in the other part of the earth.

As to the geotectonic significance of mountain ranges there are still many conflicting theories among the geologists and geophysists. In view of this important problem, the very fact that the ρ-φ relation throws many mountain-ranges into the same batch with the islands arcs in the respectively associated regions will be worthy of notice, as it may serve as a new item among the many pros and cons for and against the existing rival theories.

---

[3] I.e. least curvature or largest ρ.

---

11. 嶋弧の曲率に就て

地震研究所　寺田寅彦

世界中の主なる嶋弧の概略の曲率半徑 ρ を求め、此れと其の弧の中心の緯度 φ_m との關係を圖示して見ると、(ρ, φ_m) 點の分布は全く無秩序ではなく、凡そ三つの群に分れ、それそれの群は地球上での纒まつた區域に相當する。さうして統計的には各群に就き ρ が φ_m と共に增すやうに見える。又山脈弧に就ても同樣の結果が得られる。此結果から考へて、ρ は地殼表面の流動の局部異同によつて生じたものと想像され、もしさうだとすると、上記の ρ-φ_m 關係は、地球の部分により地殼移動の程度に差違あることを示すものと考へられる。

12. A Note on the Results of the Repeated Precise Levellings across the Itô Earthquake Area.

By Chûji **TSUBOI**,

Earthquake Research Institute.

(Read March 17, 1931.—Received March 20, 1931.)

Since February of 1930, an abnormally abundant number of weak earthquakes have taken place in a region near Itô on the east coast of the Idu Peninsula. This seismic activity lasted till the end of May of the same year. There were irregular fluctuations in the daily numbers of the earthquakes during this period. Generally speaking, however, there were two conspicuous maxima in them, the one in the middle of March and the other in the middle of May. The Itô earthquakes which were recorded during this period by a seismograph at Misaki, some 50 km. ENE of Ito, were no less than 6,000 in number. This rather unusual seismic activity seemed to have quited down until the middle of November of the same year when there happened to occur another earthquake swarm. According to the seismometric observations by N. Nasu of our Institute, most of these earthquakes originated from a region some 10 km. N of Itô and it would seem that this seismic activity was an apparently independent one from that of the former Itô earthquake swarms. On Nov. 26th, 1930, on the other hand, a destructive earthquake occurred in the northern part of the Idu Peninsula. The causal relations between these three seismic activities are not yet clear.

With the hope of obtaining, if possible, some information regarding the change of land levels connected with these seismic activities, precise levellings have been carried out three times in 1930 along the eastern coast of the peninsula across the Itô seismic area by the Land Survey Department of the Imperial Army. The levelling route meassured was from B. M. 9328 to B. M. 9344 and is shown in Fig. 1. The results of

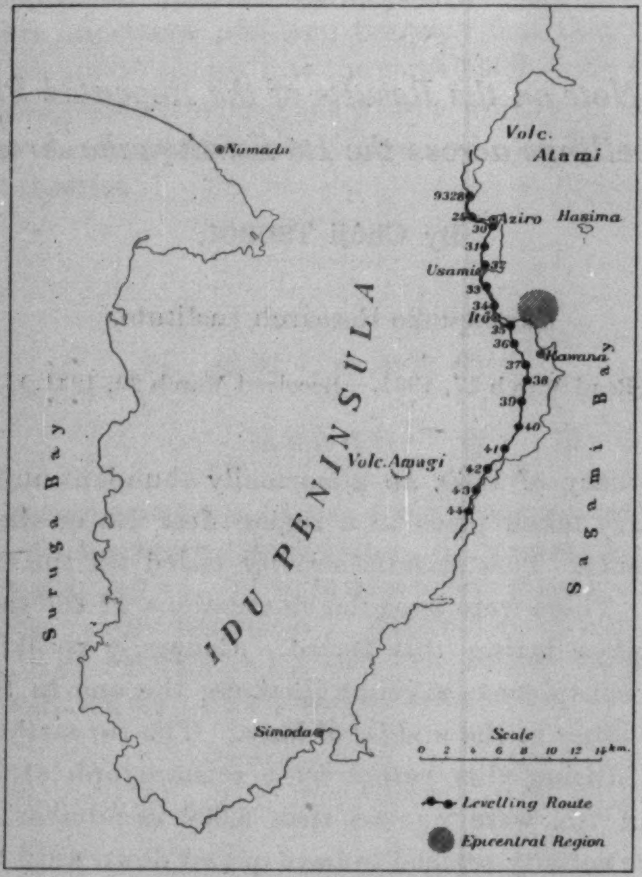
Numadu
Volc. Atami
9328
29
Aziro
Hasima
30
31
Usami
32
33
34
Itô
35
36
Kawana
37
38
39
40
41
42
43
44
Suruga Bay
IDU PENINSULA
Volc. Amagi
Sagami Bay
Simoda
Scale
0 2 4 6 8 10 12 14 km.
Levelling Route
Epicentral Region

Fig. 1.

these measurements, when combined with former levellings of 1903 and 1923, indicate the mode of successive changes of land levels in the region now in question. These five measurements will be referred to as I, II, III, IV and V in chronological order. The time of the respective measurements are as follows:

I 1903
← Kwantô Earthquake
II 1923
III 1930 April
Itô Earthquake Swarms
IV 1930 November
← Idu Earthquake
V 1930 December

The changes of heights of bench marks between successive two surveys are shown in Table I. These values have already been published elsewhere.[1]

Table I.

B. M.	II–I	III–II	IV–III	VI–V
9328	assumed to be stationary	—	—	—
	mm.	mm.	mm.	mm.
9329	– 23·6	– 3·6	+ 6·3	– 21·6
9330	+ 97·6	– 4·9	+ 5·6	+ 9·1
9331	+ 67·1	– 10·5	+ 21·5	+ 17·4
9332	+ 61·6	+ 1·7	+ 35·6	+ 26·9
9333	+ 41·1	+ 10·6	+ 59·4	+ 27·2
9334	—	+ 33·9	+ 81·0	+ 25·0
9335	+ 2·8	+ 72·6	+ 102·3	+ 13·6
9336	0	+ 93·8	+ 118·1	+ 6·8
9337	– 19·5	+ 96·9	+ 122·1	+ 4·3
9338	– 34·4	+ 74·8	+ 88·1	– 2·5
9339	– 59·8	+ 47·5	+ 56·1	– 0·7
9340	– 53·5	+ 21·5	+ 31·8	– 4·5
9341	– 48·2	+ 5·7	+ 6·0	– 8·0
9342	– 42·2	– 7·3	– 11·5	– 8·0
9343	– 31·1	– 11·8	– 17·8	– 10·1
9344	– 24·7	– 26·5	– 21·4	– 14·5

---

1) *Bull. Earthq. Res. Inst.*, **8** (1930), 375.
EARTHQUAKE RESEARCH INSTITUTE, *Proc. Imp. Acad.*, **6** (1930), 399.

The successive changes of heights of the bench marks are graphically shown in Fig. 2. The remarkable upheaval of B. M. 9337 between

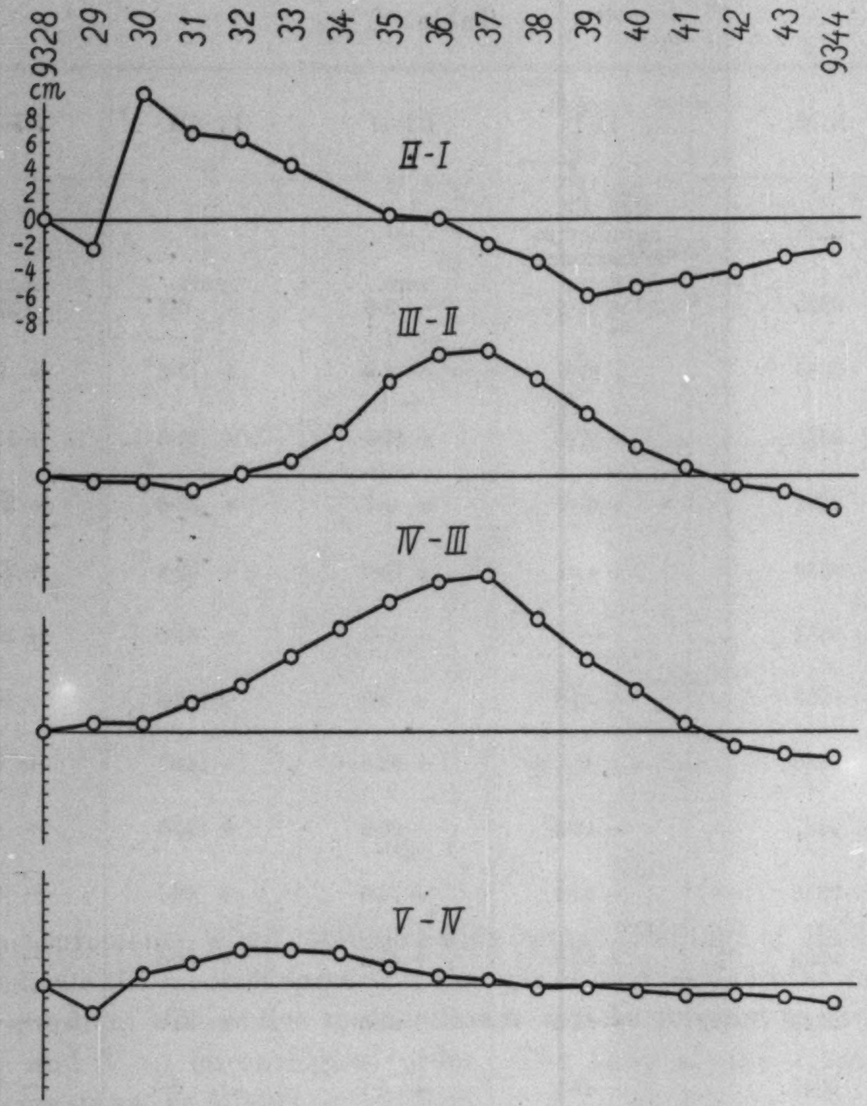

Fig. 2.

II and III, III and IV is at once apparent, and this is no doubt connected with the occurrence of the Itô earthquake swarms. The curves III–II and IV–III are remarkably similar in their forms and thus it is clear that a movement of the same mode was taking place in this district during these two periods. But if we compare the two curves in some detail, there is found a little difference between them. The chief difference is one in the curvatures of the curves in the northern part of the curves. It is concave upward in the curve III–II while it is convex upward in the curve IV–III. How these two curves are similar in one part and is not similar in the other is to be seen in Fig. 3 in which

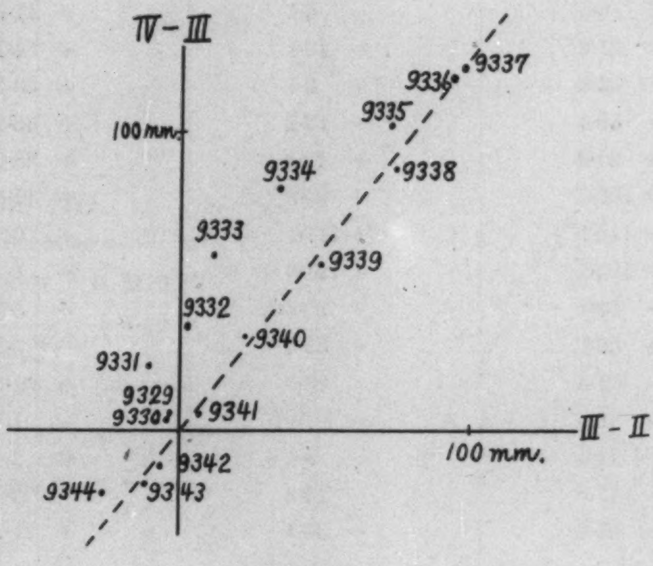

Fig. 3.

the vertical displacements of the bench marks in the period III–II are taken in abscissa and those in the period IV–III in ordinate. If the curves are exactly similar in their forms, the points in the figure should have to lie on one straight line passing the origin of the axes. In our case, we have points 9335, 9334, 9333, 9332, 9331, 9330, 9329 which do not lie on this straight line. These points correspond to the vertical movements of the bench marks on the northern part of the levelling route. On the other hand, in the southern part of the route, the similarity of the two curves is almost exact. The maximum elevations in these curves are 96·9 mm and 122·1 mm respectively, the ratio between them being approximately 0·8. For the purpose of making distinct the difference of the two curves, the values in curve III–II were divided by 0·8 and subtracted from the corresponding values of curve IV–III.

Table II.

IV–III	(III–II) ÷ 0·8	Dif.
mm	mm	mm
0·0	0·0	0·0
+ 6·3	− 4·5	+ 10·8
+ 5·6	− 6·1	+ 11·7
+ 21·6	− 13·1	+ 34·7
+ 35·6	+ 2·1	+ 33·5
+ 59·4	+ 13·2	+ 46·2
+ 81·0	+ 42·4	+ 38·6
+ 102·3	+ 90·8	+ 11·5
+ 118·1	+ 117·2	+ 0·9
+ 122·1	+ 121·0	+ 1·1
+ 88·1	+ 93·6	− 5·5
+ 56·1	+ 59·4	− 3·3
+ 31·8	+ 26·9	+ 4·9
+ 6·0	+ 7·1	− 1·1
− 11·5	− 9·1	− 2·4
− 17·8	− 14·8	− 3·0
− 21·4	− 33·1	+ 11·7

The curve Dif. in Fig. 4 was obtained in this way.

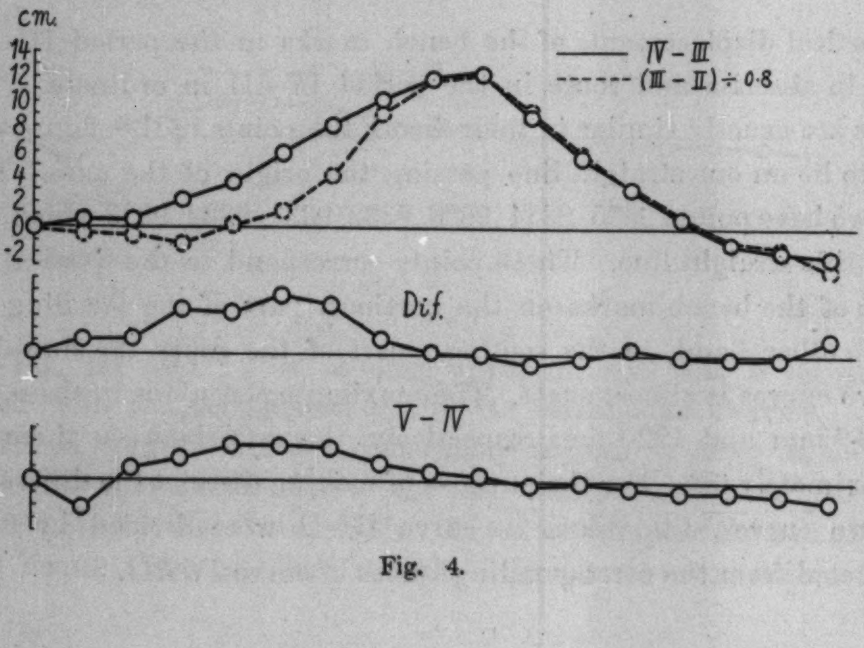

Fig. 4.

The difference is largest at the B. M. 9333. When the curve of difference is compared with the curve V–IV, the similarity in their forms is at once apparent. From these facts, it is naturally concluded that in the interval of the levelling III and IV, two different kinds of level changes took place simultaneously, the one similar to that between III and II and the other similar to that between IV–V. The successive upheavals of the B. M. 9337 and 9333 are thus shown in the following table.

Table III.

	B. M. 9337		B. M. 9333	
	mm	integrated		
II				
	96·9	96·9	—	—
III				
	122·1	219·0	46·2	46·2
IV				
	4·3	223.3	27·2	73·4
V				

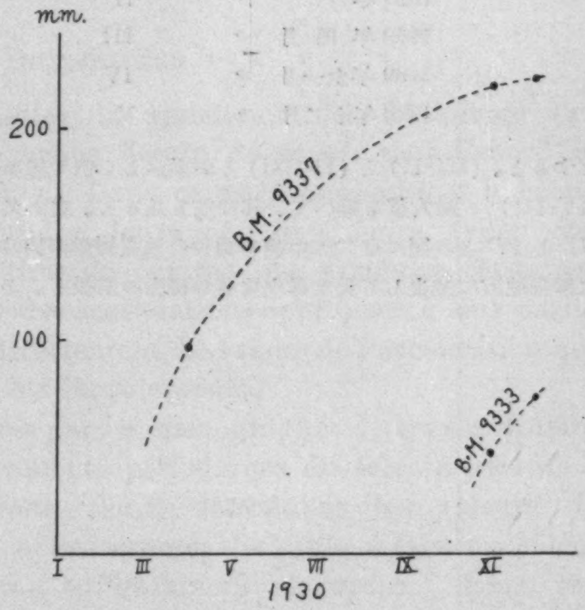

Fig. 5.

These changes in the rate of upheaval of these bench marks are in good accordance with the variation of the recent seismic activities. As was described before, the Itô earthquake swarms began to display their activities from February of 1930 and they seemed to have become apparently dormant at the end of May. On the other hand, another swarm of earthquakes occurred N of Itô in November of 1930. The different location of the seismic active centres and the rate of the upheaval of the respective bench marks seem to be in a close correlation with each other.

In conclusion, the writer wishes to express his sincere thanks to Professor T. Terada for his interests in this work.

12. 伊東地方の水準測量の結果に就いて

地震研究所　坪井忠二

伊豆半島の東海岸に沿つて行はれた水準測量は、既に五回にも達したが、此の小論文は夫等の結果に就いて二三の考察を加へたものである。今

1903年	に行はれたもの	I
1923年	〃	II
1930年四月	〃	III
1930年十一月	〃	IV
1930年十二月	〃	V

とすると、(III-II) と (IV-III) とが形がよく似て居る。それで (III-II) に適當な常數を乘じて (IV-III) と極大値を揃へて、其の差を見ると、之が又 (V-IV) と形が大變よく似る。それで III と IV との間には二つの型の違つた地殼變動が同時に行はれ居たと看做し得る。之等の事實は伊東地方に發生して居た群生地震の勢力の消長と、よく調和する様に見える。

13. *Etude préliminaire sur l'accélération des séismes*

par **Mishio ISHIMOTO,**

Institut de Recherches sur les Tremblements de terre.

(Lu le 16 septembre 1930.—Reçu le 20 mars 1931.)

1. Introduction.

Quand nous voulons étudier la résistance des bâtiments aux ébranlements sismiques, nous avons besoin de savoir tout d'abord les caractéristiques des ébranlements. Dans ce cas, nous sommes habitués à les définir par leurs amplitudes, leurs périodes, leurs types etc. Cependant, considérant les bâtiments comme des systèmes élastiques dont la destruction se réalise par des accélérations appliquées à leur partie basse, nous voulons mesurer directement la valeur de l'accélération qui varie à chaque instant pendant les ébranlements.

Les ébranlements enregistrés par les sismographes de type ordinaire représentent surtout les déplacements périodiques du terrain relatifs à l'espace. Quand nous désirons, donc, déterminer les valeurs de l'accélération correspondantes, nous sommes habitués à faire un calcul qui n'est pas considéré comme suffisamment rigoureux. Dans ces circonstances, nous espérons avoir construit un appareil qui pourra enregistrer directement la valeur de l'accélération des ébranlements.

Bien qu'il y ait deux ou trois appareils[1] construits dans ce but, nous ne trouvons presque pas de mémoires montrant des enregistrements de séismes: cela résulte sans doute de la difficulté qu'il y a à tenir les appareils dans des conditions permanentes pendant les observations.

Supposons qu'il y ait une masse M tenue verticalement par un ressort R (Fig. 1). Pour rendre la condition simple, considérons le cas où la masse est concentrée en un point et où la force restitutive du ressort est assez grande pour

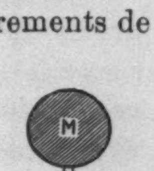

Fig. 1.

---

[1] B. Galizine. *Proc. Roy. Soc.*, A 45 (1919), 492: T. Tamaru, *Proc. Imp. Acad.*, Japan, 3 (1927), 35: J. Obata, *Proc. Phys.-Math. Soc.*, Japan, [3], 9 (1927), 83.

que la force de gravité demeure négligeable. De plus, le déplacement de M est assez petit pour que M puisse être considéré comme décrivant une ligne droite au lieu d'un arc. Designons par ξ le déplacement de M par rapport à l'espace et par x le déplacement du sol par rapport à l'espace. $y=\xi-x$ sera le déplacement relatif de M par rapport au sol et l'équation du mouvement sera

$$M\ddot{\xi}+2\varepsilon(\dot{\xi}-\dot{x})+k(\xi-x)=0,$$

ou

$$M\ddot{y}+2\varepsilon\dot{y}+ky=-M\ddot{x}.$$

Cette équation nous montre que le mouvement de M sous l'action d'une accélération sismique n'est autre que celui de M sous l'action d'une même accélération appliquée directement à la masse, le sol étant immobile. Posons $\frac{2\varepsilon}{M}=2\lambda$, $\frac{k}{M}=n^2$ et $\ddot{x}=-ap^2\sin pt$; de plus si n est assez grand par rapport à p, nous aurons pour solution :

$$y=\frac{ap^2}{n^2}\sin pt+\text{terme d'oscillation propre.}$$

Cette solution nous apprend que nous pouvons évaluer l'accélération sismique par la mesure du déplacement de la masse d'un tel système relativement au sol. Autrement dit, il prouve que nous pouvons observer directement l'accélération sismique à l'aide d'un tel système dont l'oscillation propre est amortie.

Nous avons déjà publié un mémoire[2] sur un accéléromètre capillaire construit dans les conditions rapportées plus haut; mais trouvant qu'il est difficile de faire avec cet appareil des observations continues, nous avons construit une autre appareil qui sert surtout aux études sur les propriétés sismiques. Comme nous nous limitons à constater les caractéristiques des ébranlements au point de vue accélérométrique, nous avons installé une seule composante d'appareil pendant quatre mois dans une pièce souterraine de notre Institut. Nous avons, alors, réussi à enregistrer une vingtaine de séismes répartis dans la région de Kantô. Nous pouvons donc constater certaines caractéristiques des ébranlements qu'on ne peut déduire des sismogrammes ordinaires.

---

[2] M. Ishimoto, *Bull. Earthq. Res. Inst.*, 3 (1927), 87

2. Appareil.

Désiront construire un appareil provisoire, nous choisissons un système tout à fait simple (Fig. 2). Un cylindre de cuivre jaune (M) d'une masse de 3·2 kg est tenu verticalement au moyen de deux lames d'acier (L) fixées séparément le long d'une génératrice de ce cylindre. En faisant tailler les lames, nous sommes arrivés à amener la période de ce système à moins de 0·1 seconde qui n'est pas comparable à celle des oscillations sismiques. Nous avons un bras d'alminium (B) attaché à la masse : son extremité porte une tige (t) qui tourne d'un angle correspondant aux mouvements relatifs de la masse. Un miroir (m) attaché à la tige réfléchit le faisceau lumineux et les mouvements sont enregistrés optiquement sur du papier sensible enroulé sur un tambour tournant (T). La transformation du mouvement de la masse en rotation de la tige est réalisée par un aimant (a) qui ne permet aucun glissement, sans introduire de pression sur la tige. Pour donner une rotation favorable à la tige, nous réalisons un réglage fin au moyen d'un ressort auxiliaire (r) placé sur la pince portante. Naturellement, nous intercalons un prisme rectangulaire (P) sur le passage de la lumière pour en changer la direction.

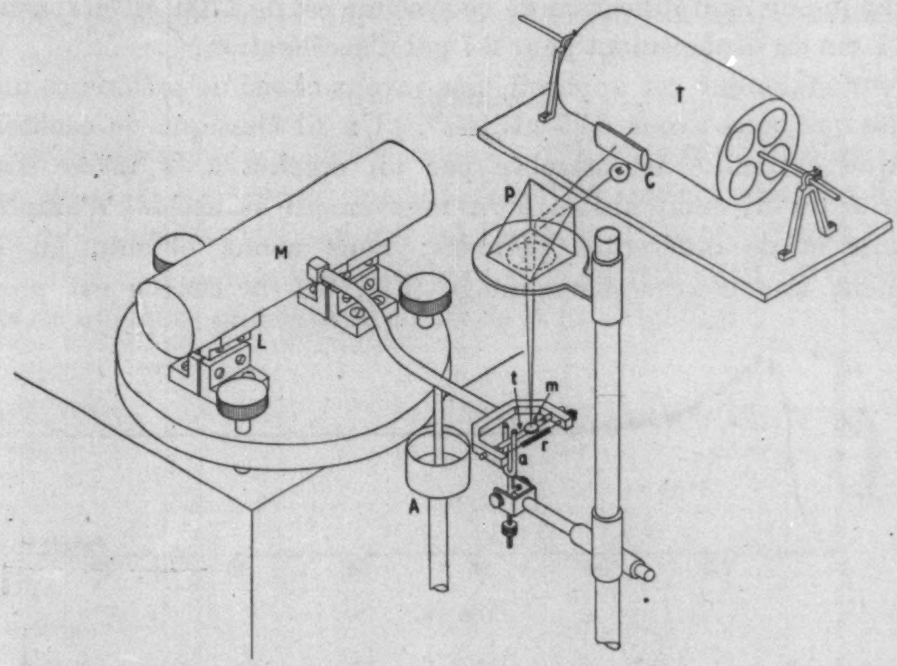

Fig. 2.

Afin d'amortir l'oscillation propre de ce système, nous l'avons muni d'un amortisseur (A) comportant un cylindre léger plongeant dans une petite cuve remplie d'huile. La viscosité du liquide varie certainement énormément avec la température ; mais il n'y aucun moyen d'amortir une si petite période d'oscillation sans utiliser de liquide. Le rapport géométrique de l'amplification de ce système est de 1700 et la sensibilité est de 1 cm de déplacement pour 2·7 gal d'accélération.

Pour étalonner cet appareil, nous avons choisi de préférence un des procédés que nous avons déjà utilisés[3]. Un fil élastique de caoutchouc dont une extrémité est attachée par un crochet à la masse, l'autre extrémité du fil étant animé d'un mouvement sinusoïdal d'amplitude constante et de différentes périodes: nous avons obtenu, en effet, facilement une courbe d'étalonnage (Fig. 3): la courbe est presque horizontale dans la région considérée[4]. Nous n'avons pas réalisé cette fois-ci d'expériences sur une plate-forme oscillante.

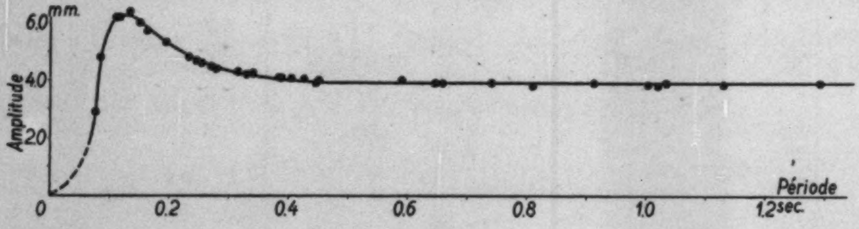

Fig. 3.

Les observations sont exécutées, alors, avec cet appareil installé sur un bloc de ciment dans la cave. Nous nous sommes heurtés toujours au problème de la source lumineuse dont l'intensité demeure insuffisante. Bien que les enregistrements soient assez nets pendant les périodes tranquilles, ils deviennent faibles au moment des ébranlements du fait que leurs périodes sont assez courtes et que leurs amplitudes deviennent assez grandes.

Pour économiser le papier photographique, nous l'avons enroulé sur un tambour qui se déplace le long de son axe avec 2 mm de pas. Ce procédé nous oblige à laisser le papier photographique exposé une dizaine de fois à la fenêtre d'entrée du faisceau. Comme le champ de la fenêtre n'est pas absolument noir pendant l'observation, il y a une certaine limite à la longueur de pas bien que nous nous éfforcions de faire le champ aussi sombre que possible. Comme source lumineuse, nous avons pris finalement un phare d'automobile alimenté sous 10 volts de tension. Nous mettons une fente juste en face de la lampe pour rendre la source linéaire et une lentille cylindrique (c) en face du papier photographique qui sert à transformer son image en un point.

---

[3] *loc. cit.*

[4] La variation de longueur du fil correspond à 3·44 × 980 dynes donnant 3·9 mm de déviation d'image. Suivant le calcul, en effet, nous avons 1 cm de déviation pour 2·7 gal d'accélération.

3. Résultats.

Les observations ont été effectuées du 17 juillet au 13 octobre et nous avons réussi à enregistrer une vingtaine de séismes apparus dans la région de Kantô: les séismes ont été ressentis à Tôkyô. Leurs données sont représentées dans le tableau ci-joint, et la reproduction des enregistrements de quelques uns dans le cliché de la fin (Fig. 5).

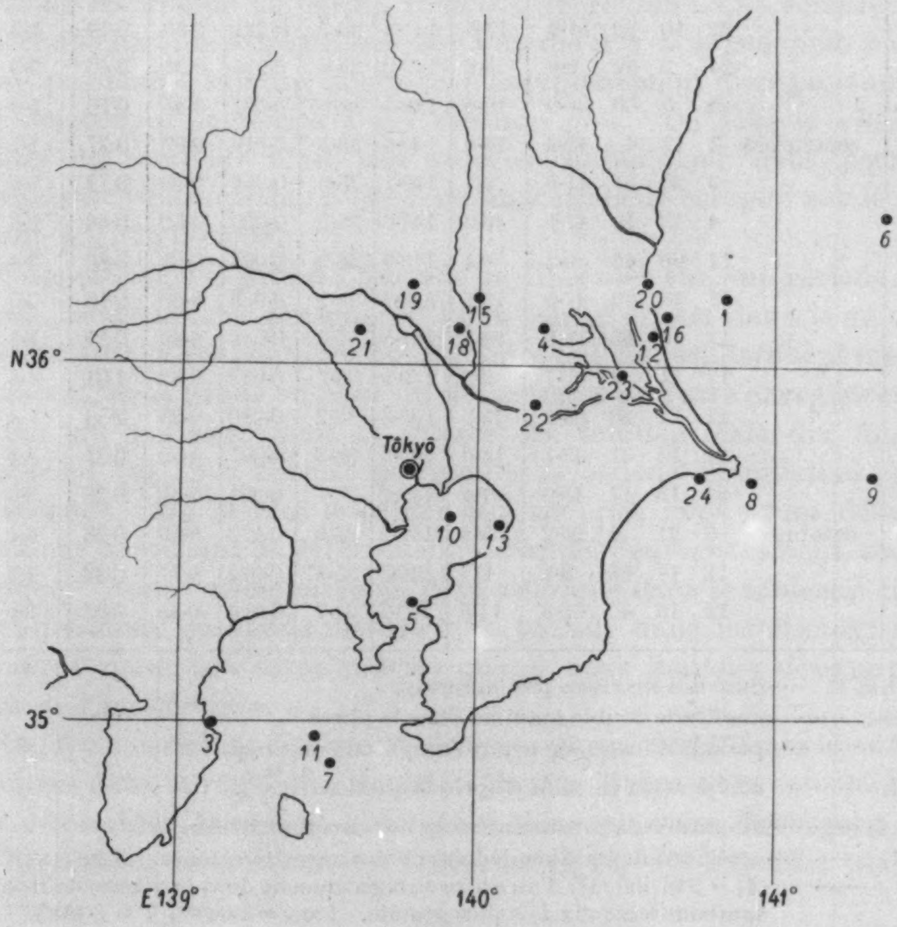

Fig. 4.

Tableau I.

No.	Observations des sismographes (d'après M. Yasuda)											Observations accélérometriques	
	Temps d'occurence (à Tôkyô)					D.S.P.	Epicentre		$2a_m$	T	A_1	$2A_0$	A_2
							λ(E)	φ(N)					
	(1930)	j	h	m	s	s	°	°	mm	s	gal	mm	gal
1	juillet	27	0	10	20·8	14·9	140·8	36·2	0·016	0·43	0·17	2·3	0·31
2	août	4	21	17	3·7	8·7	—	—	0·020	0·41	0·23	1·5	0·20
3		15	11	43	24·3	13·0	139·1	35·0	0·062	0·48	0·53	3·0	0·40
4		16	12	14	21·9	8·8	140·2	36·1	0·016	0·33	0·29	1·5	0·20
5		17	18	28	45·0	8·5	139·8	35·3	4·67	1·40	4·70	31·0	4·18
6		19	4	42	31·2	20·0	141·2	36·4	0·080	0·80	0·25	3·0	0·40
7		19	21	40	30·6	12·0	139·5	34·9	0·096	0·65	0·45	3·0	0·40
*8		20	2	41	52·3	15·2	140·9	35·7	0·560	0·48	4·81	41·4	5·59
9		22	10	30	51·9	17·5	141·3	35·7	0·024	0·50	0·19	1·5	0·20
10		24	2	52	9·0	5·8	140·0	35·6	0·028	0·35	0·45	3·0	0·40
11		24	5	00	36·9	10·8	139·4	34·97	0·001	0·45	0·16	1·0	0·14
12	septembre	3	17	4	43·9	10·6	140·6	36·1	0·019	0·37	0·27	1·1	0·15
13		3	20	31	11·3	9·3	140·1	35·6	0·056	0·39	0·73	5·8	0·78
14		4	13	18	47·1	40·0	143·0	38·3	0·060	0·52	0·44	2·5	0·34
15		17	00	46	9·2	8·4	140·0	36·2	0·024	0·28	0·60	3·8	0·51
16		17	13	56	47·5	13·7	140·7	36·1	0·029	0·60	0·16	3·0	0·40
17		17	19	55	16·8	26·2	141·8	37·9	0·048	0·70	0·19	1·3	0·18
18		17	21	3	47·7	9·2	139·9	36·1	0·052	0·32	1·01	4·5	0·61
19		22	12	26	53·7	13·7	139·8	36·2	0·080	0·25	2·53	5·4	0·73
20		24	15	31	43·1	14·0	140·6	36·3	0·097	0·72	0·37	3·4	0·46
21		26	13	17	43·0	7·4	139·6	36·1	0·024	0·41	0·28	3·0	0·40
22	octobre	5	21	4	25·2	9·8	140·2	35·9	0·172	0·59	0·98	6·4	0·86
23		12	17	58	8·2	9·8	140·5	35·97	0·082	0·71	0·32	4·3	0·58
24		12	18	40	49·3	11·5	140·7	35·7	0·026	0·88	0·07	2·0	0·27

D. S. P. ……duré des secousses préliminaires.

$2a_m$ ………amplitude double maxima dans la phase S.

T ……………période d'une onde ayant l'amplitude maxima.

A_1 …………accélération calculée d'après l'équation $\frac{4\pi^2 a_m}{T^2}$.

$2A_0$ …………amplitude double mesurée sur nos enregistrements.

A_2 …………accélération maxima déduite de nos enregistrements. $A_0(\text{cm}) \times 2·7$

* ……………$A_1 = 5·91$ calculé d'un autre enregistrement dont la vitesse de rotation du tambour était dix fois plus grande. ($2a_m = 0·64^{\text{mm}}$, $T = 0·463^{s}$)

Tout sont dans la composante N-S.

Nous distingons tout de suite certaines différences de type parmi eux. Naturellement nous savons qu'il y a différents types parmi les sismogrammes ordinaires: mais ils sont particulièrement exagérés dans les enregistrements accélérométriques. De plus nous trouvons une différence distincte d'amplitude entre les secousses préliminaires et les secousses principales.

Nous essayons d'abord de comparer les accélérations maximas des sismogrammes calculées suivant l'équation $A=\frac{4\pi^2 a}{T^2}$ et celles obtenues par nos observations. Pour calculer l'accélération maxima, nous avons l'habitude de prendre une amplitude maxima dans le domaine de la phase S, c'est-à-dire dans les secousses principales; il est donc certain que la secousse dont l'amplitude est maxima ne correspond pas toujours à celle dont l'accélération est maxima.

Dans le procédé de calcul, il faut d'abord faire une remarque sur l'exactitude de la mesure du temps. Comme il y a à peu près 6 cm de course pendant 1 minute, la vitesse d'enregistrement n'est pas suffisante pour déterminer le temps à 0·1 seconde près. De plus la vitesse de rotation du tambour n'est pas assez constante pour nous permettre d'avancer nos discussions: il est donc impossible de compter sur le 0·1 de seconde pour la période.

Supposons qu'il y ait 0·1 seconde de différence sur une période de 0·5 seconde, nous aurons presque 50 pour cent d'erreur dans la valeur de l'accélération. Cela peut être nous montre que les résultats sont inexacts. Cependant, nous avons eu pour un des séismes un autre enregistrement[5] fait sur un tambour dont la vitesse de rotation était dix fois plus grande: ce qui nous permet de calculer la période d'oscillation jusqu'à 0·01 seconde. En suivant le calcul déjà indiqué, nous avons déterminé une valeur aprochant de celle obtenue d'après l'enregistrement accélérometrique. Nous l'avons marquée d'un astérique dans le tableau. Il faut donc faire attention que la mesure de la période dans les sismogrammes ordinaires n'est pas assez précise quand nous voulons déterminer la valeur de l'accélération.

Or, il y a certaines différences de types parmi des séismes ayant leurs épicentres dans la région de Kantô. Nous utilisons cette caractéristique pour déterminer la région sismique. Nous pouvons distinguer d'une part les séismes de la région de Tonégawa (E 140°, N 36°) dont plusieurs

---

5) exécuté par Prof. Suyehiro avec un procédé spécial.

ondes prédominent dans la phase de S avec une durée de secousses assez longue; d'autre part les séismes de la région du golfe de Tôkyô dont une seule onde est très remarquable dans la phase de S avec la durée des secousses très courte. Toutes les deux sont représentées dans Fig. 5; les Nos. 19, 21 et 22 sont des exemples des premiers, et le No. 13 un du dernier.

Nous voyons surtout dans les enregistrements accélérométriques, des ondes solitaires dans les séismes de Tonégawa. Il nous semble que ce phénoméne est difficile à comprendre; mais si on nous permet d'imaginer une explication, nous ferons remarquer tout d'abord l'hétérogénéité de la composition de la croûte terrestre. Bien que les ondes produites au centre hypocentral soient pareilles, il est possible que l'hétérogénéité des passages fasse varier les secousses observées: cela probablement nous montre les différences de types ainsi que l'origine des ondes solitaires.

En tout cas, l'observation préliminaire des séismes au point de vue accélérométrique nous donne une nouvelle conception des mouvements sismiques. Il nous semble que la méthode photographique d'enregistrement n'est pas commode pour continuer nos observations; d'une part parce qu'elle est très coûteuse et d'autre part par ce que la courbe enregistrée sur le papier recouvert de noir de fumée se trouve plus fine que celle enregistrée sur le papier photographique, quoique nous réduisions les dimensions de la source lumineuse ainsi que son image. Nous préférons utiliser maintenant l'autre procédé d'enregistrement qui pourra remplir nos intentions.

Pour terminer, nous voulons exprimer nos vifs remercîments à Monsieur le Professeur K. Suyehiro, directeur de notre Institut, dont les suggestions et les discussions nous ont été infiniment précieuses.

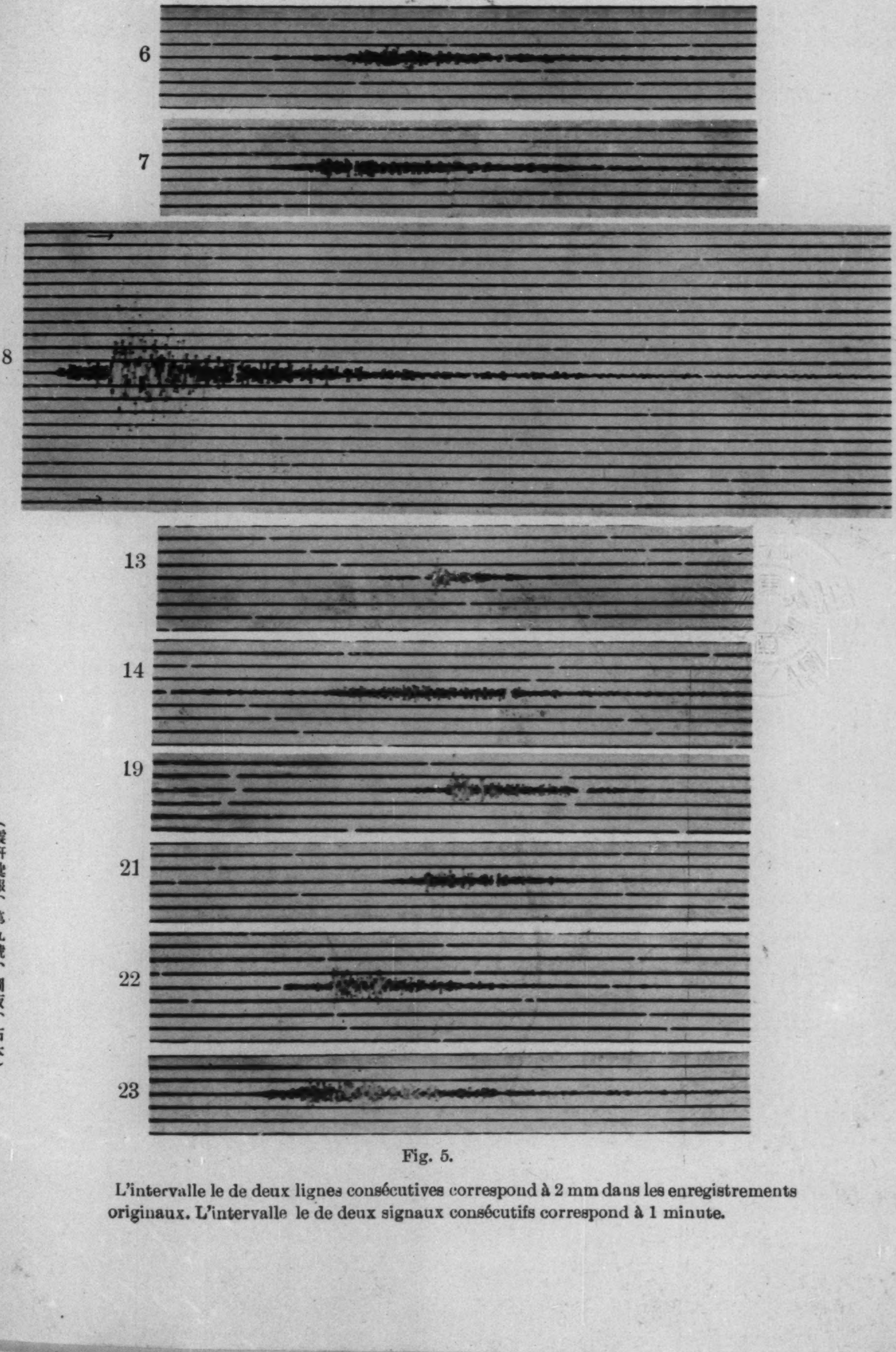

Fig. 5.

L'intervalle le de deux lignes consécutives correspond à 2 mm dans les enregistrements originaux. L'intervalle le de deux signaux consécutifs correspond à 1 minute.

（震研彙報、第九號、圖版、石本）

13. 地震加速度の觀測

地震研究所　石本巳四雄

1. 工作物の地震に對する抵抗を研究する場合、地震動の加速度が問題となる事が多い。現在加速度を求めるには一般地震計の記象から計算するのであるが此れには多少不滿足の點がある。地震の加速度を直接記錄するために二三の器械か考案されて居るが、其等による地震動觀測の記象は未だ發表されて居ない。

地震動の加速度測定は其の周期に比較してもつと小な周期をもつ振動系の變位を測定する事によつて達せられるが、此の振動系の自由振動は充分減衰してなくてはならない。

2. 吾々は地震の速度が如何なる性質のものであるかを見るために極めて簡單な裝置（第二圖）を製作した。重錘は 3·2 kg. 幾何倍率は 1700, 感度は 1 cm. の振れが 2·7 gal に相當して居る。豫め行はれた感度試驗は各周期に對して同等の値を有する事が知れた。（第三圖）

3. 寫眞裝置を採用した事によつて多少の困難は伴つたが結局昭和五年七月十七日より十月十三日に至る間において二十數個の地震を記錄する事を得た。其等の要素は第一表に、記象は第五圖に示してある。

一般地震計記象から計算によつて決定した最大加速度の値と今回得た値とを比較したがよく合はない。夫れは地震計においては測時上 0·1 秒以下は信用出來ないと云ふ事によるらしい。地震の加速度記象において直ちに氣の附く事は初期微動と主要動との間に明瞭な區別のつく事及び地震型の區別が明かである事等である。なほ利根川方面に震央を有するの地震動の中に加速度の大きな獨立波の見られる事は注意すべきであらう。

14. On Sound Phenomena of the Idu Earthquake of Nov. 26th, 1930.

By Win INOUYE and Tomonori SUGIYAMA,

Earthquake Research Institute.

(Read Feb. 17, 1931.—Received March 20, 1931.)

1. On Mt. Tukuba which lies in the north-eastern part of the Kwantô district, some characteristic earth-sound is heard accompanying about a half number of sensible earthquakes. Sometimes, we notice some such noises even on the occasion of insensible earthquakes.

They generally begin almost simultaneously with the arrival of the primary phase of each earthquake. They continue during its principal portion with fluctuating intensities and subside gradually in their intensities. The duration of these sounds ranges generally from 10 to 15 seconds and occasionally amounts to as long as 30 seconds.

A destructive earthquake occurred at 4h 03 m on Nov. 26th in Idu Peninsula. On the early morning of this very day we experienced characteristic sounds at several minutes after the beginning of the moderately intense earth trembling.

According to the report on this earthquake of the Central Meteorological Observatory, sounds were heard in the epicentral area and in two zonal areas far from it, the one lying from 120 kms. to 170 kms. to the north-east, the other between 160 kms. and 300 kms. to the west of the origin.

In order to obtain some informations regarding the geographical distribution of the limit of audibility, we send letters to the headmasters of the primary schools in the neighbouring districts asking to inform us about the nature of the sounds and the time when they were heard. The reports received from them were 102 in number, and this number may not be sufficient for getting a full information regarding the distribution of the places where the sounds were heard, but we may be allowed to discuss a little about the nature of them from these data.

In Fig. 1, the cross represents the place where no sound was perceived, the circle represents the place where the sounds were noticed which did not differ from those heard on the occasion of the ordinary near earthquakes, and the double concentric circles represent the place

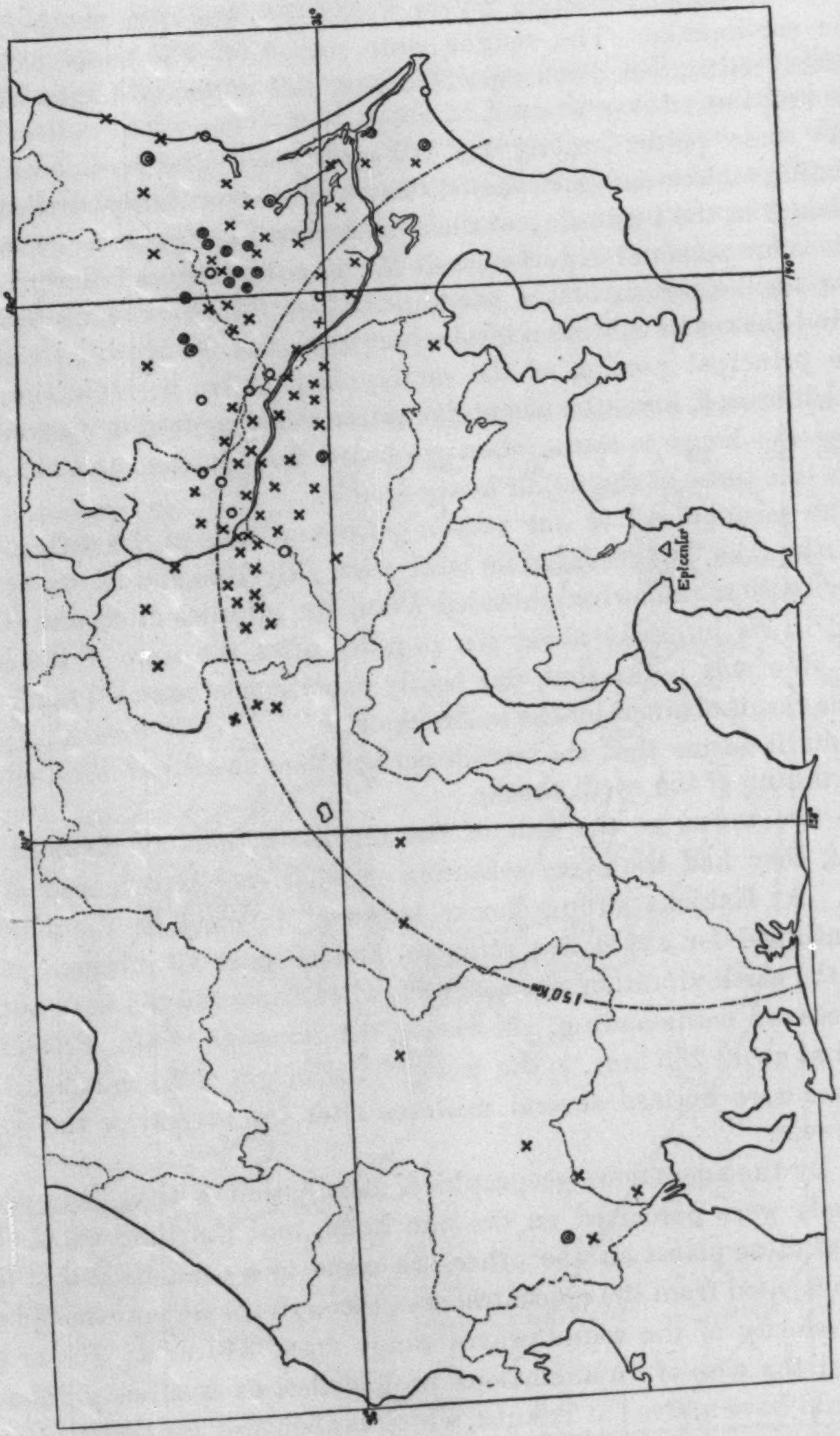
140°
Epicenter
150 Km

Fig. 1.

where the peculiar rumbling noises were perceived after the beginning of the earthquake. The sounds were somewhat like those of distant thunders, continuous discharges of a gun, fall of heavy blocks of rock, or the eruption of Asamayama.

At some places among the last mentioned places, not only the detonating noises as above stated, but also the ordinary earth-sounds were heard at the beginning of the earthquake.

2. Our personal experiences at Mt. Tukuba were as follows.

At the beginning of the earthquake the sliding-doors rattled fairly long and then slow vibration of the house was felt, indicating the arrival of the principal portion of the earthquake. After a while the earth vibration ceased, and after about five minutes had passed it was renewed making the house to rattle, when we heard three intense and two feeble sounds like those of the fall of heavy stones.

The seismometer at our station got out of scale at the early part of the earthquake, but recorded its later part. By this record we see the earth vibration somewhat subsided about six minutes after, and then it revived in its intensity about ten minutes after the time of the occurrence. We may notice that, our bodily experiences coincide fairly well with the result obained by the seismometer.

Thus it seems that the sounds arrived here about ten minutes after the beginning of the earth shocks.

At two towns at the foot of the mountain, namely Kakioka and Tanikai, they had the same sensation as what was experienced at our station. At Kakioka strong shocks began at 4 o'clock in the morning and continued for about five minutes, and then at 10 minutes past 4 o'clock the earth vibration was renewed, when three sounds were noticed like those of cannonading. Moreover, at Akasaka, Gifu Prefecture, situated at about 235 kms. to the west of the origin of the earthquake, a few noises were noticed several minutes after the arrival of the earthquake waves.

3. By the anomalous geographical distribution of the places where the sounds were perceived on the one hand, and the time when they noticed at these places on the other, we came to a conclusion that they were propagated from the epicentral area through the upper atmosphere. As the velocity of the sound waves range from 240 m to 310 m per second in the case of an anomalous propagation as is already known,[1] they should have arrived at Tukuba, which is about 160 kms. distant from the earthquake origin, at 8 m 36 s to 11 m 6 s after they had started, and this was actually the case.

---

[1] Wien-Harms, Handbuch der Experimentalphysik, XXV, Teil 3.

Although the sound waves may be generated in the atmosphere by the refraction of the earthquake waves of high frequency particularly as in the case now in question where the hypocentre had been laid shallow under the hard andesite rock in the volcanic area, owing to the lesser dissipation of energy of the earthquake waves, it may rather be plausible to attribute the source of the sound waves which were intense enough to be propagated to so distant places, to the landslips which had occurred at many places in the epicentral area either during or perhaps shortly after the destructive earth concussion.

In Fig. 2 is shown the weather chart at 6 a.m. of Nov. 26th, publi-

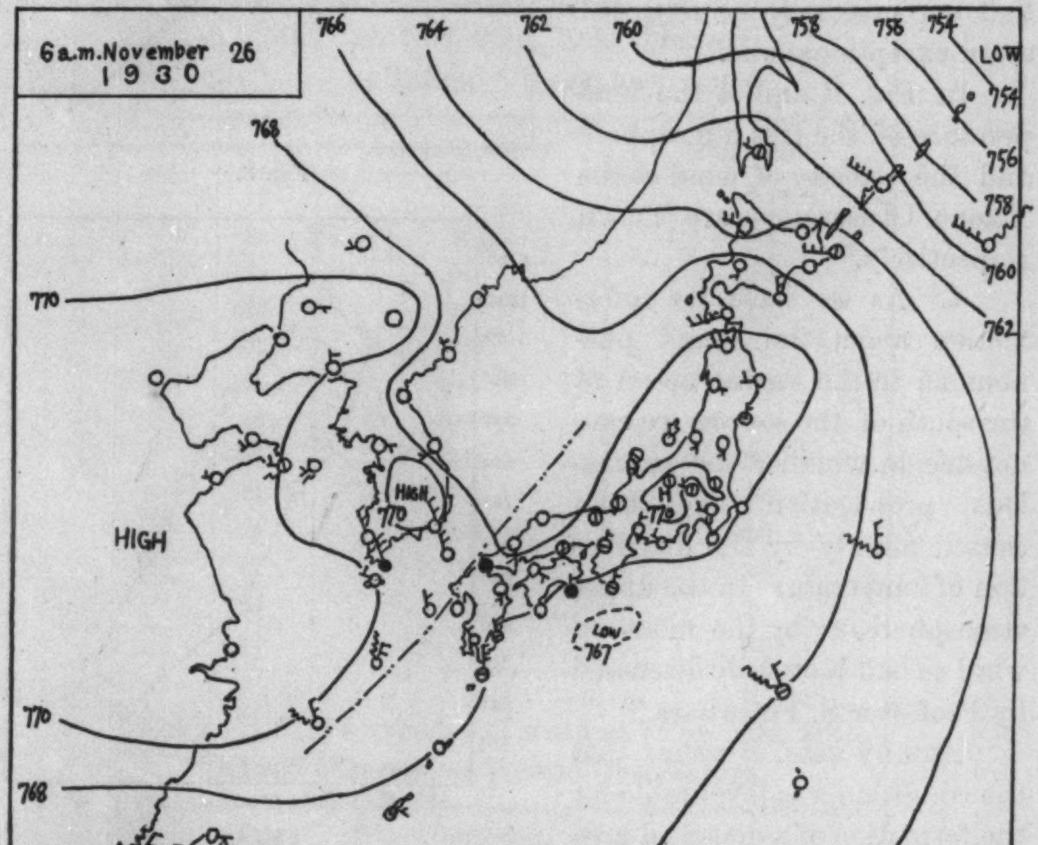
6a.m.November 26
1930
766
764
762
760
758
758
754
LOW
754
756
758
760
762
768
770
HIGH
770
HIGH
770
LOW
767
770
768
766
764
LOW
764
764

Fig. 2.

shed by the Central Meteorological Observatory. As is to be seen from the figure, the weather at that time was of the normal winter type, and calm under a detached high over the central Japan.

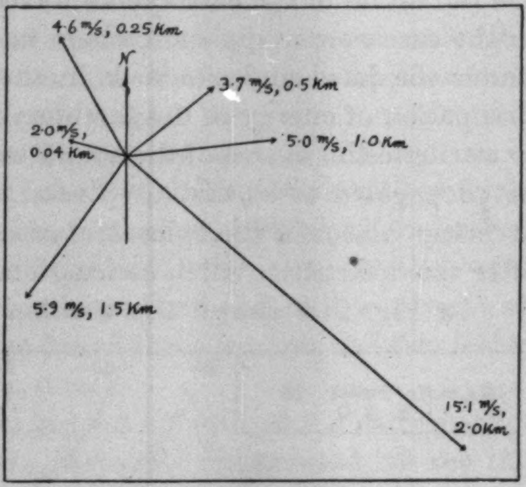

Fig. 3.

According to Fujiwhara's[2] classical study on the abnormal propagation of sound waves in the atmosphere, the region of audibility is generally continuous in winter and no detached region appears except when a powerful cyclone exists in the vicinity of the sound source, so that our case may be regarded as an exceptional one.

In Fig. 3 and 4 the temperature of the free atmosphere and the velocity of wind at the Tateno Observatory are shown respectively.[3]

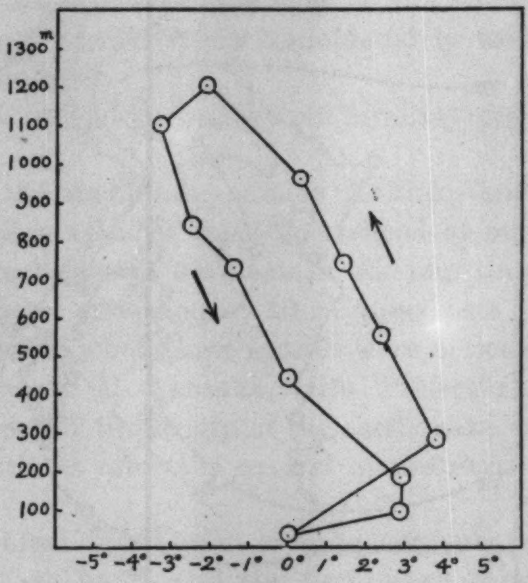

Fig. 4.

4. As we have no information about the sound phenomena in the Pacific ocean at the south of the source, we cannot decide whether the anomalous propagation had been caused mainly by the distribution of temperature in the upper atmosphere, or by the monsoon wind as had been fully discussed by Professor S. Fujiwhara.[4]

At any rate, it seems that the condition was favourable for the formation of a detached area of audibility to the northern side of the source, as at Tateno Observatory up to 1 km. from the ground the northern wind, and above it the southern wind respectively had been blowing and the velocity of the wind had been increasing with the increasing height.

---

[2] S. FUJIWHARA, *Bull. Cent. Met. Obs.*, Japan, 2 (1916), 39.

[3] As is to be seen from Fig. 4 there was a inversion of the atmospheric temperature which may have been caused by the night cooling. We confirmed by simple calculation that the sound waves have not been transmitted to so distant places by this inversion of temperature.

[4] S. FUJIWHARA, *Bull. Cent. Met. Obs.*, Japan, 2 (1912) & 2 (1916).

In conclusion, the authors wish to express their most cordial thanks to Professors Torahiko Terada and Chûji Tsuboi for their valuable advices and discussions which they have kindly given, and to the Director of the Tateno Observatory for his kindness in informing us the whether condition there.

Appendix.

Table I. The temperature of the free atmosphere at 7^h on Nov. 26th, 1930 observed at Tateno Observatory.

time	height in meter	temperature
7^h 12^m	26	0·0°C
18	282	3·8
19	548	2·4
20	743	1·4
21	961	0·3
23	1205	− 2·1
23	1097	− 3·3
24	844	− 2·5
25	726	− 1·4
29	444	1·0
31	180	2·9
33	94	2·9
37	26	0·0

Table II. The velocity of wind at 7^h on Nov. 26th, 1930 observed at Tateno Observatory.

height	direction	speed
0·04 km	285°C	2·0 m/s
0·25	331	4·6
0·5	51	3·7
1·0	174	5·0
1·5	214	5·9
2·0	132	15·1

Table III. List of places where the sounds were heard.

In Ibaraki prefecture.

Tukuba: Above stated.

Kakioka: Ditto.

Tanikai: I was staying for the night in my school. I was frightened to get up with a start by the servere shocks, and went into the office-room to examine the remaining fire in a brazier.

When I was going to get out of door, the shakings had been fairly subsided, and I went to bed. After several minutes had passed, the shakings was renewed, and sliding doors were forced to open by and by making rattling noises, and I was obliged to get up again to shut them. At that time, according to my vague memory, I heard feeble sounds accompanied by vertical shakings of the floor.

Makabe: Although the time was uncertain, I heard several detonating noises like those of cannonading or an eruption of a volcano.

A few of my colleagues also heard the similar noises. The noises were quite different from the ordinary earthquake sound.

Inada: Immediately after the earthquake, I heard a few detonating noises. I supposed that they may have been caused by an eruption of a volcano.

Ogawa: After the beginning of the earthquake, I heard several sounds.

Oo: I noticed a few noises.

Oota: Before and during the earthquake I heard a few detonating noises, which made the doors, especially sliding-doors, to rattle.

Koise: Shortly after the beginning of the earthquake I heard noises which seemed to come from beneath the ground. Some men who are living in the neighbouring district had the same experience.

Kasama: 1. Before the beginning of the earthquake I heard distant noises.

2. It shaked mostly in NS direction during about one minute. The pendulum clock was stopped. The bodies on shelves fell down.

3. After the shaking had ceased, I heard a few detonating noises like those of an eruption of Asamayama.

4. Afterwards, after-shocks were felt.

Hiraiso: According to the experiences of two teachers of our school, the feeble shocks were felt after they heard noises in the early morning on Nov. 26th.

Koga: The earthquake occurred at the same time when I heard noises in the early morning on Nov. 26th.

Iwase: Here the noises were noticed at the beginning of the earthquake.

Mizukaido: Only a single sound was heard before the earth shaking became strong. After 10 seconds had passed, the earthquake began to shake violently in EW direction.

In Tiba prefecture.

Yôkaitiba: Here many people heard several sounds after the earthquake.

Omikawa: I heard noises during several minutes like those caused by strong wind. Supposing that the wind has been getting up, I got up and opened the door.

Iioka: Some of the teachers of our school heard noises like those caused by a revolving propeller of an aircraft at the NE. Others did not notice them.

In Totigi prefecture.

Maoka: Shortly after the occurrence of the earthquake, some men heard continuous explosive noises at the south. The noises likened to those of the cannonading at some distant place, the distant thunders, or the continuous explosions of a volcano.

Mibu: Some men heard noises like those of cannonading immediately after the earth trembling has ceased.

Isibasi: They say that they heard noises as caused by a coming train just before the occurrence of the earthquake, and they heard a few explosive noises at the early part of the earthquake. Two after-shocks were felt, the first one was slightly stronger than the second.

Kuzuu: Here the noises were heard fairly intensely before the arrival of the earthquake waves.

Hudioka: Here we heard uncommonly long and intense earth-sounds. We talked with one another that a destructive earthquake must has occurred somewhere. No casualties occurred to men and beasts.

In Gumma prefecture.

Kiryû: The earthquake occurred at 3 h 57 m on Nov. 26th accompanied by earth-sounds. The earth vibration was not severe and continued for about two and half minutes.

Oniisi: An earthquake occurred after a noise was heard like the detonation caused by the eruption of Asamayama.

Yabutukamoto: All of seventeen teachers of our school heard noises like those with the ordinary earthquake.

Isezaki: A slight earthquake continued for one minute and thirty seven seconds. A single earth-sound was heard before the occurrence of the earthquake and continued for about ten seconds.

In Saitama prefecture.

Matuyama: Here earth-sounds were heard after the earthquake.

In Gifu prefecture.

Akasaka: At Akasaka a few noises were noticed at several minutes after the arrival of the earthquake waves.

---

14. 昭和五年十一月二十六日伊豆地震に伴つた音響異常傳播に就いて

地震研究所 井上宇胤
杉山友紀

地震研究所筑波山支所に於て十一月二十六日午前四時三分の伊豆大地震の發震後約十分程して數回音を聞いた。主に關東地方の小學校長あてに手紙を出して此の音に關する報告を貰つた。それによると筑波に於ける音と同樣な音を聞いた場所が可成りあつた事を知つた。それ等の場所の分布及び音を聞いた時間からして、此の音は普通近地地震に伴ふ地鳴とは異なり震源地附近の音元から大氣の上層を傳つて來たものと思ふ。尙此の音は地震波によつて直接に起されたものとするよりも、震源地附近に非常に澤山に起つた山崩によるものと思ふ。

---

15. 昭和五年十一月廿六日伊豆地震に伴ひたる光の現象に就て

地震研究所　武者金吉

（昭和六年三月十七日發表—昭和六年三月二十日受理）

I. 資料聚集の動機と聚集の方法

大地震に光の現象を伴ふたと云ふことは、洋の東西を問はず、古來の地震記錄に散見する所で、Galli の如きも若干の資料を聚集し之を發表して居る。Montessus はこの現象に對して疑を抱いて居るが、自分は十五六年前地震現象に興味を感じ始めた當時、此等の記載が單なる流言浮說に非ずして、或る程度まで事實に基いたものであらうことを考へたのであつた。1) 爾來地震史料を涉獵するに當り、常にこの事實に對して注意を怠らなかつたのであるが、親しく其の現象を目擊する機會を摑むことは出來なかつた。然るに昭和五年十一月廿六日伊豆地震に際し、全く偶然の事情から、この現象を觀察することが出來た。なほ他にもこの現象を見た者が少くないことが分つたので、十一月廿七日末廣所長の許可を得て、資料を聚集することになつた。

ついては成るべく勞少くして多くの資料を集めたいと云ふ考から、東京府、神奈川縣、靜岡縣、及び千葉縣(但し一部)の各中等學校に宛てゝ照會狀を發送し、回答を求めた。特に中等學校を選んだのは、小學校の生徒では、其の報告が餘りに不得要領であらう事を懼れたためである。震央附近は中等學校の少ない所なので、特に靜岡縣田方郡のみは、各町村役場に書類を一括して送り、管內の各小學校に分配すべく依賴した。發送した照會狀は約百五十通であつたが、回答を送つて與れた學校は約三分の一に過ぎなかつた。それも全校の生徒について調査して與れた所

---

1) 音響を伴つたとか山が崩れたとか云ふのならいざ知らず、地震に際して空が光つたとか火の玉が飛んだとか云ふ事は、到底根據なくして想像し得べきことでなく、また歷史の編纂者が机上で造り出せる文句ではないと信ずる。

もあり、單に一教員の觀察を送附して來た所もある。其の外友人及び未知の人々から惠與されたものを加へて、約千五百の報告と若干のスケッチを聚集することが出來た。

II.　光の觀察された範圍と觀察者の分布

光の現象の觀察された範圍は、照會狀を發送した範圍が狹かつたのと、回答を送つて呉れぬ學校が少なからずあつたゝめに、確實には分らない。集め得た資料の範圍では、北は埼玉縣北足立郡白子村、南は靜岡縣下田附近、東は千葉縣市原郡千種村、西は靜岡縣燒津である。尤も更に廣い範圍に亘つて照會し、回答を集めたとしても、この點に關して充分なる結果は得られなかつたであらうと思はれる。何故ならば、震度の餘り強くなかつた土地では、戸外に出る者もなく、雨戸を開くこともしないので、見えるべき光も見ずにしまつたであらうからである。

次に光を見て報告して呉れた人々の數を、東京橫濱の兩市は區に、其他は町或は村に纏めて、地圖の上に記入して見た。其の結果を見るに、光を見た人々の數が、場所によつて著しく違ふ。勿論これは回答を送つて呉れた學校が全地域に平等に分布されて居ないこと、また學校によつて全校の生徒について調査して呉れた所と呉れない所とがあつた等の事情も考慮しなければならぬ。多分この事情が與つて力があるのだらうとは思ふが、併しそれだけでは多少說明に困難な點もあるやうに思はれる。其の中最も著しいのは多摩丘陵と相模川流域である。

多摩丘陵に於ては光を見た人々の數が著しく少ない。この丘陵は、かなり dissect された丘陵で、人口が比較的少ないことは勿論であるが、或は寺田敎授の御說の如く、この地域が比較的震度が小であつたのかも知れない。相模川流域に於ては厚木中學校、厚木高等女學校、大根村の奈珂中學校、藤澤町の藤澤中學校及び湘南中學校が、孰れも熱心に調査して呉れたのであるが、光を觀た人々がこの地域全體に平等に分布しないで、相模川の右岸に多く、左岸には比較的少ない。この理由は今のところ不明である。尤も町村の全人口と其の町村の中等學校生徒の數との割合等をも調べて見なければ、確實な事は分らない。

III. 光の出現時間及び繼續時間

光の現象の現はれたのが十一月廿六日午前四時三分の地震の前であつたか、地震と同時であつたか、また地震の發した後であつたかと云ふ事については、餘り多くの資料がない。發震の時間が曉方であつて、其の當時起床して戸外に出て居た者の少ない事も、この調査を困難にする一つの理由である。兎に角今までに集まつた僅かな資料に基いて見るに、午前四時三分の地震の前に既に光の現象が現はれたのではあるまいかと考へられる。其の推論の基礎となつた資料は次ぎの如くである。

(1) 十一月廿五日午後五時頃靜岡縣田方郡長岡に於て大仁高女の一生徒が南東の方向に電光の如き色彩の光を認めた。

(2) 十一月廿五日午後九時頃小田原より北方に餘り强からざるオレンジ色の光を認めた。

(3) 十一月廿五日午後十時頃、富士大宮口五合目と御殿場との間に於て、箱根山方面に物凄い青い光を暫くの間認めた人が二人ある。

(4) 十一月廿六日午前一時頃、牛込區山吹町通に於て、北方の空に强烈な光を認めた人が多くある。

(5) 十一月廿六日午前三時五十分頃、横須賀市逸見町から西北に一種異樣の光を認め、地震の發した頃には、大部分消失して居た。

(6) 網代沖に出漁中の一漁夫は、地震の直前に電光の如き光を認めた。

(7) 熱海初島附近に出漁中の一漁夫は、始め箱根の方から光り出し、天城山の方へ光つて行き、又天城山の方から箱根山の方へ光つて行つたのを見て、不思議な現象だと思つて居ると、間もなく船が動搖した。

(8) 平塚町火薬廠内を巡廻して居た一吏員は、大きな地震の起る少し前に、箱根の上空と東の上空とに光を認めた。

尤も光の速度より地震波の速度の方が遲いから、(4) 及び (5) の如く地震の直前に光を見たと云ふのは除外すべきであらう。地震の前から光が現はれたと云ふ事は、昔の記錄にもあつて、元祿十六年關東地震、天保元年七月二日畿內地震、弘化四年善光寺地震、安政二年江戸地震等に

其の例がある。[2] 但し今回の地震には多くの「先き搖れ」を伴つたのであるから、或は「先き搖れ」に伴ふた光であつたかも知れない。

大多數の報告者が光を見たのは、地震に驚いて戸外に飛出したり、雨戸を開いたりした時であるが、それがどの位の間繼續したかについては、正確な事は分らない。資料の中から、これに關係のあるものを拾ひ出して時間の順に竝べて見ると次ぎの如くなる。

(1) 發震直後より十五分位の間小田原から箱根方面及び八幡山方面に光を認めた。

(2) 四時十五分頃千葉縣君津郡眞舟村より三浦半島の方に光を認めた。

(3) 發震後二十分頃府下荏原郡駒澤町より東南に、神奈川縣足柄上郡岡本村より西方に、同足柄下郡下府中村より(方向不明)、靜岡縣田方郡韮山村より南方に、同郡中郷村より西から東に光を認めた。

(4) 四時二三十分頃沼津市より東方に光を認めた。

(5) 發震後三十分頃神奈川縣足柄下郡下曾我村より南東に、小田原より南方に、平塚町より箱根山の上空に、千葉縣君津郡湊町より浦賀方面に光を認めた。

(6) 四時四十分頃小田原町より西方に光を認めた。

(7) 箱根町では發震後四十分位を經て霰が降つて來た時分に、漸く四邊の暗いのに氣がついた。

(8) 發震後一時間頃神奈川縣足柄下郡吉濱村より伊豆半島方面に光を認めた。

(9) 伊東町役場の報告によれば、光は發震後一時間位繼續したと云ふ。

(10) 五時頃靜岡縣田方郡內浦村より北北東に光を認めた。

此等の資料は、各〻の報告者が正確な時計を持つて居た譯ではないから、もとより嚴密な意味に於て正確なものとは云はれない。幾分の割引をして考へなければならないが、少くも震央附近に於て、發震後相當に長い間光が繼續したことは認められると思ふ。併し地震の最中が最も顯著であつたことは、多數の報告によつて疑ない事である。

---

[2] 古記錄との比較參照。

IV. 光を見た方向

各報告者が光を認めた方向を、市は區に、其他は町或は村に纏めて、之を五萬分の地形圖に記入し、矢の方向は光を見た方向を示し、矢の長さは其の方向に光を認めた人の數に比例させた。併しそれでは餘り複雜になつて、全體を大觀するに不便であるから、寺田教授の御注意によつて、五萬分地形圖を四等分し、各〻のセクションの中に含まれる矢を纏めて、其のセクションの中央に記入する方法を採つた。爰に揭げるものは卽ち其れである。

其の結果を見るに、箱根天城を連ねる地域を圍繞する所では、大多數の矢が其の地域を指し、其の地域に著しい光の現はれたことを示して居る。この事は前に記した初島附近に於ける漁夫の觀察や、神奈川縣足柄下郡吉濱に於ける小田原中學校生徒の觀察とよく一致する。[3] 殊に箱根に於ては、Caldera の中で旺に發光したのであつて、この事は箱根町の人々が確實に認めて居る。同地の人々の語る所によると、三島道の方でも、東の方でも、また神山駒ヶ嶽の中腹でも光つた。其の光り具合は大體輪廓は圓くて、或る一ヶ所で光り、それが消えると他の場所と云ふ風に位置を變へて光つた。形も大きいのと小さいのとあつた。小田原町からの報告にも、この光は箱根山上に出たものとは思はれない、Caldera の中の低い場所から發したのだと思ふと云ふのがある。[4]

箱根より天城にかけての地域に光を發したことは、前述の如く確實と認められるが、其他の地域に於ては、不可解の點が少くない。第一に、海の方を向いて居る矢が少なからずあることである。また海の方に光を認めたと云ふ事を明記してある報告も二三ある。茅ヶ崎海岸では、互に全く關係のない二人の報告者が海の方で光つたと云つて居る。横濱久保山及び大森海岸でも海の方で光つたのを認め、品川では東京灣の方から光つたと云ふ人と房州館山方面に光を認めたと云ふ人がある。海中から發光したとすれば、この謎は至極無雜作に解けてしまふが、其の可能性があるかないか、自分には分らない。海岸にある家は、多くは海に面し

---

3) 伊東上空より日金山上空にかけて著しい光の現はれたことを報告して居る。

4) 「この電光は箱根山上に出たものとは思はれず內輪山中の低き場所からだと思ひます」。

て建てゝあるから、自然海の方が光るやうに感ぜられたのかも知れない。或は寺田教授の御說の如く、海上に雲があつて其れに光が映じたのだと、斯う解釋も下される。これについては、神奈川縣三浦郡秋谷の一中學生の觀察した所は中々重要である。それに依ると、地震が起ると同時に、火の樣なものが箱根の少し左の方(秋谷から見て)から上り、またゴーと云ふ音と共に、前と同じやうなものが上り、次いでサーチライトの光の樣な一線となつて延び、葉山の上空あたりを通つて、横須賀方面に於て燃え映るやうに強く光つて消えた。光は二本出たと云ふことである。若しこの報告に誤りがなければ、(1) 横須賀上空あたりに雲があつた。(2) 丹那の邊からサーチライト狀の光を放射した。(3) 其の光が前記の雲に映じた。而して小田原から茅ケ崎邊にかけて、海の方に認めたと云ふ光は、この「一線となつて延びた」光であつたかも知れない、と斯う解釋することも出來る。

また相模川流域に於ては、光を見た方向の大多數が南東である事は、極めて著しい事實であつて、これまた一の謎である。これは前記の如く、横須賀方面の雲に映じた光を觀察したのだと解すれば、一應は說明がつくが、それだけでは未だ不充分の感がある。どうしても三浦半島北部あたりに著しい光を發したとしなければ、說明は出來ないやうに思はれる。これについて興味のあるのは、神奈川縣伊勢原町で厚木中學校の一生徒の觀察したものである。彼は箱根方面と東京方面に光を認め、横須賀方面にはサーチライトの光を認めたとて、其の狀況を圖示して居るが、其れは眞のサーチライトには非ずして、正しく自分が假にオーロラ狀と名づけた光である。[5] また逗子開成中學校の一生徒は逗子より北三十度東に、オーロラの如き光を認めて居る。

東京附近に於て光を認めた人々が、主として南と南東に見たことも一つの不可解な點である。これも矢張東京から南及び南東方向の地域に實際に光が現はれたとしなければ、充分に說明が出來まいと考へる。併し斯くの如く震央を距ること遠い所に、何故に光が現はれたかと云ふことも今のところ說明が出來ない。また光を發した地點も目下のところ明かにすることが出來ない。

---

5) 發光の狀況參照。

V. 發光の狀況

A. 形狀

各〻の報告者の記載して居る形狀は隨分まちまちであるが、大別すると次ぎの如くなる。（但しこれは報告者の記して居る所を其のまゝ分類したのであつて、これだけの種類の光が實際に現はれたと云ふ意味ではない）(1) オーロラ狀、(2) 電光狀、(3) 線狀及び帶狀、(4) サーチライト狀、(5) 喇叭狀、(6) 火球狀、(7) 雲狀、(8) 其他。

(1) オーロラ狀と假に名づけたものは、「放射狀」「太陽の昇る時の如し」「扇形に擴がつた」「地雷火の爆發したやうな形」等と形容されて居るものである。オーロラを親しく見たことのある或る科學者が、大層よく似て居ると云はれた相であるし、自分も同樣の感を起したので、斯く名づけたのである。

(2) 電光狀と稱するものは頗る曖昧なもので、必ずしもジグザグの電光と云ふ意味ではない。幕電の如きものも勿論含まれて居るに相違ない。從つてこの中にはオーロラ狀の中に分類すべきものが少なからずあると思ふが、識別することが出來ないから暫くこの儘にして置く。また空の光である故に、直ちに電光を聯想して、電光狀と記載したのも少なくないに相違ない。故にこの種類は最も確實性に乏しいものと考へる。

(3) 線狀及び帶狀と名づけたものも、充分要領を得ないものが多い。「細長く」光つた、「帶狀」に光つたと云つても、オーロラ狀の光を、森や家屋を距てゝ其の上部だけを眺めた場合もあるだらうと思はれる。

(4) サーチライト狀と稱するものは、文字通りサーチライトの光の如きもので、これは確かにあつたらしい。靜岡縣多賀小學校の報告によると「探照燈より白光を帶び、柱狀に天空に輝光を放出し」云々とある。また靜岡縣田方郡中鄕村々長清水吉彥氏は「丹那盆地の稍南方の山の東側、卽ち箱根山脈の向ふ側と思はるゝ地點に、南下より北上に斜めに發射するサーチライト狀の火光を見ました」云々と報告して居る。但しこの中でも「探照燈の如く數列」「探照燈の光の如くパッと上方に」「探海燈より幅が廣く長さ短し」等はオーロラ狀の中に入るべきものかと考へる。

(5)　喇叭狀と名づけたものは「ラッパ形」「漏斗形」「カップ形」等と形容されて居るもので、或はサーチライト狀の光が雲の塊を照射した場合かとも思はれるが、暫くこの儘にして置く。

(6)　火球狀と命名したものは文字通り火の玉である。この種の光を觀察したと云ふ報告が數例ある。其の一二を記せば、靜浦の一漁夫は鷲巣山からトテモ大きな火の玉が飛び出し、南に向つて飛んだのを海上から見た。靜岡縣庵原郡松野村の天野八代氏は、眞東から少し北へ寄つた方向に、星より大なる青色の火の玉が昇り、其の玉からサーチライトの如き青い光が二三回發し、忽ち赤色に變じ、電光の如くなること數回、その後久しく空が淡紅色であつたと報告して居る。[6]

(7)　雲狀と名づけたものは、多分雲の塊に光が映じたものであらうと思ふ。

(8)　其他と稱するのは (1) から (7) までの孰れにも屬せしめられぬものを總て含めたのであるが、この中には隨分如何はしいものもあるやうである。

便宜上以上の如く分類はしたもの丶、餘りに簡單な記載が多いために、充分確實のものとは云はれない。併し少くもオーロラ狀、サーチライト狀、火球狀の三種は、實際に現はれたものらしく自分には思はれる。資料の中から形狀に關する記載を摘出して表にすると次ぎの如くなる。

(1)　オーロラ狀　(37%)

1.	スパークの如し	22
2.	スパークに似て非なり	1
3.	パツと パーツと　光つた	71
4.	圓くパツと	3
5.	サツと光つた	1
6.	ポーツと光つた	3
7.	ポーツと明るく	1
8.	ポカツと發したやうに	1
9.	太陽の昇る時の如し	6

---

[6] 火の玉が出た後暫く空が赤かつたと云ふ例が他にもある。其の理由は自分には不明である。

10.	日の出の如く放射狀に	2
11.	太陽地平線より昇る時と同じ、大さも殆んど太陽に等しく、圓くピカピカ光れり、但し太陽より薄ボンヤリの感あり	1
12.	太陽の沒した瞬間の如し	1
13.	湧出すやうに光つた	1
14.	青い樣な光が噴出すやうに光つた	1
15.	扇形に擴がつた、光芒に縞あり	1
16.	扇形	6
17.	扇形電光の如し	1
18.	輪廓は平い末廣形	2
19.	放射狀	7
20.	オーロラ狀	3
21.	一點より四方に散るやうに	2
22.	地雷火が爆發したやうな形	1
23.	稻妻が曲線でなく集つて火藥が爆發したやうである	1
24.	物が破裂したやう	1
25.	遠くの電光を見る如き光	1
26.	半圓形	4
27.	地平線を圓心とせる平圓形	1
28.	圓形	8
29.	橢圓形	3
30.	球狀	2
31.	やゝ圓形	1
32.	圓の如く境が明瞭でない	1
33.	マグネシウムを焚いた時の樣にパアと光つた	2
34.	セルロイドを燃したやう	1
35.	パツと瓦斯の燃え上つたやう、またセルロイドの燃えた時のやう	1
36.	電光の光り方と少し違つて横の線のやうでなくポーツと光つた	1
37.	圓のくづれた形	1
38.	圓い形をしてギザギザがあつた	1
3 .	少し圓い樣な形でギザギザがあつた	1
40.	柳の出る花火のはねた時の樣にパツと四方に擴る、但し光に筋なし	1
41.	120°-130° の形で擴がつた	1

42.	160°位の形で擴つた	1
43.	大きな焰のやうな形	1
44.	焰形で電光形を示さず	1
45.	球形に火花のやうに	1
46.	遠くの火事のやうにボーッと明るく圓く	1
47.	火災の如き形、色青く暫くの後ピカピカと二三回輕く輝き忽ち消ゆ	1
48.	火災の如く明るく火災にしては出現の時期早すぎ、消ゆることも早し	1
49.	遠くの火事の如し	2
50.	雲の間に明るく薄赤色にボーッと現はれて直ぐ消ゆ	1
51.	横に一時パッと光つた	1
52.	細長くして半圓形 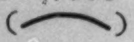	1
53.	最初圓形暫時にして横に擴りて消ゆ	1
54.	始め圓くだんだん擴がりボーッと消ゆ	1
55.	パッと圓形に波狀に流る	1
56.	はじめ圓く次第に楕圓形になり飛散す	1
57.	始め圓い様であつたが急に其がくづれて長い棒のやうになり消ゆ	1
58.	輪狀でゆらめきパッと消ゆ	1
59.	輪狀にパッと光つて消ゆ	1
60.	横に一面擴つてパッパッと	1
61.	三角のやうに	2
62.	動く度に長い三角や稻妻のやうに變る	1
63.	半月形に光り時々電光を交ゆ	1
64.	チカチカやつて居て、終りにパーと虹の様な色になつた	1
65.	穹窿狀（府下豐多摩郡大久保町より東南に）	1

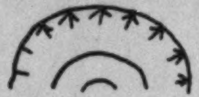

66.	（府下荏原郡世田ケ谷町より東に）	1

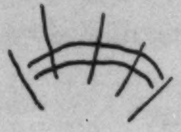

67. （神奈川縣中郡秦野町より東に） 1

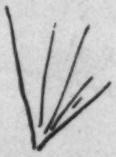

68. （神奈川縣中郡大根村より南東に） 1

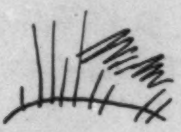

69. （神奈川縣中郡成瀬村より南東に） 1

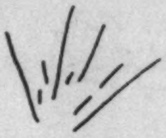

70. （神奈川縣中郡比々多村より南西に） 1

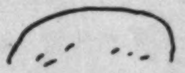

71. （府下南多摩郡町田町より東 25°南に） 1

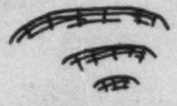

72. （神奈川縣高座郡海老名村より南東に） 1

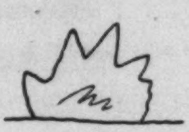

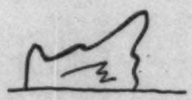

73. （千葉縣君津郡湊町より富士方向に） 1

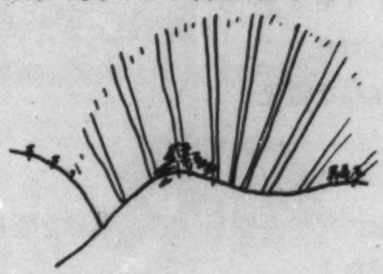

74. （神奈川縣三浦郡逗子町より北30°東に） 1

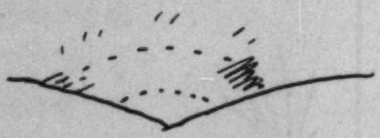

75. （神奈川縣高座郡茅ヶ崎より箱根及び海の方に） . . . 1

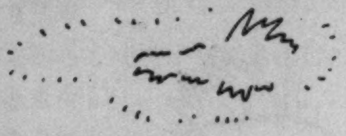

76. （茅ヶ崎より大山方面に） 1

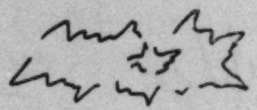

77. （神奈川縣中郡岡崎村より東に） 1

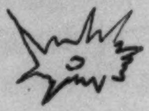

合計 209

(2) 電光狀 (27 %)

1.	普通の電光	1
2.	普通の電光のやうにシユツシユツと	1
3.	電光の如く光つた	98
4.	ピカツと光つた	6
5.	線香花火のやうにピカツと光つた	1
6.	電光に似る、但しジグザグを認めず	1
7.	電光の如くチカチカ光つた	1
8.	電光の如くチラチラ光つた	1
9.	電光に似たる閃光	1
10.	ジグザグの强烈な電光	1
11.	落雷の如し	1
12.	電光の大きいやうな形	2
13.	閃光的で稍振れたやうに思はる、電形を認めず	1
14.	電光に似て非なり	1

15.	普通の電光と色が違ふ、紫色	1
16.	電光に似て少しユツクリ光つた	6
17.	マグネシユームを燃したる如く電光より發光時間長し	1
18.	電光の様で細長い	2
19.	電光の如く横に長く	1
20.	電光に似た光が縱に見えた	1
21.	稲妻の様にピカツと下から上へ眞直の線になつて	1
22.	斜めに閃いた	1
23.	一筋の電光を認め、二三秒の後空明るくなつたが、光條を認めず	1
24.	稲妻の様なもので下より上へ光つた	1
25.	横に電光狀	1
26	普通の電光よりも細く强く横に直線的に	1
27.	電光の淡きが如し	1
28.	電光より幅廣く電光ほど鋭からず	1
29.	電光に似る（電光ほど光の帶强くなく寧ろ電光が雲へでも反映したやう）	1
30.	稲妻のやうに廣く光つた	1
31.	雲の中に電光の發せる如く（夏の雷鳴なき時の稲妻の如し）パツと光りて忽ち消ゆ	1
32.	遠くの電光のやうに	1
33.	電光よりも稍鈍き閃光	1
34.	電光の如く線香花火の如くパーと	1
35.	夕燒と强烈なる電光とを一所にしたやうな光	1
36.	南國の夏の夜の空模様のわるい時にある電光の光り方と殆んど同じ、比較的低く向ふの山蔭に沿ふて横に長く見えた	1
37.	電光の如きモヤ長く續く	2
38.	（本所區柳島元町より南及び南東に）	1

39. （神奈川縣鎌倉郡川口村片瀨より） 1

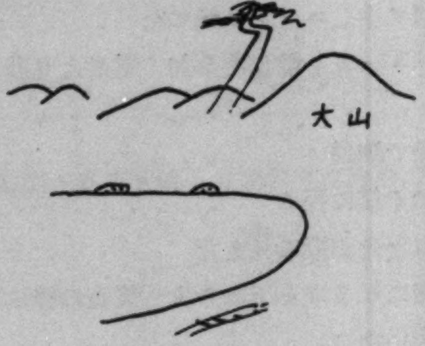

合計 149

(3) 線狀及び帶狀 (19 %)

1. 細長い 7
2. 細長く光つた 5
3. 細い光 1
4. 靑白き曲線、細き光 1
5. 細長く西方に走つて消ゆ 1
6. 細長く擴つた 3
7. 筋となつて光つた 1
8. 線狀 5
9. 橫に細く 2
10. （府下北豐島郡板橋町より南々東に） 1

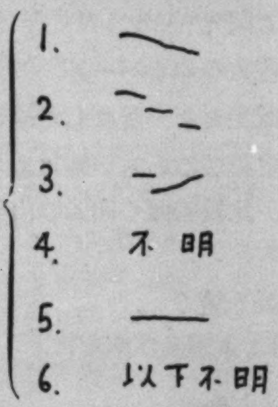

11. （府下北豐島郡瀧ノ川町より西に） 1

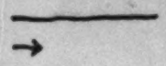

12. （神奈川縣中郡大磯町より東京横濱方面に） 1

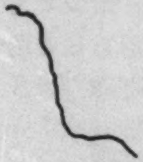

13. 細長く上に昇る 1

14. （府下豐多摩郡大久保町より東南東に） 1

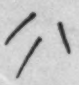

15. 1, 2, 3 の順序で圖の如く光つた（府下北豐島郡高田町より南 2°-3° 西に） 1

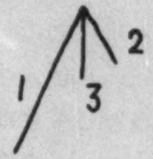

16. 短い糸の樣に光つた 1

17. 鏡に光の反射したる時の樣な狀態、幾分水平の線をなしたる時もあり 1

18. 電光に似て細長い 1

19. 太い線狀 2

20. 直線狀に上空に昇る 1

21. 横に棒狀 2

22. 棒の如く横に（府下豐多摩郡淀橋町より南に） . . . 1

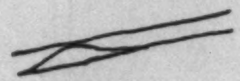

23. 流星の如く棒を横へし形 1

24. 縱の棒の如き形、電光より稍長時光る 1

25. 太い棒の樣な光が縱に光る 1

26. 上の方を向きて棒狀をなす（神奈川縣愛甲郡荻野村より南 30° 東に） 1

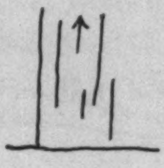

27.	太く長い	9
28.	太く長く光つて來てパツと擴つて光つた	2
29.	水平線のやうに横に長い形をして光つた	2
30.	（芝區二本榎西町より東—西に）	1

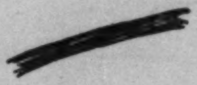

31.	眞直より少し斜め（神奈川縣中郡平塚町より西に）	1

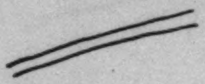

32.	帶狀をなす	11
33.	水平に帶狀	1
34.	細長き帶狀	1
35.	三條の帶狀をなす	1
36.	青味を帶びた帶の様な光	1
37.	帶狀で細長く彎曲せり	1
38.	幅廣く筋を引く	1
39.	眞中が稍廣く左右に長く	1
40.	南北に細長く兩端は尖る	1
41.	一面に横に擴る	2
42.	長い光	1
43.	縱に走る	1
44.	横に走る	4
45.	横に長く光つた	12
46.	横に廣し	1
47.	横に眞直	1
48.	幅廣く長い	1
49.	長く引いて大きく擴つた	1
50.	東北に向つて光が流れた様に見えた	1
51.	眞直の様に見えた	1
52.	弧を描いて東へ進み東南で消ゆ	1
	合計	106

(4) サーチライト狀 (9%)

1.	青白き光直立す	1

2.	斜めに發射するサーチライト狀の火光ボーとして暫くの間光を投ぐ	1
3.	細長き柱狀	2
4.	探照燈より白光を帶び柱狀に天空に輝光を放出す	1
5.	探照燈を照したやうな放射狀	1
6.	探照燈のやうに元が細く先の方が太くなつて居た	2
7.	探照燈のやうに細長く	1
8.	二つの探照燈の交錯したるが如く二條の稍黄色の光束より北にかけて二筋	1
9.	探照燈の如く數列	1
10.	燈臺の光の樣な形	1
11.	縦に光る、探照燈の如く下はせまく上するに從ひ幅廣くなる	1
12.	上が太い柱狀	1
13.	サーチライトの光形	1
14.	火の燃ゆるが如き光を認め、次いで探照燈の光の如き一線となり消失	1
15.	細長く眞直に立ち、稻妻の如く白色を帶び、其の光は等幅に非ずして、横面に凸凹あり、下にやゝ細く上に太くして、傘を開いたやうであつた	1
16.	（府下豐多摩郡長崎町より西方に）	1

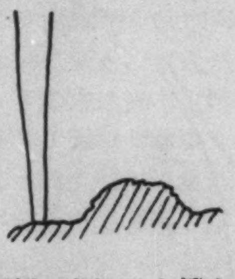

17.	（府下豐多摩郡幡ケ谷町より眞南に神奈川縣小田原町より東に）	2

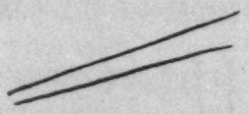

18.	（靜岡縣田方郡函南村丹那より南西に）	1

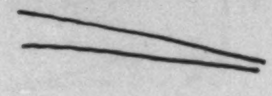

19. 一直線狀に赤色の火光立昇る 1

20. 火柱が立つた 1

21. 花火のやうな火柱 1

22. 大人の三抱位の火柱立ち其の先彎曲して消ゆ . . . 1

23. 探海燈の光の如くパツと上方に 3

24. 箒の樣にボーツと大きく 2

25. サーチライトの如く 10

26. 丁度探海燈の樣、探海燈より幅が廣く長さ短し . . 1

27. 父は「探海燈かな？」と云つた 1

28. 電光の如き火柱、赤色、雲間にありて下まで屆かず、
二三回斜に見ゆ 1

29. 上から下へ、上の尖つた 1

30. （神奈川縣横須賀市より西南西に、同縣中郡大根村よ
りほゞ南に、同郡北秦野村より東南東に） 3

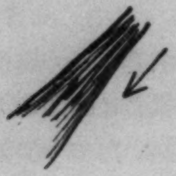

31. （神奈川縣中郡平塚町より南西に） 1

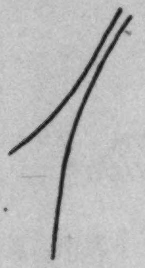

32. 圖の如し（靜岡縣田方郡修善寺町より箱根方面に） . 1

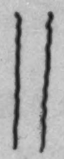

合計 48

(5) 喇叭狀 (1％)

1. ラツパ形	1
2. 漏斗形	1
3. カツプ形	1
4. （神奈川縣中郡西秦野村より伊勢原方面に）	1

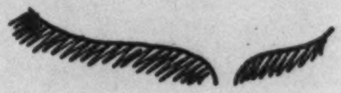

5. （丹那より東に）	1

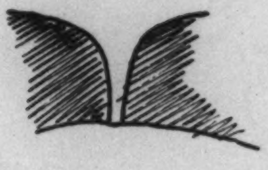

合計	5

(6) 火球狀 (1％)

1. 花火を揚げた時の如く圓い形をして上る、玉形のものゝ側に橙色をしたものがついて上つた	1
2. 青色の星より大なる玉より探照燈の如く二三度青い光を發し、忽ち赤色に變じ、電光の如くなること數回、其後久しく空淡紅色を呈す	1
3. 始めは火の玉の如く見え、だんだん擴がつて空一帶あかるくなり、下の方は赤く夕燒のやうに見え、稻妻のやうに光つて十數秒で消ゆ	1
4. 玉が昇ると共に一面に明るくなつた	1
5. 大きな火の玉が鷲巣山より出て南に飛んだ	1
合計	5

(7) 雲狀 (2％)

1. 雲形	1
2. （府下荏原郡大崎町より西方に）	1

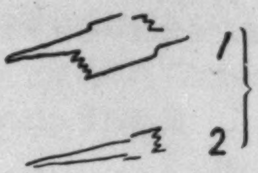

3. (府下荏原郡碑衾町より南々西に) 1

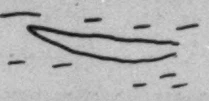

4. (イ、ロ、交互に明滅)(府下荏原郡東調布町より殆ど南に) 1

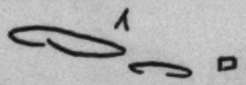

5. 細長く割合に短い(神奈川縣足柄下郡足柄村より箱根方面に) 1

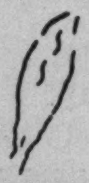

6. (神奈川縣中郡大根村より南に) 1

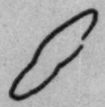

7. 圖の如くで割れたやうに見えた(神奈川縣高座郡小出村より東に) 1

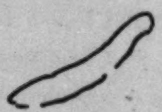

8. 一團の白雲あり、その雲全體が地震最中淡赤色(雲に反映せる火事の如く)を呈し、瞬時にして止む . . 1

9. 雲の動いて居る様に 1

10. 雲の塊が三回ばかりパツと明るくなつた 1

合計 10

(8) 其他 (4%)

1. 山の中腹に圓く光る、但し大小あり 2

2. 圓い光が一直線に並んで其の一つはクルクル廻つた、高さは電柱の頭部位 1

3. 丸い光るもの 1

4. 太陽よりズツト大きい圓い光 1

5.	（神奈川縣 愛甲郡高峰村より南東に、同郡中津村より南東に）	2

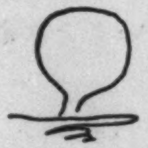

6.	（神奈川縣中郡高部屋村より東に）	1

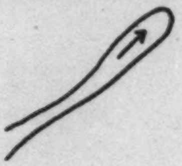

7.	槍の穗先のやう	1
8.	煙狀	1
9.	火を燃す時煙が昇る如く	2
10.	ゆらめくやうな光	1
11.	線香花火のやうにキラキラ光る	1
12.	花火のやう	1
13.	電燈のやうに光つた	1
14.	三線交叉、短冊形	1
15.	長方形	2
16.	四角	1
17.	（神奈川縣足柄上郡櫻井村より南東に）	1

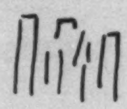

18.	（神奈川縣中郡岡崎村より南東に）	1

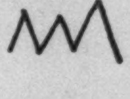

19.	三角形の長い棒の樣なものが光つて雲へ入つた	1
20.	クチヤクチヤに亂れて居た	1
21.	アミーバの如き形の光	1
	合計	25

B. 色　　彩

色彩についての記載を各々の報告の中から摘出して大別すると、次表の如くなつて、青色殊に靑白色が多いことがわかる。

(1) 青 (28%)

1.	青色	61
2.	眞青	1
3.	澄み亘つた青	1
4.	青白色	138
5.	青い様な色	4
6.	青みがゝつた色	3
7.	青味を帶ぶ	7
8.	稍青味を帶ぶ	3
9.	青つぽい色	1
10.	青い様な銀の様な色	1
11.	空色	1
12.	淡青色	2
13.	水色	1
14.	濃い水色	1
15.	淡い水色	3
16.	淡い水色に青色を混ず	1
17.	淺黃色	1
18.	銀青色	1
19.	青味を帶びたネオンサイン式の色	1
20.	白の様な青の様な色	2
21.	淡青白色	5
22.	青白く殊に白色が多い	1
23.	銀白青みがゝる	1
24.	灰青白色	1
25.	白青色	4
26.	燈用瓦斯の光に似て淡く、光澤ありて硝子を通して見るが如し	1
27.	マグネシウムを燃やした時の様	5
	合計	252

(2) 赤+黄 (12%)

1. 橙色	15
2. オレンヂ色	3
3. 黄橙色	2
4. 橙色を帯ぶ	2
5. 淡い橙色	2
6. 橙色に白が混つたやう	2
7. 薄い桃色の様な橙色の様な混合色	1
8. 青橙色	1
9. 青味を帯びた橙色	3
10. 橙色の中に黄青白色等	1
11. 赤黄	18
12. 赤黄の混合色	7
13. 淡赤黄色	1
14. 赤に稍黄色を帯ぶ	3
15. 赤味を帯びた黄色	2
16. 赤い様な黄い様な	1
17. 赤色と卵色の混り	1
18. 薄紅に黄味を帯びた色	1
19. 赤黄がゝる	1
20. 赤く少し黄	1
21. 黄赤色	12
22. 淡黄赤色	1
23. 黄に赤を帯びた様な色	6
24. 黄がゝつた赤	2
25. 黄色で少し赤味がさす	2
26. 淡い黄赤色	1
27. クリーム色に赤味を帯ぶ	1
28. 黄色赤色	1
29. 黄、赤	1
30. 黄白赤色	1
31. 樺色	2
32. 黄色に樺色を帯ぶ	1
33. 赤に樺色	1
34. 赤茶色	2
35. 赤褐色	1

36.	赤と褐色の混り	1
37.	帶黃褐色	2
38.	褐色を帶び青も少し混ず	1
39.	紫がゝつた褐色	1
40.	夕燒の金色に近し少し赤い	1
41.	夕燒に黃色を帶び少し青が入る	1
42.	火炎の色に黃味を帶ぶ	1
43.	火災の時の空の色に黃を混ず	1
44.	上は黃色じみ、だんだん赤色になる	1
45.	上が樺、下が黃	1
46.	金色に赤色の混つたもの	1
47.	紫黃色	1
	合計	116

(3) 黃色 (12%)

1.	黃色	33
2.	黃金色	3
3.	濃黃色	1
4.	電氣のやうに黃色	1
5.	淡黃色	6
6.	淡黃色のやうな色	1
7.	やゝ黃色	7
8.	黃味を帶ぶ	3
9.	黃色つぽい	1
10.	金づんで居た	1
11.	黃白色	11
12.	明るい黃白色	3
13.	淡黃白色	3
14.	帶黃白色	6
15.	黃みがゝつた白	1
16.	黃い樣な白い色	2
17.	白黃色	4
18.	金色に白色を混ず	1
19.	淡白黃	1
20.	白淡黃色	1
21.	白みがちの黃色	1

22.	白色、黄色がゝつて居る	1
23.	白色に近い黄色	1
24.	白に少し黄混る	2
25.	白と黄の混合色	1
26.	白がゝつた黄色	2
27.	Chrome-yellow tint No. 1	1
28.	Dark yellow	1
29.	黄色白色	1
30.	黄に白みを帯ぶ	1
	合計	102

(4) 電光色 (11%)

1.	電光色	67
2.	明るい電光の色	1
3.	電氣の火花の如き色	2
4.	電光より鈍し	1
5.	電光より少し色は弱い	1
6.	電光の濃い色	3
7.	電光よりやゝ淡き色	1
8.	電光に赤味を帯ぶ	9
9.	電光のやうで幾分赤色(黄色)を帯ぶ	1
10.	電光より黄がゝつて居た	2
11.	電光より青味を帯ぶ	9
12.	電光の様でやゝ黒み走つた色	1
13.	電光より白色を帯ぶ	1
	合計	99

(5) 赤+青 (9%)

1.	赤みがゝつた青	19
2.	赤青い色	6
3.	赤と青とを合せたやうなもの	4
4.	赤く青く	2
5.	赤い様な青い様な	1
6.	赤青	2
7.	桃色に淡青色	1

8.	青と赤の斑	1
9.	花色	1
10.	青赤い色	5
11.	青に赤を帯ぶ	1
12.	青色に少し赤のかゝつた色	1
13.	青白色と赤色とが混じて居た	2
14.	青白く少し赤し	2
15.	紫	4
16.	薄紫	1
17.	少し紫がゝる	1
18.	白色紫色を帯びた色	1
19.	紫色と白色の混色	1
20.	青紫色	5
21.	紫青	1
22.	白に青紫を混ぜたみたいな色	1
23.	青紫にやゝ黄色の入つた色	1
24.	赤味を帯びた青紫色	1
25.	赤紫	4
26.	紫に少し赤味を帯ぶ	10
27.	青くやゝ青紫色を帯ぶ	1
28.	銀色と薄紫に薄い赤を混ぜた色	1
29.	赤に放電の時の色を混ぜた様な色	1
	合計	82

(6) 青＋黄 (9%)

1.	青黄色	13
2.	青く黄く	1
3.	青く幾らか黄みがかる	1
4.	青みを帯びた黄色	1
5.	青白黄	2
6.	空色に黄色まじる	1
7.	水色と黄色の混つた様な色	2
8.	黄色と青色の混つた色	1
9.	青の少し入つた電氣の色より少し黄色い様な色	1
10.	青白い黄色い様な色	1
11.	青白い色と黄色の光が入亂れて居た	1

12.	青白く黄味を帶ぶ	1
13.	蒼白色にやゝ黄を帶ぶ	1
14.	青白黄色	1
15.	青色にて周圍黄みがかる	1
16.	白と青と黄色を帶ぶ	1
17.	黄青	6
18.	黄青い光	2
19.	帶黄青色	2
20.	黄に青味を帶ぶ	1
21.	黄色に少し青味がかる	2
22.	黄がかつた青	16
23.	黄い様な青色のかかつた色	1
24.	黄味を帶びて青白い	1
25.	薄く黄みがゝつた蒼白色	1
26.	薄黄色い様な青い様な色	1
27.	黄色を帶びた淡い空色	1
28.	黄に青	1
29.	黄と青、赤も少し含む	1
30.	綠色	1
31.	綠青色	1
32.	黄がかつた綠色	1
33.	黄色の混つた綠色	1
34.	淡黄綠白色	1
35.	黄綠色に白を帶びた如き色	1
36.	黄綠を混じたやうな色	1
37.	黄色に紫の混つた色	1
38.	紫黄色	1
39.	紫白色	1
	合計	76

(7) 赤色 (7 %)

1.	赤色	30
2.	眞赤	2
3.	焰色	2
4.	普通の火の色	1
5.	淡赤色	11

6.	桃色	2
7.	赤色か桃色	1
8.	赤みがかる	1
9.	赤みを帶ぶ	3
10.	鈍い赤色	1
11.	赤色づいた色	1
12.	火色より稍淡色	1
13.	やゝ赤味を帶ぶ	2
14.	赤白色	4
15.	赤い様な白い様な色	1
16.	白い様でポーツと赤い色を帶びた色	1
17.	黑味を帶びた赤	1
	合計	65

(8) 電燈色 (4%)

1.	電燈色	10
2.	電氣の光の様な色	17
3.	ガス入電球より發する色	1
4.	艶消電球の如き色	1
5.	電燈より濃い色	1
6.	電氣の光より淡し	1
7.	白い電燈のやうな色	1
8.	電球の光つた色に少し赤色を帶ぶ	1
9.	電氣の光に赤を混ず	1
10.	電燈の光に少し黄色の入つた様な色	1
11.	電燈の光に少し青味を含む	2
12.	電氣の光と螢の光を合せた様な色	1
13.	電氣の薄い黄色で、すぐ紫色になる	1
	合計	39

(9) 白色 (4%)

1.	白色	28
2.	白い様な色	2
3.	白みがかつた色	1
4.	白銀の様な色	1

5.	白熱	1
	合計	33

(10) 其他 (4％)

1.	サーチライトの様	4
2.	サーチライトの弱い様な色	1
3.	サーチライトより白光を帶ぶ	1
4.	セルロイドを燃したやう	1
5.	最も强い瓦斯燈のやうな色	1
6.	瓦斯の如き色	1
7.	レントゲンの光線に少し赤味を加へたやう	1
8.	日光のやうな色	1
9.	曇ガラスのやうな色	1
10.	星の光の様な色	2
11.	金星の色	1
12.	虹のやうな色	1
13.	上が紫で下が黄	1
14.	螢光(弱きもの)	4
15.	紫、白、黃色	1
16.	黃白紫色	1
17.	青黃赤	3
18.	何とも云へぬ土色と黃色と混ぜたやうな色	1
19.	赤黃綠白空色	1
20.	赤に青黃を混ず	2
21.	赤色薄黃色紫等混合	1
22.	燈色	1
	合計	32

C. 光度其他

各地で觀察された光の光度は頗る强烈であつたらしい。東京附近に於ても「其の光が家の中を照して如何にも恐ろしかつた」(府下井荻町)、「近くの人の顏が見える程」(府下品川町)であり、また「物凄きこと何とも譬へやうがなかつた」と云ふ(赤坂區)。厚木町では「晝間の様で」あつた。靜岡縣大仁から約十キロの距離にある達磨山がありあり見えた。靜岡縣賀茂郡稻生澤村本鄉では、五六町距つて居る中村の家々がよく見えた。

光の現はれた大體の位置と其の光を觀察した位置との距離が相當に正確にわかつて居る例として、三浦半島秋谷に於ける逗子中學校生徒の報告は極めて貴重なるものである。その報告によれば、箱根の左の方から光が出て、其の時には月の光以上に一面に明るくなつたと云ふことである。この「箱根の左」を假に丹那盆地とすると、秋谷との間の距離は約五十五キロである。また伊豆山邊としても四十八キロである。千葉縣君津郡巖根村に於ては、箱根方面に光を認めたが、其の光景は「壯觀にして形狀しがたき程」であつたと云ふ。この光が眞に箱根より發したとすれば、其の距離は約八十五キロである。箱根と巖根村とを連ねる線は丁度三浦半島北部を過ぎるが、若し其の光が三浦半島北部に發したとしても、約三十キロである。震央附近に於ては、其の光度は一層强烈であつて、丹那盆地で聞いた所によると、「腰が拔ける程光つた」相である。また箱根町に於ては、光つて居る間は用を辨ずるに一向不自由を感じなかつた。地上に切れて落ちて居る電線まで明らかに見えて、其を避けて歩むことが出來た。無電局から舊本陣石内家に人が駈けつけて來るのに、滅茶々々に裂け崩れて居る道を恙なく駈けて來ることが出來た程に明るかつたと云ふことである。

各〻の光の發光時間については、各報告者の記すところ區々として一定しないが、時間を數量的に記載したものには、「二秒」、「十秒位」、「約一分弱」、「二三分」等がある。沼津市の吉井幸吉氏は、同地から丹那方面に見えた光について詳しい報告を寄せられたが、同氏によると、光り續けた時間は一分間餘、或は其れ以上であつたと云ふ。また丹那盆地の一農家で自分が親しく聞いた所によると、東の山の後ろから朝顏の花のやうな光が出て、十分位續いて居たと云ふことである。

發光時間を電光と比較したものも少くない。

(1) 「電光に似て少しゆつくり光つた」(府下中野町)
(2) 「電光に似て速度ゆるやか」(府下大久保町)
(3) 「緩漫なる稻妻樣」(府下杉並町)
(4) 「稻妻のやうにしてピカピカするのが稍遲し」(神奈川縣足柄上郡酒田村)
(5) 「電光より少し遲く光り」(神奈川縣高座郡海老名村)
(6) 「稻妻より光る時間長し」(神奈川縣箱根湯本)
(7) 「電光より稍長時に亘つて見ゆ」(靜岡縣庵原郡庵原村)

(8) 「電光より發光時間長し」(千葉縣安房郡國府村)

以上の資料によると、今回現はれた光は、電光の如く瞬間的の現象にあらずして、やゝ緩漫な光であつたらしい。

發光と震動との間に相互關係があるらしい資料も若干ある。卽ち下の如くである。

(1) 「地震の搖れ方激しき毎に光る樣に思はれた」(府下豐多摩郡上井草)

(2) 「震動する度毎に光る」(府下荏原郡駒澤町)

(3) 「强く搖れが來る毎に光りたるやうに感ず」(府下荏原郡大井町)

(4) 「震動の度毎にパッパッと光る」(赤坂區高樹町)

(5) 「餘震の來る度毎に光つた」(箱根湯本)

(6) 「搖れ方と時間的に一致したと思ふ」(荏原郡碑衾町)

(7) 「地の動くと同じ樣に(光が)動き」(神奈川縣中郡川瀨村)

(8) 「光つたり消えたりし、其と同時に地震が搖つた」(神奈川縣中郡城島村)

(9) 「震動につれて光つたり消えたり」(橫濱市)

(10) 「光の起つた際は殊に震度が大であつた」(鎌倉町)

(11) 「振動毎に光を放つ」(神奈川縣三浦郡田浦町)

(12) 「搖れる毎に光が湧き出す樣な氣がした」(神奈川縣鶴見)

(13) 「怪光につれて地震起る」(前同)

(14) 「搖れて居る其の周期を同じうして明るくなり暗くなる」(千葉縣君津郡周南村)

(15) 「搖れる度毎に」(千葉縣君津郡貞元村)

(16) 「グラグラ振動する度毎にパッパッと輝く」(千葉縣君津郡湊町)

(17) 「地震の搖れる度に光つた」(芝區白金町)

(18) 「地面の動く度にピカリピカリと光りました」(府下荏原郡荏原町)

(19) 「地震の震動と共に明暗」(日本橋區北島町)

(20) 「强い地震が來る度毎に光つた」(府下豐多摩郡代々幡町)

(21) 「地震が相當激しくなる時に見え始め、ゆるやかになれば消えた」(府下荏原郡世田ヶ谷町)

(22) 「强震の襲來毎に數回に亘つて光を發せり」(府下豐多摩郡杉並町)

(23) 「ひどく搖れる度毎に稻光のやうに廣く見えた」（府下荏原郡世田ヶ谷町）

また搖れ方の强弱と光の光度とが比例したと云ふ報告には次ぎのものがある。

(1) 「劇震と電光の强さと比例するやうであつた」（箱根町）
(2) 「最も强く搖れた時が最も光が强かつた」（神奈川縣足柄上郡酒田村）
(3) 「地震の强弱に應じて輝光に强弱を生ず」（靜岡縣田方郡多賀村）

D. 音響の有無

今回の地震に伴つた光は音響を隨伴したかどうかと云ふ事については、照會をする際に特に注意を促すことをしなかつたゝめに、明かに記載してあるものは少ない。兎に角音響についての記載は次ぎの如くである。

(1) 「光つてから約一分の後遠鳴のやうな音を聞いた」（府下南葛飾郡小松川町）
(2) 「光が現はれる時に無氣味な人の呻く樣な轟きがあつた、但し最初に現はれた時」（府下南多摩郡町田町）
(3) 「火の燃えるやうな形の光が見え、同時にゴーと云ふ音と共に前の如き光が出た」（神奈川縣三浦郡秋谷）
(4) 「稻光の消えた後地の底でボーと音がした」（神奈川縣高座郡寒川村）
(5) 「先づ電燈が消え、大きな音が聞え、直ちに大地震が起つた」（神奈川縣高座郡綾瀨村）
(6) 「韮山の方に火柱が立ち、地鳴がし、家屋が震動した」（靜岡縣駿東郡淸水村）
(7) 「ボーッと明るく雲の間に光る、ウナリの聞ゆる十秒前」（靜岡縣淸水市）
(8) 「音はしなかつた」（神奈川縣厚木町）
(9) 「何かの爆發かと噂し合つたが爆音は聞えなかつた」（靜岡縣沼津市）
(10) 「この前送電線に鳥が引かゝつた時は大きな音がしたが、今回の光には全く音を伴はなかつた」（神奈川縣箱根町）

(11) 「午前四時三分ゴウーッと山鳴りがして間もなくゴロゴロと大きな地震があつた、其の時皆家から飛び出すとバアと光るのを認めた」(神奈川縣足柄下郡湯河原)

此等の資料に基いて考へて見るに、今回現はれた光には音響を伴はなかつたらしい。「遠鳴」「ウナリ」「地鳴」「山鳴」などゝ云ふものは、普通に地震に伴ふ地鳴であらうと考へる。

VI. 古記録との比較

地震に伴ふ光の現象の文獻は、自分が今日まで聚集した所のものが、本邦の例だけで九十一例、其の中明治以前のもの六十七例である。この數は、少しく努力すれば、倍にすることは大して困難でないと信ずる。其等の資料について見るに、地震に伴ふ光の現象には、大別して四種あるらしく思はれる。即ち

(1) 單に地震に伴ふもの。
(2) 地震のために生じた山崩れに伴ふもの。
(3) 地震津浪に伴ふもの。
(4) 地震によつて生じた裂罅から火焔を噴出するもの。

今回の伊豆地震に觀察されたものは、其の中 (1) 及び (2) の二種であつて、孰れも古記録に記す所と著しい類似を示して居る。

1. 地震に先つて光の現はれたこと

今回の光の現象が十一月二十六日午前四時三分の地震の前から既に現はれたのではなからうかと云ふことは、前に記した通りであるが、昔の記錄にも次ぎの如き例がある。

(1) 「廿二日大地震以前より折々光り物白氣夜半に相見へ申候所に、廿二日の夜月の色かわり、光り物相見へ、星ながれ候事繁く」(元祿十六年關東地震)

(2) 「大地震の發りは五六日前より日々暮時頃より夜四時頃迄西北之空電いたし、此光り常之稻光よりは分而强く、何れも怪敷思候許に而御座候」(天保元年畿內地震)

(3) 「又京の人の言を聞くに、大震の前夜には空一面に光り物ありて、地面よりも光り出現し、大體晝の如なりしゆゑ人々訝りて

何なることやと云合ひしが果して翌日にかの大震なりしと是も飛州の話」(前同)

(4) 「夜に相成四時前電光有之候をは須坂陶器場職人久兵衛米子村におゐて見受、其外見受候者有之、正四ッ時頃滔々の音とひとしく大地震に而……」(弘化四年善光寺地震)

(5) 「飯綱山の方に火の如き雲出候間、不思議に存、見つめて居候處、其雲くるくると廻り消るや否山鳴致し、直に大地震になり」(前同)

(6) 「地震の少し前に洋の方に四斗樽といふものゝ大さなる物ありて、左右へわかる、一つは房總の方へ赴き、一つは江戸の方へ赴くと見えしが間もなく大地震あり」(安政二年江戸地震)

(7) 「二日の夕海上へ漁獵に出たりしが、地震の前東北の方一時に明るくなり、各著たる衣服の染色模樣迄鮮かに見え分る程也しが、やがて海底より鳴渡りて船底へ砂利を打當る樣に聞えて恐ろしかりしが、又一團の火炎空中を鳴渡りしかば、彌恐ろしく成て、船を陸へ付しに、はや地震の後にて」(前同)

2. 光度極めて强烈なりしこと

光の光度の强烈なりしことは前述の通りであるが、この點も古記錄の記載とよく一致する。

(1) 「流光如晝」(貞觀十一年陸奧地震)
(2) 「大體晝の如く」(天保元年畿內地震)
(3) 「屋の內隅々まで晝の如く見へ」(弘化四年善光寺地震)
(4) 「衣服の染色模樣まで鮮かに見分けられ」(安政二年江戸地震)

3. 山崩れに著しき光を伴ひたること

山崩れに伴ふ發光は、今回の地震に於ては、靜岡縣田方郡梶山に於て觀察されて居るが、慶長元年七月九日豐後薩摩の地震には速見高崎山崩壞して火が出たと云ひ、また弘化四年善光寺地震には、岩倉山崩壞して、家の隅々まで晝の如く明るくなつたと云ふ記錄がある。

4. 形狀の類似すること

a. 「東西雲なくして稻光の如くひかり有之候」(元祿十六年關東地

震）、「電光の様には無之、空惣ひかりに光」（天正十七年駿河遠江地震）、「電の如ならず、その幅何十丈とも量りがたきが、一面に火氣たちて須臾に消る」（安政二年江戸地震）、「月輪之如く空光申候」（弘化四年善光寺地震）等の記錄があるが、これは多分自分の所謂オーロラ狀の光であらうと考へる。後法興院記に明應七年八月廿六日東海道地震に現はれた光を記載して、其の中に「カラカサノセイ」と云ふ言葉が用ひられてあるが、これは「傘の精」で、オーロラ狀の光が恰もサッと傘を開くに似て居るから、斯く呼ばれたのであらうと想像する。

b.　今回の地震に火球狀の光の觀察せられたことは、前に記した通りであるが、この例も古來の記錄に少なからず發見せられる。

(1)　「東をさして飛ぶものあり、其の形提灯のごとし」（寬文十二年江戸地震）

(2)　「大地震動して車輪の如くなる火の玉飛違ふこと透間なし」（元祿十一年土佐地震）

(3)　「何やら火の玉の如きもの飛ぶを見ると云ふ」（享保十九年江戸地震）

(4)　「大なる火の玉折〻飛行致候」（弘化四年善光寺地震）

(5)　「大釜程の光物飛出申候」（前同）

(6)　「火玉南より北にとぶ」（安政元年十一月五日南海道地震）

(7)　「四斗樽といふものゝ大きさなる物ありて左右にわかる」（安政二年江戸地震）

(8)　「蹴鞠ほどの光り物」（前同）

(9)　「坊主の首火の付たる木を喰へて東より西の方へ飛行」（前同）

c.　サーチライト狀の光ではないかと思はれるものも、僅か一例ではあるが、安政二年江戸地震の記錄にあつて、「虹の如くその長十丈ほどなるすぐの氣」と記してある。また「火柱」と稱するものも、或はこの種の光を云ふのではなからうかと考へる。

d.　彎曲した光を認めたと云ふ例が今回の地震に一つある。即ち小田原で、大人の三抱へ位の火柱が立ち、其の先きが伊豆半島の方に曲つて消えたのを見たと云ふ人がある。これに類似するものは安政二年江戸地震の記錄にあつて、「數丈の火氣赤く見へ、鍋つるの如く曲りて折れたるを看たり」とある。

VII. 結語

(1)　昭和五年十一月廿六日午前四時三分に發した伊豆地震には著しい光の現象が現はれた。

(2)　其の光は地震の發する前から現はれ、發震後暫くの間繼續した。

(3)　其の光は五十キロを距てた所でも尚ほ月光以上の光度を有した。

(4)　形狀は少くもオーロラ狀、サーチライト狀、火球狀の三種があつた。

(5)　色は青白色と見た者が最も多い。

(6)　音響は伴はなかつたらしい。

(7)　昔の記錄と比較するとよく一致する。

(8)　當時この地域に雷雨はなかつたから、この光は普通の電光ではない。

(9)　この光は送電線のない所でも見られた。

(10)　送電線から著しく發光するのを見たと云ふ報告が一つもない。

(11)　故に自分はこの光の現象が直接地震と關係あるものではないかと考へる。

(12)　但し發光の機巧は自分には分らない。

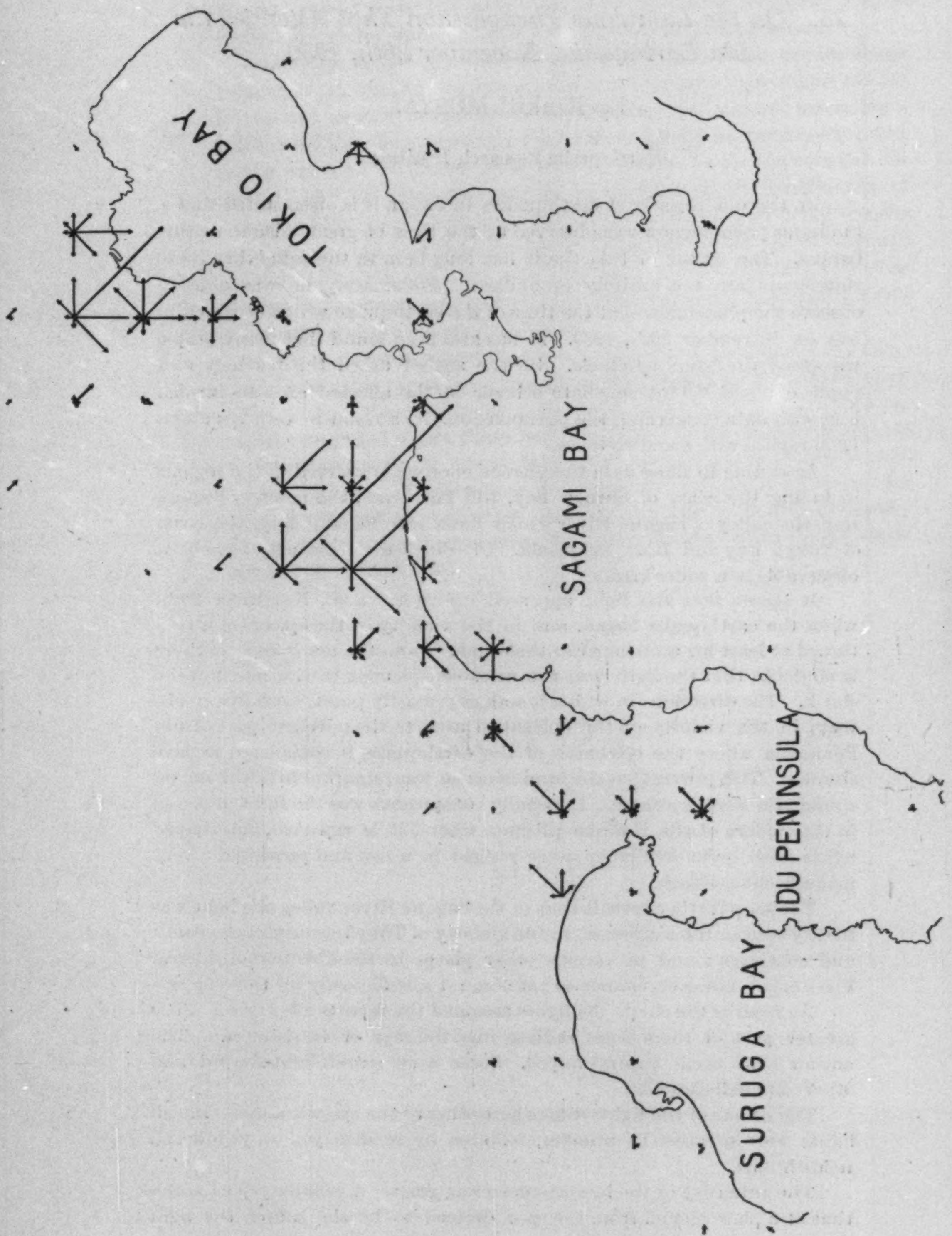
TOKIO BAY
SAGAMI BAY
IDU PENINSULA
SURUGA BAY

光を見たる方向

矢は光を見たる方向を示し矢の長さは同じ方向に光を見たる人の數に比例させてある

15. *On the Luminous Phenomenon That Attended the Idu Earthquake, November 26th, 1930.*

By Kinkiti MUSYA,

Earthquake Research Institute.

In the old records of earthquakes in Japan it is often stated that a luminous phenomenon was observed at the time of great seismic disturbances. The writer of this thesis has long been in the belief that those statements are not entirely groundless. Fortunately he was able to observe the phenomenon at the time of the earthquake which occurred in Idu on November 26th, 1930. It has also been found that many people witnessed the same spectacle. So the author asked the teachers and pupils of about 150 intermediate schools in the affected area to furnish him with data concerning the phenomenon. As a result he received about 1,500 replies with some sketches.

According to those data the phenomenon was observed in the regions including the coast of Suruga Bay, Idu Peninsula, the coast of Sagami Bay, the valley of Sagami River which flows into Sagami Bay, the coast of Tôkyô Bay and Bôsô Peninsula. Of course the light may have been observable in a wider area.

It seems that the light appeared before 4:3 a.m., November 26th, when the earthquake began, and in the vicinity of the epicentre it continued at least for an hour after that time. From the many reports there is no doubt that the light was the most conspicuous in the midst of the shock. The directions in which it was seen mostly point, as shown in the map, in the vicinity of the epicentral area, to the northern part of Idu Peninsula where the epicentre of the earthquake is considered to have situated. This proves that the luminescence was remarkable in the region round the seismic centre. Especially conspicuous was the light observed in the caldera of the Hakone volcano. where, it is reported, ball-shaped lights with great brilliancy were ranged in a row and presented a very magnificent spectacle.

The map further reveals that in the Sagami River valley the light was mostly seen in the southeast; in the vicinity of Tôkyô mostly in the south and southeast; and in various other places in the direction of the sea. The author, however, cannot as yet account satisfactorily for these facts.

As regards the shape the lights assumed the reports are varied. The greater part of them were radiate like the rays of the rising sun. The author calls them aurora-shaped. Some were search-light-shaped and others fire-ball-shaped.

The colour of the lights differs according to the eye-witnesses. Bluish lights were greatest in number, followed by reddish yellow, yellow and reddish blue.

The intensity of the luminescence was great. A reliable report states that at a place 50 km. from the spot deemed to be the source the light was greater than the moonlight.

The duration of each light was longer than lightning. Some careful observers report that the same light was perceived for more than a minute. No sound seems to have accompanied the luminescence.

According to the old records of earthquakes in Japan the luminous phenomenon accompanying seismic disturbances seem to be of four kinds: (1) the one merely attending an earthquake; (2) the one attending a landslip; (3) the one attending a tsunami caused by an earthquake; and (4) the emission of flames from fissures formed in an earthquake. Of these (1) and (2) were observed on the occasion of the earthquake of November 26th, 1930, and they coincide with the accounts in old records in four points: (a) that the light began to appear before the earthquake occurred; (b) that the light was very strong; (c) that landslips were attended by luminescence; and (d) that there were aurora-shaped, searchlight-shaped and fire-ball-shaped lights.

It has been ascertained by the investigation of the Central Meteorological Observatory that there was no thunderstorm in the affected area at the time of the earthquake. So those lights could not be lightning. The light appeared where there were no high-voltage electric wires, nor has there been a single report stating that those wires were seen to emit considerable light. The phenomenon, therefore, cannot be accounted for by the sparks from electric wires. Although he is as yet unable to explain the mechanism of the phenomenon, the writer believes them to be directly related to the earthquake.

16. 昭和5年10月17日加賀南西部の强震調査報告

岸上冬彦

(昭和六年三月二十日受理)

加賀南西部卽ち石川縣能美郡、江沼郡及び福井縣坂井郡附近に、昭和5年10月17日午前6時32分及6時36分頃に强震があつた。被害は少なかつたが、此の地方は從來地震の少なかつた所である爲と、大正14年の但馬地震、昭和2年丹後地震を想起し地震活動の東方へ移動することを考へ、此の地震は注意を引いた。筆者は其の調査を命ぜられ、10月21日に東京を出發し一週間實地踏査をすると共に、筆者の考案した携帶用地震計を持つて行き、22日から26日まで大聖寺町に於て地震觀測をした。

此の地方の地震 今回の地震の最も激しかつた地域は金澤、福井兩市の中間にあつて、此の附近は海岸に沿うて洪積紀の低い丘陵のある地方である。東方約50 km. には白山火山が加賀、飛彈の國境に聳え、其の東は我が國中部の高地に續いてゐる。

所謂內側地震は能登半島の北部を過り海上を通つて丹後半島に到り更に西に走つてゐる。又之と殆ど垂直に、明治24年の濃尾大地震の斷層線は陸地測量部によつて行はれた水準測量の結果、伊勢灣から福井附近まで續いてゐると考へられてゐる。[1]

今迄此の附近で著しい地震は第一表の如くである。

尙以上の他にも小さい地震は[2]あつた樣であるが、此處には記錄の確かなもののみを記した。此等の中で震原が此の地方にあると考へられるものは 1, 3, 8, 10 で、其の他は他の地方に起つた大地震の餘波をうけたものと思はれる。

---

[1] A. Imamura, "On the Seismic Activity of Central Japan," *Jap. Journ. Astr. Geophys.*, 6 (1928), 119.

[2] 岸上冬彥「石川縣大聖寺町の地震記錄」地震 3 (1931), 220.

第 一 表

	日本暦	西暦	震原又は被害地域の地名	此地方に於ける被害
1	寛永 16. XI	1639, XII	越前	福井城破損
2	寶永 4. X 4	1707, X 28	東海道・畿內・南海道及東山・西海兩道の一部	潰家あり
3	寛政 11. V 26	1799, VI 29	加賀(金澤)	宮越浦に津浪あり
4	文政 2. VI 12	1819, VIII 2	伊勢・美濃	不明
5	安政 1. XI 4	1854, XII 23	畿內及東海・東山・北陸・山陽・山陰・西海・南海諸道	潰家あり
6	安政 5. II 26	1858, IV 4	飛彈・越中・越前	家屋破損多し
7	明治 24. X 28	1891, X 28	美濃・尾張	家屋破損多し
8	明治 25. XII 9	1892, XII 9	能登西南部	羽咋郡にて家屋破損す
9	明治 33. III 22	1900, III 22	越前鯖江	今立・吉田兩郡にて家屋破損す
10	明治 5. IX 27	1930, IX 27	能登	富山灣沿岸弱震

今回の地震前後の氣象 北陸地方に於ては一般に十月頃は曇天の時が多いのであるが、今回の地震前には 760 mm. 位の低氣壓が遠く南洋にあり、高氣壓は 766 mm. 以上で北支那から東に進行中であつて、地震の起つた頃はその中心が日本海上にあり、此の季節として珍らしくよく晴れてゐた。

被害狀況及び地變 當時新聞の報導する所によれば被害は小松町と大聖寺町とに於て多く、又地震記象を見れば前述の如く二回つゞいて起り、そして普通の場合の本震と餘震の强さと反對に、後の地震の方が大きかつた。そこで或は二つの地震が少し隔つた二個所から起つたといふ疑があつた。併し實地に見聞した所によれば小松町に多數ある九谷燒の賣店では商品の毀れたものが少ない程で、他にも別に大した被害もなかつた。之に反して大聖寺町では棚の上にあつたものは殆ど全部落ち戸障子の大多數は外れたといふことである。此等の事實や後で述べる如く金澤・福

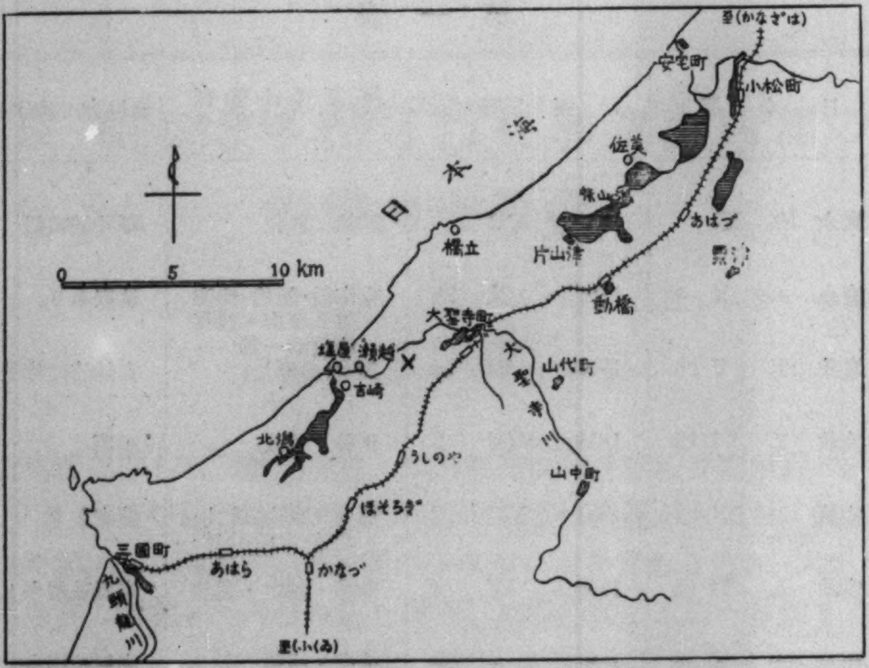
至(かなざは)
安宅町
小松町
日本海
佐美
柴山
あはづ
橋立
片山津
0 5 10 km
動橋
大聖寺町
塩屋
瀬越
×
吉崎
山代町
大聖寺川
北潟
うしのや
山中町
ほそろぎ
三國町
あはら
かなづ
九頭龍川
至(ふくゐ)

第一圖　× 震央推定位置

井兩測候所の地震記象によつて二回の地震の震原は略同じ所にあり、大聖寺町に近い所であらうと考へられた。

此の地震の爲に片山津溫泉に於て二歲の小兒が金庫の倒れた下敷になつて壓死した。此の金庫の脚は狹い石の臺の上にあつたので、震動によつて臺から外れ、金庫が倒れたので、此の犧牲は金庫の置き方に不注意の點があつた爲であるといふことを聞いた。

構造物の被害としては、煙突の破損、石塔籠・墓石の轉倒等はあつたが、家屋では壁が落ち、柱のずれたものがあつた程度である。家屋の倒潰したものは、數戸の古い納屋の如きもので、此の爲の被害は僅少である。

小松町の南端に於て高さ約 20 m. 徑約 4 m. の六角壔の煉瓦積の煙突が二本あり、その中一本は上部約 2 m. が崩れ落ち、それから更に 2 m. 下で回轉した。他の一本は上部約 6 m. の間が膨れた。此の破壞の起つたのは目撃した人によると、地震がすんでしまつたと思つた時であつたといふ。又鹽屋村の鑛泉宿の屋根上の土管をつなぎ合せた約 4 m. の煙突は、二度目の地震で三・四遍搖れたときに最上部の土管が北に約 4 m. とばされたといふ。此等の話が事實ならば、地震が主要部になつてから煙突は被害をうけたと考へられる。又吉崎村及び大聖寺町の墓地に於て

墓石の積み重ねてある部分が別々に變位·囘轉してゐたことは、此の如きものを動かし得る地震動が何囘か續いたことを示すであらう。

地變として著しかつたものは、道路の龜裂と崖崩れの多かつたことである。此等の原因としては、海岸の近くに砂丘が多く、此が崩れ易い性質であるからである。崖崩れの最も大きなものは、小松町の南西約5km. 石川縣御幸村字佐美の佐美山に生じたものである。(圖版XXIX第4圖)此の山は柴山潟に沿うて佐美から同村字柴山に行く道路の西側の高さ約20 m. の砂丘である。道路をつくるときに崖を削つて表面を以前より急傾斜にした所が地震の時に平衡を破られたのであらう。崩壊個所は約150 m. の幅で、崩れた部分の上方は水平面に對して約80°の傾斜の絶壁となり、下方は約35°の傾きをなして堆積してゐた。上方の急傾斜の部分は手で觸れても少しも崩れない程度に固く、2–3 cm. の長さの小さな角柱を竝べた様な形狀をなしてゐる。(圖版XXIX第5圖)一般に筆者の見た砂丘の崩れは前記の様に上部が急傾斜し、下部は崩壊した土砂が緩傾斜で堆積してゐた。

他に注意すべき地變としては、小松町にある小松高等女學校の運動場に於て地震後水を噴出したことである。運動場は約50 m. 平方の正方形に近い形をなし、その西方に校舍がある。地震當日宿直した教員に會つて筆者の聞いた所によれば、地震の直後に運動場に出て見ると一面に網目狀に細い龜裂が生じ、その中に運動場の北隅に近くS 60° Eの方向に一條、それより少し南方にEWの方向に一條、合計二條の大きな割目が出來てそれより北側は約5 cm. の沈下をした。S 60° Eの割目に於いては十一個所から灰白色の濁水を噴出し、その噴水の高さは約30 cm. で噴出は何時始まつたか知らなかつたが、地震後10分か15分間繼續した。その他に割目の線の延長上で、運動場の北東隅に三個所清水を噴き出した。噴水の時間は前述のものと同様で、但噴水の終つた跡は噴火口狀であつた。此の運動場の沈下した部分は城の內堀の跡を明治43年頃コークスと砂とを略等量に混じて埋立てた所であるといふ。埋立の厚さは約1 m. で、その下には赤色の土があり、運動場外ではあるが此の附近で井戸を堀つたときに、噴水した濁水と似た色の土が約30 m. の地下にあつたといふ。

以上と同様に噴水の現象が柴山潟の南部にある片山津溫泉にもあつたといふことである[3]。そして此處に於ても湖畔の沈下した所があつたこ

とを聞いたので、噴水の原因について考へるに、地面の不同沈下によつて地下水の水準面に變化を生じ、その爲に地下水が流動を始め、割目から噴出することが推察される。地下水の流路に軟い土砂があれば、それを含んで濁水となることもあり、十分水が流れ再び地下水が平衡狀態に復すれば噴水は全く止んでしまふのであらう。氣體が地中に生じてその壓力によつて噴水することも想像されるが、氣體の生じた證據はなかつた。

地震計測　東京帝國大學に於ける觀測によれば10月17日 6時33分11·1秒に初動が到着し、次いで6時36分46·5秒に前者より大きな地震を記錄した。その觀測結果は第二表の如くである。

第二表

東京到着時	初期微動繼續時間	最大全振幅	
		EW	NS
6 h　33 m　11·1 s	39·6 s	0·06 mm	0·05 mm
6　36　46·5	39·9	0·74	1·67

前の地震で强震を感じた區域[4]は大聖寺町を中心として大體北は小松町、南は福井市の範圍內である。併し人體に感じた區域は相當に廣く、京都·大阪·名古屋等に達してゐる。後者は更に廣く、强震の區域は加賀·越前は勿論、能登・越中・飛彈・美濃・近江・山城・丹後・若狹を含み、人體の感じた所は高田・長野・大阪・神戸・洲本・境・多度津等である。

震原の位置を求める爲に、各地の初動の方向·走時·初期微動繼續時間等を調べた。先づ初動の方向については最も震原に近い福井・金澤兩測候所に於て、前震では福井は S 47° W 金澤は SW, 次の地震では福井は S 36° W, 金澤は不明であつた。東京では初動は非常に小さい爲に測れなかつた。又他の觀測所でも測れない所が多い。二回目の地震の初動は前震の表面波の上に重なり、其爲に計測が困難になつた樣である。走時曲線を引くと觀測結果が不規則にならび、殊に第二震を遠距離で觀測したものは偏差が大きいのは以上の理由によることと思はれる。走時曲線に

---

3) 吉田宏彥・井村次一郎「昭和五年十月十七日の北陸地方の地震に就て」建築雜誌 No. 540 (Dec. 1930), 2196.

4) 東京以外の觀測結果は氣象要覽（昭和五年十月）に依る。但し福井・金澤は兩測候所長の好意によつて筆者の記象を調べたものである。

よつて推定すると第一震の震央に於ける發震時は約 6 時 32 分 20 秒、第二震は約 6 時 36 分 0 秒となる5)。初期微動繼續時間と震央距離との圖(第二圖・第三圖)を畫いても走時曲線の場合と同樣に相當不規則である。圖に於て S-P の走時曲線を震央の方に延長すると、圖の原點の近くを過る。これは震原の淺いことを示すのであらう。

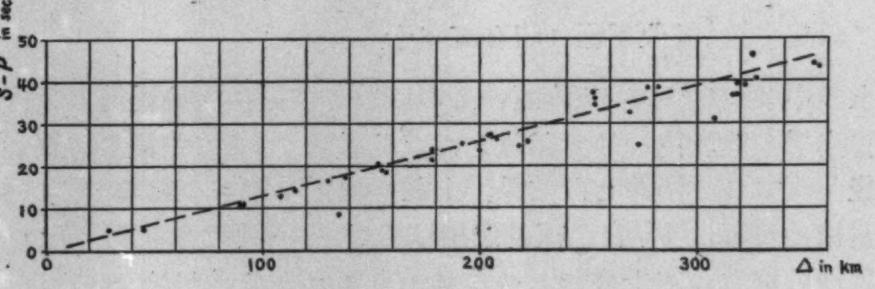

第二圖　1930 X 18.　6 h 32 m の地震

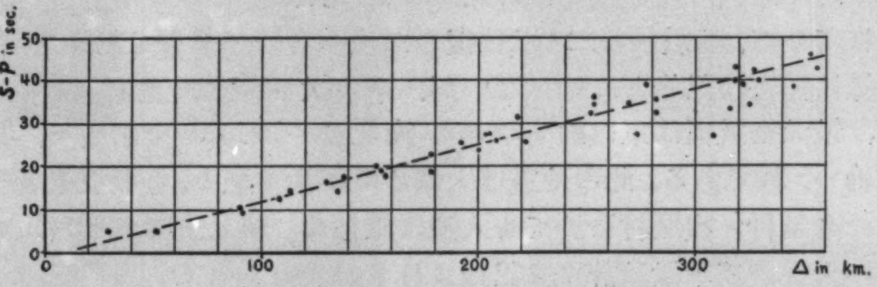

第三圖　1930 X 17.　6 h 36 m の地震

初期微動繼續時間は二回の地震について各地に於て殆ど等しい。福井では 4·8 秒、金澤では 4·9 秒である。震原距離は初期微動繼續時間の長さに比例するといふ一般に用ひられる假定によれば、震原は大聖寺町附近に當り、距離と時間の比、即ち距離係數は福井と金澤とについては約 7·0 km./sec. となる。此の値は震原の深さを考へに入れゝば少し大きくなるべきである。第 2 圖、第 3 圖によつて遠距離の觀測を用ひれば約 7·7 km./sec. となる。

二回の地震の他に、所謂餘震は下に示す如く少數であつた。

X月	17日	15時	10分	*
	17	19	23	*
	18	11	38	*
	18	12	50	*

---

5) 圖は略す、氣象要覽（昭和五年十月）參照。

18日	13時	22分
20	11	07
		*
20	12	00
22	9	10
25	11	33

但し * は氣象要覽（昭和五年十月）による

以上の中25日11時33分頃のものは前述の携帶用地震計6)によつて大聖寺警察署の建物內に於て記錄した。地震計で22日午後1時頃から26日午後3時頃まで觀測した結果、上記の地震を唯一つ記錄することを得た。器械の倍率は45, 自己振動週期は東西動5·0秒、南北動5.7秒であつた。器械の据方の不十分であつた爲か東西動は地震が始まると同時に記錄する針が傾き、他の一つは針先が時刻の合圖に用ひる電磁石の爲に上げられてゐて、地震動の二・三往復した後から針が落ちて記錄を始めた。此の樣に完全な記錄とはいへないが、初期微動繼續時間を測れば約1·4秒で、最大全震幅は東西動0·22 mm. 南北動0·13 mm. であつて、其の週期は約0·5秒である。此の地震は大聖寺町が最も强く、その頃筆者の步いてゐた瀨越村・鹽屋村に於ても人體に感じた。併し金澤測候所にある倍率35の大森式簡單微動計には記錄されてゐないといふことである。土地の人に聞く所によつても大聖寺町附近が最も多數の地震を感じてゐる樣であつたが、正確な時刻を聞くことは出來なかつた。前記の餘震表は氣象要覽によつて補つたから或は全部の地震を記し得たと考へられる。以上の事實から考へるに餘震は大聖寺町附近に起つたので、被害狀態も大聖寺町・吉崎村間が比較的甚しいことも此の考を確めるであらう。

又地震の際に吉崎と橋立附近の漁夫は海上に於て衝動を感じたといふが、他の土地ではその樣な話は聞かれなかつた。吉崎では海岸近くに居た船の漁夫は海鳴を聞いたので、急いで陸に上つたら陸上に居た人に地震があつたことを聞いたといふ。此の事も前述の震原の推定を確めるであらう。

---

6) 筆者の考案により地震研究所に於て製作したもの、詳細については地震研究所彙報に掲載される豫定である。

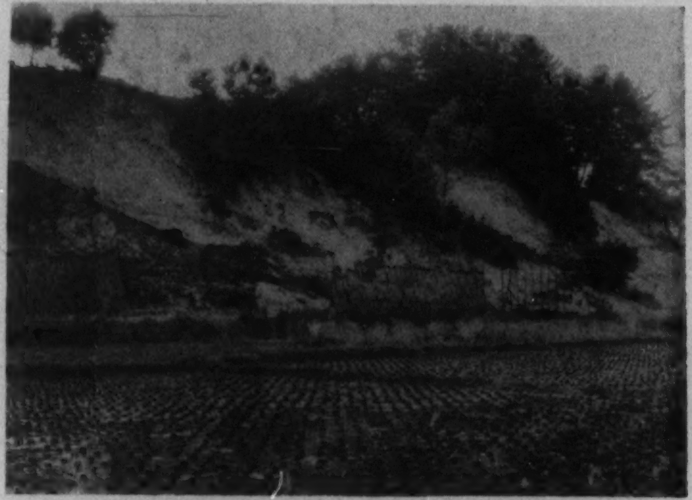

第四圖　佐美山の崖崩れ（北端）

崖の高さ約 20 m. 樹木のない所は崩れた跡

第五圖　佐美山の崖崩れに於て土砂の落ちた跡に生じた模樣

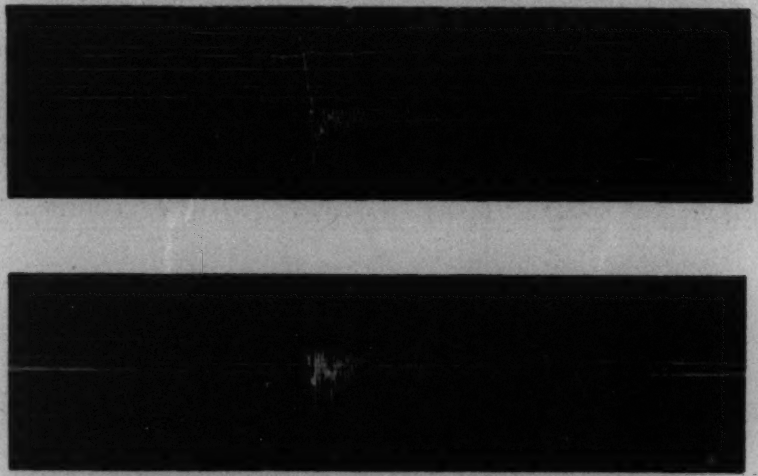

第六圖　昭和5年10月25日11時33分大聖寺附近に起つた地震の記象

地震計の倍率×5, 1 min.=37·8 mm.

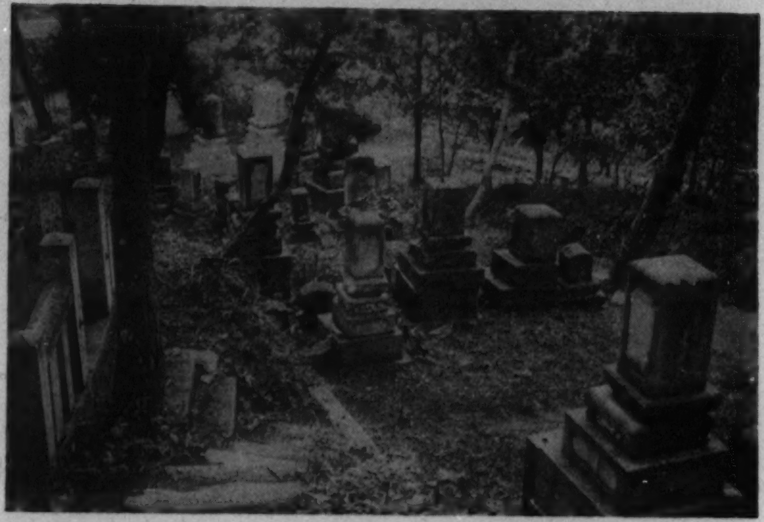

第七圖　吉崎村墓地に於ける墓石の廻轉

積み重ねた石が各〻異つた變動をした

（震研彙報、第九號、圖版、岸上）

16. *Report of the Strong Earthquake in the Southwestern Part of Kaga Province, Oct. 17, 1930.*

By Fuyuhiko KISHINOUYE.

An earthquake occurred at about 6 h 32 m 20 s on Oct 17, 1930, in the southwestern part of Kaga province, and soon after it, at about 6 h 36 m 0 s, stronger one took place. Epicentre of the both earthquakes were deduced to be near *Daisyôzi.* Its co-ordinates obtained were $\varphi=36°\ 18'$ N, $\lambda=136°\ 17'$ E.

Fissures in roads, marginal collapse of sand dunes which lie along the coast of the Japan Sea, were found in many places. Only several barns fell down, and human lives were not lost, except a baby was crushed to death by falling of a safe at *Katayamazu,* near *Daisyôzi.*

After-shocks occurred were only seven in number, and most of them were felt in a very small area near *Daisyôzi.* The author made a seismological observation with a portable seismometer during Oct. 22, and 26 in the building of the *Daisyozi* police station. An earthquake which occurred at 11 h 33 m on Oct. 25 was recorded on the seismogram. The record is shown on Plate XXIX. The duration of preliminary tremors of the earthquake obtained was 1·4 sec., so the origin would be within the range of several kilometres from the place where the instrument was set up.

17. *On Luminous Phenomena Accompanying Earthquakes.*

By **Torahiko TERADA,**

Earthquake Research Institute.

(Read Dec. 16, 1930.—Received June 20, 1931.)

AERONAUTICAL RESEARCH INSTITUTE · LIBRARY · OCT 10 1931 · TOKYO ·

Introduction.

Among the historical documents regarding severe earthquakes of the past, in Japan as well as in the other parts of the worlds, we find not infrequently some descriptions of remarkable luminous phenomena observed in the sky or on the ground before, during, or after the time of severe shocks. The phenomena were observed sometimes in the immediate vicinity of the epicentre and sometimes in very remote quarters. The descriptions of the form, colour, intensity, duration, motion and fluctuation of the luminosity observed are extremely variegated as the case may be. Still, it is interesting to remark that among these chaos of testimonies we may pick up almost parallel statements of quite independent witnesses. Thus, for example, we may cite a number of testimonies recorded in Galli's collection[1] of such data, which have their respective facsimiles among the Japanese data collected by Mr. Musya[2] and the present author. The agreement between the independent witnesses is not only referred to vague statements of the general features of the luminosity, but also to very detailed descriptions only capable for keen observers.

Notwithstanding these almost superfluously abundant materials of testimonies, the phenomena failed to attract any serious attention from the majority of seismologists, who apparently did not care for these documents at all. Even among those who came eventually to be confronted with some examples of the phenomena, skeptical opinions usually prevailed. Psychological or physiological illusions were often quoted, without proof. Distant lightnings, firebrands, camp-fires will be often mentioned, again mostly without proof. In the recent years, the possibility of short-circuiting of electric transmission lines has furnished a new item for these would-be causes of the phenomena in question. For those who does not spare the trouble of examining these documents with open mind, it will be, however, found difficult to discard the phenomena a priori as utterly unreal or independent from the earthquakes. Thus, for example, A. Sieberg[3] spared a special chapter in his book on seismology for this phenomenon and states that there are some examples for which the usual explanation by the trivial causes seems to fail. He concludes by saying rightly enough that this luminous phenomenon is just the darkest chapter in seismology.

---

[1] Ignazio Galli, "Raccolta e classificazione di fenomeni luminosi osservati nei terremoti," *Bolletino della Società Italiana*, 14 (1910), 221.

[2] K. Musya, *Bull. E.R.I.*, 9 (1931), 177, (in Japanese, with English abstract).

Mr. Kinkiti Musya of our Institute was early interested with the luminous phenomena frequently described in the historical documents of our country concerning earthquakes and has made an excellent collection of these materials. The present writer was also of the opinion that the phenomena may be well worth a serious study and at least cannot be discarded as trivial without scrutiny. The Idu Earthquake of Nov. 26 1931 occurred just at this time when our attentions towards this particular phenomenon was ripening, and at once furnished us with so many conspicuous examples that any doubt about the physical reality of phenomena was completely removed and, moreover, their physical connection with the earthquake became a matter beyond any question. It seems, therefore, not without interest to attempt here a brief review of the literatures regarding the matter and also to make some discussions regarding them though the results of Mr. Musya's investigation are already published in the previous number of this Bulletin.

Occidental Literatures regarding the Phenomena.

Besides 148 examples given in Galli's collections and those cited in Sieberg's Erdbebenkunde, there are a number of other data at the hand of the writer for which the reference is made in the footnote.[4]

---

3) A. SIEBERG, "Erdbebenkunde," Kap. 14, Jena, 1923. See also A. SIEBERG u. R. LAIS, "Das mitteleuropäische Erdbeben von 16 Nov. 1911," *Veröff. Reichsanst. f. Erdb. fors. i. Jena*, Heft 4.

4) S. GÜNTHER, "Geophysik," I, (Stuttgart 1897), 477; CORN. TACITUS's Annali cited regarding the luminous phenomena observed on the occasion of an earthquake in Achäian cities in 373 B.C., which is the earliest example; literatures on allied matters found in citate

Examining these numerous materials it will be seen that the phenomena recorded are of extremely variegated features but may be conveniently classified into a number of types, which are represented on different occassions in different nuances of forms and combinations. I. Galli classified:[5] (I) indefinite instantaneous illumination, (II) well-defined and mobile luminous mass, (III) bright flame and emanation and (IV) phosphorescence of sky and clouds. The class (I) was subdivided into (a) lightning (lampi e bagliori), (b) sprinkles (sprazzi luminosi) and (c) streamer (strisce luminosi sottili). The class (II) contains (d) fire-ball (globo di fuoco) (e) fire-column (colonna di fuoco), (f) beam of fire (trave di fuoco) and (g) luminous funnel (tromba luminosa). The class (III) including those phenomena which appear from the earth and last for a sensible duration of time, is subdivided as (h) flame (fiamme), (i) little flame (fiamelle) (j) spark (scintille numerose) and (k) luminous vapour (vapori luminosi). Lastly, the class (IV) is divided into (l) diffused light in the sky (luce diffusa nell'aria) and (m) luminous cloud (nube luminosa). These classifications seem to cover almost all the examples in the occidental literatures above cited as well as in our collection of the Japanese documents and testimonies. Though such a classification is liable to much ambiguity, as the meaning of the same words used by different witnesses may have more or less different contents, we will sometimes conveniently refer to this classification in the following description of Japanese examples.

Examples in Japan.[6]

Above forty examples of documents concerning the luminous phenomena observed in connection with severe earthquakes dated up to the

---

at the end of Chap. 4. Urbanitzsky, "Die Elektrizität des Himmels u. d. Erde," (1888), 358. R. Hoernes, "Erdbebenkunde," (1893), 113–116. E. Hennig, "Erdbebenkunde," (1909), 111–113. J. Milne, "Seismology," 330. K. Futterer, "Das Erdbeben vom 22 Jan. 1896," Karlsruhe 1896, 32. " On Earthquake of Dec. 17, 1896," *Symons's Met. Mag.*, (1897), 183. W. Gaw, "Atmospheric Phenomena during the Chili Earthquake," *Symons's Met. Mag.*, (1906), 228. A. Sieberg u. R. Lais, *loc. cit.* Myron L. Fuller, "The New Madrid Earthquake," *Bull. U.S. Geol. Surv.*, **494** (1912), 46. Baily Willis, "Earthquake Condition in Chile," 30. I. Galli, *loc. cit.* It is said that luminous phenomena were also observed on the occasions of San Fransisco Earthquake of 1906 and the recent Italian Earthquake of 1930, though the reliable documents are not at hand. For an example of Chinese earthquake, we may cite 童振藻, 雲南地震考 (1926), in which it is stated that on the occassion of Yunnan earthquake of March 1925, immediately before each of the severe shocks sulphurous smell was felt and fiery light discovered in the sky which moved from N to S.

[5] The numbering of the classes and the alphabetical denominations are not given in Galli's paper, but introduced here for the sake of convenience.

[6] Most of these examples are cited from "Dainihon-Disin-Siryô", some from Musya's collection and the rest from other miscellaneous sources

beginning of Meidi Era (1868), are found in Musya's collection, of which about twenty refer to the Ansei Earthquakes (1854 and 1855). The earliest record in Sandai-Zituroku (三代實錄) states that on the occasion of the severe earthquake in Mutu, N. Japan, in 869 A. D., "streaming light was seen as if it was daytime" and its intensity seems to have shown some sensible fluctuation (流光如晝隱映). The phraseology suggests that the luminosity was something unusual and different from that of lightning, perhaps belonging to Galli's class I or IV. In Kamakura Earthquake of 1257, bluish flames were seen to emerge from the fissures opened on the ground⁷⁾. This belongs apparently to Galli's class III. In the case of an earthquake in Suruga and Tôtômi 1589, the luminosity observed from a distant quarter is expressedly stated as "not like lightning" and also "whole sky illuminated." Flying luminous bodies are mentioned in connection with two local earthquakes in Yedo in 1630 and 1672; as these occurred in winter, the connection with thunderstorm is improbable. In the case of 1672, a fire-ball resembling paper-lantern is mentioned which was seen flying through the sky towards E. In the case of Tosa Earthquake of 1698, a number of fire-balls like wheel were seen flying in different directions. In the case of Great Genroku Earthquake of 31 Dec., 1703, in Tôkaidô, luminous "bodies" and "air" were frequently seen in the nights preceding the day of the severest shock⁸⁾ and, afterwards, a kind of luminosity like the sheet-lightning continued to be seen for about twenty days, even when there was no cloud to be seen. This earthquake occurred also in the season when the thunderstorms are extremely rare. It is needless to say that there existed no electric transmission lines. Galli's "fiamme" is again met with in the case of Sandyô Earthquake of 1828 and Sinano Earthquake of 1847. In the latter case, "lampi e bagliori" are also reported. One of the records states: "Under the dark sky, a fiery cloud appeared in the direction of Mt. Iduna. It was seen to make a whirling motion⁹⁾ and then disappeared. Immediately afterward, a roaring sound was heard, followed by severe earthquakes." Again, "the luminosity accompanying the enormous land-slide of Mt. Iwakura was of so strong intensity that it was as bright as daylight to

---

7) *Cf.* GALLI, N. 128: "……par les fentes que l'on me montrait (fentes causées par le tremblement de terre et qui n'existaient pas auparavant) on avait vu sortir du feu"; and many others.

8) See foot-note, p. 235.

9) *Cf.* resolving motion mentioned in p. 240.

every corner of houses." At the time of earthquake of 19 Aug. 1830 in Kyôto and its vicinity, it is stated that in the night preceding to the earthquake luminous phenomena were seen in the whole sky and some kinds of luminosity were emitted also from the ground which were so bright as to be compared with daylight. The people were wondering at the unusual phenomena until the severe earthquake was experienced on the next day. In the case of Ansei earthquake of Nov., 1855, different forms of luminous phenomena[10)] were reported and, in this case also, the season was near the minimum of thunderstorm frequency.

As for the examples recorded after the Restoration of Meidi, we may cite the following.

1889, July 28, Kumamoto Earthquake: According to "Kumamoto Meidi Sinsai Nikki", a fearful lightning flash (or flashes ?) was seen towards E immediately before the arrival of shocks. Afterwards, lightnings were observed towards W till the next dawn. In the previous (?)

---

10) We may cite a few examples from Musya's collections: "At the time of the earthquake, a luminosity resembling lightning was seen towards E which disappeared after a short time". "Before the noon, something like a vertical rainbow was seen towards SE". "An witness, who were afishing off Sinagawa, saw flashes like lightnings towards Yedo (Tôkyô) at three or four places." "A party of 19 persons went to sea on the eve of the earthquake. Before the time of the shock a sudden luminosity was seen towards NE, which was so bright that the coloured patterns of their clothes could be well discerned. Soon afterwards, a horrible roaring sound was heard from underneath the sea, which gave them an impression as if a mass of gravels were impinging upon the bottom of the boat. At the same time a mass of flame went flying through the sky accompanied with sounds." "A person in Ikenohata, Sitaya, observed at the time of the shocks a luminosity towards NNW which was quite unlike a lighting. "At Yosiwara, fissures were formed on the ground, from which a beam of white 'air' (luminosity) emerged. It moved aslant toward Asakusa Temple." "A man in Usigome was surprised to see the window illuminated. Towards S he saw a slender beam of ruddy light which was bent like the handle of a kettle. He was wondering at the phenomenon when the sudden shaking of the ground was felt." It seems that the luminosity preceded the first shock; moreover, the curved beam of light mentioned resembles to a similar phenomenon observed by Mr. Hattori on the occasion of Tanzawa-yama Earthquake of Jan. 15, 1924, cited later. "A traveller on his way through Koisikaw at midnight saw some 'dark air containing bluish luminosity' which moved rapidly from NE to S accompanied with a sound like strong gusts of wind. Soon afterwards, the earthquake shock was felt." There are several witnesses who state to have seen some dark object flying through the sky which is rarely mentioned on the other occasions. It is possible that a physiological effect might here be concerned. "In the night of the earthquake, fire was seen to be emitted from the ground somewhere near Gyôtoku, Simôsa. On approaching the spot where the flame seemed to emerge, nothing could be found, but the similar fire was seen in front again at some distance from thence."

night, a fire-column had been seen to pierce the cloud, while it was raining. In the night of the earthquake which occurred at about 12h, the sky was at first clear with abundunt shooting stars and afterwards it begun to rain. The season was near the maximum of thunderstorm frequency and we are not in possession of the weather chart of that time so that it is difficult to tell whether the light seen was not the usual lightning.

1891, Oct. 28, Nôbi Earthquake: In the preceding night lightnings were seen towards W from the village Miyake. Frequent lightnings were also seen at Tusima-Mati.

1896, June. 15, Sanriku Earthquake with tunamis: Fishermen 30–40 ri off the coast saw something like burning fire and after a short time heard a sound like cannonading towards the land.

1909, Aug. 14, Kônô or Anegawa Earthquake: According to Prof. Koto's report, the western slope of Mt. Ibuki slided down and some luminous phenomena observed.

1917, May 18, Earthquake in Suruga and its vicinity: Fire-column was seen in the mountain north of Siduoka.

1918, Sept. 11, Oomati Earthquake: According to Prof. S. Tsuboi's report, at the time of the second severe shock, a kind of luminosity was seen in the directions of mountains in Hida and Sinano to W. of Ikeda-Mati.

1923, Sept. 1, Kwantô Earthquake: Fishermen of Awa saw several fire-column appearing in (?) the sea in a part of the Sagami Bay near the mouth of the Bay of Tôkyô, on 1 (or 2) Sept. A staff-member of the Central Meteorological Observatory observed a kind of stationary fire-ball in the sky of Tokyo. A woman in Hukagawa saw a flashing light on the sea in the morning, i.e. before the earthquake, of Sept. 1. A student observed unusual luminous phenomena towards the direction of Bôsyû in the night of Sept. 2 (?).

1924, Jan. 15, earthquake in Tanzawa-yama district: A luminosity was seen in Yokosuka at the time of shocks. Such was also seen from C.M.O., Tôkyô, towards W. Fishermen off the coast of Kôdu saw a strong light on the southern slope of Mt. Tanzawa. Mr. K. Hattori, Assistant in Aeron. Res. Inst., who was dwelling at that time in Terazima-mati on the E-side of R. Sumida, was awakened by the first shocks and hurried out of door, when he happened to observe a pillar of fire over the roof of a house towards N. It was slightly bent with its concave side to the right and its upper end merged into a diffuse sheet of light attaining a considerable altitude. The colour of the light was pale white. The sky was clear. Two persons saw the same phenomenon. It is interesting to notice that this latter example bears a remarkable similarity with that depicted in Fig. 58 of Sieberg's book cited.[11]

1925, May 23, Tazima Earthquake: At the time of one of the severest after-shocks which occurred during the night, Mrs. Yamamoto of Hukutiyama observed a luminous ball, reminding her of a foot-ball, in the sky in the direction opposite to Kinosaki, i.e. the epicentral region. It moved rapidly from NE to S like a shooting star and disappeared somewhere.

1927, March 7, Oku-Tango Earthquake: Mr. S. Sawada of Hirakata-Mati, observed at Huse-Mati a luminosity towards E which he supposed to be due to sparking of an electric transmission line in the neighbourhood. Mr. K. Saito of Kyôto was in an electric car running from Kôbe to Osaka at the time of earthquake. He observed an unusual luminosity of night sky towards Mts. Muko and Rokkô, not quite unlike a distant fire-brand, but of quite unusual colour. Fishermen of Taiza who were fishing off the mouth of R. Asamo observed a luminosity above the sea towards E, which was more reddish in hue than the usual lightning flash, and paler compared with a candle light.

1928, May 21, a local earthquake in the NE part of the Tokyo Bay: Mr. Hattori, Aeron. Res. Inst., observed a diffuse illumination of sky a few second after the first severe shock. The flashes which seemed to be of longer duration than that of a lightning, were repeated two or three times; they also seemed to occur nearly simultaneously with the maxima of earth's disturbances. Dr. S. Yamaguti of our Institute observed a flickering luminosity in the southern sky which continued during the shocks and abated with it. The colour was like that of an electric spark and the luminosity seemed to reach an alititude of about 10°.

1930, Dec. 20, a local earthquake in Hirosima Prefecture: Mr. B. Takeda of Syôbara-Mati states that several persons observed some luminous phenomena towards N at the time of the severest shocks as well as during some of the aftershocks. It is stated by several witnesses that the northern sky was illuminated by a ruddy light as in the case of a fire-brand. Some one is said to have seen a fire-ball. Elecric light was extinguished at the time of earthquake. Mr. K. Nozaka, the Master

---

11) A similar kind of curved fire-column was seen at the time of Ansei Earthquake (see foot-note p. 229); another, probably of the same class, was seen in the present case of Idu Earthquake (see p. 232).

of Syôbara Common School, reports that a fire-ball was seen from the school towards NNW, which moved upward and vanished, followed by a luminosity in all directions. A member of the Village Office in Syôbara observed a purple flash of radiating light towards WNW. Mr. N. Emura of Kimita School saw white light of indefinite extention towards SE, NW and E respectively. The report from Kimita Village Office states that immediately after the severe shock of 20 Dec., an illumination of the sky towards NE was seen resembling a distant fire and the similar phenomenon was also seen in the night of 21st. in two directions N and S. Lastly, Mr. M. Hara of Kutikita-Mura, Hiba District, observed immediately after the shock a beam of light like an inverted brush or a signal fire rising upward and illuminating the clouds with a hue similar to a fire-brand. The light gradually faded upwards. Besides, a faint general illumination was seen in the lower sky just above the mountains, first in SW direction and then in SE and N.

In most of the above examples, no strong evidence could be brought forth against the criticism which may be applied as regards the suspicions whether they were not due to lightning, electric short-circuiting etc. In this respect the recent Idu Earthquake of Nov. 26, 1931, may be cited as an unique case in which the abundance in number of testimonies far surpassed the total sum of all the above cited and the detailed features of evidences allows no room for suspicion as to the physical reality of the phenomena as an immediate appendage of earthquake shocks.

Examples from Idu Earthquake of 1930.

Immediately after the earthquake of Nov. 26, 1930 in Idu district, Mr. K. Musya sent a circular inquiring after detailed informations regarding any form of luminosity observed in connection with the earthquake, adressed chiefly to the masters of the boys' and girls' middle schools in the neighbouring prefectures. The data accumulated in this way amount to 1168 in number.[12] Mr. K. Musya made a thorough study of these data and already published a summary of his results of investigations in the preceding number of this Bulletin.[13] The present author also examined these data which was kindly placed at his disposal, and confirmed Musya's results in the essential points. Besides, the author was able to obtain about 15 data from the sides of persons more or less trained in scientific observations. Besides, about twenty other reports were also gathered from the side of laymen witnesses among the inhabitants of Tokyo as well as of different localities in Sagami and Idu. Moreover, another set of valuable data was obtained by the courtesy of the Central Fire-Brigade Station of Tôkyô which consists of the testimonies of the firemen who were in charge of night watch on the watching towers of different local fire-brigade stations situated in different quarters of the city. The latter data are especially valuable, as the witnesses were awake before the arrival of the earthquake shocks and they could be expected to be especially alert to any trace of unusual luminous phenomena of night. These additional data taken altogether bring, however, nothing essentially new to the summary given by Musya.

---

[12] On examining these data from the school boys and girls, it was noticed that their testimonies are neither always original nor independent from each other, being apparently influenced by the effect of mutual conversations and inquiries, so that the coincidence of testimonies is not necessarily the proof of their truth.

[13] In the following his paper will be as K.M.

With regards to all these testimonies of witnesses, it must be always kept in mind that people are naturally alive to all kinds of phenomena observed at the time of a severe earthquake and apt to regard them as something connected with the catastrophal occurrence, while they forget to consider that the same phenomena are frequently observed on many other occasions not at all connected with earthquake. On the other hand, we learn from the results of investigations by psychologists in what a ludicrous manner the testimonies of people, otherwise quite normal in mentality, may appear distorted when compared with the bare truth. These points taken into due account a sufficiently numerous independent testimonies may still give at least a general outlines of what really happened.

In the following will be given a review of the essential features of the phenomena with some discussions.

(*1*) *The extent of localities where the phenomena were observed:*

The phenomena were seen as far as 80 km. to E, 110 km. to NE and 70 km. to W of the epicentral region. The geographical distribution of the observers shows a peculiarity which seems to be due to different factors such as the density of population and the intensity of shocks felt. Abundance of data in the city and suburb of Tôkyô may naturally be explained by the former factor. The same factor seems to explain the decided superiority in number of data on the western side of R. Sagami compared with the eastern side. Extreme scantiness of the reports from the Tama Terrace, situated between Tôkyô and Sagami River Plain, may probably be due to both the causes above mentioned. The observers in Bôsô Peninsula are confined within a zone with a breadth of 5–10 km. along the coast of the Bay of Tôkyô, extending to the mouth of R. Yôrô to N and to Tateyama to S. The western-most point of observation was at Yaidu in Siduoka Prefecture and the southern-most at the vicinity of Simoda, Idu. No report was obtained from the mountainous districts to N of the line connecting Mt. Ooyama with Hatano, Yamakita and Gotenba.

(*2*) *The time of observation:*

The greatest majority of witnesses were those who were awakened by the severe shocks, and hurried to open the door and get out. There are a few who became aware of the phenomena by looking out through glass windows immeditately after awakening. A watch-man who was in charge on the top of the watch-tower of Sibaura Branch Fire-Brigade Station, Minami-Hamatyô 18, states that he has observed a flash of light towards S about 10 minutes[14] before the shocks, and afterward four or five spark-like flashes during the earthquake. He also states that the peculiarity of the time relation drew his special notice. Another report due to Mr. T. Makino of Itô is worth of special notice, which states that a number of fishermen who were about to set their boat afloat in the evening previous to the earthquake observed a spherical luminous body to W of Mt. Amagi which moved towards NW with considerable speed. This fire-ball was seen at about 4 o'clock pm. of 25th. while the severe shock occurred at 4 h. 3 m in the next morning.[15] Three other examples of unusual light phenomena seen before the midnight of 25th. in different places near the epicentral district are given in Musya's paper, K.M. p. 179.

---

[14] The examples abunduntly cited in GALLI's collection as well as in ours in which the shocks were felt immediately after the luminosity, may be explained by the time required by the earthquake waves to traverse the distance from the origin to the observer. The time here stated seems to be too long. It is, however, not clear whether the luminosity began to appear so early, or some kind of illusion was committed.

[15] This testimony of the fisherman reminds us of an article in NANKEI TATIBANA's "Tôyûki" (橘南谿, 東遊記 A Journey to Eastern Countries) in which a luminous phenomenon is described as a foreboding of a dreadful landslide. The fishermen of Nadati, Etigo, who were afishing off the coast observed a remarkable ruddy glow towards the land which they considered to be due to a great conflagration. On landing and returning to their native village they were surprised to found that nothing unusual has happened in the vicinity. On the next day, however, a landslide of enormous scale took place in the same locality and buried the unfortunate fishermen who could not understand the fearful omen of the previous night. It may be supposed that the landslide had already been commenced preceding the final catastroph, somewhere in remote regions devoid of popula-

In this connection, a very singular fact may be recorded that Mr. Mukuhira in Tango, an amateur in "earthquake prediction" sent in the afternoon of 25th. a telegram adressed to the Director of the Science College of the Imperial Kyôto University giving the warning of an earthquake to be expected in Idu districts at about 4 o'clock next morning, which turned out to be true. The photogram of the telegram was reproduced in *Oosaka Mainiti* of 28th. Nov. According to the newspaper he based his prediction on the observation of a certain rainbow-like phenomenon which was seen in the morning of 25th. Though we are unable to trace any scientific basis in his way of prediction, the coincidence is nevertheless quite remarkable. It must be remarked, however, that vague anticipations of a severe earthquake to occur in Idu was prevalent among the laymen interested, on account of the frequent repetition of swarm earthquake in that region since the spring of the year. What is remarkable is that the exact time of occurrence was "predicted" and moreover that he was so convinced and determined as to send the telegram stating this very time. From the present status of our science we cannot but attribute this coincidence to a rare chance, but it is too rare and interesting to be entirely discarded from the literatures of earthquake phenomena, especially because it is connected with some luminous phenomena in the sky, though his "rainbow" was seen in the daytime and belongs to none of Galli's classification above cited.(16)

---

tion. In the present example of Idu Earthquake above cited, it may also be conjectured that somewhere in the mountainous district of the epicentral zone a conspicuous sliding has happened on the eve of the day of the earthquake though there is no positive evidence available. At any rate it is desirable in view of such a possibility to pay due attention to any luminous phenomenon reported to have been observed preceding a severe earthquake and not to cast away such data too hastily as a priori improbable. In this respect, cf. for example, GALLI, No. 72, in which different luminous phenomena are given which were seen in the evening before the severe shocks.

16) According to the newspaper "*Tôkyô Asahi*" of June 8, a telegram from London states that an unusual luminous phenomenon was observed in London in the night two days before the earthquake of 7th. June. A detailed description of the phenomena, if real, is desirable, whatever may be their actual causes. Here, we may add a case of an apparent prediction of the earthquake of Genroku 16 (1703 Dec. 31) by SUKEZAEMON SIBUKAWA, the Astronomer of that age in service of Syôgun. It is stated in a document recorded in "Dainihon-Disin-Siryô" that on the eve of the great earthquake, he gave a positive warning to the officers in the residence of Syôgun to the effect that a severe thunderstorm or earthquake is expected in the course of that night. It is also stated that he was constantly in the habit of watching the night sky, as is natural for an astronomer. It is worthy of notice that he apparently treated thunderstorms and earthquakes under the common category (cf. ARISTOTELES: Meteororum, lib. II, cap. 9). This suggests that his premonition

(3) *Varieties of phenomena observed.*

Almost all the varieties of phenomena classified by Galli were represented in the present occasion (cf. K. M. pp. 183–197). Most numerous examples seem to belong to Galli's (Ia) lampi e bagliori, i.e. the sky was illuminated in a manner not unlike the usual sheet-lightning. The greatest majority of the observers remote from the epicentral region describe the phenomena as such. Most witnesses in Tôkyô observed one of the flashes immediately after the first shock which was followed by three or four similar flashes with irregular intervals of few seconds, varying from 1 sec. to 10 sec. according to the estimation by a number of physicists. Almost all agree in saying that the duration of a single flash was decidedly longer than that of a usual lightning. The unusual duration has also attracted the attention of some laymen who positively emphacize this point in their reports. On the other hand, some state that a single flash was steady and showed no fluctuation, while other speak to the contrary. This latter point may depend upon some physiological effect so that it is not easy to decide which was right. Or, the different descriptions may refer to different phenomena. As to the extent of the part of sky illuminated, there are some testimonies which state that it reached 20–30 degrees from the horizon, but it must be kept in mind that probably no one would care to look towards the zenith in such an occasion. The directions in which this kind of phenomena was observed are extremely various and contradicting with each other even among the observers in the same locality. It seems to depend on the direction at which the observer happened to be facing at the time of the occurrence of flash. Thus, it will depend on the direction towards which the window or door opens, and also on the topographical conditions, such as the slope of the land as well as the vicinity of sea. There will also come into play a probable psychological moment of the inhabitants of suburban districts to look involuntarily towards the city centre in the case of occurrences arousing general alarm. It is, therefore, hopeless to decide upon the position of the source of these " lampi " from the data at

---

was based on some luminous phenomena not unlike lightnings. As already mentioned, it is recorded also in other documents regarding this very earthquake that luminous phenomena were frequently observed in the night (or nights?) preceding the catastroph, notwithstanding that the season was just near the minimum of thunderstorm frequency. All these examples as such are certainly not able to stand the criticism of scientists, but it will not be legitimate to cast away these cases on account of mere prejudical reasoning, especially when there are more than one physical possibility of premonitory phenomena as are discussed in the present paper.

hand. It will not be far from the truth to assume that in Tôkyô and its western suburb almost the entire sky was illuminated at the moment of flash.

On the other hand, the distribution of clouds at that time must be taken into consideration with regard to the above question. Mr. Kita, Student of Physics, reported from Takinogawa Observatory that the sky was generally clear with KC 3 towards SE–SW at 4h 5 m. Another reliable testimony by Dr. Wadati who observed about four flashes at his dwelling in the western suburb, states that the sky towards S was overcast with greyish stratified clouds and the light seemed to be emitted from one of the strata. According to the data kindly furnished by Mr. Saki of C. M. O., the cloudiness at 2h am. was: Numadu 10, Yokohama 4, Iida 0, Kôhu 1, Kumagaya 0; at 6 am., however, a remarkable change had occurred, i.e. it was 10 for Hamamatu, Numadu, Nagatoro, Tigasaki, Yokosuka, Yokohama, Misima, Tôkyô, Mera, Tateyama, Hakoneyama, Kumagaya, Oome, Tokorozawa and Titibu, 9 for Katuura, Tyôsi, Mito, 8 for Tukubasan, and 6 for Maebasi. Mr. Kita went out of door again at 4h 10 m and was surprised to notice the rapid change in cloudiness within so short a time, as the cloudiness now attained about 8 and beside KC in the sourthern sky there was seen a *thin sheet of SC* which was moving towards SW with the speed 5. On more flash was observed at that time which was decidedly longer in duration than ordinary lightning.

Looking at the map constructed by Mr. Musya giving the statistical distribution of the directions of light observed, a tendency may be observed that a large number of the data point either towards the Bay of Tôkyô or to the Sagami-gawa Plain. As the hour was just at the minimum of daily temperature, it may be suspected that there was some component of ascending air current above the bay and the river plain, resulting in somewhat earlier cloud formation in these region compared with the others.

A phenomenon reminding us of auroral streamers diverging from a point on horizon is described accompanied with a sketch, by a witness at Minato-mati in Awa on the eastern side of the Bay of Tôkyô (see K. M. p. 187, No. 73). The radiant point is identified by reference to the profile of hills in the background of the sketch and may be traced to the direction of the epicentral region. Similar sketches are given by others.

Beams (trave) and columns (colonna) were also seen at different places with different forms, directions and modes of motion (cf. K. M., pp. 190–

194). Several observers compare the phenomena to the beam of a search light. Fire-balls (globo di fuoco) are also repeatedly mentioned (K. M. pp. 195, 196–197). It may be noticed that the ball-form and also the funnel-or trampet-form (tromba, K.M. p. 195) of luminosity were mostly seen near the epicentral districts. A witness in Odawara observed a fire-column, one (upper ?) end of which was bent towards Idu Peninsula. This reminds us of what was seen by Mr. Hattori on the occasion of Tanzawa-yama Earthquake (p. 230) of 1924 and also of another similar example of Ansei Earthquake (p. 229 foot-note).

Highly variegated forms of luminosity which may belong to Galli's (IV m) "nube luminosa" (K. M. pp. 195–196, also pp. 188) are abundantly reported, often apparently with fantastic exaggerations. Some positively state that detached clouds were illuminated. Mr. Musya is in possession of an oil painting by an observer in Hibusuma-Mura, which may be cited as an example of this same class. Another remarkable example probably belonging to this class is reported by an observer at Hongô, a few km. to N of Simoda in Idu, who observed three blinding flashes of light towards S, i.e. in the direction opposite to that of the epicentral region. He gives a well depicted pen-drawing sketch, according to which it seems that the luminosity was concentrated to a portion of the sky with considerable altitude, giving the impression of a luminous cloud. It is stated that the luminosity was so strong that different objects at a distance of about 250 m. could be well discerned. Another observer in Otiai, near the former place, saw "a funnel-shaped light (sic) resembling a beam of search-light" also to S.

In the districts not far from the epicentral region, the descriptions of the phenomena assume more or less definite form instead of an indefinite flashing of sky. One of the class of phenomena is represented by the personal observation of Dr. S. Nasu of our Institute who happened to be staying in Itô at the time of earthquake. Immediately after the severe shock he observed a ruddy glow above the profile of mountain ridges towards NW and WSW, which remained for a few minute.[17] Mr. Makino, the observer in charge of the seismograph in that town, observed the same phenomena. He had once happened to observe somewhat similar phenomena on the occasion of a great fire in Numadu (27 km.

---

[17] *Cf.* GALLI No. 121: "Si videro delle fiammelle sortire dal suolo, e queste durarono per qualche minuto dopo cessato il terremoto." "Sopra questo monte poco dopo il terremoto fu vista una luce rossastra per brevissima durata di tempo, che illumina il paese di Pioraco e sembrava uscire dal medesimo monte."

NW). "Comparing the two phenomena the glow due to the fire-brand was characterized by frequent fluctuations of intensity, whereas the glow seen in the present case of the earthquake was kept nearly steady in luminosity showing no sensible flickering." The colour of the light was dark red with orange tint, according to a colour match made by Mr. Watanabe of Itô Common School. It seems rather strange that the flashing light was not stated by these witnesses. Another example of the same kind of glow is given by Prof. Saem. Nakamura in Vol. 3, No. 2 of "Disin" with a coloured sketch by the observer Mr. S. Nisimura in Ubako, Hakone. In the same Plate is shown a similar sketch by Dr. Nasu of his personal observation in Itô above mentioned.

A very vivid description of the most remarkable phenomena observed at Hakone-Mati which was one of the most severely shaken places, is given by one of Musya's collection which is due to Mr. Isiuti, his son and others. His son who hurried out of door and was clinging to a tree to keep his equilibrium observed a flashing luminosity on the slope on the NE side of the Lake ranging from Komagadake (4 km. N) to Kami-yama (5 km. N) now in a spot and then in another, thus successively in different places. The intensity of light was such that trees and clouds illuminated by it could be sharply discerned. The sources of light seemed to be of a round shape sometimes large and sometimes small. According to Mr. Musya there is no electric transmission line passing this side of the lake. On the other hand, numerous land-slides took place on the slopes of mountains facing to the Lake. Again, according to the testimonies of the others the following details are given.

"Luminosities were seen on the mountains in different directions. The brightest one was at a spot near the wireless tower (1·5 km. SW). They were seen towards Kurakake (1·5 km. S) as well as on the mountains in SW. The colour of the light was limpid blue."

"The garden and the pond of the neighbouring Hakone Hotel were clearly seen on account of the illumination so that the observer was not aware of the fact that the electric light was extinguished."

"The illumination was so strong that the *broken electric transmission line* lying on the ground was clearly seen and the witness took care not to touch it on his way. The brightness was similar to that at the time of full moon. Everything in the neghbourhood could be well discerned."

"While a staff-member of the wireless station was hurrying to Mr. Isiuti's house, he could make his way without the aid of a lantern," which is apparently needed in a dark night. "He became aware of the darkness only when hails began to fall, about 40 minutes after the earthquake. Up to that time, he could attend to his affairs without the aid of a candle."[18]

"The light appeared to be emitted from below, during the earthquake. It was after a considerable time that it was seen in higher quarter."

"When the earthquake was at its height, *a straight row of round masses of light*[19] was seen towards the Manpukuzi Temple (SW). Each of these luminous bodies was seen to be in revolving motion. The brightness was considerable. Their heights seemed to be equal to the top of poles of transmission lines."

"Formerly, it had once happened that a crow caused the sparking of a transmission line. A loud noise was heard at that time. In the pressent occasion, however, no unusual sound was heard."

There are some reports regarding the observations made off the coast of Idu, which are interesting in many respects. According to Mr. R. Nisizima of Aziro, a number of fishermen afishing off the coast near the island Hasima at the time of the earthquake, observed a fearful display of luminous phenomena all along the mountainous districts of the epicentral zone. According to the manuscript of a fisherman, as reported from Kawana Common School, the phenomena were observed from the beginning on a boat off the island Hasima. The light first appeared above Mt. Hakone and it was seen to be propagated southwards, towards Mt. Amagi.[20] Then it was reversed in its direction of propagation and went back towards Mt. Hakone. The light which was white in colour was seen only near the ground. When he was wondering at the unusual sight, sudden shaking of the boat was felt, which he attributed to an earthquake. While talking with the others about the unusual nature of the shock felt, they saw fiery displays at three spots of the land, which he considered to be due to some volcanic eruptions accompanied by the earthquake. On landing, he found that there was no eruption, but a firebrand was caused by the earthquake." As a matter of fact, fire broke out in the town of Itô after the earthquake by which a number of houses were destroyed. Another conflagration seems to have taken place in Kôdu which was however due to other cause than the earthquake, and had been almost extinguished at the time of the earthquake shocks. Again, a fisherman of Siduura on the western coast of Idu is said to have observed on sea a large fire-ball starting from Mt. Wasidu and moving towards S.

---

[18] *Cf.* GALLI, No. 54: "Poco prima delle furiosissime scosse... quelli, que avevano gli scuri o sportelli delle fenestre aperti, veddero nella loro camera tal chiarore, che per non breve spazio di tempo poterono distinguere tutti gli oggetti anchorchè piccoli, che si presentavano alla loro vista, in modo che qualcheduno credette che fosse già cominciato il giorno." "... un grandissimo chiarore, col quale vedeva distintamente tutto il paese, e che tale si mantenne nel tempo ch'egli impiegò a percorrere lo spazio di 20 passi, dopo del quale senti egli tremare la terra."

[19] *Cf.* GALLI, No. 59: "osservato di sera venir fuora certe fiammette della grandezza e similitudine di quelle di una picciola candela, situate una presso d'altra quasi in eguale distanza e direzione, formando una linea retta.

[20] *Cf.* GALLI, No. 141: "... si vedere di notte delle striscie di fuoco attraversare il M. Nerone in senso orizzontale, fenomeno che si ripetè poche ore prima della scossa successiva..." Also No. 127, last paragraph. Again, No. 146: an observation, made on sea, of "una luce come un faro luminoso, che lentamente procedeva da Sud-Est verso Nord-West, lasciando dietro una gran fascia di luce donde cadeva una pioggia di scintille." The latter description reminds us of the description of land-slide in Siroyama, Oohito (p. 241).

There are a few reports regarding the light observed in apparent connection with land-slides, inspite of the fact that the latter were quite numerous in the epicentral region. According to the newspaper, "*Misima Asahi Sinbun*," a minor land-slide at Siroyama in front of Oohito Station was accompanied by a display of light similar to that of a pyrotechnic show initating a waterfall; it is stated that light was produced by the mass of small stones falling down along the rocky slopes of the mountain. In Mr. K. Hasimoto's letter to Mr. Musya, the testimony of a newspaper-saler is given who saw a luminosity at the moment when a land-slide took place at a distance of about one km. and he attributes the light to the heat produced as the effect of sliding. Another example is given by the testimony obtained by Mr. Musya from a chauffeur at Yugasima, who states that a large fire-column appeared at the time of great land-slide at Kadiyama. The same fact was also stated by another witness in Nakaômi.

The row of round luminous bodies observed by the family of Mr. Isiuti above mentioned (p. 240) may also be connected with land-slides which took place in numerous spots on the slopes facing the Lake.

On the other hand, according to the statement of a witness in Kadiyama recorded by Mr. Musya, no one in the immediate neighbourhood of that place seems to have observed the luminous phenomena at the time of the great land-slide, while those at distant places saw such phenomena towards the direction of Kadiyama.

It is rather remarkable that among the thousand data accumulated there are few reliable testimony of those witnesses who happened to observe remarkable electric sparks actually caused by breaking or short-circuiting of electric transmissoin lines, though there are superfluous number of reports stating that the light was much *alike* the flash produced by such a sparking. It is said that a man at Misaki actually saw a broken electric line sparking at the ground. Another reporter from Matuda near Kôdu writes to the effect that the luminosity observed was due to the short-circuiting, but it is not clear whether he actually observed such thing. A similar report from Mera Observatory is equally not quite convincing. On the other hand, there are some reports stating that the light was seen towards the direction at which there is passing no transmission line. As a matter of fact, in the circular send out asking for informations there was no special item inquiring after such accidences, so that it might be supposed that the report regarding this point was naturally eliminated.

There are, on the other hand, a few reports stating the conditions of the electric lighting at the time of earthquake. In a village named Seya (瀬谷), Kamakura-Gôri, a transformer was seen to be sparking and immediately afterwards, the electric light went out. In Hudisawa and Kugenuma, the electric light dimmed awhile at the time of shock and recovered after a short time. Prof. N. Mononobe who was awaken and reading in his residence in Azabu, Tôkyô, noticed a momentary dimming of light. The light soon recovered and then the preliminary tremor of the earthquake was felt.

The author made an inquiry at the Department of Communication with the purpose of ascertaining whether any powerful trasmission line was seriously affected by the earthquake. No positive evidence could however been obtained up to this day. Perhaps it is not practicable to confirm this point after the lapse of several months.

(4) *Colour and intensity of light observed.*

The colour of the light observed is reported by a great majority of of observers, in the case of flashing "lampi", as pale blue, white, or as similar to that of electric sparking or lightning. There are also a large number of witnesses who state positively that the light was decidedly of reddish or orange colour compared wiih the usual lightnings or sparks. In the case of that kind of glow which was observed over the mountain ridges the ruddy colour predominates. Sieberg and Lais emphacized the reddish tint of the light observed on the occasion of the earthquake as one of its characteristics. The present examples seem to confirm their opinion.

It is well known that a faint light is perceived mainly by the peripheral region of retina which is devoid of colour sense. The colour of lightnings or sparks usually described as blue, pale blue, greenish grey, etc. seems to be really connected with this colourless luminosity.

In this connection it may be added that an electric spark may sometimes show an apparent propagation of luminosity along its track due to an optical illusion,21) while the actual discharge phenomena is completed within a very short interval of time, 10^{-6} sec. say, and no such propagation can be detected by means of ordinary rotating mirror or the like. Some of the descriptions regarding the apparent propagation of luminosity *along* the track or beam of light, may be due to this kind of illusion.

As to the intensity of luminosity observed at distant quarters, it is stated by a number of reliable witnesses in Tôkyô that different objectss in the room illuminated through glass windows could be discerned (cf. foot-note 18). At that time, the eyes of the most observers were completely accustomed to darkness, so that the light might have been quite weak, though it is difficult to give any reliable quantitative estimation. Assuming, for example, that the illumination of a wall in Tokyo was of the same degree as that due to a single candle placed at a distance of 10 m. and that the source of the luminosity was in Idu at 100 km. distance the candle power of the source will amount to $10.^8$ According to the estimation of an expert in naval engineering, the total candle power of a certain squadron in full display of festival illumination amounts to about 3.10^7 CP. If a light source of these orders of magnitude were placed in an elevated mountain region with comparatively clear atmosphere, it may probably produce a considerable illumination of sky even at 100 km. distance, especially when there was a suitable distribution of clouds to catch and reflect the light. The question is how a source of light of such an enormous candle power could be produced by earthquake.

(5) *Probable and possible causes of luminosity accompanying earthquake.*

From the superfluous number of testimonies, among which we may cite those given by most reliable scientists, it will be beyond any doubt that the luminous phenomena reported are neither entirely due to the illusion of untrained minds struck by the earthquake shocks, nor due to

---

21) T. TERADA, *Nature*, **125** (1930), 528; *Bull. Inst. Phys. Chem. Res.*, 9 (1930), 287.

some purely physiological effects, though much distortion or exaggeration might have slipped into the descriptions of the phenomena especially in the case of laymen witnesses. We may, therefore, safely take the phenomena as physically real and inquire after their probable causes.

There are left many points still obscure as to the true nature of the phenomena observed, as is quite natural if we consider that they happened utterly unexpected at the moment of general alarm and passed away rapidly before a few of the witnesses could recover the coolness of mind. Hence, it will not be legitimate to draw any decisive conclusion for the present, but it will be plausible and desirable to enumerate and discuss as many causes as are conceivable, either probable or possible, and thus prepare for the next occasion on which we may hope to obtain more accurate data from those witnesses who are well prepared for observations of the rare phenomena and well aware of the variety of causes as are here enumerated.

(a) Fire-brand. As already mentioned, a conflagration took place in Kôdu before the earthquake which was already extinguished at the monent of the first shock. Fire-brand in Itô broke out after the earthquake and might have been seen from some observers at distant quarters and confounded with the other luminous phenomena. It is, however, difficult to attribute to this cause all kinds of luminosity observed in wide extent, especially those flashes resembling lightning. The ruddy glow seen from Itô above the mountain ridges and the similar phenomena observed at the other localities near the epicentral region coincide in their directions with no fire-brand reported. Besides, the characteristic difference of the nature of the glow compared with that of a fire is emphacized by more than one reliable witnesses. Thence, it may be safely concluded that fire-brand could not have been the main cause of the phenomena observed by the majority of witnesses.

(b) Lightnings. There is no room for the doubt whether some of the luminosity observed were not due to lightning flashes of a remote origin. Consulting the weather maps of that time it is found that the weather in the night was such as is characteristic to any calm and clear winter night, the central part of Honsyû being under the reign of an anticyclonic area. Moreover, according to the reports from local meteorological observatories, no thunderstorm could be traced within the range possible of such a suspicion. It was only in the night of 26th. that thunders are reported from Hatidyôzima and Miyadu, i. e. above 200 km. from the epicentral district, but nowhere else. Thus, the ambiguity due to the simultaneous occurrence of lightning is fortunately got rid of in the present case.

(c) Electric sparking. The question regarding the possibility that the short-circuiting of a powerful transmission line might have been responsible for the flash-light observed in wide extent, cannot be too hastily discarded, though indeed positive testimonies to this effect are yet wanting. There are evidences showing that the electric light got dimmer for a short time or extinguished at the time of earthquake in some locatilies at least. Some state that a transmission line was broken and the others that sparks actually were observed on the line or transformer. Moreover, it seems to be of quite common occurrence that sparkings of transmission lines are observed during an earthquake. It must, therefore, be admitted that at least a part of the luminosity observed was actually due to such causes. At the time of the earthquake no electric tramway was running, so that the usual sparking at the pole of an electric car is quite out of question. The question arises as regards the possible intensity of the light emitted by sparking of a transmission main. In the case of the full display of illumination of a squadron the estimation of the total candle power amounts to 3.10^7 CP. when the electric power consumed is 3000 kw. in round number. In the case of a spark caused by short-circuiting, the efficiency as a light source must be low compared with the above case. Estimating the latter efficiency at 1/10 of that of the former and assuming that a transmission main of 30 000 kw. was made to spark, the result will be same as that of the squadron illumination above quoted and may be sufficient for the sensible illumination of sky to a considerable extent. There is, however, no evidence for assuming that any such powerful main was actually short-circuited and brought about a general extinction of light for a very wide area depending on such a main. Moreover, the above provisory estimation may be probably too high.

On the other hand, there is a class of luminosity observed especially in the epicentral region and described as resembling that of a firebrand and having a considerable duration of time compared with an electric spark, which cannot by all means be explained by an electric sparking. Again, the testimony above given of Mr. Isituti, as reported by Mr. Musya, shows that the light source of another class was seen also at the side of the Lake where no transmission line is running. These phenomena are utterly impossible to be explained by the short-circuiting as above considered. Again, Mr. Kita's observation of a flash at 4 h 10 m seems to be difficult to be attributed to this cause. Prof. T. Itô of the Mineralogical Institute, College of Science, Tôkyô, observed the flash-light at the western suburb of Tôkyô, which was seen to emerge from the distant horizon in the direction of the epicentral region. He observed a sensible after-glow of the sky in in the same direction which he compares to the after-glow of an aurora observed by him in Norway. Such an remarkable after-glow is again utterly difficult to be explained by electric sparking. His observation gives at the same time an evidence to the effect that the after-glow was not quite independent from the flash-light. Hence, it must be admitted that the spark theory cannot cover the entire ground of the phenomena observed.

Lastly, it appears to the author very remarkable that there are so many records of luminous phenomena which are described as resembling to lightnings, but not quite similar to these, either with regards to their duration, or to their colour, and moreover, that the descriptions of these phenomena by the modern witnesses agree in many essential points with those given by the documents, either Japanese or European, dating back to the time when no electric transmission line existed at all.

(c) Land-slides and triboluminecences produced by them. It is known that considerable luminosity is observed on the occasion of land-slides. O. Vogler's and C. L. Griesbach's papers are cited in Sieberg's book in this very respect. The luminosity emitted from chalk-pits, which is mentioned in Milne's "Seismology," may probably belong to the same category. In Prof. B. Kotô's report on Kônô Earthquake, it is stated that some luminous phenomena were seen in connection with the land-slide on the slope of Mt. Ibuki. In the present occasion, some examples have already been given which positively state that some kinds of such phenomena were actually seen accompaying land-slides. It seems, therefore, that the most probable cause of some kinds of the luminosity observed in the present occasion may be attributed to this effect of land-slides. According to the map prepared by the Land Survey Department showing the geographical distribution of land-slides caused by the present earthquake they are quite numerous along the meizoseismal zones, i.e. over seventy, even if we only take the most conspicuous ones into account. The question of after-glow could also be solved by this effect, if we consider that a land-slide may be followed by subsequent series of minor slidings and it may take a sensible time before settling down to the stable state of equilibrium, especially when the earthquake is still continuing to disturb the equilibrium. It is not necessary to inquire after the after-glow effect of triboluminescence itself, which seems to be not yet fully investigated. The question is, however, whether this effect may quantitatively suffice to explain the enormous intensity of luminosity observed. In this respect, the author devised a provisory experiment which was carried out in the Institute of Physical and Chemical Research by the able hands of Dr. M. Hirata and Mr. T. Utigasaki, to whom the best thanks of the author are due. Different kinds of rocks at hand were subjected to grinding by means of a usual tool-grinder in form of a disc which is revolved with an electric motor. The light emitted from the line of contact between the rock specimen and the cylindrical surface of the grinder disc (5 mm. in thickness) was compared with that of 100 lighted "senkô" (incense sticks used by Buddists), by means of a simple Bunsen photometer, as a candle or Hefner lamp was not convenient for the direct comparison. The "100 senkô" light was afterwards compared with a candle by the same photometer. Though the measurement was very rough, it was deemed sufficient for determining the order of magnitude of the luminosity, as such only is here in question. The results of the experiments show firstly that the luminosity is almost independent on the

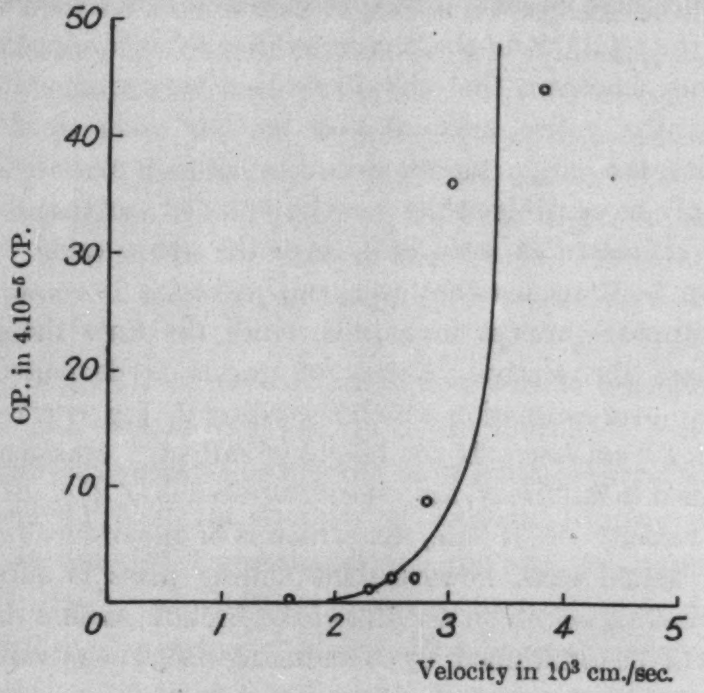

Fig. 1.

pressure between the specimen and the grinder, at least within the range practicable without stopping the motor by the braking action. Secondly, the intensity of light emitted increase with the peripheral velocity of the grinder, first slowly and later rapidly, as shown by Fig. 1, in which the abscissa gives the peripheral velocity in 10^3 cm./sec. and the ordinates in a provisional unit of "100 senkô" which is roughly equivalent to 4.10^{-5} CP. The order of magnitude is not much different for different kinds of rocks tested. Assume now for the sake of estimation that in the area disturbed by a land-slide, every unit area contains l cm. of the luminous line-element similar to that of the line of contact between the rock specimen and the grinder. It will not matter much that in the case of the experiment the two pieces in contact were of different substances. Take the emission per 5 mm. as $p \times 4.10^{-5}$ CP. Then the emission per 1 cm.^{2} of the area will be $pl \times 8.10^{-5}$ CP. Assuming one of the land-slide to be of an area equal to that of a semicircle with the radius of 100 m., the total area of a single slide will be $1{\cdot}57.10^8$ cm.^{2} Thence, the total light for the single slide area will be about $pl \times 12{\cdot}8.10^3$ CP. If one hundred similar land-slides may be assumed to cooperate at the same time, the total will make $pl \times 1{\cdot}28.10^5$ CP. Hence if we put $p=10$ and $l=10$, the result may become $1{\cdot}28.10^7$ CP. which is of the same order of magnitude as the total CP. of the luminous display of a squadron above cited. It seems, however, that the above is a very exaggerated estimation. Firstly, the entire area affected by land-slide cannot become luminous, since the large relative velocities between consecutive masses of rock can only be sensible at the very slip-plane,[22] so that the effective area must be estimated at most at 1/10 of the above value. Secondly, the assumption $l=10$ means that every cm.^{2} contains 10 cm. of luminous lines, which appears almost incredible, since the finer the grains produced, the more the relative velocity of grains is decreased. Again, $p=10$ is also an over-estimation which according to Fig. corresponds to a velocity of 3×10^3 cm./sec. If the height of fall of a rock mass be h m. which is assumed to fall freely, the velocity aquired is $\sqrt{2hg}$. If $h=50$ m., we obtain a velocity of $31{\cdot}3$ m./sec. which is of the order of magnitude required. In actual case, however, the sliding mass is subjected to a considerable braking action on account of the friction, so that the effective acceleration will be multiplied by a reducing factor equivalent to the difference between the static and kinetic coefficients of friction. Even if $v=20$ m./sec., p is only of the order of unity. Thirdly, it is also an over-estimation to assume that 100 land-slides took place simulaneously to contribute to a single flash of illumination of the sky at a given direction, a fortiori because the solid angle of illumination is always limited by the topographical configurations.

---

[22] Different kinds of beam or column of light can be explained if we assume that the light is emitted from the interior of the crevasse formed at the instant of its opening and sliding. A fire-ball might be due to an illuminated spot of cloud.

Thus, putting $l=1$, $p=1$ and the effective area$=1/10$ of the value above assumed, the total candle power is reduced to the order of 10^4. This is still no small figure, but it seems doubtful whether the source of these order of magnitude may explain the observed intensity at a distance of 100 km. The illumination of a source of 10^4 CP. at 100 km. will be equivalent to that of a single candle at 1 km., even if there were no absorbing medium. Hence, the light observed within a house in Tôkyô is difficult to be attributed to this cause. On the other hand, there are some evidences already mentioned showing that at least some of the flash-light observed in Tôkyô are originated from somewhere in epicentral region and not connected with electric sparks.

In the above, the estimation of p was based on the laboratory experiment and given as the function of the relative velocity of sliding. A possibility must be kept in reserve that in the actual case of land-slides in a great scale, another kind of mechanism for producing luminosity may come into play and contribute to increase the value of p to a considerable amount. If some of the old documents, stating emission of light from fissures on ground, may be true, we must take account of such effect which does not depend on the velocity of sliding. Even in that case, it is difficult to assume that the order of magnitude of the luminosity can be quite different. A thorough investigation is, however, desirable on this very respect.

Lastly, it may be remarked that there are some phemomena observed which are not easy to be explained by the luminosity due to land-slides even in qualitative sense, such as the strong luminosity observed towards the southern sky from the vicinity of Simoda, Idu, as no remarkable land-slide is reported from that region and also it is improbable judged from the intensity of shocks in that district. It is, indeed, not yet certain whether a sparking of electric line has not occurred somewhere near Simoda. If we may rely upon the fine sketch made by the witness, the altitude of the concentrated luminosity is seems to have been far too greater than that of any transmission line possible.

(d) A possible cause of luminosity due to the motion of water in the earth's crust.

In the early stage of the author's present investigations, the data from the immediate vicinity of the epicentral region could not yet be obtained; especially, no report was at hand regarding the luminosity observed in connection with land-slides. While seeking then after all conceivable causes of luminosity which may come into play on such an occasion, the author hit upon a possibilty which seems to have been utterly neglected to be taken in account in all previous discussions concerning the phenomena. A preliminary discussion was therefore made on this point and the result was communicated to the Proceedings of Imperial Academy, Vol. VI, 1930, No. 10, p. 401–404.[23] It was shown that the motion of water through subterranean layers containing a network of capillary channels may, under favourable conditions, produce an enormous potential difference in the upper atmosphere and excite a luminous electric discharge in a higher region. The dscussion will be reproduced in the following with little modification.

According to the investigations of Wiedemann, Quincke, Helmholtz and the recent students of "surface chemistry," a potential difference called "Strömungspotential" is established between the two ends of a capillary tube, through which a liquid is made to flow under a pressure gradient. The P.D. is given by

$$E = \frac{\varphi D p \sigma}{4\pi\eta},$$

where φ is the kinetic potential (mostly 0·01–0·05 volts), p the total hydrostatic pressure difference, D, σ and η respectively the dielectric constant, specific resistance, and coefficient of viscosity of the liquid.

For application to the case of earthquake, we will consider here two kinds of "models," for which the juvenile and meteorological waters are the respective working liquids.

(1) The disturbance of a severe earthquake will affect the earth crust to a depth comparable with the linear dimension of the megaseismic

---

[23] When later consulting GALLI's paper, loc. cit. the author came across the following passages among the article No. 128, regarding to Andalusian Earthquake of 25 Dec., 1884, quoted as "dai rapporti ufficiali di Formes, Murchas, Nigüelas e Periana": "...ne abbiamo una spiegazione semplicissima quando si ammetta la teoria geodinamica, fondata principalmente sul vapore d'acqua. Questo, infatti, salendo con sufficiente pressione per le fessure, può dare origine ad una manifestazione elettrica, come si ottiene artificialmente nei gabinetti di fisica colla machina Armstrong."

area. We will assume, for example, that the water is displaced vertically upwards through numerous capillary channels existing, or freshly set free in the crust due to the deformation, under a pressure which is of the order of that prevailing in the depth of 100 km. or may be much larger at least for a short time in the case of a catastroph. In that case, P.D. calculated from the above formula will be established between the upper and the lower layers and maintained as long as the flow is continued.

For a rough estimation, we will take $\varphi=0{\cdot}05$ volts, $D=81$, $\sigma=1000$ ohms/cm^3., $\eta=10^{-3}$ c.g.s.[24] For p we take $p=ap_0$, where a is an unknown numerical factor and p_0 the hydrostatic pressure due to 100 km. column of rock with the density of 3, i.e. $p_0=3.10^{10}$ c.g.s.[25] In this case we obtain $E \doteqdot 3{\cdot}3\ a.\ 10^6$ volts. Thus, even if $a=1$, we have a value of 3000 KV.

The value of the potential in the atmosphere depends on the geometrical form of the equipotential surface on the ground. If it be assumed as spherical, with a radius R, the potential at a height H will be $E_H = ER/(R+H)$ and the field $F_H = -ER/(R+H)^2$. The sparking potential of atmosphere is the least at about 60 km. height, where the pressure is of the order of 0·1 mm. Hg. Putting $R = H = 5$ km., the field at the height H is $F_H = -5E.10^{-8}$. If we take the value of E above obtained, then $F_H = -0{\cdot}165$ volts/cm. In the case of the Moore vacuum light, the driving field is about 2 volts/cm. which will require $a = 12$, a value a little too large to be expected. This is, however, not necessary in the present case. The sparking is facilitated by many circumstances such as the heterogeneity[26] in conductivity and the presence of ionisation and

---

24) We take this value, since the water may be of a temperature higher than 100°C. For σ we have no available data for subterranean water. Besides, the conductivity of rock in the depth is unknown and if it be large the result of calculation will be sensibly modified. On the other hand, the subterranean water may be in gaseous form in which case no experimental data are available. The fact that an enormous P.D. is produced along the pillar of volcanic dust on the occasion of eruption will show that the kinetic potential between the rock materials and the superheated steam must be of a large value, as in this case also the P.D. is produced by the relative flow of the gas along the heated rock material.

25) The strength of rock materials against one-sided crushing load is usually of the order of 1000 kg./cm^2. $=10^9$ c.g.s. The hydrostatic pressure in the depth corresponding to such an order of stress difference may be of a higher degree than this strength. This will also support the above assumption for p.

26) In this repect, the readers are referred to a paper: T. Terada, U. Nakaya and K. Yumoto "Some experiments on spark discharge in heterogeneous media—a hint on the mechanism of lightning discharge," *Sci. Pap. Inst. Phys. Chem. Res.*, 4 (1926), 129–160. It is demonstrated that an abnormally long spark may be drawn under suitable conditions.

space charge. For example, we may expect a considerable increase of the field near the lower boundary of the Heaviside layer. At any rate, the value of P.D. between the layer above the epicentral region and the surrounding atmosphere is far greater than the ordinary cathode fall of any vacuuam discharge, even if we take $a<1$.[27)]

The duration of the above phenomena may be short and could not affect the usual recording instrument of the atmospheric potential. Again, the horizontal potential gradient is small, so that the telegraphic lines might not necessarily be sensibly affected.[28)]

(2) The meteorological water contained in the water-bearing layer near the ground surface may be forced to a horizontal displacement under the pressure gradient caused by earthquake. In this case the process may be of a more gradual one than in (1). Here we may take $a=1$ and $\eta=0{\cdot}01$ ($t=15^\circ$). Then, $E=3\times10^5$ volts. The head and end of the canal may be compared with a dipole, in roughly estimating the effect at the a great distance. If the length of the dipole be l, we may take $E/l=F_m$ for the field in the middle point of it and compare F_m with the field F_d at a distance ρl. For $l=20$ km. $F_m=1{\cdot}5\times10^{-1}$. K. Shiratori[29)] observed a change in earth's potential gradient of about 4.10^{-7} volts/cm. at Sendai, on the occasion of the Kwantô Earthquake of 1923. Thus $F_d/F_m=2{\cdot}7\times10^{-6}$. As the distance of Sendai from the epicentre is about 800 km., $\rho=40$. On the other hand, the field due to a dipole varies as $\rho^{-3}F_m$, disregarding the factor due to the azimuth. The above ρ will therefore give $F_d/F_m=4{\cdot}7\times10^{-6}$, which is of the same order of magnitude as derived above from the observed F_d. Hence, it is possible that the effect observed by Shiratori cannot be merely due to the change in contact potential or resistance of electrodes, but might well have been produced by the real electrical effect of the earthquake.

The case of quadruplets as well as of octuplets may also happen, especially the former in the case of Shida's " pull-push " model.

At the present moment, the above may be taken as a suggestion regarding to a physical possibility, which must at any rate be taken in

---

27) In the above model, the case was considered as statical. It may also be possible that a disruptive discharge may take place somewhere in an underground layer and induce an additional field in the atmosphere. Moreover, a large P.D. may already exist in the upper atmosphere before the seismic disturbance, and the latter may then act as a kind of trigger. For the present we may better leave these possibilities as open questions.

28) The magnetic effect may also be small due to the radial nature of the current sheet.

29) K. SHIRATORI, *Jap. Journ. Astr. Geoph.*, **2** (1924), 173.

account, if we attempt to make a thorough investigation of the problem at hand, though the author is far from venturing to explain all the phenomena observed in the present case by this special possible cause[30].

In this connection, it will be of some interest to remark that on the occasion of the Idu Earthquake an unusual fluctuation of current were recorded by the recording system for the submarine cable of Guam Line, though it cannot be ascertained whether it was not due to a merely mechaanical cause. Again, on the occasion of an earthquake in the neighbourhood of Tôkyô on 30th January of this year, a remarkable oscillation was revealed in the recording system[31] of earth-current between Tôkyô and Hôya, while the similar system between Tôkyô and Yokohama showed no trace of such fluctuation of the current. The former circuit is perpendicular to the direction of the epicentre, while the latter is nearly parallel to it. Similar cases may be found frequently in the earlier literatures[32] of earthquake phenomena, though regarded mostly as trivial and neglected by modern students of seismology. It seems, however, not quite superfluous to resume the investigations in this line with improvements of the method which will be possible in these days to be applied for ensuring the reliability of the results far greater than was attainable in the past.

Another fact already mentioned that the cloudiness of sky showed a remarkable abrupt change at the time of earthquake, cannot be overlooked as purely accidental without a further inquiry. It is well known[33] that the formation of cirrus cloud is frequently connected with an auroral display which is a mode of electric discharge in upper air, though the real physical connection between these two phenomena is still obscure.

---

30) There remains to be mentioned another electro-capillary effect which is complementary to that of "Strömungspotential," i.e. of "electro-endosmose," by which a hydrostatic pressure gradient may be generated by an electric current. The fact that severe earthquakes seems to take place frequently associated with thunderstorm may be worth attention when viewed under the stand point of the present note.

31) The self-recording apparatuses of the earth-currents have recently been installed by the authorities of the Department of Communication. The records here mentioned were kindly shown to the author by Mr. S. INADA of that Department for which the author feels greatly obliged. The earthquake occurred at 10h 10 m. 41 sec., 30th. Jan., 1931; the epicentre is located at the Kokai-gawa basin; the maximim amplitude in Tôkyô was about 0.4 m.m.

32) Some of them are mentioned in URBANITZKY's book, *loc. cit.*, 917.

33) ARRHENNIUS, "Lehrbuch der komischen Physik," (1903), 907; E. MATHIAS, "Traité d'electricité atmosphérique et tellurique," (1924), 346; Handbuch der Experimental-Physik, Bd. 25, Teil 1, 472. Also GALLI, *loc. cit.*, 439.

It seems therefore interesting to pay attention on this special point in future occasions of severe earthquakes accompanied with, or without, luminous phenomena, and to make a thorough investigation regarding the clouds as well as the general weather conditions before and after the earthquakes.34)

In concluding, we may repeat that certain classes of the luminous phenomena observed on the occasion of severe earthquakes are physically real and directly connected with the earthquake. The question as to the true cause of the phenomena is not yet settled. The ultimate solution of the problem must be reserved for a future when a more sufficient reliable material of observations would have been accumlated. It is, therefore, desirable that on any future occasion of severe earthquake the seismologists as well as the other scientists capable of reliable observations with open mind would be keenly alive to the appearance of such phenomena and keep detailed records of what were observed.

The author's cordial thanks are due to Mr. Musya who kindly placed his entire collection of data at the author's disposal and not less to many of the scientific members of different Institutes, among which our Earthquake Research Institute, Aeronautical Research Institute and Central Meteorological Observatory must be especially mentioned, for the most reliable data of their personal observations. For the valuable informations regarding the literatures of the subject, he is greatly obliged to Prof. T. Okada, Director of the Central Meteorological Observatory.

17. 地震に伴ふ發光現象に就て

地震研究所 寺 田 寅 彦

地震の際に空中又は地上に著しい發光を伴ふことがあるといふことは、日本のみならず西洋諸國の地震に關する記事中に多數に發見され、しかも其記事の內容が古今東西を通じて共通な諸點を具備して居るのは興味のあることである。それにも拘らず此現象は從來學者の側からは餘り注意されず、稀に注意されても多くは初から疑の眼をもつて見られ、充分に檢討されなかつた場合が多いやうに見える。昭和五年十一月の伊豆地震に際しても此種の現象が到處で觀測され、此れ

---

34) A similar change of weather happened in the case of Kumamoto Earthquake of 1889 above cited. Other parallel cases are not wanting, e.g. B. Willis, Chile earthquake, loc. cit., though a thorough statical investigation must be carried out in order to make this point clear.

に關する多數の報告を纒めた武者金吉氏の報文は旣に本誌前號に掲載された。著者も武者氏蒐集材料と、並に、少數ではあるが若干の信頼すべき科學者の觀察した材料とを併せ調べた結果、武者氏の結果を確かめることが出來た。

本篇では先づ古來西洋諸國に於ける此現象の文獻を略記し、次には本邦に於ける古來の記錄中から若干の例を採錄し、特に明治以後のものは詳しく列記した。

次に今回の伊豆地震に關する諸資料に就て著者の所見を述べた。(1) 光の見へた場所の分布 (2) 光の現はれた時刻 (3) 光り方の種類 (4) 光の色と (5) 强度等に就て多少の考察を試みた。

又此現象の原因に就て考察した結果は次の通である。(1) 火事と (2) 雷雨に伴ふ電光とは此際問題にならない。(3) 送電線の接觸又切斷によるスパークは、現象の一部を説明するとしても、此れでは説明されない著しい現象がある。さうして其等は (4) 山崩れ地辷りによる tribolumin scence として説明すれば多くの場合に質的には容易に説明されさうである。併し著者が行つた簡單な實驗を基礎として試みた量的の計算 (勿論或假定の下に) の結果では、此れだけで凡ての現象を説明するのは困難であるやうに見える。それで電線のショートと山崩と兩方で凡てを説明すれば一應は尤らしいやうである。併し充分强力な放電に關する確證が得られないのみならず、又電線の存在しなかつた時代に於ける東西兩洋の記錄の共通圏内に多數に現はれる閃光的現象が、今日の場合にショートで説明されるものと殆同一であり、しかもそれが雷雨の疑のない時にでも度々あつたと考へられるところに困難がある。

以上の原因の外に從來全く考慮されなかつたと思はるゝ一つの可能な原因がある。それは毛管電氣現象に關するもので、地殼内に於ける水の運動の爲に地殼中、從て空中に著しき電位差を起こし、場合によつては高層の空中放電を生ずることが可能であるといふのである。此に關する若干の考察をした結果を述べてある。現在では確に此の爲と考へるべき實證はないが、多少の手掛と見られる二三の現象を附記して將來の參考とした。

武者氏並に著者の調査によつて、「地震に伴ふ發光現象」の少くも大部分が單なる幻覺ではないこと、又此れが、凡ての場合に火事や、電光や、電線の故障等だけで説明することは出來ないので、兎も角、直接に地震によつて惹起される一つの發光現象が存在することが明になつたと思はれる。

此樣な發光が主なる地震の前から現はれることもありはしないかと疑はせるに足るやうな若干の例もあるので、此點から見ても、此現象は、地震學上必ずしも輕視することの出來ない一つの問題を提供するものであらう。

此研究に關して貴重な材料を供給された武者氏其他多數の舊知又未知の諸君の好意ある援助に對して茲に深謝の意を表する。

18. *Blocks in the Earth's Crust and their Movements. Part I.*[1]

By **Naomi MIYABE,**

Earthquake Research Institute.

(Read March 17, 1931.—Received June 20, 1931.)

In Kwantô, Tango and other districts, where the leveling or triangulation surveys were carried out more than twice in the same districts, the vertical displacements of bench-marks or triangulation points are generally found which may be considered to have occurred during the time interval of the two successive surveys.

In the preceding paper,[2] the present writer pointed out that the apparent discontinuities in the vertical displacements of bench-marks are due partly to the configuration of the leveling routes. In the present paper, the writer introduced a method to analyse the data of vertical displacements of bench-marks, which might not be affected by the configuration of the leveling routes. Then he investigated block movements of the earth's crust referring to the data of vertical displacements of triangulation points in Bôsô Peninsula.

1. A Method for determining Blocks.

When vertical displacements of bench-marks or triangulation points are given, there may be a number of methods for determining the extent and form of each constituent block and also for investigating its movement. The present writer employed a method described as follows.

Taking pairs of triangulation points, we measure the distance s and the difference of vertical displacements δh between the two triangulation points, together with the azimuth θ of the direction of the line connecting the same pair of triangulation points, with reference to some definite direction, for instance, N. δh is divided by s, the distance between the two triangulation points, and the quotient is put equal to $\tan\phi$, where ϕ denotes the angle of inclination of the line connecting the corresponding pair of the triangulation points.

---

[1] An abstract of the present paper was already appeared in *Proc. Imp. Acad.*, 7 (1931), 150.

[2] N. MIYABE, *Bull. E. R. I.*, 9 (1931), 1.

When a number of triangulation points are situated on the same block, θ's and $\tan\phi$'s measured between every pair of these triangulation points are connected by a relation expressed by an equation

$$\tan\phi = \tan\phi_m \cos(\theta-\theta_m), \qquad (1)$$

where ϕ_m and θ_m denote the magnitude and the direction of the tilting of the block, respectively.

Conversely, if a number of triangulation points are such that the measured $\tan\phi$'s and θ's between every pair of them are connected with the relation (1), they are regarded as situated on a single block, ϕ_m and θ_m of which being estimated on the θ-$\tan\phi$ diagramme.

The relation (1), however, holds exactly right when the surface of the block is horizontal before its movement. If the surface of the block is inclined, or, two triangulation points of a pair are situated at portions of different heights, the slope may be expected to affect the value of $\tan\phi$ to some extent. To investigate the effect of the topographical slope, we consider two points A and B situated at different heights (Fig. 1). After a block-movement, B comes to B' relative to A. Let the height-difference measured between A and B and that measured A and B' be h and $h+\delta h$ respectively, and AC be s, then we have

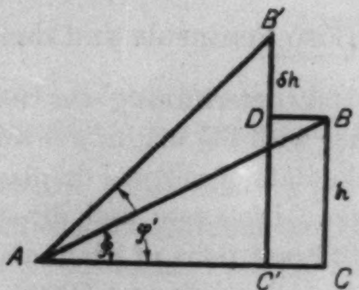

Fig. 1.

$$\tan\phi = \delta h/s \fallingdotseq B'D/AC = (B'C'-DC')/AC = (B'C'-BC)/AC,$$

$$B'C' = AB'\sin\varphi', \qquad BC = AB\sin\varphi,$$

$$AC = AB\cos\varphi, \qquad AB' = AB.$$

Therefore, $\tan\phi = (\sin\varphi' - \sin\varphi)/\cos\varphi$.

Put $\varphi' = \varphi + \Delta\varphi = \varphi + \phi,$

and we get $\sin\varphi' = \sin(\varphi+\phi) = \sin\varphi\cos\phi + \cos\varphi\sin\phi$.

Now ϕ is small enough for expanding $\cos\phi$ and $\sin\phi$ in terms of ϕ. Hence, we have for the approximation of second order

$$\tan\phi = \frac{\sin\varphi\,(1-\phi^2/2)+\phi\cos\varphi-\sin\varphi}{\cos\varphi}$$

$$= \phi - \phi^2/2\tan\varphi, \qquad (\tan\varphi = BC/AC = h/s)$$

where $-\phi^2/2\tan\varphi$ is a term of correction due to the topographical slope between the two points A and B. The value of the term of correction tends to be infinite, when φ approaches to $\frac{\pi}{2}$. Therefore, the correction due to the slope may not be disregarded when the topographical slope, φ, of the surface of the block is very near to $\frac{\pi}{2}$. But, in most cases, at least in our present case, magnitudes of φ's rarely exceed $\frac{\pi}{4}$. Hence, the correction due to the topographical slope, φ, may be disregarded in our present case.

2. Blocks in Bôsô Peninsula and their Movements.

The above method for determining the form and extent of each constituent block, together with the magnitude and direction of its tilting, was applied to analyse the data of vertical displacements of triangulation points in Bôsô Peninsula. Distances and directions, with reference to N., of lines connecting different pairs of triangulation points are measured on the topographical maps of the scale of 1/50000. Fig. 2 shows the block structure and tilting of each constituent block in Bôsô Peninsula obtained. Lengths and directions of arrows in the figure denote the magnitudes and directions of tiltings of constituent blocks. Dotted lines are probable boundaries of the groups of triangulation points which are regarded as

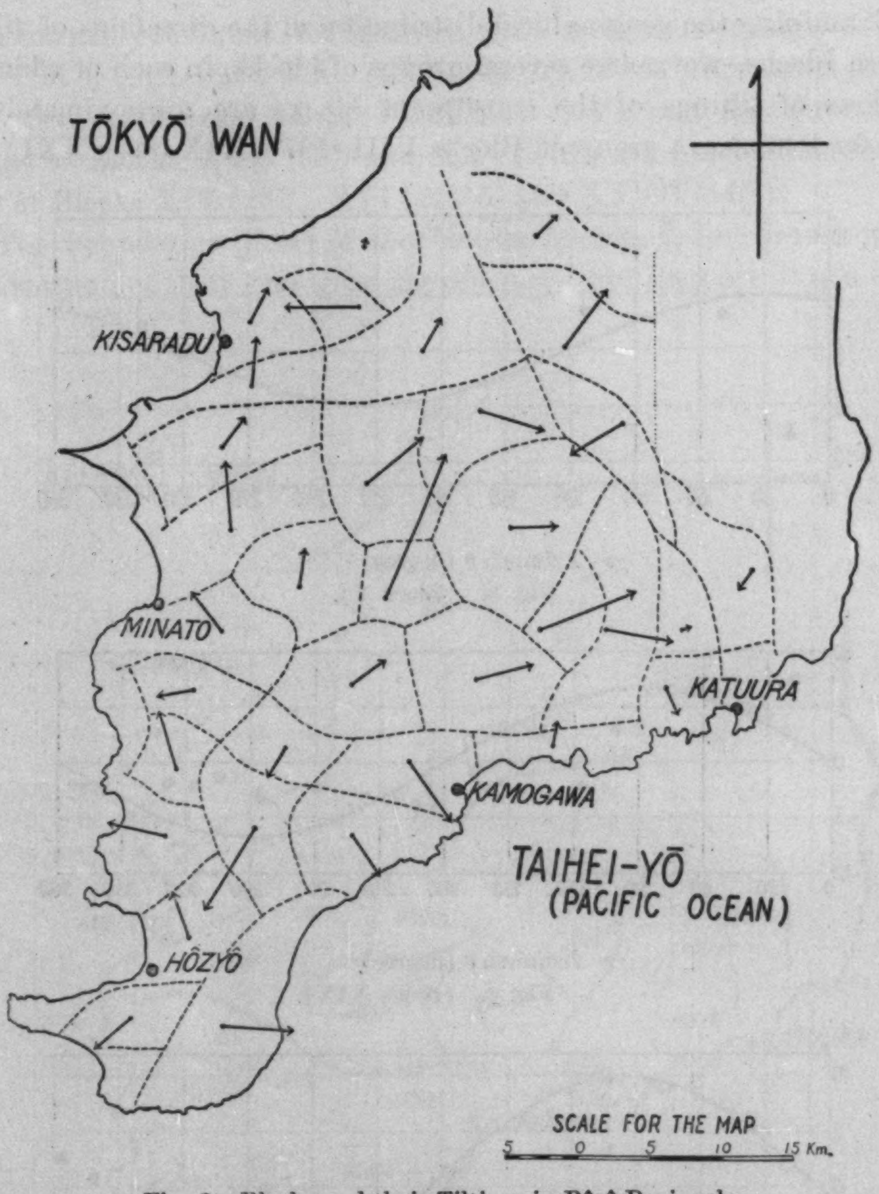
TŌKYŌ WAN
KISARADU
MINATO
KATUURA
KAMOGAWA
TAIHEI-YŌ
(PACIFIC OCEAN)
HÔZYÔ
SCALE FOR THE MAP
5 0 5 10 15 Km.

Fig. 2. Blocks and their Tiltings in Bôsô Peninsula.
(The Magnitudes and Directions of the Arrows correspond to those of Tiltings of the Blocks.)

situated on respective blocks. The relation (1) holds in each group of triangulation points or in each constituent block, as shown in Figs. 3, 4 and 5, which correspond to Blocks V, XIX and XXXIII respectively. In these figures, ○'s are the marks for the triangulation points which are regarded as situated on the respective blocks, the tiltings of which are represented by the curves drawn with thick full lines, while, ●'s are the marks for the triangulation points which are not on the same blocks as represented by the curves and the marks ○'s.

Examining the geographical distribution of the directions of tiltings of these blocks, we notice several groups of blocks, in each of which the directions of tiltings of the constituent blocks are approximately the same; for instance, a group of Blocks VIII (107°), XIX (89°), XXI (100°), XXII (73°), XXV (70°) and XXVI (76°) and another group of Blocks V (31°), VI (46°), VII (38°), IX (52°), XVII (55°) and XVIII (23°). The numerical figures in brackets are the values of θ_m's of the blocks. In several other cases, however, the directions of tiltings of adjacent blocks

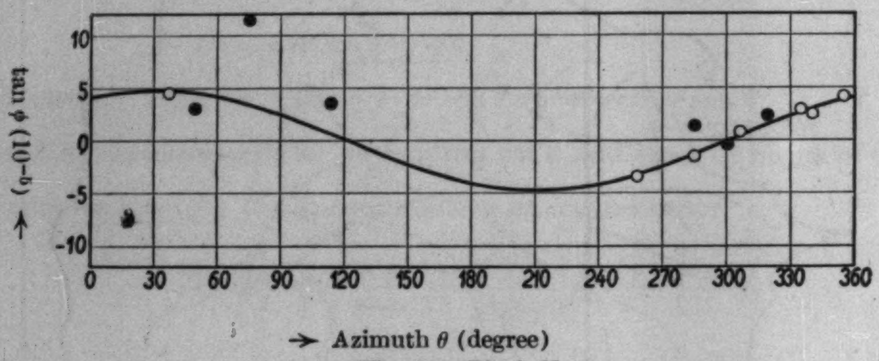

Fig. 3. (Block V).

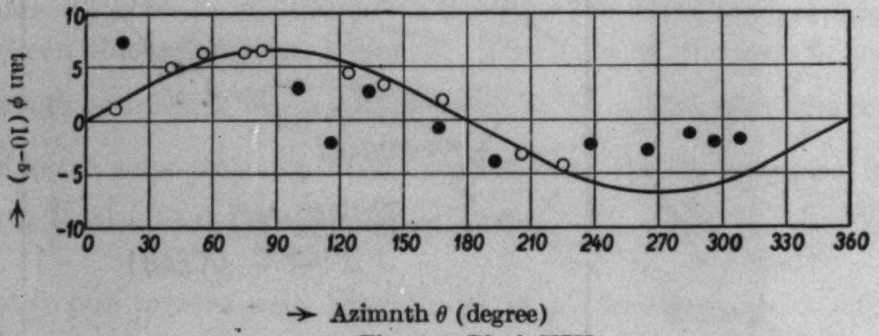

Fig. 4. (Block XIX).

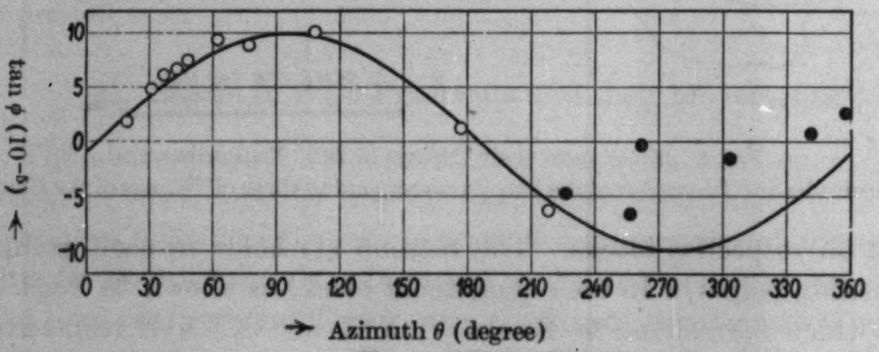

Fig. 5. (Block XXXIII).

are remarkably different; for instance, the directions of tiltings of Blocks VIII (107°), XIX (89°), XXI (100°) and XXII (73°) are much different from those of Blocks XX (240°), XXIII (215°), and the directions of tiltings of Blocks XVII (55°) and XXVI (76°) are much different from those of Blocks XIV (261°), XVI (211°.5) and XXVII (145°).

The boundaries (dots) of the blocks, in Fig. 2, are drawn with no consideration of their geological significances, but they are drawn only to

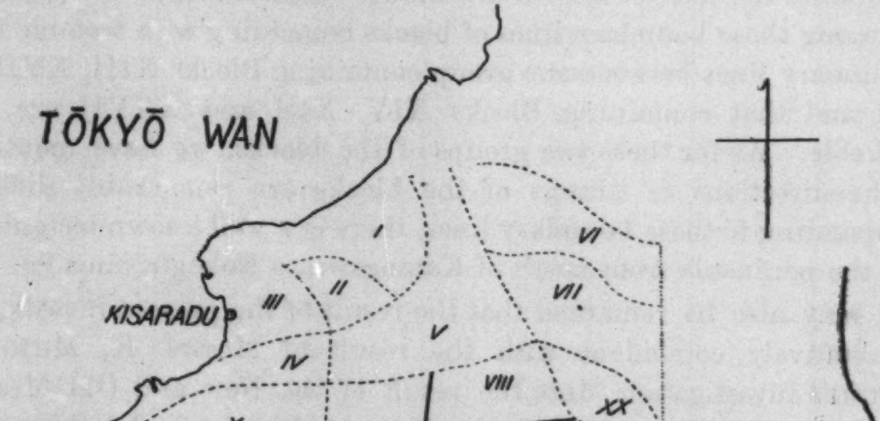
TŌKYŌ WAN
KISARADU
MINATO
HÔZYŌ
KAMOGAWA
KATUURA
TAIHEI - YŌ
(PACIFIC OCEAN)
I
II
III
IV
V
VI
VII
VIII
IX
X
XI
XII
VIII
XIV
XV
XVI
XVII
XVIII
XIX
XX
XXI
XXII
XXIII
XXIV
XXV
XXVI
XXVII
XXVIII
XXIX
XXX
XXXI
XXXII
XXXIII
XXXIV
SCALE FOR THE MAP
5 0 5 10 15 Km.

Fig. 6.

Probable Boundaries of the Blocks in Bôsô Peninsula. (The Boundaries coinciding with Tectonic Lines are drawn with Thick Full Lines.)

distinguish the areas within which the triangulation points belonging to respective groups or blocks are distributed. Among them, however, there are found several boundaries which are approximately coincident with the discontinuities significant in geologic structure. In Fig. 6, the boundaries of the blocks which are approximately coincident with geological faults located by Prof. H. Yabe and his collaborators,[3] are drawn with full lines, while the boundaries with which the coincident tectonic lines are not yet known are shown by dotted lines.

Among these boundary lines of blocks coinciding with tectonic lines, the boundary lines between the group containing Blocks XIII, XVII and XXVI and that containing Blocks XIV, XVI and XXVII are most remarkable. As for these two groups of the blocks, we have mentioned that the directions of tiltings of the blocks are remarkably different. Corresponding to these boundary lines, there is a well known tectonic line across the peninsula from north of Kamogawa to Nokogiriyama.[4]

It may also be remarked that the result of the present investigation is qualitatively coincident with the result of Messrs. K. Mutô and K. Atumi's investigation "into the result of the New and Old Measurements of the Levelling Net in the Kwantô District." In the present paper, block movements of the earth's crust in Bôsô Peninsula were investigated in more detail than the case of Messrs. K. Mutô and K. Atumi's investigation.

3. Vertical Movements of Blocks.

In the preceding pages, we have exclusively dealt with the tiltings of the blocks. To interprete the full significance of the observed vertical displacements of triangulation points, it is necessary to consider also the translational vertical movements of the blocks as a whole besides the tiltings.

The vertical movement of a block is, in the present investigation, given by the mean value of vertical displacements of triangulation points distributed on the block.

Table I contains vertical movements of the blocks together with

---

3) Prof. H. Yabe was kind enough to lend me the geological maps of northern part of Bôsô Peninsula compiled by him and his collaborators, at the writer's disposal.

4) R. Tayama, *Saitô Hôonkwai, Gakuzyutu Kenkyu Hôkoku*, No. 9 (1930), etc.

5) K. Mutô and K. Atumi, *Bull. E. R. I.*, *7* (1929), 495.

Table I.

Block	φ_m	θ_m (degree)	Vertical Movement
	$\times 10^{-5}$		cm.
I	1·75	10·0	13·7
II	10·44	270·0	25·3
III	5·20	28·0	15·8
IV	6·60	5·0	31·0
V	4·80	31·0	28·3
VI	4·20	46·0	24·8
VII	9·60	38·0	20·7
VIII	9·50	107·0	27·8
IX	10·00	52·0	69·7
X	5·20	38·0	58·3
XI	9·30	355·0	2·7
XII	5·10	7·0	125·6
XIII	6·90	321·5	125·3
XIV	5·10	261·0	126·5
XV	8·20	343·0	132·0
XVI	4·80	211·5	123·3
XVII	5·60	55·0	118·4
XVIII	21·40	23·0	83·3
XIX	6·60	89·0	32·2
XX	8·50	240·0	39·0
XXI	10·20	100·0	54·6
XXII	1·28	73·0	30·8
XXIII	3·10	215·0	29·0
XXIV	4·00	156·0	28·8
XXV	14·40	70·0	32·0
XXVI	8·30	76·0	63·3
XXVII	10·20	145·0	87·2
XXVIII	3·50	11·0	45·7
XXIX	7·00	145·0	102·7
XXX	13·10	212·0	128·3
XXXI	8·20	282·0	128·0
XXXII	6·60	340·0	141·9
XXXIII	9·95	94·0	128·6
XXXIV	6·60	230·0	154·5

the directions and magnitudes of their tiltings. Fig. 7 shows the geographical distribution of vertical movements of the blocks. In Fig. 7,

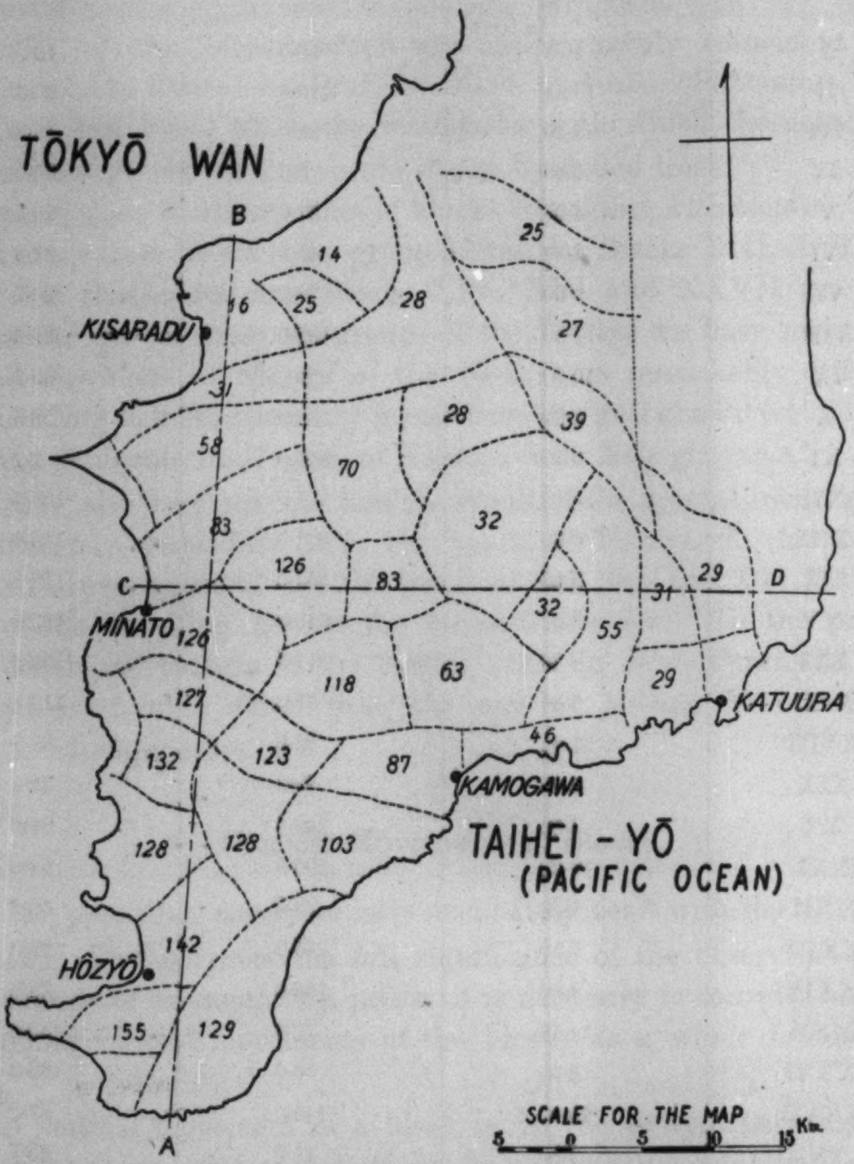
TŌKYŌ WAN
B
14
16
25
28
25
27
KISARADU
31
28
39
58
70
32
83
C
126
83
31
29
D
MINATO
126
32
55
118
63
29
KATUURA
127
46
132
123
87
KAMOGAWA
TAIHEI - YŌ
(PACIFIC OCEAN)
128
128
103
142
HÔZYÔ
155
129
A
SCALE FOR THE MAP
5 0 5 10 15 Km.

Fig. 7. Translational Vertical Movements of the Blocks in Bôsô Peninsula. (The Numeral Figures are the Amounts of the Vertical Movements in cm.)

we notice three groups of blocks, in each of which the vertical movements of the block are approximately the same.

They are:

1) A group of the blocks situated in the southwestern part of the peninsula, of which the vertical movements are 120–130 cm, including Blocks XXXII (142 cm) and XXXIV (155 cm) with exceptional upheavals;

2) A group of the blocks adjacent to N. and E. of the group 1), of which the vertical movements are 60–80 cm; and

3) A group of the blocks adjacent to N. and E. of the group 2), of which the vertical movements are 20–30 cm, except for Blocks XXI (55 cm) and XXVIII (45 cm) with greater upheavals. Blocks situated in the northern part of this group are less in amounts of vertical movements than those situated in the southern part, by 10 cm or more.

From the result obtained above, we can build a model of block movements in Bôsô Peninsula. Figs. 8 and 9 show the elevations of the model of block movements along the sections *AB* and *CD* of Fig. 7, the scales for the vertical movements and tiltings being much enlarged.

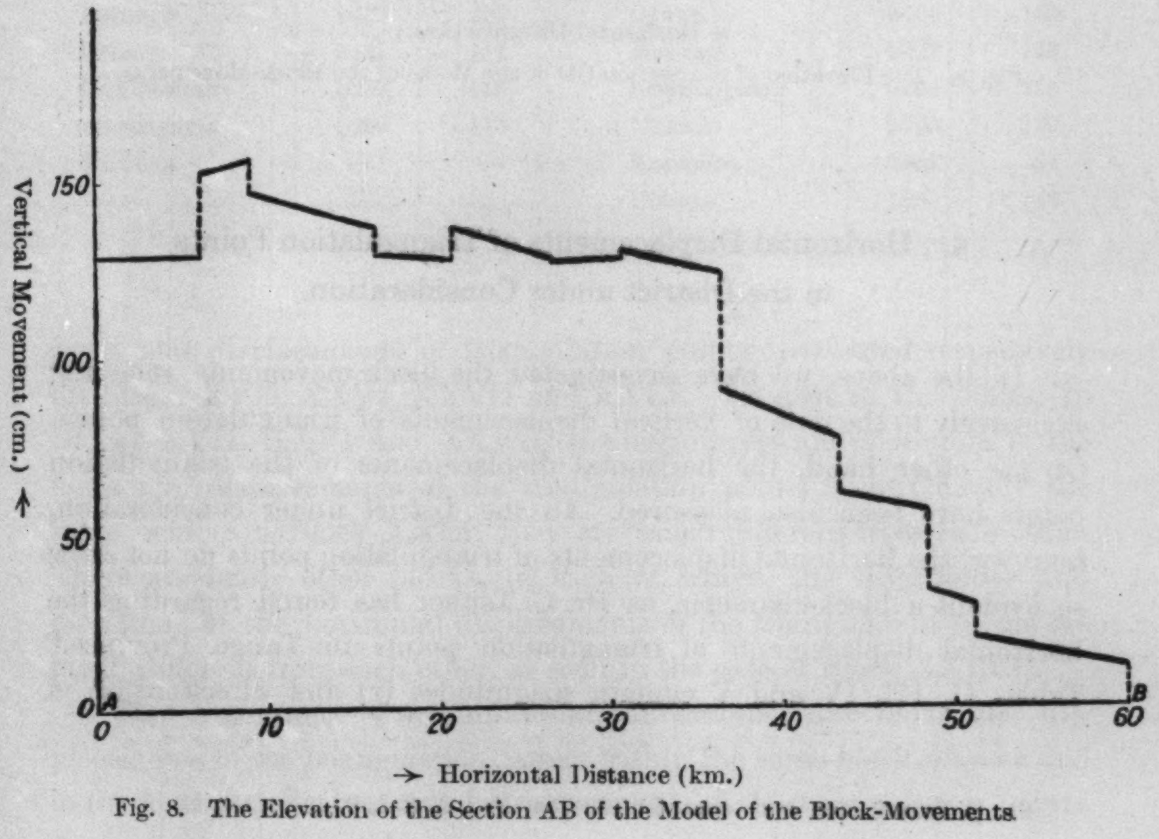

Fig. 8. The Elevation of the Section AB of the Model of the Block-Movements.

are measured relative to certain fixed points,7) while the block might be deformed in itself. We consider, for simplicity's sake, the case that there is no horizontal deformation in the block. In this case, horizontal displacements of the triangulation points in the block may be the same in both magnitudes and directions, if the horizontal movement of the block was purely translational relative to the fixed points. When, however, the block was rotated about a vertical axis, magnitudes and directions of the horizontal displacements of the triangulation points are expected to be much different from each other. Fig. 10 shows a plan of an ideal case in

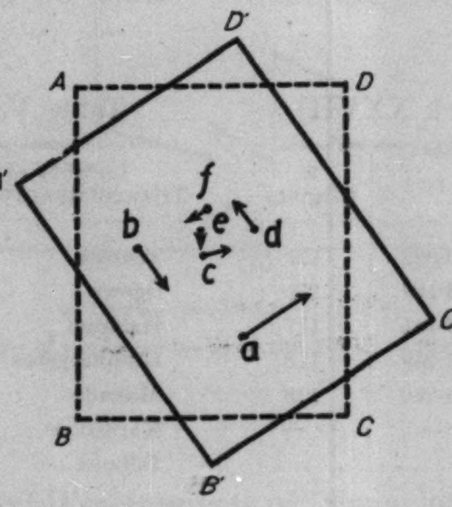

Fig. 10.

which the position of a rectangular block *ABCD* (dotted) has changed its position to *A' B' C' D'* (full), after a block movement. The points ***a***, ***b***, ***c***, ***d***, ***e*** and *f* on the block are found to have moved in the directions of respective arrows, the lengths of which denote the magnitudes of the horizontal displacements of the points.

---

7) On calculating the present data of horizontal displacements of triangulation points in Kwantô District, 6 primary triangulation points were taken as fixed, which are situated in the outermost zone, surrounding the district, where the triangulation points with their horizontal displacements measured are distributed.

As a matter of fact, we notice a similar phenomenon near Rokudizô, one of the fixed primary triangulation points. Fig. 11 shows the horizontal displacements of triangulation points in the neighbourhood of Rokudizô.

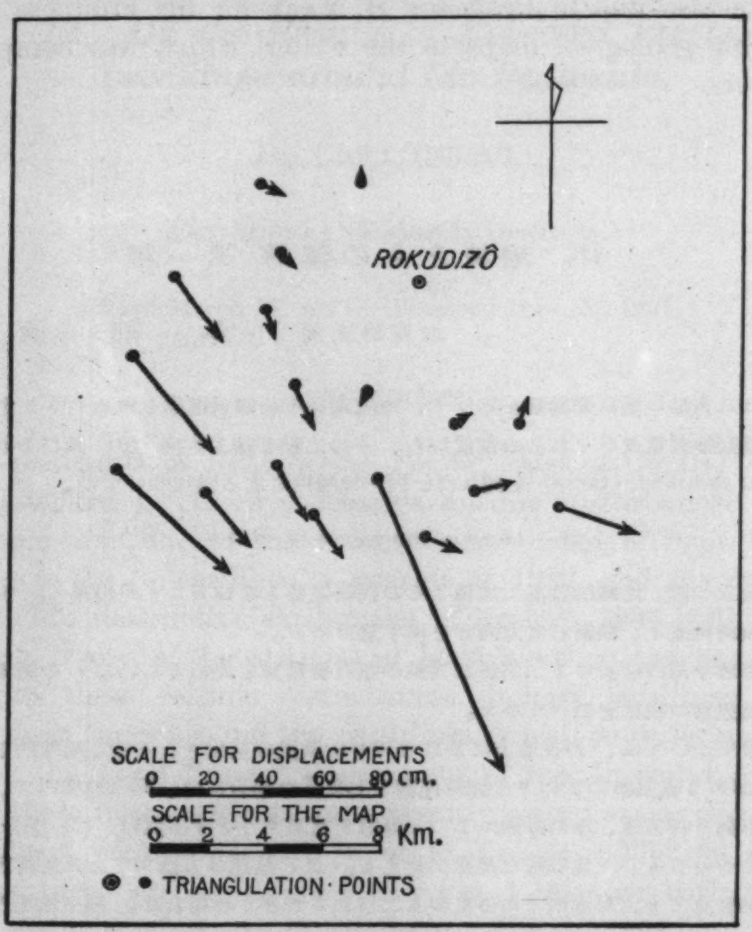

Fig. 11. Horizontal Displacements of Triangulation Points in the Neighbourhood of Rokudizô.

Thus we cannot say that the triangulation points are not on a single block by the mere fact that the magnitudes and directions of their horizontal displacements are much different from each other. Hence, the horizontal displacements of triangulation points are not convenient for determining the forms and extents of constituent blocks in the earth's crust, at least in our present case.

As for the horizontal deformation of each constituent block, the investigation is reserved for a future communication.

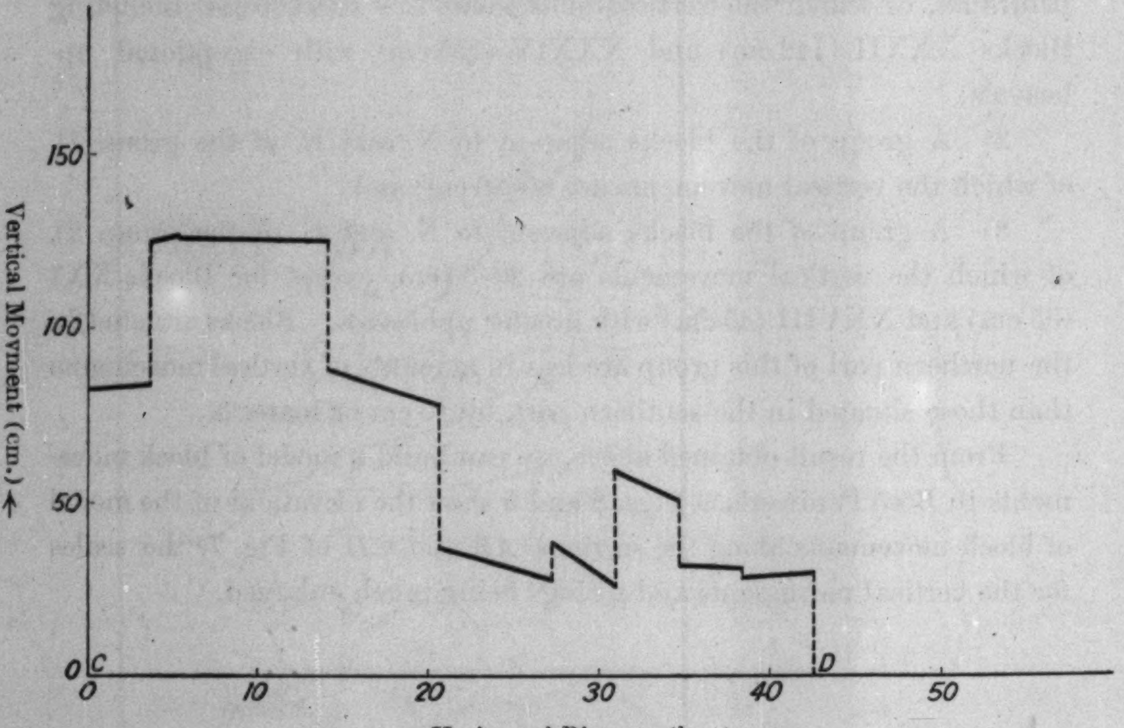

Fig. 9. The Elevation of the Section CD of the Model of the Block-Movements.

4. Horizontal Displacements of Triangulation Points in the District under Consideration.

In the above, we have investigated the block movements referring exclusively to the data of vertical displacements of triangulation points. On the other hand, the horizontal displacements of the triangulation points have been also measured. In the district under consideration, however, the horizontal displacements of triangulation points do not show so evident a block-character, as Dr. C. Tsuboi has found regarding the horizontal displacements of triangulation points in Tango Province.[6] Tables II, III, IV and V contain magnitudes (r) and directions (λ) of

---

[6] C. Tsuboi, *Proc. Imp. Acad.*, 6 (1930), 56; *Bull. E. R. I.*, 8 (1930), 153.

Table II. (Block XVII)

Locality of Triangulation Points	$r\,(m)$	λ (degree)
Narikawa	1·320	128
Komatimine	1·358	124
Higasikuti	1·270	128
Uenohara	1·310	129
Terakado	1·407	132
Toyooka	1·447	138

Table III. (Block XXVI)

Locality of Triangulation Points	$r\,(m)$	λ (degree)
Izumi	1·301	119
Motokiyosumi	1·434	118
Utizumi	1·398	117
Simidu	1·332	119
Kase	1·346	120
Takatenzin	1·258	118
Nisino	1·259	118
Oomi	1·264	121
Suzuri	1·278	124

Table IV. (Block XXVII)

Locality of Triangulation Points	$r\,(m)$	λ (degree)
Asamiduka	1·292	127
Issenzyô	1·127	121
Uehara	1·141	117
Hotokeduka	1·259	118
Sengenyama	1·259	118
Mineoka	—	—

Table V. (Block XXIX)

Locality of Triangulation Points	$r\,(m)$	λ (degree)
Tenmen	0·781	129
Ogawa	0·706	139
Hasiragi	1·422	148
Kaminoyama	0·564	116
Makado	0·790	129
Karasuba	0·981	134
Dôbone	1·230	143

horizontal displacements of triangulation points distributed respectively on Blocks XVII, XXVI, XXVII and XXIX. As seen in the tables, in Blocks XVII, XXVI and XXVII, the magnitudes and directions of the horizontal displacements of the triangulation points approximately the same, while, in Block XXIX, they are much different from each other. There are many other blocks, in each of which, the magnitudes and directions of the horizontal displacements of the triangulation points are much different from each other, as seen in the case of Block XXIX.

This discordance of magnitudes and directions of the horizontal displacements of the triangulation points within the same block may be due to the facts that the horizontal displacements of the triangulation points

In conclusion, the writer wishes to express his sincere thanks to Professor T. TERADA for his kind advices and guidance. The writer's thanks are also due to Professor H. YABE for his kindness in lending the valuable geological maps to the writer, which was compiled by his collaborators.

---

18. 地塊とその運動 第一報

地震研究所 宮部直巳

水準點又は三角點の垂直變動量を知つて、地塊及びその傾斜運動を求めやうとする時に、近接する二點の垂直變動量及びそれらの位置から、その二點を結ぶ方向 (θ) 及びその方向に於ける垂直變動量の gradient ($\tan\phi$) を測れば、同一地塊内に在る點については、

$$\tan\phi = \tan\phi_m \cos(\theta - \theta_m) \qquad (1)$$

なる關係が成立つ故、比較的容易に地塊とその傾斜運動とを知ることが出來る。ϕ_m, θ_m は夫々、その地塊の傾斜角度と、傾斜した方向とを示す量である。

筆者は、房總半島内に於ける二三等三角點の垂直變動量を資料とし、(1) の關係を用ひて、同半島内の地塊運動の模樣を調べてみた。

水平移動量については、丹後地方に於ける坪井助教授の見出された樣な地塊的な模樣は見られない。地塊がある垂直軸のまわりに廻轉運動をした樣な場合には、同一地塊内で、水平移動の大いさも方向も異り得る故、水平移動によつて地塊を定めやうとする試は、この場合不適當である。實際の場合についても、上述の樣な模樣が見える。又、前述の方法で定めた地塊内に於ける三角點の水平移動を見ても、そろつてゐるものも二三あるが多くの場合は、同一地塊内で方向も大いさも著しく異つてゐる。

19. On the Results of Repeated Precise Levellings around Idu Peninsula.

By Chûji **TSUBOI**,

Earthquake Research Institute.

(Read March 17, 1931.—Received June 20, 1931.)

Introduction.

The peninsula of Idu, on the Pacific coast of Central Japan, was recently attacked by three successive seismic disturbances. The first one of them was due to the Kwantô earthquake of Sept. 1, 1923, the second due to the Ito earthquake swarms of 1930, and the third due to the North Idu destructive earthquake of Nov. 26, 1930. With the hope of detecting, if any, of the changes of land levels in the peninsula connected with these seismic disturbances, precise levellings have been repeated three times around the peninsula as well as in its neighbouring regions by the Land Survey Department of the Imperial Army. The results of these measurements were recently placed at our disposal which are the object of the present paper to discuss. The levelling route covered by these surveys is shown in Fig. 1 together with the ordinal numbers of the bench-marks in the route. The first levelling survey was made about 30 years ago, the second one immediately after the occurrence of the Kwantô earthquake of 1923 but before that of the Idu earthquake of 1930, and the third one after the occurrence of the last mentioned earthquake. These three surveys will be referred to in this paper as I, II, and III according as their chronological orders. The changes of heights of the bench-marks on the levelling route as found by means of these levellings are tabulated in the following tables. The changes of heights of the bench marks are graphically shown in Figs. 2, 7, and 10. Generally speaking, the peninsula has been dipping southwards, especially in the interval (III–II). Remarkable changes of heights of bench-marks are found at B.M. 9400 in Fig. 2, B.M. 55.1 in Fig. 7, and B.M. 9337 in Fig. 10. They will be discussed in detail in the following chapters.

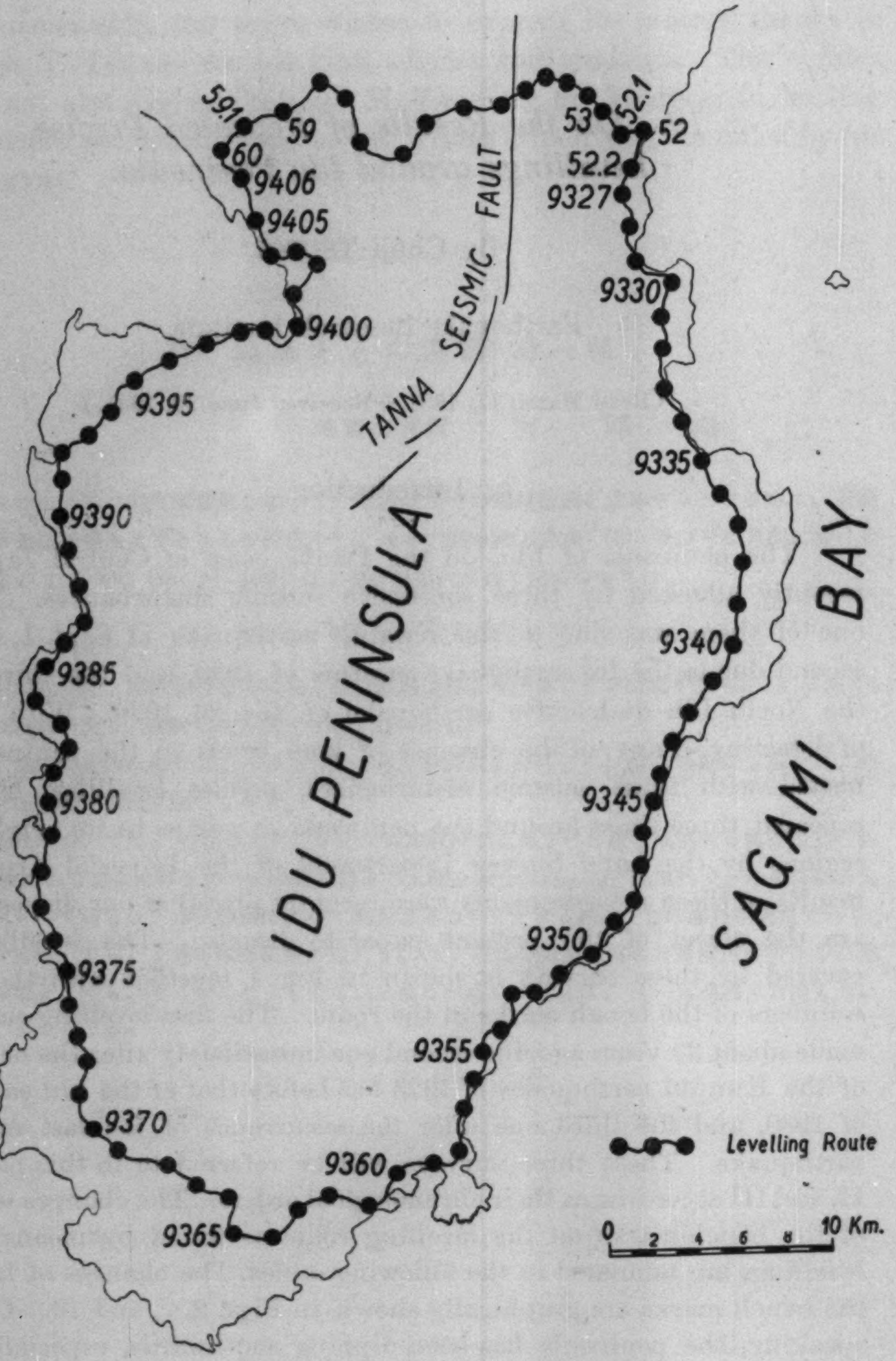
59.1
59
60
9406
9405
9400
9395
9390
9385
9380
9375
9370
9365
9360
9355
9350
9345
9340
9335
9330
9327
52.2
53
52.1
52
TANNA SEISMIC FAULT
SURUGA BAY
IDU PENINSULA
SAGAMI BAY
Levelling Route
0 2 4 6 8 10 Km.

Fig. 1.
Levelling Route Around and Across Idu Peninsula.

Table I.

Change of Heights along the Western Coast of the Peninsula.

B. M.		I	II–I	II	III–II	III
			mm		mm	
60	Numadu	1903	− 84·3	1924	+ 17·0	Dec. 21, 25, 1930
9406		"	− 91·9	"	+ 14·2	" 20, 21
9405	Sisigahama	"	− 89·7	"	+ 20·2	" 20
9404		"	−114·2	1929	+ 27·8	" 18
9403		"	−109·0	"	+ 46·1	" 17, 18
9402		"	−110·1	"	+ 64·3	" 17, 19
9401		"	−106·9	"	+ 64·9	" 11, 12
9400	Mito	"	− 94·4	"	+ 74·6	" 12, 16
9399		"	−104·8	"	+ 61·6	" 14
9398		"	−113·6	"	+ 51·2	" 9, 10
9397	Kou	"	−126·0	"	+ 34·2	" 10, 12
9396		"	−125·7	"	+ 30·8	" 12, 14
9395		"	−101·7	"	+ 21·4	" 14, 18
9394		"	− 98·6	"	+ 19·2	" 20, 26
9393		"	−113·6	"	+ 12·5	" 17, 20
9392	Hata	"	−132·5	"	− 3·0	" 21, 23
9391		"	−114·3	"	+ 4·9	{Dec. 27, 1930, {Jan. 10, 1931
9390		"	−125·1	"	− 1·8	Jan. 4, 1931,
9389		"	−102·2	"	− 3·4	" 2, 4
9388	Tohi	"	−113·7	"	− 12·3	" 5
9387		"	−126·1	"	− 23·0	" 7
9386		"	−102·4	"	− 11·9	" 8, 12
9385	Kosimoda	"	−101·4	"	− 8·8	" 12, 13
9384		"	− 99·2	"	− 8·3	" 14, 15
9383		"	− 96·0	"	− 4·5	" 16, 22
9382	Ukusu	"	− 84·5	"	− 15·7	" 18, 19
9381		"	− 91·6	"	− 14·2	" 18, 22
9380		"	− 88·1	"	− 10·0	" 14, 15
9379		"	− 79·5	"	− 10·4	" 11, 13
9378	Tago	"	− 76·0	"	− 13·3	" 15, 16
9377		"	− 86·6	"	− 14·8	" 17
9376		"	− 80·8	"	− 17·3	" 5
9375		"	−110·3	"	− 19·9	" 2
9374	Matuzaki	"	− 92·5	"	− 20·5	Dec. 28, 31, 1930
9373	Iwasina	"	− 90·8	"	− 22·1	" 28, 31
9372		"	− 83·5	"	− 23·4	Jan. 3, 7, 1931
9371		"	− 72·8	"	− 29·8	Dec. 24, 26, 1930
9370	Zyaisi		− 78·6		− 28·7	

Table II.

Change of Heights across the Tanna Seismic Fault.

B. M.		I	II–I	II	III–II	III
			mm		mm	
52	Atami	1896	+ 43·5	1924	+ 92·1	Dec. 10, 12, 1930
52.1		„	− 40·0	„	+ 89·1	„ 11, 13
53		„	− 6·1	„	+101·4	„ 14, 13
53.1		„	− 39·9	„	+ 94·5	„ 16, 18
54		„	− 48·3	„	−	„ 23, 25
54.1		„	− 55·6	„	+ 47·7	„ 22, 26
55	Karuizawa	„	−	„	−132·8	„ 26, 37
55.1		„	− 80·8	„	−197·8	„ 27, 31
56		„	− 95·5	„	− 52·5	Jan. 3, 1931
56.1	Hirai	„	− 77·9	„	− 7·7	„ 2, 5
57	Daiba	„	− 74·0	„	+ 36·1	„ 2, 5
57.1		„	−125·6	„	− 0·6	„ 2, 5
58		„	−110·1	„	− 10·6	„ 7,
58.1	Misima	„	− 96·4	„	− 6·1	„ 9,
59		„	− 88·6	„	+ 6·5	„ 10, 11
59.1		„	− 80·7	„	+ 19·5	„ 12,
60	Numadu		− 84·3		+ 17·0	

Table III.

Change of Heights along the Eastern Coast of the Peninsula.

B. M.		I	II–I	II	III–II	III
			mm		mm	
52	Atami	1903	+ 43·5	1923	+ 92.1	Dec. 9, 10, 1930
52.2		„	− 25·5	„	+ 72·7	„ 10, 16
9327		„	+ 18·8	„	+ 58·0	„ 12, 15
9328	Kamitaga	„	− 9·6	„	+ 69·0	„ 19, 20
9329		„	− 33·2	„	+ 50·7	„ 19, 20
9330		„	+ 88·0	„	+ 77·6	„ 21, 25
9331		„	+ 57·5	„	+ 93·8	„ 22, 24
9332	Aziro	„	+ 52·0	„	+134·4	„ 26, 27

(*to be continued.*)

Table III. (*continued.*)

B. M.		I	II-I	II	III-II	III
			mm		mm	
9333		1903	+ 31·5	1923	+168·0	Dec. 26, 27
9334		„	–	„	+210·5	„ 26, 27
9335	Itô	„	– 6·8	„	+259·7	Dec. 28, 1930. Jan. 2, 1931.
9336		„	– 9·6	„	+288·3	Dec. 28, 31
9337	Yosida	„	– 29·1	1924	+292·5	„ 30, 31
9338		„	– 44·0	„	+250·8	Jan. 3, 15 1931
9339	Sakihara	„	– 69·4	„	+193·0	„ 3, 15
9340		„	– 63·1	„	+140·7	„ 4, 16
9341	Yawatano	„	– 57·8	„	+ 97·2	„ 4, 13
9342		„	– 51·8	„	+ 68·0	„ 5, 13
9343		„	– 40·7	„	+ 54·3	„ 10, 11
9344	Ookawa	„	– 34·3	„	+ 33·2	„ 17, 18
9345		„	– 33·4	„	+ 30·2	„ 15, 18
9346		„	– 33·4	„	+ 24·7	„ 11, 18
9347	Katase	„	– 33·5	„	+ 16·9	„ 12, 13
9348		„	– 36·1	„	+ 17·2	„ 9, 12
9349	Inatori	„	– 31·5	„	+ 16·8	„ 5, 10
9350		„	– 24·4	„	+ 11·1	Dec. 30, 31, 1930
9351		„	– 26·5	„	+ 11·0	{Dec. 28, 1930, Jan. 2, 1931
9352		„	– 25·6	„	+ 3·9	Dec. 27, 28, 1930
9353	Kôduhama	„	– 36·4	„	+ 0·6	Dec. 26, 27, 1930
9354		„	– 42·3	„	+ 4·5	„ 23, 26
9355		„	– 35·8	„	+ 2·1	„ 19, 22
9356		„	– 32·4	„	+ 0·5	„ 16, 17
9357	Sirahama	„	– 37·1	„	– 2·8	„ 14, 15
9358		„	– 47·0	„	– 0·3	„ 11, 13
9359	Simoda	„	–	„	– 5·7	„ 10
9360		„	– 47·4	1929	– 5·1	„ 10, 12
9361		„	– 46·9	„	– 10·0	„ 12
9362		„	– 48·6	„	– 12·3	„ 13
9363	Simogamo	„	– 61·1	„	– 17·5	„ 15
9364		„	– 61·6	„	– 17·9	„ 16, 18
9365		„	– 67·9	„	– 21·9	„ 17
9366		„	– 61·7	„	– 21·9	„ 18
9367	Simoono	„	– 63·3	„	– 20·6	„ 20
9368		„	– 64·4	„	– 20·8	„ 20, 21
9369		„	– 69·2	„	– 30·0	„ 22, 23
9370	Zyaisi		– 78·6		– 28·7	

The Results of the Levelling along the Western Coast of Idu Peninsula.[1]

The changes of heights of the bench-marks along the western coast of the peninsula are shown in Fig. 2. The curve (II–I) shows the changes in the interval between II and I, while the curve (III–II) those in the interval between III and II. The former changes are to be regarded as mainly due to the effect of the earthquake of 1923 and the latter ones to that of the earthquake of 1930. If we compare these two curves, we find that a number of segments or portions such as A, B, C, D, and E that are quite similar in their forms for both curves are commonly involved in them. For the segment B, the form of the curve is very much characteristic. The levelling route from B.M. 9404 to B.M. 9396 corresponding to the segment B is not straight but goes winding as may be seen in Fig. 1, thus the peculiar form of the curves of Fig. 2 corresponding to the segment B may be produced purely as a geometrical effect even if the land

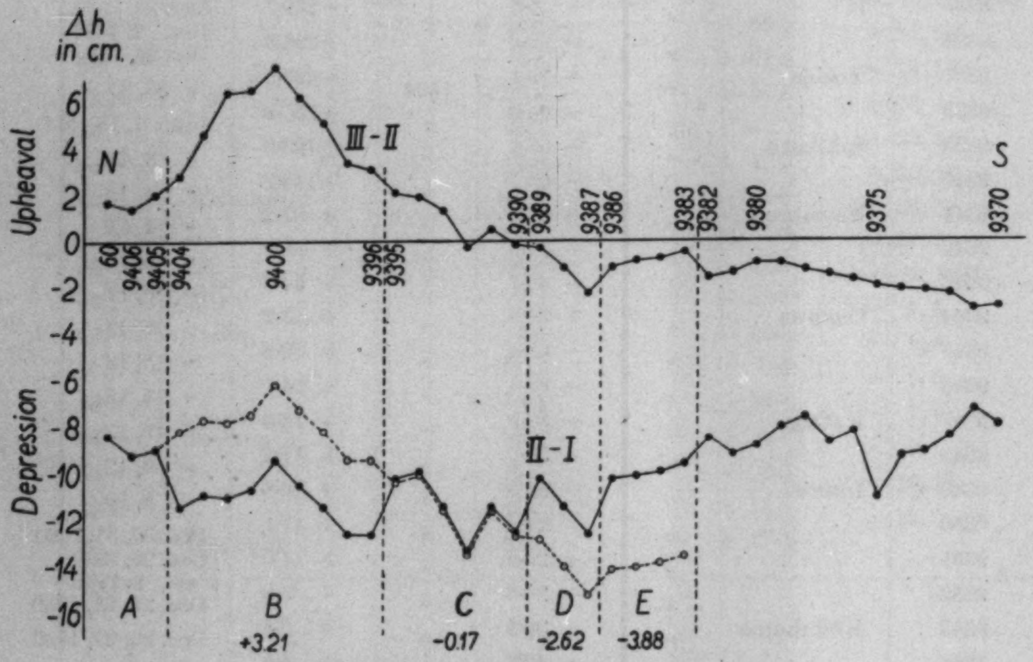

Change of Level along the Western Coast of Idu Peninsula

Fig. 2.

---

[1] C. TSUBOI, *Proc. Imp. Acad.*, 7 (1931), 158.

between B.M. 9404 and B.M. 9396 is subjected to a single tilting as a whole. For the purpose of determining whether this is actually the case or not, the method due to my colleage Mr. N. Miyabe[2] is exclusively effective. If the land between B.M. 9404 and B.M. 9396 is assumed to have undergone a single tilting, then the difference of changes in heights of any two points lying on this land whose distance is of a unit length, must be a sinusoidal function of the directional azimuth of the line connecting these two points with respect to a definite reference direction, say E. The difference per unit distance of changes in heights in different azimuths may be obtained by dividing the difference of changes of heights of any two of the bench-marks between B.M. 9404 and B.M. 9396 by the distance between these marks. In Table IV will be given these quotients obtained for (II–I) and (III–II) together with the corresponding azimuths, distances, and differences in height changes.

---

[2] N. Miyabe, *Proc. Imp. Acad.*, 7 (1931), 150.

Table IV.

Section B. Bench-Marks 9396; 9397; 9398; 9399; 9400; 9401; 9402; 9403: 9404.

Azimuth

To From	9396	9397	9398	9399	9400	9401	9402	9403	9404
9396	–	+25°	+23°	+15°	+12°	+27°	+32°	+ 41°	+ 46°
9397	−155°	–	+22°	+ 9°	+ 7°	+27°	+33°	+ 45°	+ 53°
9398	−157°	−158°	–	− 4°	− 1°	+30°	+37°	+ 53°	+ 64°
9399	−165°	−171°	+176°	–	+ 2°	+55°	+53°	+ 71°	+ 87°
9400	−168°	−173°	−179°	−178°	–	+94°	+72°	+ 90°	+107°
9401	−153°	−153°	−150°	−125°	− 86°	–	+50°	+ 88°	+117°
9402	−148°	−147°	−143°	−127°	−108°	−130°	–	+139°	+162°
9403	−139°	−135°	−127°	−109°	− 90°	− 92°	−41°	–	−169°
9404	−134°	−127°	− 16°	− 93°	− 73°	− 63°	−18°	+ 11°	–

Distance in km.

To From	9396	9397	9398	9399	9400	9401	9402	9403	9404
9396	–	1·65	3·10	4·45	5·65	6·10	7·70	7·25	6·40
9397	1·65	–	1·50	2·85	4·05	4·40	5·90	5·70	4·90
9398	3·10	1·50	–	1·45	2·70	3·00	4·45	4·35	3·70
9399	4·45	2·85	1·45	–	1·25	1·95	3·50	3·75	3·40
9400	5·65	4·05	2·70	1·25	–	1·55	2·85	3·50	3·50
9401	6·10	4·40	3·00	1·95	1·55	–	1·50	1·95	2·00
9402	7·70	5·90	4·45	3·50	2·85	1·50	–	1·20	2·00
9403	7·25	5·70	4·35	3·75	3·50	1·95	1·20	–	2·00
9404	6·40	4·90	3·70	3·40	3·50	2·00	2·00	2·00	–

Difference of Change of Height for (II-I) in mm.

To From	9396	9397	9398	9399	9400	9401	9402	9403	9404
9396	–	+ 0·3	+12·1	+20·9	+31·3	+18·8	+15·6	+16·7	+11·5
9397	− 0·3	–	+12·4	+21·2	+31·6	+19·1	+15·9	+17·0	+11·8
9398	−12·1	−12·4	–	+ 8·8	+19·2	+ 6·7	+ 3·5	+ 4·6	− 0·6
9399	−20·9	−21·2	− 8·8	–	+10·4	− 2·1	− 7·3	− 4·2	− 9·4
9400	−31·3	−31·6	−19·2	−10·4	–	−12·5	−15·7	−14·6	−19·8
9401	−18·8	−19·1	− 6·7	+ 2·1	+12·5	–	− 3·2	− 2·1	− 7·3
9402	−15·6	−15·9	− 3·5	+ 7·3	+15·7	+ 3·2	–	+ 1·1	− 4·1
9403	−16·7	−17·0	− 4·6	+ 4·2	+14·6	+ 2·1	− 1·1	–	− 5·2
9404	−11·5	−11·8	+ 0·6	+ 9·4	+19·8	+ 7·3	+ 4·1	+ 5·2	–

Table IV.

Inclination for (II-I) in 10^{-6}

From \ To	9396	9397	9398	9399	9400	9401	9402	9403	9404
9396	–	+0·2	+3·9	+4·7	+5·5	+3·1	+2·0	+2·3	+1·8
9397	−0·2	–	+8·3	+7·4	+7·8	+4·3	+2·7	+3·0	+2·4
9398	−3·9	−8·3	–	+6·1	+7·1	+2·2	+0·8	+1·1	−0·2
9399	−4·7	−7·4	−6·1	–	+8·3	−1·1	−2·1	−1·1	−2·8
9400	−5·5	−7·8	−7·1	−8·3	–	−8·1	−5·5	−4·2	−5·7
9401	−3·1	−4·3	−2·2	+1·1	+8·1	–	−2·1	−1·1	−3·7
9402	−2·0	−2·7	−0·8	+2·1	+5·5	+2·1	–	+0·9	−2·1
9403	−2·3	−3·0	−1·1	+1·1	+4·2	+1·1	−0·9	–	−2·6
9404	−1·8	−2·4	+0·2	+2·8	+5·7	+3·7	+2·1	+2·6	–

Difference of Change of Height for (III-II) in mm.

From \ To	9396	9397	9398	9399	9400	9401	9402	9403	9404
9396	–	+ 3·4	+20·4	+30·8	+43·8	+34·1	+33·5	+15·3	− 3·0
9397	− 3·4	–	+17·0	+27·4	+40·4	+30·7	+30·1	+11·9	− 6·4
9398	−20·4	−17·0	–	+10·4	+23·4	+13·7	+13·1	− 5·1	−23·4
9399	−30·8	−27·4	−10·4	–	+13·0	+ 3·3	+ 2·7	−15·5	−33·8
9400	−43·8	−40·4	−23·4	−13·0	–	− 9·7	−10·3	−18·5	−46·8
9401	−34·1	−30·7	−13·7	− 3·3	+ 9·7	–	− 0·6	−18·8	−17·1
9402	−33·5	−30·1	−13·1	− 2·7	+10·3	+ 0·6	–	−18·2	−36·5
9403	−15·3	−11·9	+ 5·1	+15·5	+18·5	+18·8	+18·2	–	−18·3
9404	+ 3·0	+ 6·4	+23·4	+33·8	+46·8	+17·1	+36·5	+18·3	–

Inclination for (III-II) in 10^{-6}

From \ To	9396	9397	9398	9399	9400	9401	9402	9403	9404
9396	–	+ 2·0	+ 6·6	+ 7·0	+ 7·8	+ 5·6	+ 4·4	+ 2·2	− 0·4
9397	− 2·0	–	+11·4	+ 9·6	+10·0	+ 7·0	+ 5·0	+ 2·0	− 1·4
9398	− 6·6	−11·4	–	+ 7·2	+ 8·6	+ 4·6	+ 3·0	− 1·2	− 6·4
9399	− 7·0	− 9·6	− 7·2	–	+10·4	+ 1·6	+ 0·8	− 4·2	−10·0
9400	− 7·8	−10·0	− 8·6	−10·4	–	− 6·0	− 3·6	− 5·2	−13·4
9401	− 5·6	− 7·0	− 4·6	− 1·6	+ 6·0	–	− 0·4	− 9·6	− 8·6
9402	− 4·4	− 5·0	− 3·0	− 0·8	+ 3·6	+ 0·4	–	−15·2	−18·2
9403	− 2·2	− 2·0	+ 1·2	+ 4·2	+ 5·2	+ 9·6	+15·2	–	− 9·2
9404	+ 0·4	+ 1·4	+ 6·4	+10·0	+13·4	+ 8·6	+18·2	+ 9·2	–

The results given in Table IV are shown graphically in Figs. 3 and 4. As a matter of fact, the points in the figures are distributed approximately on a sine-curve whose equations are

$$y = 1.''8 \sin (50^\circ - \alpha) \qquad \text{for (II—I)}$$
$$y = 3.''5 \sin (50^\circ - \alpha) \qquad \text{for (III—II)}$$

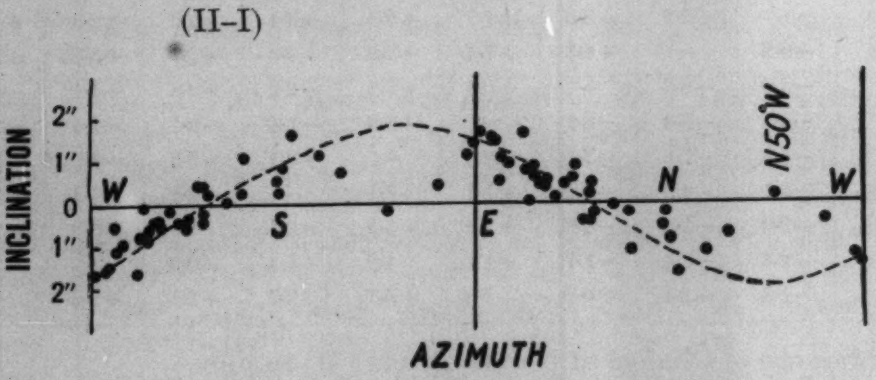

Fig. 3.

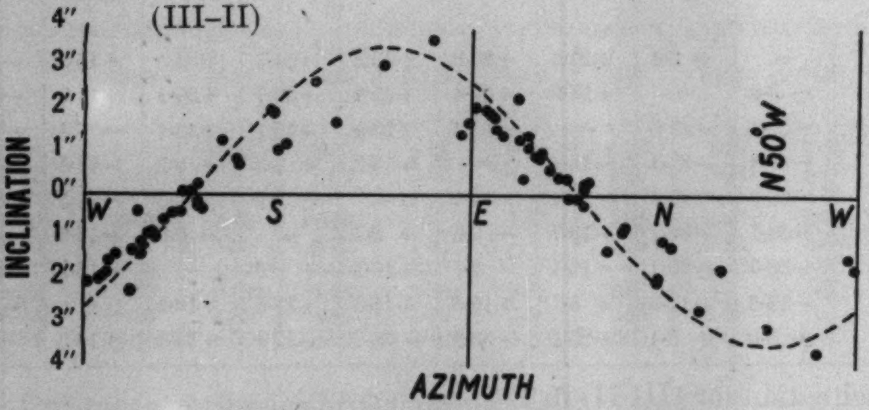

Fig. 4.

This is evidently a proof that the land between B.M. 9404 and B.M. 9396 underwent for both intervals (II—I) and (III—II), a tilting as a whole making a movement what we call a block movement. The tilting was evidently down towards N 50°W for both cases and it was about 2″ and 3.5″ in its amount for the former and latter intervals respectively. It is interesting that the directions of the tiltings were just the same for both of the intervals. For other sections of the levelling routes, such as A, C, D, and E, the tiltings were similarly calculated. The results of these calculations are summarised in Tables V, VI, VII, VIII and some of them are graphically shown in Figs. 5 and 6.

Table V.

Section A. Bench Marks, 60 ; 9405 ; 9406.

Azimuth

From \ To	9405	9406	60
9405	−	111°	116°
9406	−69°	−	122°
60	−64°	−58°	−

Inclination for (II-I) in 10^{-6}

From \ To	9405	9406	60
9405	−	− 1·2	+ 1·5
9406	+ 1·2	−	+ 4·8
60	− 1·5	− 4·8	−

Direction of Tilting: N 70° E

Magnitude of Tilting: 4″

Inclination for (III-II) in 10^{-6}

From \ To	9405	9406	60
9405	−	− 3·2	− 0·9
9406	+ 3·2	−	+ 1·8
60	+ 0·9	− 1·8	−

Direction of Tilting: N 60° E

Magnitude of Tilting: 4″

Table VI.

Section C. Bench Marks, 9390 ; 9391 ; 9392 ; 9393 ; 9394 ; 9395.

Azimuth

From \ To	9390	9391	9392	9393	9394	9395
9390	−	84°	89°	66°	60°	59°
9391	− 96°	−	95°	54°	50°	51°
9392	− 91°	− 85°	−	26°	33°	41°
9393	−114°	−126°	−154°	−	43°	50°
9394	−120°	−130°	−147°	−137°	−	55°
9395	−121°	−129°	−139°	−130°	−125°	−

Table VI.

Inclination for (II-I) in 10^{-6}

To From	9390	9391	9392	9393	9394	9395
9390	−	+ 6·8	− 2·6	+ 2·9	+ 5·1	+ 3·4
9391	− 6·8	−	− 14·6	+ 0·3	+ 4·2	+ 2·3
9392	+ 2·6	+14·6	−	+ 9·5	+10·9	+ 6·4
9393	− 2·9	− 0·3	− 9·5	−	+10·7	+ 3·8
9394	− 5·1	− 4·2	−10·9	−10·7	−	− 1·7
9395	− 3·4	− 2·3	− 6·4	− 3·8	+ 1·7	−

Direction of Tilting N 60° W, Magnitude of Tilting 4·5″

Inclination for (III-II) in 10^{-6}

To From	9390	9391	9392	9393	9394	9395
9390	−	+ 4·2	− 0·4	+ 3·6	+ 4·0	+ 3·3
9391	− 4·2	−	− 6·3	+ 3·1	+ 3·6	+ 2·9
9392	+ 0·4	+ 6·3	−	+ 7·9	+ 7·2	+ 5·1
9393	− 3·6	− 3·1	− 7·9	−	+ 4·8	+ 2·8
9394	− 4·0	− 3·6	− 7·2	− 4·8	−	+ 1·2
9395	− 3·3	− 2·9	− 5·1	− 2·8	− 1·2	−

Direction of Tilting N 70° W, Magnitude of Tilting 2.″5

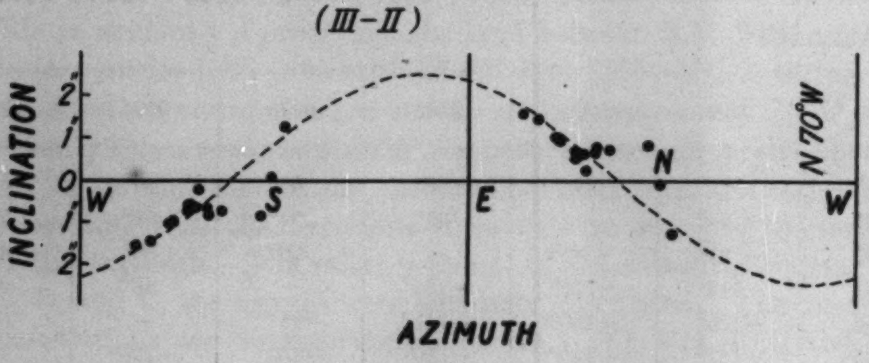

Fig. 5.

Table VII.

Section D. Bench Marks, 9389 ; 9388 ; 9387.

Azimuth

To From	9389	9388	9387
9389	−	−74°	−77°
9388	106°	−	−81°
9387	103°	99°	−

Inclination for (II-I) in 10^{-6}

To From	9389	9388	9387
9389	−	−7·2	−7·6
9388	+7·2	−	−7·8
9387	+7·6	+7·8	−

Direction of Tilting: S 20° W

Magnitude of Tilting: 2″

Inclination for (III-II) in 10^{-6}

To From	9389	9388	9387
9389	−	−5·6	−6·2
9388	+5·6	−	−6·7
9387	+6·2	+6·7	−

Direction of Tilting: S 40° W

Magnitude of Tilting: 2″

Table VIII.

Section E. Bench Marks, 9386 ; 9385 ; 9384 ; 9383.

Azimuth

To From	9386	9385	9384	9383
9386	−	−132°	−120°	− 96°
9385	48°	−	−109°	− 77°
9384	60°	71°	−	− 46°
9383	84°	103°	134°	−

Table VIII.

Inclintion for (II-I) in 10^{-6}

From \ To	9386	9385	9384	9383
9386	–	+ 0·7	+ 1·1	+ 1·8
9385	– 0·7	–	+ 1·4	+ 2·1
9384	– 1·1	– 1·4	–	+ 2·1
9383	– 1·8	– 2·1	– 2·1	–

Direction of Tilting: N 30° W
Magnitude of Tilting : 0·″4

(II–I)

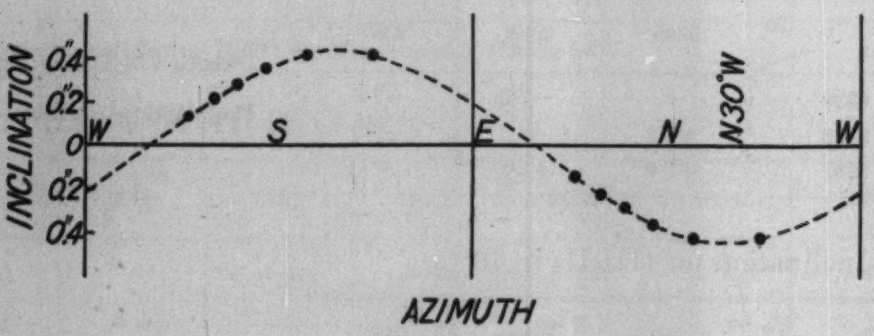

Fig. 6.

Inclination for (III-II) in 10^{-6}

From \ To	9386	9385	9384	9383
9386	–	+ 2·1	+ 1·2	+ 2·0
9385	– 2·1	–	+ 0·3	+ 1·7
9384	– 1·2	– 0·3	–	+ 2·5
9383	– 2·0	– 1·7	– 2·5	–

Direction of Tilting N 30° W
Magnitude of Tilting 0.″5

We have now determined the extents of land blocks which respectively underwent a tilting as a whole. We can find another evidence of the existence of such more or less rigid land blocks in the results of the repeated levellings here. If we displace in Fig. 2, the sections B, C, D, and E in the lower curve (II—I) along the vertical axis by 3·21 cm., –0·17 cm., –2·62 cm., and –3·88 cm. respectively, we have the curve in Fig. 2 that is shown in dotted lines. The curve obtained in this way is evidently similar to the upper curve (III—II) in its form. Thus it is concluded that these land blocks were subjected to independent vertical movements simultaneously with the tilting movements. The facimile of such movements may be visualised by an aggregate of wooden blocks floating side by side on a disturbing water surface. From B.M. 9382 south down, no evidence of block movements is apparent and this is rather a striking contrast with the structure of the northern part of the levelling route, on which the evidence of block movements is so pronounced.

Results of the Levelling across the Tanna Seismic Faults.

The change of land levels along this route is shown in Fig. 7. At the time of the earthquake of Nov. 26, 1930, a system of remarkable seismic faults was produced in the northern part of the peninsula in approximately NS trend. The fault was about 30 km. in length and crossed the levelling route from B.M. 52 to B.M. 60 between the bench-marks 55 and 55.1. The land to the east of the fault was displaced northwards relative to the land to the west of it, the amount of the dislocation being about 100 cm. as measured on the surface of the ground. The new seismic fault was right along the well-known Tanna tectonic line. The vertical movement along the recent seismic fault was not simple but of a type of a hinge, the western block, relative to the eastern one being depressed at the northern part of the fault whereas elevated at the southern part. The movement in the neighbourhood of the fault was, so far as the levelling is concerned, of a V-shaped depression. It is to be noted that a movement somewhat similar to the recent one may be found in the neighbourhood of the fault in the interval between the first and second levellings which includes in it the event of the Kwantô earthquake of 1923. Prof. A. Imamura has long emphasised

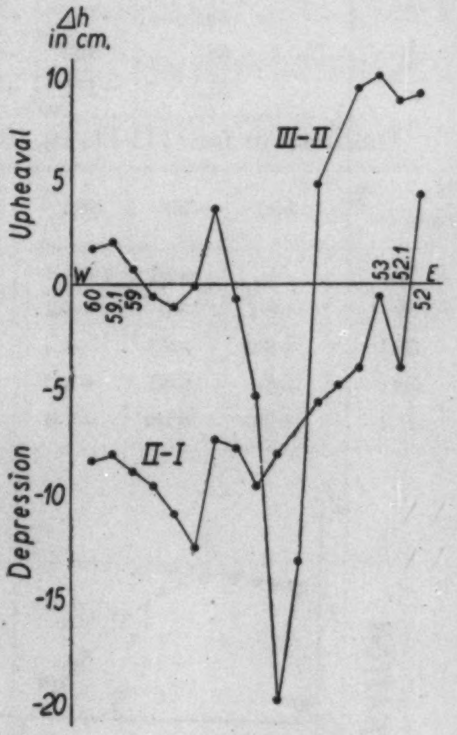

Fig. 7.
Change of Level across the Tanna Seismie Fault

that there are at least two types in the movement at a fault found by means of levelling, the one he called N-type, and the other V-type, according to the similarity in forms of the profile of the change of land levels to these characters. The present case for the Tanna fault may correspond to the category of V-type. In this route, the tilting of land blocks were also determined similarly as in the preceding chapter. The

Table IX.

Bench Marks 59.1 ; 59 ; 58.1 ; 58 ; 57.1 ;

Azimnth

From \ To	59.1	59	58.1	58	57.1
59.1	–	20°	29°	13°	−9°
59	−160°	–	40°	8°	−23°
58.1	−151°	−120°	–	−35°	--55°
58	−167°	−172°	145°	–	−69°
57.1	−171°	+157°	125°	111°	–

Inclination for (III-II) in 10^{-6}

From \ To	59.1	59	58.1	58	57.1
59.1	–	−6·1	−6·2	−6·1	−3·6
59	+6·1	–	−6·3	−6·1	−1·9
58.1	+6·2	+6·3	–	−3·0	+1·6
58	+6·1	+6·1	+3·0	–	+2·4
57.1	+3·6	+1·9	−1·6	−2·4	–

Direction of Tilting N 50° E

Magnitude of Tilting 1.″5

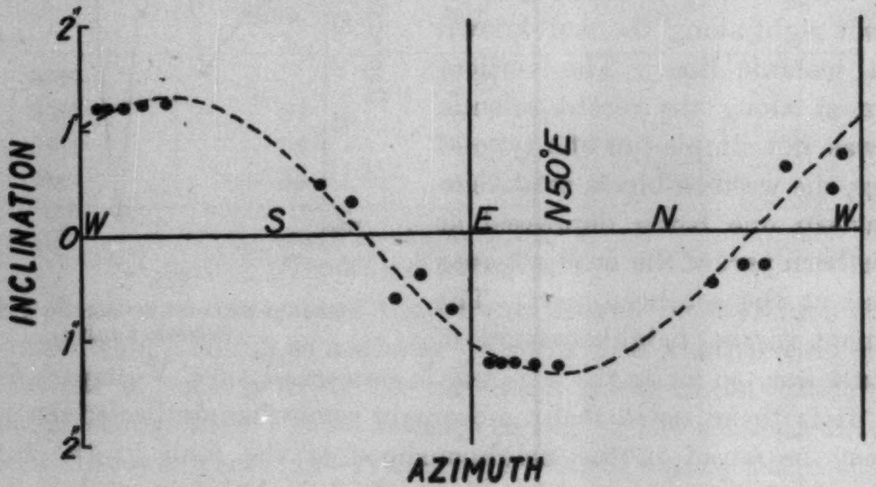

Fig. 8.

Table X.

Bench-Marks 57 ; 56.1 ; 56 ; 55.1.

Azimuth

From \ To	57	56.1	56	55.1
57	–	47°	36°	30°
56.1	−133°	–	23°	21°
56	−144°	−157°	–	18°
55.1	−150°	−159°	−162°	–

Inclination for (III-II) in 10^{-6}

From \ To	57	56.1	56	55.1
57	–	−24·4	−25·3	−45 4
56.1	+24·4	–	−27·1	−54·4
56	+25·3	+27·1	–	−78·6
55.1	+45·4	+54·4	+78·6	–

Direction of Tilting S 50° E

Magnitude of Tilting 28″

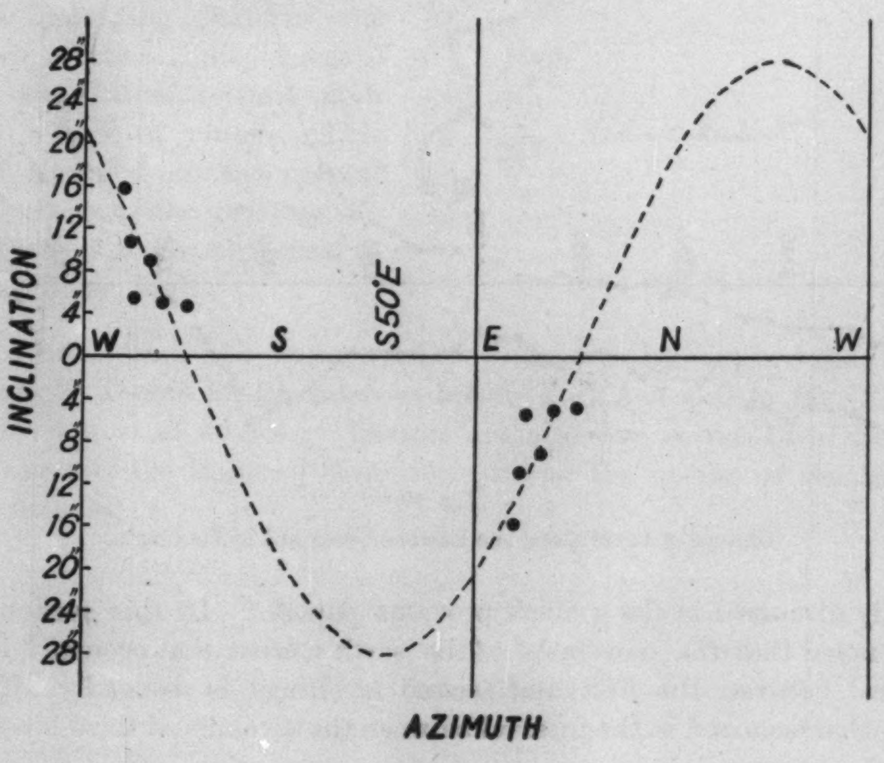

Fig. 9.

results of the calculations are shown in Tables IX and X. The results of these calculations are shown in Figs. 8 and 9.

The Results along the Eastern Coast of the Peninsula.

The change of land levels along the eastern coast of the peninsula is shown in Fig. 10. The results of the levellings along this route were

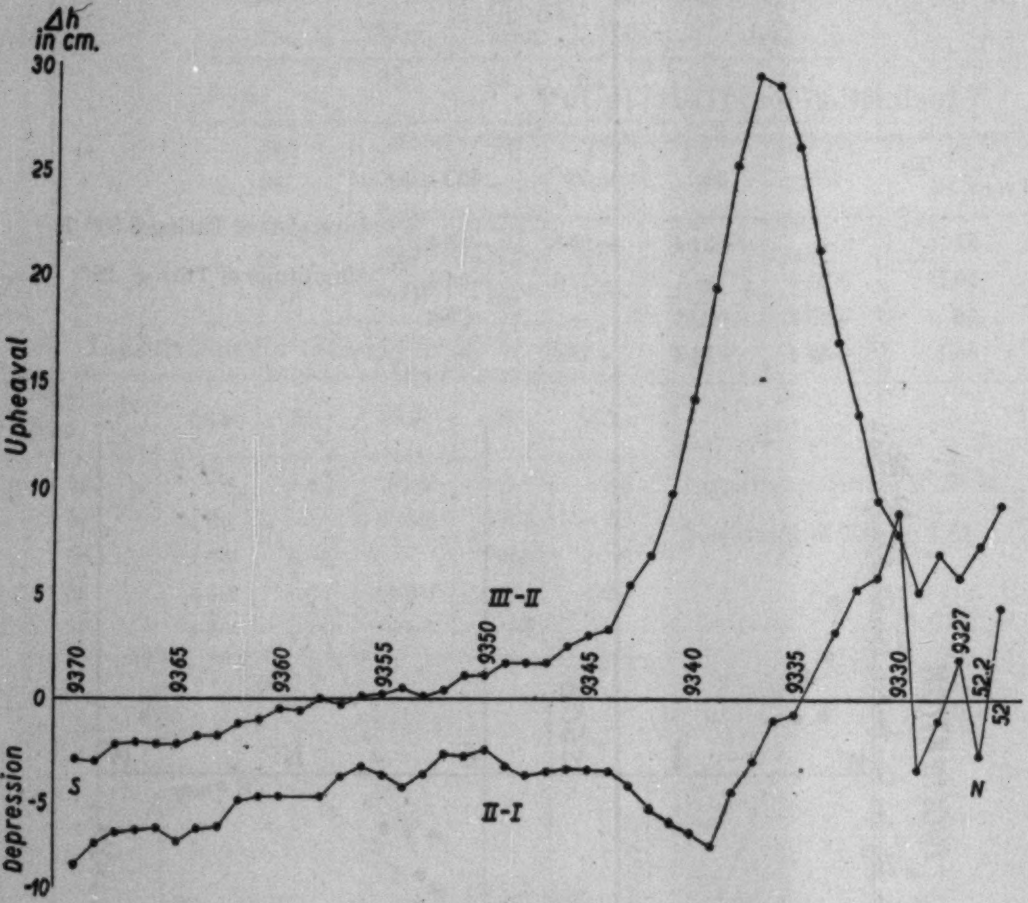

Fig. 10.

Change of Level along the Eastern Coast of Idu Peninsula.

already discussed in the writer's previous papers.[3] In this section it is to be noted that the movement of the earth's crust that occurred in the interval between the first and second levellings is decidedly different from what occurred in the interval between the second and third levellings.

---

[3] C. TSUBOI, *Proc. Imp. Acad.*, 7 (1931), 153; *Bull. Earthq. Res Inst.*, 9 (1931), 151.

Idu Earthquake of 1930 and Tilting of Land Blocks.

The writer has often pointed out[4] the block-structure of the outer part of the earth's crust especially in earthquake districts. These individual land blocks seem to move apparently independently, yet their movements must be in some order when viewed as a whole. We have here a good example of such a case. We have determined the directions and magnitudes of tilting of land blocks in the northwestern part of the peninsula. They are shown by arrows in Fig. 11. A remarkable feature is at once apparent that the arrows change the directions clockwise as we go from the southern blocks to the northern. This shows that the land as a whole was twisted like a plate. As was described in one of the preceding chapters, the relative vertical displacement along the Tanna seismic fault was of a type of a hinge. This can be regarded now as a natural consequence of the twisting deformation of the earth's crust to the west of the fault.

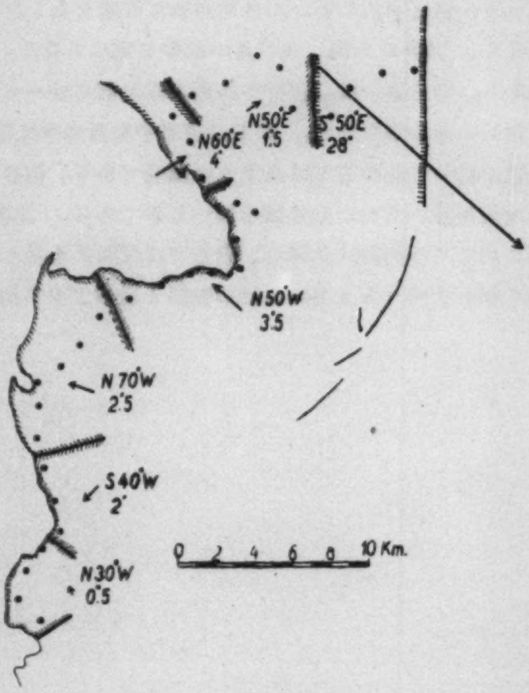

Fig. 11.

In conclusion the writer wishes to express his sincere thanks to Professor T. Terada for his interests in this work and also to Mr. N. Miyabe for his kind advices. Thanks are also due to the Land Survey Department of the Imperial Army for placing the results of the survey at our disposal.

---

[4] C. Tsuboi. *Bull. Earthq, Res. Inst.*, 6 (1929), 71; 7 (1929), 103; 8 (1930), 153; *Proc. Imp. Acad.*, 4 (1928), 529.

19. 伊豆半島に於ける水準測量の結果に就いて

地震研究所　坪井忠二

伊豆半島の周圍に沿つた水準測量は既に三度も繰返されたが、此の論文は夫等の結果に就いて若干の考案を加へたものである。特に昭和五年十一月二十六日の北伊豆地震によつて生じたと信ぜらるゝ垂直變動に就いては稍詳細に吟味をなした。宮部理學士が考案した方法に從つて地塊の大きさ、傾斜の方向、及び其の量等を定めて見た。その内稍大切な結果と思はれるのは次の二點である。即ち第一は、伊豆半島西海岸北部に於いては地塊構造が著しいが、南部には之が認められないと云ふ事である。第二は伊豆半島西海岸北部に於ける地塊を全體から大きい目で見ると、大體に於いて北の方では東下りの傾斜であり、南の方では西下りの傾斜であつて、宛も此の近傍の地殼が捩れたかの如き觀を與へる事である。北伊豆地震に關聯した丹那斷層は、北方では西が東に對して相對的に沈降し、南方では反對に上昇してゐると報ぜられたが、之も斷層の西側の地殼の捩れを考へると其の自然の結果と看做す事が出來る。

20. *Movement of the Ground due to Atmospheric Disturbance in a Sea Region.*

By **Katsutada SEZAWA** and **Genrokuro NISHIMURA**,

Earthquake Research Institute.

(Read April 21, 1931.—Received June 20, 1931.)

1. In a previous paper[1] one of us studied some problem of the transmission of seismic waves on the bottom surface of an ocean and it was found that the problem is of a great importance in connection with the dispersive nature of distant earthquakes. It occurred us very recently that the problem, if somewhat extended, may also be significant on the pulsatory motion of the ground occurring in disturbed weather in a sea region. Geophysical investigations of microseisms have already been made fully by Prof. Gutenberg,[2] [3] Dr. Banerji[4] and others, chiefly by examining the data of the actual seismic records. It seems, however, that the accurate mathematical study concerning microseisms has not yet been made probably on account of the reason that the action of the water waves on the ground and on the steep coast is of a complex nature. Although it has already been concluded by Professor Gutenberg and others that the cause of the microseisms is the action of the surf against steep coasts but not the direct action of the wind pressure or of the water upon the bottom ground, yet we are now to study the problem of the movement of the ground due to the disturbed sea in rough weather for the purpose of ascertaining to what extent the change of the air pressure and also of the resulting water waves influence the microseisms in the neighbourhood of the sea.

From the result of calculation, however, it has been ascertained that even the shallow water waves give no much effect directly on the generation of microseisms and that the principal cause of those microseisms, in fact, as Professor Gutenberg[5] suggested, seems to be of a kind such as the surf at the rocky cliff of a coast.

---

[1] K. Sezawa, "On the Transmission of Seismic Waves on the Bottom Surface of an Ocean," *Bull. Earthq. Res. Inst.*, 9 (1931), 115–143.

[2] B. Gutenberg, "Bodenunruhe durch Brandung und durch Frost," *ZS. Geophys.*, 4 (1928), 246–250; and a number of his papers.

[3] B. Gutenberg "Die seismische Bodenunruhe," *Gerl. Beitr. Geophys.* 11., (1912), 414.

[4] S. K. Banerji, "Microseisms Associated with Disturbed Weather in the Indian Seas," *Phil Trans. Roy. Soc.*, 229 (1930), 287–328.

We shall assume that the horizontal surface of a sea, whose depth is h_0, is subjected to a pulsatory pressure:

$$p = f(r)e^{in_1t}, \quad \cdots\cdots\cdots\cdots\cdots\cdots(1)$$

where r is the radial distance of a point from the pressure centre and $2\pi/n_1$ the period of the pulsation. The resulting movements of the sea water and of the surface of the solid will give us long water waves as well as microseisms of the ground caused by the atmospheric disturbance in a sea region.

2. Referring to the axes which are shown in the figure and using the same notations as in the preceding paper,[6] we may write the expressions of the displacement of the ground and the water, besides the potential of the water waves, in the following forms:

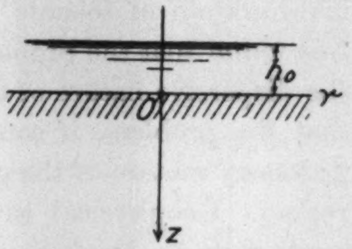

Fig. 1.

$$\left.\begin{aligned} u_1 &= -A_m\frac{1}{h^2}\frac{\partial H_m^{(2)}(kr)}{\partial r}\,e^{-\alpha z+int}\left.\begin{matrix}\cos\\ \sin\end{matrix}\right\} m\theta, \\ v_1 &= A_m\frac{m}{h^2}\frac{H_m^{(2)}(kr)}{r}\,e^{-\alpha z+int}\left.\begin{matrix}\sin\\ -\cos\end{matrix}\right\} m\theta, \\ w_1 &= A_m\frac{\alpha}{h^2}H_m^{(2)}(kr)\,e^{-\alpha z+int}\left.\begin{matrix}\cos\\ \sin\end{matrix}\right\} m\theta, \end{aligned}\right\}\cdots\cdots\cdots\cdots(2)$$

$$\left.\begin{aligned} u_3 &= C_m\frac{\beta}{mj^2}\frac{\partial H_m^{(2)}(kr)}{\partial r}\,e^{-\beta z+int}\left.\begin{matrix}\cos\\ \sin\end{matrix}\right\} m\theta, \\ v_3 &= -C_m\frac{\beta}{j^2}\frac{H_m^{(2)}(kr)}{r}\,e^{-\beta z+int}\left.\begin{matrix}\sin\\ -\cos\end{matrix}\right\} m\theta, \\ w_3 &= -C_m\frac{k^2}{mj^2}H_m^{(2)}(kr)\,e^{-\beta z+int}\left.\begin{matrix}\cos\\ \sin\end{matrix}\right\} m\theta, \end{aligned}\right\}\cdots\cdots\cdots\cdots(3)$$

---

[5] B. GUTENBERG, "Microseisms in North America," *Bull. Seism. Soc. Amer.*, 21 (1931), 1-24.

[6] K. SEZAWA, *loc. cit.*

$$\left.\begin{aligned}
\phi &= (D_m \operatorname{ch} k_1 z + E_m \operatorname{sh} k_1 z) J_m(kr) \left.\begin{matrix}\cos\\ \sin\end{matrix}\right\} m\theta\, e^{int},\\
u' &= \frac{i}{n}(D_m \operatorname{ch} k_1 z + E_m \operatorname{sh} k_1 z) \frac{\partial J_m(kr)}{\partial r} \left.\begin{matrix}\cos\\ \sin\end{matrix}\right\} m\theta\, e^{int},\\
v' &= -\frac{im}{n}(D_m \operatorname{ch} k_1 z + E_m \operatorname{sh} k_1 z) \frac{J_m(kr)}{r} \left.\begin{matrix}\sin\\ -\cos\end{matrix}\right\} m\theta\, e^{int},\\
w' &= \frac{ik_1}{n}(D_m \operatorname{sh} k_1 z + E_m \operatorname{ch} k_1 z) J_m(kr) \left.\begin{matrix}\cos\\ \sin\end{matrix}\right\} m\theta\, e^{int},
\end{aligned}\right\} \cdots(4)$$

where

$$k_1^2 = k^2 - \frac{n^2}{c^2}. \quad \cdots\cdots\cdots\cdots\cdots\cdots\cdots\cdots(5)$$

The boundary conditions are such that

$$z = 0\,; \quad w = w', \quad \cdots\cdots\cdots\cdots\cdots\cdots\cdots\cdots\cdots\cdots(6)$$

$$z = 0\,; \quad \lambda\Delta + 2\mu\frac{\partial w}{\partial z} + g(\rho - \rho')w' - \rho'\frac{\partial \phi}{\partial t} = 0, \cdots\cdots\cdots\cdots(7)$$

$$\left.\begin{aligned}
z = 0\,; \quad & \frac{\partial u}{\partial z} + \frac{\partial w}{\partial r} = 0,\\
& \frac{1}{r}\frac{\partial w}{\partial \theta} + \frac{\partial v}{\partial z} = 0,
\end{aligned}\right\} \cdots\cdots\cdots\cdots\cdots\cdots(8)$$

$$z = -h_0; \quad p = e^{in_1 t} f(r) \left.\begin{matrix}\cos\\ \sin\end{matrix}\right\} m\theta, \cdots\cdots\cdots\cdots\cdots\cdots\cdots\cdots(9)$$

where p is the pulsatory pressure on the surface of water.

From (8), we get

$$\frac{C_m}{m}\bigg/ A_m = \frac{2\alpha j^2}{h^2(2k^2 - j^2)}. \quad \cdots\cdots\cdots\cdots\cdots\cdots(10)$$

From (6),

$$k_1 E_m = -in\left(\frac{\alpha}{h^2}A_m - \frac{k^2}{j^2}\frac{C_m}{m}\right). \quad \cdots\cdots\cdots\cdots\cdots(11)$$

From (7),

$$\left(\lambda - \frac{2\mu\alpha^2}{h^2}\right)A_m + \frac{2\mu k^2\beta}{mj^2}C_m + \frac{ik_1}{n}g(\rho - \rho')E_m - in\rho' D_m = 0. \cdots(12)$$

Comparing (10), (11), (12), we find

$$D_m = \frac{\mu(2k^2-j^2)^2-4\mu k^2\alpha\beta+g(\rho-\rho')\alpha j^2}{\rho' n^2\alpha j^2}\times k_1E_m. \quad\cdots\cdots\cdots\cdots(13)$$

By the use of the relation (13), we get the equation of the pressure distribution of the sea water as follows:

$$\begin{aligned} p &= \rho'\frac{\partial\phi}{\partial t}+\rho' g w' \\ &= iE_m\times\Bigg[\left(nk_1 \operatorname{ch} k_1z+\frac{k_1^2 g}{n}\operatorname{sh} k_1z\right) \\ &\qquad\times\frac{(2k^2-j^2)(2\mu\alpha^2-\lambda h^2)-4\mu k^2\alpha\beta+g(\rho-\rho')\alpha j^2}{n^2\alpha j^2} \\ &\qquad+\left(n\rho' \operatorname{sh} k_1z+\frac{\rho' k_1 g}{n}\operatorname{ch} k_1z\right)\Bigg]\times J_m(kr)\left.\begin{matrix}\cos\\ \sin\end{matrix}\right\} m\theta\, e^{int}. \quad\cdots\cdots\cdots(14) \end{aligned}$$

When $z=-h_0$, this may be written in the form:

$$p = XJ_m(kr)\left.\begin{matrix}\cos\\ \sin\end{matrix}\right\} m\theta\, e^{in_1t}, \quad\cdots\cdots\cdots\cdots\cdots\cdots\cdots\cdots(15)$$

where n is equated to n_1 and

$$\begin{aligned} E_m &= \frac{X}{i\mu k_1(n_1^2-gk_1^2h_0)} \\ &\times\frac{n_1^3\alpha j^2}{\left[(2k^2-j^2)^2-4k^2\alpha\beta-\dfrac{g\alpha j^2}{\mu}+\dfrac{\rho'\alpha j^2}{\mu}\left(g-n_1^2\times\dfrac{g-n_1^2h_0}{n_1^2-gk_1^2h_0}\right)\right]}\cdots(16) \end{aligned}$$

Now, write

$$F(k)\equiv(2k^2-j^2)^2-4k^2\alpha\beta-\frac{g\rho\alpha j^2}{\mu}+\frac{\rho'\alpha j^2}{\mu}\times\frac{n_1^4h_0-g^2h_0k_1^2}{n_1^2-gh_0k_1^2}, \cdots\cdots\cdots(17)$$

or, neglecting $gh_0k_1^2/n_1^2$, write

$$F(k)\equiv(2k^2-j^2)^2-4\alpha\beta k^2-\frac{g\rho j^2}{\mu}\alpha+\rho'\frac{h_0\alpha j^4}{\rho}, \cdots\cdots\cdots\cdots\cdots\cdots(18)$$

then, by means of Fourier's integral expression of p on $z=-h_0$, such that

$$p = e^{in_1t}\left\{\int_0^\infty J_m(kr)kdk\int_0^\infty f(\sigma)J_m(k\sigma)\sigma d\sigma\right\}\left.\begin{matrix}\cos\\ \sin\end{matrix}\right\} m\theta, \cdots\cdots\cdots\cdots\cdots\cdots(19)$$

we obtain the expressions of the displacement of the water surface in the forms:

$$u'_{z=-h_0} = e^{in_1t} \left.\begin{matrix}\cos\\ \sin\end{matrix}\right\} m\theta$$

$$\times \int_0^\infty \frac{[\{\mu(2k^2-j^2)^2 - 4\mu k^2\alpha\beta + g(\rho-\rho')\alpha j^2\}k_1 \operatorname{ch} k_1h_0 - n_1^2\rho'\alpha j^2 \operatorname{sh} k_1h_0]}{\rho'\mu k_1(n_1^2 - gk_1^2h_0)F(k)} \frac{\partial J_m(kr)}{\partial r} kdk$$

$$\times \int_0^\infty f(\sigma)J_m(k\sigma)\sigma d\sigma, \quad \cdots\cdots\cdots\cdots(20)$$

$$v'_{z=-h} = -e^{in_1t}\, m \left.\begin{matrix}\sin\\ -\cos\end{matrix}\right\} m\theta$$

$$\times \int_0^\infty \frac{[\{\mu(2k^2-j^2)^2 - 4\mu k^2\alpha\beta + g(\rho-\rho')\alpha j^2\}k_1 \operatorname{ch} k_1h_0 - n_1^2\rho'\alpha j^2 \operatorname{sh} k_1h_0]}{\rho'\mu k_1(n_1^2 - gk_1^2h_0)F(k)} \frac{J_m(kr)}{r} kdk$$

$$\times \int_0^\infty f(\sigma)J_m(k\sigma)\sigma d\sigma, \quad \cdots\cdots\cdots\cdots(21)$$

$$w'_{z=-h_0} = e^{in_1t} \left.\begin{matrix}\cos\\ \sin\end{matrix}\right\} m\theta$$

$$\times \int_0^\infty \frac{[\rho' n_1^2\alpha j^2 \operatorname{ch} k_1h_0 - \{\mu(2k^2-j^2)^2 - 4\mu k^2\alpha\beta + g(\rho-\rho')\alpha j^2\}k_1 \operatorname{sh} k_1h_0]}{\rho'\mu(n_1^2 - gk_1^2h_0)F(k)} J_m(kr)kdk$$

$$\times \int_0^\infty f(\sigma)J_m(k\sigma)\sigma d\sigma, \quad \cdots\cdots\cdots\cdots(22)$$

and similar expressions of the elastic body at the bottom surface of the sea in the forms:

$$u_{z=0} = e^{in_1t} \left.\begin{matrix}\cos\\ \sin\end{matrix}\right\} m\theta$$

$$\times \int_0^\infty \frac{n_1^2\{(2k^2-j^2)^2 - 2\alpha\beta\}}{\mu(n_1^2 - gk_1^2h_0)F(k)} \frac{\partial J_m(kr)}{\partial r} kdk \int_0^\infty f(\sigma)J_m(k\sigma)\sigma d\sigma, \quad \cdots\cdots(23)$$

$$v_{z=0} = -e^{in_1t}\, m \left.\begin{matrix}\sin\\ -\cos\end{matrix}\right\} m\theta$$

$$\times \int_0^\infty \frac{n_1^2\{(2k^2-j^2)^2 - 2\alpha\beta\}}{\mu(n_1^2 - gk_1^2h_0)F(k)} \frac{J_m(kr)}{r} kdk \int_0^\infty f(\sigma)J_m(k\sigma)\sigma d\sigma, \quad \cdots\cdots(24)$$

$$w_{z=0} = e^{in_1t} \left.\begin{matrix}\cos\\ \sin\end{matrix}\right\} m\theta$$

$$\times \int_0^\infty \frac{n_1^2 \alpha j^2}{\mu(n_1^2 - gk_1^2 h_0)F(k)} J_m(kr) k dk \int_0^\infty f(\sigma) J_m(k\sigma)\sigma d\sigma. \cdots\cdots\cdots\cdots(25)$$

When the depth h_0 is comparatively small, we find

$$u'_{z=-h_0} = \frac{e^{in_1t}}{\rho'\mu} \left.\begin{matrix}\cos\\ \sin\end{matrix}\right\} m\theta$$

$$\times \int_0^\infty \frac{[\mu(2k^2-j^2)^2 - 4\mu k^2 \alpha\beta + g(\rho-\rho')\alpha j^2 - \rho' n_1^2 \alpha j^2 h_0]}{(n_1^2 - gk_1^2 h_0)F(k)} \frac{\partial J_m(kr)}{\partial r} k dk$$

$$\times \int_0^\infty f(\sigma) J_m(k\sigma)\sigma d\sigma, \cdots\cdots\cdots\cdots(26)$$

$$v'_{z=-h_0} = -\frac{e^{in_1t}}{\rho'\mu} m \left.\begin{matrix}\sin\\ -\cos\end{matrix}\right\} m\theta$$

$$\times \int_0^\infty \frac{[\mu(2k^2-j^2)^2 - 4\mu k^2 \alpha\beta + g(\rho-\rho')\alpha j^2 - \rho' n_1^2 \alpha j^2 h_0]}{(n_1^2 - gk_1^2 h_0)F(k)} \frac{J_m(kr)}{r} k dk$$

$$\times \int_0^\infty f(\sigma) J_m(k\sigma)\sigma d\sigma, \cdots\cdots\cdots\cdots(27)$$

$$w'_{z=-h_0} = \frac{e^{in_1t}}{\rho'\mu} \left.\begin{matrix}\cos\\ \sin\end{matrix}\right\} m\theta$$

$$\times \int_0^\infty \frac{[\rho' n_1^2 \alpha j^2 - k_1^2 h_0 \{\mu(2k^2-j^2)^2 - 4\mu k^2 \alpha\beta + g(\rho-\rho')\alpha j^2\}]}{(n_1^2 - gk_1^2 h_0)F(k)} J_m(kr) k dk$$

$$\times \int_0^\infty f(\sigma) J_m(k\sigma)\sigma d\sigma, \cdots\cdots\cdots\cdots(28)$$

$$u_{z=0} = \frac{e^{in_1t} n_1^2}{\mu} \left.\begin{matrix}\cos\\ \sin\end{matrix}\right\} m\theta$$

$$\times \int_0^\infty \frac{(2k^2-j^2) - 2\alpha\beta}{(n_1^2 - gk_1^2 h_0)F(k)} \frac{\partial J_m(kr)}{\partial r} k dk \int_0^\infty f(\sigma) J_m(k\sigma)\sigma d\sigma, \cdots\cdots\cdots\cdots(29)$$

$$v_{z=0} = -\frac{e^{in_1t}n_1^2}{\mu}\, m \left.\begin{matrix}\sin \\ -\cos\end{matrix}\right\} m\theta$$

$$\times \int_0^\infty \frac{(2k^2-j^2)-2\alpha\beta}{(n_1^2-gk_1^2h_0)F(k)}\,\frac{J_m(kr)}{r}kdk \int_0^\infty f(\sigma)J_m(k\sigma)\sigma d\sigma, \quad\cdots\cdots\cdots\cdots(30)$$

$$w_{z=0} = \frac{e^{in_1t}n_1^2}{\mu} \left.\begin{matrix}\cos \\ \sin\end{matrix}\right\} m\theta$$

$$\times \int_0^\infty \frac{\alpha j^2}{(n_1^2-gk_1^2h_0)F(k)}\, J_m(kr)kdk \int_0^\infty f(\sigma)J_m(k\sigma)\sigma d\sigma. \quad\cdots\cdots\cdots\cdots(31)$$

When the disturbed pressure is accumulated in the neighbourhood of $r=0$ and symmetrical with respect to the vertical axis passing through the pressure centre, we may have

$$m = 0\,; \qquad \int_0^\infty f(\sigma)2\pi\sigma d\sigma = 1, \quad\cdots\cdots\cdots\cdots\cdots\cdots(32)$$

so that

$$\left.\begin{aligned}
u'_{z=-h_0} &= \frac{e^{in_1t}}{2\pi\rho'\mu} \\
&\times \int_0^\infty \frac{[\mu(2k^2-j^2)^2-4\mu k^2\alpha\beta+g(\rho-\rho')\alpha j^2-\rho' n_1^2\alpha j^2 h_0]}{(n_1^2-gk_1^2h_0)F(k)}\,\frac{\partial J_0(kr)}{\partial r}kdk, \\
v'_{z=-h_0} &= 0, \\
w'_{z=-h_0} &= \frac{e^{in_1t}}{2\pi\rho'\mu} \\
&\times \int_0^\infty \frac{[\rho' n_1^2\alpha j^2-k_1^2h_0\{\mu(2k^2-j^2)^2-4\mu k^2\alpha\beta+g(\rho-\rho')\alpha j^2\}]}{(n_1^2-gk_1^2h_0)F(k)}\, J_0(kr)kdk,
\end{aligned}\right\} \quad (33)$$

$$\left.\begin{aligned}
u_{z=0} &= \frac{e^{in_1t}n_1^2}{2\pi\mu}\int_0^\infty \frac{(2k^2-j^2)-2\alpha\beta}{(n_1^2-gk_1^2h_0)F(k)}\,\frac{\partial J_0(kr)}{\partial r}kdk, \\
v_{z=0} &= 0, \\
w_{z=0} &= \frac{e^{in_1t}n_1^2}{2\pi\mu}\int_0^\infty \frac{\alpha j^2}{(n_1^2-gk_1^2h_0)F(k)}J_0(kr)kdk,
\end{aligned}\right\} \cdots\cdots\cdots(34)$$

Since we know the expression

$$J_m(kr) = -\frac{i}{\pi}\int_0^\infty\left(e^{i\left(kr\,\mathrm{ch}\,f-\frac{m\pi}{2}\right)} - e^{-i\left(kr\,\mathrm{ch}\,f-\frac{m\pi}{2}\right)}\right)\mathrm{ch}\,mfdf,^{7)} \quad\cdots\cdots\cdots(35)$$

we obtain

$$\left.\begin{aligned}
u'_{z=-h_0} &= \frac{e^{in_1t}}{2\pi^2\rho'\mu}\int_0^\infty \mathrm{ch}\,fdf \\
&\times\int_{-\infty}^\infty \frac{[\mu(2k^2-\jmath^2)^2-4\mu k^2\alpha\beta+g(\rho-\rho')\alpha\jmath^2-\rho' n_1^2\alpha\jmath^2h_0]}{(n_1^2-gk_1^2h_0)F(k)}\,e^{ikr\,\mathrm{ch}\,f}\,kdk, \\
w'_{z=-h_0} &= -\frac{ie^{in_1t}}{2\pi^2\rho'\mu}\int_0^\infty d \\
&\times\int_{-\infty}^\infty \frac{[\rho' n_1^2\alpha\jmath^2-k_1^2h_0\{\mu(2k^2-\jmath^2)^2-4\mu k^2\alpha\beta+g(\rho-\rho')\alpha\jmath^2\}]}{(n_1^2-gk_1^2h_0)F(k)}\,e^{ikr\,\mathrm{ch}\,f}\,kdk,
\end{aligned}\right\}\quad(36)$$

$$\left.\begin{aligned}
u_{z=0} &= \frac{e^{in_0t}n_1^2}{2\pi^2\mu}\int_0^\infty \mathrm{ch}\,fdf\int_{-\infty}^\infty \frac{(2k^2-\jmath^2)-2\alpha\beta}{(n_1^2-gk_1^2h_0)F(k)}\,e^{ikr\,\mathrm{ch}\,f}\,kdk, \\
w_{z=0} &= -\frac{ie^{in_1t}n_1^2}{2\pi^2\mu}\int_0^\infty df\int_{-\infty}^\infty \frac{\alpha\jmath^2e^{ikr\,\mathrm{ch}\,f}}{(n_1^2-gk_1^2h_0)F(k)}kdk.
\end{aligned}\right\}\quad(37)$$

The evaluation of the integrals of the types :

$$\int_{-\infty}^\infty \frac{[\rho' n_1^2\alpha\jmath^2-\{\mu(2k^2-\jmath^2)^2-4\mu k^2\alpha\beta+g(\rho-\rho')\alpha\jmath^2\}k_1^2h_0]}{(n_1^2-gk_1^2h_0)F(k)}\,e^{ikr\,\mathrm{ch}\,f}\,kdk, \cdots(38)$$

$$\int_{-\infty}^\infty \frac{\alpha\jmath^2\,e^{ikr\,\mathrm{ch}\,f}\,kdk}{(n_1^2-gk_1^2h_0)F(k)}, \quad\cdots\cdots\cdots\cdots\cdots\cdots\cdots\cdots\cdots(39)$$

where $k_1^2 = k^2 - n_1^2/c^2$, can be performed in the following manner. Consider, for example, the integral

$$\int_c \frac{\sqrt{Z^2-h^2}\,e^{iZr\,\mathrm{ch}\,f}\,ZdZ}{\left\{n_1^2\left(\frac{c^2+gh_0}{c^2gh_0}\right)-Z^2\right\}F(Z)} \quad\cdots\cdots\cdots\cdots\cdots\cdots\cdots\cdots\cdots(40)$$

---

7) WATSON, "Theory of Bessel Functions", (1922), 180.

taken round a contour shown in Fig. 2. In (40),

$$F(Z)=(2Z^2-j^2)^2-4Z^2\sqrt{(h^2-Z^2)(j^2-Z^2)}$$

$$-\frac{g\rho}{\mu}\sqrt{h^2-Z^2}\,j^2+\frac{\rho'\sqrt{h^2-Z^2}}{\mu}\,j^2\,\frac{n_1^4h_0-g^2h_0(Z^2-n_1^2/c^2)}{n_1^2-gh_0(Z^2-n_1^2/c^2)},\quad\cdots\cdots(41)$$

and $h^2=\rho n_1^2/(\lambda+2\mu)$, $j^2=\rho n_1^2/\mu$. ……………………………………………(42)

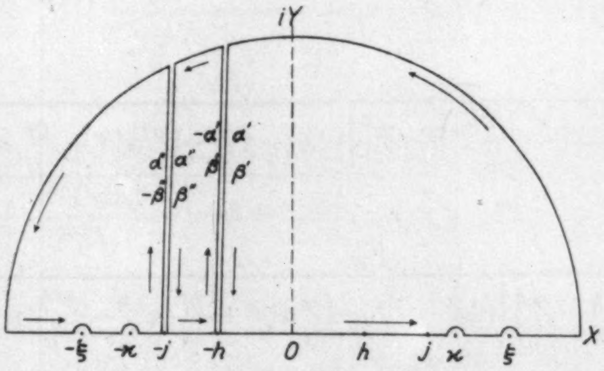

Fig. 2.

In Fig. 2, $h, j, -h, -j$ are branch points corresponding to the integrand of (40); $\pm\varkappa$ and $\pm\xi$ poles of the same integrand, namely $\pm\varkappa$ are a pair of real roots of the equation (41), while $\pm\xi$ are a pair of the roots of the equation $n_1^2\left(\frac{c^2+gh_0}{c^2gh_0}\right)-Z^2$. If we assume that there are certain terms of insensible frictional damping in the equations of the vibrations of the solid body, it will be clear that the branch points $Z=h$, $Z=j$ are shifted in the space of the lower quadrant of Fig. 2, so that these points do not influence the contour integration. The two grooves running between $(-h, 0)$, $(-h, i\infty)$ and between $(-j, 0)$, $(-j, i\infty)$ are branch lines. The positive and negative signs of $\alpha', \beta', \alpha'', \beta''$ on both sides of the lines $Z=-h$ and $Z=-j$ are taken suitably so as to satisfy the conditions of continuity. The resultant of these lines, when composed, may be equivalent to a branch line joining two points $(-h, 0)$, $(-j, 0)$. The result of the contour integral shows that

$$I=\int_{-\infty}^{\infty}\frac{\alpha j^2e^{ikr\,\mathrm{ch}\,f}\,kdk}{\left\{n_1^2\left(\frac{c^2+gh_0}{c^2gh_0}\right)-k^2\right\}F(k)}$$

$$=\frac{i4\pi\alpha_1j^2\xi}{\phi'(\xi)}\cos(\xi r\,\mathrm{ch}\,f)+\frac{i4\pi\alpha_2j^2\varkappa}{\phi'(\varkappa)}\cos(\varkappa r\,\mathrm{ch}\,f)$$

$$+e^{-ijr\,\mathrm{ch}\,f}\int_0^\infty\Bigg[\frac{j^2\alpha''}{\left\{n_1^2\left(\frac{c^2+gh_0}{c^2gh_0}\right)-Z^2\right\}\left\{(2Z^2-j^2)^2-4Z^2\alpha''\beta''-\frac{g\rho}{\mu}\alpha''j^2+\frac{\rho'h_0}{\rho}\alpha''j^4\right\}}$$

$$-\frac{j^2\alpha''}{\left\{n_1^2\left(\frac{c^2+gh_0}{c^2gh_0}\right)-Z^2\right\}\left\{(2Z^2-j^2)^2+4Z^2\alpha''\beta''-\frac{g\rho}{\mu}\alpha''j^2+\frac{\rho'h_0}{\rho}\alpha''j^4\right\}}\Bigg]Ze^{-Yr\,\mathrm{ch}\,f}i\,dY$$

$$+e^{-ihr\,\mathrm{ch}\,f}\int_0^\infty\Bigg[\frac{j^2\alpha'}{\left\{n_1^2\left(\frac{c^2+gh_0}{c^2gh_0}\right)-Z^2\right\}\left\{(2Z^2-j^2)^2-4Z^2\alpha'\beta'-\frac{g\rho}{\mu}\alpha'j^2+\frac{\rho'h_0}{\rho}\alpha'j^4\right\}}$$

$$+\frac{j^2\alpha'}{\left\{n_1^2\left(\frac{c^2+gh_0}{c^2gh_0}\right)-Z^2\right\}\left\{(2Z^2-j^2)^2+4Z^2\alpha'\beta'+\frac{g\rho}{\mu}\alpha'j^2-\frac{\rho'h_0}{\rho}\alpha'j^4\right\}}\Bigg]Ze^{-Yr\,\mathrm{ch}\,f}i\,dY$$

$$=i\frac{4\pi\alpha_1j^2\xi}{\phi'(\xi)}\cos(\xi r\,\mathrm{ch}\,f)+i\frac{4\pi\alpha_2j^2\varkappa}{\phi'(\varkappa)}\cos(\varkappa r\,\mathrm{ch}\,f)$$

$$+8ie^{-ijr\,\mathrm{ch}\,f}\int_0^\infty\frac{j^2\alpha''e^{-Yr\,\mathrm{ch}\,f}\alpha''\beta''Z^3dY}{\left\{n_1^2\left(\frac{c^2+gh_0}{c^2gh_0}\right)-Z^2\right\}\left[\left\{(2Z^2-j^2)^2-\frac{g\rho}{\mu}\alpha''j^2-\frac{\rho'h_0}{\rho}\alpha''j^4\right\}^2-16Z^4\alpha''^2\beta''^2\right]}$$

$$+2ie^{-ihr\,\mathrm{ch}\,f}\int_0^\infty\frac{j^2\alpha'e^{-Yr\,\mathrm{ch}\,f}Z(2Z^2-j^2)^2dY}{\left\{n_1^2\left(\frac{c^2+gh_0}{c^2gh_0}\right)-Z^2\right\}\left[(2Z^2-j^2)^4-\left(4Z^2\alpha'\beta'+\frac{g\rho}{\mu}\alpha'j^2-\frac{\rho'h_0}{\rho}\alpha'j^4\right)^2\right]},$$

$$\cdots\cdots\cdots\cdots\cdots\cdots(43)$$

where

$$\alpha_1=\sqrt{\xi^2-h^2},\quad \alpha_2=\sqrt{\varkappa^2-h^2}.\ \cdots\cdots\cdots\cdots(44)$$

It is known that, for small values of Y,

$$\left.\begin{aligned}\alpha'&=-\sqrt{2hY}\,e^{-\frac{1}{4}i\pi},\quad \beta'=i\sqrt{(j^2-h^2)},\\ \alpha''&=\sqrt{(j^2-h^2)},\qquad \beta''=-\sqrt{2jY}\,e^{-\frac{1}{4}i\pi}\end{aligned}\right\}\ \cdots\cdots\cdots(45)^{8)}$$

may be taken with approximation. Hence we get

---

8) H. LAMB, *Phil. Trans. Roy. Soc.*, 203 (1904), 20.

$$I = i\frac{4\pi\alpha_1\ddot{j}^2\xi}{\phi'(\xi)}\cos(\xi r\,\mathrm{ch}\,f) + i\frac{4\pi\alpha_2\ddot{j}^2\varkappa}{\phi'(\varkappa)}\cos(\varkappa r\,\mathrm{ch}\,f)$$

$$-\int_0^\infty \frac{\ddot{j}^2(\ddot{j}^2-h^2)\sqrt{2jY}(-j+iY)^3e^{-\frac{1}{4}i\pi-Yr\,\mathrm{ch}\,f}df}{\left\{n_1^2\frac{(c^2+gh_0)}{c^2gh_0}-(-j+iY)^2\right\}\left[\left\{(2(-j+iY)^2-\ddot{j}^2)^2-\frac{\rho g}{\mu}\ddot{j}^2\sqrt{\ddot{j}^2-h^2}-\frac{\rho' h_0}{\rho}\ddot{j}^4\sqrt{\ddot{j}^2-h^2}\right\}^2-32(\ddot{j}^2-h^2)jYe^{-\frac{i\pi}{2}}(-j+iY)^4\right]}$$

$$-\int_0^\infty \frac{\sqrt{2h}\,\ddot{j}^2(-h+iY)\{2(-h+iY)^2-\ddot{j}^2\}^2Y^{\frac{1}{2}}e^{-\frac{1}{4}i\pi-Yr\,\mathrm{ch}\,f}df}{\left\{n_1^2\frac{(c^2+gh_0)}{c^2gh_0}-(-h+iY)^2\right\}\left[\{2(-h+iY)^2-\ddot{j}^2\}^4-2hYe^{-\frac{i\pi}{2}}\left\{4i(-h+iY)^2\sqrt{\ddot{j}^2-h^2}+\frac{\rho g}{\mu}\ddot{j}^2-\frac{\rho' h_0}{\rho}\ddot{j}^4\right\}^2\right]}.$$

$$\cdots\cdots\cdots\cdots(46)$$

We know again

$$\int_0^\infty Y^{1/2}\chi(Y)e^{-Yx}dY = \frac{\Pi(1/2)}{x^{3/2}}\chi(0) + \frac{\Pi(3/2)}{x^{5/2}}\frac{\chi'(0)}{1!} + \frac{\Pi(\ /2)}{x^{7/2}}\frac{\chi''(0)}{2!} + \cdots \qquad (47)^{9)}$$

Hence

$$I = \frac{i4\pi\alpha_1\ddot{j}^2\xi}{\phi'(\xi)}\cos(\xi r\,\mathrm{ch}\,f) + \frac{i4\pi\alpha_2\ddot{j}^2\varkappa}{\phi'(\varkappa)}\cos(\varkappa r\,\mathrm{ch}\,f)$$

$$+\frac{\Pi(1/2)}{(r\,\mathrm{ch}\,f)^{3/2}}\left[\frac{\sqrt{2j}\,(\ddot{j}^2-h^2)e^{-\frac{1}{4}i\pi}\ddot{j}^5}{\left\{n_1^2\frac{(c^2+gh_0)}{c^2gh_0}-\ddot{j}^2\right\}\left\{\ddot{j}^2-\frac{\rho g}{\mu}\ddot{j}^2\sqrt{\ddot{j}^2-h^2}-\frac{\rho' h_0}{\rho}\ddot{j}^4\sqrt{\ddot{j}^2-h^2}\right\}^2}\right] + \text{etc.}$$

$$+\frac{\Pi(1/2)}{(r\,\mathrm{ch}\,f)^{3/2}}\left[\frac{h\ddot{j}^2\sqrt{2h}\,e^{-\frac{1}{4}i\pi}}{\left\{n_1^2\frac{(c^2+gh_0)}{c^2gh_0}-h^2\right\}(2h^2-\ddot{j}^2)^2}\right] + \text{etc.} \qquad \cdots\cdots\cdots\cdots(48)$$

Substituting this in (37), we obtain

---

9) H. Lamb, *loc. cit.*

$$w_{z=0}=-\frac{ie^{in_1t}n_1^2}{2\pi^2\mu g h_0}\Bigg[\frac{i4\pi\alpha_1 j^2\xi}{\phi'(\xi)}\int_0^\infty\cos(\xi r\operatorname{ch}f)df+\frac{i4\pi\alpha_2 j^2\varkappa}{\phi'(\varkappa)}\int_0^\infty\cos(\varkappa r\operatorname{ch}f)df$$

$$+\frac{8i\Pi(1/2)(j^2-h^2)\sqrt{2j}\,j^5e^{-\frac{i\pi}{4}}}{r^{3/2}\left\{\frac{n_1^2(c^2+gh_0)}{c^2gh_0}-j^2\right\}\left\{j^4-\frac{\rho g}{\mu}j^2\sqrt{j^2-h^2}-\frac{\rho' h_0}{\rho}j^4\sqrt{j^2-h^2}\right\}^2}\int_0^\infty\frac{e^{-ij\operatorname{ch}f}}{(\operatorname{ch}f)^{3/2}}df$$

$$+\frac{2i\Pi(1/2)\sqrt{2h}\,hj^2e^{-\frac{i\pi}{4}}}{r^{3/2}\left\{\frac{n_1^2(c^2+gh_0)}{c^2gh_0}-h^2\right\}(2h^2-j^2)^2}\int_0^\infty\frac{e^{-ihr\operatorname{ch}f}}{(\operatorname{ch}f)^{3/2}}df\Bigg].\cdots\cdots(49)$$

The integrals of the first and second terms of the right-hand side of this expression are easily obtained by means of the formula:

$$Y_0(\xi r)=-\frac{2}{\pi}\int_0^\infty\cos(\xi r\operatorname{ch}f)df.\cdots\cdots(50)$$

To evaluate the third and fourth integrals, we consider

$$K=\int_c\frac{e^{-\xi Z}dZ}{Z^{3/2}\sqrt{1+Z^2}}\quad\cdots\cdots(51)$$

taken round the contour shown in this page. Thus we know

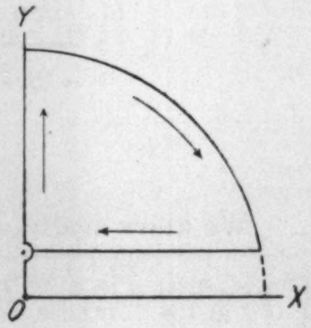

Fig. 3.

$$\int_0^\infty\frac{e^{i\xi\operatorname{ch}f}}{(\operatorname{ch}f)^{3/2}}df=e^{-i\left(\xi+\frac{\pi}{4}\right)}\sqrt{\frac{\pi}{2\xi}}\left(1+\frac{7}{4}i\frac{1}{2\xi}-\frac{15}{8}\frac{1\cdot3}{4\xi^2}+\cdots\cdots\right).\quad(52)$$

Substituting from (50), (52) in (49), we get

$$w_{z=0}=\frac{ie^{in_1t}n_1^2}{2\pi^2 u g h_0}\Bigg[\frac{i2\pi^2\alpha_1 j^2\xi}{\phi'(\xi)}Y_0(\xi r)+\frac{i2\pi^2\alpha_2 j^2\varkappa}{\phi'(\varkappa)}Y_0(\varkappa r)$$

$$-\frac{4i\pi(j^2-h^2)je^{-i\left(jr+\frac{\pi}{2}\right)}}{r^2\left\{\frac{n_1^2(c^2+gh_0)}{c^2gh_0}-j^2\right\}\left\{j^2-\frac{\rho g}{\mu}\sqrt{j^2-h^2}-\frac{\rho' h_0}{\rho}j^2\sqrt{j^2-h^2}\right\}^2}$$

$$-\frac{\pi hj^2e^{-i\left(hr+\frac{\pi}{2}\right)}}{r^2\left\{\frac{n_1^2(c^2+gh_0)}{c^2gh_0}-h^2\right\}(2h^2-j^2)^2}+\cdots\cdots\Bigg].\quad\cdots\cdots(53)$$

This expression is suitable to the problem of transmission of waves of finite extent of disturbances. To get progressive waves of an infinite extent, we add to this expression other systems of standing vibrations corresponding to the water waves as well as the surface waves of the elastic solid body, the wave lengths and the amplitudes of both systems being respectively equal to the first and the second terms of the right-hand side of the equation (53), but the phases of the additive systems differ from the original ones about $\pi/2$. The final solution is thus expressed by

$$w_{z=0} \approx -\frac{ie^{in_1t}n_1^2}{2\mu g h_0}\left[\frac{\alpha_1 j^2\xi}{\phi'(\xi)}H_0^{(2)}(\xi r)+\frac{\alpha_2 j^2\varkappa}{\phi'(\varkappa)}H_0^{(2)}(\varkappa r)\right.$$

$$+\frac{4i(j^2-h^2)je^{-i\left(jr+\frac{\pi}{4}\right)}}{\pi r^2\left\{\frac{n_1^2(c^2+gh_0)}{c^2gh_0}-j^2\right\}\left\{j^2-\frac{\rho g}{\mu}\sqrt{j^2-h^2}-\frac{\rho' h_0}{\rho}j^2\sqrt{j^2-h^2}\right\}^2}$$

$$\left.+\frac{ihj^2e^{-i\left(hr+\frac{\pi}{2}\right)}}{\pi r^2\left\{n_1^2\frac{(c^2+gh_0)}{c^2gh_0}-h^2\right\}(2h^2-j^2)^2}\right], \quad\cdots\cdots\cdots\cdots\cdots\cdots\cdots\cdots(54)$$

provided

$$\phi(k)=\left\{\frac{n_1^2(c^2+gh_0)}{c^2gh_0}-k^2\right\}\left\{(2k^2-j^2)^2-4\alpha\beta k^2-\frac{g\rho}{\mu}\alpha j^2+\frac{\rho' h_0}{\rho}\alpha j^4\right\}. \cdots(55)$$

In the same manner of mathematical treatment we get the horizontal component of displacement of the surface of the solid, $u_{z=0}$, the similar component of the surface of water, $u'_{z=-h_0}$, and the vertical component of the surface displacement of the water, $w_{z=-h_0}$, as in the following forms:

$$u_{z=0} \approx \frac{ie^{in_1t}n_1^2}{2\mu g h_0}\left[\frac{(2\xi^2-j^2-2\alpha_1\beta_1)\xi^2}{\phi'(\xi)}H_1^{(2)}(\xi r)+\frac{(2\varkappa^2-j^2-2\alpha_2\beta_2)\varkappa^2}{\phi'(\varkappa)}H_1^{(2)}(\varkappa r)\right], \quad (56)$$

$$u'_{z=-h_0} \approx \frac{ie^{in_1t}}{2\rho'\mu g h_0}\left[\frac{\{\mu(2\xi^2-j^2)^2-4\mu\xi^2\alpha_1\beta_1+g(\rho-\rho')\alpha_1 j^2-\rho' n_1^2\alpha_1 j^2 h_0\}\xi^2}{\phi'(\xi)}H_1^{(2)}(\xi r)\right.$$

$$\left.+\frac{\{\mu(2\varkappa^2-j^2)^2-4\mu\varkappa^2\alpha_2\beta_2+g(\rho-\rho')\alpha_2 j^2-\rho' n_1^2\alpha_2 j^2 h_0\}\varkappa^2}{\phi'(\varkappa)}H_1^{(2)}(\varkappa r)\right], \cdots\cdots(57)$$

$$w'_{z=-h_0} \eqsim -\frac{ie^{in_1t}}{2\rho'\mu g h_0}$$

$$\times\left[\frac{\left\{\rho' n_1^2\alpha_1\bar{\jmath}^2-\left[\mu(2\xi^2-\bar{\jmath}^2)^2-4\mu\xi^2\alpha_1\beta_1+g(\rho-\rho')\alpha_1\bar{\jmath}^2\right]\left(\xi^2-\frac{n_1^2}{c^2}\right)h_0\right\}\xi}{\phi'(\xi)}H_0^{(2)}(\xi r)\right.$$

$$\left.+\frac{\left\{\rho' n_1^2\alpha_2\bar{\jmath}^2-\left[\mu(2\varkappa^2-\bar{\jmath}^2)^2-4\mu\varkappa^2\alpha_2\beta_2+g(\rho-\rho')\alpha_2\bar{\jmath}^2\right]\left(\varkappa^2-\frac{n_1^2}{c^2}\right)h_0\right\}\varkappa}{\phi'(\varkappa)}H_0^{(2)}(\varkappa r)\right]$$

$$\cdots\cdots\cdots\cdots(58)$$

in which

$$\beta_1=\sqrt{\xi^2-\bar{\jmath}^2},\quad \beta_2=\sqrt{\varkappa^2-\bar{\jmath}^2},\cdots\cdots\cdots\cdots(59)$$

and the terms corresponding to the dilatational and the distortional waves are neglected.

3. It may be seen from (54) (or other expressions) that the movement of the solid body (or of water) is composed of four kinds of displacements, namely the displacement due to the transmission of shallow water waves, that due to Rayleigh-waves on the bottom surface of the water superposed upon a solid body, that due to distortional waves through the body and also that due to dilatational waves through the same body. The velocities of transmission of the waves of these displacements are, of course, equal to those peculiar to the respective kinds of waves. Thus the velocity of transmission of the waves of the displacement of the solid due to the shallow water waves is exceedingly slow in comparison with that of the Rayleigh-type deformation.

The amplitudes of the deformation of the solid body due to Rayleigh-waves and also to the shallow water waves change as inverse square root of the epicentral distance, while those due to the dilatational and distortional waves diminish as inverse square of the epicentral distance, so that it may be concluded that the principal movement at a certain distance from the centre of the pulsating pressure should be caused by the transmission of Rayleigh-waves as well as shallow water waves.

It is important to know the relative magnitudes of the deformations of the solid due to the transmission of shallow water waves and to that of Rayleigh-type waves, because it is yet uncertain, whether the microseisms occurring in a disturbed weather may be the effect of the seismic waves transmitted directly from the region of the original disturbance, or may be the vibratory motion of the ground due to the disturbed water waves approaching from the origin to the locality of the observing station, or even due to some other cause such as the surf against the steep coast.

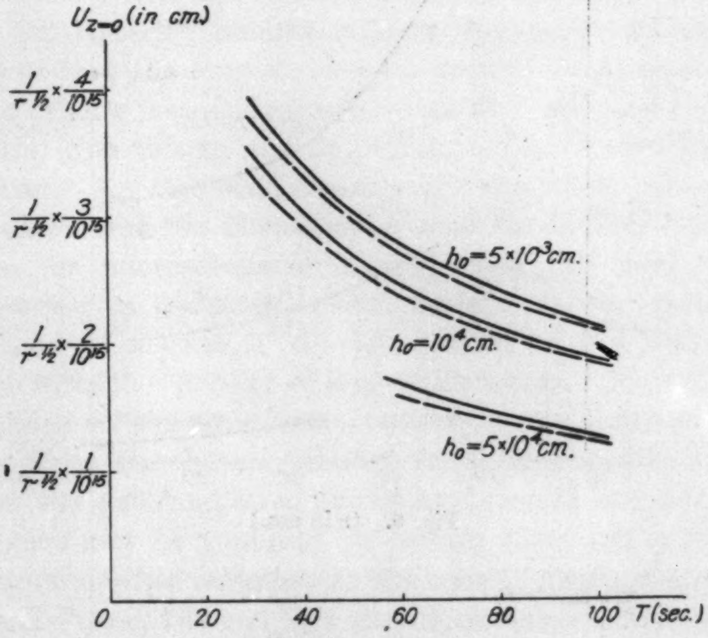

Fig. 4. (r in cm.)

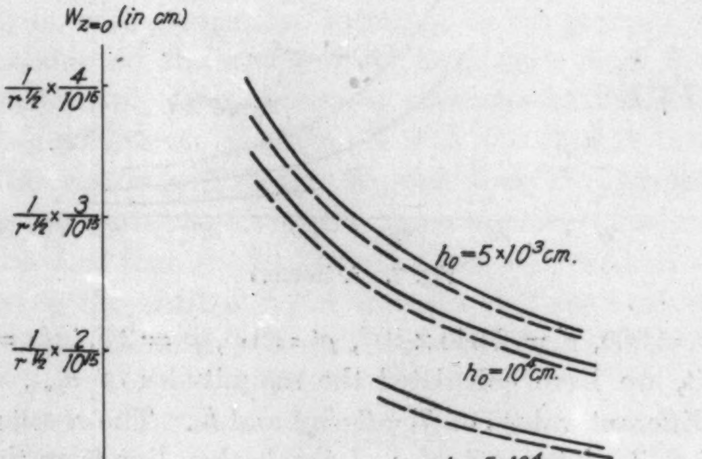

Fig. 5. (r in cm.)

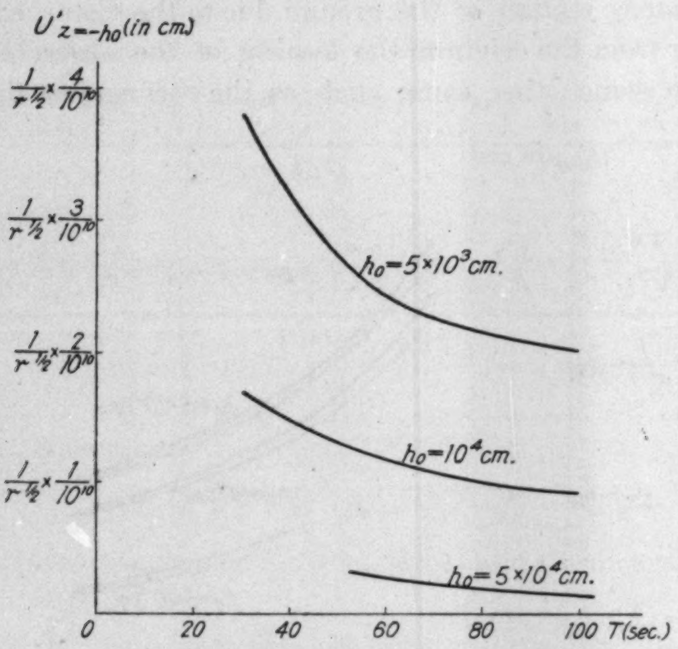

Fig. 6. (r in cm.)

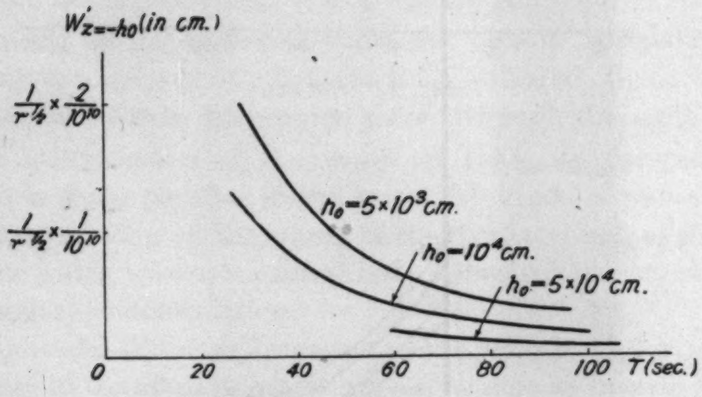

Fig. 7. (r in cm.)

Assuming $g = 980$, $c^2 = 2{\cdot}045\times10^{10}$, $\rho' = 1{\cdot}0$, $\rho = 2{\cdot}5$, $\mu/\rho = 3{\cdot}14^2\times10^{10}$ in C.G.S. unit, we have calculated the magnitudes of $u_{z=0}$, $w_{z=0}$, $u'_{z=-h_0}$, $w'_{z=-h_0}$ for different values of $T(=2\pi/n_1)$ and h_0. The results are plotted in Figs. 4, 5, 6, 7. The ordinates of the broken line from the base gives the effect due to the term involving $H_0^{(2)}(\xi r)$ and the vertical distance between the full line and this broken line indicates the effect due to the term containing $H_0^{(2)}(\varkappa r)$. In Figs. 6 and 7 the broken line coincides practically with the full line. The former cause, however, is principally of statical and special to shallow water, so that this is not yet sufficient for the full explanation of the microseisms. From these figures it will be clearly seen that the microseisms are rather due to long water waves near the observing station which are transmitted from the region of the disturbed weather, but not due to the seismic waves directly transmitted from such a region. Dr. Banerji(10) seemed to have the similar opinion. It is also to be noticed that the amplitude of the ground due to pulsatory original disturbance of long periods is smaller than that due to the disturbance of short periods, even though the amplitude of the disturbing pressure is kept constant. As Professor Gutenberg(11) suggested, this only fact is in good accordance with the phenomenon that the breakers play an important *rôle* on the microseisms of short periods. In fact, the pulsatory motion observed at a station seems partly to be the radiation, in the neighbourhood of a coast, of the deformation of the ground, which is transmitted with the velocity of long water waves. Besides the action of the surf against a steep coast, some portion of the shock of the breakers themselves must also be contributed from these radiated waves. The radiation of the deformation of the bottom ground and that of the shock due to breakers may be combined in certain cases owing to their approximately simultaneous radiation at the coast. Again, the comparison of Figs. 4, 5 and Figs 6, 7 shows that the displacement of the surface of the water is greater than that of the surface of the bottom ground about 10^4 times. Although it is obvious that the amplitude of water waves is exceedingly large in comparison with that of the ground, yet we may get some knowledge on the order of its magnitude from the result of the present calculation. It is, however, understood that the deformation of the bottom ground never corresponds with the statical head of the wave height. This reason will clearly be seen from the elementary theory of hydrodynamics with respect to the wave motion. The analytical treatment of the fact that the radiation of the deformation of the bottom ground due to the shallow water waves is still small compared with the shock of the surf against a steep coast, will be published in a future paper.

Summary.

We may now complete this paper with a brief summary.

1. The movement of the ground is composed of four kinds of displacements; namely the displacement due to the transmission of

---

10) S.K. Banerji, *loc. cit.*

11) B. Gutenberg, *loc. cit.*

shallow water waves, that due to Rayleigh-waves, that due to distortional waves and that due to dilatational waves.

2. The velocity of the transmission of the displacement of the body due to shallow water waves is equal to that of shallow water waves, while the transmission of the displacements of other kinds have their own velocities peculiar to the respective waves.

3. The amplitudes of the deformation of the solid body due to Rayleigh-waves and also to shallow water waves change as inverse square root of the epicentral distance, while those due to the dilatational and distortional waves diminish as inverse square of the epicentral distance.

4. Microseisms due to a disturbed weather occurring in a different region are chiefly due to long water waves, including breakers at the coast, advancing near the observing station, but not the seismic waves directly transmitted from the region of the disturbed weather. The action of the long water waves is, however, relatively small compared with that of breakers.

5. The amplitude of the ground due to pulsatory original disturbance of long periods is smaller than that due to short periods, even though the amplitude of the disturbing pressure is kept constant.

20. 海面大氣壓の擾亂によつて起る地動に就て

地震研究所 {妹澤克惟
西村源六郎

遠方の洋上に低氣壓が起つてゐる時、たとひ觀測點の附近は平穩であつても、地震計に脈動がよく現はれるといふ事が既に知られて居る。しかし其脈動は低氣壓の中心地方から直接地震波として來たものであるか、又は擾亂が一度海洋波として送られて來てから後其附近の海岸に於て地動に變化したものか未だ充分わかつて居らぬ樣に思はれる。

その機構を確める目的を以て筆者等は、半無限固體上に水の層を置き、其水面に適當な分布をなす氣壓の週期的變化を與へた場合に生ずる水の波と固體の變形とを計算し、脈動に對して如何なる原因をなすべきかを考へて見たのである。勿論この氣壓の週期的變化といふ事は、實際にはもつと複雜なものを簡單な形で代表させたまでである。

計算の結果によれば、固體の動き方は四種類の變位から成り、第一のものは淺海波の傳播によつて與へられる影響であつて其傳はる速さは恰度其淺海波の速度に等しいのである。第二のものはレーリー波の速度を以て傳はる固體其自身の波であり、他の二種は夫々固體の縱波と横波とである。

淺海波に伴つて起る波動とレーリー波に相當する波動とは擾亂氣壓の中心からの距離の平方根に反比例して振幅が減じて行く。然るに縱波と横波とは距離の二乘に反比例して振幅が少くなる。從て脈動が縱波や横波に基くものでない事は明である。

次に原點からのレーリー波による土地の振幅は、淺海波に伴つて起る振幅に比較する時は非常に小さい。從て脈動は原點から擾亂が一度淺海波として送られ、其に相當する土地の變形が傳はる事及び淺海波が海岸で碎けて生ずる振動とが非常に勢力のある原因をなす事がわかるのである。しかしこの論文では淺海波が碎けて斷崖などに直接衝動を與へる場合は態と避けた。これが主要な原因である事は明であるけれども餘りわかり切つた現象であるからである。實は淺海波による土地の變形が其儘傳播する事と淺海波が海岸で碎けて生ずる振動とは其生成の時間が大體同じである爲に之を分離する事は殆ど不可能といつても差支がない。しかし兩方とも同じ種類の原因であるから强ひて分る必要もないと思ふ。

尙大氣壓の擾亂振幅が同じでも、擾亂振動の週期が短いもの程土地の振幅卽ち脈動の振幅が大になる事は注意を要する事と思ふ。

21. *A Kind of Waves transmitted over a Semi-infinite Solid Body of Varying Elasticity.*

By **Katsutada Sezawa**,

Earthquake Research Institute.

(Read July 5, 1927 and April 21, 1931.—Received June 20, 1931.)

In this paper I am going to study the propagation of surface waves over a semi-infinite solid body whose elastic constants are functions of the position of a material point of the body below its free surface. There are, of course, several kinds of waves according with the forms of the functions of varying elasticities and also with the types of the propagated waves; yet we now confine ourselves to the case such that

$$\varDelta = 0, \qquad w = 0; \quad \cdots\cdots\cdots\cdots\cdots\cdots\cdots\cdots(1)$$

$$\mu = c(d+z_1), \quad \cdots\cdots\cdots\cdots\cdots\cdots\cdots\cdots(2)$$

where $\varDelta$ is the dilation, w the vertical component of the displacement, μ the modulus of rigidity, and z_1 the depth of a material point below the free surface, c and d being certain constants. Although a similar kind of waves has already been dealt with by Meissner[1] and Aichi,[2] yet their cases belong to a one-dimensional problem and the methods of integration of differential equation are quite different from that of the present paper.

The differential equation of motion of a semi-infinite solid body, when the conditions in (1) are to be satisfied, are expressed by

$$\rho\frac{\partial^2 u}{\partial t^2} = -\frac{2\mu}{r}\frac{\partial \varpi_z}{\partial \theta} + 2\frac{\partial(\mu\varpi_\theta)}{\partial z}\,, \quad \cdots\cdots\cdots\cdots(3)$$

$$\rho\frac{\partial^2 v}{\partial t^2} = -2\frac{\partial(\mu\varpi_r)}{\partial z} + 2\mu\frac{\partial \varpi_z}{\partial r}\,, \quad \cdots\cdots\cdots\cdots(3)$$

---

[1] E. Meissner, "Elastische Oberflächen-Querwellen," *Verh. 2. int. Kongr. f. tech. Mech.*, (Zürich, 1926), 3-11; and also *Vierteljahr. Nat. Forsch. Ges.*, Zürich, 67 (1921), 181.

[2] K. Aichi, "On the Transversal Seismic Waves travelling upon the Surface of Heterogeneous Material," *Proc. Phys.-Math. Soc.*, Japan, [3], 4 (1922), 137-142.

provided

$$2\varpi_r = -\frac{\partial v}{\partial z}, \quad 2\varpi_\theta = \frac{\partial u}{\partial z}, \quad 2\varpi_z = \frac{1}{r}\left(\frac{\partial (rv)}{\partial r} - \frac{\partial u}{\partial \theta}\right), \quad (4)$$

in which ρ is the density of the solid and u, v are the radial and azimuthal components of the displacement. From the condition of the problem we have the identical relation such that

$$\frac{1}{r}\frac{\partial (ru)}{\partial r} + \frac{1}{r}\frac{\partial v}{\partial \theta} = 0. \quad \cdots\cdots\cdots\cdots(5)$$

Eliminating u, v between (3) and (4), we obtain

$$\rho\frac{\partial^2 \varpi_z}{\partial t^2} = \mu\left(\frac{\partial^2 \varpi_z}{\partial r^2} + \frac{1}{r}\frac{\partial \varpi_z}{\partial r} + \frac{1}{r^2}\frac{\partial^2 \varpi_z}{\partial \theta^2}\right) + \frac{\partial}{\partial z}\mu\frac{\partial \varpi_z}{\partial z}, \quad \cdots(7)$$

$$\rho\frac{\partial^2 \varpi_r}{\partial t^2} = \frac{\partial^2}{\partial z^2}\left(\mu\,\varpi_r\right) - \frac{\partial}{\partial z}\left(\mu\frac{\partial \varpi_z}{\partial r}\right), \quad \cdots\cdots\cdots\cdots(8)$$

$$\rho\frac{\partial^2 \varpi_\theta}{\partial t^2} = \frac{\partial^2}{\partial z^2}\left(\mu\,\varpi_\theta\right) - \frac{1}{r}\frac{\partial}{\partial z}\left(\mu\frac{\partial \varpi_z}{\partial \theta}\right). \quad \cdots\cdots\cdots\cdots(9)$$

These differential equations are satisfied by

$$\varpi_z = B_m \Phi(z) H_m^{(2)}(kr) \left.\begin{matrix}\sin\\ -\cos\end{matrix}\right\} m\theta e^{ipt}, \quad \cdots\cdots\cdots\cdots(10)$$

$$\varpi_r = \frac{B_m}{k^2}\frac{\partial \Phi(z)}{\partial z}\frac{\partial H_m^{(2)}(kr)}{\partial r} \left.\begin{matrix}\sin\\ -\cos\end{matrix}\right\} m\theta e^{ipt}, \quad \cdots\cdots\cdots\cdots(11)$$

$$\varpi_\theta = \frac{B_m m}{k^2}\frac{\partial \Phi(z)}{\partial z}\frac{H_m^{(2)}(kr)}{r} \left.\begin{matrix}\cos\\ \sin\end{matrix}\right\} m\theta e^{ipt}, \quad \cdots\cdots\cdots\cdots(12)$$

where p is frequency of waves, $2\pi/k$ wave length, B_m a constant and $\Phi(z)$ is a certain function which satisfies the differential equation

$$\frac{d^2\Phi(z)}{dz^2} + \frac{1}{\mu}\frac{d\mu}{dz}\frac{d\Phi(z)}{dz} + \left(\frac{\rho p^2}{\mu} - k^2\right)\Phi(z) = 0. \quad \cdots\cdots(13)$$

The components of the displacement (u, v) are found from (4) in the following forms:

$$u = 2B_m \frac{m}{k^2}\, \Phi(z)\, \frac{H_m^{(2)}(kr)}{r} \left.\begin{matrix}\cos\\ \sin\end{matrix}\right\} m\theta e^{ipt}, \cdots\cdots\cdots\cdots(14)$$

$$v = -2B_m \frac{1}{k^2}\, \Phi(z)\, \frac{\partial H_m^{(2)}(kr)}{\partial r} \left.\begin{matrix}\sin\\ -\cos\end{matrix}\right\} m\theta e^{ipt}, \cdots\cdots\cdots(15)$$

When z is taken vertically downwards and $z = d$ is assumed to be the free surface, the boundary conditions at that surface are written by

$$z = d: \left\{\begin{aligned} &\lambda\Delta + 2\mu\frac{\partial w}{\partial z} = 0\,, \cdots\cdots\cdots\cdots\cdots\cdots\cdots\cdots\cdots(16)\\ &\frac{1}{r}\frac{\partial w}{\partial \theta} + \frac{\partial v}{\partial z} = 0\,, \cdots\cdots\cdots\cdots\cdots\cdots\cdots(17)\\ &\frac{\partial w}{\partial r} + \frac{\partial u}{\partial z} = 0\,. \cdots\cdots\cdots\cdots\cdots\cdots\cdots\cdots(18)\end{aligned}\right.$$

From the nature of the problem, (16) is identically satisfied, and (17) and (18) are simply written by

$$z = d: \quad \frac{\partial v}{\partial z} = 0\,, \qquad \frac{\partial u}{\partial z} = 0\,; \cdots\cdots\cdots\cdots(19)$$

and therefore

$$\left[\frac{d\Phi(z)}{dz}\right]_{z=d} = 0 \cdots\cdots\cdots\cdots\cdots\cdots\cdots\cdots\cdots(20)$$

is the only condition of the boundary.

When the distribution of the elastic constants is defined by (2), i.e.

$$\mu = cz \qquad (z = d + z_1), \cdots\cdots\cdots\cdots\cdots\cdots\cdots\cdots(2')$$

the equation (13) can be transformed to

$$z\frac{d^2\Phi(z)}{dz^2} + \frac{d\Phi(z)}{dz} + \left(\frac{\rho p^2}{c} - k^2 z\right)\Phi(z) = 0. \cdots\cdots\cdots\cdots(21)$$

Putting

$$\Phi(z) = e^{kz}\,\Phi_1(z), \cdots\cdots\cdots\cdots\cdots\cdots\cdots\cdots\cdots(22)$$

we get

$$z\frac{\Phi_1^2(z)}{dz^2} + (1+2kz)\frac{d\Phi_1(z)}{dz} + k\left(1 + \frac{\rho p^2}{kc}\right)\Phi_1(z) = 0. \cdots\cdots(23)$$

Writing

$$1+\frac{\rho p^2}{kc}=2\alpha, \quad \cdots\cdots\cdots\cdots\cdots\cdots(24)$$

the appropriate solution of (23) is expressed by

$$\Phi_1(z)=\left\{1-\frac{\alpha}{1.1}(2kz)+\frac{\alpha(\alpha+1)}{1.2.1.2}(2kz)^2-\cdots\cdots\right\}$$

$$={}_1F_1(\alpha\,;\,1\,;-2kz). \quad \cdots\cdots\cdots\cdots\cdots\cdots(25)^{3)}$$

Substituting (22) and (25) in (20), we have

$$\frac{d}{dz}\Big[e^{kz}\,{}_1F_1(\alpha\,;\,1\,;-2kz)\Big]_{z=d}=0, \quad \cdots\cdots\cdots\cdots(26)$$

which is to be written by

$$\frac{d_1F_1(\alpha\,;\,1\,;-2kz)}{dz}+k\,{}_1F_1(\alpha\,;\,1\,;-2kz)=0 \quad \cdots\cdots(27)$$

at $z=d$.

When kd is very small, the solution of (27) is approximately expressed by

$$2\alpha=1. \quad \cdots\cdots\cdots\cdots\cdots\cdots(28)$$

The second approximation gives us

$$2\alpha=1+\frac{1}{2}(kd). \quad \cdots\cdots\cdots\cdots\cdots\cdots(29)$$

The third approximation shows that

$$2\alpha=1+\frac{1}{2}(kd)+0. \quad \cdots\cdots\cdots\cdots\cdots\cdots(30)$$

The fourth approximation gives us

$$2\alpha=1+\frac{1}{2}(kd)-\frac{1}{48}(kd)^3 \quad \cdots\cdots\cdots\cdots\cdots\cdots(31)$$

---

3) E. W. Barnes, *Camb. Trans.*, **20**, 253: H. Lamb, *Proc. Roy. Soc.*, London, **86** (1911), 551.

From (24) and (31), we obtain

$$\left(\frac{p}{k}\right)^2=(2\alpha-1)\frac{1}{k}\,\frac{c}{\rho}$$

$$=\frac{1}{2}\left\{1-\frac{1}{24}(kd)^2\right\}\frac{cd}{\rho}\,.\quad\cdots\cdots\cdots\cdots\cdots(32)$$

If we write the modulus of rigidity at the free surface by $\mu_0(=cd)$, we have

$$\text{Velocity of propagation}=\sqrt{\frac{1}{2}\left\{1-\frac{1}{24}(kd)^2\right\}}\sqrt{\frac{\mu_0}{\rho}}\,,\cdots\cdots\cdots(33)$$

the calculated results being shown in the table below:

kd	0	0·1	0·5	1·0	1·5
Velocity $\Big/\sqrt{\frac{\mu_0}{\rho}}$	0·713	0·713	0·708	0·696	0·679

The components of the displacement are written by

$$\left.\begin{aligned}u&=2B_m\frac{m}{k^2}e^{kz}{}_1F_1(\alpha\,;\ 1\,;-2kz)\frac{H_m^{(2)}(kr)}{r}\left.\begin{matrix}\cos\\ \sin\end{matrix}\right\}m\theta e^{ipt},\\ v&=-2B_m\frac{1}{k^2}e^{kz}{}_1F_1(\alpha:\ 1\,;-2kz)\frac{\partial H_m^{(2)}(kr)}{\partial r}\left.\begin{matrix}\sin\\ -\cos\end{matrix}\right\}m\theta e^{ipt}.\end{aligned}\right\}\cdots(34)$$

In some cases, we have

$$e^{kz}{}_1F_1(\alpha\,;\ 1\,;-2kz)\rightarrow 0 \qquad (35)$$

as $z\rightarrow\infty$, on account of the reason that, in such cases, the value of ${}_1F_1(\alpha\,;1\,;-2kz)$ decays more quickly than that of e^{-kz} as z is increased continuously. Thus the waves written by (34) may have the characteristic of surface waves.

From the expression of (35) it may be noticed that the radial component of the displacement of the waves of the present type quickly disappears as the waves proceed outwards from the epicentre, while the transverse component is transmitted in the manner of the ordinary Love-waves, the azimuthal distribution of the azimuthal displacement being maintained for all radius. It may no doubt be significant on seimology that this kind of waves, in which the vertical displacement and the dilatation do not exist, and the velocity of propagation is different for different wave length, is possible to be transmitted over the free surface whose elastic constant increases continuously along the depth of the body.

21. 彈性が深さに從て變る半無限固體上に傳はる一地震波

地震研究所　妹澤克惟

半無限固體の彈性が其表面からの深さに從て變化する場合に其ダイレテーションと上下の變位とが零になる樣な場合に一種の地震波の存在し得る事を確めた。多少似た場合の研究はマイスナーや愛知博士などによつても行はれて居るけれども、其等は一次元的の問題であり、且つ一般の微分方程式の積分の方法などに於ても可なり違つて居る。さて地震波の性質をよくしらべて見ると波動の進行方向の變位は震央からの距動が遠くなるに從つて急に少くなるけれども、其方向に直角な向の水平變位はそれ程減少せず、普通の二次元傳播の法則に從つて居る事がわかる。又其樣な横變位は震央からの距離に無關係に其割合が保持される事が示されて居る。波動の速度は波長が長くなる程多少は速くなるとはいへ、それ程大きくはならぬ樣である。一體ラブ波の如く違つた物質から成る表面層を特別に置かなくても物質が連續的に變化しさへすればラブ波に似た波の存在し得る事は驗震學上無意味の事とは思はれぬ次第である。

22. Un sismographe accélérométrique et ses enregistrements

par **Mishio ISHIMOTO,**

Institut de Recherches sur les Tremblements de terre.

(Lu le 21 avril 1931.—Reçu le 20 juin 1931.)

1. Introduction.

On sait que les accélérations des secousses sismiques ont un rapport étroit avec les catastrophes; mais les enregistrements accélérométriques des secousses ne sont pas encore réalisés de manière permanente dans les observations sismiques. Actuellement, les estimations de la valeur de l'accélération sont faites suivant le degré de destruction des bâtiments ou de glissement des pierres dans les cimetières.

Les deux ou trois procédés existant pour la mesure directe des accélérations sismiques, ne nous semblent pas encore bien au point pour les observations permanentes. Nous avons déjà publié une étude[1] préliminaire sur la valeur accélérométrique des secousses ainsi que les caractéristiques des ondes ; dans ce cas-là ils sont fait avec des enregistrements optiques. Comme nous l'avons signalé dans ce mémoire, ce procédé d'enregistrement n' a pas été trouvé très commode pour continuer nos observations, d'une part parce qu'il est très couteux et d'autre part parce que les courbes enregistrés ne sont pas assez fines.

Pour enregister les accélérations dans les secousses sismiques, on considère habituellement le déplacement d'une masse d'un système vibratoire dont la période propre est assez courte par rapport à celle de secousses à étudier. On amplifie suffisamment ce déplacement pour apercevoir le passage des secousses enregistrées sur un tambour tournant. L'équation du mouvement sera :

$$M\ddot{y} + 2\,\varepsilon\dot{y} + ky = -M\ddot{x}, \quad \cdots\cdots\cdots\cdots\cdots\cdots\cdots(1)$$

où y est le déplacement relatif de M par rapport au sol et x le déplacement du sol par rapport à l'espace. Posons dans (1) $\frac{2\varepsilon}{M} = 2\lambda$, $\frac{k}{M} = n^2$, et $x = a \sin pt$, on aura

---

[1] M. ISHIMOTO, *Bull. Earthq. Res. Inst.*, 9 (1931), 159.

$$\ddot{y} + 2\lambda\dot{y} + n^2 y = ap^2 \sin pt, \cdots\cdots\cdots\cdots\cdots(2)$$

et on obtient la solution

$$y = \frac{ap^2 \sin(pt - \delta)}{\sqrt{(n^2 - p^2)^2 + 4\lambda^2 p^2}} + \text{terme d'oscillation propre.} \cdots(3)$$

Considérons le cas où n est très grand par rapport à p, on a

$$y = \frac{ap^2}{n^2} \sin pt, \cdots\cdots\cdots\cdots\cdots\cdots\cdots\cdots(4)$$

qui nous montre que le déplacement de la masse est proportionnel à la valeur de l'accélération. Cependant comme ce déplacement reste toujours assez petit, on est obligé choisir un procédé qui poura enregistrer de manière visible les secousses sismiques. Par conséquent il semblait très difficille d'enregistrer les accélérations des secousses par un procédé purement mécanique. Pour cela on utilise le phénomène piézo-électrique ou le changement de capacité électrique d'un diaphragrame métallique bien tendu : mais ces procédés se heurtent toujours à la difficulté de maintenir les appareils dans des conditions favorables aux observations permanentes.

Pour réaliser un sismographe accélérométrique, on remarque d'une part qu'il n'y a presque plus d'ondes sismiques de période inférieure à 0·2 seconde et d'autre part que les ondes sismiques de petite période ne jouent pas un rôle important sur la destruction des bâtiments. Autrement dit, la valeur de l'accélération n'est importante qu'autant que sa période d'oscillation demeure assez longue par rapport à celle des maisons et dans ce cas l'action des secousses sismiques est considéré comme une force statique.

Considérant ces conditions réelles, on peut alors fixer la période propre de l'appareil à 0·15 seconde, période inférieure à celles des secousses sismiques. Quant à la sensibilité de l'appareil, il nous semble qu'il est suffisant d'avoir 1 mm de déplacement à l'extrémité de la plume pour 1 gal d'accélération. Désignons par ξ_m le déplacement maximum de la pointe correspondant à l'accélération $-A \sin pt$ du sol, par T_0 la période d'oscillation propre de l'appareil et par R le rapport d'amplification géométrique ; on a la relation :

$$\xi_m = \frac{T_0^2}{4\pi^2} A{\cdot}R. \cdots\cdots\cdots\cdots\cdots\cdots\cdots\cdots(5)$$

Posons $T_0 = 0{\cdot}15$, $\xi_m = 1$ mm et $A = 1$ gal dans (5), on obtient $R = 175$ qui est réalisable avec une amplification mécanique ; car cet ordre d'amplification est toujours adopté dans un sismographe de haute sensibilité.

Après avoir discuté la grandeur de la masse, le moment d'inertie des leviers et le procédé d'amortissement, la construction de l'appareil a été exécutée dans l'atelier de notre Institut. Puis on a exécuté les étalonnages de l'appareil achevé et il a été installé dans une cave. On a, en effet, réussi à enregistrer un certain nombre de séismes apparus aux environs de Tôkyô. Nous allons alors rendre compte de la construction de cet appareil et des enregistrements obtenus avec.

2. Dimensions de l'appareil.

Il est certain qu'on est tout à fait libre quant au choix des dimensions de l'appareil. On a d'abord une masse oscillant sous l'action d'une force restitutive, dont la période n'est pas sensiblement modifiée par les moments d'inertie des leviers. Certes la grandeur de la masse dépend entièrement de la valeur du moment d'inertie du levier attaché et on peut donc réaliser un appareil comportant une masse relativement petite quand on adopte les leviers très légers.

On a pris un type de pendule représenté dans la Fig. 1, dont le cylindre (M) ayant 27·2 cm de longueur et 7·5 cm de diamètre, pèse 13 kg.

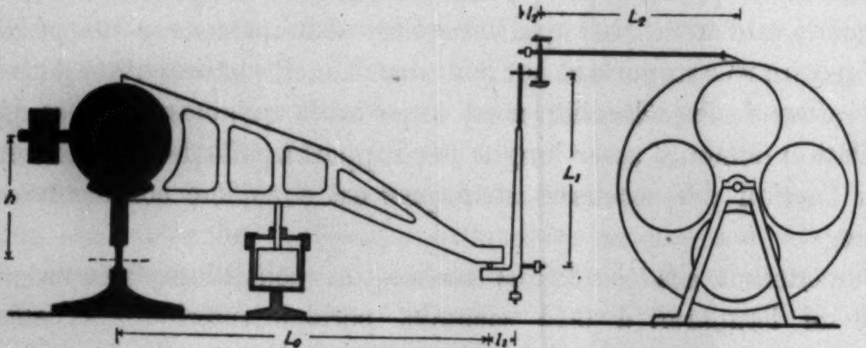

Fig. 1.

Il est tenu verticalement au moyen de deux lames d'acier fixées séparément le long de sa génératrice. En faisant tailler les deux lames, on peut amener la période de ce pendule à 0·15 seconde en la comparant par le procédé de Lissajous à un étalon vibratoire.

Il y a trois leviers qui servent à amplifier le déplacement de la masse : leurs dimensions sont :

leviers	bras inférieur	bras supérieur
1 er	h (9·2 cm)	L_0(28 cm)
2 me	l_1 (2 cm)	L_1(14 cm)
3 me	l_2 (1·5 cm)	L_2(15 cm)

Désignons par y le déplacement de la masse M, par ξ celui de l'extrémité du troisième levier et par θ_0, θ_1 et θ_2 les valeurs de la rotation de chacun des trois leviers, on a donc

$$\begin{array}{ll} y = h\theta_0, & L_0\theta_0 = l_1\theta_1, \\ L_1\theta_1 = l_2\theta_2, & \xi = L_2\theta_2. \end{array} \quad \cdots\cdots\cdots\cdots\cdots\cdots (6)$$

Par suite le rapport d'amplification géométrique totale devient ;

$$\frac{\xi}{y} = \frac{L_0L_1L_2}{hl_1l_2} = 213 \quad \cdots\cdots\cdots\cdots\cdots\cdots\cdots\cdots (7)$$

Les valeurs du moment d'inertie des leviers sont déterminées d'une part par l'augmentation de la période du pendule quand on ajoute le premier levier ; d'autre part par le procédé d'oscillation d'un pendule tortionnel :

$$\begin{aligned} I_0 &= 71500 \text{ c. g. s.} \\ I_1 &= 212, \\ I_2 &= 9{\cdot}8. \end{aligned}$$

Naturellement tous les leviers sont disposés de manière que leurs centres de gravité soient sur les axes de rotation ; autrement les secouses pourraient influer directement sur la rotation des leviers.

3. Equations du mouvement.

L'expression générale de l'équation du mouvement d'un sismographe donné par l'équation (1) sera suffisante, sauf s'il n'y a pas de levier ou de frottement à l'extrémité de la plume. Dans le cas actuel, on est obligé de modifier plus ou moins l'équation (1). Le Prof. S. Ono[2] a déjà donné une série d'équations du mouvement qui sont applicables à des cas plus généraux. Mais comme il n'y a presque plus d'occasions d'utiliser un grand nombre de leviers, il est mieux de limiter les calculs à des conditions simples. On a les équations :

$$\left.\begin{array}{lll} I_0\ddot{\theta}_0 + 2\,k_0\dot{\theta}_0 + n^2{}_0\theta_0 & = & -F_{01}L_0 - Mh\ddot{x}, \\ I_1\ddot{\theta}_1 & = & F_{01}l_1 - F_{12}L_1, \\ I_2\ddot{\theta}_2 \pm k_\xi L_2 & = & F_{12}l_2, \end{array}\right\} \cdots\cdots\cdots (8)$$

---

[2] S. Ono, *Kisyô-syûsi*, [2], **5** (1927), 39.

où F_{01} et F_{12} sont les forces de réaction existant entre les deux leviers consécutifs, k_0 le coefficient dû à un amortisseur spécialement attaché au premier levier et k_ξ le coefficient du frottement mécanique à l'extrémité du troisième levier.

En éliminant F_{01} et F_{12}, et représentant θ_1, et θ_2 par θ_0, on obtient tout de suite l'équation suivante :

$$\left(I_0 + I_1 \frac{L_0^2}{l_1^2} + I_2 \frac{L_0^2 L_1^2}{l_1^2 l_2^2}\right)\ddot{\theta}_0 + 2\,k_0\dot{\theta}_0 + n_0^2\theta_0 \pm k_\xi \frac{L_0 L_1 L_2}{l_1 l_2} = -Mh\ddot{x}.$$

Prenons le cas où k_ξ est négligiable ; on a

$$\ddot{\theta}_0 + 2\,\lambda\dot{\theta}_0 + n^2\theta_0 = -\frac{Mh}{I}\ddot{x}, \quad \cdots\cdots\cdots\cdots\cdots\cdots(9)$$

où $$I = I_0 + I_1 \frac{L_0^2}{l_1^2} + I_2 \frac{L_0^2 L_1^2}{l_1^2 l_2^2}, \quad \lambda = \frac{k_0}{I} \text{ et } n^2 = \frac{n_0^2}{I}.$$

En posant $x = a \sin pt$, on a la solution du mouvement forcé :

$$\theta_0 = \frac{Mh}{I} \frac{ap^2 \sin(pt-\delta)}{\sqrt{(n^2-p^2)^2 + 4\,\lambda^2 p}}, \quad \cdots\cdots\cdots\cdots\cdots(10)$$

où $$\delta = \tan^{-1}\frac{2\,\lambda p}{n^2-p^2},$$

dans le cas où $n >> p$,

$$\theta_{0m} = \frac{Mh}{n_0^2}\,a^2p = \frac{T_0^2}{4\,\pi^2 h}\,ap^2, \cdots\cdots\cdots\cdots\cdots\cdots(11)$$

où T_0 est la période d'un système dont la masse M est concentrée en un point à la distance h de l'axe de rotation. Conséquemment la sensibilité d'un sismographe accélérométrique a toujours la même valeur, que l'on considère ou non le moment d'inertie des leviers qui amplifient le déplacement de la masse.

D'autre part, cependant, il est certain que la période propre de ce système augmente, si on ajoute des leviers comme le montre dans l'équation suivante :

$$\frac{T_0^2}{T_r^2} = \frac{Mh^2}{I} = \frac{Mh^2}{I_0 + I_1 \frac{L_0^2}{l_1^2} + I_2 \frac{L_0^2 L_1^2}{l_1^2 l_2^2}}.$$

On a donc besoin d'une assez grande masse dans un sismographe accélérométrique seulement pour que sa période propre ne varie pas sensiblement par l'adjonction d'un certain nombre de leviers. On peut, donc, réaliser un sismographe accélérométrique avec une petite masse à condition de chercher quelque moyen permettant l'enregistrant avec des leviers très légers.

Alors, on peut diviser I_0 en deux parties ;

$$I_0 = M\left(h^2 + \frac{r^2}{2}\right) + I_0',$$

où la première partie est le moment d'inertie du cylindre et la seconde partie est celui du premier levier ; on peut connaître la première d'après ses dimensions tandis qu'il faut faire une expérience pour connaître la valeur de la seconde. On a, enfin, pour les moments effectifs d'inertie des éléments :

$$\begin{aligned} Mh^2 &= 1{\cdot}100 \times 10^6 \\ M\frac{r^2}{2} &= 0{\cdot}091 \quad ,, \\ I_0' &= 0{\cdot}072 \quad ,, \\ I_1\frac{L_0^2}{l_1^2} &= 0{\cdot}041 \quad ,, \\ I_2\frac{L_0^2 L_1^2}{l_1^2 l_2^2} &= 0{\cdot}167 \quad ,, \\ \hline I &= 1{\cdot}471 \times 10^6 \end{aligned}$$

On a 0·15 s. pour la période d'un pendule comportant un cylindre tenu verticalement par deux lames d'acier et de suite la période réelle sera ;

$$T_r = 0{\cdot}15\sqrt{\frac{I}{M\left(h^2 + \frac{r^2}{2}\right)}} = 0{\cdot}167 \text{ seconde.}$$

Cette période sera convenable pour exécuter nos observations ; en tout cas le troisième levier donne une influence maxima faisant varier la période. On a adopté une tige de paille pour le troisième levier afin de diminuer le moment d'inertie le plus possible : mais il nous a semblé qu'il était presque impossible d'avoir une tige de 15 cm de longneur ayant un moment d'inertie inférieur à 8 c.g. s.

4. Amortisseur.

Pour amortir l'oscillation propre de ce système on met un amortisseur comportant un piston cylindrique plongeant dans une petite cuve remplie d'huile. Naturellement, le coefficient de viscosité varie énormément avec la température ; néanmoins on ne peut pas rejeter ce liquide à cause de cet inconvénient. Quand on adopte un amortisseur à air, on est obligé de réduire l'espace entre le piston et la paroi, et on ne peut empêcher que le contact entre l'un et l'autre ne se produise. Pour cette raison il est mieux d'utiliser une matière visqueuse. On fixe l'amortisseur à peu près au milieu du premier levier. La force d'amortissement γ rapportée à l'unité de vitesse est représentée par,

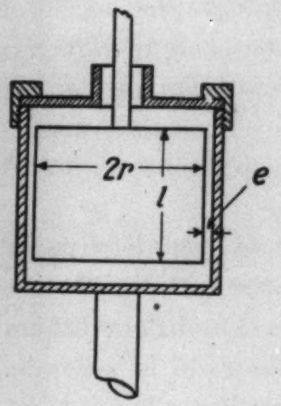

Fig. 2.

$$\gamma = \frac{6\pi l \eta r^3}{e^3}, \text{.................................}(13)$$

où l est la longueur du cylindre, r son rayon, e l'espace entre le cylindre et la paroi et enfin η le coefficient de viscosité de liquide. La condition d'amortissement critique sera,

$$2\left(\alpha \frac{\gamma}{I}\right)^2 = \frac{4\pi^2}{T_r^2}, \text{.............................}(14)$$

où α est le rapport entre la vitesse du piston et celle de la masse. En posant $r=2$ cm, $l=3$ cm, $e=1$ mm, $\alpha=1{\cdot}3$, $T=0{\cdot}16$ s et $I=1{\cdot}47\times10^6$, on peut estimer $\eta=1{\cdot}4$ c. g. s. près qui est une valeur habituelle pour la viscosité des huiles lourdes. En mélangeant du pétrole à l'huile à mécanisme, on obtient un liquide ayant la viscosité exigée. Après cette manipulation on a réussi à amortir le système, comme l'étalonnage exécuté nous l'a fait constater.

5. Frottement de la plume.

Comme l'extrémité du troisième levier glisse sur le papier recouvert de noir de fumée afin d'enregistrer les secousses, il faut considérer le frottement à la pointe ; cela joue un rôle important dans l'estimation du degré de précision des enregistrements obtenus.

La plume est en acier ou en tungustène, ce qui donne une pointe très fine, et un frottement aussi petit que possible. Certes, ce genre de frottement n'est autre que celui dû au contact de deux solides et il augmente à peu près propertionellement avec la pression de la pointe sur le papier, pression due au poids de la plume. Il est, en effet, préférable de la construire légère et cela nous a conduit à exécuter une expérience pour déterminer la valeur du frottement.

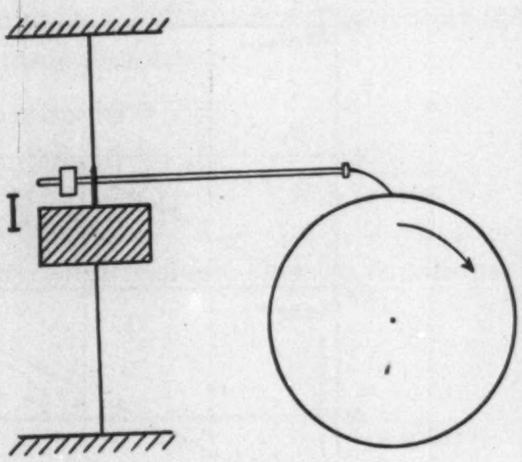

Fig. 3.

Une masse ayant un moment d'inertie (I) peut osciller comme le montre la Fig. 3. On attache à la masse un levier muni d'une plume dont la pointe est destinée à écrire l'oscillation sur le papier enroulé sur un tambour tournant. L'équation du mouvement est :

$$I\ddot{\theta} + n\theta \pm fL = 0, \quad \cdots\cdots\cdots\cdots\cdots\cdots(15)$$

où on prend + pour $\dot{\theta} > 0$, − pour $\dot{\theta} < 0$. La solution de cette équation sera

$$\theta = \left(\theta_0 \mp \frac{fL}{n}\right)\cos\sqrt{\frac{I}{n}}\,t \pm \frac{fL}{n}, \cdots\cdots\cdots(16)$$

et

$$f = \frac{\pi^2 I}{2NT^2L^2}(2a_0 - 2a_N), \quad \cdots\cdots\cdots\cdots(17)$$

où N est le nombre d'oscillations, a_0 et a_N correspondent respectivement à la première et à la N^{me} amplitude. Avec une expérience on peut tout de suite déterminer la valeur de f; mais il y a en général un amortissement visqueux qui nous est indifférent pour notre but et on est obligé de considérer la valeur ultième de l'amplitude comme l'indique la Fig. 4. On prend l'amplitude d'oscillation pourl'abscisse et $2(a_n - a_{n+20})$ pour l'ordonnée. Dans la figure on trouve deux lignes droites dont l'inclinaison représente le degré d'amortissement visqueux qui est constante pour les deux lignes ; tandis que les valeurs ultièmes montrent ceux correspondant aux valeurs de frottement solide de deux plumes ayant des poids différents. Ces valeurs nous montrent que le frottement solide varie sensiblement avec le poids de la plume et enfin on a adopté une plume ayant le coefficient de frottement le plus petit. D'après cela, on a calculé la valeur de f: 0·19 dyne. Quoiqu'elle soit petite, il est necéssaire de considérer cette valeur qui est une cause de flexion des leviers.

L'action de ce frottement réagit sur la masse et la pointe n'enregistra

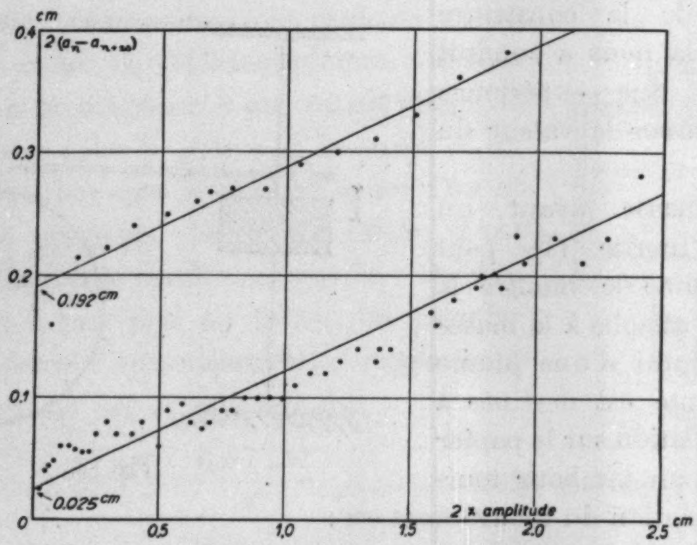

Fig. 4. $T=0{\cdot}714$ s. $I=3580$
$L=15$ cm $N=20$

plus d'accélérations inférieures à cette force. Cette accélération est $A=\dfrac{f}{M}\times 213=0{\cdot}0031$ gal qu'on peut considérer comme négligeable pour le but que nous poursuivons.

6. Flexion des leviers.

Il y a trois leviers dans notre sismographe accélérométrique qui servent amplifier le déplacement de la masse. Comme ils sont constitués par un corps élastique, il se produit des flexions sous l'action du frottement à l'extrémité du troisième levier ainsi que sous celle de rotation non-uniforme des leviers à cause de leur moment d'inertie.

Désignons par α la diminution du déplacement à l'extrémité du troisième levier, due à la flexion des leviers. On peut alors diviser α en trois parties correspondant aux trois leviers.

$$\left.\begin{aligned} \alpha &= \alpha_0+\alpha_1+\alpha_2, \\ \alpha_0 &= F_{01}\,D_0\,\frac{L_1L_2}{l_1l_2}, \\ \alpha_1 &= F_{12}\,D_1\,\frac{L_2}{l_2}, \\ \alpha_2 &= k_\xi D_2, \end{aligned}\right\} \quad \cdots\cdots\cdots\cdots\cdots\cdots\cdots\cdots (18)$$

où D_0, D_1 et D_2 sont les valeurs de la flexion déterminée expérimentalement sur chaque levier et rapportées à l'unité de force ;

$$\begin{aligned} D_0 &= 2{\cdot}5\times10^{-9} \\ D_1 &= 6{\cdot}9\times10^{-7} \\ D_2 &= 1{\cdot}7\times10^{-4} \end{aligned}$$

F_{01} et F_{12} sont les valeurs déterminées définitivement dans les équations (8). On a :

$$\left.\begin{aligned} F_{12} &= I_2\frac{\ddot{\theta}_2}{l_2} + k_\xi\frac{L_2}{l_2}, \\ F_{01} &= I_1\frac{\ddot{\theta}_1}{l_1} + I_2\frac{\ddot{\theta}_2 L_1}{l_1 l_2} + k_\xi\frac{L_1L_2}{l_1 l_2}. \end{aligned}\right\}\cdots\cdots(19)$$

Quand le mouvement de la pointe sera représenté par l'oscillation sinusoïdale, on a

$$\ddot{\theta}_2 = \frac{4\pi^2\xi_m}{L_2T^2}\sin\frac{2\pi}{T}t.$$

Introduisons ces relations dans les équations (18), on obtiendra tout de suite,[3]

$$\begin{array}{rl} \alpha_{0m} = & \dfrac{\xi_m}{T^2}\,26{\cdot}8\times10^{-6}+2{\cdot}45\times10^{-6} \\ \alpha_{1m} = & \dfrac{\xi_m}{T^2}\,11{\cdot}9\times10^{-5}+1{\cdot}38\times10^{-5} \\ \alpha_{2m} = & \qquad\qquad\qquad\quad +3{\cdot}4\times10^{-5} \\ \hline \alpha_m = & \dfrac{\xi_m}{T^2}\,14{\cdot}6\times10^{-5}+5{\cdot}0\times10^{-5} \end{array}$$

D'autre part, on a $\alpha_m=\xi_m-\xi_m'$ où ξ_m' représente le déplacement maximum de l'extrémité de la plume en tenant compte la flexion des leviers ; on a donc

$$\frac{\xi_m'}{\xi_m} = 1-\frac{a}{T}-\frac{b}{\xi_m}, \quad\cdots\cdots\cdots\cdots\cdots\cdots(20)$$

où $a = 14{\cdot}6\times10^{-5}$ et $b = 5{\cdot}0\times10^{-5}$. On représente cette relation dans la Fig. 5 montrant la dimunition de ξ_m rapportée à T. La diminusion de ξ_m ne dépasse pas de 4 pour cent, même dans le cas où $T=0{\cdot}1$ s, $\xi_m = 0{\cdot}1$ mm.

---

[3] nous avons pris k_ξ : 0·2 dyne.

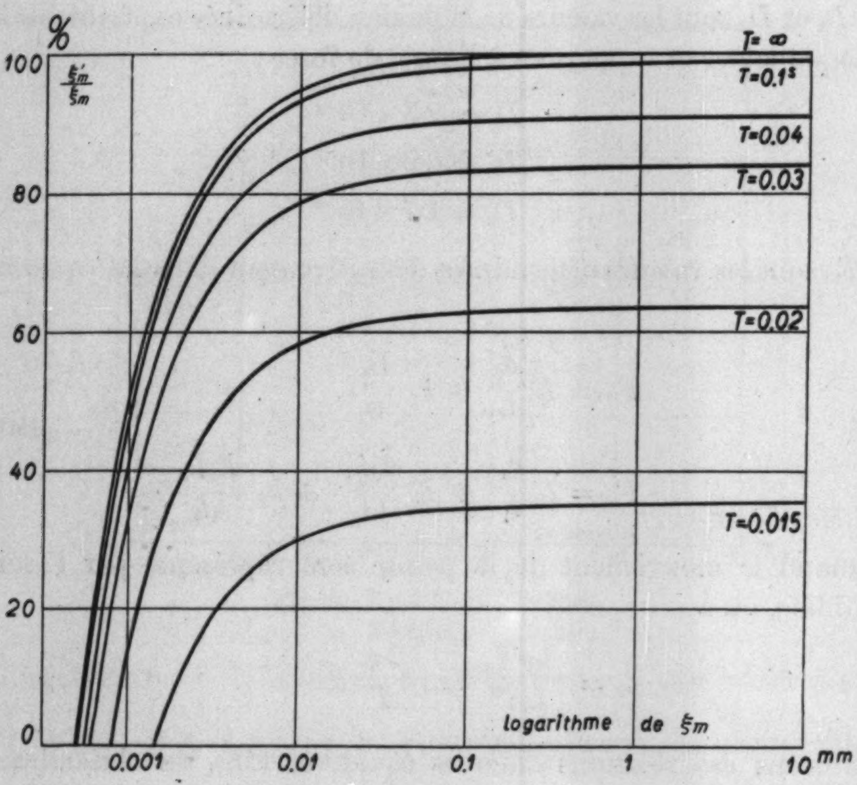

Fig. 5.

Tous les calculs sont faits jusqu'ici suivant l'hypothèse que les forces sinusoïdales agissent comme les forces statiques : ils sont appliquables, cependant, dans le cas où la période d'oscillation des leviers est très petite par rapport aux périodes des secousses sismiques. On a donc exécuté une expérience sur le troisième levier pour connaître sa période propre d'oscillation. Elle était $T = 1{\cdot}06 \times 10^{-2}$ s. qui est assez petite par rapport à celle des secousses sismiques.

7. Montage.

On a construit deux systèmes vibratoires identiques disposés de manière à enregistrer les deux composantes des secousses sur un seul tambour tournant. Le système pour la composante verticale est maintenant en construction et les détails seront publiés dans un prochain mémoire.

Les connections de deux leviers consécutifs sont faites avec beaucoup de précaution pour qu'il n'y a aucun jeu entre eux. Le premier est en contact avec le deuxième par l'intermédiaire d'une petite bille d'acier qui est maintenue pressée entre les deux au moyen d'un petit ressort. Le bras inférieur du troisième levier est constitué par un aimant qui fait un contact par pression avec le bras supérieur du deuxième levier.

Le tambour fait un tour complet en 10 minutes à l'aide d'un moteur synchrone[4] qui fait 300 révolutions par minute ; sa vitesse est, en effet, diminuée par deux étages de vis sans fin. On constate que la vitesse de rotation du tambour demeure assez constante pour qu'on puisse mesurer le temps très exactement sur les enregistrements obtenus. On a 5·65 cm de course par minute à la surface du tambour. La Fig. 6 est une photographie de cet appareil.

8. Etalonnages.

Pour verifier la sensibilité de cet appareil, on a exécuté une série d'étalonnages.[5]

La première expérience consiste à faire agir une force statique : soit une force de pesanteur, soit une force due à l'élongation d'un fil élastique de caoutchouc. Au crochet de la masse, on a attaché un fil de soie transmettant la force de pesanteur par l'intermédiaire d'une poulie ou simplement par la force d'un fil de caoutchouc dont l'élongation pour une force donnée est connue. Les résultats obtenus sont indiqués dans la Fig. 7 : ils nous prouvent que les déviations sont proportionelles à la force appliquée, et on peut donc calculer tout de suite la valeur de l'accélération représentée par les déviations de la plume.

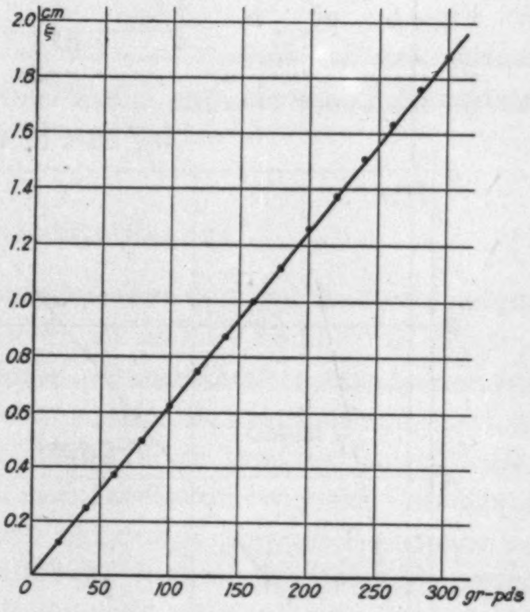

Fig. 7.

---

[4] F. Kishinouye, *Disin*, 2 (1930), 487.

[5] Nous avons exécuté l'étalonnage sur No. 2 dont nous avons mis un petit ressort en contact des premier et deuxième leviers, cela nous a donné un peu de diminution de sa période ainsi que sa sensibilité.

On a alors 1 mm de déviation pour 1·20 gal d'accélération pour No. 2 A d'après la formule suivante:

$$\textit{Sensibilité} \text{ (déviation de plume pour l'unité de l'accélération)} = \frac{mg}{M\xi}$$

La deuxième expérience est exécutée à l'aide d'un fil élastique de caoutchouc dont une extrémité est attachée au crochet, l'autre extrémité du fil étant animée d'un mouvement sinusoïdal d'amplitude constante et de différentes périodes ; ce procédé d'expérience est déjà expliqué dans les mémoires précédents. Une courbe d'après les données est représentée dans la Fig. 8 où la courbe est toujours horizontale dans la

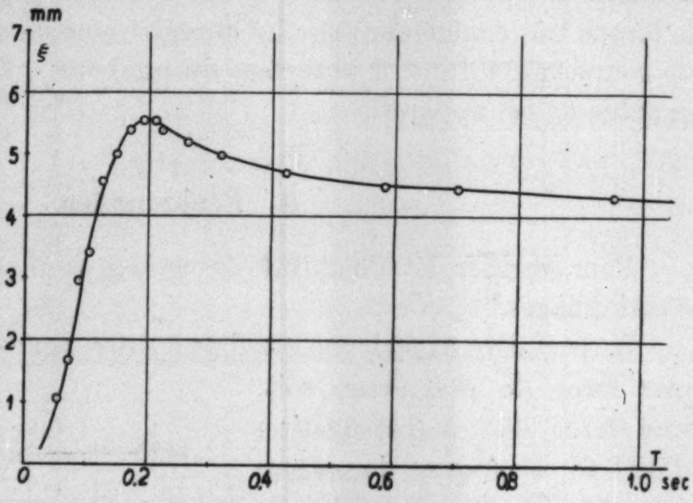

Fig. 8.

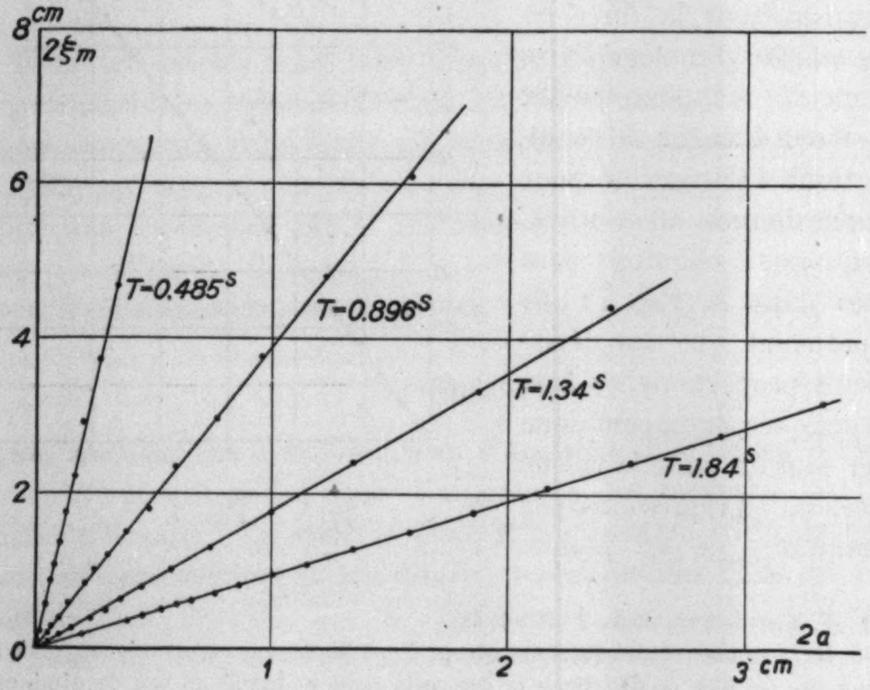

Fig. 9.

région considérée. On constate une diminution brusque de la sensibilité dans la région de période inférieure à 0·2 seconde. Cette caractéristique dépend simplement de ce que le système a une période propre d'une certaine valeur ; une telle relation a été déjà montrée théoritiquement dans un des mémoires précédents.

La troisième expérience a été faite sur une plate-forme oscillante suspendue par quatre montants de bois et le changement de sa période est réalisée en attachant un certain nombre de tiges donnant la force restitutive ; la force est à peu près proportionelle au nombre des tiges. Les résultats obtenus sont montrés dans la Fig. 9. De ces résultats nous pouvons tirer une certaine relation entre ξ_m et T. Pour 10 mm. de double amplitude de plate-forme on a :

$2\xi_m$	T	T^2	$2\xi_m T^2 (=4\pi^2 2a)$
cm	s.		
0·93	1·84	3·39	3·22
1·79	1·34	1·80	3·21
3·96	0·896	0·803	3·13
13·6	0·483	0·233	3·20

où $\xi_m T^2$ est presque constante. Nous avons enfin la sensibilité de cet appareil comme $\xi=1$ mm correspond à 1·23 gal.

9. Enregistrements obtenus.

En installant notre appareil[6] dans une cave de notre Institut pendant quatre mois, on a réussi à enregistrer un certain nombre de séismes dont malheureusement les intensités demeuraient comparativement petites. On a déjà parlé de la comparaison de l'accélération maxima déduite des enregistrements d'un sismographe de type ordinaire à celle obtenue directement par les enregistrement accélérométriques.[7] Constatant qu'il n'y a aucune coïncidence entre eux, on a proposé l'existence de deux sources d'erreurs ; il y a 1° la difficulté de connaître une onde ayant l'accélération maxima ; 2° l'inéxactitude de la rotation du tambour. On a, en effet, été obligé de comparer les ondes l'une après l'autre dans les deux sortes d'enregistrements.

Les trois enregistrements montrés dans les figures 10, 11, et 12 sont les secousses des séismes apparus dans la région de Kantô donnant des secousses perceptibles à Tôkyô. Leurs éléments sont

---

[6] Cet appareil était le premier, et sa sensibilité n'st pas la même que celle du second surlequel on a montré les résultats d'étalonnage.

[7] *loc. cit.*

	Temps d'occurence (1931)	Epicentre[8]	
Fig. 10	mars 25^j 15^h 30^m 36·8^s	E 139°·1	N 36·°2
Fig. 11	„ 27 5 25 35·9	E 140·4	N 35·3
Fig. 12	avril 4 9 16 41·9	E 139·3	N 35·5

Quand on compare les deux enregistrements de même composante, on s'aperçoit que toutes les petites ondes se correspondent l'une après l'autre. Naturellement, on ne peut pas distinguer les ondes dont la période est assez grande dans les enregistrements accélérométriques ; c'est parce que les accélérations des grandes ondes sont toujours petites.

D'autre part, dans les enregistrements obtenus par un sismographe de type ordinaire, les ondes de petite période disparaissent quand les ondes de grande amplitude et de grande période prédominent ; tandis qu'on trouve toujours les ondes de petite période dans les enregistrements accélérométriques. On accepte de ce fait deux sortes d'explications : l'une due au défaut mécanique d'enregistrement du sismographe, l'autre due au fait que les mouvements dus aux grandes ondes masquent les petites ondes. Il nous semble en tout cas que la vraie source du fait sera le dernier.[9] On peut adopter un sismographe accélérométrique pour étudier surtout les petites ondes des séismes ; autrement dit, les études sur les séismes voisins seront mieux exécutées avec un sismographe accélérométrique : car on trouve que ce sont toujours les ondes de petite période qui y prédominent.

10. Remarques.

Nous avons l'intention d'exécuter des observations simultannées sur les séismes avec plusieurs stations munies des sismographes accélérométriques, afin de connaître les caractéristiques des secousses sismiques. On a déjà signalé des caractéristiques des secousses qui sont probablement des conséquences de l'hétérogéniété du milieu où les ondes sismiques se propagent. Il est certain, donc, qu'on peut inversement imaginer que la croûte terrestre est composés de substances diverses ayant des paramètres d'élasticité différents.

---

[8] déterminés par M. C. Yasuda.

[9] Quand on regarde un sismographe pendant un séisme, on apprecoit souvant la plume qui oscille avec deux périodes de mouvements, mais il semble qu'elle écrit seulement les plus grandes ondes.

Des enregistrements d'une seule station, on peut simplement classer les séismes en différents types rapportés à la direction de leurs hypocentres ; mais avec un certain nombre de stations, on peut avancer nos discussions sur les caractéristiques rapportées aux mêmes positions hypocentrales. En tout cas, quand on aura plusieurs enregistrements accélérométriques pour chaque séisme, on pourra aisément tirer quelques faits rapportés à la constitution de la croûte terrestre.

Pour discuter le phémomène de l'influence de l'accélération sismique sur la destruction des bâtiments, il nous faut attendre qu'un séisme assez fort nous permette des observations.

Pour terminer nous voulons exprimer nos vifs remercîments au Professeur K. Suyehiro, directeur de notre Institut, pour l'obligeance avec laquelle il nous a donné des suggestions de valeur et des discussions précieuses.

---

22. 加速度地震計及び其の記象

地震研究所　石本巳四雄

1. 地震の加速度は其の周期より比較的短い周期を有する振動系の重錘の變位を目標として測定する事が出來るが、此の變位は極めて小である事から適當の方法を以て擴大する事が必要である。變位を器械的に擴大する事は困難であるが、地震動として考へられるものの中には 0·2 秒より小な周期を持つものが少ないと云ふ理由の下に振動系の周期も 0·15 秒附近であつて差支へない。今擴大率を 175 とすれば記象上 1 gal の加速度が 1^{mm} に相當する事となり、感度として適當なものとなる。而して此の程度の器械的擴大率は比較的高倍率地震計にも採用されて居る事から實現は可能となる。

2. 考案された加速度地震計の重錘は 13 kg の質量を有し、固有振動周期は約 0·15 秒に保たれて居る。重錘の變位は三つの桿杆によつて 213 倍に擴大される。桿杆の回轉能率は重錘に近きものから夫れ夫れ 71500, 212, 9·8 (c.g.s.) の値を有して居る。

3. 運動の式からすれば加速度地震計の感度は附加した桿杆の影響は無いが其の固有周期が大となつて目的に副はない事となる。即ち重錘の質量を大として周期の大とならぬ方法が講ぜられる一方、桿杆の回轉能率を極度に小にする事によつて質量を比較的小となす事が出來る。

4. 此の振動系の減衰は器械油を使用したピストン型の制動器によつて行はれて居る。油の粘度が溫度によつて多少は變化するが、此れは止むを得ない。

5. ペン先きが回轉圓壔上に振動を記錄するため、此所に固體摩擦がある。摩擦は實驗により測定され、小なるものの一例としては一回毎の振動に對して 0·38 dyne の力が働くと云ふ結果が得られた。

6. ペン先きの摩擦と桿杆に回轉能率とがある事から、振動を記錄する場合に桿杆に撓みが生ずる。此の結果周期の小なるものと振幅の小なるものとに對して影響が大である。此の減少率を實際の桿杆の有する諸量について計算したが、周期=0·1 秒 變位 $\xi_m=0·1^{\mathrm{mm}}$ と云ふ場合でも 4% の減少である事が判明した。

7. 加速度地震計は二つの水平成分を別々に記錄する二つの振動系から成るが、記錄圓壔の回轉は小型同調電動機によつて行はれ、調時上極めて精度のよい結果を與へて居る。

8. 感度試驗は三種類のものが行はれた。第一は重錘に加へられた靜力によるものであるが、結局 1^{mm} の變位が 1·20 gal に相當して居る。第二の試驗はゴム糸によつて周期の異つた振幅の等しい力を重錘に與へて行はれ、其の結果は吾々の要求する範圍においては感度は一定である事が判つた。第三の試驗は振動臺上に器械を設置して行はれた。此の場合何れの周期に對しても殆ど同樣の感度が得られ、1^{mm} のペンの振れは 1·23 gal に相當して居る。

ニ

9. 器械は研究所地下室に設置して四ケ月間の觀測がなされたが、此の期間には比較的小さな地震の發生のみであつた。今村式50倍地震計と比較すると加速度記象は比較的小周期の波動のみを記錄するに反し、變位記象中には別に大周期の波が多分にする存事が判つた。後者においては大周期の波が小周期の波を隱蔽する傾向があるため、兩者の間に大なる隔絕を生ぜしめる如くであるが、其れは外觀上の問題と思はれる。大周期の波動に隱蔽されない部分においては明かに小周期の波動が一波毎に相當せしめる事が出來る事から見ても明かであらう。近地地震は多く小周期の波動を多分に有して居る事から、加速度地震計を以て記象せしめる方が有利である。記象が各震源方向に對して同一でない事は地震波の通過する地殼において彈性不均一の存在する結果と考へられる。

10. 加速度地震計を各地に設置する時は其等の記象から地殼の不均等狀況を推察し、又地殼構造に對して何等か研究が進められると期待される。家屋の破壞と加速度との問題に關しては適當な地震を待つ外はない。

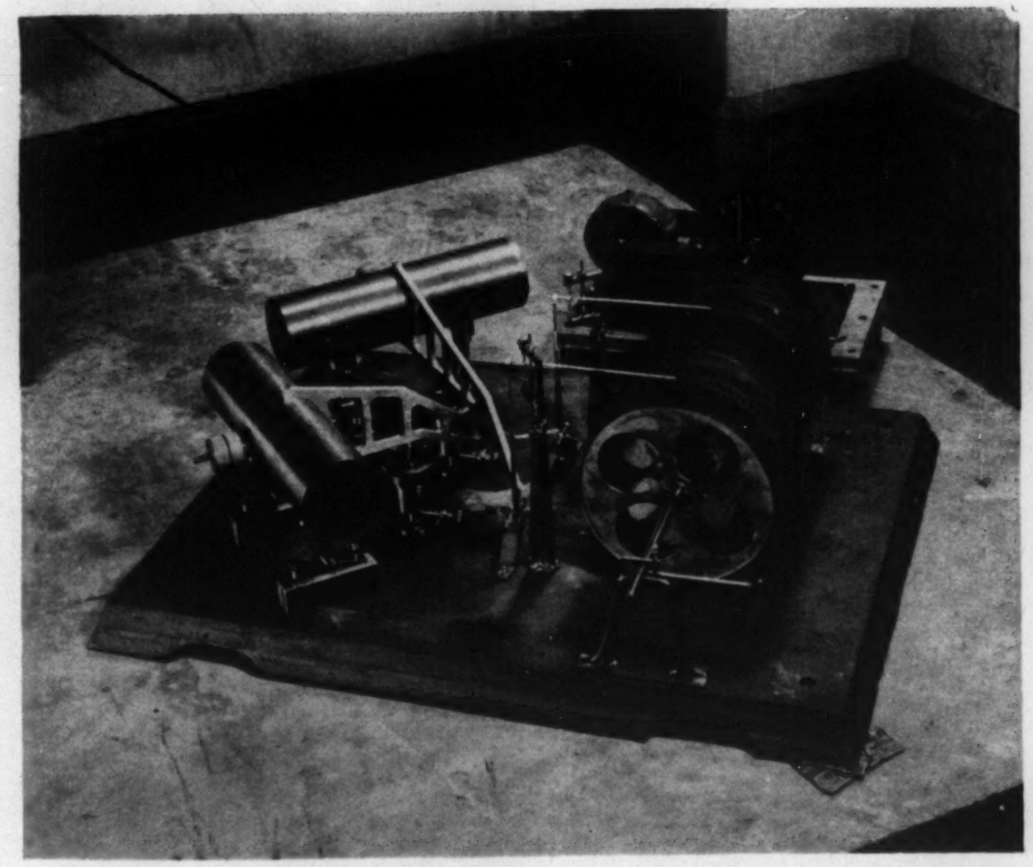

Fig. 6. Vue générale du Sismographe accélérométrique. Masse: 13 kg. Amplification géométrique: 213. Sensibilité 1 ^{mm} sur l'inscription≡ 1·23 gal. Période propre de l'oscillation: 0·15 s.

（震研彙報、第九號、圖版、石本）

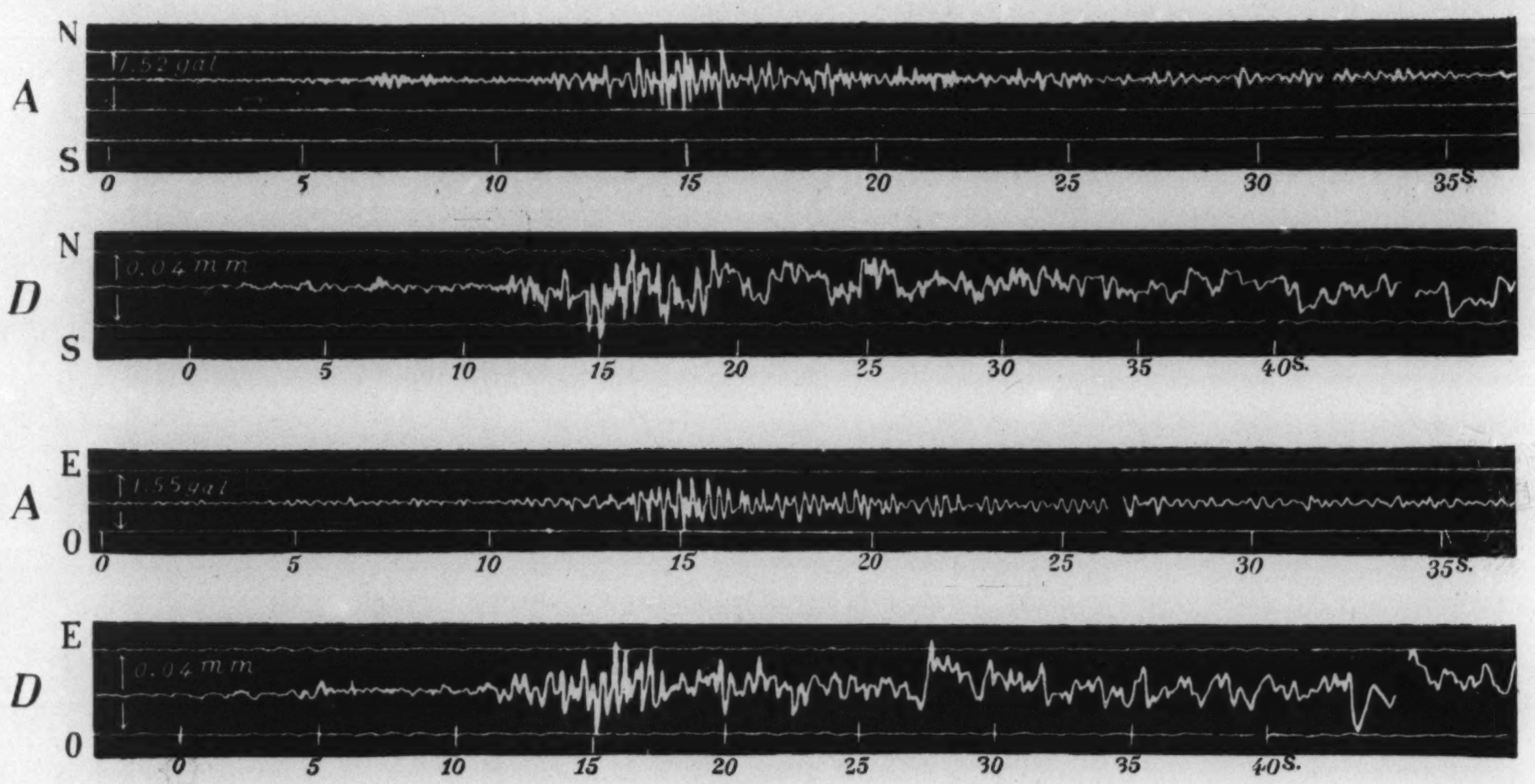

Fig. 10

Temps d'occurence: 26 mars 1931, $15^h30^m36{\cdot}8^s$ Epicentre: près de Maebasi E 139°·1 N 36°·2
A: Inscription accélérométrique; D: Inscription par le déplacement.

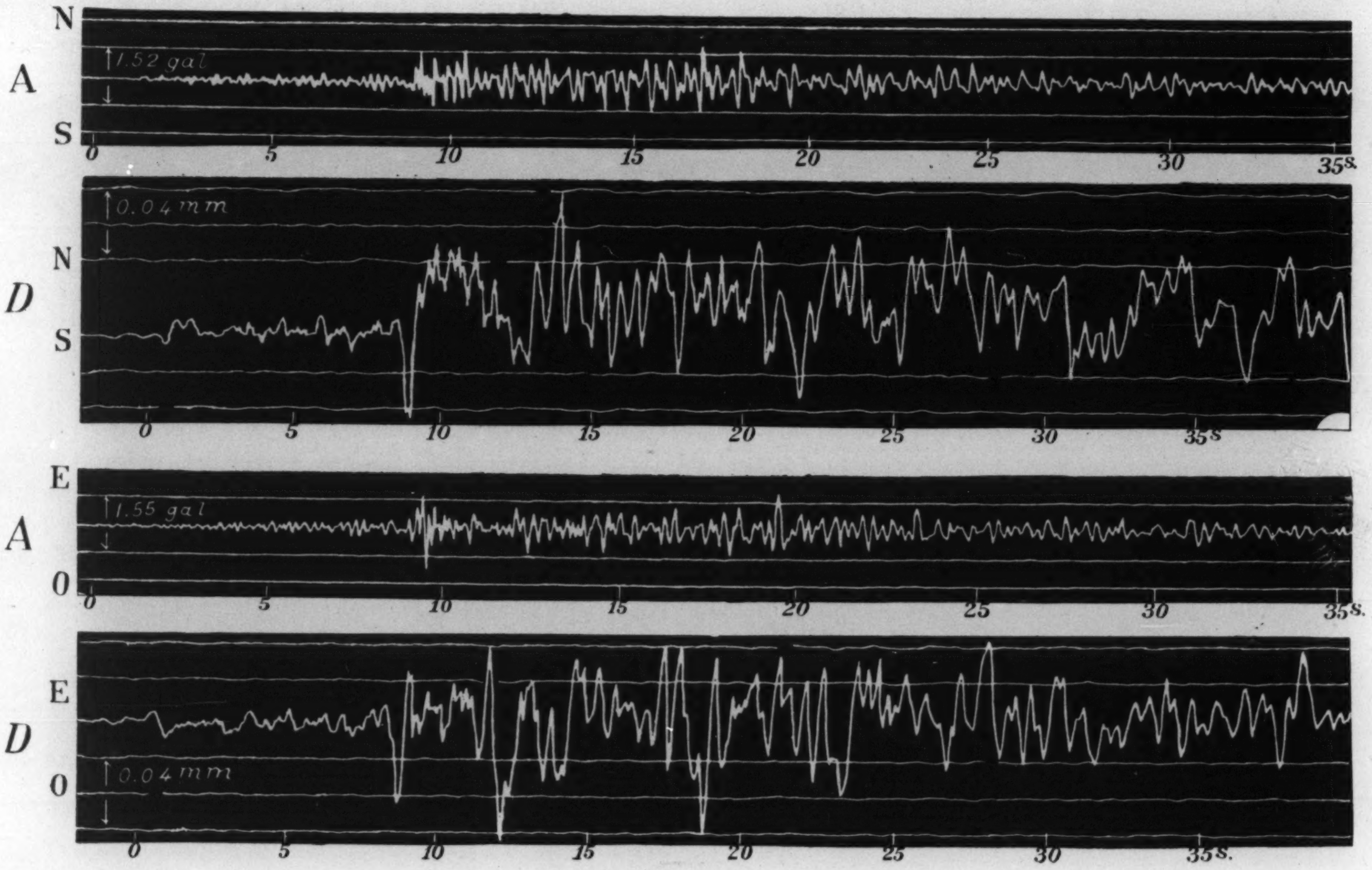

Fig. 11.

Temps d'occurence: 27 mars 1931, $15^h25^m35{\cdot}9^s$ Epicentre: près d'Itinomiya E 140·°4 N 35·°3
A: Inscription accélérométrique; D: Inscription par le déplacement.

（震研彙報、第九號、圖版、石本）

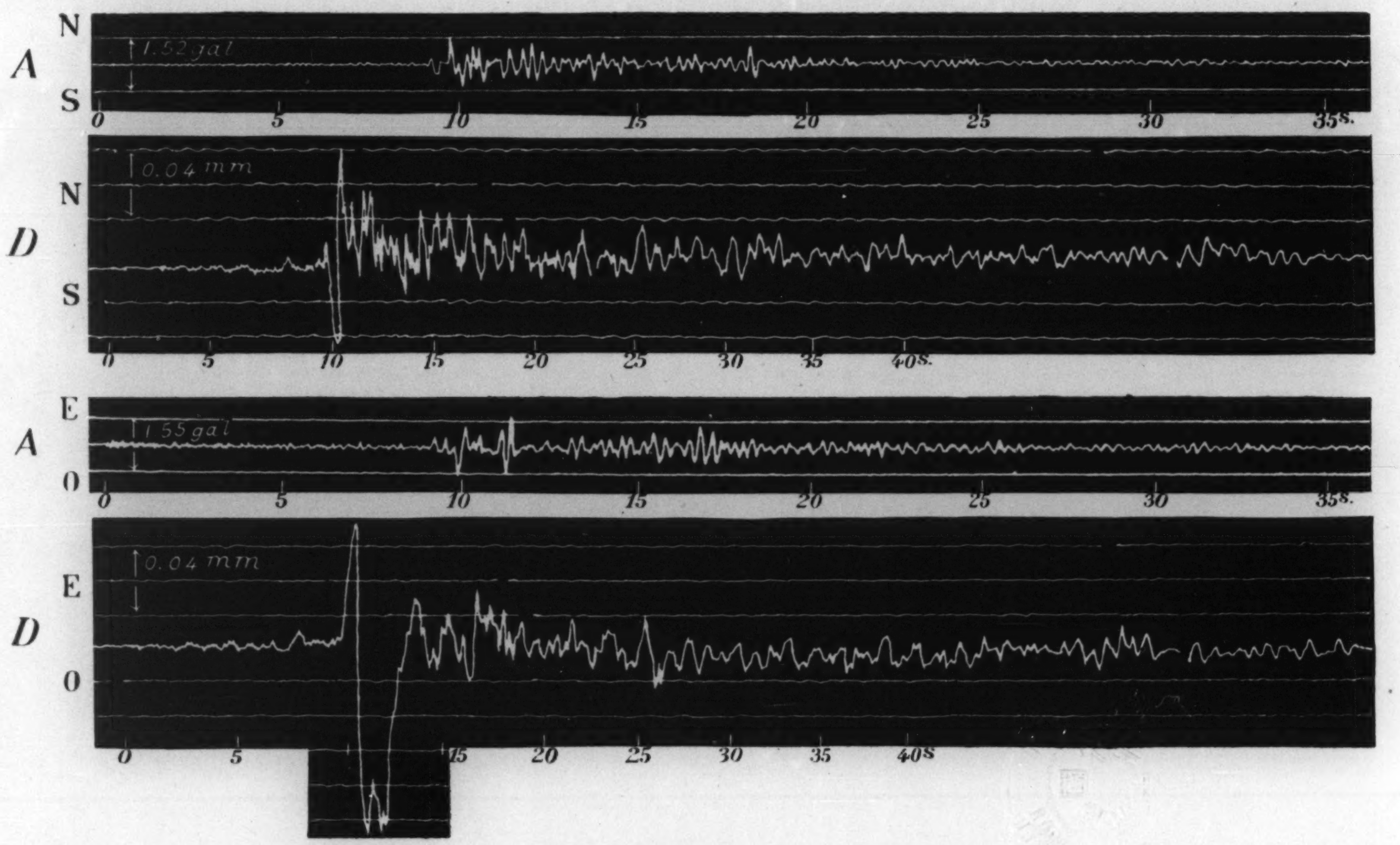

Fig. 12.

Temps d'occurence: 4 avril 1931, $6^h16^m41{\cdot}9^s$ Epicentre: près de Kawasaki E 139·°8 N 35·°5
A: Inscription accélérométrique; D: Inscription par le déplacement.

23. *Geological Growth of the Tôkyô Bay.*

By **Hisakatsu YABE**,

Earthquake Research Institute.

(Read May 19, 1931.—Received May 17, 1931.)

The Tôkyô Bay is a rectangular depression in the Kwantô tectonic basin,[1] with an extension of 50 km. from north-east to south-west and 30 km. from north-west to south-east. Its four borders are more or less irregular; while the major irregularities are due to prograded deltaic deposits of the Sumida-gawa, Rokugô-gawa and several other rivers as well as to the sand spit of Futtsu, minor ones are the consequence of a land-submergence of 150± m., thereby the depression of the Tôkyô Bay and the ancient valley anteceding the Uraga Channel being invaded by transgressing marine water. This submergence of land was followed by an emergence of at most 20 m. The outline of the Tôkyô Bay with rectilinear borders suggests its tectonic origin; it is probably controlled by faults in two systems, one of NE-SW trend and the other of NW-SE. It may also deserve our attention that all the large swamps and lagoons (Tega-numa, Imba-numa, Kasumiga-ura and Kita-ura), dependent to the drainage system of the Tone-gawa, are situated on the north-eastern extension of this depressed zone.

The higher, Tama-, and the lower, Musashino-terraces[2] into which the plateau-surface of the Kwantô tectonic basin is divided are arranged in discordance with the area occupied by the Tôkyô Bay; this fact is a remarkable testimomy to the essential youth of the Tôkyô Bay, suggesting that its foundering dated later than the building of the two terraces, or in other words, later than the tectonic movements which led to the building of the Kwantô basin by basin-shaped uplift of the marine Narita Series; or more correctly, it may be considered as an episode of a later date intervening this long continued tectonic movement which gave rise to the Tama- and Musashino terraces. Perhaps it was also anteceded by the deposition of the Kwantô loam upon the surface of the two terraces.

---

[1] H. Yabe and R. Aoki, "The Great Kwantô Earthquake of September 1, 1923, Geologically Considered," *Ann. Rep. Saitô Gratitude Foundation*, No. 1 (1926).

[2] R. Aoki and R. Tayama, "Topography and Geology of the Kwantô Tectonic Basin with Special Reference to Its Western Border," *Saitô Gratitude Foundation, Scientific Report*, No. 8 (1930), (in Japanese).

Hence the Tôkyô Bay is not a relic sea of the older, Palaeo-Tôkyô Bay,[3] in which the marine sediments of the Narita Series are thought to have been deposited.

The Tôkyô Bay is shallow, not exceeding 60 m. in depth; the basin was in terrestrial condition before the land submergence referred to above, as indicated by the drowned valley in the Uraga Channel.[4]

The Uraga Channel is zigzag-shaped, parallel-sided and 10 km. broad on the average; its floor gently descends from 60 m. at the north to 80 m. at the south, and has a drowned valley running lengthwise on its floor. There is no trace of the Tama- and Musashino-terraces fringing the periphery of the channel, and it has in common with the outer sea and the Tôkyô Bay only the coastal topography of the last land-submergence and raised-beaches telling younger, the last emergence.

The silt beneath the soil of the Downtown of Tôkyô is an estuarine deposit of the time of the last land-submergence, later uplifted; it occasionally contains numerous mollusca characteristic of a muddy bottom, as that once excavated at Yûraku-chô, Kôjimachi-ku[5]; it is a kind of bay-head deposits in drowned valleys, and contemporaneous deposits of similar nature occur also along the both sides of the Uraga Channel, for instance, at Uraga on the west side and Minato on the east. The molluscan fauna of these raised beaches does not essentially differ in its constitution from the recent one living in the Tôkyô Bay under the same physical condition.

The contemporaneous raised beaches exist not only along the Sagami Bay coast of Sagami and the Miura Peninsula, and around the Bôsô Peninsula outside the Uraga Channel, but also almost everywhere around the Japanese Islands where they were not destroyed by later abrasion, either marine or subaerial; there are primarily absent only where a local crustal disturbance caused the shifting of the strand line more in opposite sense, as, for instance, in the southernmost part of the Kitakami Mountainland and in the Matsushima-Shiogama district.[6]

---

[3] In Ôiso block, Miura and Bôsô Peninsulas, the grouping of the strata shows that we are dealing with the surviving remnants of the late Neogene range that ran along the northern border of the present Sagami-nada and crossed the Uraga Channel; this horst mountain struck farther south-south-eastward into the Pacific. The crust-block sunken north of it converted into a bay, open to east and south-east; for this Pleistocene bay, the name Palaeo-Tôkyô Bay was proposed by me many years ago. H. YABE, "Bôsô Peninsula" *Gendai no Kwagaku*, 2 (1914), No. 4, (in Japanese).

[4] H. YABE and R. TAYAMA, "On Some Remarkable Examples of Drowned Valleys found around the Japanese Islands," *Records Oceanogr. Wks.*, Japan, 2 (1929), No. 1.

[5] G. YAMAKAWA, "Alluvial Mollusca from Yûraku-chô," *Jour. Geol. Soc.*, Tôkyô (1909), (in Japanese).

The raised beaches constitute one particular group of terraces which are geologically the youngest ones among the so-called "Post-Kwantô loam terraces" of Messrs. R. Aoki, and R. Tayama,[7] and may hereafter be called "the 15 m. beaches" for the sake of brevity, though their altitude much differs from place to place and ranges usually from less than 5 m. to 20 m. in the Kwantô region.

One of the "15 m. beaches", which is the most instructive of all, is the coral bed, or more correctly coral reef, of Noma near Tateyama and along the Tateyama-wan, in the province of Awa, where an alluvial plain has its surface some 20 m. higher than the present sea-level. As shown by many excavations at Okanoma and several other places near by, there is in a more or less extended distribution an incipient fringing reef of reef-building corals beneath the alluvial silt, which had once grown in drowned valleys, cut into Neogene rocks, at the time of the last land submergence, referred to above.

The semifossil reef is about 2–3 m. thick and consists of coral heads or stocks in upright position, the basal ones of which attach directly to the rock-floor, Neogene tuffs of the Miura Series, or to angular or subangular blocks of the same rocks torn off from the very floor and rolled.

Other common organic remains in association with these corals are thick-shelled mollusca, all found in fresh condition, not seldom with colour pattern and bivalves having both valves usually intact. The corals are likewise well preserved, even delicate spinules of septal margin usually showing no trace of damage. Worthy of special note is further the circumstance that there are almost no rolled pieces of coral stocks around the reef; at least these were not seen in an excavation of Okanoma which I had an opportunity personally to examine a score of years ago, and in another one very recently prosecuted by members of the Institute of Geology and Palaeontology, Tôhoku Imperial University. All these facts seem to support the view that we have here an incipient fringing reef grown in a rather calm water immediately after the land submergence.

---

[6] H. Yabe, "Excursion to Matsushima and Sendai; Geological Guide," Guide-Book, Excursion C 3, published by the Pan-Pacific Science Congress, 1926.

[7] R. Aoki and R. Tayama, *op. cit.* R. Tayama, "Topography of the Bôsô Peninsula, with Special Reference to the Correlation of Abrasion Planes," *Saitô Gratitude Foundation, Scientific Reports*, No. 9 (1930), (in Japanese).

There is a divergence of opinions as to the geological age of the Noma coral reef. Dr. M. YOKOYAMA at first maintained the Pleistocene warm age instead of glacial in Japan on the evidence of this formation, but later assigned it to the youngest Pleistocene.[8] In my opinion it is early Holocene as already expressed elsewhere.[9] Mr. T. KURODA of the Institute of Geology and Mineralogy, Kyôto Imperial University, verbally communicated me that the molluscan fauna of the semifossil reef of Noma is similar to the recent one living in the adjacent warm water. The question of the geological age of the coral reef is intimately related to the larger problem how to mark the Pleistocene-Holocene boundary in the Japanese Islands, where we have no trace of past glaciation else than scanty small cirques on the high peaks of the Hida-Shinano Mountains or the so-called Japanese Alps[10] and the Hidaka Mountains of Hokkaidô. The topographical relation of these cirques to the valley-terraces in the mountains and that of the latter to the Tama and Musashino terraces have not yet been thoroughly studied by any of us, though these are topics of our keen interest.

In this connection, very interesting is a comparison between the British Islands (especially of non-glaciated areas) and the Japanese Islands as to the change of sea-level and climate during the latest Cenozoic. Our 15 m. beaches and terraces may approximately correspond to the so-called Neolithic beaches of the British Islands and the stage of land-submergence preceding to the emergence has its exact copy in the land-submergence by which the stage of the Neolithic beaches is separated from the so-called Forest stage, while the Forest stage seems to found its counterpart in the time during which our Tama and Musashino terraces were formed. Then the best way from the stand-point of diastrophism is, I think, to mark the dawn of the Holocene with the last land-submergence in the Japanese Islands, as already definitely stated by me several years ago.[11] So far as I am now aware, all the neolithic human sites and shell mounds in the Kwantô region with dressed and polished stone implements as well as potteries are situated on the 15 m. beaches and terraces or on the Kwantô loam covering the Tama- and Musashino-terraces.

---

[8] M. YOKOYAMA, "Climatic Changes in Japan since the Pliocene Epoch," *Jour. Coll. Sci. Imp. Univ.*, Tôkyô, 32 1911), Art. 5 M YOKOYAMA, "Mollusca from the Coral-Bed of Awa," *ibid.*, 45 (1924), Art. 1.

[9] H. YABE and R. AOKI, "A Summary of the Stratigraphical and Palaeontological Studies of the Cenozoic of Japan, 1920 to 1923," *Proc. Pan-Pacific Sci. Congr.*, Australia (1923).

[10] N. YAMASAKI, "Glaciation of the Hida Mountains," *Geol. Soc.*, Tôkyô, 21 (1 14), (in Japanese). K. ÔSEKI, "Some Notes on Glacial Phenomena in the North Japanese Alps," *Scot. Geogr. Mag.*, 31 (1915).

Finally it remains to settle the relative antiquity of the depression of the Tôkyô Bay and the building of the older terraces of the " Post-Kwantô loam terraces ", because the latter, like the former, is a geological event preceding the last land-submergence. An answer to this question can be obtained by a glance of the terrace map of the northern part of the Bôsô Peninsula by Mr. R. TAYAMA,[12] which distinctly shows that the older terraces of the " Post-Kwantô loam terraces " are nearly conformant in their areal distribution with the present drainage system of the district, fringing even small, apparently young side-valleys. Hence there is almost no doubt about that the older terraces of the " Post-Kwantô loam terraces ", like the younger ones, are of the later origin than the depression of the Tôkyô Bay, at least in this district now we specially concern, though of course it is never the truth to say that every one of the terraces of this category has the same history, because we have good reason to believe that the emergence of land was continuously in progress in the Kwantô basin as before as after the foundering of the Tôkyô Bay, and the possibility is by no means excluded that some of the terraces are decidedly of an earlier date.

Summary.

From the foregoing remarks it appears reasonable to subdivide the Shikishima Period (the Japanese Pleistocene + Holocene)[13] by the use of various diastrophic criteria in the following way, in so far as the Kwantô region is concerned.

---

[11] H. YABE and R. AOKI, " A Summary of the Stratigraphical and Palaeontological Studies," *loc. cit.*

[12] R. TAYAMA, " Topography of the Bôsô Peninsula," *loc. cit.*

[13] H. YABE and R. AOKI, " A Summary of the Stratigraphical and Palaeontological Studies," *loc. cit.*

1. Land submergence in the early Shikishima Period and the deposition of the marine Narita Series in the Palaeo-Tôkyô Bay on the submerged land surface called by YABE the Pre-Narita and believed to be equivalent to the Pre-Tama of Messrs. AOKI and TAYAMA.[14]

2. Land emergence, elevating the Narita Series above the sea level; subaerial denudation and the building of the Tama terraces.

3. Crustal disturbance as indicated by the different behaviours of the Tama and Musashino terraces.

4. Land emergence and subaerial denudation continued; building of the Musashino terraces.

5. Deposition of the Kwantô loam upon the surface of the Tama and Musashino terraces.

6. Land emergence and subaerial denudation continued; depression of the Tôkyô Bay and building of the older ones of the "Post-Kwantô loam terraces".

7. The last land submergence; giving rise to the drowned valleys of the higher level[15]; the deposition of the sediments of the 15 m. beaches and terraces; growth of the Noma fringing reef. Early Holocene.

8. The last land-emergence; building of 15 m. beaches and the other terraces of the younger group of the "Post-Kwantô loam terraces".

23. 東京灣の出現

地震研究所 矢部長克

今日の東京灣の占むる地域は、其の輪廓より窺ふに、北西—東南及び北東—西南の二組の地質構造線の間に挾まれたる沈下地塊の如し。然して此の沈下は青木及田山兩氏の多摩及び武藏野臺地の形成後にして且つ後關東ローム段丘の內、新期のものに先んず。此れ東京灣盆地の出現の時期にして此の盆地が海水の浸す所となりたることは上述最後の段丘の一種たる十五米隆起汀線海成堆積層の示す陸地沈降卽ち海浸の時期なり。

此の日本群島最近地史の上に著るしき陸地沈降及び上昇は英群島の所謂ネオリシツク、、ビーチの示す水準變化と全く其の軌を一にして又同時代のものなるべし。

---

[14] R. AOKI and R. TAYAMA, "Geology and Topography of the Kwantô Tectonic Basin," *loc. cit.*

[15] H. YABE and R. TAYAMA, "On Some Remarkable Examples of Drowned Valleys," *loc. cit.*

成田層堆積當時に於ては、箱根の北より大磯地塊、三浦及び房總兩半島を連ぬる東西趨向の山地又は丘陵地ありて、其の北に成田層の沈積を見たる一大海灣あり。東及東南太平洋に開く。然して上記の事實より現在の東京灣は此の所謂古東京灣とは全く別個の成生に係り前者は後者の遺跡ならざるを知る。

24. *Early Pliocene Crustal Movement in the Outer Zone of Southwest Japan and in the Naumann's Fossa Magna.*

By **Yanosuke ÔTUKA,**

Earthquake Research Institute.

(Read June 16, 1931.—Received June 20, 1931.)

The object of this communication is to describe an interesting structural feature of the lower Pliocene strata in the Outer Zone of Southwest Japan[1] and in the Naumann's Fossa Magna.[2]

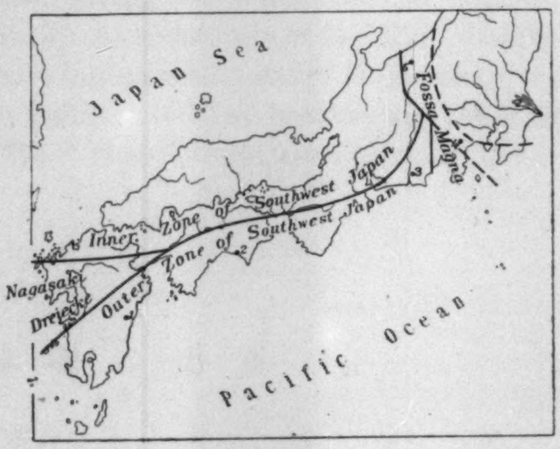

Fig. 1.

The areas dealt with are plotted on the accompanying index map (Fig. 1); these are:—

1. The northeastern part of Miyazaki prefecture, along the southeastern coast of Kyûsyû.
2. The eastern part of Kôti prefecture along the Tosa bay.
3. The Kakegawa district, west of Siduoka.
4. The Asigara district, adjoining to the north of the volcano Hakone.
5. The Nagano prefecture.

The first three districts of the above list are sited in the Outer Zone of Southwest Japan and the latter two are in the Fossa Magna.

---

[1] Dr. H. Yabe divided the southwest Japan into two parts, the inner or northern side and the outer or southern side, with his median dislocation line, which is the boundary line between the Izumi sandstone and gneiss on one side and the crystalline schists and the lower Chichibu series on the other.

[2] The term "Fossa Magna" was proposed originally by E. Naumann to the transverse divisional zone between the southwest Japan and the northeast Japan. Western border of the Fossa Magna is the Itoigawa-Siduoka line of Dr. H. Yabe.

1. The northeastern part of Miyazaki prefecture, along the southeastern coast of Kyûsyû.

The northeastern part of Miyazaki prefecture is built up of Mesozoic deposits, of which the precise geological age is still unknown, porphyrite, older and younger Tertiary and Quaternary in ascending order.

Dr. T. Iki[3] who first studied the geology of this district gave some accounts of the younger Tertiary in his explanatory text to the geological map of Japan, 1 : 200.000, the Sadowara sheet, 1896, published from the Imperial Geological Survey. Later Dr. H. Yabe[4] made a reference to an *Operculina*-rocks in Japan, and Dr. M. Yokoyama[5] published in 1928 the result of his thorough study of fossils collected by Mr. T. Kobayashi from the formation, thereby describing 119 species. The following accounts of the younger Tertiary formation of this district is an outcome of my field work carried on late in the spring of 1930.[6]

The area occupied by Neogene strata is a dissected raised coastal plain, called the Hyûga coastal plain, drained by the rivers Omaru and Hitotuse ; it is trianguler in outline, bounded by the Hyûga-nada (Hyûga sea) coast on the east and Osuzu mountainland and Higasimorogata mountainland on the other two sides.

The general sequence of the younger Tertiary deposits as observed between the Omaru and Hitotuse is as follows, in descending order :

Takanabe group { Heki beds
Kôonzi beds
Sadowara beds

Tuma group

The Takanabe group which occupies the eastern portion of the area (Fig. 2) is divisible into Heki beds, Kôonzi beds and Sadowara beds. The upper member, Heki beds, is essentially gray sandy mud, intercalating two pumiceous zones and sometimes enclosing calcareous nodules : there are many fossiliferous zones in this complex. The Kôonzi beds consist of mud and silt in thin-bedded alternation and have fossiliferous zones. The Sadowara beds consist of barren sand and mud in the northern part of the area, which gradually pass into brown fine grained conglomerates in the southern part of the area; an archætypal *Stegodon* reported by Dr. Yokoyama[7] is from the latter.

---

[3] T. Iki, *Expl. Text Geol. Map Japan*, " Sadowara " Sheet, 1: 200.000, (1904).

[4] H. Yabe, " Notes on *Operculina*-Rocks from Japan, with Remarks on *Nummulites cumingi* Carpenter ", *Sci. Rep. Tôhoku Imp. Univ.*, II ser., **5**, 1 (1918).

[5] M. Yokoyama, " Pliocene Shells from Hyûga ", *Jour. Fac. Sci. Imp. Univ.*, Tôkyô, Sect. II, **2** (1928), 331–350.

[6] Y. Ôtuka, " Some Geologic Problems in the Southwestern Coast of Kyûsyû ", *Georg. Rev.*, Japan, **6**, 7 (1930), (in Japanese).

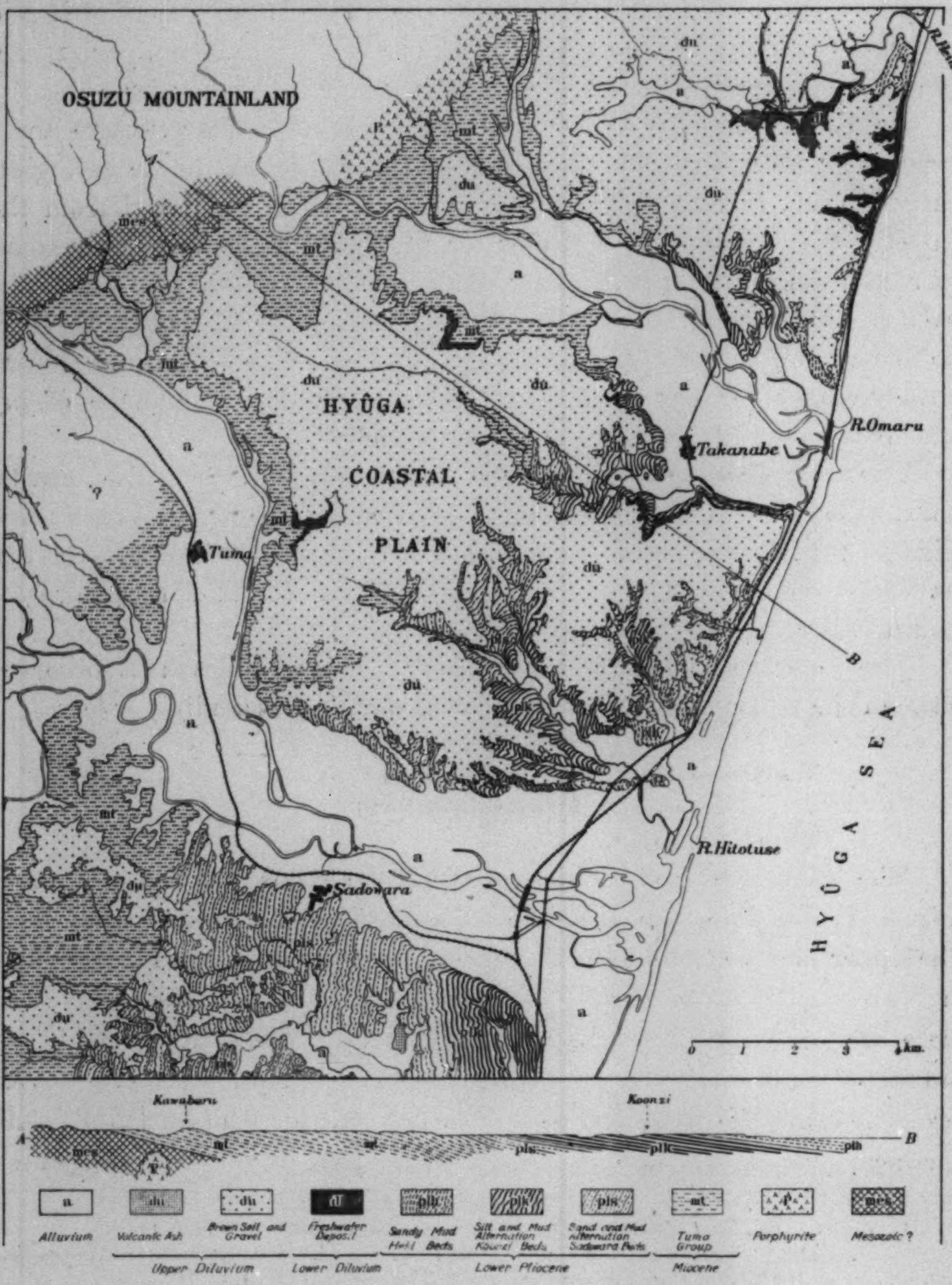
OSUZU MOUNTAINLAND
HYÛGA COASTAL PLAIN
Takanabe
R.Omaru
Tuma
Sadowara
R.Hitotuse
R.Heida
HYÛGA SEA
0 1 2 3 4 km.
Kawabaru
Koonzi
A
B
a
du
dl
plh
plk
pls
mt
P
mes
Alluvium
Volcanic Ash
Brown Soil and Gravel
Freshwater Deposit
Sandy Mud Heil Beds
Silt and Mud Alternation Koonzi Beds
Sand and Mud Alternation Sadowara Beds
Tuma Group
Porphyrite
Mesozoic ?
Upper Diluvium
Lower Diluvium
Lower Pliocene
Miocene

Fig. 2. Geological Map of Hyûga Coast by Yanosuke Ôtuka.

---

[7] M. YOKOYAMA, "*Stegodon* from Uryûno, Miyazaki Prefecture", *Jour. Geol. Soc.*, Tôkyô, 20 (1913), 236, (in Japanese).

Of numerous species of the fossil shells found in the Takanabe group, *Anadara satowi castellata* (Yokoyama), *Glycymeris nakamurai* Makiyama, *Pecten* (*Amussiopecten*) *praesignis* Yokoyama, *Venericardia panda* (Yokoyama), *Umbonium suchiense* Yokoyama, *Umbonium suchiense subsuchiense* Makiyama, *Umbonium mysticum* Yokoyama, *Clavatula dainichiensis* Yokoyama, *Latrunculus eratus* (Yokoyama) etc., are specially worthy of note, because of their being also common and characteristic species of the lower part of the Kakegawa series of Dr. J. Makiyama,[8] to be mentioned later on.

The older, Tuma Group, which occupies the western part, consists of unstratified thick dark gray muds in its upper part and stratified sands in the lower. It covers the older basement complex in clinounconformity with its base on the west almost coinciding with the topographic boundary between Osuzu mountainland and the Hyûga coastal plain.

The structural arrangements of these younger Tertiary complexes are regular, having the strike varying from N 20° E to N-S and hence generally parallel to the shoreline of the plain and the dip about 10° NE or E: the general strike and dip, however, are sometimes affected by local foldings or other disturbances. Freshwater deposits, presumably of the lower Pleistocene age, rest horizontally upon these groups in a few isolated patches. Fig. 2 is a map showing the geologic structure of this district and a profile on the line AB, which is normal to the general trend of the younger Tertiary.

2. The eastern part of Kôti prefecture along the Tosa bay.

The first geological survey of this district was prosecuted by Dr. T. Ogawa[9] and the late Y. Ôtsuki,[10] the author of the explanatory text to the geological map of Japan, 1 : 200.000, the Kôchi (Kôti) and Muroto sheet respectively, which contain many instructive geological accounts worthy of special attention.

In the explanatory texts to the geological map of Japan, 1 : 75.000, the Muroto[11] and Kôchi[12] (Kôti) sheet, Mr. T. Suzuki ascribed middle Pliocene age[13] to the upper Tertiary deposits of this field which rest unconformably upon the formation of Mesozoic ? rocks and consist of marine conglomerate and sand. Prior to this, Dr. J. Makiyama[14] found *Umbonium mysticum* Yokoyama, a characteristic fossil of his lower part of the lower Kakegawa series, and suggested the contemporaneity of one part of the fossiliferous deposits and the lower part of the lower Kakegawa series. According to Mr. T. Suzuki, the middle Pliocene beds occupy small isolated patches along the coast of Aki-gun, Kôti prefecure, with a slight seaward dip ; the strike turns from NE in the southern part to N 60° W or even to E-W in the northwestern. The younger Tertiary deposits are covered by horizontal gravel beds presumably of the Pleistocene age. Fig. 3 is a geological map, after T. Suzuki, showing the distribution of the Pliocene and Pleistocene deposits in this area.

---

[8] J. Makiyama, "Molluscan Fauna of the Lower Part of the Kakegawa Series in the Province of Tôtômi, Japan", *Mem. Coll. Sci. Kyôto Imp. Univ.*, Ser. B. 3, 1 (1927).

[9] T. Ogawa, *Expl. Text Geol. Map Japan,* "Kôchi" sheet, 1:200.000, (1905).

[10] Y. Ôtsuki, *Expl. Text Geol. Map Japan,* "Muroto" sheet, 1:200.000, (1902).

[11] T. Suzuki, *Expl. Text Geol. Map Japan,* "Muroto" sheet, 1:75.000, (1930).

[12] T. Suzuki, *Expl. Text Geol. Map Japan,* "Kôchi" sheet, 1:75.000, (1931).

[13] M. Yokoyama, "Pliocene Shells from Tônohama, Tosa", *Imp. Geol. Surv.*, Japan, Rep. 104 (1929).

3. The Kakegawa district, west of Siduoka.

It was in the explanatory text to the geological map of Japan, 1: 200.000, Shidzuoka (Siduoka) sheet (1886), that the late Dr. K. Nakajima[15] divided the Tertiary deposits of the area covered by the sheet into the upper and the lower Ôigawa. For a long time since, stratigraphical details and faunal nature of the Tertiaries had been studied by nobody. Firstseveral years ago, Mr. Y. Chitani[16] and Dr. J. Makiyama[17] independently begun their researches on the Tertiaries in the Kakegawa district, west of Siduoka, and the recent rapid progress of our

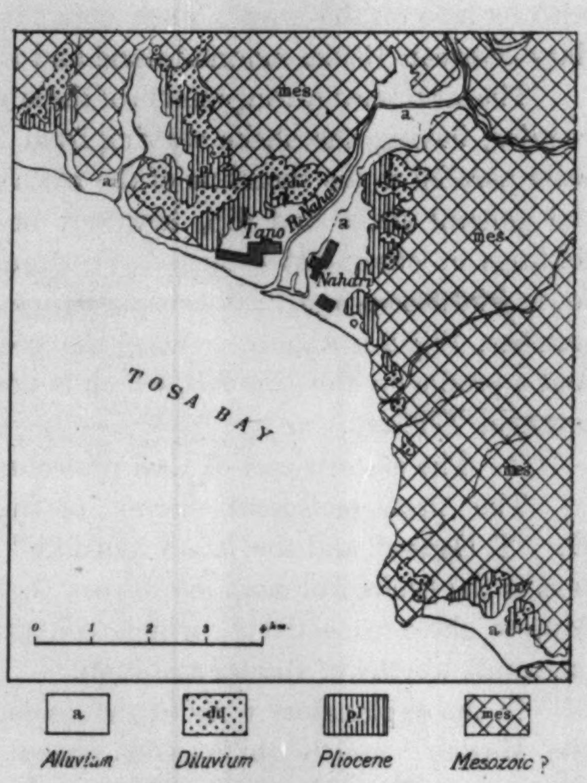

Fig. 3 Geological Map of the Eastern Part of Kôti Prefecture along the Tosa Bay. (After T. Suzuki).

---

[14] J MAKIYAMA, *op. cit.*, (1927), 21.

[15] K. NAKAJIMA, *Expl Text Geol. Map Japan*, "Shidzuoka" sheet, 1:200.000, (1886).

[16] Y CHITANI, "The Tertiary in the Vicinity of Kakegawa and Sagara, Tôtômi", *Journ. Geogr.*, **38** (1926), 84-89, (in Japanese).

[17] J. MAKIYAMA, "On the Geology near Kakegawa, Shidzuoka Prefecture", *Chikyû*, **9**, 1-2 (1928), (in Japanese).

knowledge on the subjects is essentially due to the works of the two authors.

According to Dr. J. Makiyama,[18] the Mesozoic and Cainozoic formations developed in the eastern part of Tôtômi are divisible into eight groups of Mikura (Cretaceous or Palaeogene), Ôigawa (lower Miocene or older), Sagara (upper Miocene), Horinouchi (Horinouti) (transition), Kakegawa (lower Pliocene), Soga (upper Pliocene), Ogasa conglomerate (upper Pliocene), and Pleistocene gravel deposits.

The Kakegawa series is a formation about 640 m. thick in its type locality treated by Dr. Makiyama, where it represents a complete cycle of sedimentation. Its stratigraphical relation to the underlying Soga is marked unconformity. The averaged dips of these strata are 10°–15° and the strike is usually about N 50° W. There are small dip- and strike-faults, and also very slight folding of strata.

The area covered by the geological map of Japan in 1 : 75.000, Sagara sheet (1927) by Mr. Y. Chitani[19] includes the southern part of Makiyama's field, and in the southern part of this sheet, the younger Tertiary strata have the dips 10°–30° SW and the strikes ranging from N 10° W to N–S. EF in Fig. 5 is a geologic profile, after Y. Chitani, at right angles to the main strikes of the younger Tertiary.

4. The Asigara district adjoining to the north of volcano Hakone.

A thick complex of sandstone and conglomerate occupies the area immediate north of volcano Hakone and between the Yamakita and Suruga station on the Tôkaidô railway line. Dr. T. Hirabayashi[20] who studied this formation in 1896 in connection of his geological research of the volcano Hakone, called it the Ashigara Tertiary (Asigara Tertiary) and some more detailed accounts of it was subsequently given by the late Tetsunosuke Katô[21] in his paper "Report of the geology of the vicinity of Yamakita" (in Japanese) published in the Bulletin of Imperial Geological Survey of Japan, No. 18, 1910. In 1926, Dr. M. Yokoyama[22] examined the fossil shells from this formation and expressed that the

---

[18] J. Makiyama, *op. cit.*, (1927), 5.

[19] Y. Chitani, *Expl. Text Geol. Map Japan*, "Sagara" sheet, 1:75.000, (1927).

[20] T. Hirabayashi, "Geologic Report of Hakone and Atami", *Shinsai Yobô Chôsakai Hôkoku* (*Report of the Imperial Earthquake Investigation Committee in Japanese Language*), **16** (1896).

[21] Te. Kato, "The Geologic Report near Yamakita, Sagami Province", *Bull. Imp. Geol., Surv.*, Japan, **18** (1910).

[22] M. Yokoyama, "Neogene Shells from Kôzuke and Other Provinces," *Jour. Fac. Sci. Imp Univ.*, Tôkyô, Sect. II, **1**, 7 (1926).

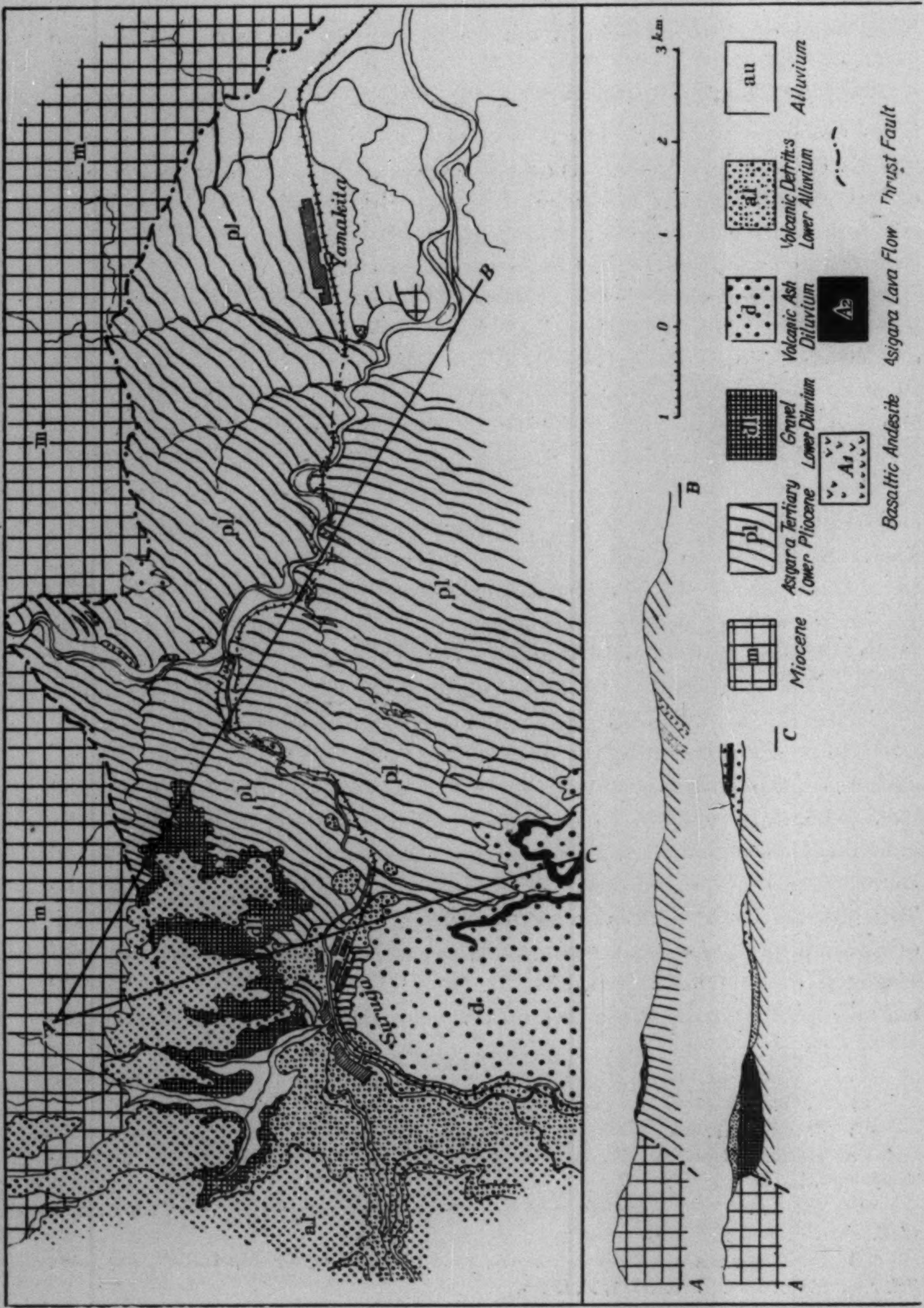
m
pl
Yamakita
al
dl
d
A
B
C
1
0
1
2
3 km
m
Miocene
pl
Asigara Tertiary Lower Pliocene
dl
Gravel Lower Diluvium
d
Volcanic Ash Diluvium
al
Volcanic Detritus Lower Alluvium
au
Alluvium
A₁
Basaltic Andesite
A₂
Asigara Lava Flow
Thrust Fault

Fig. 4. Geological Map and Profiles of the Asigara District by Yanosuke Ôtuka.

fauna, which is by no means rich in species, is certainly Pliocene in age. The "Asigara Tertiary" or better Asigara beds turn the strike from E–W in the northeastern part of the field to N 10° E–10° W in the southeastern part, the dip being almost always northwestern. Previous authors ascribed this deformation of strata to a tectonic disturbances of the late Pliocene. On the north this formation lies beneath the Miocene

Table I.

List of Fossils from the Asigara beds	a. Yôzawa	b. Yagurazawa	c. Yaga
1. *Acila mirabilis* Adams et Reeve	a	b	c
2. *Yoldia lischkei ?* Smith			c
3. *Yoldia* sp.	a		
4. *Glycymeris yessoensis* (Sowerby)		b	
5. *Ostrea gigas* Thunberg	a		
6. *Pecten* sp.		b	
7. *Thracia* sp.		b	
8. *Miltha* (*Lucinoma*) *annulata* (Reeve)	a	b	
9. *Diplodonta japonica?* Pilsbry			c
10. *Cardium braunsi* Tokunaga		b	
11. *Cardium* (*Fulvia*) sp.	a		
12. *Paphia ?* sp.		b	
13. *Macrocallista pacifica* (Dillwyn)	a		c
14. *Chamaeformis meretrix* Linné		b	
15. *Dosinia japonica troscheli* Lischke	a	b	c
16. *Macoma nasuta* (Conrad)	a		
17. *Tellina* aff. *gratiosa* (Römer)	a		
18. *Tellina nitidula* Dunker	a		
19. *Solen krusensternii* Schrenck	a		
20. *Mactra sulcataria* Reeve	a		
21. *Mya* aff. *japonica* A. Adams	a		
22. *Panope japonica* A. Adams	a		
23. *Turritella* sp.		b	
24. *Neritaeformis didyma* (Bolten)	a		
25. *Terebra bifrons* Smith	a		
26. *Umbonium suchiense* Yokoyama	a		
27. *Cancellaria spengleriana* Dunker	a		
28. *Lingula hians* Swainson	a		
29. *Carpinus yedoensis ?* Maximoviczi	a		
30. *Salix* sp.	a		
31. *Phyllites* sp.	a		

Misaka series overthrusted from the north upon it. Simultaneous with and also after these movements basaltic andesites intruded into it as dykes or intrusive sheets. The area of the Asigara beds is bordered by Pleistocene volcanic deposits elsewhere than north.

Fig. 4 is a geological map of the field now in question showing the structural relations of the Asigara beds to the other formations.

In the last winter I had an opportunity to collect fossils in the Asigara beds and obtained the species listed above (Table I) some of whith are additional to Dr. M. Yokoyama's[23] list.

One of these species, *Umbonium suchiense* Yokoyama, is a characteristic fossil of the lower part of the Lower Kakegawa series and is a lower Pliocene form in the evolutional series of its phyllum after Dr. J. Makiyama's scheme.[24]

Now in the Ôiso block northeast of the volcano Hakone, the Takatoriyama conglomerates,[25] which are the eastern extension of the Asigara beds, are covered by the middle Pliocene Nisikoiso[26] beds and the upper Pliocene Ninomiya beds in clinounconformity. Consequently the process which disturbed the Asigara beds must be accepted as having been active in the latest stage of the lower Pliocene, and this is in strong contrast with what we find in the Neogene strata of the Outer Zone of Southwest Japan.

5. The Nagano prefecture.

Tertiary deposits in the northern part of the Fossa Magna in the Nagano prefecture have recently been studied by Mr. F. Homma[27] in some details; his Sigarami and Ogawa beds too are regarded by Dr. M. Yokoyama[28] to be lower Pliocene in age on the molluscan fauna they contain, and Dr. S. Tokunaga[29] described once a *Cervus* remain of an upper Miocene type derived from either of them, whereas Dr. J. Makiyama[30] holds an eclectic

---

23) M. Yokoyama, *op. cit.*, (1926), 230.

24) J. Makiyama, "The Evolution of *Umbonium*", *Jap. Jour. Geol. Geog.*, 3-4 (1924).

25) Y. Ôtuka, "A Stratigraphical Study of the Ôiso Blocks and Its Adjacent Area," *Jour. Geol. Soc.*, Tôkyô, **36**, **434** (1929).

26) Y. Ôtuka, "On the Ôiso Bed," *Jour. Geol. Soc.*, Tôkyô, **33**, **451** (1931), (in Japanese).

27) F. Homma, "Shinano Chûbu Chishitsushi (Geology of the Middle Part of Sinano Province)," (1931), (in Japanese).

28 M. Yokoyama, "Tertiary Mollusca from Shinano and Echigo". *Jour. Fac. Soc. Imp. Univ.*, Tôkyô, Sect. II, 1, **1** (1925).

29) S. Tokunaga, "A New Form of *Cervus* from the Tertiary of Shinano", *Jour. Goel. Soc.*, Tôkyô, **33** (1926), 397-402, (in Japanese).

30) J. Makiyama, "Preliminary Report of Tertiary Fossils from Minauchi-gôri, Shinano Province," *Chikyû*, **8** (1927), 181-188, (in Japanese).

view slightly diverging from those of the two authors, refering one complex to the upper Miocene and the other to the lower Pliocene.

According to Mr. Homma, these two complexes form an anticlinorium, which is intruded by the pyroxene andesites, and the main folds are parallel to the trend of the Fossa Magna, which runs in N 30° W across the Honsyû. These folds are arranged in échelon along the eastern side of the Itoigawa-Siduoka line of Dr. H. Yabe,[31] by which the southern ends of each fold are separated from the pre-Tertiary formation on the west of the tectonic line. In this part the Itoigawa-Siduoka line is a series of thrust faults. Fig. 5 CD is a geological profile, after Homma, of this district normal to the main trend.

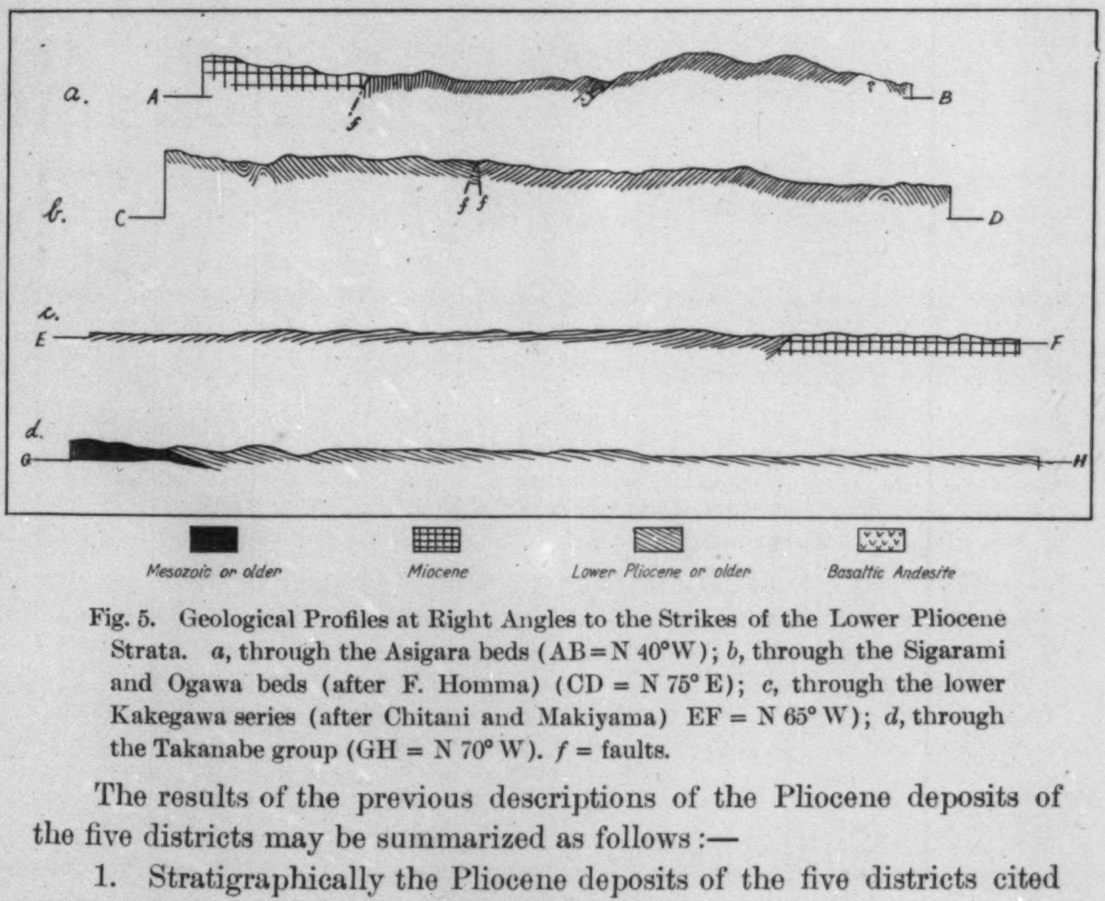

Fig. 5. Geological Profiles at Right Angles to the Strikes of the Lower Pliocene Strata. *a*, through the Asigara beds (AB = N 40°W); *b*, through the Sigarami and Ogawa beds (after F. Homma) (CD = N 75° E); *c*, through the lower Kakegawa series (after Chitani and Makiyama) EF = N 65° W); *d*, through the Takanabe group (GH = N 70° W). *f* = faults.

The results of the previous descriptions of the Pliocene deposits of the five districts may be summarized as follows :—

1. Stratigraphically the Pliocene deposits of the five districts cited above are to be correlated as follows (Table II).

2. In the latest stage of lower Pliocene, crustal movements took place in Japan. In the Outer Zone of Southwest Japan, the lower Pliocene or

---

31) H. Yabe, "Itoigawa-Siduoka Geotectonic Line", *Gendai no Kagaku*, **6**, 3 (1918), (in Japanese)

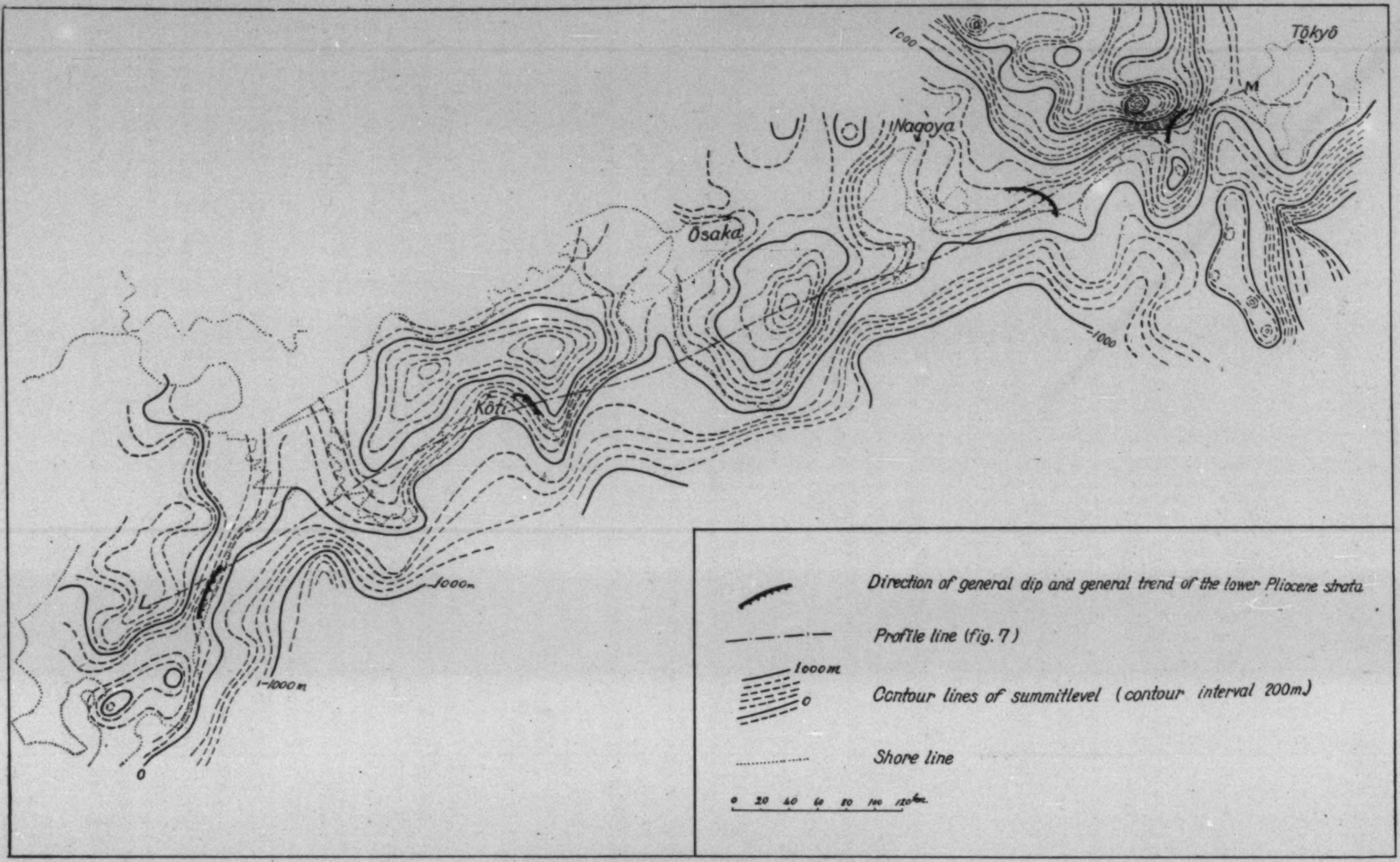
Tōkyō
M
Nagoya
Ōsaka
Kōti
1000
1000
1000m
1000m
0
Direction of general dip and general trend of the lower Pliocene strata
Profile line (fig. 7)
1000m
0
Contour lines of summitlevel (contour interval 200m)
Shore line
0 20 40 60 80 100 120km

Fig. 6 Summit-level of Southwest Japan

Table II.

Geologic Age \ Locality	(1) Miyazaki	(2) Kôti	(3) Kakegawa	(4) Asigara	(5) Nagano
Upper Diluvium	Gravel beds	Gravel beds	Gravel beds	Volcanic lava and ash	
Lower Diluvium	Freshwater deposits		Ogasa conglomerate	Gravel beds	
Upper Pliocene			Soga beds	(Ninomiya beds) Nisikoiso beds	
Lower Pliocene	Takanabe group { Heki beds Kôonzi beds Sadowara beds	Suzuki's Pliocene *Umbonium mysticum* Zone	Kakegawa series Horinouti series	Asigara beds	Sigarami beds Ogawa beds
Miocene	Tuma group		Sagara beds	Misaka beds	

Pliocene strata are usually monoclinal in low angles either to southwest, or to south with a few exception of other small displacements, while the contemporaneous deposits in the Fossa Magna form a complex anticlinorium, each pericline with the trend parallel to that of the Fossa Magna. There are many thrust- and normal-faults in association of these folds, and volcanism was often active.

3. The structural lines of the lower Pliocene deposits do not conform with the general trend of the Honsyû arc or with the main structural lines of the Outer Zone of Southwest Japan, but with the trend of contour lines of a summit level in the Outer Zone of Southwest Japan. Fig. 6 is a map showing the conformity of the structural lines of the lower Pliocene strata and the trend of contour lines of the summit-level.

4. Fig. 7 is a schematic profile from Siduoka through the Tosa bay to Miyazaki along the line LM in fig. 6. That is parallel to the main structural trend of the Outer Zone of Southwest Japan. It shows us that the inclination of the bedding plane of the Pliocene strata is steeper than that of the surface of the summit-level dipping to the same direction; and suggests that an extensive crustal movement in the form of broad swells took place in the Outer Zone of Southwest Japan along the lines rather parallel to the Ryûkyû arc than to the Honsyû arc

5. Comparing the thickness and rock facies of these lower Pliocene strata, the Fossa Magna may be regarded as a geosynclinal trough of the geological period.

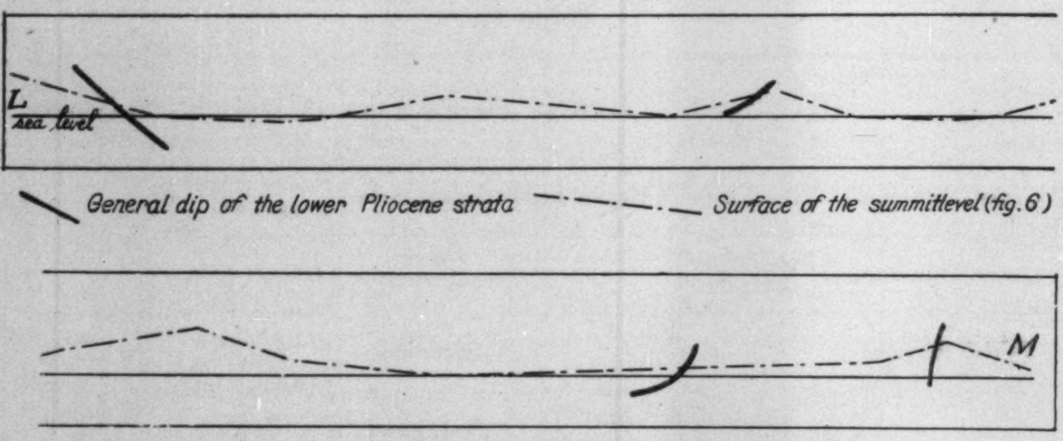
L
sea level
General dip of the lower Pliocene strata
Surface of the summitlevel (fig. 6)
M

Fig. 7. Profile along L in Fig. 6. Vertical scale × 5

24. 西南日本外帯とフォッサ・マグナとに於ける鮮新期初期末の地殼運動

地震研究所　**大塚彌之助**

西南日本外帶とフォッサ・マグナとの下部鮮新統の發達地域五ケ處(宮崎縣日向海岸平野、高知縣東部土佐灣沿岸、靜岡縣掛川地方、靜岡神奈川兩縣下足柄地方、長野縣北部）の地質を略記し、それらの地質構造の一般的特徴を述べ互に比較した。

その結果次のやうなことが知られた。

鮮新期初期末に著しい地殼運動が日本に起つた。その擾亂の程度はフォッサ・マグナに於て極めて著しく、褶曲、正逆斷層、火山活動等が生じた。外帶ではその程度が極めて弱く展張性を帶びてゐた。陸地測量部の五萬分ノ一地形圖一枚の面積を一單位として作つた切峯面と下部鮮新統の構造とを比べてみると、下部鮮新統の層向の走向とその地域の切峯面の等高線の走向とはかなり一致し、その地層の傾斜の度は、その地域の切峯面の傾斜の度より急であるが、その方向は一致してゐる、又地層の厚さはフォッサ・マグナの地域の鮮新統の方が厚い。

上記の事實から鮮新期初期末に起つた地殼運動は極めて激しかつたやうだが、西南日本外帶では展張性な廣い「うねり」があつたやうにも見える。そしてその「うねり」の峯の延び方は琉球弧に平行なものの方が、本州弧に平行なものに比べて著しく目について見える。尙フォッサ・マグナはヂオシンクラインであつたらしい。

25. *Petrographic Notes on the Sedimentary Rocks of Southwest Sagami Province. (Part II)*

By **Hiromichi TSUYA**,

Earthquake Research Institute.

(Read Jan. 20, 1931.—Received June 20, 1931.)

Introduction.

In a previous paper[1] the writer gave results of his petrographic study of the sedimentary rocks of Enosima[2], and showed that, petrographically, the rocks there have certain distinguishing characters according to their respective stratigraphic horizons.

This is a continuation of that paper and gives results of petrographic studies of the rocks of Ôiso[3], a district adjoining the northeast foot of volcano Hakoné[4], in Idu. The rock-specimens examined were not sufficient for the purpose of this study, so that publication of full results will have to be deferred to a later opportunity. Many of the rock-specimens were supplied by Y. Ôtuka[5], who is studying the geology of the district from the stratigraphic side, and to whom the writer tenders his sincere thanks.

Stratigraphic Succession of the Beds of Ôiso District.

Stratigraphic studies of the district have been made by several geologists. It being however outside the scope of this paper, the reader is referred to Ôtuka's paper[6], for a summary of it, in which a bibliography of earlier literature on the subject will also be found. Recently, Y. Ôtuka[7]

---

[1] H. Tsuya, "Petrographic Notes on the Sedimentary Rocks of Southwest Sagami Province, (Part I.)," *Bull. Earthq. Res. Inst.*, 9 (1931), 98–106.

[2] 江ノ島

[3] 大磯

[4] 箱根

[5] Y. Ôtuka, "A Stratigraphical Study of the Ôiso Block and Its Adjacent Area," *Jour. Geol. Soc.*, Tôkyô, 36 (1929), 435–456; 479–497, (in Japanese).

[6] Y. Ôtuka, *loc. cit.*

[7] Y. Ôtuka, "On Ôiso Bed," *Jour. Geol. Soc.*, Tôkyô, 38 (1931), 174–187, (in Japanese).

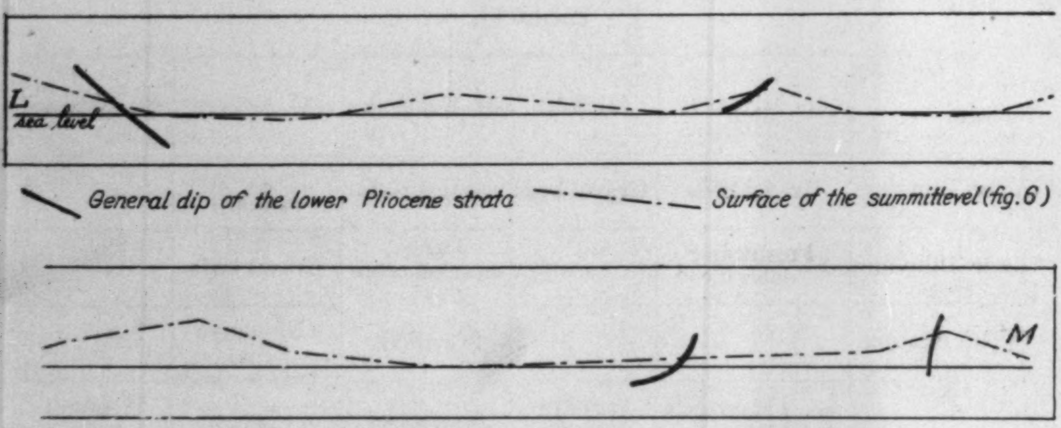
L
sea level
General dip of the lower Pliocene strata
Surface of the summitlevel (fig. 6)
M

Fig. 7. Profile along L in Fig. 6. Vertical scale × 5

---

24. 西南日本外帯とフォッサ・マグナとに於ける鮮新期初期末の地殻運動

地震研究所 大塚彌之助

西南日本外帯とフォッサ・マグナとの下部鮮新統の發達地域五ケ處(宮崎縣日向海岸平野、高知縣東部土佐灣沿岸、靜岡縣掛川地方、靜岡神奈川兩縣下足柄地方、長野縣北部)の地質を略記し、それらの地質構造の一般的特徴を述べ互に比較した。

その結果次のやうなことが知られた。

鮮新期初期末に著しい地殻運動が日本に起つた。その擾亂の程度はフォッサ・マグナに於て極めて著しく、摺曲、正逆斷層、火山活動等が生じた。外帶ではその程度が極めて弱く展張性を帶びてゐた。陸地測量部の五萬分ノ一地形圖一枚の面積を一單位として作つた切峯面と下部鮮新統の構造とを比べてみると、下部鮮新統の層向の走向とその地域の切峯面の等高線の走向とはかなり一致し、その地層の傾斜の度は、その地域の切峯面の傾斜の度より急であるが、その方向は一致してゐる、又地層の厚さはフォッサ・マグナの地域の鮮新統の方が厚い。

上記の事實から鮮新期初期末に起つた地殻運動は極めて激しかつたやうだが、西南日本外帶では展張性な廣い「うねり」があつたやうにも見える。そしてその「うねり」の峯の延び方は琉球弧に平行なものの方が、本州弧に平行なものに比べて著しく目について見える。尙フォッサ・マグナはヂオシンクラインであつたらしい。

25. *Petrographic Notes on the Sedimentary Rocks of Southwest Sagami Province. (Part II)*

By **Hiromichi TSUYA,**

Earthquake Research Institute.

(Read Jan. 20, 1931.—Received June 20, 1931.)

Introduction.

In a previous paper[1] the writer gave results of his petrographic study of the sedimentary rocks of Enosima[2], and showed that, petrographically, the rocks there have certain distinguishing characters according to their respective stratigraphic horizons.

This is a continuation of that paper and gives results of petrographic studies of the rocks of Ôiso[3], a district adjoining the northeast foot of volcano Hakoné[4], in Idu. The rock-specimens examined were not sufficient for the purpose of this study, so that publication of full results will have to be deferred to a later opportunity. Many of the rock-specimens were supplied by Y. Ôtuka[5], who is studying the geology of the district from the stratigraphic side, and to whom the writer tenders his sincere thanks.

Stratigraphic Succession of the Beds of Ôiso District.

Stratigraphic studies of the district have been made by several geologists. It being however outside the scope of this paper, the reader is referred to Ôtuka's paper[6], for a summary of it, in which a bibliography of earlier literature on the subject will also be found. Recently, Y. Ôtuka[7] made a revision of the stratigraphy of the district. According to his revised summary, the stratigraphic succession is as shown in Table I, and the distribution of the successive beds as shown in Fig. I.

---

[1] H. Tsuya, "Petrographic Notes on the Sedimentary Rocks of Southwest Sagami Province, (Part I.)," *Bull. Earthq. Res. Inst.*, 9 (1931), 98-106.

[2] 江ノ島

[3] 大磯

[4] 箱根

[5] Y. Ôtuka, "A Stratigraphical Study of the Ôiso Block and Its Adjacent Area," *Jour. Geol. Soc.*, Tôkyô, 36 (1929), 435-456; 479-497, (in Japanese).

[6] Y. Ôtuka, *loc. cit.*

[7] Y. Ôtuka, "On Ôiso Bed," *Jour. Geol. Soc.*, Tôkyô, 38 (1931), 174-187, (in Japanese).

Table I.

Geol. Periods		Beds	Rock types
Holocene	a_{II}		Dune-sands; fluviatile deposits of sands, gravels, and clay.
	a_{I}	Simohara[8] bed	Fossiliferous deposits of sands and gravels.
Pleistocene	du_{II}	Terrace bed	Gravels.
	du_{I}	Loam bed Takao[9] bed	Volcanic ashes ? and lapilli. Andesitic pumices and andesitic tuffs.
	dl_{II}	Kuroiwa[10] bed	Andesite-gravels, and others.
	dl_{I}	Tutizawa[11] bed	Fossiliferous sands and clay; dacitic tuffs.
	p-d	Ninomiya[12] bed	Fossiliferous, tufaceous sands.
Pliocene	pu pm	Nisikoiso[13] bed	Fossiliferous conglomerate.
	pl	Takatoriyama[14] bed	Andesite-gravels; andesite agglomerates and lavas.
Miocene	mu ml	Ôiso bed	Fossiliferous, tufaceous sandstone and conglomerate.
	o?	Komayama[15] bed	Dacite-dikes and lavas; dacitic tuffs. Siliceous sandstone.

Volcanic History as inferred from Petrographic Studies.

As shown in Table I, the general geologic succession of the district consists of an alternation of pyroclastic rocks and sedimentary rocks containing much volcanic material. These rocks belong to their respective stratigraphic divisions, the lowest one of which dates back to the lower Miocene or probably an older period. If they contain juvenile

---

[8] 下原 [9] 高尾 [10] 黒岩 [11] 土澤 [12] 二宮 [13] 西小磯 [14] 鷹取山 [15] 高麗山

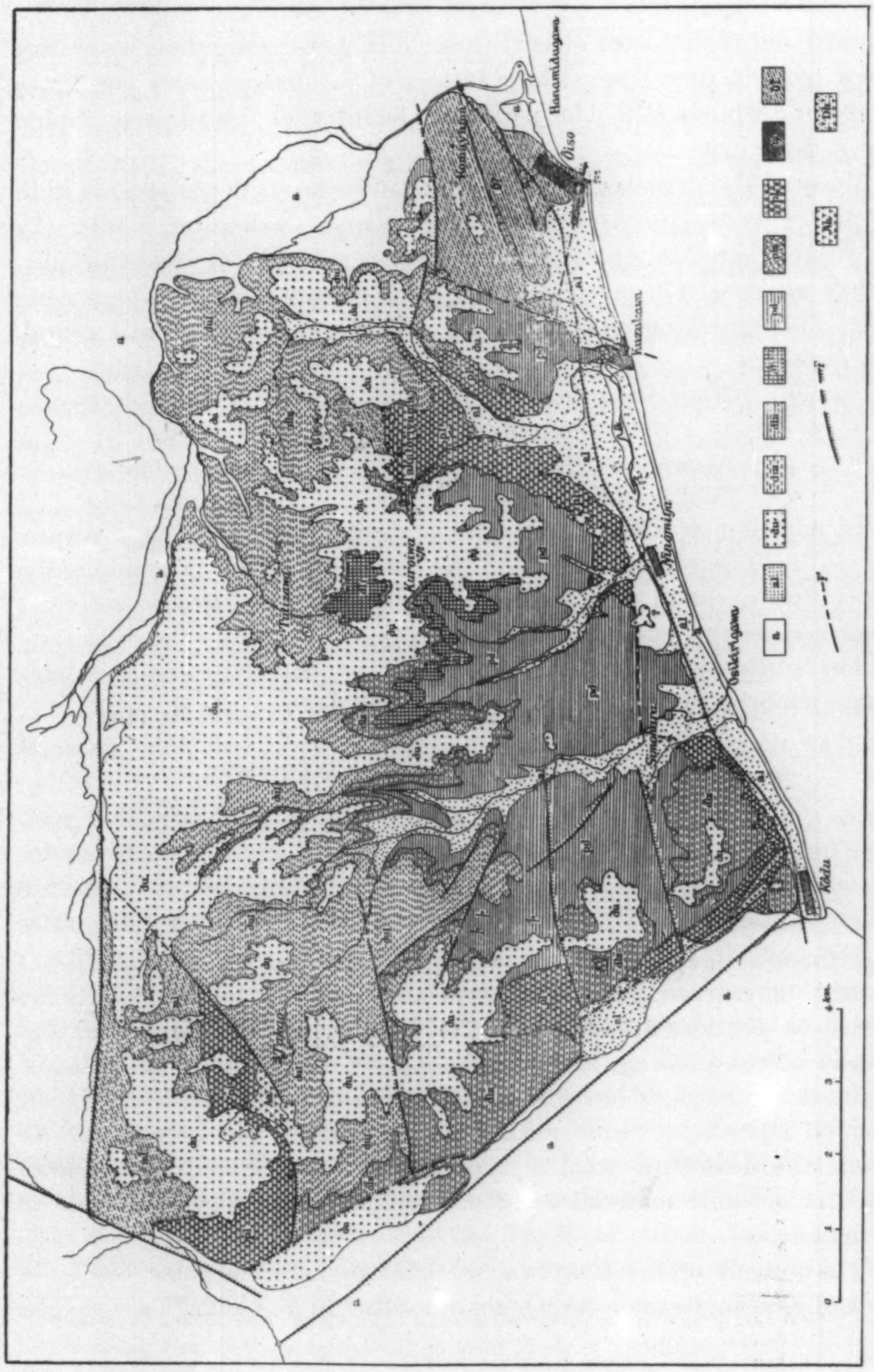
Hanamizugawa
Ôiso
Ninomiya
Kôzu
F
F′
0
1
2
3
4 km.

Fig. 1. Geologic map of the Ôiso district. (after Y. Ôtuka, 1931.) a—Alluvium, al—Simohara bed, du—Loam bed, du_I—Takao bed, dl_{II}—Kuroiwa bed, dl_I—Tutizawa bed, pd—Ninomiya bed, pm—Nisikoiso bed, pl—Takatoriyama bed, m—Ôiso bed, o?—Komayama bed, Aa—Pyroxene-andesite, Da—Dacite. F, F′—Faults.

volcanic material that were ejected from volcanoes during their respective geologic periods, then the volcanic history of the district since the lower Miocene or even of a still older period can be inferred from a petrographic study of these material.

Many of the pyroclastic rocks are of subaqueous deposition, as indicated by occasional occurrences of marine and fresh-water fossils. In these rocks, therefore, occur detritus, either volcanic or non-volcanic; but they all consist of practically the same volcanic material, possessing certain distinguishing characters as petrographic studies will reveal. These rocks are

du$_{I}$.	Andesitic tuffs and andesitic pumices	Takao bed.
pl.	Andesitic agglomerate	Takatoriyama bed.
o ?	Dacitic tuffs	Komayama bed.

In addition to these, dacite and andesite occur as lavas, respectively, in the Takatoriyama bed and the Komayama bed. Consequently, there is little question that these rocks represent the volcanic activities of their respective geologic periods.

The ordinary sedimentary rocks of the district contain sundry volcanic material in various proportions. They are

dl$_{II}$.	Andesite gravels	Kuroiwa bed.
dl$_{I}$.	Tufaceous sands and clay	Tutizawa bed.
p-d.	Tufaceous shale	Ninomiya bed.
pu.	Conglomerate	Nisikoiso bed.
mu. ml.	Tufaceous sandstone and tufaceous conglomerate	Ôiso bed.
o?.	Siliceous sandstone	

Although some explosive volcanic material, either juvenile or accessory, may occur, most of the volcanic material in these rocks are regarded as detritus arising from the weathering, disintegration, and transport of pre-existing volcanic masses. Until some of the volcanic material are proved to have been of juvenile origin at the time of their respective depositions, these rocks have no bearing on the present discussion. To determine what is juvenile and what is accessory or detrital in the volcanic material contained in such rocks is generally not an easy matter.

The gravels of the Kuroiwa bed contain much angular blocks of porous olivine-augite-andesite which, according to Y. Ôtuka[16], are suggestive of eruption at the time of their deposition. The tufaceous sands and clay of the Tutizawa bed are mixed with much pumice. These deposits pass upward into a finely stratified bed consisting entirely of pumice. Occasionally, the pumice exhibits oxidation effects, as was observed in juvenile pumiceous ejecta at the time of the eruption in 1929 of Komagataké (Hokkaidô[17]). These effects might be due to high temperatures that were maintained at the time of ejection for periods sufficiently long to bring about oxidation. These facts suggest juvenile origin for the pumice. But with the exceptions of the Kuroiwa bed and the Tutizawa bed, evidence in the district of juvenile origin for some of the volcanic constituents of the above-mentioned sedimentary rocks is entirely wanting. In the circumstances, volcanic history of the district can be inferred only partially from petrographic study. The history as far as can be traced is as follows:

---

[16] Y. Ôtuka, *loc. cit.*, 480.

Of beginning of volcanic activity during the Tertiary in the neighbouring district of Idu no trace is found in the Ôiso district; nor is there any certainty that the volcanic material (Hypersthene-augite-andesine-andesite, see p. 363) in the siliceous sandstone (o? in Table I) marks the oldest volcanic activity in the Ôiso district.

From all reliable data obtainable, volcanic activity begun before the Miocene, with eruptions of dacitic lavas and tuffs (Komayama bed, o? in Table I) which were followed by intrusions of dacite-dikes. From their calcareous nature, the dacitic tuffs seem, locally at any rate, of submarine deposition. The micro-cataclastic structure exhibited in the tuffs may be the result of later disturbances, which, according to Y. Ôtuka, threw the tuffs into complicated structures with numerous fault systems. This was followed by renewed outpourings of lava and agglomerate, but this time of more basic type, such as the two-pyroxene-bytownite-andesite (see p. 367) of the Takatoriyama bed (pl in Table I). The volcanic material in the Ôiso bed (ml-mu in Table I) and Nisikoiso bed (pm-pu in Table I) are, petrographically, of the same general type as those in the Takatoriyama bed (see pp. 367–368). Furthermore, the volcanic constituents of the Ninomiya bed (p-d in Table I) are indistinguishable from those of beds previously mentioned (see p. 369). If therefore some of the volcanic material in these three beds—the Ôiso, the Nisikoiso, and the Ninomiya beds—were of juvenile origin at the time of their respective depositions, it may be said that volcanic activity of the same general type as that represented by the pyroxene-andesite in the Takatoriyama bed occurred during the periods between the lower Miocene and the lowest Pleistocene.

---

[17] S. Tsuboi and H. Tsuya, "On the Temperature of the Pumiceous Ejecta of Komagataké, Hokkaidô, as inferred from their Mode of Oxidation," *Bull. Earthq. Res. Inst.*, **7** (1930), 271–273.

After the formation of the Ninomiya bed there was a reversion in the eruptions to rocks of more acidic character (Tutizawa bed, dl_I in Table I). This is seen in the dacitic tuff which consists of quartz, hornblende, hypersthene, augite, and labradorite, together with pumice and obsidian (see p. 369 .

Basic andesites characterized again the subsequent volcanic activities as is seen by the fresh blocks of olivine-augite-anorthite-andesite (see p. 370) in the Kuroiwa bed (dl_{II} in Table I) and also by the pumice of both hypersthene-augite-bytownite-andesite and hypersthene-augite-labradorite-andesite (see p. 371) in the Takao bed (du_I in Table I).

The last volcanic activity traceable in rocks of the district seems to be represented by the scoriaceous lapilli of augite-bytownite-andesite (?, see p. 372) in the so-called loam bed.

Comparison of Rocks of the Ôiso District with Similar Rocks of the Adjoining District.

Of centres of the above-mentioned volcanic activities, and which supplied the pyroclastic material now found in the rocks of Ôiso district, there is no trace there today. These centres may however be located in the adjoining districts where volcanic rocks occur. They are Asigara(18) on the northwest and Idu(19) on the southwest. The rocks of these two districts are of the same general type, but naturally differ in detail. It is believed that careful comparison of the rocks of Ôiso district with those of neighbouring districts may throw some light on their genetical relationship. For this purpose, further detailed studies of rocks of neighbouring districts are desirable. The following comparison is only tentative.

1. *Siliceous sandstone* (o? in Table I) and *tufaceous sandstone*(20) *in the lower Miura series of Enosima.*

The former is similar in mineral composition to the latter, both being composed of quartz, orthoclase, andesine ($Ab_{60}An_{40}$), hornblende,

---

18) 足柄
19) 伊豆
20) H. Tsuya, *loc. cit.*, 99.

and augite, together with microscopic fragments of pyroxene-andesite (see p. 363). The main difference is that the former is siliceous with much quartz fragments while the latter is tufaceous with much andesite fragments. Although their stratigraphic relation is yet uncertain, they are considered to be older than lower Miocene.

2. *Dacite of the Komayama bed* (o? in Table I) and *dacitic rocks*[21] *of Idu district.*

The acidic rock that occurs as dikes intruding into the dacitic tuffs of the Komayama bed is hypersthene-hornblende-labradorite-dacite (see p. 364). In the Idu district liparitic and dacitic rocks occur in following sequences:

Idu Peninsula[22],
Potash-liparite ⟶ biotite-plagioliparite ⟶ hornblende-dacite ⟶ augite-hornblende-dacite ⟶ hypersthene-hornblende-dacite ⟶ two-pyroxene-dacite.

Niizima[23] group of the Seven Idu Islands[24],
Potash-liparite ⟶ pyroxene-plagioliparite ⟶ hornblende-plagioliparite ⟶ biotite-plagioliparite.

In Table II is shown a comparison of the refractive indices of the

Table II.

	Plagioclase	Hornblende (n_{1D})	Augite	Hypersthene (n_{1D})
I	$Ab_{45}An_{55}$	1·6721	n.d.	1·6991
II	$Ab_{62}An_{38}$	1·6748	–	–
III	$Ab_{55}An_{45}$	1·6783	n.d.	–
IV	$Ab_{62}An_{38}$	1·6915	–	n.d.
V	$Ab_{64}An_{36}$	–	n.d.	1·6997

I. Hypersthene-hornblende-labradorite-dacite, Ôiso.
II. Hornblende-andesine-dacite, Takaneyama, Simoda, Idu[25]
III. Augite-hornblende-andesine-dacite, Warabo, Idu[26].
IV. Hypersthene-hornblende-andesine-dacite, Taga, Idu[27].
V. Augite-hypersthene-andesine-dacite, Kasiwatôgé, Itô, Idu[28].

---

[21] H. Tsuya, "Volcanoes of Kôzu-shima," *Bull. Earthq. Res. Inst.*, 7 (1929), 318–339.
[22] 伊豆半島 [23] 新島 [24] 伊豆七島
[25] 伊豆下田高根山 [26] 伊豆原保 [27] 伊豆多賀 [28] 伊豆伊東柏峠

constituent minerals in some dacitic rocks of Idu district and the dacite of the Komayama bed. The principal difference between the dacite of the Komayama bed and the similar rocks of the Idu district is in the more calcic composition of the plagioclase phenocrysts of the former and in the lower refractive indices of the phenocrystic mafic minerals of the former.

Stratigraphically, the liparitic or dacitic rocks of the Idu district, in view of their geologic ages, may be left out of consideration. As far as the writer knows, they are believed to be younger than lower Miocene, whereas, according to Y. Ôtuka, the dacite and dacitic tuffs of the Komayama bed are of lower Miocene or probably an older period. But, volcano-tectonically, the N.E.-S.W. trend of distribution of the liparitic and dacitic rocks of the Idu district is very significant in connection with the same trend noticeable in the strike, the fault systems, and in the dacite-dikes in the Komayama bed. Probably, this trend is a surface manifestation of the regional structure of the ground, and the cause of the eruption here of liparitic and dacitic rocks throughout recent geologic time.

3. *Andesitic material in the rocks of Ôiso district* and *similar material in the rocks of the neighbouring districts.*

Petrographically, the andesitic material of the Ôiso bed, the Takatoriyama bed, the Nisikoiso bed, and of the Ninomiya bed are of the same general type as the constituents of the agglomerate-tuff of the upper Miura series of Enosima. The former is also of the same general type as the andesitic material of the Asigara bed of Asigara district. But of stratigraphic relations between them, petrographic study has not yielded so far any evidence. The andesitic material of the Kuroiwa bed and of the Takao bed are similar to the basaltic andesite of the volcanoes, Hakoné, Amagi[29], etc., of the Idu district. Probably, the depositions of the former and the eruptions of the latter took place at the same general time, in middle and upper Pleistocene, when the nature of the magma regionally became strongly basic[30].

4. *Dacitic tuff of the Tutizawa bed* (dl$_1$ in Table I) and *similar rock of the Simo-Tanna*[31] *bed of Idu district.*

The occurrence of dacitic material (see p. 369) in the Tutizawa bed calls for a discussion of their possible relation to similar material in the

---

[29] 天城

[30] S. Tsuboi, " Volcano Ô-shima, Izu," *Jour. Col., Tôkyô Imp. Univ.*, 43 (1920), 139.

[31] 下丹那

Simo-Tanna bed of northern Idu. The Simo-Tanna bed develops at the western margin (Simo-Tanna) of the Tanna basin[32], under which the so-called Tanna tunnel is now being excavated. It consists of sandy tuff, tufaceous shale, and black clay. The sandy tuff contains many fragments of hornblende-pyroxene-dacite, as well as of pyroxene-andesite. The dacite is pumiceous and is similar in the refractive indices of the constituent minerals to the dacitic material in the tuff of the Tutizawa bed, as shown in Table III.

Table III.

	Glass (n_D)	Quartz	Plagioclase	Hornblende	Augite (n_{1D})	Hypersthene (n_{1D})
I	1·5083	+	$Ab_{45}An_{55}$	n_{1D} 1·6617 n_{2D} 1·6737	1·6930	1·7040
II	1·5075	+	$Ab_{43}An_{57}$	n_{1D} 1·6617 n_{2D} 1·6757	1·6930	1·7040

I. Dacitic tuff, Tutizawa bed, Ôiso.
II. Dacite pumice, Simo-Tanna bed, Idu.

Evidences of fresh-water deposition are found both in the Tutizawa bed and in the Simo-Tanna bed. The Tutizawa bed contains " *Corbicula nipponensis* Prim." and " *Juglans sieboldiana* Max.[33]" It contains also brown coal containing plant fossils. The black clay in the Simo-Tanna bed contains plant fossils.

The Tutizawa bed was subjected to a crustal movement with considerable tilting and minor faulting. It is overlain by the Takao bed which practically consists of angular blocks of olivine-pyroxene-andesite. The Simo-Tanna bed was disturbed by faulting, tilting, and flexuring. It is covered with lavas and fragmentals of olivine-pyroxene-andesite.

The above-mentioned similarities, petrological, palaeontological, and structural, suggest that the Tutizawa bed and the Simo-Tanna bed are of the same age. If these beds are entirely of detrital origin, it would then be a rare coincidence that they are similar to each other in mineral composition. But they contain dacitic pumice which suggests juvenile ejecta (see p. 370), besides many isolated crystals similar to those in the pumice. Therefore, it would seem far more reasonable to conclude that both of them had received their share of dacitic juvenile ejecta at the same time from a certain volcanic centre that happened to be active at the time of

---

32) 丹那盆地
33) Y. Ôtuka, *loc. cit.*, 455–456.

their deposition in the Pleistocene period. It is to be noted that dacitic volcanism displayed activity in the northern Idu in the Pleistocene period.

5. *The so-called loam of Ôiso district* and *similar rocks in other localities.*

The material composing the so-called loam bed of the Ôiso district is almost destitute of microscopically determinable minerals except plagioclase and augite, which are very rarely found in the scoriaceous lapilli layers in the loam bed. The writer in his previous paper[34] suggested that the material composing the loam bed of Enosima may be of detrital origin. These beds are distributed widely in the Kwantô district, and are included stratigraphically in the name "Kwantô Loam". Petrographically, they show much variation, laterally as well as vertically. In Table IV. are shown the results of optical analyses of the minerals found in some specimens of this loam.

Table IV.

	Orthoclase	Plagioclase	Augite (n_{1D})	Hypersthene (n_{1D})
I	–	$Ab_{13}An_{87}$	1·6922	–
II	–	$Ab_{30}An_{70}$	1·6920	–
III	–	$Ab_5 An_{95}$	–	–
IV	+	–	1·6970	1·6899
V	–	$Ab_{78}An_{22}$	1·6937	–
VI	–	$Ab_{35}An_{65}$	1·6925	1·6940

I. Isolated crystals in lapilli in loam bed, Sibusawa[35], Ôiso.
II. Isolated crystals in the upper horizon of the loam bed, Enosima.
III. Isolated crystals in the lower horizon of the loam bed, Enosima.
IV. Isolated crystals in the lower part of the middle horizon of the loam bed, Masukatayama, Noborito[36].
V. Isolated crystals in the upper part of the middle horizon of the loam bed, Ibid.
VI. Isolated crystals in the loam bed, Ikégayato, about 5 km. southeast of Hatiôzi[37].

---

[34] H. Tsuya, *loc. cit.*

[35] 澁澤 [36] 登戸桝形山 [37] 池ケ谷戸, 八王子.

Petrographic Descriptions of the Rocks of Ôiso District.

The petrographic descriptions of typical rocks of the Ôiso district are given in the following order:

I. Siliceous sandstone (o? in Table I.)
II. a. Dacitic tuffs
    b. Dacite (Komayama bed.)
III. Tufaceous sandstone (Ôiso bed.)
IV. Pyroxene-andesite (Takatoriyama bed.)
V. Conglomerate (Nisikoiso bed.)
VI. Tufaceous shale (Ninomiya bed.)
VII. Dacitic tuff (Tutizawa bed.)
VIII. Olivine-augite-andesite (Kuroiwa bed.)
IX. Two-pyroxene-andesite (Takao bed.)
X. Loam (Loam bed.)

I. ***Siliceous sandstone*** (o? in Table I.) (Fig. 2.)

This rock occurs at Takatoriyama, about 1 km. northeast of Ôiso railway station on the Tôkaidô line, forming the foundation of the Takatoriyama bed. It occurs with siliceous shale.

Megascopic Characters.—The rock is light gray to green, medium-grained, and is compact. Visible in it are crystals, 1·0–1·5 mm. in diameter, of quartz, felspar, hornblende, and pyroxene.

Microscopic Characters.—This rock is composed of quartz, plagioclase, orthoclase, hornblende, hypersthene, augite, and magnetite, together with a few fragments of augite-andesite. Although these constituents are commonly angular to subangular, they are sometimes well rounded.

The quartz, 0·1–1·0 mm. in diameter, is not cracked, but is pure and free from any notable inclusions.

The plagioclase, 0·1-1·5 mm. in diameter, exhibits the simple and polysynthetic twinnings according to the Carlsbad and albite laws. The extinction angle is $Y \wedge (010)=20^\circ$ and the optic character of the mineral positive. The plagioclase was identified as andesine near $Ab_{60}An_{40}$. The mineral contains a few particles of dark brown glass.

The hornblende, 0·1–0·2 mm. in length, is moderately pleochroic. Its axial colors are X′—light yellowish green, Y′—deep brownish green, Z′—green. $c \wedge Z'$ (on 110) $= 14^\circ$. The maximum extinction angle measured is 17°. The refractive indices measured with the cleavage flakes are $n_{1D}=1{\cdot}6635$, $n_{2D}=1{\cdot}6767$.

The hypersthene, 0·1–0·5 mm. in length, shows alteration along its cleavage lines. The augite, less than 0·1 mm. in diameter, is negligible in quantity.

The fragments of augite-andesite, 0·3–0·5 mm. in diameter, contain a few plagioclase phenocrysts scattered through the groundmass which consists of plagioclase, augite, magnetite, and a brown glass base.

Another sample of the siliceous sandstone is free from isolated crystals of hornblende and hypersthene, but it contains abundant rock-fragments, chief among which are vitreous andesite, silicified rock, and quartz-orthoclase-oligoclase-hornblende-rock.

Fig. 2. Microphotograph of siliceous sandstone. × 30. p—andesine, ho—hornblende, hy—hypersthene, a— augite, q—quartz.

II. Dacitic tuffs and Dacite (Komayama bed.)
(Figs. 3 and 4.)

a. Dacitic tuffs. This rock occurs as disturbed strata at Komayama and its environs near Ôiso, and occurs with siliceous shale and breccia.

Megascopic Characters.—The dacitic tuffs are white. Angular fragments of plagioclase, quartz, and pyroxene are scattered through the white matrix.

Microscopic Characters.—There are two types of dacitic tuffs, the α-type and β-type.

α-type. Dacitic tuff of this type consists of plagioclase, quartz, hypersthene, augite, and colorless splinters of glass. The minerals are 0·1–1·0 mm. in diameter, quartz being the most abundant.

The plagioclase is twinned according to the albite laws. Zoning of less and more calcic plagioclases is absent. The refractive indices are $n_{1D}=1{\cdot}5573$, $n_{2D}=1{\cdot}5644$. Accordingly, the mineral was identified as labradorite $Ab_{45}An_{55}$. It contains minute inclusions of brown glass.

The hypersthene is moderately pleochroic. Its axial colors are X—yellowish green, Y—brownish green, Z—green. Optical plane parallel to the c-axis : the refractive index $n_{1D}=1{\cdot}7152$. The augite is light green. It is subordinate in amount.

The groundmass consists of angular splinters, 0·1–0·3 mm. in diameter, of pumiceous glass, perlitic glass, and light brownish obsidian. The refractive index of the pumiceous glass is $n_{1D}=1{\cdot}5070$.

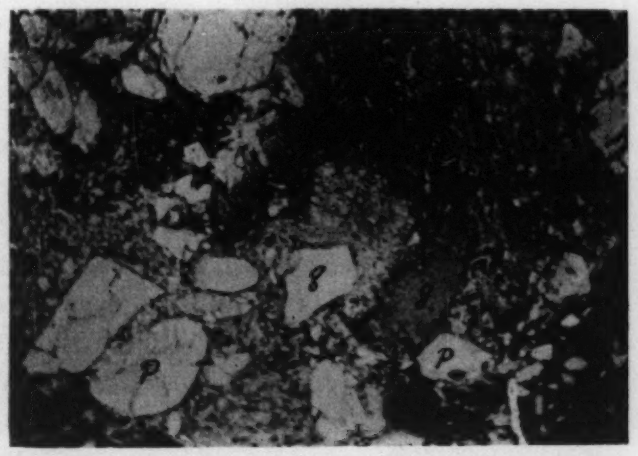

Fig. 3. Microphotograph of dacitic tuff (*α-type*). ×32. p—labradorite, q—quartz, hy—hypersthene, g—glass.

β-type. Dacitic tuff of this type consists of quartz, plagioclase, hypersthene, augite, and biotite, together with splinters of glass and a few fragments of hypersthene-andesite. These constituents are crushed into angular pieces and their interstices filled with calcite.

The plagioclase shows faint zoning of less and more calcic plagioclases. It is twinned according to the albite and Carlsbad laws. The optical character of the mineral is positive. It was identified as bytownite $Ab_{25}An_{75}$, with $n_{1D}=1{\cdot}5675$. Small particles of brown glass are included in the mineral.

The hypersthene is pleochroic. Its axial colors are X—brownish green, Y—brownish green, Z—green. Optical plane parallel to the c-axis: the refractive index $n_{1D}=1{\cdot}6998$. The augite occurs in subordinate amount as fragments of about 0·5mm. in diameter, with refractive index $n_{1D}=1{\cdot}6928$.

The biotite occurs in negligible amount as distorted flakes of about 0·5 mm. in length.

The glass splinters are obsidian with $n_D=1{\cdot}4980$. They are light brownish and contain microlites. The hypersthene-andesite, which occurs sporadically as angular fragments, 1·0–1·5 mm. in diameter, is porphyritic with phenocrysts of plagioclase and hypersthene scattered through a glassy groundmass.

b. Dacite. This rock occurs as dikes intruding into the Komayama bed.

Megascopic Characters.—The rock is white, medium-grained, and is fragile. It is percrystalline and is porphyritic with phenocrysts of quartz, plagioclase, hornblende, and hypersthene

Microscopic Characters.—The rock is sempatic to dosemic, and is composed of closely packed phenocrysts of quartz, plagioclase, hornblende, augite, and hypersthene, together with magnetite grains and interstitial glass base.

The plagioclase phenocryst, 0·5 mm. in diameter, is twinned according to the albite and Carlsbad laws. Zonal structure due to the chemical difference is exhibited. Recurrent zoning is often noticed. The less calcic shell part of the zonally built phenocryst was identified as labradorite $Ab_{45}An_{55}$ with the following optical properties: $n_{1D}=1{\cdot}5569$, $n_{2D}=1{\cdot}5620$. Extinction angle on section perpendicular to X is $Y \wedge (010)=28°$. The optical character is positive. The more calcic plagioclase (bytownite) forms the core part of the plagioclase phenocryst. Small enclosures of brown glass are arranged in zones parallel to the outline of the host mineral. The quartz, 0·3–0·6 mm. in diameter, is irregularly cracked, and has irregular outline either with rounded corner or with sharp edge. Rarely, the bipyramidal form of the mineral is incompletely developed. The mineral is almost free from inclusions except sporadic enclosures of a deep brown opaque mass.

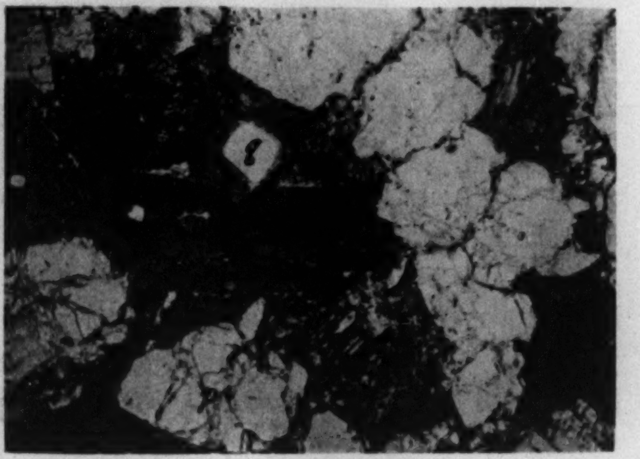

Fig. 4. Microphotograph of dacite. ×30. p—labradorite, q—quartz, ho—hornblende, hy—hypersthene.

The hornblende, 0·5–1·0 mm. in diameter, is euhedral to subhedral, but is frequently split along the prismatic cleavage lines. Lamellar twinning is often exhibited. The mineral shows a distinct pleochroism with the axial colors X′—pale greenish brown, Y′—green, Z′—dark green. Absorption $X' < Y' < Z'$: maximum extinction angle measured in thin section $c \wedge Z'=24°$: refractive indices $n_{1D}=1{\cdot}6587$, $n_{2D}=1{\cdot}6721$. The mineral contains inclusions of plagioclase.

The hypersthene, 0·1–1·0 mm. in length, occur as stout prisms, euhedral to subhedral, and shows distinct cleavage lines. Optical plane is parallel to the c-axis. The mineral is pale brown with faint pleochroism X—pale brown, Y—pale yellowish brown, Z—pale green. The refractive index $n_{1D}=1{\cdot}6991$. Enclosures are plagioclase prismoids and colorless glass. The augite, 0·1–0·5 mm. in diameter, is negligible in amount.

The groundmass is colorless glass in which are disseminated magnetite grains and plagioclase microlites. Angular fragments (1·0 mm. in diameter) of a microgranular rock and composed practically of quartz, albite, and chlorite are found though rarely.

III. ***Tufaceous sandstone*** (Ôiso bed.) (Fig. 5.)

This rock occurs at Sigitatusawa[38] and Terugasaki[39] near Ôiso as alternating layers of fine and coarse sands.

Megascopic Characters.—The rock is light gray and compact. It is porphyritic with pumiceous fragments (1·0–10 mm. in diameter) of pyroxene-andesite scattered through the tufaceous matrix in which are found plagioclase and pyroxene.

Microscopic Characters.—The rock is characterized by its numerous angular constituents, of which the following are noted:

Isolated crystals,

Plagioclase (bytownite), augite ($c \wedge Z = 45°$), hypersthene, hornblende, and quartz.

Rock-fragments,

Pumiceous two-pyroxene-andesite with phenocrysts of plagioclase ($Ab_{23}An_{77}$) augite ($n_{1D} = 1{\cdot}6940$), and hypersthene. Scoriaceous pyroxene-andesite. Microgranular quartz-rock. Pumice glass.

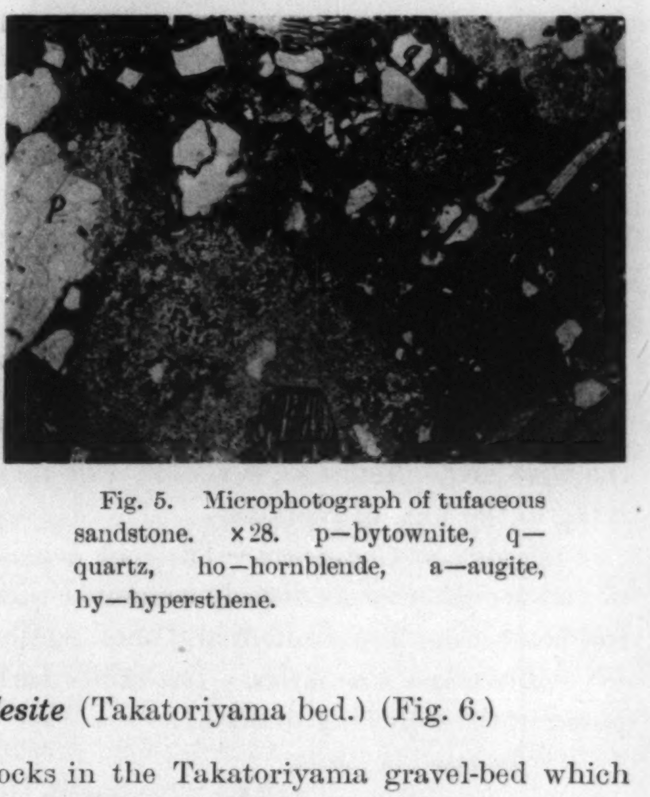

Fig. 5. Microphotograph of tufaceous sandstone. ×28. p—bytownite, q—quartz, ho—hornblende, a—augite, hy—hypersthene.

IV. ***Pyroxene-andesite*** (Takatoriyama bed.) (Fig. 6.)

This rock occurs as blocks in the Takatoriyama gravel-bed which passes laterally into agglomerate and downwards into lava of the pyroxene-

---

38) 鳴立澤 39) 照ヶ崎

andesite. It is exposed only in the southern part of the district at Takatoriyama and southwards. At Takatoriyama it rests on siliceous sandstone, the oldest bed (o? in Table I) of the district.

Megascopic Characters.—This rock is dark gray, and is free from phenocrysts except plagioclase, which however is very rarely found.

Microscopic Characters.—Plagioclase occurs as phenocrysts scattered through the groundmass. The plagioclase phenocryst, 0·1–0·3 mm. in diameter, is twinned according to the albite and Carlsbad laws. Very faint zoning of less and more calcic plagioclases is exhibited. The mineral was identified as bytownite $Ab_{18}An_{82}$ with $n_{1D}=1{\cdot}5710$ and $n_{2D}=1{\cdot}5775$.

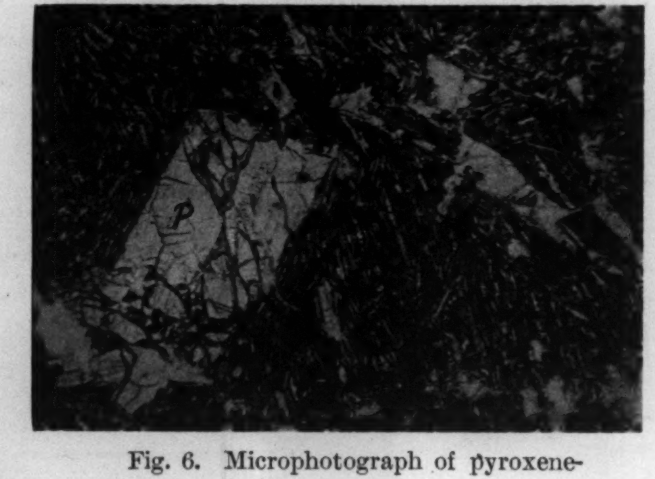

Fig. 6. Microphotograph of pyroxene-andesite. ×56.
p—bytownite.

The groundmass consists of plagioclase laths (0·1–0·3 mm. in length), augite prismoids (0·01 mm. in length), magnetite grains, and a brown glass base. The refractive index of the glass is a little higher than 1.5276.

V. *Conglomerate* (Nisikoiso bed.)

This rock occurs as a basal gravel-bed, resting unconformably on the Ôiso bed. As far as is visible, this rock exists only in a small area lying to the west of Nisikoiso.

Megascopic Characters.—The rock consists of round blocks or pebbles of various other rocks, loosely cemented with sands and calcareous material containing foraminifera and shell fossils.

Microscopic Characters.—The sandy part of the conglomerate is composed of the following material:

- Isolated crystals,
  - Plagioclase ($Ab_{45}An_{55}$), augite ($n_{1D}=1{\cdot}6930$–$1{\cdot}6945$), hypersthene and quartz.
- Rock-fragments,

Pumiceous hypersthene-andesite with phenocrysts of plagioclase ($Ab_{16}An_{84}$) and hypersthene ($n_{1D}=1{\cdot}7053$). Scoriaceous augite-andesite.

VI. ***Tufaceous shale*** (Ninomiya bed.) (Fig. 7.)

This rock occupies the greater part of the Ninomiya bed and is distributed in Azumamura[40] adjoining Ninomiya and westwards.

Megascopic Characters.—The rock is light gray, fine-grained to medium-grained, and is compact. A sandy part of this rock consists of plagioclase and pyroxene, together with rock-fragments, angular and round, besides a fine tufaceous matrix.

Microscopic Characters.—The rock is composed of the following material:

Isolated crystals,

Plagioclase ($Ab_{15}An_{85}$) and augite ($n_{1D}=$ 1·6948).

Rock-fragments,

Augite-andesite with phenocrysts of plagioclase ($Ab_{17}An_{83}$) and augite. Scoraceous hypersthene-andesite with phenocrysts of plagioclase ($Ab_{27}An_{73}$) and hypersthene. Brown glass pieces.

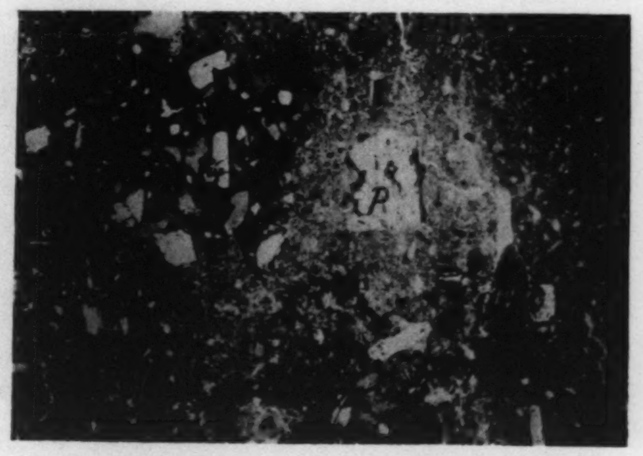

Fig. 7. Microphotograph of tufaceous shale. ×26. p—bytownite. hy—hypersthene in a scoriaceous fragment of hypersthene-andesite.

VII. ***Dacitic tuff*** (Tutizawa bed.) (Fig. 8.)

This rock occurs as sandy and clayey beds at Tutizawa, where it is associated with brown coal. The sandy part of the tuff passes laterally into tufaceous clay containing fossils of "*Corbicula nipponensis* Prim." and "*Juglans sieboldiana* Max.[41]" In a little higher horizon than the beds of sandy tuff and tufaceous clay there occurs a finely stratified bed of pumice which is also found abundantly in the lower tuff.

---

40) 吾妻村

41) Y. Ōtuka, *loc. cit.*, 455–456.

Megascopic Characters.—It is light yellowish gray, fine-grained to coarse-sandy, and is moderately congealed. In its sandy part are found crystals, usually less than 1 mm. in diameter, of plagioclase, hornblende, and pyroxene, together with pumice-fragments up to 2·5 cm. in diameter.

Microscopic Characters.—The rock contains much pumice. The pumice hold a few phenocrysts of plagioclase, hornblende, hypersthene, and augite. The plagioclase phenocryst, 0·4–1·0 mm. in diameter, is euhedral, and is twinned according to the albite and Carlsbad laws. Zonal structure due to the chemical difference is exhibited. The less calcic shell part of the mineral was identified as labradorite ($Ab_{45}An_{55}$), and the more calcic core part as bytownite ($Ab_{25}An_{75}$). The hypersthene, 0·1–0·2 mm. in length, is very weakly pleochroic with its optical plane often normal to the c-axis. Augite and hornblende occur as very minute crystals. The groundmass of the pumice is colorless glass with refractive index $n_D = 1{\cdot}5083$. In addition to the pumice, the tuff contains angular fragments of pyroxene-andesite.

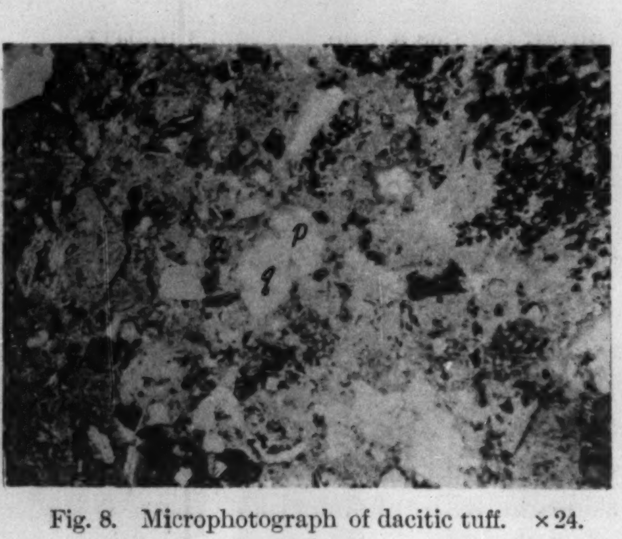

Fig. 8. Microphotograph of dacitic tuff. × 24.
q – quartz, p—labradorite, a – augite, g – pumice.

Isolated crystals contained in the tuff are plagioclase ($Ab_{38}An_{62}$-$Ab_{45}An_{55}$), hornblende ($n_{1D} = 1{\cdot}6617$, $n_{2D} = 1{\cdot}6737$), hypersthene ($n_{1D} = 1{\cdot}7045$), augite ($n_{1D} = 1{\cdot}6930$), and quartz (bipyramidal form).

VIII. Olivine-augite-andesite (Kuroiwa bed.) (Fig. 9.)

This rock occurs in the vicinity of Kuroiwa as the main constituent of the Kuroiwa gravel-bed.

Megascopic Characters.—The rock is dark gray, and is very porous. It is porphyritic with phenocrysts of plagioclase, pyroxene, and olivine.

Microscopic Characters.—The rock is sempatic, percrystalline, and consists of phenocrysts of plagioclase, augite, and olivine, together with a groundmass consisting of plagioclase, augite, magnetite, and a little glass base.

The plagioclase phenocryst is euhedral and is twinned in polysynthetic lamellae according to the albite law. Zonal structure due to the chemical difference is very faintly exhibited. The mineral was identified as anorthite Ab_4An_{96} with $n_{1D}=1{\cdot}5780$. The less calcic shell part is bytownite-anorthite Ab_{10}-An_{90} with $n_{1D}=1{\cdot}5750$.

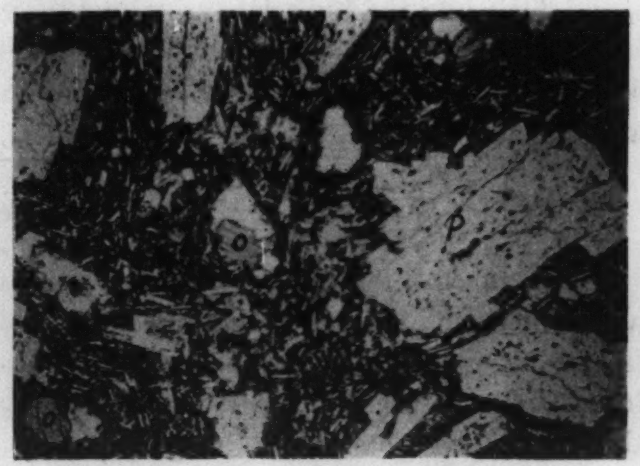

Fig. 9. Microphotograph of olivine-augite-andesite. ×30. p – anorthite, o – olivine.

The olivine has a refractive index $\alpha_D=1{\cdot}6804$. The augite phenocrysts are subordinate in amount.

IX. ***Two-pyroxene-andesite*** (Takao bed.) (Fig. 10.)

This rock occurs in the northern half of the Ôiso district as a pumice-bed 10 m. or more in thickness.

Megascopic Characters —The rock is pumiceous and is white to light gray. It is slightly porphyritic with phenocrysts of plagioclase and pyroxene.

Microscopic Characters.—The rock is dopatic, consisting of a few phenocrysts of plagioclase, augite, and hypersthene, together with an entirely glassy groundmass.

The plagioclase phenocryst, 0·1–0·3 mm. in diameter, is euhedral. Zonal structure due to the chemical difference is absent. The mineral was

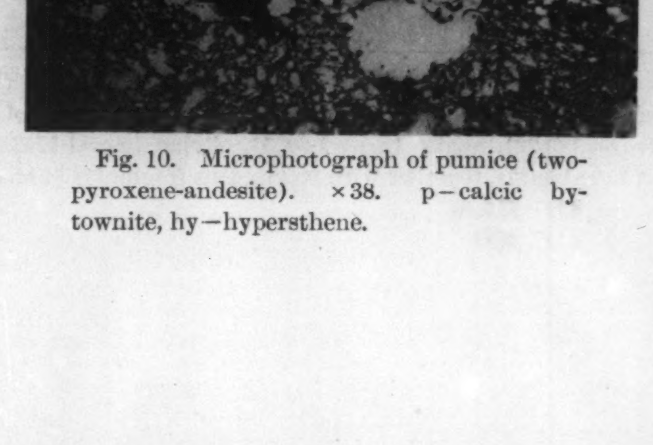

Fig. 10. Microphotograph of pumice (two-pyroxene-andesite). ×38. p – calcic bytownite, hy—hypersthene.

identified as calcic bytownite $Ab_{12}An_{88}$ with $n_{1D}=1{\cdot}5742$. It contains inclusions of brown glass. The augite phenocryst has a refractive index $n_{1D}=1{\cdot}6955$, and the hypersthene $n_{1D}=1{\cdot}6939$.

In addition to the pumice of two-pyroxene-andesite, the Takao bed[42] contains a few-fragments of hypersthene-augite ($n_{1D}=1{\cdot}6928$)-anorthite-andesite and of olivine ($\alpha_D=1{\cdot}6790$)-augite ($n_{1D}=1{\cdot}6966$)-anorthite-andesite.

X. ***Loam*** (Loam bed.)

The so-called loam bed of the Ôiso district rests on the Takao bed almost horizontally, and covers unconformably other beds older than the latter. A specimen of the loam collected from the upper horizon of the loam bed at Sinseiko[43] adjoining Hatano[44] was free from any minerals that could be determined megascopically or microscopically. Thin layers of black scoriaceous lapilli are found in some horizons of the loam bed. In the lapilli are seen a few isolated crystals of plagioclase ($Ab_{13}An_{87}$) and augite ($n_{1D}=1.6922$), together with pieces of obsidian ($n_D=1.5078$).

---

25. 相模國南西地域の堆積岩の岩石學的研究（二）

地震研究所 津屋弘逵

この論文は大礒地塊の地層を構成する岩石の岩石學的研究の結果である。大塚彌之助理學士の研究によれば大礒地塊は新第三紀層及び第四紀層より成る。これらの地層を構成する岩石は主として火山物質を材料とする堆積岩である。大塚理學士の研究されたこの地方の地質層序に從つて各地層を代表する岩石を檢べた結果、新第三紀層以後この地方に少くとも次の四期の火山活動が行はれたものと推定される。

1） 中新期一或はそれ以前・・・・・・・・・・石英安山岩の噴出
2） 中新期一鮮新期・・・・・・・・・・・・・基性安山岩の噴出
3） 洪積期前期・・・・・・・・・・・・・・・石英安山岩及び基性安山岩の噴出
4） 洪積期後期・・・・・・・・・・・・・・・最基性安山岩の噴出

現在では以上の四期以上に細分する確かな材料がない。然しこの地方に比較的酸性の火山岩と

---

[42] In a little lower horizon than the pumice-bed (Takao bed) there occurs a yellowish gray tuff-bed. The tuff contains abundant crystals of anorthite (Ab_7An_{93}), hypersthene ($n_{1D}=1{\cdot}6892$), augite ($n_{1D}=1{\cdot}6925$), olivine ($\alpha_D=1{\cdot}1743$, $\beta_D=1{\cdot}6905$), and a few fragments of hornblende, together with scoriaceous fragments of olivine-pyroxene-andesite.

[43] 震生湖

[44] 秦野

基性の火山岩とが新第三紀以後交互に噴出してゐることはかゝる堆積岩の研究によつて明かにせられた。この事實は伊豆半島の第三紀及びそれ以後の火山岩の噴出順序にも認められ、伊豆七島の新しい火山島に於ても認められてゐる。

所謂大磯地塊内にはその地層を構成する岩石に含まれてゐる火山物質を供給したと考へられる火山が存在しない。從つて、かゝる火山物質の本源は隣接地方に存在するに相違ない。大磯地塊の西隣には足柄地方及び伊豆地方の火山岩地域があるから、これらの地方の火山岩を研究すれば大磯地塊内の岩石に見られる火山物質の本源を推定し得るかも知れない。本論ではまだそこまで研究を進めてゐないが次の如き二、三の比較を試みた。

1. 大磯地塊で最古（中新期或はそれ以前）の地層と考へられてゐる珪質砂岩は筆者の前報告に記載した江ノ島第三紀層のうち下部三浦層の凝灰質砂岩に岩石學的に可なりよく一致してゐる。著しい相違は前者が石英を多量に含んで珪質なるに反し、後者は中性安山岩片を多量に含んで凝灰質であることである。

2. 大磯地塊の岩石より推定される最古の火山活動を代表する石英安山岩（中新期或はそれ以前）は伊豆地方に發達する數種の石英安山岩に比して斜長石斑晶、有色鑛物斑晶共に結晶作用の早期のものである。伊豆地方に於ても中新期或はその前後の火山活動に屬する石英安山岩は認められるが大磯地塊のそれと岩石學的に又層位學的に如何なる關係にあるかは今後の研究に俟たねばならぬ。

3. 大磯地塊の中新層及び鮮新層に多量に含まれてゐる基性安山岩質の火山物質は何れも類似してゐて層序學的細分に從つて區別し得る特徴を示さない。これらは足柄地方に發達する足柄層及び江ノ島の上部三浦層を構成する岩石に含まれてゐる火山物質に類似してゐる。從つて足柄層及び江ノ島の上部三浦層が大磯地塊の中新層及び鮮新層の何の層位に相當するかは岩石學的に確言し得ない。然し、江ノ島の上部三浦層と足柄層とは少くとも岩石學的には略對比され得るから、足柄層が大磯地塊の下部鮮新層に層位學的に對比されるならば江ノ島の上部三浦層も亦後者に對比されても不都合ではない。

4. 大磯地塊の下部洪積層には石英安山岩質の火山物質が含まれてゐる。これは北伊豆の下丹那附近に發達する洪積層中に含まれてゐる石英安山岩質の火山物質に極めてよく類似してゐる。また前者は植物化石、淡水性の貝化石等を含み、後者は植物化石を含む。地層の採め方も兩者略同程度である。從つて、兩地層は略對比れさ得るものでその堆積時代に石英安山岩の噴出があつたと推定される。大磯地塊ではこの地層の上に最基性の安山岩物質を含む地層が發達してゐるが北伊豆に於ても箱根、熱海附近の新期の最基性安山岩は下丹那の石英安山岩を含む洪積層より新しい。故に一般に伊豆地方の最基性の玄武岩質安山岩は下部洪積層後の噴出で伊豆七島に於ける大島、三宅島等に於ける如く現在まで續いてゐる。

5. 大磯地塊に發達する所謂ローム層は安山岩質スコリアの如き火山物質を含んでゐるが一般に顯微鏡下にても鑑定し得る鑛物少く他の地方の類似層と十分比較し得ない。

26. *Seismometrical Report.*

地震觀測報告

(Earthquake Research Institute, Tôkyô, Japan.)

(January 1—March 31, 1931.)

Introduction.

The object of this new column is to report all earthquakes that have been felt without instrumental aid as registered at stations in the seismic network framed over the Kwantô districts by the Earthquake Research Institute of the Tôkyô Imperial University. In the case of important earthquakes, their seismograms will be reproduced, while, as of possible aid to international co-operation, distant earthquakes will also be reported.

As shown in List I, there are eight permanent seismological stations in the Kwantô district, and these will supply us with the necessary data. Data from such temporary stations as Wakayama and Idu will not be reported.

(1) *Seismological stations in the Kwantô districts.*

List I.

Station	Coordinates		Approximate distance from Tôkyô (Hongô)
	Longitude (E)	Latitude (N)	
Tôkyô (Hongô)	139° 45′ 59″	35° 42′ 40″	0 km.
Kamakura	139° 32′ 39″	35° 18′ 32″	48
Kiyosumi	140° 09′ 02″	35° 09′ 22″	70
Misaki	139° 37′ 05″	35° 09′ 26″	62
Titibu	139° 04′ 54″	35° 58′ 56″	69
Tôgane	140° 21′ 38″	35° 34′ 00″	55
Tukuba	140° 06′ 36″	36° 12′ 39″	64
Mitaka	139° 32′ 32″	35° 40′ 20″	20

(2) ***Instruments.***

List II.

(A) Tôkyô (Hongô).

No.	Name or type component	Weight of the bob (kg.)	Magnification or minification	Natural period (sec.)	Damping ratio	Time scale mm./min.	Remarks
1	(E.W.) (N.S.) (Vert.)	2 2 1	1/2 1/2 1/2	10 10 6	2·0 2·0 2·0	50	With oil damper.
2	(E.W.) (N.S.) (Vert.)	2 2 0·45	2 2 2	10 10 5	2·5 2·5 2·0	40	With oil damper.
3	(E.W.) (N.S.)	15 15	1½ 1½	50 50	1·5 1·5		With oil damper.
4	(E.W.) (N.S.)	7 7	50 50	7 7	1·3 1·3	60	
5	(E.W.) (N.S.) (Vert.)	7 7 7	50 50 28	7 7 7	1·5 1·5 1·5	50	With magnetic damper.
6	(E.W.)	30	300	12	1·7	100	
7	(N.S.)	30	300	12	1·7	100	
8	(E.W.)	15	15	50	2·0	15	
9	(N.S.)	15	10	50	2·0	25	
10	(N.S.)	30	120	18	2.0	60	
11	Wiechert (E.W.N.S.)	200	120	14	5·0	10	With air damper.
12	Ewing-Gray type (E.W.) (N.S.) (Vert.)	 2 2 0·8	 3½ 3½	 5 5	 1·5 1·5	 600	Record-receiver starts automatically.
13	Tanakadate (E.W.) (N.S.) (Vert.)	 1.5 1.5 1.5	 1 1 1		 1·5 1·5 1·2	 150	Ditto.
14	(E.W.)	17	15	60	3·2	27	With magnetic damper.
15	(N.S.)	42	20	60	2·0	25	Ditto.
16	(E.W.)	10	5	210	1·5	50	
17	(N.S.)	15	1½	210	1·2	40	
18	(E.W.)	40	120	25	2·0	25	

(to be continued.)

(A) Tôkyô (Hongô). (*continued.*)

No.	Name or type component	Weight of the bob (kg.)	Magnification or minification	Natural period (sec.)	Damping ratio	Time scale mm./min.	Remarks
19	(N.S.)	60	120	20	2·5	25	
20	Wiechert (Vert.)	1300	120	6	5·0	15	With air damper.
21	(Vert.)	10	20	15	1·7	22·5	
22	(Vert.)	45	7½	20	3·0	4·0	With magnetic damper.
23	Galitzin. (E.W.)	13		Pendul. 24 Galva. 24	∞	27	With magnetic damper.
24	Galitzin. (N.S.)	13		Pendul. 24 Galva. 24	∞	27	Ditto.
25	Galtzin (vert.)			Pendul. 13 Galva. 13	∞		
26	Long Pendulum	300	50	6·7		60	
27	Ishimoto Acceleration seismograph (E.W. N.S.)	13		0·15	∞	57	1 mm. deviation of the index end =1 gal ca.
28	Clinograph (E.W.)	8	15	32			
	(N.S.)	8	15	32		0·12	

(B) Kamakura.

No.	Component	Weight of the bob (kg.)	Magnification	Natural period (sec.)	Damping ratio	Time scale mm./min.	Remarks
1	(E.W.)	2	2	10	2·0	40	With oil damper.
	(N.S.)	2	2	10	2·0		
	(Vert.)	0·45	2	5	2·0		
2	(E.W.)	15	10	30	1·2	15	
3	(Vert.)	4	10	10	2·0	25	
4	(E.W.)	7	50	10	1·5	50	
	(N.S.)	7	50	10	1·5		

(C) Kiyosumi.

No.	Component	Weight of the bob (kg.)	Magnification	Natural period (sec.)	Damping ratio	Time scale mm./min.	Remarks
	(E.W.)	7	50	7	1·5	50	
	(N.S.)	7	50	7	1·5		

(D) Misaki.

No.	Component	Weight of the bob (kg.)	Magnification	Natural period (sec.)	Damping ratio	Time scale mm./min.	Remarks
	(E.W.)	12	120	4	1·5	50	
	(N.S.)	12	120	4	1·5		

(E) Titibu.

No.	Component	Weight of the bob (kg.)	Magnification	Natural period (sec.)	Damping ratio	Time scale mm./min.	Remarks
1	(E.W.)	7	50	7	1·3	60	
	(N.S.)	7	50	7	1·3		

(F) Tôgane.

No.	Component	Weight of the bob (kg.)	Magnification	Natural period (sec.)	Damping ratio	Time scale mm./min.	Remarks
1	(E.W.)	7	50	7	1·5	50	
	(N.S.)	7	50	7	1·5		

(G) Tukuba.

No.	Component	Weight of the bob (kg.)	Magnification	Natural period (sec.)	Damping ratio	Time scale mm./min.	Remarks
1	(N.S.)	35	120	21	2·0	25	
2	(E.W.)	35	120	21	2·0	25	

(H) Mitaka.

No.	Component	Weight of the bob (kg.)	Magnification	Natural period (sec.)	Damping ratio	Time scale mm./min.	Remarks
1	(E.W.)	7	50	7	1·3	60	
	(N.S.)	7	50	7	1·3		
	(Vert.)	7	28	7	1·3		
2	(E.W.)	40	80	18	2·0	25	
3	(N.S.)	40	80	18	1·9	25	

(3) *Sensible earthquakes in Tôkyô for the period January 1—March 31, 1931.*

List III.

Time = Central standard time of Japan (Civil mean time of the meridian 135° E).

Notation:

prel. tr. = Preliminary tremors.
N.S. = North-south component.
E.W. = East-west component.
2A = Range of motion.
T = Period of earthquake motion.
λ = Longitude.
φ = Latitude.
D = Depth.

Intensity: I (slight), II (rather weak), III (weak), IV (rather strong), V (strong), VI (violent).

No.	Station	Date	Time of occurrence	Duration		Maximum motion				Epicentre		D	Intensity
				Prel. tr.	Total	N.S.		E.W.		λ (E)	φ (N)		
						2A	T	2A	T				
			h m s	s	m	μ	s	μ	s	°	°	km.	
1	Tôkyô	Jan. 5	17 14 59·3	15·0	2	32	(0·3)	34	(0·3)	139·6	35·00	90	I
	Kamakura			11·6	2·7	28	(0·3)	48	(0·3)				
	Misaki			12·0	3	21	(0·5)	22	(0·6)				
	Kiyosumi			13·2	2	4	(0·6)	13	(0·9)				
	Titibu			20·8	2			12	(0·8)				
	Tôgane			15·8	2	8	(0.4)	8	(0·4)				
	Tukuba		15 4·8	12·8	1·5								
	Mitaka		17 15 0·6	14.4	2	28	(0·2)	23	(0·2)				
2	Tôkyô	23	1 59 35·4	31·4	12	56	(0·6)	74	(0·6)	141·81	36·80		I
	Kamakura			37·0	14	30	(0·7)	34	(0·6)				
	Misaki			37·5	10	43	(0·7)	38	(0·6)				
	Kiyosumi			31·5	11	12	(0·9)	20	(0·9)				
	Titibu			35·0	6			68	(0·8)				
	Tôgane			24·8	10	26	(0·8)	16	(0·7)				
	Tukuba		1 59 22·1	21·5	5								II
	Mitaka		1 59 39·0	32·5	10	116	(2·4)	86	(2·1)				
3	Tôkyô	30	10 40 29·5	6·9	4	294	(0·4)	340	(0·4)	139·90	36·06	40	II
	Kamakura			13·2	3	10	(0·5)	8	(0·5)				
	Misaki			13·8	4	37	(0·5)	29	(0·7)				
	Kiyosumi			14·2	5	24	(0·5)	20	(0·6)				
	Titibu			8·4	5	44	(0·2)	22	(0·2)				
	Tôgane			9·1	3	44	(0·3)	46	(0·3)				I
	Tukuba		10 40 25·0	6·2	1·8								III
	Mitaka		10 40 32·2	8·7	3·5	86	(0·3)	128	(0·6)				II

List III. (*continued.*)

No.	Station	Date	Time of occurrence	Duration		Maximum motion				Epicentre		(D)	Intensity
				Prel. Tr.	Total	N.S.		E.W.		λ (E)	φ (N)		
						2A	T	2A	T				
			h m s	s	m	μ	s	μ	s	°	°	km.	
4	Tôkyô	Feb. 4	8 33 55·8	12·7	3	36	(0·4)	28	(0·4)	140·00	35·00	50	I
	Kamakura												
	Misaki			8·1	3	20	(0·6)	28	(0·6)				I
	Kiyosumi												
	Titibu												
	Tôgane			11·6	3	22	(0·6)	10	(0·6)				
	Tukuba												
	Mitaka		8 33 56·8	11·7	2·5	15	(0·6)	27	(0·6)				
5	Tôkyô	4	13 37 32·3	12·2	2·5	44	(0·3)	36	(0·3)	139·91	35·29	90	I
	Kamakura												
	Misaki			9·9	3	17	(0·4)	15	(0·4)				
	Kiyosumi		13 37 21·0	11·8	2·5	8	(0·3)	6	(0·2)				
	Titibu			15·4	1	4	(0·3)	4	(0·3)				
	Tôgane			12·1	2	10	(0·3)	10	(0·3)				
	Tukuba												
	Mitaka		13 37 33·0	11·5	2	14	(0·3)	26	(0·3)				
6	Tôkyô	9	23 45 15·0	20·9	3	32	(0·3)	28	(0·3)	139·46	35·27	143	I
	Kamakura			19·3	3	20	(0·6)	30	(0·6)				
	Misaki			19·6	3	29	(1·7)	42	(0·6)				
	Kiyosumi			21·3	3	12	(1·2)	12	(1·2)				
	Titibu			22·3	3	16	(0·9)	12	(0·7)				
	Tôgane			22·5	3	22	(0·8)	20	(0·8)				
	Tukuba		23 45 16·6	25·4	1·6								
	Mitaka		23 45 14·9	20·2	3	32	(0·3)	38	(0·3)				
7	Tôkyô	20	6 42 33·4	5·0	1·5	66	(0·3)	90	(0·3)	139·73	35·79	40	
	Kamakura			8·0	1·5	11	(0·4)	8	(0·4)				
	Misaki			10·0	2	15	(0·8)						
	Kiyosumi			12·0	1·5	6	(0·8)	6	(0·8)				
	Titibu												
	Tôgane			9·6	2	30	(0·5)	25	(0·7)				
	Tukuba		6 42 35·9	8·6	1								
	Mitaka		6 42 33·7	4·8	1	50	(0·3)	62	(0·3)				
8	Tôkyô	20	14 35 34·0	99·7	90	3200	(5·8)	2500	(6·8)	137·60	43·40		I
	Kamakura			103·0	60	900	(4·8)	1100	(3·9)				
	Misaki			110·4	40	360	(1·4)	290	(1·4)				
	Kiyosumi		14 35 39·9	108·5	60	620	(5·0)						
	Titibu			97·5	30	1360	(7·4)	736	(4·8)				
	Tôgane			102·0									II
	Tukuba		14 35 28·0	93·5	29								I
	Mitaka		14 35 35·5	76·2	70								I
9	Tôkyô	23	20 08 07·3	15·3	7	61	(0·3)	40	(0·3)	140·61	36·30	50	
	Kamakura			20·7	7	32	(0·4)	48	(0·4)				
	Misaki			24·2	7	40	(0·6)	30	(0·6)				
	Kiyosumi			19·5	7	64	(3·3)	80	(2·6)				
	Titibu												
	Tôgane			14·9	6	40	(1·8)	46	(1·8)				
	Tukuba		20 07 55·5	9·6	3·5								
	Mitaka		20 08 09·0	17·5	6	48	(2·1)	28	(0·3)				

List III. (*continued.*)

No.	Station	Date	Time of occurrence	Duration		Maximum motion				Epicentre		D	Intensity
				Prel. Tr.	Total	N.S.		E.W.		λ (E)	φ (N)		
						2A	T	2A	T				
			h m s	s	m	μ	s	μ	s	°	°	km.	
10	Tôkyô	Mar. 4	5 39 56·3	25·6	7	70	(0·6)	46	(0·6)				I
	Kamakura			29·0	9	70	(0·5)	62	(0·7)				
	Misaki			31·0	7	57	(0·6)	54	(0·6)				
	Kiyosumi		5 39 59·2	28·3	8	10	(1.2)	20	(1·2)				
	Titibu			27·3	7	24	(0·6)	46	(0·8)				
	Tôgane			24·0	5	100	(1·9)	120	(1·9)				
	Tukuba		5 39 30·2	20·4	6								II
	Mitaka		5 39 59·2	25·0	6	86	(1·0)	54	(0·5)				
11	Tôkyô	7	1 13 37·2	14·8	20	160	(0·5)	104	(0·5)	138·8	35·0		I
	Kamakura			11·7	20	370	(1·2)	140	(1·1)				
	Misaki			11·6	9	164	(0·5)	117	(0·5)				
	Kiyosumi			16·4	15	90	(3·5)	180	(3·5)				
	Titibu			12·2	5	86	(1·2)	11	(1·2)				
	Tôgane			22·3	15	44	(0·8)	26	(0·7)				
	Tukuba		1 13 44·5	20·2	7								
	Mitaka												
12	Tôkyô	7	1 53 49·7	15·4	15	620	(1·0)	310	(1·0)	138·9	35·0		II
	Kamakura			10·2	10	526	(1·1)	414	(1·5)				
	Misaki			10·1	10	455	(0·6)	262	(0·6)				
	Kiyosumi			16·2	10	170	(3·3)	192	(3·3)				
	Titibu			12·6	7	200	(1·0)	290	(1·1)				
	Tôgane			20·1	15	100	(1·0)	120	(1·1)				I
	Tukuba		1 53 54·5	20·0	9								II
	Mitaka		1 53 46·5	11·6	15	950	(1·7)	645	(1·6)				
13	Tôkyô	9	12 50 06·2	82·0	60	5600	(4·0)	8300	(4·7)	142·70	40·75		
	Kamakura			65·5	30	4250	(2·5)	3500	(2·6)				
	Misaki			75·5						(Off the coast of Hatinoye)			
	Kiyosumi		12 50 16·8	82·0									
	Titibu			72·0									
	Tôgane			86·6						(See Fig. 1)			I
	Tukuba		12 49 52·8	65·0	56								I
	Mitaka		12 50 05·8	77·5									I
14	Tôkyô	10	3 41 01·7	9·1	6	164	(0·3)	434	(0·3)	139·23	35·74	45	II
	Kamakura			9·4	6	65	(0·5)	62	(0·5)				
	Misaki			10·6	3	—	—	42	(0·6)				
	Kiyosumi			15·5	6	20	(0·8)	48	(0·9)				
	Titibu			7·4	4	100	(0·4)	108	(0·4)				
	Tôgane												
	Tukuba		3 41 04·8	10·8	2.3								
	Mitaka		3 41 01·3	8·8	4	248	(0·4)	326	(0·7)				II
15	Tôkyô	12	14 06 21·1	13·2	4	80	(0·7)	60	(0·7)	140·30	36·07	80	
	Kamakura												
	Misaki			17·6	3	58	(0·6)	46	(0·6)				
	Kiyosumi		14 06 21·8	16·9	2	4	(0·6)	10	(0·6)				
	Titibu			15·9	3	34	(0·4)	28	(0·5)				
	Tôgane			13·6	2			28	(0·9)				
	Tukuba		14 06 14·7	9·6	2								I
	Mitaka		14 06 22·2	14·1	2·5	62	(0·3)	50	(0·3)				

List III. (*concluded.*)

No.	Station	Date	Time of occurrence	Duration		Maximum motion				Epicentre		D	Intensity
				Prel. Tr.	Total	N.S.		E.W.		λ (E)	φ (N)		
						2A	T	2A	T				
			h m s	s	m	μ	s	μ	s	°	°	km.	
16	Tôkyô	Mar. 23	17 28 41·8	7·5	4	52	(0·4)	61	(0·4)	140·2	36·0	30	
	Kamakura			13·4	3	20	(0·9)	20	(0·9)				
	Misaki			13·9	3	18	(0·7)	13	(0·6)				
	Kiyosumi			13·4	4	6	(0·6)	6	(0·6)				
	Titibu			10·4	3	24	(0·3)	20	(0·2)				
	Tôgane			9·0	3	15	(0·8)	26	(0·8)				
	Tukuba		17 28 39·1	5·7	1.7								
	Mitaka		17 28 43·1	9·3	3	15	(0·4)	46	(0·8)				
17	Tôkyô	23	20 24 43·7	6·9	3	24	(0·5)	30	(0·5)	139·83	36·05	20	I
	Kamakura			11·7	3	14	(0·6)	8	(0·6)				
	Misaki			15·3	3	5	(0·5)	3	(0·5)				
	Kiyosumi			14·1	1	4	(1·0)	3	(0·6)				
	Titibu			9·4	2	18	(0·2)	16	(0·2)				
	Tôgane			10·2	3	4	(0·4)	6	(0·5)				
	Tukuba		20 24 35·8	6·2	1.4								
	Mitaka		20 24 39·6	8·8	2·5	10	(0·4)	10	(0·7)				
18	Tôkyô	25	1 29 01·1	3·6	1	36	(0·4)	36	(0·4)				
	Kamakura			6·3	1.2	12	(0·3)	12	(0·3)				
	Misaki			8·1	1	10	(0·6)	10	(1·2)				
	Kiyosumi												
	Titibu												
	Tôgane												
	Tukuba												
	Mitaka		1 29 01·3	5·0	1	36	(0·2)	28	(0·2)				
19	Tôkyô	26	15 30 36·8	11·2	4	64	(0·3)	106	(0·3)	139·09	36.19	15	I
	Kamakura			14·4	3	32	(0·5)	48	(0·5)				
	Misaki			16·9	4	19	(0·9)	13	(0·9)				
	Kiyosumi			20·2	3	4	(0·6)	6	(0·5)				
	Titibu			3·8	3	112	(0·5)	140	(0·5)				
	Tôgane			18·1	2	20	(0·7)	25	(0·7)				
	Tukuba												
	Mitaka		15 30 33·1	11·1	3·5	40	(0·2)	32	(0·2)				
20	Tôkyô	27	5 25 35·9	9·3	4	81	(0·3)	96	(0·3)	140·36	35·34	30	II
	Kamakura			10·4	5	90	(0·6)	145	(0·6)				
	Misaki			9·7	5	57	(0·5)	71	(0·5)				
	Kiyosumi		5 25 31·1	4·9	4	420	(0·5)	448	(0·5)				II
	Titibu			18·0	4	30	(1·3)	20	(0·9)				
	Tôgane			5·0	3	650	(0·2)	550	(0·2)				III
	Tukuba		5 25 37·5	12·0	1.7								
	Mitaka		5 25 40·0	13·5	3·5	166	(0·5)	72	(0·5)				
21	Tôkyô	29	20 14 25·9	6·2	2.5	40	(0·5)	36	(0·5)	139·49	35·54	32	I
	Kamakura			5·7	2	40	(0·4)	24	(0·4)				
	Misaki			7·3	2	22	(0·7)	19	(0·7)				
	Kiyosumi			11·4	3	4	(0·6)						
	Titibu			9·5	2.5	2	(0·5)	4	(0·7)				
	Tôgane			11·5	3	12	(0·5)	8	(0·9)				
	Tukuba		20 14 36·4	10·1	1								
	Mitaka		20 14 25·1	3·8	2	84	(0·5)	105	(0·3)				I

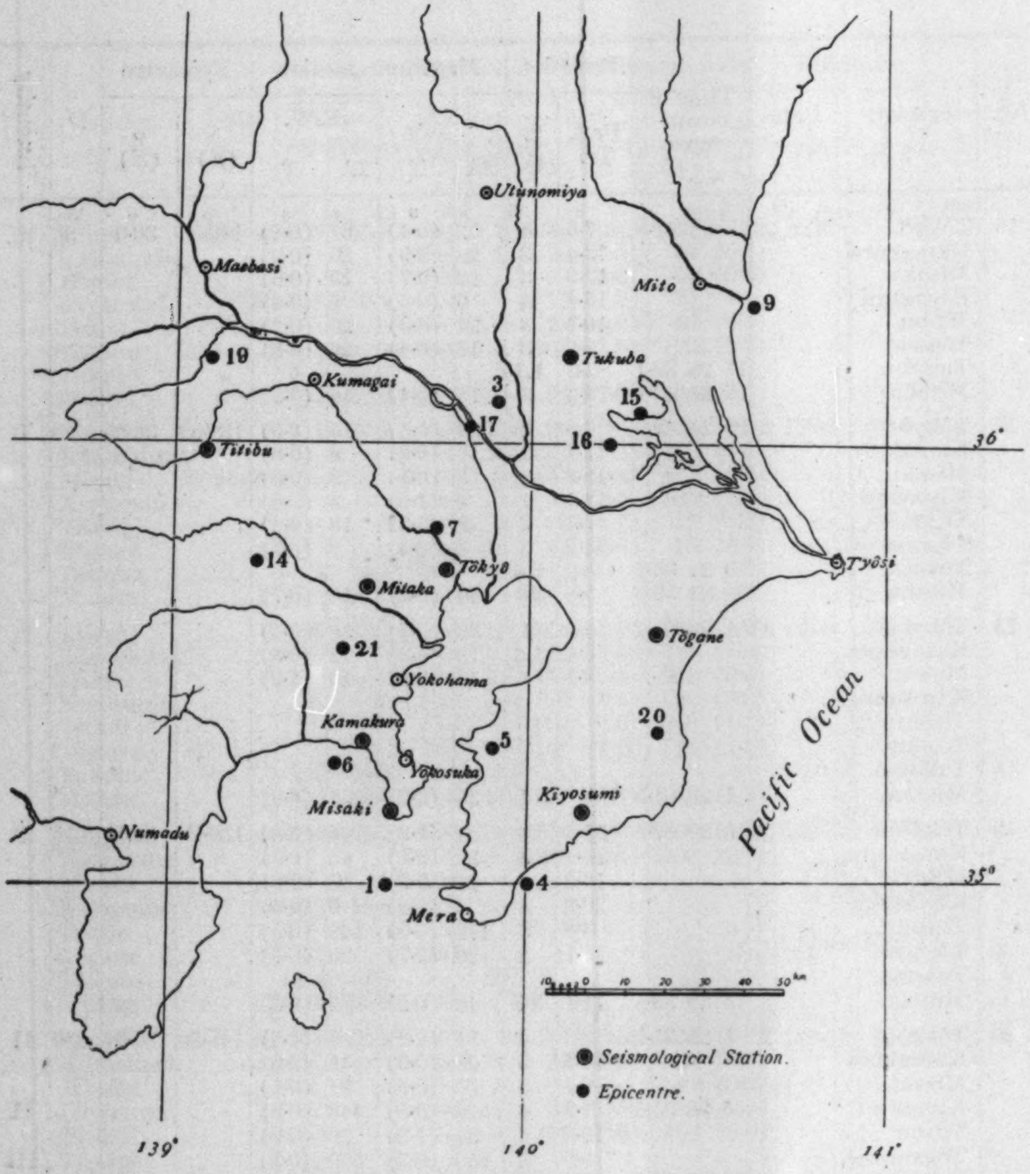
Utunomiya
Maebasi
Mito
9
19
Tukuba
Kumagai
3
15
17
16
Titibu
36°
7
Tôkyô
14
Mitaka
Tyôsi
Tôgane
21
Yokohama
Pacific Ocean
20
Kamakura
5
6
Yokosuka
Kiyosumi
Misaki
Numadu
1
4
35°
Mera
10 0 10 20 30 40 50 km
Seismological Station.
Epicentre.
139°
140°
141°

Fig. 2. Distribution of the epicentres of the sensible earthquakes that originated within 160 km. from Tôkyô for the period January 1-March 31, 1931. (Figures attached to each epicentre correspond to earthquake number in List III.)

(4) *Important distant earthquakes as observed in Tôkyô (Ĥongô).*

List IV.

Notation: EW = East-west component.
+ = towards east.
− = towards west.
NS = North-south component.
+ = towards north.
− = towards south.
G.M.T. = Greenwich mean time.

Date	Phase	Time of occurrence. (G. M. T.)	Amplitude (2A)	Period	Probable epicentre and remarks
		h m s	μ	sec.	
Jan 15	P	2 05 22·2			Mexico.
	S	2 16 52·2			
	L	2 34 33·7			
	M(EW)	2 45 01·5	+ 400	25·2	
	M(NS)	2 35 22·2	− 550	23·3	
15	P	21 02 32·8			
	S	21 08 28·5			
	M(EW)	21 10 43·3	− 343	10·7	
	M(NS)	21 11 03·6	+ 363	10·6	
15	P	22 49 23·7			
	S	22 56 16·2			
	L	23 00 13·7			
	M(EW)	23 01 57·6	− 100	23·0	
	M(NS)	23 01 56·2	+ 225	25·0	
27	P	20 16 21·0			
	S	20 23 10·7			
	L	20 28 19·6			
	M(EW)	20 32 02·4	+1170	12·0	
	M(NS)	20 31 27·1	+1300	13·0	
28	P	21 29 21·9			
	S	21 33 57·1			
	L	21 35 21·4			
	M(EW)	21 35 36·2	−3000	25·0	
	M(NS)	21 36 46·2	+2167	27·0	
Feb. 2	P	22 59 09·6			New Zealand, Hawkee Bay.
	S	23 09 20·2			
	L	23 21 37·0			
	M(NS)	23 26 10·0	+1300	43·0	(See Fig. 3, 4)
	M(EW)	23 26 24·0	−1000	37·0	
	M(Vert.)	23 26 29·0	70	32·0	
	M(EW. max.)	23 32 0 (approx.)	2500	21·0	
	M(NS. max.)	23 28 30 (approx.)	1800	27·0	
	M(Vert. max.)	23 29 0 (approx.)	250	26·0	

(*to be continued.*)

List IV. (*concluded.*)

Date	Phase	Time of occurce (G. M. T.)	Amplitude (2A)	Period	Probable epicentre and remarks
10	P	6 44 23·0			
	S	6 51 56·0			
	L(?)	7 05 28·0			
	M(?)	7 08 38·0			
Mar. 19	P	6 30 19·8			
	S	6 35 08·8			
	L	6 37 00			
28	P	12 46 41·0			
	S	12 53 08·0			
	L(EW)	12 57 46·0	2100	58·0	
	L(NS)	12 57 46·0	300	59·0	
	M(EW)	13 00 00	600	63·0	
	M(NS)	13 00 00	1400	60·0	

(5) *Preliminary notes on the strong earthquake of June 17, 1931.*

After the previous report had already been written Tôkyô was strongly shaken by an earthquake in the evening of June 17. This earthquake caused no serious damage. In some parts of Tôkyô, however, electric lights went out owing to breakage of wires on account of shock. It is reported that in Itabasi, a suburb northwest of Tôkyô, a poultry-yard was burned down by fire through overturning of a petroleum lamp. It seemed that the shock was especially strong at the west or northwest suburb of Tokyo. In Yokohama the intensity was somewhat lighter than at Tôkyô, but all the electric lights and all street cars were put out of service for about ten minutes following the shock. Duration of the preliminary tremors at Hongô was 6,8 seconds, the beginning of which was felt strongly as an up-and-down motion. Duration of the sensible shocks at Tôkyô was about 40 seconds.

Times of occurrence of this earthquake at Hongô, Tukuba, Mitaka, Kamakura and Kiyosumi were as follows: These stations are supplied with wireless signals.

Station	Time ot occurrence		
Tôkyô	21^h	09^m	$50{\cdot}3^s$
Mitaka	21	09	49.0
Tukuba	21	09	54·3
Kamakura	21	09	52·5
Kiyosumi	22	09	55·3

Durations of the preliminary tremors and directions of the initial motion.

Station	Duration of preliminary tremors	Direction of initial motion
Tôkyô	6·8 sec.	N 73° W down
Mitaka	6·7 ?	N 32° W down ?
Kamakura	10·3	N 21° W down
Titibu	8·1	N 56° W
Kiyosumi	13·5	N 35° W
Tôgane	12·1	N 66° W
Misaki	—	N 15° W
Tukuba	10·0	S 19° W
Koyama	9·6	E
Tanna	11·5	N 40° E down
Itô	11·6	N 32° E

(See Figs. 7—10.)

Maximum Range and period of the earthquake at Hongô.

All the seismographs having magnifications larger than ten-time were put out of order by the strong shock. The pointers of these seismographs were bent and gave only registers of the preliminary portion. The periods and the maximum ranges of component earthquake motions as registered by the strong motion seismograph (No. 3 in List II) were as follows:

Component	Range	(Period)
N. S.	42·1 mm.	(2·4 sec.)
E. W.	20·2 mm.	(2·4 sec.)
Vert.	8·3 mm.	(2.4 sec.)

(See Figs. 5 and 6)

Intensity (Acceleration) of the earthquake.

According to the Ishimoto acceleration seismograph diagram, (see Fig. 11), maximum accelerations of the horizontal component motions at Tôkyô (Hongô) were as follows:

Component	Max. Acceleration	Direction	Time from beginning of the earthquake.
E. W.	49·5 gal.	towards E.	10·4 sec.
N. S.	45·5 gal.	towards S.	9·5 sec.

Intensity of this earthquake was V (strong) in the intensity scale, or VII in the Rossi-Forel scale.

Probable origin of the earthquake. From the data above given the position of the epicentre and the approximate depth work out as follows:

Epicentre	Depth (approx.)
$\lambda = 139{\cdot}6°$ E $\varphi = 35{\cdot}7°$ N	45 km.

Epicentre is probably a point about 20 km. distant from Hongô in a westerly direction.

(N. Nasu and Ch. Yasuda are responsible for this report.)

Fig. 1. Tôkyô Observation of the Northeast Japan earthquake of March 9, 1931.
a · · · · · · · · beginning.

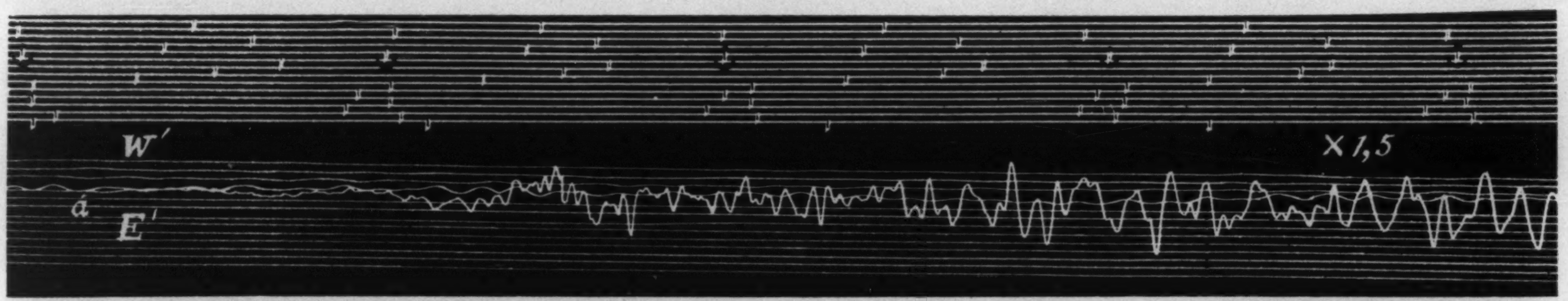

E′ = N 77° E, W′ = S 77° W

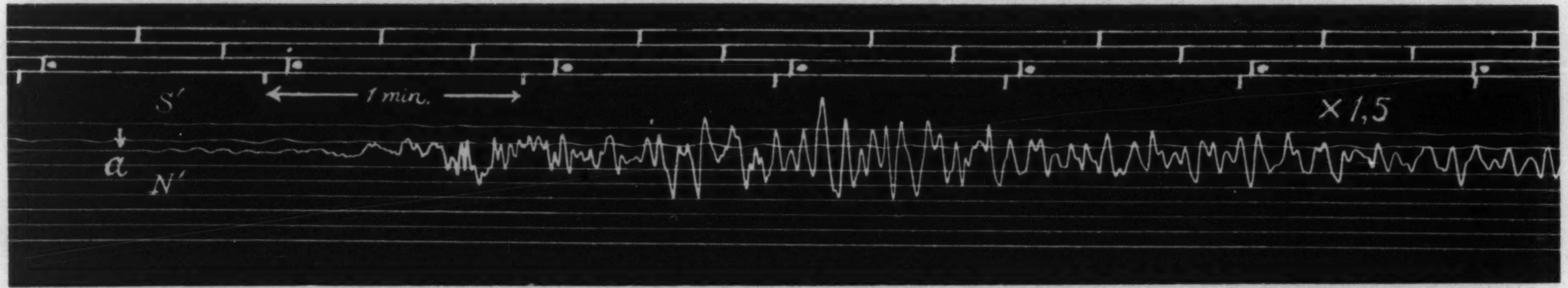

N′ = N 13° W, S′ = S 13° E

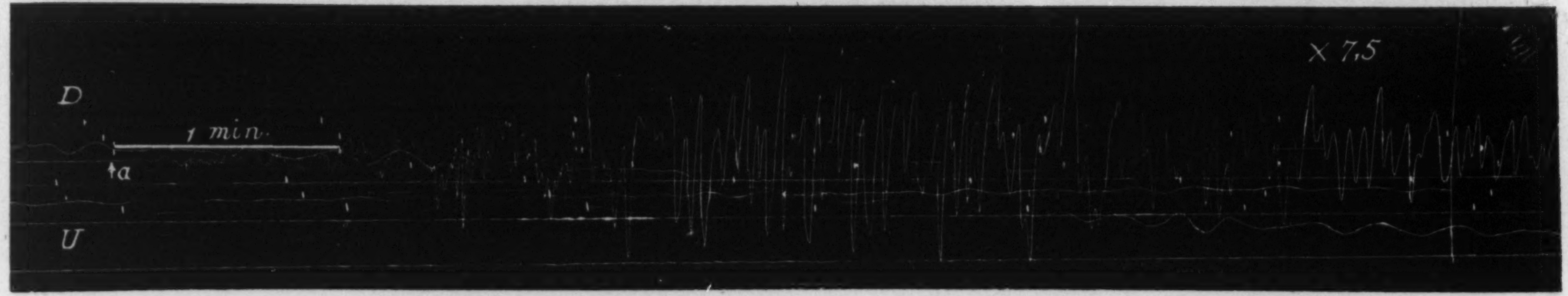

(*Full size of the original diagrams*)

Instrumental constants: E. W. Component [See No. 3 in List II (A)]. N. S. Component [See No. 3 in List II (A)].
Vertical Component [See No. 22 in List II (A)].

（震研彙報、第九號、圖版、那須）

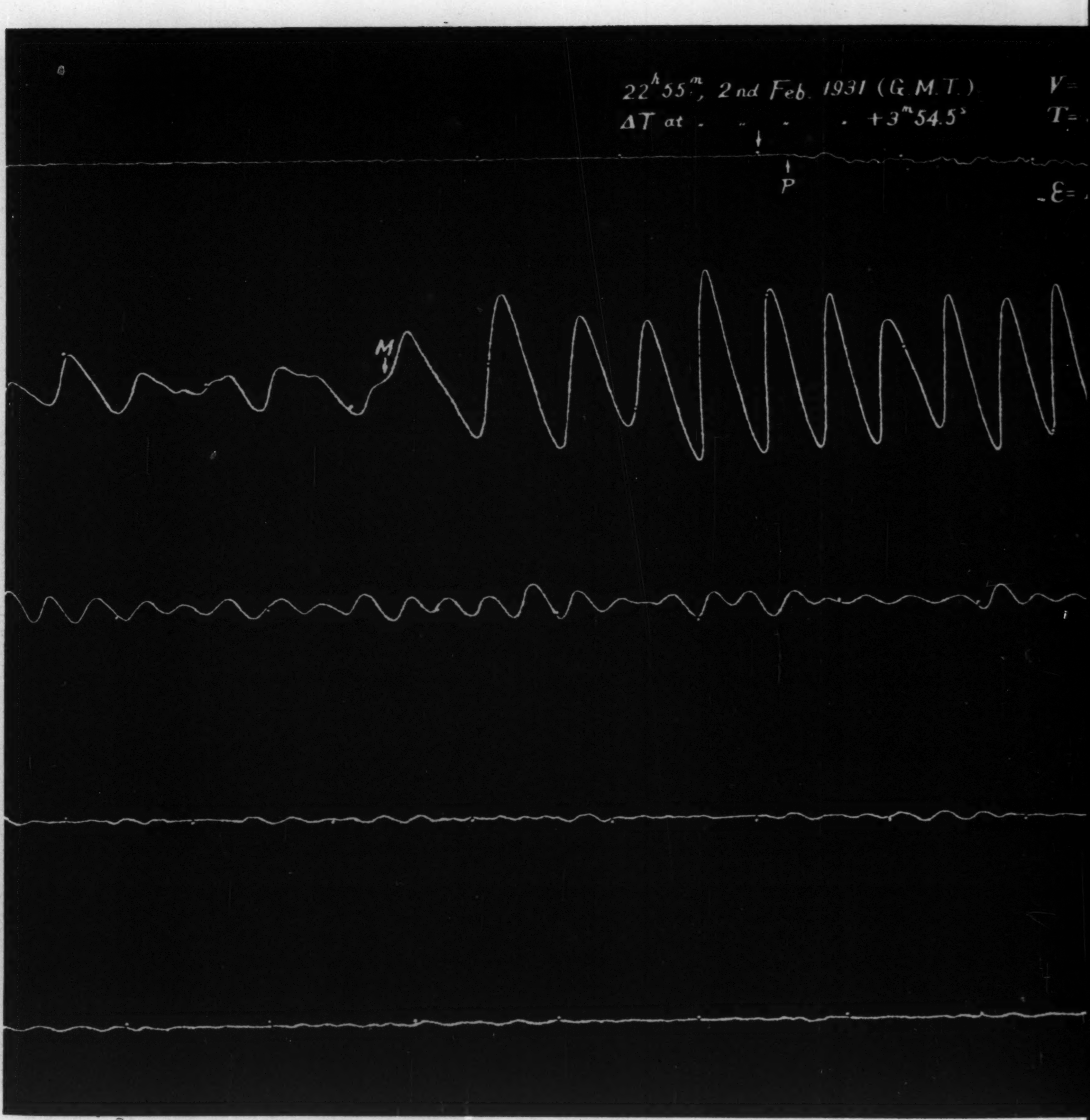

（震研彙報、第九號、圖版、那須）

Fig. 3. T

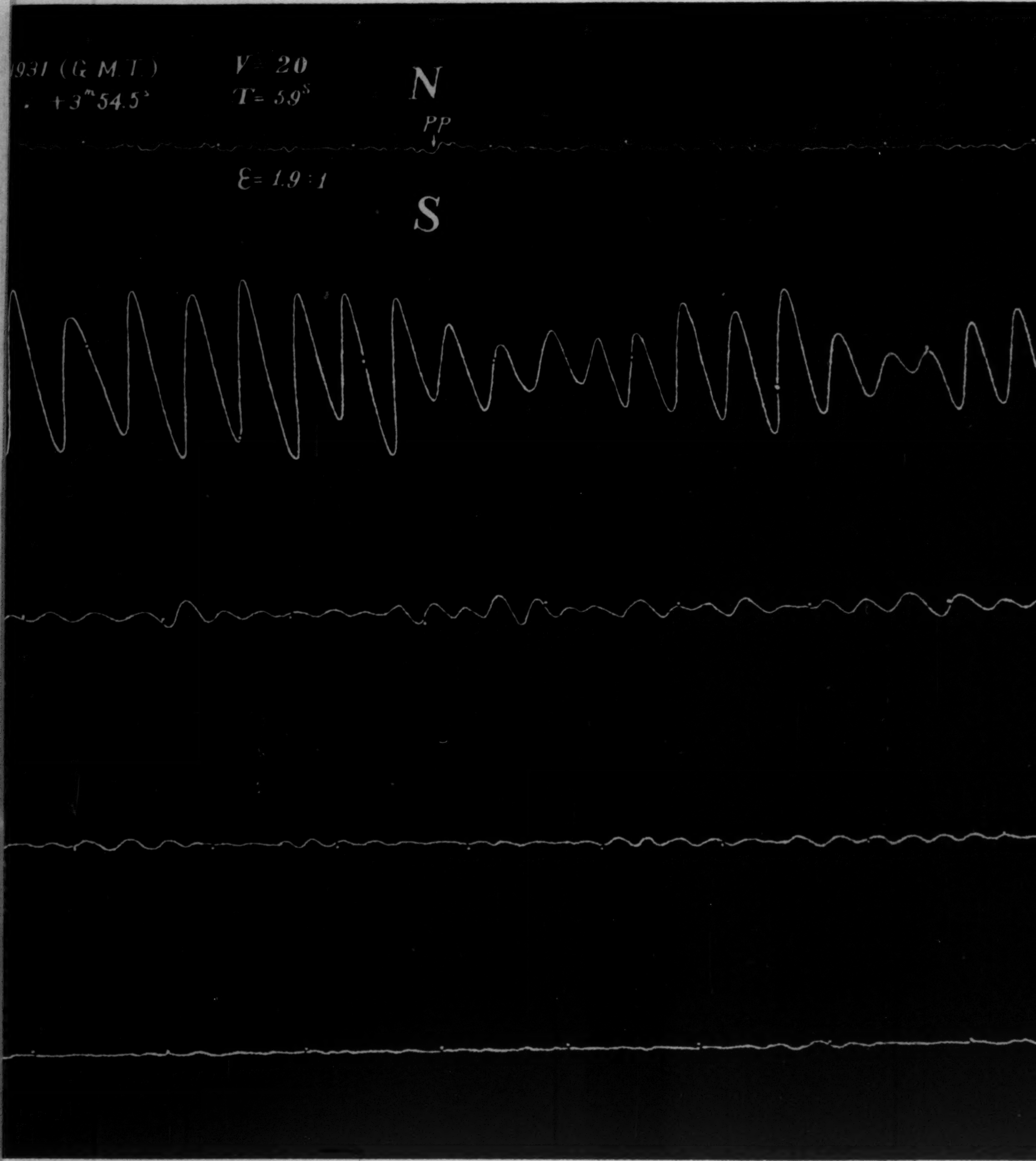

Instruments: [No. 15 in List II (A

. Tôkyô Observation of the New Zealand Earthquake of Feb. 2, 1931.

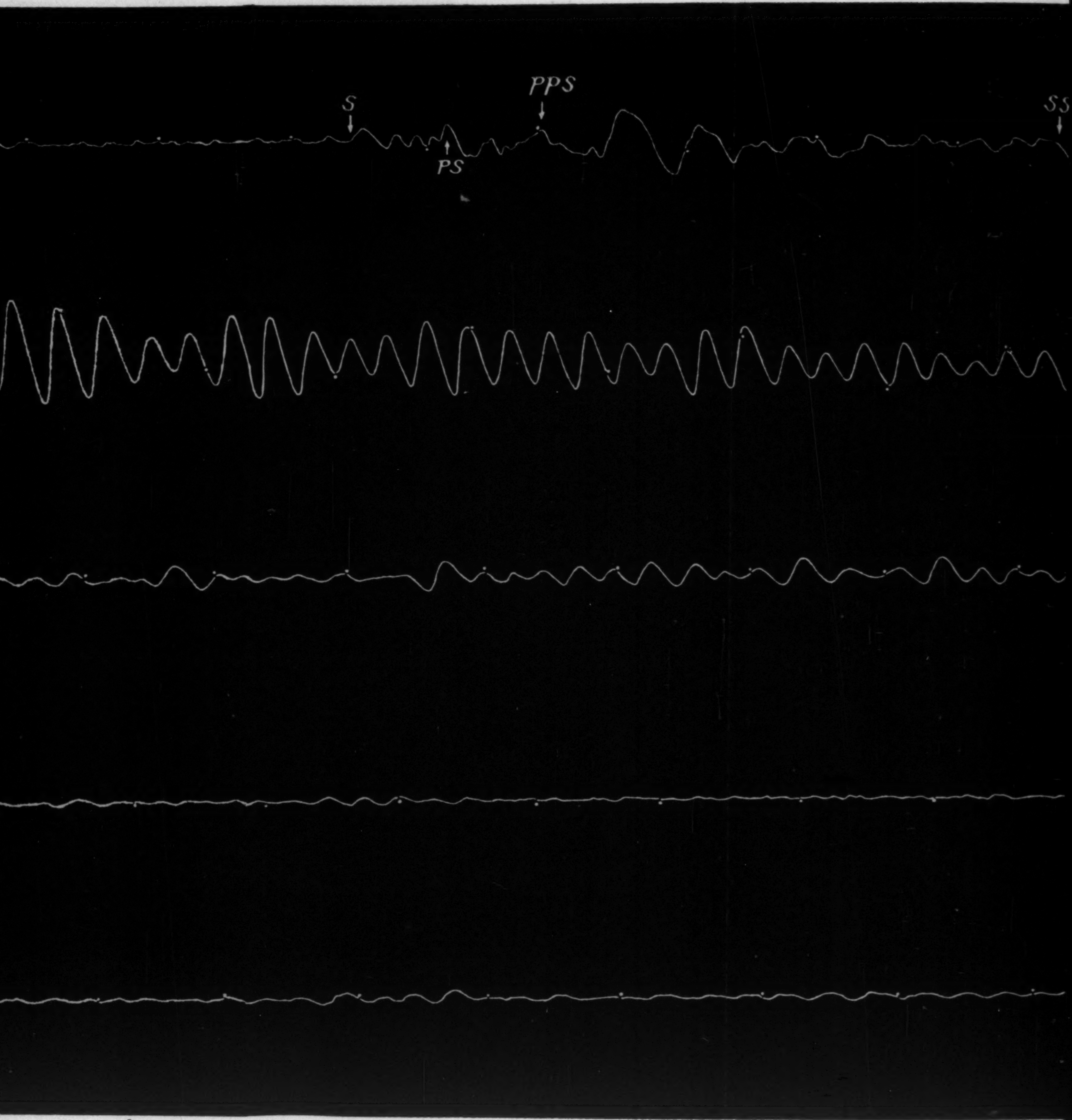

(A)]. Instrumental constants determined on Feb. 2 are shown on the upper left of this diagram.

land Earthquake of Feb. 2, 1931.

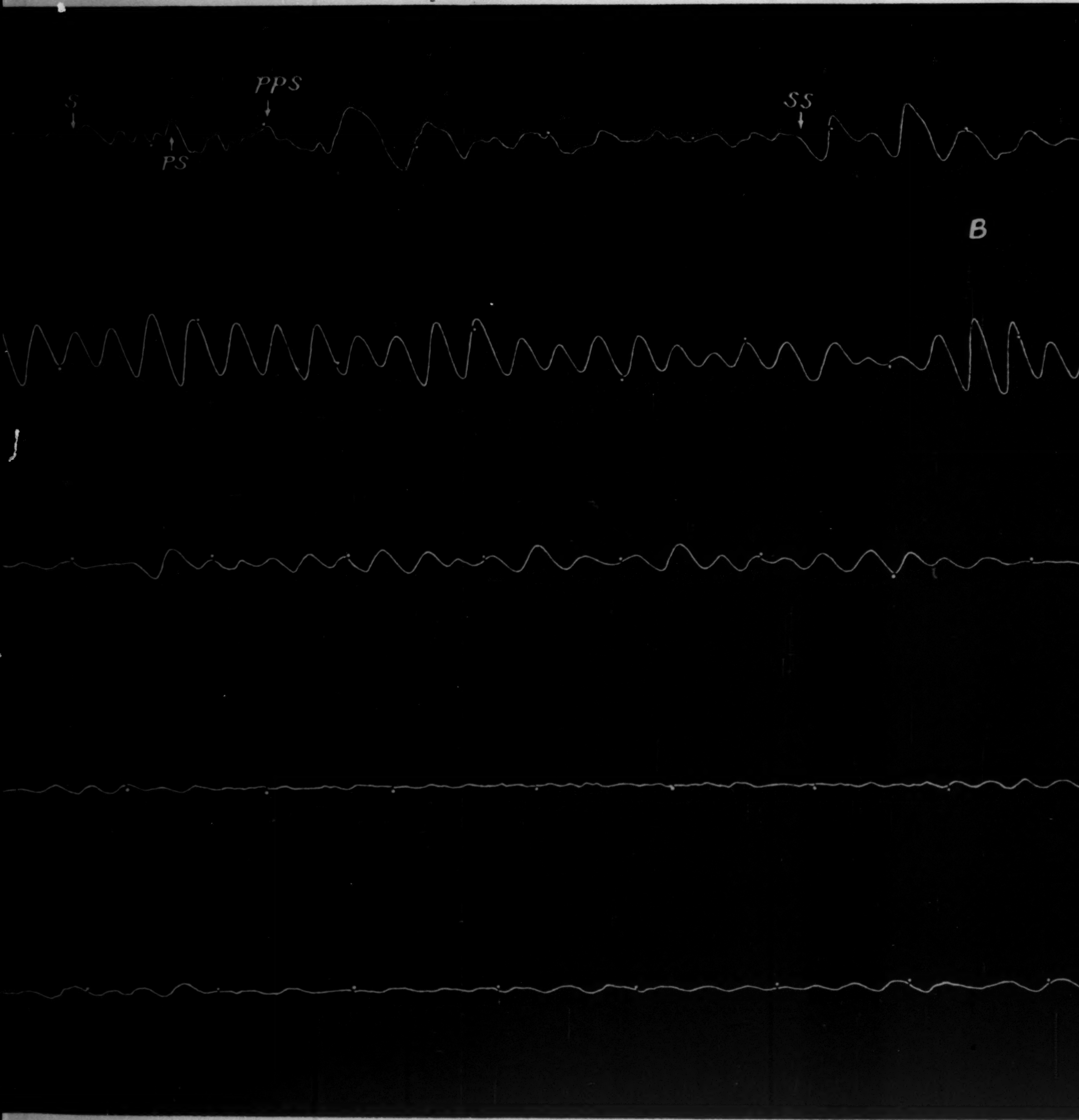

nined on Feb. 2 are shown on the upper left of this diagram.

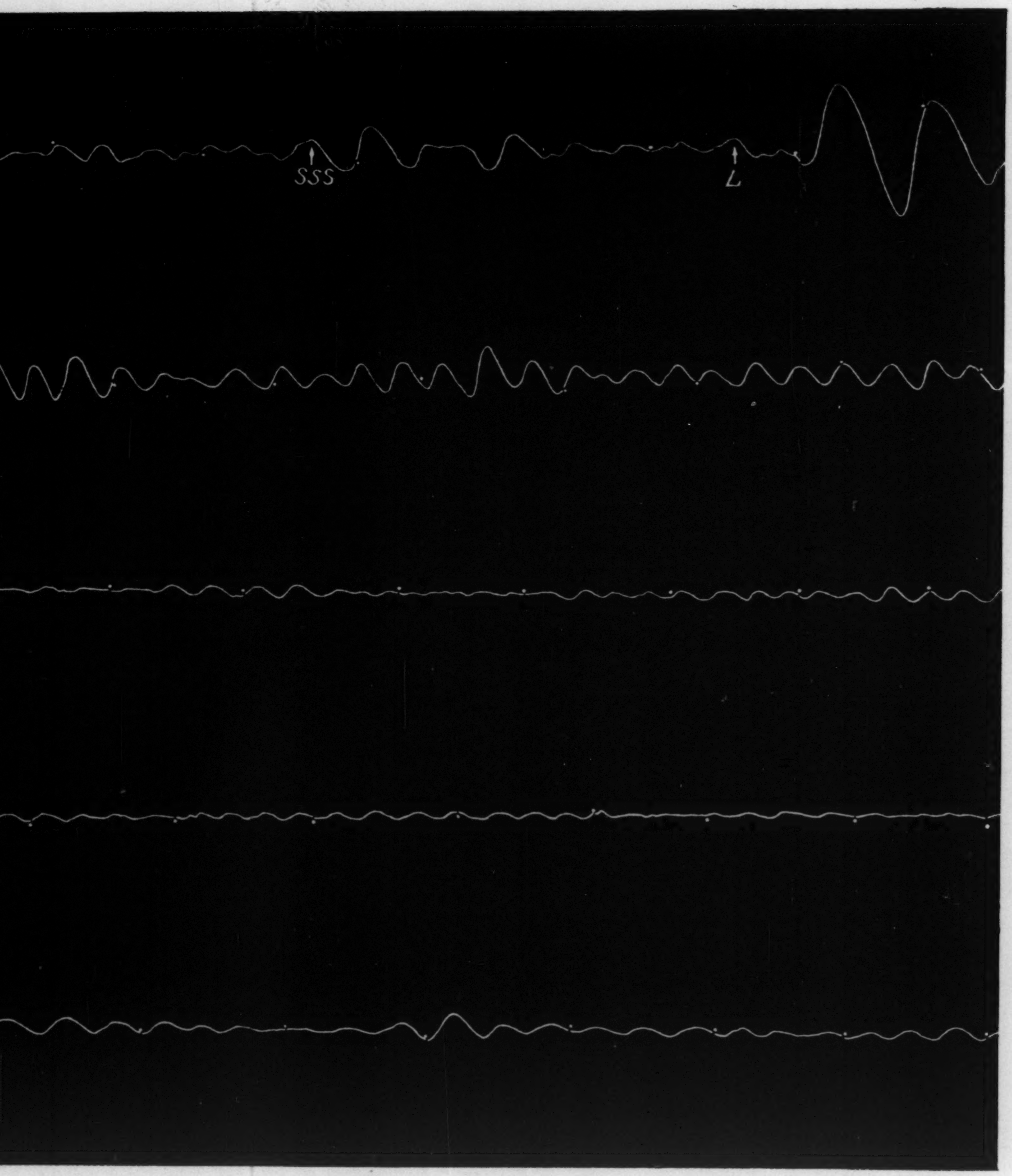
SSS
L

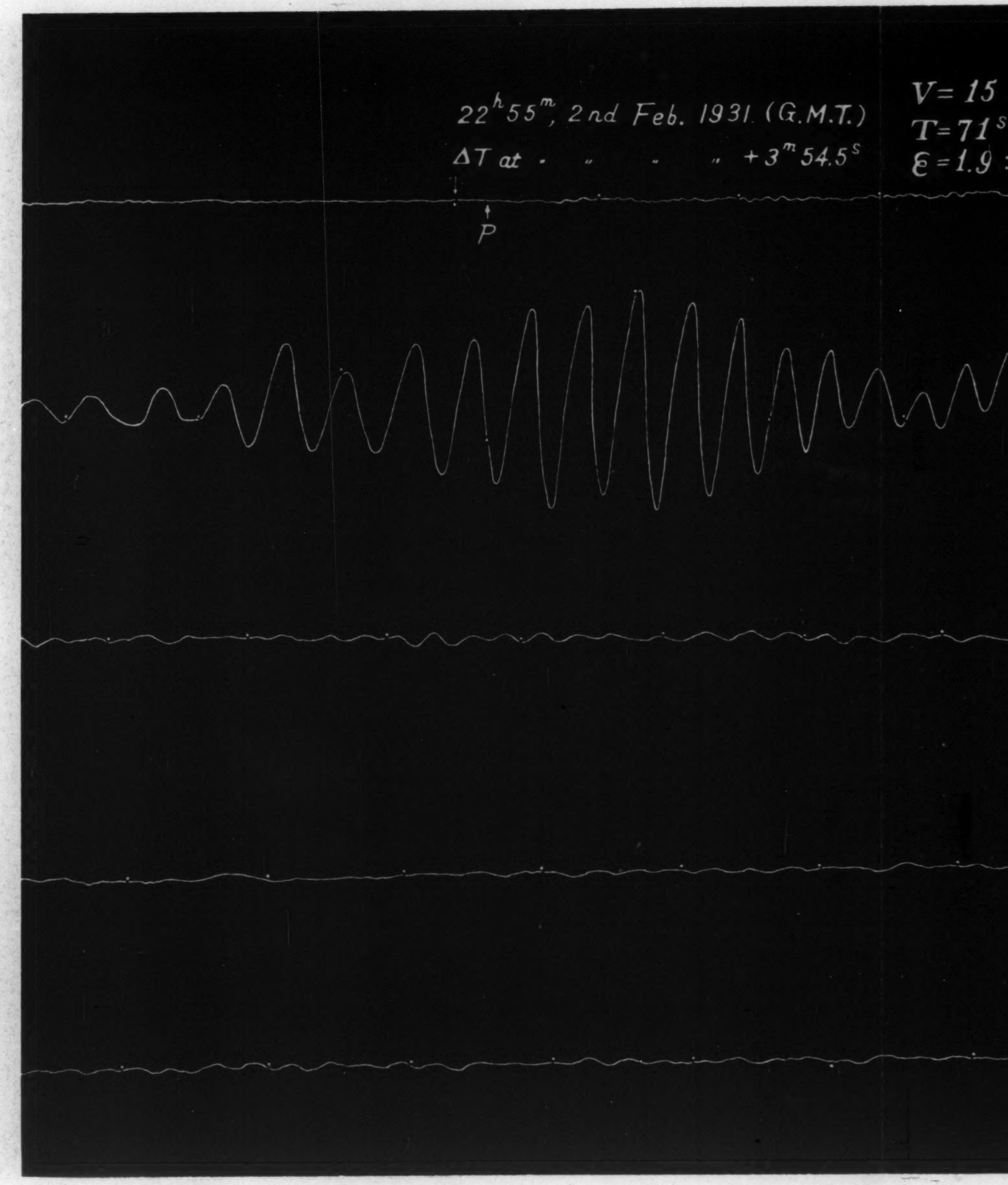
22h55m, 2nd Feb. 1931 (G.M.T.)
ΔT at " " " " +3m54.5s
V= 15
T=71s
ε=1.9
P

Fig. 4.

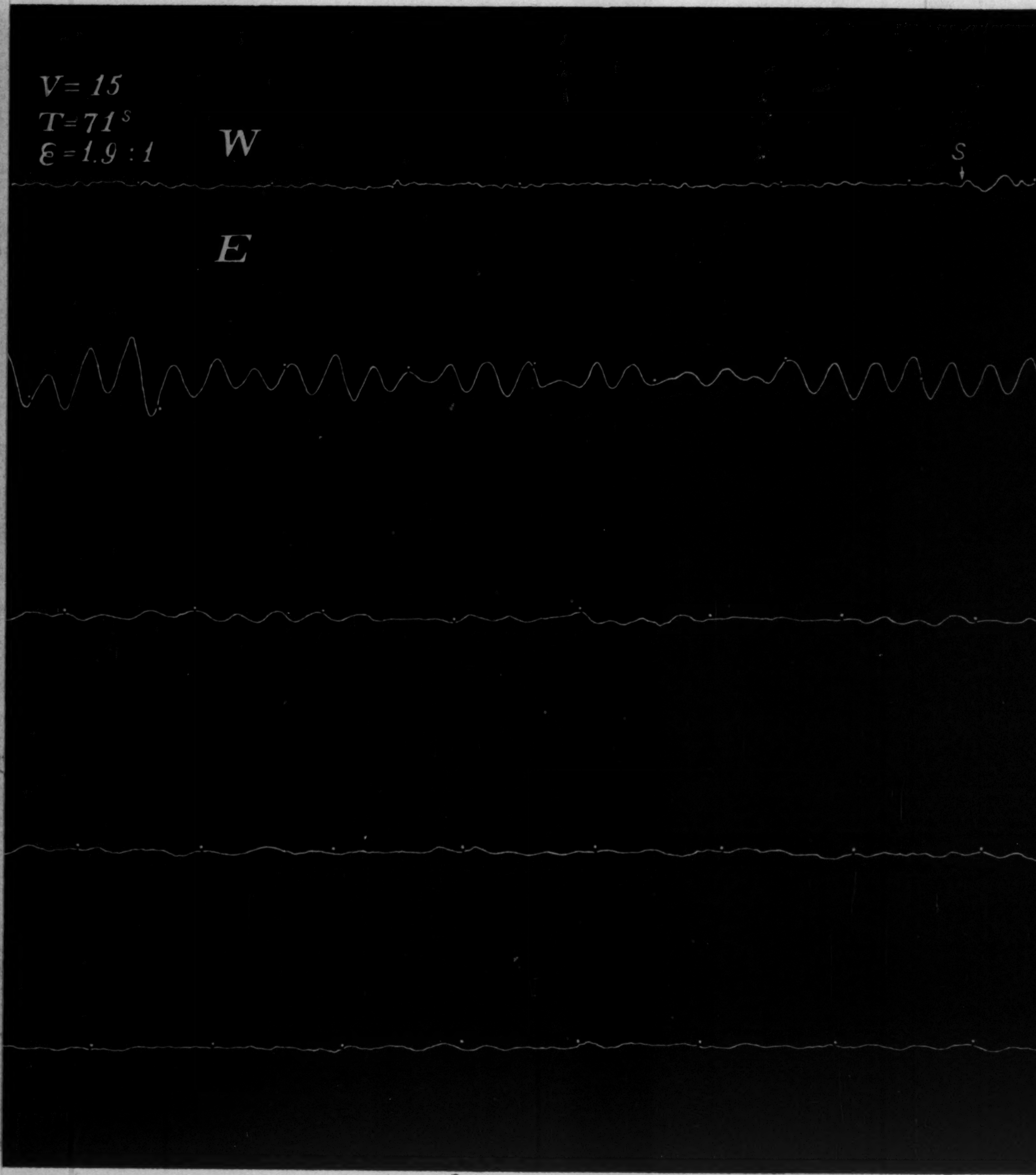

Instrument: [No. 14 in List II (
Interval between co

4. Tôkyô Observation of the New Zealand Earthquake of Feb. 2, 1931.

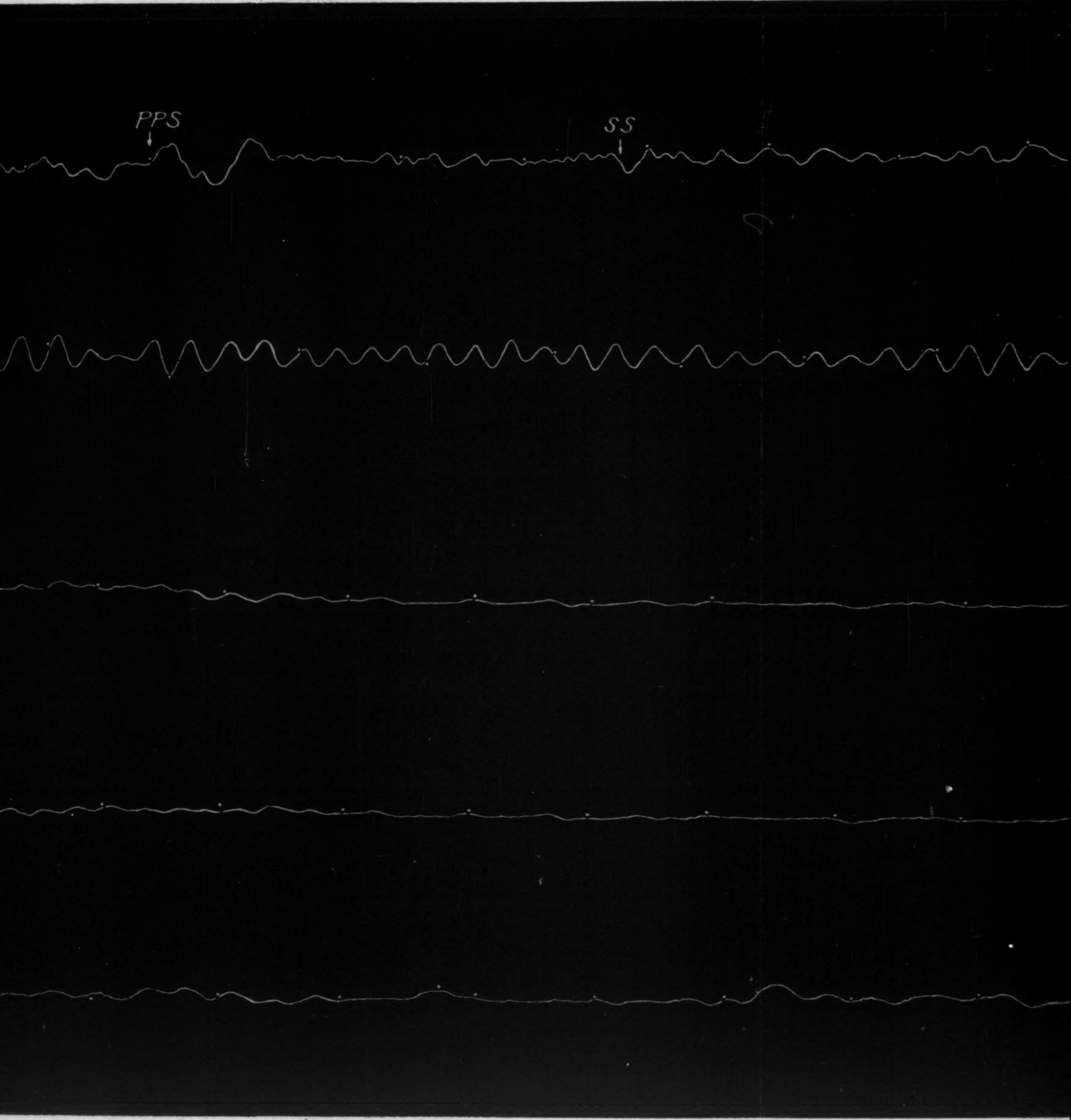

II (A)]. Instrumental constants determined on Feb. 2 are shown on the upper left of this diagram.
n consecutive two breaks equals 1 minute.

land Earthquake of Feb. 2, 1931.

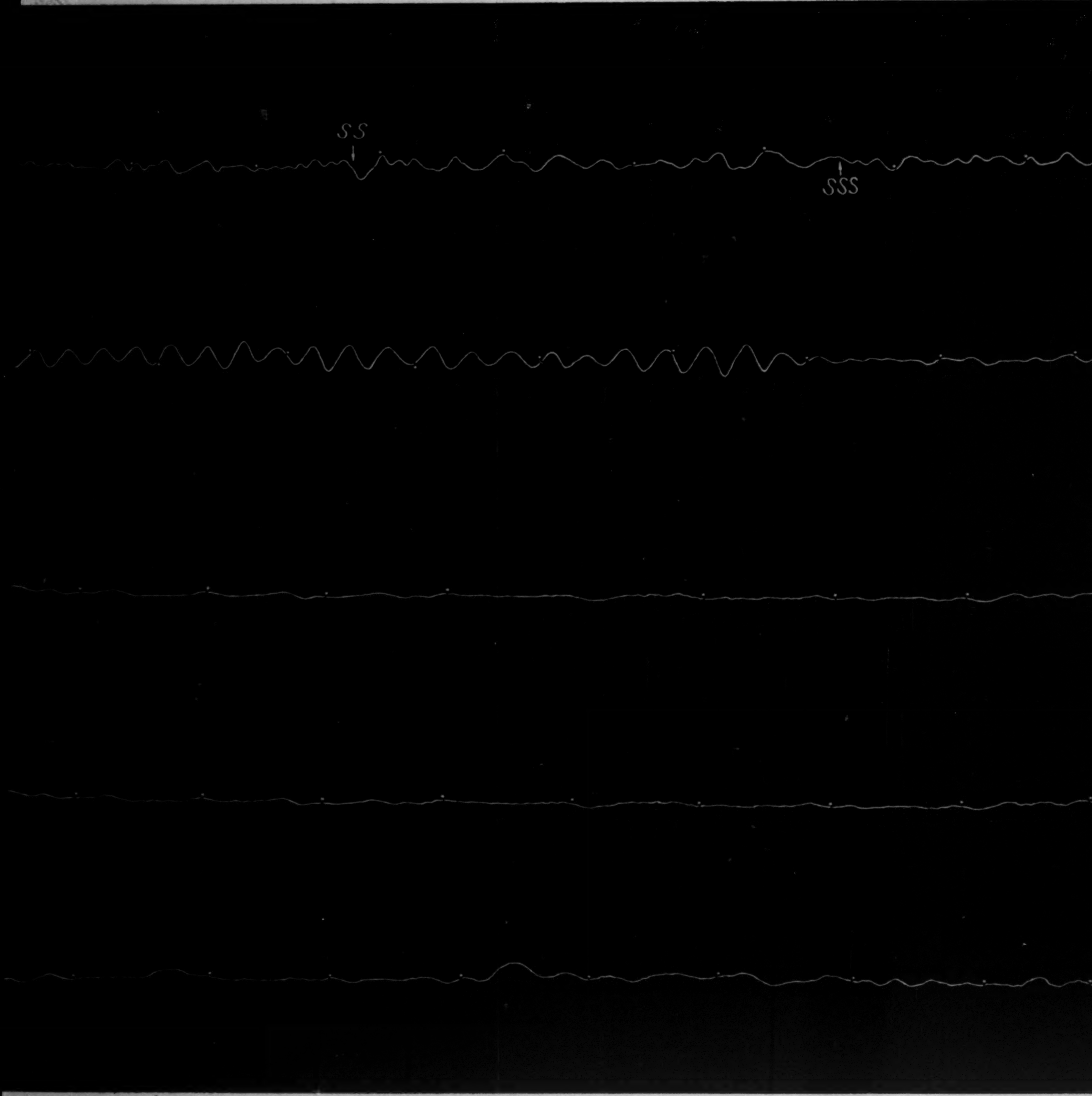

ermined on Feb. 2 are shown on the upper left of this diagram.
nute.

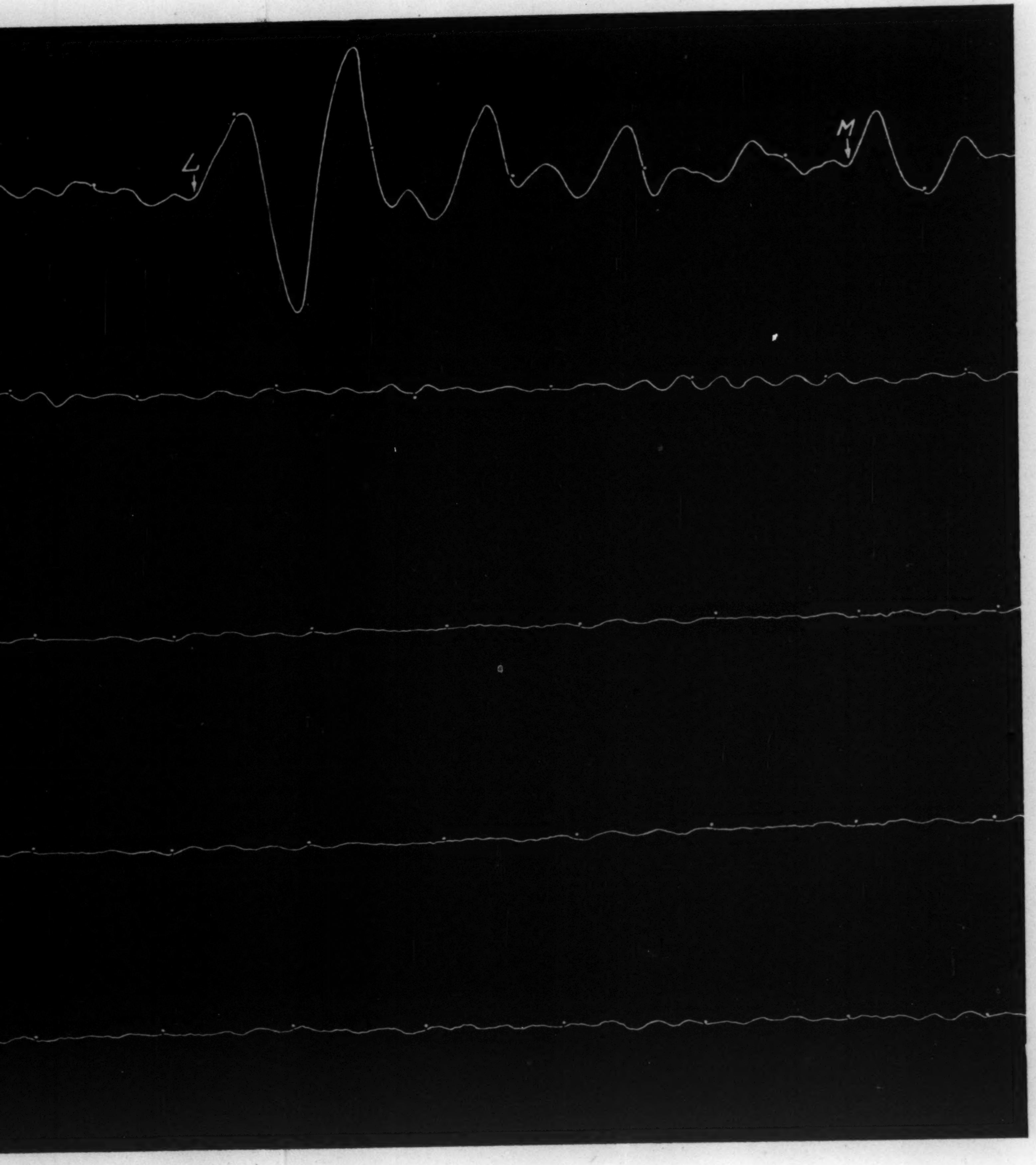
L
M

Fig. 5. Tôkyô (Hongô) Observation of the Strong Earthquake of June 17, 1931.
Horizontal Pendulum Strong Motion Seismograph Diagrams.

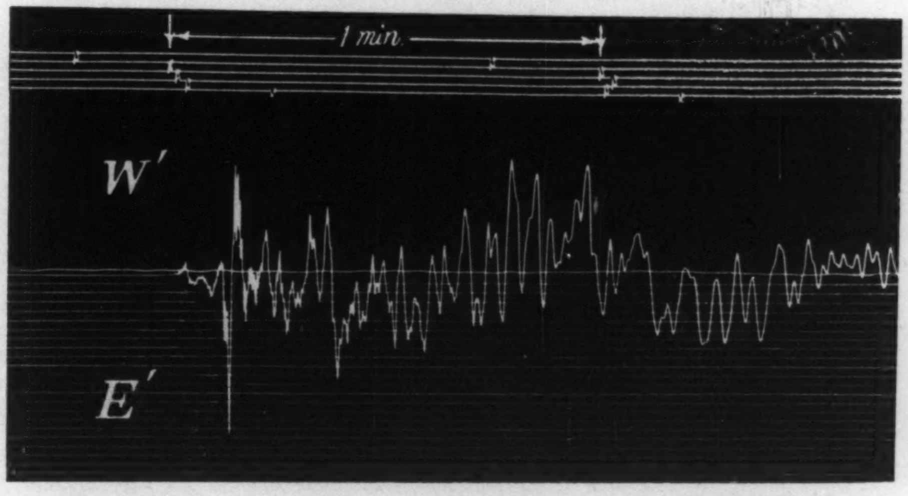

E′ = N 77° E, W′ = S 77° W (*Full size of the original diagram*)

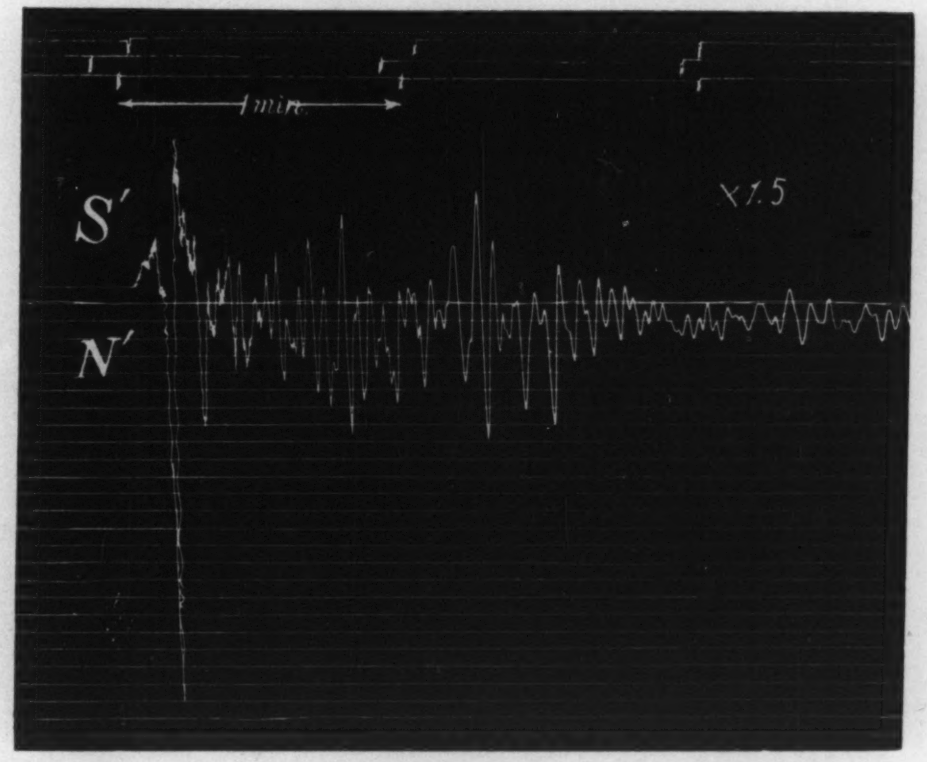

N′ = 13° W, S′ = S 13° E (*Full size of the original diagram*)

Instrumental constants: E. W. Component [See No. 3 in List II (A)].
N. S. Component [See No. 3 in List II (A)].

（震研彙報、第九號、圖版、那須）

Fig. 6. Tôkyô Observation of the Strong Earthquake of June 17, 1931.
Vertical Seismograph Diagram.

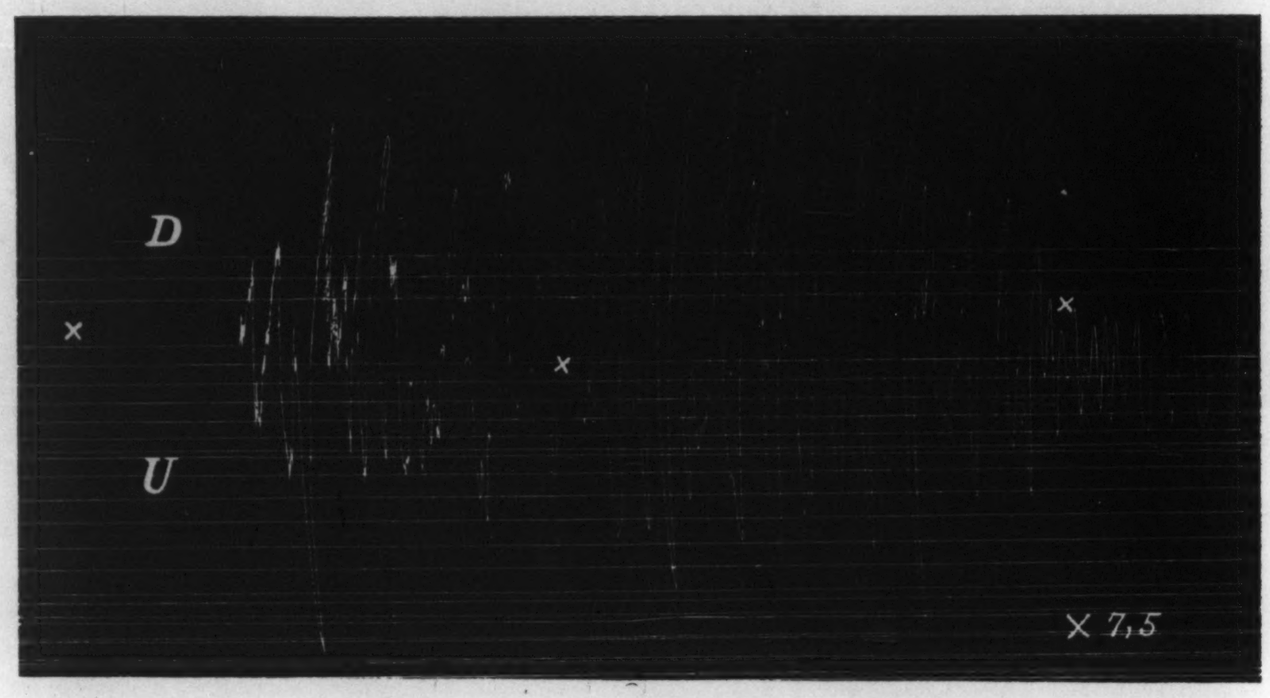

(*Full size of the original diagram*)

Instrumental constants: [See No. 22 in List II (A)]. In erinal between consecutive two breaks indicated by × equals to 1 minute.

Fig. 7. Tôkyô Observation of the Strong Earthquake of June 17, 1931.
Three Component Motions Seismograph Diagram.

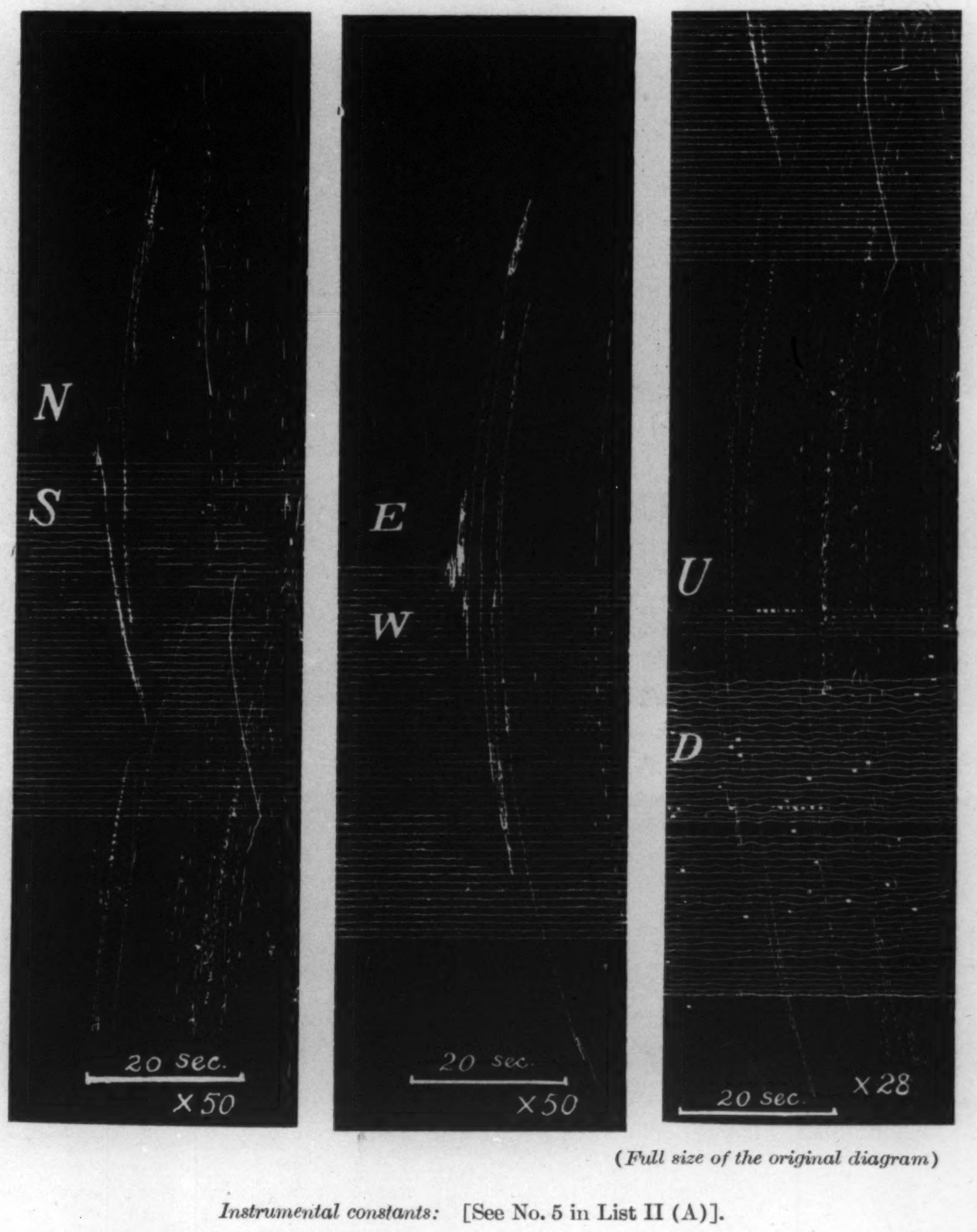

(*Full size of the original diagram*)

Instrumental constants: [See No. 5 in List II (A)].

Fig. 8. Kamakura Observation of the Strong Earthquake of June 17, 1931
Strong Motion Seismograph Diagram.

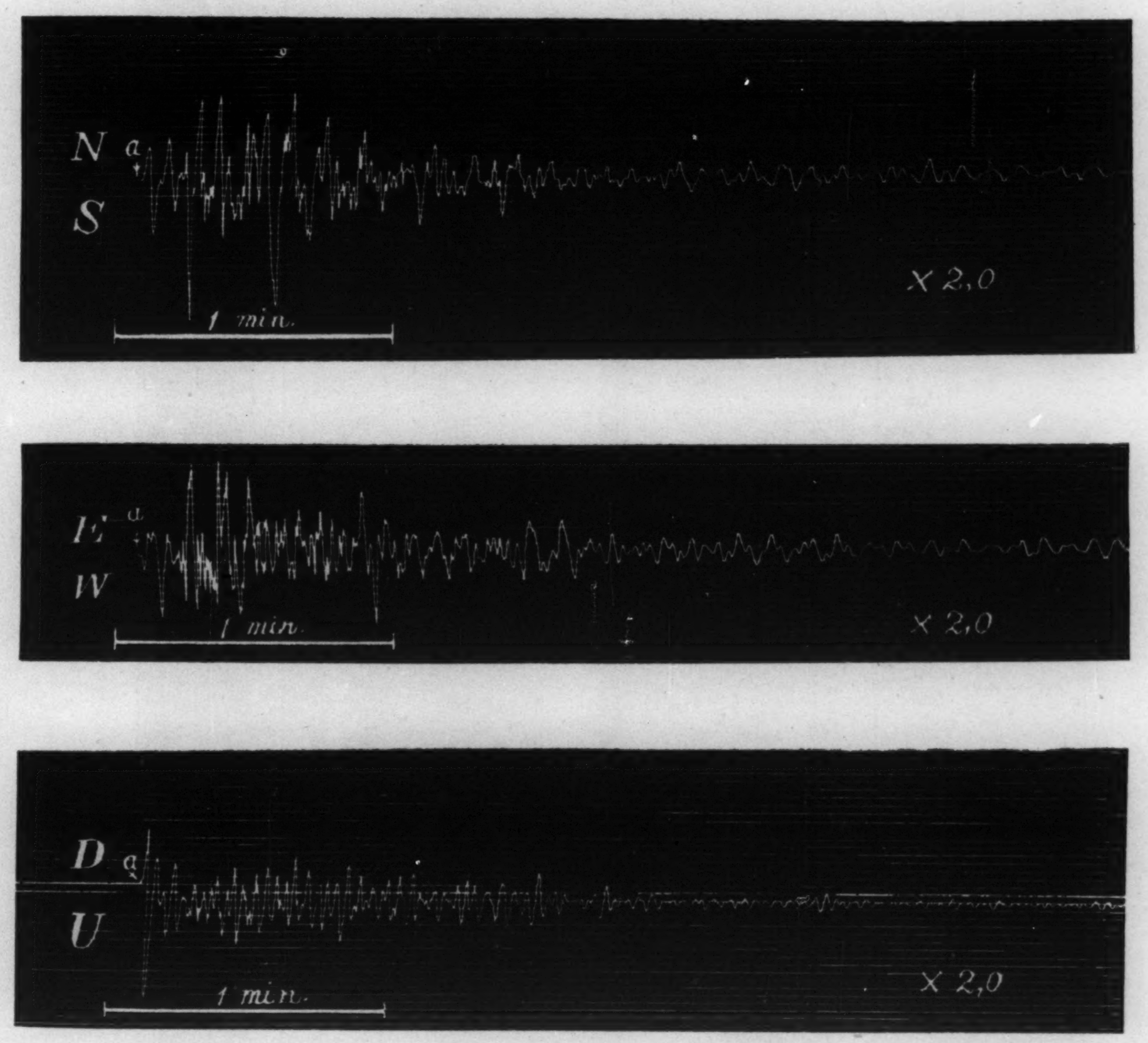

(Full size of the original diagram)

Instrumental constants: [See No. 1 in List II (B)].

（震研彙報、第九號、圖版、那須）

Fig. 9. Itô Observation of the Strong Earthquake of June 17, 1931.
Horizontal Motion Seismograph Diagram.

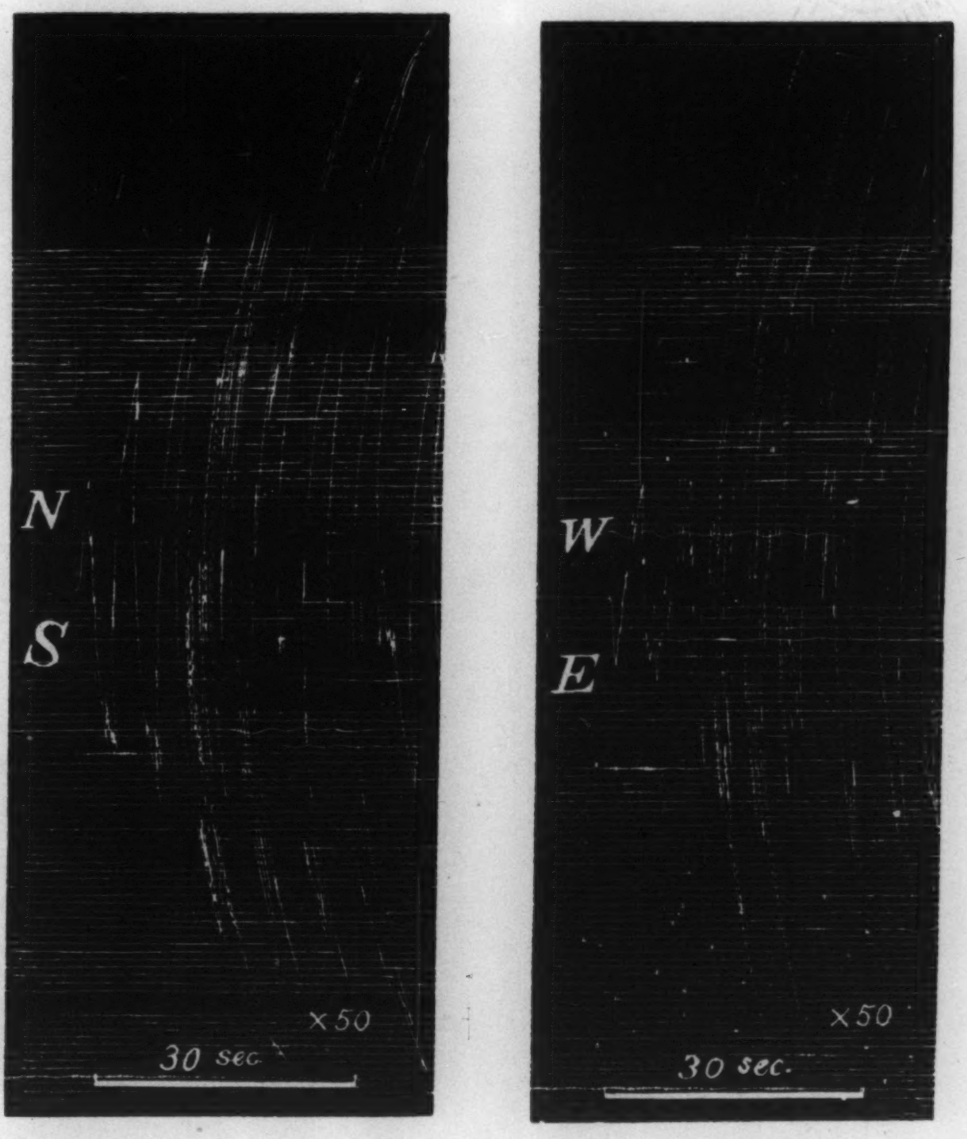

(Full size of the original diagram)

Instrumental constants:

Component	Natural Period	Magnification	Damping Ratio
E.W.	6·5 sec.	50	1·30
N.S.	6·5 sec.	50	1·20

Fig. 10. Tanna Observation of the Strong Earthquake of June 17, 1931.
(A) Strong Motion Seismograph Diagram.
(B) Three Component Motions Tromometer Diagram.

(A)

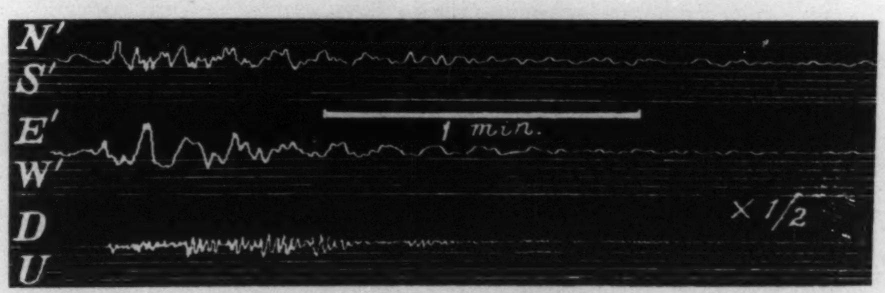

(Full size of the original diagram)

(B)

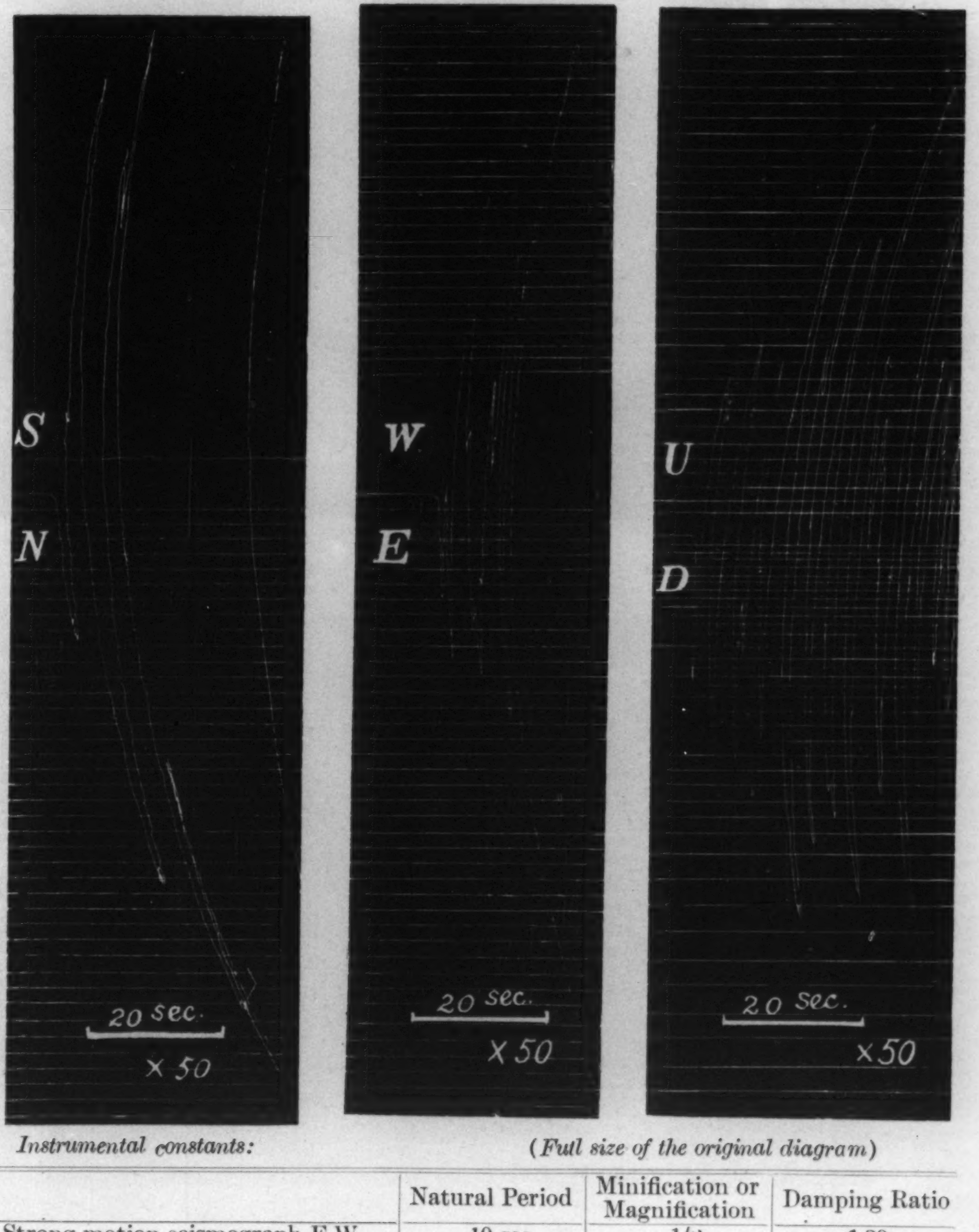

(震研彙報、第九號、圖版、那須)

Instrumental constants:

(Full size of the original diagram)

	Natural Period	Minification or Magnification	Damping Ratio
Strong motion seismograph E.W.	10 sec.	1/2	1·30
N.S.	10	1/2	1·30
Vert.	4	1/2	1·20
Tromometer E.W.	5·8	50	1·40
E.S.	5·4	50	1·58
Vert.	3·5	50	1·20

Fig. 11. Tôkyô (Hongô) Observation of the Strong Earthquake of June 17, 1931.

Ishimoto Acceleration Seismograph Diagram.

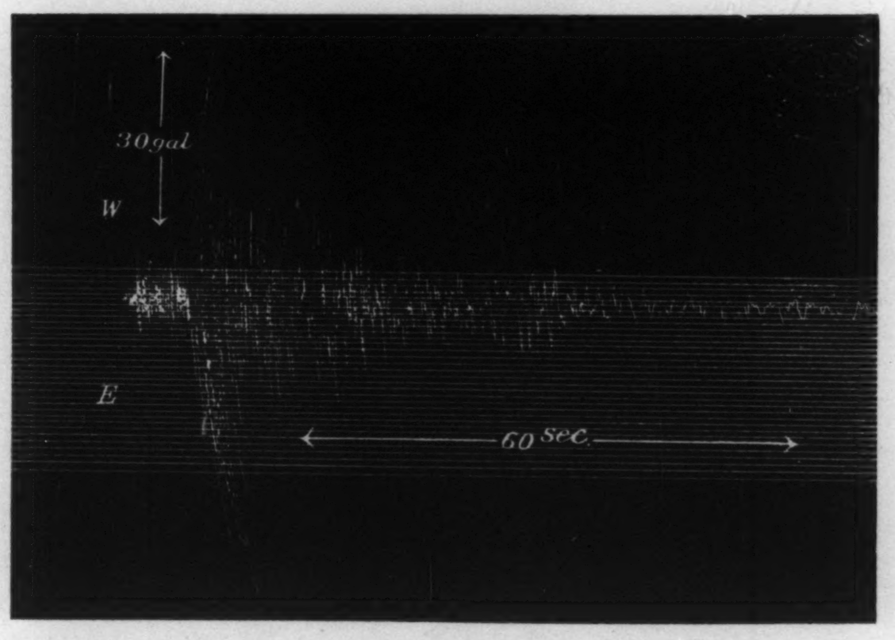

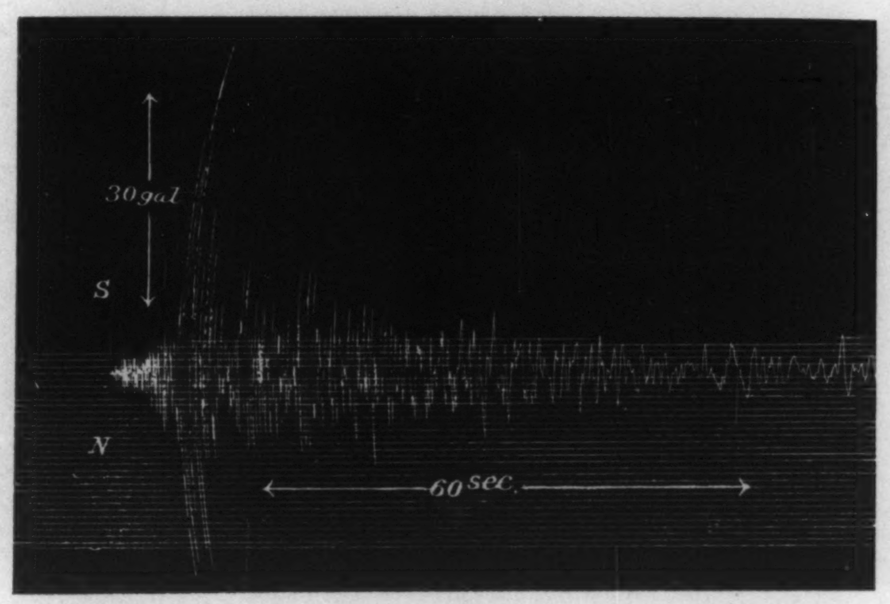

（震研彙報、第九號、圖版、那須）

27. *Earthquake and Thunderstorm.*

By Torahiko **TERADA**,
Earthquake Research Institute.

(Read Apr. 21, 1931.—Received Sept. 14, 1931.)

Relations between the occurrence of earthquake and the status of different meteorological elements prevalent at the time of, or before, the earthquake have been investigated in many details as one of the favourite subjects of seismological statistics. Tidal effects have also been treated by many previous investigators with more or less success.[1] Many years ago, the present author made some study[2] on an apparent relation between the occurrence of earthquake and the mode of distribution of sunspots on the solar hemispheres. In view of the superfluous number of these literatures, it appears rather strange that the possibility of a relation, direct or indirect, between thunderstorm and earthquake has rarely been inquired, at least as far as the knowledge of the author is concerned.[3]

Firstly, the occurrence of a thunderstorm is associated with a certain type or types of barometric pressure distribution and on this account we may expect some statistical relation between thunderstorm and earthquake, as it is already established beyond doubt that there exist some definite relations between the occurrence of earthquake and the barometric gradient prevailing in the region of a certain extent including the epicentral district. Secondly, it is not altogether inconceivable that an electrical effect of thunderstorm may exist which could give rise to an additional mechanical stress in the earth's crust and thus play a sensible role as one of the secondary causes for inducing the seismic activity well ripened for its display. The electrostatic traction normal to the earth's surface due to the atmospheric potential gradient may be shown to be apparently negligible in comparison with the amount of variation of the atmospheric pressure which is considered to be effective in affecting the mechanism of earthquake and thus acting as one of the secondary cause. The effect of the horizontal gradient of this normal stress may, however, be not quite negligible in comparison with that of the barometric gradient as may be seen from an estimation made in the Appendix of this paper. There is also another effect related to the phenomena of electro-endosmose,[4] which must be here taken into account and tested whether its amount may or may not suffice for enlisting this factor as one of the competent secondary causes. A rough estimation made in the Appendix shows that though the effect is generally small, it is not so small that we could discard it as a priori negligible.

---

[1] Special mention may be made of the recent investigations by S. Yamaguti, *Bull. E.R.I.*, 9 (1931); N. Nasu, F. Kishinouye and T. Kodaira, *ibid.*, 9 (1931), 22; K. Hukutomi and Z. Kawase, *Disin*, 3 (1931), 484.

[2] T. Terada, *Journ. Coll. Sci.*, Imp. Univ., Tokyo, 44, Art. 6 (1923), 1.

[3] Aristoteles considered wind, earthquake and thunder to be of the same nature: " Nos autem dicimus eandem esse naturam: super terram quidem ventum; in terra autem terraemotum; in nubibus autem tonitruum. Omnia, enim esse haec, secundum substantiam, idem: exhalationem siccam." (Meteororum lib. II, cap. 9). The same idea seems to have been handed down to the end of 18 century and led l'ab. Bertholon to contrive his para-tremblements-de-terre.

These considerations led the author to undertake a preliminary statistical study of the suspected relation between thunderstorm and earthquake, at first with respect to the Kwantô District, for 1915–1930, as this district is characterized by the great frequency of earthquakes. The years before 1915 were excluded because the available data of thunderstorms are not based on the same system of regional classification as for the later years.

The data are exclusively taken from Kisyô-Yôran issued by the Central Meteorological Observatory of Tôkyô. As for thunderstorm frequency, the monthly numbers of thunderstorms observed and recorded within the said district, comprising the Provinces of Musasi, Sagami, Kadusa, Simoosa, Awa, Hitati, Kôduke and Simotuke were taken for the basis of comparison. The three months, July, August and September, were only referred to in the present preliminary study, as the monthly numbers for the other months are generally too small to be subjected to the present method of statistical analysis. As for the earthquake frequency to be compared with the above thunderstorm data, those earthquakes were picked up, of which the epicentres are located in the region within or near the district specified for the thunderstorm data and the intensities are denoted by the usual designations "conspicuous" (顯著) and "rather conspicuous" (稍顯著) in Kisyô-Yôran. It may appear that there is involved a large margin of ambiguity concerning the choice of the extent of the geographical area within which the epicentres are to be picked up for the comparison at hand. From the practical point of view, however, the difficulty is not at all serious, as the number of earthquakes of which the origins are situated outsides of the above specified districts and still so near the margin of this area that it seems not plausible to discard them, is comparatively small. Thus, though the epicentres in the Provinces of Idu, Kai and Iwaki were included in the present statistics, omission of these will not sensibly affect the general feature of the results of comparison which will be shown later. A point which deserves a more serious consideration, is concerned with the question, whether we should include, or not, those earthquakes of which the epicentres are situated in the sea area off the coast of these land districts, in the present statistics. Those earthquakes which are originated in such deep-sea areas as Iwaki-nada, Kasima-nada, Tyôsi-oki, Bôsô-oki, Kuzyûkuri-oki and the sea near Oosima, Idu, are by no means small in comparison with the total number for the entire region in question. Thence, the comparisons were made for the two kinds of data, one including and the other excluding the sea area above mentioned. On the other hand, those earthquakes of which the origins are located at different points within the Bay of Tokyo, such as Uraga Channel, Haneda-oki, Estuary of the R. Naka etc. were enlisted as land earthquakes, as will appear quite natural if we consider the shallowness of this bay.

---

[4] T. TERADA, *Proc. Imp. Acad.*, 6 (1930), 401; *Bull. E.R.I.*, 9 (1931), 225, v. footnote (30) in p. 253.

Fig. 1 shows the graphs

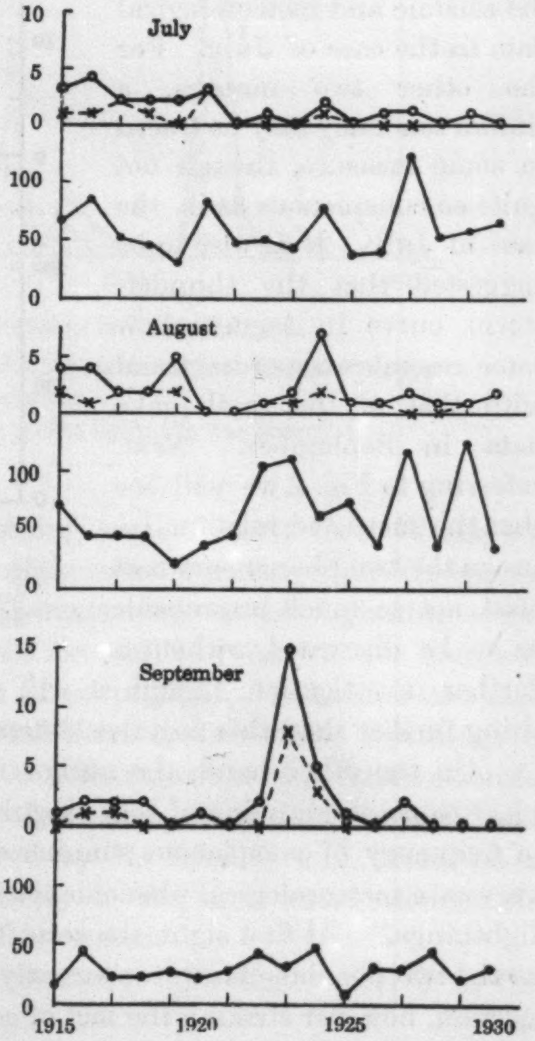

Fig. 1. Yearly Frequencies of Earthquakes and Thunderstorms in Kwantô Region, for July, August and September respectively.

○: Earthquakes, including those originated in sea area.
×: Earthquakes, excluding those originated in sea area.
●: Thunderstorms.

of the yearly variations of the frequencies of thunderstorms and earthquakes respectively, for the three months named above separately, while Fig. 2 gives the said variations for the three months taken together.

Referring to Fig. 1, we may notice some parallelism, especially the coincidence of frequency maxima, between the seismic and meteorological data in the case of July. For the other two months, a similar tendency may be traced in some measure, though not quite so conspicuous as in the case of July. It is also to be suggested that the thunderstorm curve in August show some resemblance of its trend with that of the earthquake data in September. Next, referring to Fig. 2 we will see that the suspected relation between the two phenomena is at least not so much improbable as to be discarded without a further investigation, though it will not be safe enough to propose anything further than this negative statements.

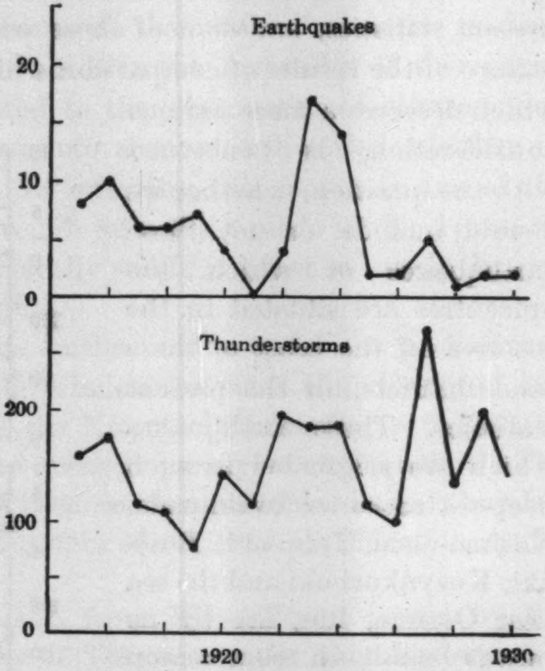

Fig. 2. Yearly frequencies of earthquakes and thunderstorms in Kwantô Region for July, August and September taken together.

On the other hand, the author may be allowed to venture in this place to point out a fact of very singular coincidence between the maxima of frequency of conspicuous summer earthquake and the appearance of a very rare meteorological phenomenon known under the name of "rocket lightnings." At first sight, the coincidence will appear quite accidental, as the two phenomena are apparently too remote in their physical connection, however striking the fact of coincidence may appear even to the majority of scientists. A little consideration will, however, lead us to assume a more cautious attitude than of a hasty negation. If there exist a physical relation between thunderstorm and earthquake, it will be of no wonder if the activity maxima of the latter would coincide with one of the rare modes of display of the former, since as a matter of fact the observation of rocket lightning here referred to happened to be made at, or near, the maxima of thunderstorm frequency, as may be seen from the comparison of Fig. 2 with Fig. 3.

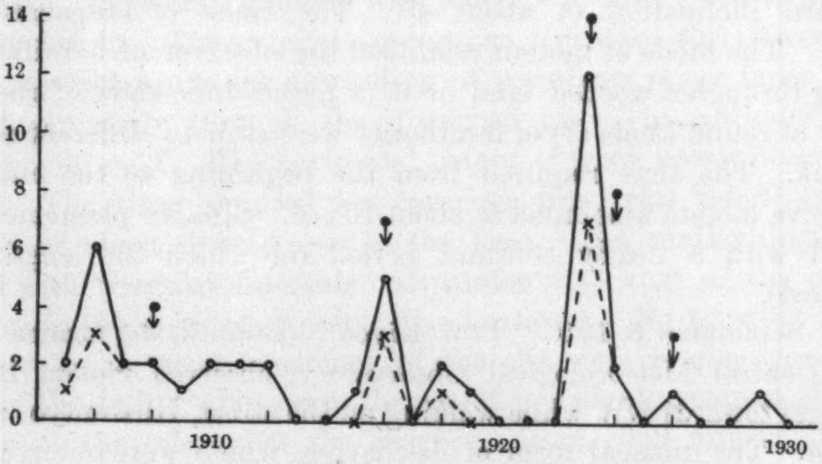

Fig. 3. Summer Earthquakes in Kwantô Region.

○ conspicuous earthquakes including those originated from sea area.
× „ „ excluding „ „ „ „ „ .
●↓ marks the year in which the rocket lightning was observed.

The phenomena of rocket lightning are extremely rare. Though it seems that there are some variety of phenomena among those designated by this name, one of the essential characteristics of this lightning is the comparative slowness with which the foremost extremity of the luminous ribbon is prolonged in its direction of propagation. Examples are rare, however, even among the occidental literatures, of those lightnings of which the descriptions are positive with regard to this latter essential point. We may only cite those observed by Everett,[5] Simpson[6] and Mack.[7] The phenomenon observed by E. Schelle[8] and described as "Schlangenblitzen" belongs probably to the same class, though the velocity of propagation is not positively stated.

Searching for the examples of the rocket lightnings observed in this country, we find the following cases.

---

[5] J. D. and W. H. Everett, *Nature*, 68 (1903), 599; cited in Humphreys, "Physics of the Air," 376.

[6] G. C. Simpson, an abstract of 32nd. Robert Boyle Lecture, delivered before the Oxford Junior Scientific Club, June 7, 1930, in *Month. Weath. Rev.*, 58 (1930), 497.

[7] K. Mack, *Met. Zs.*, 18 (1901), 427.

[8] E. Schelle *Met. Zs.*, 16 (1899), 475.

1) July 31, 1908.[9] The phenomenon was observed from the summit of Mt. Huzi (Fujiyama) towards NNE. The lightning started from the base of a mass of cumulo-nimbus and proceeded towards E with a downward inclination of about 45°. The track of propagation was sinuous. The mode of motion reminded the observer of a railway train running through a wooded land or of a pyrotechnic show of rocket. A number of round knots (?) of luminosity were seen in different points of the track. The time required from the beginning to the end of the progressive motion amounted to about 10 sec. Similar phenomena were repeated with a nearly constant period (of which the length is not mentioned).

2) September 5, 1916.[10] Prof. Kiyoo Nakamura, the former Director of the Central Meteorological Observatory, observed violent lightning discharges towards NW while walking on the street, Huzimityô, at about 8h 30 m. The unusual form of discharges, which were observed twice, attracted his attention. The sky was covered with cloud from SW to NE (via N?) up to an altitude of 30°. The discharges were frequent and sometimes the whole sky was illuminated. A large mass of cumulo-nimbus was seen towards NW, from behind of which a lightning of extraordinary form emerged towards right. It reminded the observer of the sprinkles of fire thrown up into the air on the occasion of a conflagration. Seven or eight such "particles of fire" were seen to fly off towards NE covering an area of about five or six degrees. Another similar phenomenon was observed after two or three minutes. No thunder was heard at that time, but a distant roaring was noticed after he had returned home (his residence was at Minamityô, Usigome). Though the slow motion is not positively stated, the comparison with the sprinkles of fire above mentioned may be taken as an indirect evidence for this point.

3) August 26, 1923. It was just one week before the Great Kwantô Earthquake of Sept. 1, when this unusual phenomenon was observed by the present author and his family in his dwelling Akebonotyô 24, Komagome, Tôkyô. Unfortunately, no detailed note was recorded at that time so that the following description is drawn from his sheer memory. It was near the time of sunset and the sky was not yet quite dark when the phenomenon was detected towards the western sky. A

---

[9] *Journ. Met. Soc. Jap.*, **27** (1906), 399, among the miscellaneous articles, with the name of the author given in initials only as R. W.

[10] K. NAKAMURA, *ibid.*, **35** (1916), 360.

number, five or six, of luminous tape or band were seen to start from somewhere towards W or NW and to be prolonged towards E expanding to a "fan" subtending an angle of 20 or 30 degrees. The luminous tracks were irregularly sinuous with knots and kinks which appeared especially bright. The general appearance reminded the observer of a striking resemblance to the unwinding of rolled up paper tapes thrown nearly horizontally through the disturbed air. The altitudes of the tracks were 40°—60°. The horizontal extent of track nearly amounted to 70°—90°. The time required for covering this total length may be estimated at about 3 or 4 sec. in the least. The similar display was repeated with irregular intervals comparable with that of the ordinary lightnings in the cases of average thunderstorms. No sensible thunder was heard as far as the memory of the observers is concerned. The mother of the author who was at the age of just eighty years at that time told him to the effect that she has never seen such unusual form of lightnings. The duration of the display was of the order of half an hour.

4) August 30, 1924. An extraordinary form of lightning was observed and photographed by Mr. Takayama in this evening. The phenomenon was described and discussed as "Bead and Rocket Lightnings?" by Prof. S. Fujiwhara,[11] in English, so that the readers may be referred to the original paper. In this case also the velocity of motion of the luminous spot is not stated, but comparing the photograms reproduced with the verbal descriptions of Nakamura's case we may suppose that the two cases may probably be counted under the same class of phenomena.

5) The exact date of the last example is unfortunately lacking, but it was a few days after July 27 and certainly before Aug. 7 of 1926. One of the observers is Dr. U. Nakaya, now in Hokkaidô University, who lately wrote to the author describing the details of the phenomena observed, at the author's inquiry. Dr. Chûji Tsuboi of our Institute and also Mr. R. Yamamoto of the Institute of Physical and Chemical Research were the witnesses of the same phenomena on the same occasion, and they also took the trouble of writing down the descriptions of their own observations. According to these most reliable descriptions, the phenomena seem to have been an almost exact facsimile of what were observed by the present author in the summer of 1923 and described in

---

[11] *Journ. Met. Soc. Jap.*, ii, 2 (1924), 189, (in Japanese), 197, (in English). Mr. T. TAKAYAMA, who is the Member of our Institute, was as that time in C.M.O.

the above paragragh. The three witnesses state independently that the track of lightning was branched, and judging from the sketches drawn by Nakaya and Tsuboi, the mode of branching was not unlike that of a tree, or of some usual branched sparks. The characteristic feature was the unusually long time of development. Nakaya and Tsuboi state that the motion could be followed with ease by the eyes. Tsuboi estimates the duration at 2 or 3 sec. and Yamamoto at 5 or 6 sec. whereas Nakaya's estimation seems to have been much shorter (1/2 sec.), though his description on this point is not positive.

The altitudes of the tracks were 20° to 40° above the southern horizon and its horizontal extents, W to E, were 50°–90°, taking the data of the three observers together. The hour of observation was 8h or 9h p.m. Nakaya saw the similar discharge repeated two or three times, and heard the thunders which appeared not quite remote. Tsuboi states that the discharges were repeated with an interval of about 5–10 sec. and continued for about 20 min. gradually decreasing in frequency towards the end of the display. He describes the colour of the luminosity as greenish blue. The progressing end or tip of the track was brighter than the other part which did not disappear instantly but seemed to remain luminous for a considerable time. Tsuboi considers this latter duration too long to be attributed to the usual persistence of image by retina.

Fig. 3 shows the yearly fluctuation in the frequency of the "conspicuous" earthquakes of which the origins were located in the region above specified. The full line curve refers to the total number of earthquakes including those originated in the sea area as above mentioned, while the dotted line represents those earthquakes originated in the land area. The arrow with black circle marks the year in which the rocket lightning was observed. Though the material is still too scanty to allow us any definite conclusion, it seems nevertheless interesting to observe that the unusual electric phenomema occurred at the period of enhanced seismic activity.

In the case of Example (1) of rocket lightnings, a conspicuous earthquake occurred on August 12, i.e. 12 days after the day of the lightning, in the northern part of Simôsa and also in the sea off Awa. For (2), a conspicuous earthquake is recorded on Sept. 15, i.e. 10 days after the lightning in SE part of Bôsô Peninsula. For (3), we have the Great Kwantô Earthquake six days after the lightning observed by the author. Lastly, for (4) a conspicuous shock was felt in Tôkyô of which the origin was located in the Bay of Tôkyô near Haneda, on August 3, i.e. very near the day of the extraordinary lightning for which the exact date is wanting but falls certainly within a definite period of ten days.

Of course, the occurrence of conspicuous earthquakes in the region here in question is rather frequent as may be judged from the graphs above shown, so that the probability of some accidental phenomenon occurring within a few days before or after the earthquake, is by no means negligibly small and therefore, the above apparent coincidence might be of no significance further than arousing our curiosity. Still, it seems to the present author of some interest to point out this mere fact, either significant or not, and to draw the attention of seismologists towards a domain of research which has been left unnoticed inspite of the physical possibility underlying the nature of the problem.

A further statistical investigation is now going on.

Appendix.

The normal tension acting upon the earth's surface due to the Faraday-Maxwell stress of the earth's electric field prevailing on the surface is given by $\varepsilon E^2/8\pi$ per cm²., where E is the potential gradient and ε the dielectric constant which may be put equal to unity for the present case. If E be $A \times 100$ volts/cm. the normal tension per unit area amounts to $A^2/226$. In the case of a thunderstorm E may attain 10 000 volts/cm. so that $A=100$, for which the tension becomes 44·3 dynes/cm². On the other hand, the atmospheric pressure of 1 mm. Hg is $1{\cdot}33 \times 10^3$ dynes/cm². Thus, the electric tension may attain at most a few per cent. of one mm. barometric pressure in its absolute magnitude and may be safely neglected in comparison with the variation of the atmospheric pressure as far as its direct mechanical effects in affecting the stress and strain of the earth's crust is in question.

On the other hand, it is well known that the barometric *gradient* of a few mm. per 100 km. may affect the occurrence as a significant secondary cause. Hence, if the above traction be applied at a locally limited area, a gradient of an amount may be produced which is comparable with the above atmospheric pressure gradient. For example, 44·3 for 3·33 km. corresponds to 1330 per 100 km. Such a steep horizontal gradient of the earth's electric field cannot be quite exceptional in the case of thunderstorm weather.

Hence, we cannot *a priori* reject the possibility of some earthquake being connected with thunderstorm phenomena, though it will be equally absurd to draw any positive conclusion from the above hypothetical consideration.

As to the horizontal pressure gradient due to the phenomenon of electro-endosmose, it is difficult at present to make any reliable estimation based upon observed data as these are utterly wanting. We may, however, show that the effect is at least worth a further investigation.

The hydrostatic pressure difference between the two ends of a capillary tube is given by

$$p = \frac{2\varphi D \varDelta V}{\pi r^2} \times \frac{1}{(300)^2} \text{ dynes/cm}^2.$$

where φ (volts) is the kinetic potential, $\varDelta V$ (volts) the potential difference, D the dielectric constant and r (cm.) the radius of the capillary. p is independent of the length of the tube. Assume $\varphi = 0{\cdot}03$, $D = 81$, $\varDelta V = 10^4$ volts[12] and $r = 10^{-2}$ cm. Then $p = 1{\cdot}72 \times 10^3$ dynes per cm²., i.e. attains the same order of magnitude as 1 mm. Hg.

The assumption tacitly made above that the rock material consisting the wall of the capillary is of an infinite specific resistance does not hold. However, it seems that the conductivity should rather enhance the pressure effect under the given potential difference. The assumption as to the dimensions of the capillary is a matter of great uncertainty. When, however, a distance of some ten or hundred km. along the earth's crust is involved, we may scarcely conceive any larger canal of subterranean water communication, so that it seems rather natural to assume such an effective radius of the order as above tentatively chosen, or perhap still less.

To avoid misunderstanding it must be emphasized that the above estimations were made only to demonstrate the plausibility of undertaking a statistical study of the relation between earthquake and thunderstorm, which may sound at first sight rather too fantastic. At least there is no reason to disprove such a relation from the beginning.

It must be remarked also that even if some relation between the two phenomena may actually exist, the relation cannot be necessary so simple as to allow an immediate explanation.

It may occur that the monthly frequencies run parallel, whereas the

---

12) A P.D. of this order of magnitude may easily be established for a distance of some 100 km. on the occasion of thunderstorm, at least for a short duration of time.

daily frequency does not. The relation might again depend upon seasons as well as localities. Before we may say anything definitive about these points the statistical materials must be gradually accumulated. For the latter purpose, the cooperation is desirable of as many investigators as possible.

---

27. 地震と雷雨との關係

地震研究所　寺田寅彦

地震と氣象要素との關係の統計的研究は從來少くないが、地震と雷雨との關係に就ては文献が少いやうである。著者は理論上から考へて此の二現象間に關係があるかも知れないと思つたので、試に關東地方だけに就て、1915-1930 の期間に就き、七、八、九の三箇月に於ける顯著及稍顯著地震の月回數と雷雨の月回數との年變化の模樣を對應させて見た。其結果は幾分でも著者の豫想を確かめるやうに見える。本文第二圖だけを見ても、少くも、此關係が初めから全然否定は出來ないものだといふことを示すには十分であらうと思ふ。

火箭電光 (rocket lightning) と稱する稀有の現象が雷雨の盛な年、又顯著地震の多い年に起るのではないかといふ疑問を提出して置く爲に第三圖を作つた。

附錄として、空中電位による地面に直角な力、又毛管電氣現象に歸因する水平方向の壓力差の大さに關する概算を行つた結果を示す。此等の電氣的直接影響も一概に初めから否定することは出來ないことだけは分ると思ふ。併し、實際上地震と雷雨との統計的關係が確立したとしても、それは雷雨の發生を促がす氣壓配置狀態が地震に影響する爲として、それだけで說明されるか、或は又上記の電氣的作用も參加するか、此れに就ては將來十分の調査をしなければ何事も云はれない。唯地震と雷雨との關係といふ從來余り注意されなかつたことが將來一つの研究題目として採用する價値のあるものだといふことは今回の豫備的調査だけでも明になつたことと思はれる。

28. *The Plastico-Elastic Deformation of a Semi-infinite Solid Body due to an Internal Force.*

By **Katsutada SEZAWA**,

Earthquake Research Institute.

(Read July 7, 1931.—Received Sept. 19, 1931.)

In this paper I am going to find mathematically the deformation of the ground in the neighbourhood of a volcano due to internal pressure at its nucleus, if exists, the material of the ground being assumed to be of plastic as well as of elastic nature.

1. We shall take first a two-dimensional problem, in which the axis of x resides on the horizontal surface of a simi-infinite ground and the axis of y is drawn vertically upwards. Let the centre of the pressure nucleus be at a depth ξ from the free surface and the radius of the nuclelus be a, the distribution of the pressure at the nucleus being assumed to be symmetrical with respect to its centre. The state of the material in the very vicinity of the nucleus must be purely plastic, so that we have the equations of the equilibrium such that

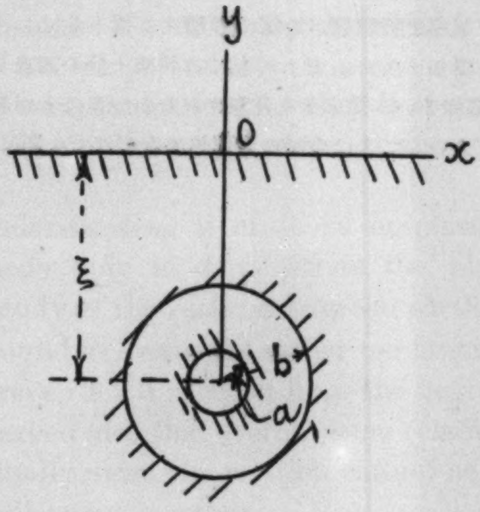

Fig. 1.

$$\left.\begin{aligned}\frac{d}{dr}(r\sigma_r)-\sigma_t &= 0,\\ \sigma_r-\sigma_t &= 2k,\end{aligned}\right\}\quad [a<r<b]\quad\cdots\cdots\cdots\cdots(1)$$ [1]

where $r^2=x^2+(y+\xi)^2$ and k is the constant of the plastic state such that the maximum shearing stress takes this value in such a state. σ_r and σ_t are the radial and transverse components of the symmetrical stress in the region, $a<r<b$. In the region, $r>b$, the state of the material is assumed to be elastic owing to the fact that the maximum shearing stress does not reach the value k.

At the inner boundary, $r=a$, we may put

$$r=a\,; \qquad \sigma_r=-p. \quad\cdots\cdots\cdots\cdots(2)$$

From (1) and (2) we have

$$\left.\begin{aligned}\sigma_r &= -p+2k\log\frac{a}{r},\\ \sigma_t &= -p-2k\left(1-\log\frac{a}{r}\right).\end{aligned}\right\}\quad [a<r<b]\quad\cdots\cdots\cdots(3)$$

At the outer elastic region we have

$$\frac{\partial}{\partial r}\left(\frac{\partial U}{\partial r}+\frac{U}{r}\right)=0, \qquad [r>b]\cdots\cdots\cdots\cdots(4)$$

the solution of which is

$$U=\frac{B}{r}, \quad\cdots\cdots\cdots\cdots(5)$$

and therefore the radial and the transverse stresses in this region are

$$\sigma_r'=-\frac{2\mu B}{r^2}, \qquad \sigma'=\frac{2\mu B}{r^2}. \quad\cdots\cdots\cdots\cdots(6)$$

At the surface, $r=b$, we get

$$r=b\,; \qquad \sigma_r=\sigma_r', \qquad \sigma_r'-\sigma_t'=2k. \quad\cdots\cdots\cdots\cdots(7)$$ [2]

---

[1] St. Venant, *C. R.*, 70 (1870) and 73 (1871). These equations are not contradictory with laws in recent metallurgy and strength of materials; no other criterion than that involved in these equations can seem to explain the phenomena of slip bands and the stress-strain relation of the strained materials and also the behaviour of a material under hydrostatic external pressure.

[2] In the case of special materials such as mild steel, in which the critical stress of the elastic region is different from the constant maximum shearing stress of the plastic region, we have to take, in place of (7), the forms:

$$r=b; \qquad \sigma_r=\sigma_r', \qquad \sigma_r'-\sigma_t'=2\mu k,$$

where μ is the ratio of the critical stress of the shear of the elastic region to the maximum shearing stress of the plastic region.

From (3), (6), (7) we find

$$\left.\begin{aligned} B &= \frac{pb^2}{2\mu}+\frac{kb^2}{\mu}\log\frac{b}{a}, \\ \frac{b}{a} &= e^{\left(\frac{1}{4}+\frac{p}{2k}\right)}. \end{aligned}\right\} \qquad \cdots\cdots\cdots\cdots (8)$$

x- and y-components of the displacement U are expressed by

$$\left.\begin{aligned} u_0 &= U\frac{x}{r} = B\int_0^\infty e^{-k(y+\xi)}\sin kx\,dk, \\ v_0 &= U\frac{y+\xi}{r} = B\int_0^\infty e^{-k(y+\xi)}\cos kx\,dk. \end{aligned}\right\} \quad [-\xi<y] \quad \cdots\cdots\cdots (9)$$

We may now suppose at $y=\xi$ the image of the previous nucleus, all conditions being to be similar. Then the radial displacement U' and its x- and y-components (u', v') are expressed by

$$U' = \frac{B'}{r'}, \qquad [r'^2 = x^2+(\xi-y)^2] \quad \cdots\cdots\cdots\cdots (10)$$

$$\left.\begin{aligned} u' &= U'\frac{x}{r'} = B'\int_0^\infty e^{-k(\xi-y)}\sin kx\,dk, \\ v' &= -U'\frac{\xi-y}{r} = -B'\int_0^\infty e^{-k(\xi-y)}\cos kx\,dk. \end{aligned}\right\} \quad [y<\xi] \quad \cdots\cdots\cdots (11)$$

The effect of the image on the conditions in the neighbourhood of the nucleus is not so great on account of its large distance from the image.

Add (11) to (9), and consider the tangential and vertical stresses on $y=0$. Then we have

$$\frac{\partial(v_0+v')}{\partial x}+\frac{\partial(u_0+u')}{\partial y}=0, \quad \cdots\cdots\cdots\cdots (12)$$

provided

$$B = B'; \quad \cdots\cdots\cdots\cdots (13)$$

and hence we get

$$\lambda\Delta+2\mu\frac{\partial(v_0+v')}{\partial y} = -4\mu B\int_0^\infty e^{-k\xi}\cos kx\,k\,dk. \quad \cdots\cdots\cdots\cdots (14)$$

To annul the stress in (14), we shall introduce the following displacement which is mainly accumulated in the neighbourhood of the free surface.

$$\left.\begin{aligned} \Delta_1 &= Ce^{ky}\cos kx, \\ u_1 &= C\left(\frac{\lambda+\mu}{2\mu}y+\alpha\right)e^{ky}\sin kx, \\ v_1 &= -C\left(\frac{\lambda+\mu}{2\mu}\,y+\beta\right)e^{ky}\cos kx, \end{aligned}\right\} [y<0] \quad \cdots\cdots\cdots\cdots(15)$$

where

$$k(\alpha-\beta) = \frac{\lambda+3\mu}{2\mu}. \cdots\cdots\cdots\cdots(16)$$

This displacement makes

$$\frac{\partial v_1}{dx}+\frac{\partial u_1}{\partial y} = 0. \cdots\cdots\cdots\cdots(17)$$

When the vertical component of the stress formed by this displacement is added to the expression (14), and the sum :

$$\lambda\Delta_1+2\mu\frac{\partial v_1}{\partial y}+\lambda\Delta+2\mu\frac{\partial(v_0+v')}{dy} \cdots\cdots\cdots\cdots(18)$$

is made zero, we find

$$\alpha = \frac{1}{2k}, \quad \beta = -\frac{\lambda+2\mu}{2\mu k}, \quad C = \frac{4\mu B}{(\lambda+\mu)}e^{-k\xi}k\,dk. \cdots\cdots\cdots\cdots(19)$$

Substituting these values in (15) and evaluating the total displacement $(u_0+u'+u_1,\ v_0+v'+v_1)$, we obtain

$$\left.\begin{aligned} u = u_0+u'+u_1 &= \frac{2B(\lambda+2\mu)}{(\lambda+\mu)}\int_0^\infty e^{-k\xi}\sin kx\,dk \\ &= 2B\,\frac{(\lambda+2\mu)}{(\lambda+\mu)}\,\frac{x}{(\xi^2+x^2)}, \\ v = v_0+v'+v_1 &= \frac{2B(\lambda+2\mu)}{(\lambda+\mu)}\int_0^\infty e^{-k\xi}\cos kx\,dk \\ &= \frac{2B(\lambda+2\mu)}{(\lambda+\mu)}\,\frac{\xi}{(\xi^2+x^2)} \end{aligned}\right\} \cdots\cdots\cdots\cdots(20)$$

on $y=0$, where the constant B, and hence the boundary, $r=b$, can be found from the expression (8).

2. Secondly, we shall consider a three-dimensional problem, in which r is taken in lieu of x and z in lieu of y, both of the foregoing case. As we are to study the case of a symmetrical nucleus, we can easily construct the equations of equilibrium of the plastic region, such that

$$\left.\begin{aligned} \frac{\partial\sigma_R}{\partial R}+\frac{2(\sigma_R-\sigma_t)}{R}&=0,\\ \sigma_R-\sigma_t&=2k, \end{aligned}\right\}\quad [a<R<b] \quad\cdots\cdots\cdots\cdots(21)$$

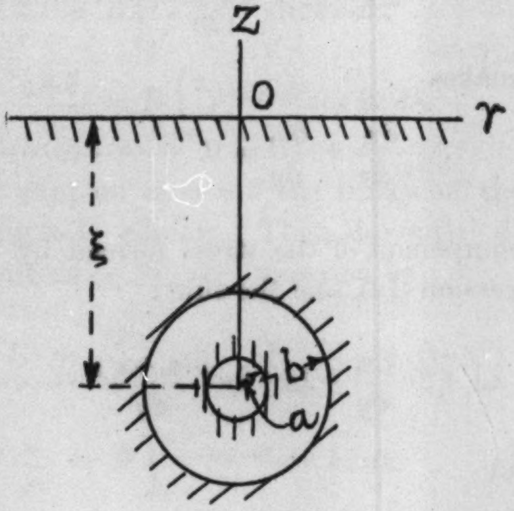

Fig. 2.

where $R^2=r^2+(z+\xi)^2$ and σ and σ_t are the radial and the transverse components of the stress. From the conditions that

$$R=a\,;\qquad \sigma_R=-p,\quad\cdots\cdots\cdots\cdots\cdots\cdots(22)$$

we get

$$\left.\begin{aligned} \sigma_R&=-p+2k\log\frac{a}{R},\\ \sigma_t&=-p-2k\left(1-\log\frac{a}{R}\right). \end{aligned}\right\}\quad\cdots\cdots\cdots\cdots\cdots(23)$$

At the elastic region we have

$$\frac{\partial}{\partial R}\left(\frac{\partial U}{\partial R}+\frac{2U}{R}\right)=0,\qquad [R>b]\quad\cdots\cdots\cdots\cdots\cdots(24)$$

the solution of which is

$$U=\frac{B}{R^2},\quad\cdots\cdots\cdots\cdots\cdots\cdots\cdots\cdots(25)$$

so that we obtain

$$\sigma_R{}' = -\frac{4\mu B}{R^3}, \qquad \sigma_t{}' = \frac{2\mu B}{R^3} \quad \cdots\cdots\cdots\cdots\cdots(26)$$

At the surface $R = b$ we get

$$R = b\,; \quad \sigma_R = \sigma_R{}', \qquad \sigma_R{}' - \sigma_t{}' = 2k. \cdots\cdots\cdots\cdots\cdots(27)$$[3]

From (23), (26), (27), we find

$$\left.\begin{aligned} B &= \frac{pb^3}{4\mu} + \frac{kb^3}{2\mu}\log\frac{b}{a}, \\ \frac{b}{a} &= e^{\left(\frac{1}{6}+\frac{p}{4k}\right)}. \end{aligned}\right\} \cdots\cdots\cdots\cdots\cdots(28)$$

r- and z-components of the displacements U are expressed by

$$\left.\begin{aligned} u_0 &= U\frac{r}{R} = B\int_0^\infty e^{-k(z+\xi)} J_1(br)k\,dk, \\ v_0 &= U\frac{y+\xi}{R} = B\int_0^\infty e^{-k(z+\xi)} J_0(kr)k\,dk. \end{aligned}\right\} \quad [\xi < z] \cdots\cdots\cdots(29)$$

Suppose the image at $z = \xi$, then the radial displacement U' and its r- and z-components (u', w') due to the image are written by

$$U' = \frac{B'}{R'^2}, \qquad [R'^2 = r^2 + (\xi - z)^2] \cdots\cdots\cdots\cdots\cdots(30)$$

$$\left.\begin{aligned} u' &= U'\frac{r}{R'} = B'\int_0^\infty e^{-k(\xi-z)} J_1(kr)k\,dk \\ v' &= -U'\frac{\xi - z}{R'} = -B'\int_0^\infty e^{-k(\xi-z)} J_0(kr)k\,dk. \end{aligned}\right\} \quad [z < \xi] \cdots\cdots(31)$$

Add (31) to (29) and take the tangential and the vertical stresses on $z = 0$. Then, we get

$$\frac{\partial(w_0 + w')}{\partial r} + \frac{\partial(u_0 + u')}{dz} = 0, \quad \cdots\cdots\cdots\cdots\cdots(32)$$

---

[3] For special materials as already cited concerning the equation (7), we have to put the following forms in place of (27),

$$R = b; \qquad \sigma_R = \sigma_R', \qquad \sigma'_R - \sigma_t' = 2\mu k,$$

where μ has the same meaning as that of the preceding case.

provided

$$B = B' ; \quad\cdots\cdots\cdots\cdots(33)$$

and hence we obtain

$$\lambda\varDelta + 2\mu\frac{\partial(w_0 + w')}{\partial z} = -4\mu B\int_0^\infty e^{-k\xi}J_0(kr)k^2\,dk. \quad\cdots\cdots\cdots\cdots(34)$$

We shall again consider the displacement which is accumulated in the neighbourhood of the surface, $z = 0$, such that

$$\left.\begin{aligned} \varDelta_1 &= Ce^{kz}J_0(kr) \\ u_1 &= C\left(\frac{\lambda+\mu}{2\mu}z + \alpha\right)e^{kz}J_1(kr), \\ w_1 &= -C\left(\frac{\lambda+\mu}{2\mu}z + \beta\right)e^{kz}J_0(kr), \end{aligned}\right\} \quad [z<0] \quad\cdots\cdots\cdots\cdots(35)$$

where

$$k(\alpha - \beta) = \frac{\lambda + 3\mu}{2\mu}. \quad\cdots\cdots\cdots\cdots(36)$$

This displacement naturally satisfies the condition :

$$\frac{\partial w_1}{\partial r} + \frac{\partial u_1}{\partial z} = 0, \quad\cdots\cdots\cdots\cdots(37)$$

and, when the vertical component of the stress is added to (34), and the sum is made zero, such that

$$\lambda\varDelta_1 + 2\mu\frac{\partial w_1}{\partial z} + \lambda\varDelta + 2\mu\frac{\partial(w_0 + w_1)}{\partial z} = 0, \quad\cdots\cdots\cdots\cdots(38)$$

we get

$$\alpha = \frac{1}{2k}, \quad \beta = -\frac{(\lambda+2\mu)}{2\mu k}, \quad C = \frac{4\mu Be^{-k\xi}}{(\lambda+\mu)}k^2\,dk. \quad\cdots\cdots\cdots\cdots(39)$$

We find finally the components of the displacement on $z = 0$ in the forms :

$$\left.\begin{aligned} u = u_0 + u' + u_1 &= \frac{2B(\lambda+2\mu)}{(\lambda+\mu)}\int_0^\infty e^{-k\xi}J_1(kr)k\,dk \\ &= \frac{2B(\lambda+2\mu)}{(\lambda+\mu)}\frac{r}{(\xi^2+r^2)^{\frac{3}{2}}}, \quad (a) \\ w = w_0 + w' + w_1 &= \frac{2B(\lambda+2\mu)}{(\lambda+\mu)}\int_0^\infty e^{-k\xi}J_0(kr)k\,dk \\ &= \frac{2B(\lambda+2\mu)}{(\lambda+\mu)}\frac{\xi}{(\xi^2+r^2)^{\frac{3}{2}}}, \quad (b) \end{aligned}\right\} \quad\cdots\cdots\cdots(40)$$

where the constant B and hence the boundary $r = b$ can be determined from (28).

3. From the preceding calculation it may be easily concluded that

i) When the plastic region is mainly localised in the neighbourhood of the pressure nucleus, the general character of the distribution of the displacements on the free surface is not altered due to the size of the (spherical) nucleus or of the (spherical) plastic region; but the absolute value of the surface displacement changes considerably due to the size of the above elements and also due to the internal pressure at the nucleus.

ii) When the radius of the pressure nucleus is a, its pressure is p and the plastic constant is k, the boundary separating the solid into plastic and elastic regions is denoted by

$$b = a\,e^{\left(\frac{1}{4}+\frac{p}{2k}\right)}$$

in a two-dimensional case; and

$$b = a\,e^{\left(\frac{1}{6}+\frac{p}{4k}\right)}$$

in a three-dimensional case.

iii) In the two-dimensional case the vertical component of the displacement on a point on the free surface is proportional to the inverse square of the distance of that point from the centre of the nucleus, while in the three-dimensional case this component is inversely proportional to the cube of the distance.

To ascertain the validity of the present result for the practical purpose, I have introduced the result of the levelling survey which was carried out by Dr. C. TSUBOI[4] at the very vicinity of Volcano Komagatake at the epoch shortly after its eruption. The observed result concerning the movement being substituted in the formula (40b), I have found that the centre of the nucleus resides at 0∼3 km vertically downwards from the summit of the volcano. Owing to the seismometrical observation made by Dr. F. KISHINOUYE[5] at Komagatake at the same epoch, the focal depths of the frequent seismic shocks seem to be very near to the depths of the nucleus which I have calculated here, so that, I think, my

---

[4] C. TSUBOI, Part V of the paper "The Eruption of Komagatake, Hokkaidô, in 1929," *Bull. Earthq. Res. Inst.*, 8 (1930), 298–300.

[5] F. KISHINOUYE, Part III of the same paper, 274–289.

mathematical result is not without value to the geophysical problem of the volcanoes.

It may be added that the equilibrium of the boundary separating the plastic and the elastic regions is in general of a somewhat complex nature, especially in some cases of metals; but in the case of the rocks the problem is very simple and the present analysis will be sufficient at least for the purpose of the geophysical investigation. For the discussion of the separation boundary of the general substances the result due to Robertson and Cook[6] will be of some interest.

---

28. 內部に力核を有する半無限プラスチコ彈性體の變形

地震研究所 妹澤克惟

火山に內核(若しありとすれば)があつて、其爲に半無限固體である地殼が如何なる變形をなすべきかといふ事を計算して見たのである。固體はプラスチック性と彈性とを有するものと假定してあるのであり、從てこの樣な靜力學的の問題に可なりあてはまると思ふ。

內核の附近は應力が大である爲に最大剪斷應力がプラスチックの常數 k に達する。其等の所をプラスチックの領域と考へ、それから外の部分は彈性の領域としてよい譯である。此等の各々に平衡の微分方程式を應用し、又內核の壓力の加はる所の條件や、上述の兩領域の接ぎ目や半無限體表面の條件等を滿足する樣な解を求めたのである。

計算の結果の重要な事項を擧げて見ると、i) プラスチックの領域が餘り擴つて居らぬ時に、固體表面の變位の分布の割合は、內核の大さ、壓力及びプラスチック彈性兩領域境界面の大さなどに無關係となる。 ii) 內核の半徑を a とし、其壓力を p、プラスチックの常數を k と書く時、プラスチック、彈性兩領域境界面の半徑 b は次式で表はされる。

$$b = a\,e^{\left(\frac{1}{4}+\frac{p}{2k}\right)} \qquad \text{(二次元)}$$

$$b = a\,e^{\left(\frac{1}{6}+\frac{p}{4k}\right)} \qquad \text{(三次元)}$$

iii) 固體表面上の點の上下の變位は二次元の時には其點から核心までの距離の二乘に反比例し、三次元の時にはその距離の三乘に反比例する。

この計算結果の適合性を確める爲に、駒ケ岳火山爆發後坪井忠二所員が行つた水準測量結果から火山の核心の深さを求めて見た。それが 0〜3 粁と出るのである。此を岸上所員が大體同じ頃に同火山の地震の源點を地震計的に觀測せる結果と比較して見ると可なり近い値を取る樣に思はれるのである。

---

6) A. Robertson and G. Cook, "The Transition from the Elastic to the Plastic State in Mild Steel," *Proc. Roy. Soc.*, London, **88** (1913), 462.

29. *Blocks in the Earth's Crust and their Movements.*
Part II.
(*Post-Seismic Crustal Movements in Bôsô Peninsula*)

By **Naomi Miyabe**,

Earthquake Research Institute.

(Read July 7, 1931.—Received Sept. 6, 1931.)

1. At the time of the Kwantô Earthquake of 1923, the earth's crust was found much disturbed in the district lying near the Bay of Sagami where the epicentre of the earthquake was located. The earth's crust in Bôsô Peninsula was also much disturbed. The disturbance of the earth's crust was measured, among others[1] as the vertical displacements of the bench-marks distributed along the leveling routes passing through the peninsula, with which the writer deals in the present paper. The leveling route passing through Bôsô Peninsula, along which vertical displacements of the bench-marks were measured, is shown in Fig. 1. The surveys of this leveling route was carried out for the first time in 1898. The second survey of the same leveling route was carried out in 1924, and thence the vertical displacements of the bench-marks which had occurred during 1898-1924 were determined. The vertical displacements of the bench-marks obtained as the result of the second survey contain the effect of the " acute " crustal movement due to the Kwantô Earthquake.

An urgent need was felt, after the lapse of these several years since the second survey, to know the post-seismic crustal movement in Bôsô peninsula. In 1931, the long wanted third survey of the same leveling route was carried out[2] by means of the research fund granted to the Earthquake Research Institute from the Authority of the Imperial Academy, for which the present writer's best thanks are due.

---

[1] On the other hand, we know horizontal and vertical displacements of triangulation points, which we used as the data for investigating the crustal disturbance in Kwantô Districts.

T. Terada and N. Miyabe, *Proc. Imp. Acad.*, 6 (1930), 49. N. Miyabe, *Proc. Imp. Acad.*, 6 (1930), 305; 7 (1931), 150. *Bull. Earthq. Res. Inst.*, 9 (1931), 1; 9 (1931), 256.

[2] The result of the third survey was communicated by Colonel Suzuki of the Military Land Survey, at the Meeting of the Colloquium of the Earthquake Research Institute, April 17, 1931.

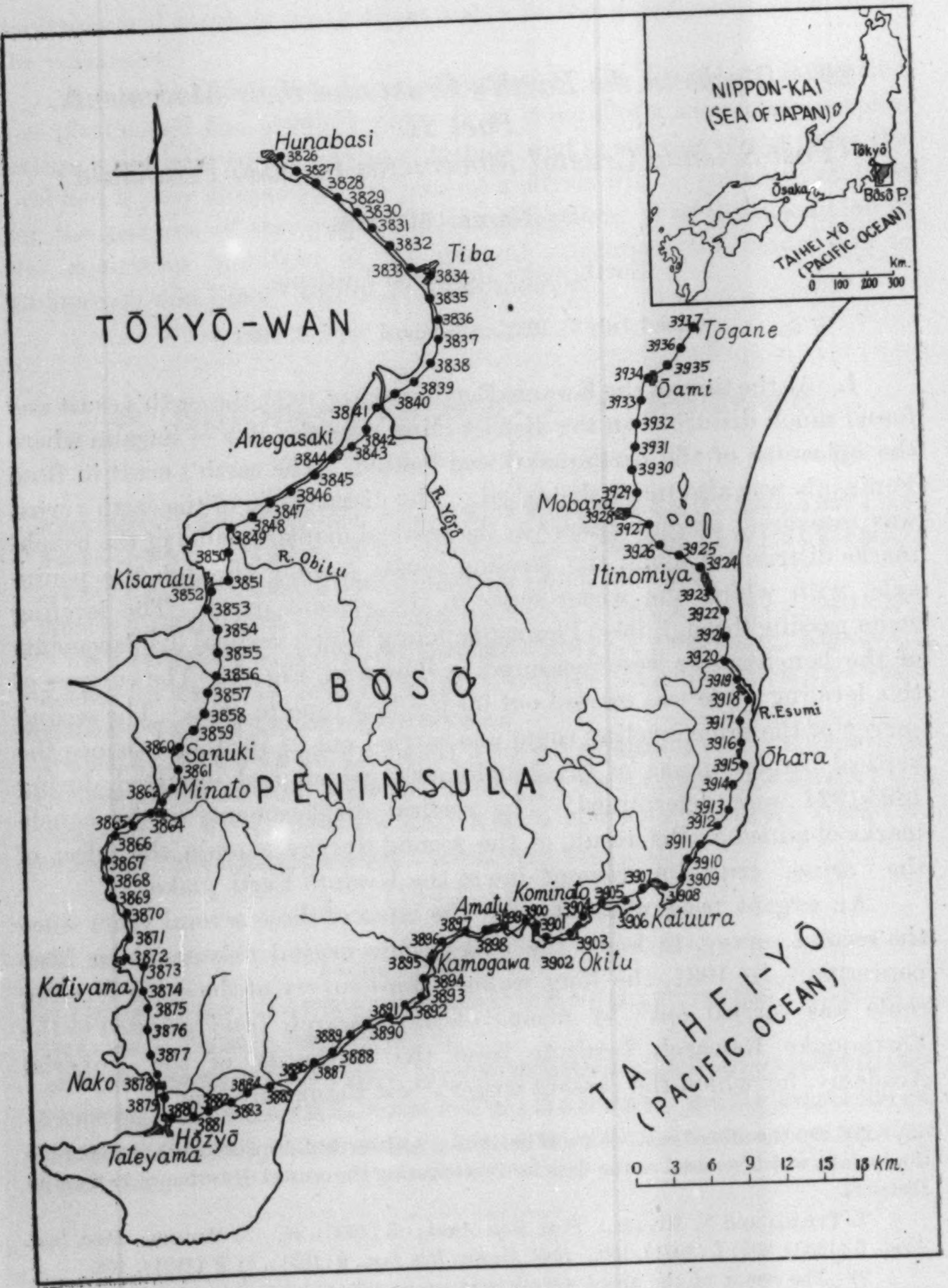
NIPPON-KAI
(SEA OF JAPAN)
Tôkyô
Ôsaka
Bôsô P.
TAIHEI-YÔ
(PACIFIC OCEAN)
km.
0 100 200 300
TÔKYÔ-WAN
Hunabasi
Tiba
Anegasaki
R. Yôrô
R. Obitu
Kisaradu
BÔSÔ
PENINSULA
Sanuki
Minato
Katiyama
Nako
Tateyama
Hôzyô
Kamogawa
Amatu
Kominato
Okitu
Katuura
Ôhara
R. Esumi
Itinomiya
Mobara
Ôami
Tôgane
TAIHEI-YÔ
(PACIFIC OCEAN)
0 3 6 9 12 15 18 km.
3826
3827
3828
3829
3830
3831
3832
3833
3834
3835
3836
3837
3838
3839
3840
3841
3842
3843
3844
3845
3846
3847
3848
3849
3850
3851
3852
3853
3854
3855
3856
3857
3858
3859
3860
3861
3862
3864
3865
3866
3867
3868
3869
3870
3871
3872
3873
3874
3875
3876
3877
3878
3879
3880
3881
3883
3884
3886
3887
3888
3889
3890
3891
3892
3893
3894
3895
3896
3897
3898
3900
3901
3902
3903
3904
3905
3906
3907
3908
3909
3910
3911
3912
3913
3914
3915
3916
3917
3918
3919
3920
3921
3922
3923
3924
3925
3926
3927
3928
3929
3930
3931
3932
3933
3934
3935
3936
3937

Fig. 1.

Bôsô Peninsula and the Distribution of the Bench-marks.

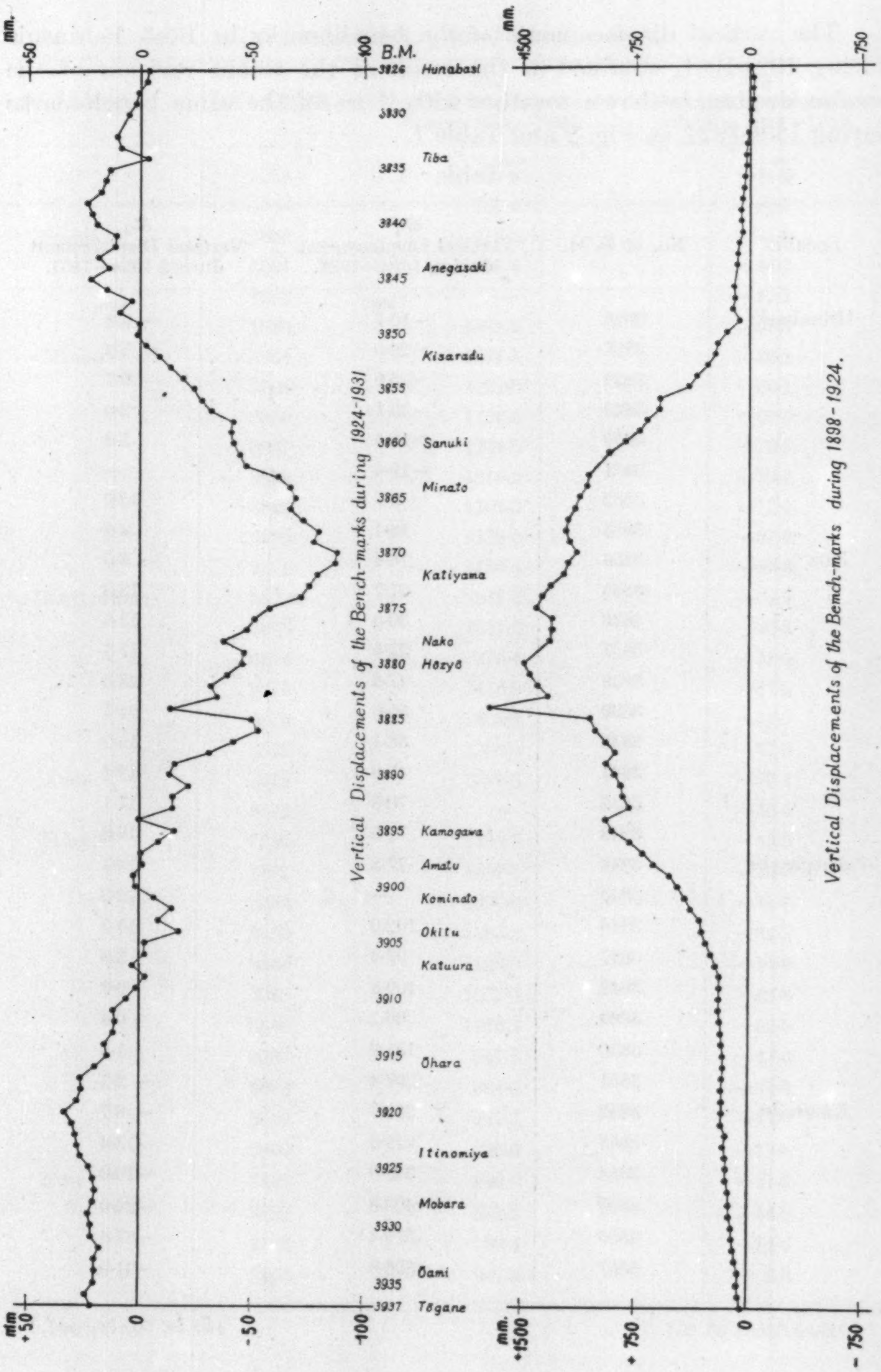

Vertical Displacements of the Bench-marks during 1924-1931

Vertical Displacements of the Bemch-marks during 1898-1924.

Fig. 2.

The vertical displacements of the bench-marks in Bôsô Peninsula during 1924-1931, obtained as the result of the recent revision of the precise leveling, is shown, together with those of the same bench-marks during 1898-1924, in Fig. 2 and Table I.

Table I.

Locality	No. of B. M.	δh_1 Vertical Displacement during 1898—1924.	δh_2 Vertical Displacement during 1924—1931.
		mm.	mm.
Hunabasi	3826	−10·7	− 3·8
	3827	−26·0	− 3·3
	3828	−23·9	0·7
	3829	−23·1	2·0
	3830	−12·4	5·3
	3831	−10·4	—
	3832	5·7	10·2
	3833	16·1	8·9
Tiba	3834	16·4	− 3·6
	3835	21·7	13·6
	3836	30·8	15·5
	3837	37·5	17·5
	3838	47·6	23·3
	3839	55·6	21·7
	3840	53·1	19·2
	3841	45·8	10·8
	3842	70·3	11·1
	3843	77·5	18·8
Anegasaki	3844	77·3	14·1
	3845	—	22·2
	3846	102·0	14·9
	3847	97·3	3·8
	3848	100·8	9·2
	3849	66·7	0·6
	3850	151·9	1·2
	3851	207·4	− 2·7
Kisaradu	3852	226·7	− 8·7
	3853	279·0	−13·4
	3854	343·0	−19·0
	3855	409·8	−24·0
	3856	519·4	−27·8
	3857	596·8	−31·9

(*to be continued.*)

Table I. (*continued.*)

Locality	No. of B. M.	δh_1 Vertical Displacement during 1898—1924.	δh_2 Vertical Displacement during 1924—1931.
		mm.	mm.
	3858	677·8	−41·5
	3859	727·0	−40·5
Sanuki	3860	816·2	−41·8
	3861	925·8	−44·2
	3862	—	−47·1
	3863	1061·9	−61·5
Minato	3864	1077·1	−66·8
	3865	1122·7	−69·1
	3866	1156·6	−67·0
	3867	1204·5	−72·6
	3868	1215·2	−79·4
	3869	1192·9	−77·2
	3870	1139·0	−87·9
	3871	1199·4	−86·8
Katiyama	3872	1242·3	−78·9
	3873	1311·2	−75·5
	3874	1376·4	−71·9
	3875	1413·5	−57·5
	3876	1308·8	−51·0
	3877	1306·0	−47·8
Nako	3878	1319·3	−37·4
	3879	—	−46·5
Hôzyô	3880	1482·0	−45·3
	3881	1457·1	−38·9
	3882	1396·8	−31·7
	3883	1335·2	−34·2
	3884	1726·0	−14·6
	3885	1057·0	−49·8
	3886	1016·8	−52·6
	3887	947·1	−41·8
	3888	884·0	−31·0
	3889	941·7	−15·8
	3890	890·6	−13·4
Emi	3891	840·0	−21·5
	3892	831·3	−14·8
	3893	799·4	−14·6
	3894	947·8	0·3

(*to be continued.*)

Table I. (*continued.*)

Locality	No. of B. M.	δh_1 Vertical Displacement during 1898—1924.	δh_2 Vertical Displacement during 1924—1931.
		mm.	mm.
Kamogawa	3895	905·9	−15·5
	3896	789·1	−8·2
	3897	703·7	−0·7
Amatu	3898	629·4	−1·3
	3899	525·2	2·6
	3900	470·0	1·6
Kominato	3901	421·8	−6·6
	3902	380·3	−14·7
	3903	318·5	−8·6
Okitu	3904	310·4	−17·6
	3905	283·7	−2·3
	3906	249·8	−2·5
	3907	233·5	3·0
Katuura	3908	193·9	−2·5
	3909	196·1	1·2
	3910	192·9	5·8
	3911	195·8	11·4
	3912	186·1	10·9
	3913	183·6	11·5
	3914	174·3	15·1
Ôhara	3915	169·0	14·3
	3916	165·4	19·5
	3917	174·9	26·0
	3918	161·0	25·7
	3919	160·3	27·8
	3920	171·3	33·2
	3921	170·3	30·0
	3922	146·2	28·1
Itinomiya	3923	159·2	27·7
	3924	147·8	26·0
	3925	148·8	22·4
	3926	160·9	20·4
	3927	130·7	19·5
Mobara	3928	126·1	20·6
	3929	116·1	22·4
	3930	106·7	21·3
	3931	99·8	21·1

(*to be continued.*)

Table I. (*continued.*)

Locality	No. of B. M.	δh_1 Vertical Displacement during 1898—19.4.	δh_2 Vertical Displacement during 1924—1931.
		mm.	mm.
	3932	90·9	17·5
	3933	78·4	19·9
Ôami	3934	55·7	19·6
	3935	64·9	20·0
	3936	52·9	23·8
Tôgane.	3937	41·8	21·3

2. At a glance of the two curves in Fig. 2, i. e., the vertical displacements of the bench-marks during 1924—1931 and those of the same bench-marks during 1898—1924, we notice the general tendency that the vertical movement of the earth's crust in Bôsô Peninsula is reversed during 1924—1931 compared with that which had occurred during 1898—1924. Remembering the distribution of the bench-marks, it may be suggested that the general movement of the earth's crust in Bôsô Peninsula was SW-ward tilting during 1924—1931, while it was NE-ward tilting during 1898—1924.

To investigate the matter in more detail, Fig. 3 was constructed. In Fig. 3, the points corresponding to the bench-marks are plotted on the diagram, in which the values of vertical displacements of the bench-marks during 1924—1931, δh_2, are taken in ordinate and those of the same bench-marks during 1898—1924, δh_1, are taken in abscissa. Fig. 3, therefore, shows the relation between the vertical displacements of the bench-marks due to the crustal movement during 1924—1931, δh_2, and those of the same bench-marks due to the crustal movement during 1898—1924, δh_1, including the acute movement associated with the Kwantô Earthquake of 1923.

In Fig. 3, we notice a general tendency in distribution of the points, which may be roughly represented by the two dotted lines *AB* and *CD*. These lines are expressed numerically by

$$\delta h_1^{mm} = 210{\cdot}0^{mm} - 15{\cdot}4 \times \delta h_2^{mm} \quad (1) \text{ for } AB$$

and

$$\delta h_2^{mm} = -\, 50{\cdot}2^{mm} + 7{\cdot}8 \times \delta h_2^{mm} \quad (2) \text{ for } CD.$$

The relation (1) corresponds to the general tilting of the earth's crust

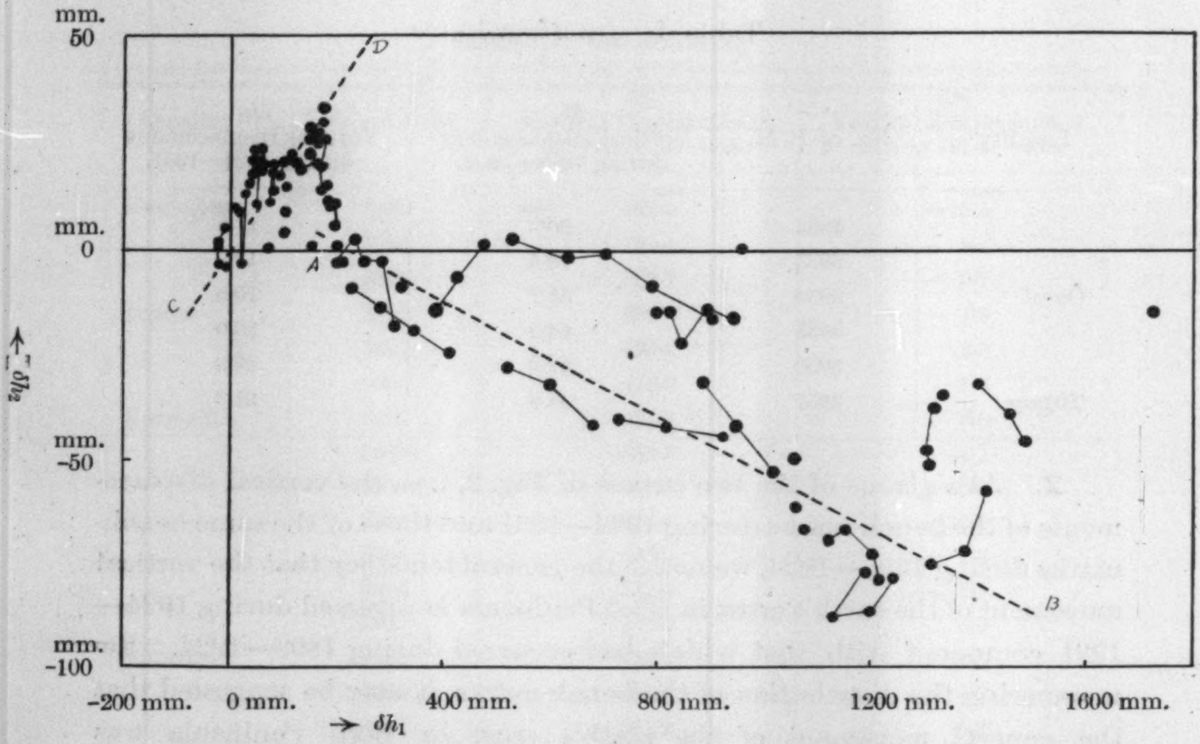

Fig. 3. The Relation between δh_1 and δh_2. Points belonging to a Group or regarded as situated on a Single Block are connected by Full Lines. Broken Lines *AB* and *CD* denote the General Tendencies in Distribution of the Points.

of the peninsula, which we noticed in Fig. 2. The relation (1) holds for a group of bench-marks, B.M. 3746—B.M. 3915, while the relation (2) holds for groups of bench-marks, B.M. 3826—B.M. 3845 and B.M. 3916—B.M. 3937. As for the bench-marks situated, in Fig. 3, between these two different groups, it cannot be determined without ambiguity to which group they belong.

From the relation (1), we have $\partial h_2 = 0{\cdot}0$ mm. for $\partial h_1 = 210{\cdot}0$ mm. The bench-marks with their amounts of vertical displacements during 1924—1931, ∂h_2, nearly equal to zero and, simultaneously, ∂h_1 approximately equal to 210·0 mm., lie near Kisaradu and also near Katuura, as they are shown in Table I.

From the fact mentioned above, the following mode of tilting of the earth's crust in Bôsô Peninsula may be suggested. If the crustal movement during 1924—1931 is mainly due to a mere tilting having its horizontal axis approximately coincident with the line connecting Kisaradu and Katuura, the crustal movement in the same district during

1898-1924 may be regarded as have consisted of two components, i.e., a translational vertical movement superposed by a tilting, the latter being the movement about the same horizontal axis as in the case of the crustal movement during 1924—1931.[3]

A similar suggestion may be given as to the movement of the earth's crust in the regions where the vertical displacements of the bench-marks for the two different time intervals are connected by the relation (2). For the boundary of the two regions, in one of which the relation (1) holds and, in the other, the relation (2) holds between the vertical displacements δh_1 and δh_2, an approximately coincident fault line was traced from Anegasaki to Ôhara by Prof. H. Yabe and his collaborators. But it is not evident whether the geological fault was significant for the boundary of the regions with different modes of crustal movements observed during 1898—1931.

3. Connecting adjoining points in Fig. 3, corresponding to adjoining bench-marks, we notice many groups which are connected by approximate straight lines, i. e., groups of bench-marks of which δh_1 and δh_2 are connected approximately by linear relations. In several groups of the bench-marks, δh_1 and δh_2 are negatively correlated, while in the other groups they are positively correlated. Bench-marks belonging to the groups with positive correlations are generally situated near Anegasaki, Mobara and Ôhara (at the neck portion of the peninsula) and near Hôzyô (near southwest end of the peninsula), while those belonging to the groups with negative correlations are generally distributed in spaces between those two regions where the bench-marks belonging to the groups with positive correlations are situated.

4. Corresponding to several groups of bench-marks mentioned in the above, blocks are determined by the method described in the previous paper[4] using as the data the vertical displacements of bench-marks. The blocks and their magnitudes and directions of tiltings are determined and shown in Fig. 4. In this figure, the double arrows show the tiltings of the blocks during 1898—1924 and the thick single arrows show the tiltings of the blocks during 1924—1931. The magnitudes

---

[3] At the May Colloquium of the Earthquake Research Institute (May 21, 1931), Prof. H. Yabe pointed out the existence of tilting motion of the earth's crust about the horizontal axis conneting Kisaradu and Katuura in this district, in connection with the geological and geotectonic evidences.

[4] N. Miyabe, *Proc. Imp. Acad.*, 7 (1931), 150; *Bull. Earthq. Res. Inst.*, 9 (1931), 256.

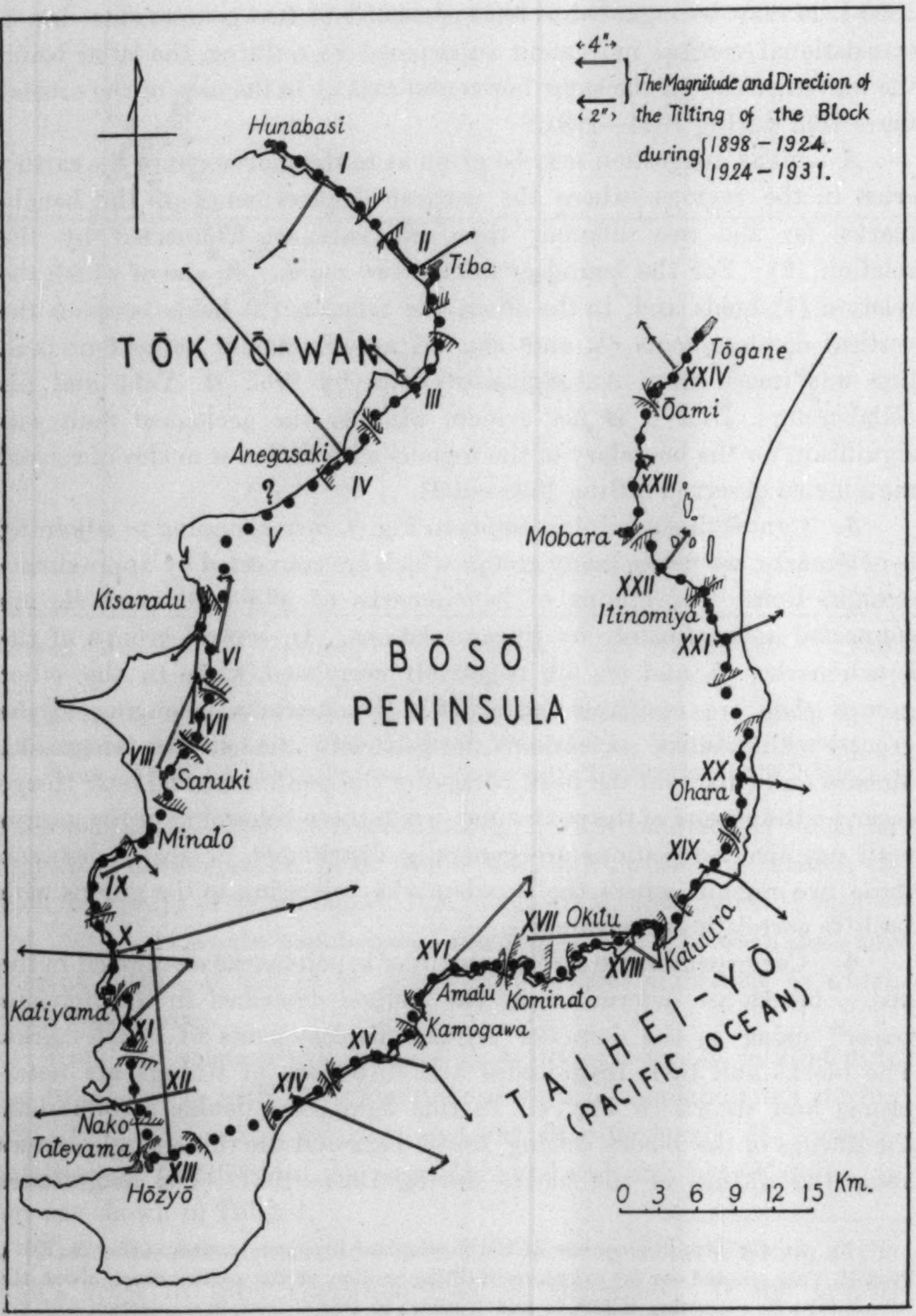
4"
2"
The Magnitude and Direction of the Tilting of the Block during 1898 – 1924. 1924 – 1931.
Hunabasi
I
II
Tiba
TŌKYŌ-WAN
Tōgane
XXIV
Ōami
III
Anegasaki
IV
?
V
XXIII
Mobara
XXII
Itinomiya
Kisaradu
XXI
BŌSŌ PENINSULA
VI
VII
VIII
Sanuki
XX
Ōhara
Minato
XIX
IX
X
XVII Okitu
XVI
Katuura
XVIII
Amatu
Kominato
Kamogawa
Katiyama
XI
XV
TAIHEI-YŌ (PACIFIC OCEAN)
XII
XIV
Nako
Tateyama
XIII
Hōzyō
0 3 6 9 12 15 Km.

Fig. 4. Blocks and their Tiltings during 1898–1924 (Double Arrows) and those during 1924–1931 (Thick Single Arrows). Bench-marks situated on the same Block are connected by Lines.

and directions of tiltings, mean vertical movements and the differences of the directions of tiltings of the blocks for the two different time intervals, $\varepsilon=\theta_{m2}-\theta_{m1}$, are shown in Table II. Examining the mode of block movements during 1898–1924, it is natural to notice that the movements are similar to those determined by using as the data the vertical displacements of the triangulation points[5], except for several cases of discordances. These discordances in block movements, determined by the different data, may be due partly to the difference between the duration of the time interval of the successive leveling

Table II.

Block	B. M.	1924—1931			1898—1924			$\varepsilon=\theta_{m2}-\theta_{m1}$
		$\tan\varphi_{m2}$	θ_{m2}	$\overline{\delta h_2}$	$\tan\varphi_{m1}$	θ_{m1}	$\overline{\delta h_1}$	
I	3826—3830	$0{\cdot}9\times10^{-5}$	223·5°	0·2 mm	$5{\cdot}3\times10^{-5}$	215·5°	−19·2 mm	8·0
II	3832—3835	1·5	60·0	7·3	0·4	5·5	15·0	54·5
III	3837—3841	1·0	310·5	18·5	1·8	320·0	47·9	9·5
IV	3842—3844	5·2	318·3	14·7	3·0	320·5	75·0	2·2
V	?	?	?	?	?	?	?	?
VI	3852—3855	0·3	259·5	−16·3	4·0	12·5	314·6	247·0
VII	3856—3858	1·0	225·5	−33·7	4·6	5·5	598·0	220·0
VIII	3859—3861	0·1	167·0	−42·2	5·3	23·0	823·0	144·0
IX	3865—3868	0·6	138·7	−72·0	2·3	65·5	1174·8	73·2
X	3869—3872	1·8	84·3	−82·7	9·6	75·5	1193·5	8·8
XI	3873—3875	4·1	272·3	−68·3	4·3	50·5	1367·0	221·8
XII	3876—3878	2·0	265·8	−45·4	4·7	259·5	1311·4	6·3
XIII	3880—3882	0·5	225·0	−38·6	11·0	355·3	1445·3	130·0
XIV	3886—3888	0·6	238·5	−41·8	8·9	112·0	949·3	126·5
XV	3889—3893	1·7	146·5	−16·0	3·2	115·0	860·6	31·5
XVI	3895—3899	0·5	187·0	− 4·6	6·1	44·0	710·7	143·0
XVII	3900—3902	0·7	102·0	− 6·6	4·6	87·0	424·0	15·0
XVIII	3904—3908	1·1	352·5	− 4·4	2·1	126·0	254·3	226·5
XIX	3910—3913	1·7	125·5	9·9	2·0	118·5	189·6	7·0
XX	3914—3918	0·8	113·5	20·1	1·9	98·5	168·9	15·0
XXI	3921—3924	0·2	53·5	28·0	3·4	68·0	155·9	−14·5
XXII	3924—3927	0·2	263·5	22·3	2·7	37·5	147·1	226·0
XXIII	3928—3933	0·4	280·0	20·5	0·6	35·0	103·0	245·0
XXIV	3934—3937	0·4	327·5	21·2	2·2	320·0	53·8	7·5

---

[5] *loc. cit.* 4)

surveys and that of the successive triangulation surveys, during which the vertical displacements of bench marks or triangulation points are considered to have occurred, and partly to the accuracies in determining the blocks and their tiltings. The time intervals of the successive surveys is 36 years for the triangulation surveys and 26 years for the leveling surveys.

In our present cases, the accuracy in determining the blocks may mainly depend on numbers of the points (bench-marks or triangulation points) and the range of variation of azimuths of lines connecting the adjoining points in a single constituent block. For blocks determined by using as the data the vertical displacements of the triangulation points, conditions are favourable for insuring a higher order of accuracy than those determined by using as the data the vertical displacements of the bench-marks, for the triangulation points are distributed in areas.

5. As obtained in the above, the directions of tiltings of the block for the two different time intervals are not the same. Now the preliminary assumption that the bench-marks of which δh_1 and δh_2 are connected approximately by a linear relation are situated on a single block, should be a little modified.

For the vertical displacements of the bench-marks situated on a single block, the following relation is required:

$$\frac{\delta h - \delta h_0}{s} = \tan\varphi = \tan\varphi_m \cos(\theta - \theta_m)$$

as we have shown in the preceding paper[6], where s is the distance between the two bench-marks of which the vertical displacements are δh and δh_0 respectively, θ the azimuth referring to N of the line connecting the bench-marks under consideration, and φ_m and θ_m are the magnitude and the direction of tilting of the block.

Now, for the block movements during 1898—1924 and 1924—1931, we have

$$\frac{\delta h_1 - \delta h_{10}}{s} = \tan\varphi_{m1} \cos(\theta - \theta_{m1})$$

and

$$\frac{\delta h_2 - \delta h_{20}}{s} = \tan\varphi_{m2} \cos(\theta - \theta_{m2})$$

---

6) *Loc. cit.* 4) 5).

Then we have for the ratio K

$$K=\frac{\delta h_2-\delta h_{20}}{\delta h_1-\delta h_{10}}=\frac{\tan\varphi_{m2}}{\tan\varphi_{m1}}\frac{\cos(\theta-\theta_{m2})}{\cos(\theta-\theta_{m1})}$$

$$=\frac{\tan\varphi_{m2}}{\tan\varphi_{m1}}\left\{\cos\varepsilon-\tan(\theta-\theta_{m1})\sin\varepsilon\right\},$$

where $\varepsilon=\theta_{m2}-\theta_{m1}$.

Hence, the ratio $\frac{\delta h_2-\delta h_{20}}{\delta h_1-\delta h_{10}}$ is not constant, even if the bench-marks under consideration are situated on a single block, when $\theta_{m2}\neq\theta_{m1}$, i. e., the directions of tiltings of the block for the two different time intervals are not the same.

The ratios $\frac{\delta h_2-\delta h_{20}}{\delta h_1-\delta h_{10}}$ are calculated as the function of $(\theta-\theta_{m1})$ in a single block. In Fig. 5, $[\cos\varepsilon-\tan(\theta-\theta_{m1})\sin\varepsilon]$ are plotted against $(\theta-\theta_{m1})$ for several values of ε. As seen in the graph, for smaller values of ε the ratios $\frac{\delta h_2-\delta h_{20}}{\delta h_1-\delta h_{10}}$ are nearly constant, if the values of $(\theta-\theta_{m1})$ are sufficiently

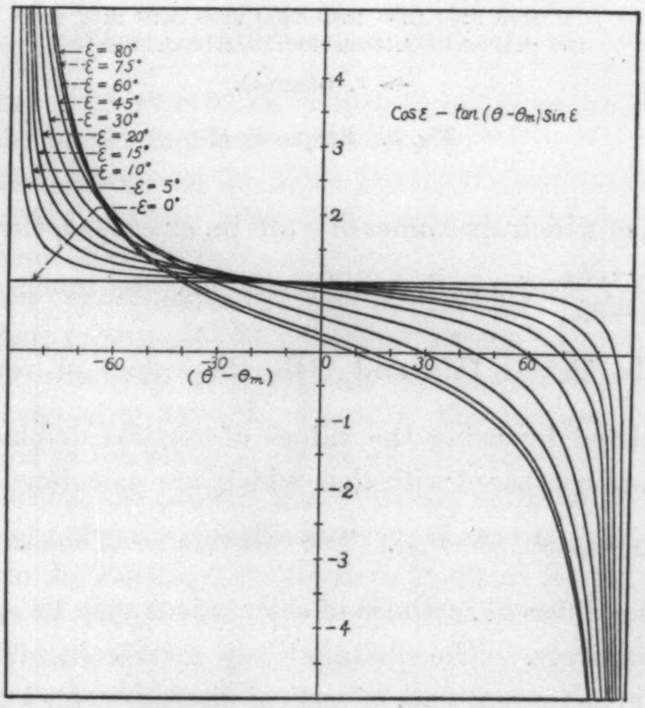

Fig. 5.

apart from $\pm\frac{\pi}{2}$. In actual cases, however, the values of ε fall frequently into the ranges 0°–10° and 30°–50°, as shown in Fig. 6. Hence, in

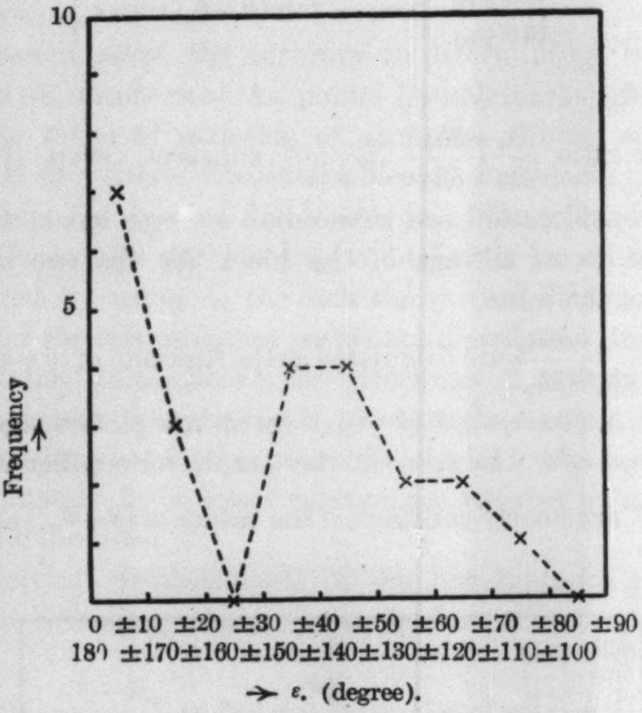

Fig. 6. Frequency of ε.

several blocks, of which the values of ε are in, or exceed, the range 30°–50°, the ratios $\frac{\partial h_2-\partial h_{20}}{\partial h_1-\partial h_{10}}$ for each bench-mark may be much different from each other. In Tables IIIa and IIIb, the values of ratios $\frac{\partial h_2-\partial h_{2,}}{\partial h_1-\partial h_{10}}$ directly calculated by using the values of vertical displacements of the bench-marks are compared with that which are calculated by using the values of ε, φ_{m1}, φ_{m2} and $(\theta-\theta_{m1})$. The coincidence of the ratios $\frac{\partial h_2-\partial h_{20}}{\partial h_1-\partial h_{10}}$ obtained by the different methods of calculations may be seen fairly good at least qualitatively. The quantitatively good coincidence cannot be expected from the present data of vertical displacements and the accuracy in determining the blocks.

Table III a. (Block X)

Vertical displacements of B. M. 3869 are taken as δh_{20} ($=-77{\cdot}2^{\text{mm}}$) and δh_{10} ($=1192{\cdot}9^{\text{mm}}$)

B. M.	$\delta h_2-\delta h_{20}$	$\delta h_1-\delta h_{10}$	$\dfrac{(\delta h_2-\delta h_{20})}{(\delta h_1-\delta h_{10})}$	The ratio calculated from magnitudes and directions of tilting of the block.
	mm	mm		
3870	−10·7	−53·9	0·199	0·271
3871	− 9·6	6·5	−1·443	−2·15
3872	− 1·7	49·4	−0·034	−0·033

Table III b. (Block XVIII)

Vertical displacements of B. M. 3904 are taken as δh_{20} ($=-17{\cdot}6^{\text{mm}}$) and δh_{10} ($=310{\cdot}4^{\text{mm}}$)

B. M.	$\delta h_2-\delta h_{20}$	$\delta h_1-\delta h_{10}$	$\dfrac{(\delta h_2-\delta h_{20})}{(\delta h_1-\delta h_{10})}$	The ratio calculated from magnitudes and directions of tilting of the block.
	mm	mm		
3905	15·3	− 26·7	−0·573	−0·799
3906	15·1	− 60·6	−0·246	−0·117
3907	20·6	− 76·9	−0·268	−0·269
3908	20·6	−116·5	−0·177	−0·090

Summary. The present investigation on block movements in Bôsô Peninsula may be summarized as follows:

i) Crustal movement in Bôsô Peninsula occurred, as a whole, in reversed direction during 1924–1931 compared with that which had occurred during 1898–1924:

ii) Closer examination of the movements of constituent blocks shows that their movements do not follow always the general tendency of the crustal movement in the peninsula taken as a whole mentioned in i):

iii) Constructing $\delta h_1-\delta h_2$ diagram, the relation between δh_1 and δh_2 is discussed as the result of the block movements.

In conclusion, the present writer wishes to express his best thanks to the Authority of the Imperial Academy from whom the research fund was granted to the Earthquake Research Institute for the present revision of the precise leveling. He also wishes to express his sincere thanks to Professor T. TERADA for his kind suggestions and guidance and to Professor K. SUYEHIRO for his kind advices and encouragements given to the writer throughout the present investigation.

29. 地塊とその運動 第二報
（關東地震後、房總半島の地殼運動）

地震研究所 宮部直巳

1923 年の關東地震後房總半島にある水準線路について測量が行はれ、その結果として、1898—1924 の間の垂直變動が知られた。其後、この地方の地殼の變動を知るために震後第二回の水準測量が待望されてゐたが、本年に至り地震研究所が帝國學士院より研究費の補助を得て、之を遂行することが出來た。その結果、1924—1931 の間の水準線路に沿ふ地殼の變動が判明した。本文に於いては、是等の結果を取扱ひ、房總半島における地殼運動の模樣を調べてみて次の樣なことを結論することが出來た。

i). 全體として、水準測量の結果の示す所は、1898—1924 には、半島の西南部が上り、東北の方向に傾斜する樣な運動であるが、1924—1931 には、大體その逆、卽ち、西南の方向へ傾斜する樣な運動である。

ii). 併し、尙些細に之を見れば、小地塊の集合體と考へられ、而して各地塊の運動は必ずしも全體としての傾向に順はない。

iii). 1898—1924 と 1924—1931 との二期の運動の模樣を比較する爲めに、δh_1 を橫軸、δh_2 を縱軸とする圖に各 Bench-mark に相當する點を盛り込んで、その點のその圖の上での分布狀態を調べてみると i) の傾向の見える他に、略ゝ直線上に並ぶ點の群がかなり多く見出される。是等の點に相當する Bench-marks は、各群別に大體一つの地塊の上に在ることが示されるが、各地塊の傾斜運動の方向が、前後二期に於いて、必ずしも一致してゐないので、同一地塊內にある Bench-mark に相當する點はこの圖の上で、常に一つの直線上に竝ぶとは言はれない。

30. *Investigation on the Deformation of the Earth's Crust in the Tango District Connected with the Tango Earthquake of 1927.*[1] (*Part III*)

By **Chûji TSUBOI.**

Earthquake Research Institute.

(Read May 19, 1931.—Received Sept. 18, 1931.)

In his previous papers,[2] the writer discussed the deformation of the earth's crust that was produced in the Tango District of northern Central Japan connected with the Tango destructive earthquake of 1927. The discussions expressed in these papers were based on the results then available of the repeated precise levellings and triangulations executed by the experts of the Land Survey Department over the Tango District by means of which the horizontal and vertical displacements of geodetic points in the district had been obtained. Since then two series of new additional data have been obtained by the same authorities. The one of them is the result of the extensive survey over the third order triangulation points in the district whose displacements were calculated by the comparison of the results of the survey with those of the older one that was made over the same triangulation points some 30 years before. The other is the result of the precise levelling that was carried out along the levelling routes in the district for the fifth time after the earthquake. The purpose of the present paper is to discuss the results of the latter survey, discussions for those of the triangulation survey being preserved for future publication.

The present levelling survey was made by a grant generously given jointly to Drs. M. Ishimoto, F. Tada, and the writer by the Imperial Academy to which the writer expresses his sincere thanks. We could thus entrust the execution of the levelling survey to the Land Survey Department of the Imperial Army which carried out the work from June 17 to Sept. 21, 1930. In Fig. 1 is shown the levelling route covered by the present survey with ordinal numbers of the bench-marks on it. The results that were obtained by the new survey were compared with those of the fourth post-seismic levelling obtained in 1929 and the following changes were found to have taken place in the heights of the bench-marks on the measured route.

---

[1] Preliminary report was published in *Proc. Imp. Acad.*, **7** (1931), 234.

[2] C. TSUBOI, *Proc. Imp. Acad.*, **4** (1928), 529; **6** (1930), 56: *Bull. Earthq. Res. Inst.*, **6** (1928), 71; **8** (1930), 153; 338.

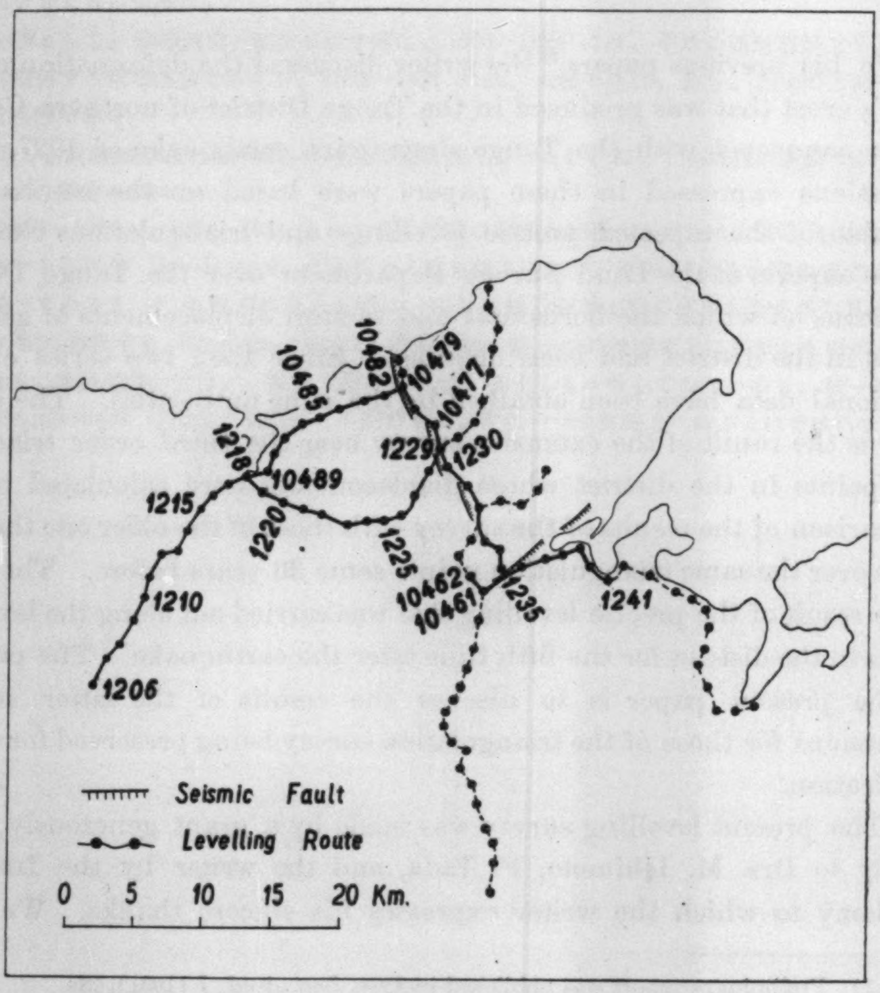
10482
10479
10485
10477
1218
1229
1230
10489
1215
1220
1225
10462
10461
1235
1241
1210
1206
Seismic Fault
Levelling Route
0
5
10
15
20 Km.

Fig. 1.

Levelling Routes Covered by the Fifth Precise Levelling.

Table I.

Change of Heights of Bench-Marks in the Tango District Between the Fourth & Fifth Precise-Levellings after the Earthquake of 1927.

Bench-Mark	(Height in 1930) −(Height in 1929)	Date of Measurement	
1206	+15·3 mm		
1207	+16·0	Sept. 7,	1930.
1208	+12·7	" 8,	"
1209	+ 9·8	" 9, 10,	"
1210	+ 7·2	" 10, 11,	"
1211	− 0·6	" 11,	"
1212	− 0·6	" 1, 2,	"
1213	+10·2	Aug. 31, Sept. 1,	"
1214	+ 8·1	Sept. 5, 6,	"
1215	+11·0	" 3, 6,	"
1216	+ 2·9	Aug. 24, 25,	"
1217	+ 1·4	" 26,	"
1218	− 2·1	" 22,	"
1219	− 0·5	" 21, 22,	"
1220	− 4·2	" 23,	"
1221	− 1·4	" 17,	"
1222	− 2·0	" 18,	"
1223	− 2·4	" 15, 19,	"
1224	+ 1·6	" 14, 16,	"
1225	+ 3·7	" 14, 15,	"
1226	+ 0·6	" 5,	"
1227	+ 4·1	" 6,	"
1228	+ 2·6	" 6, 11,	"
1229	+ 1·3	" 7, 8,	"
1230	− 0·2	" 3, 4,	"
1231	+ 0·6	" 2, 3,	"
1232	taken to be stationary	" 2,	"
1233	+ 2·4	July 25,	"
1234	+ 3·6	" 25, 26,	"
1235	+ 1·2	" 27,	"
1236	− 2·4	" 24, 30,	"
1237	− 3·0	" 23, 24,	"
1238	− 2·5	" 18,	"
1239	− 4·6	" 18, 19,	"
1240	− 3·4	" 19, 20,	"
1241	− 4·6	" 20, 21,	"

(*to be continued.*)

Table I. (*continued.*)

Bench-Mark	(Height in 1930) −(Height in 1929)	Date of Measurement
1218	− 2·1 mm	
		Aug. 29, "
10489	− 1·6	
		" 28, "
10488	− 4·0	
		" 27, 28, "
10487	+ 9·7	
		Sept. 19, 20, "
10486	+ 4·9	
		" 20, 21, "
10485	+ 4·2	
		" 18, 19, "
10484	− 1·9	
		" 16, 17, "
10483	− 1·3	
		" 15, 16, "
10482	+ 1·6	
		" 14, 15, "
10479	+ 2·1	
		" 10, "
10478	+ 3·2	
		" 10, "
10477	+ 3·5	
		Aug. 4, 8, 11, "
1229	+ 1·3	
10462	+ 1·3	
		July 28, 29, "
10461	− 3·1	
		" 29, "
1235	+ 1·2	

Generally speaking, the variations of the heights of the bench-marks in this district may be said to have become ultimately more or less dormant, though not quite stationary, after the lapse of three years since the earthquake of 1927. For comparing the present variations with those for former intervals, the following table is constructed in which are shown the calculated mean daily variations in the heights of the bench-marks on the route from B.M. 1206 to B.M. 1241 during different intervals of the levelling surveys after the earthquake.

Table II.
Mean Daily Variation of Heights of Bench-Marks in the Tango District.

Bench-Mark	(II-I)	(III-II)	(IV-III)	(V-IV)
	mm	mm	mm	mm
1206	+0·033	−0·080	−0·066	+0·039
1207	+0·002	−0·082	−0·067	+0·041
1208	−0·004	−0·076	−0·078	+0·032
1209	−0·040	−0·064	−0·077	+0·025
1210	−0·027	−0·061	−0·097	+0·018
1211	−0·056	−0·080	−0·112	−0·002
1212	−0·072	−0·084	−0·116	−0·002
1213	+0·009	−0·026	−0·086	+0·027
1214	−0·028	−0·001	−0·089	+0·021
1215	−0·083	+0·009	−0·095	+0·030
1216	−0·088	+0·009	−0·083	+0·008
1217	−0·173	+0·007	−0·077	+0·004
1218	−0·202	+0·001	−0·077	−0·006
1219	−0·121	−0·008	−0·071	−0·001
1220	−0·143	−0·014	−0·072	−0·012
1221	−0·190	+0·015	−0·072	−0·004
1222	−0·133	+0·009	−0·065	−0·006
1223	−0·061	+0·002	−0·057	−0·007
1224	−0·163	+0·004	−0·048	+0·005
1225	−0·214	+0·010	−0·050	+0·011
1226	−0·186	+0·016	−0·039	+0·002
1227	−0·059	+0·018	−0·038	+0·012
1228	+0·059	+0·027	−0·029	+0·008
1229	−0·074	−0·009	−0·029	+0·004
1230	−0·124	−0·023	−0·032	−0·001
1231	−0·135	−0·008	−0·009	+0·002
1232	taken to be stationary	—	—	—
1233	−0·032	−0·005	+0·003	+0·008
1234	−0·060	+0·010	+0·009	+0·012
1235	−0·025	+0·004	+0·013	+0·004
1236	−0·065	−0·039	−0·007	−0·008
1237	−0·080	−0·055	−0·012	−0·010
1238	−0·050	−0·036	−0·009	−0·008
1239	−0·029	−0·032	−0·006	−0·014
1240	−0·076	−0·032	−0·008	−0·011
1241	−0·083	−0·038	−0·005	−0·014

The values given in Table 2 are shown by the curves in Fig. 2, in which the gradual decrease with time in the rate of variation of the height change is evidently apparent.

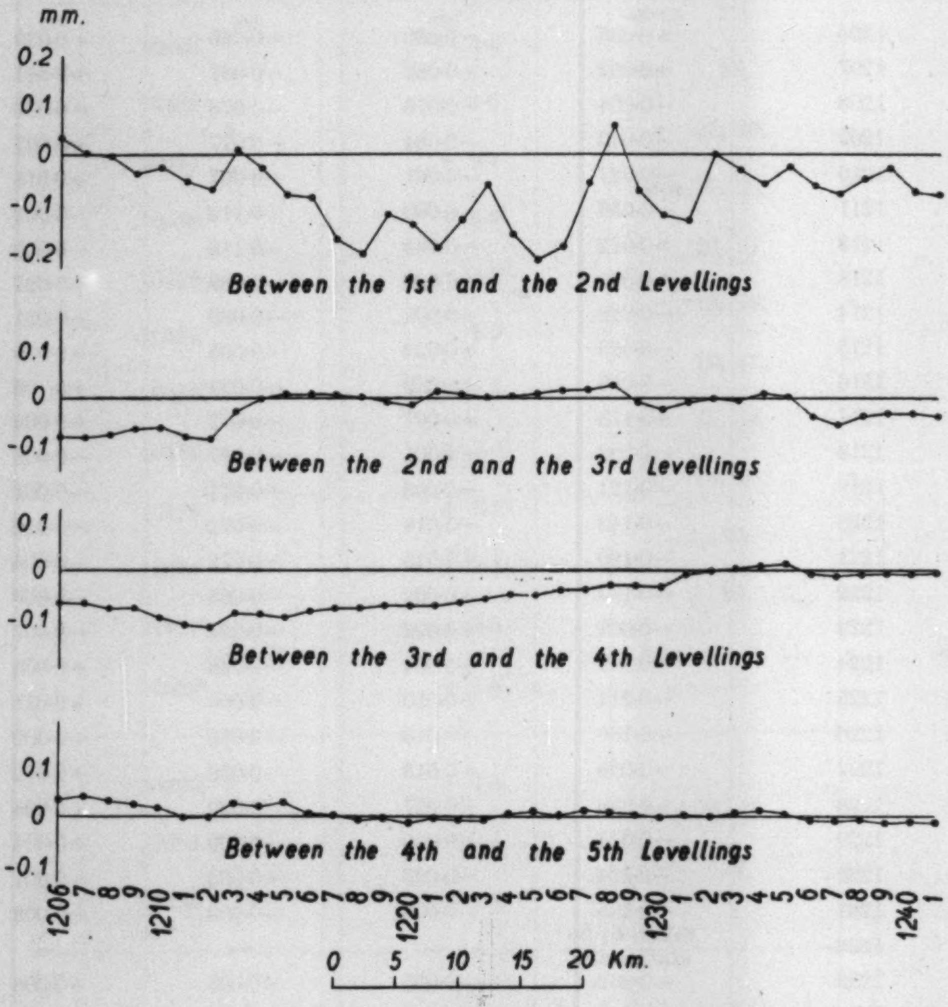

Fig. 2.

Mean Daily Variation of the Heights of Bench-Marks.

The total change of heights of the bench-marks that occurred after the earthquake along the same levelling route are given in Table 3 in which it will be compared with what was produced at the time of the earthquake of 1927.

Table III.

Comparison of the Changes of Heights of Bench-Marks that were Produced at the Time of and After the Earthquake of 1927.

Bench-Mark	Change of Height at the Time of the Earthquake	Total Change of Height After the Earthquake
1206	−197·0 mm	−37·7 mm
1207	−196·0	−39·1
1208	−254·2	−46·1
1209	−266·3	−47·2
1210	−375·3	−58·3
1211	−467·7	−79·6
1212	−832·3	−84·9
1213	−221·9	−39·7
1214	−174·3	−37·9
1215	−162·2	−37·0
1216	−162·9	−40·1
1217	−156·3	−42·7
1218	−173·8	−49·7
1219	−141·5	−44·3
1220	−194·9	−51·7
1221	− 90·6	−42·6
1222	− 84·3	−39·5
1223	− 54·6	−34·8
1224	+ 2·2	−29·9
1225	+ 31·7	−29·6
1226	+100·3	−24·2
1227	+135·4	−14·1
1228	+308·1	− 3·1
1229	−441·0	−20·2
1230	−252·8	−29·9
1231	− 76·4	−12·2
1232	taken to be stationary	—
1233	+263·4	+ 1·4
1234	+468·2	+ 8·5
1235	+784·8	+ 9·6
1236	−353·0	−20·3
1237	−277·7	−28·6
1238	−210·7	−19·9
1239	−128·6	−17·8
1240	−127·3	−18·9
1241	−151·8	−21·7

The values in Table 3 are graphically shown in Fig. 3. When the scale for the lower curve is taken ten-times reduced as that for the upper

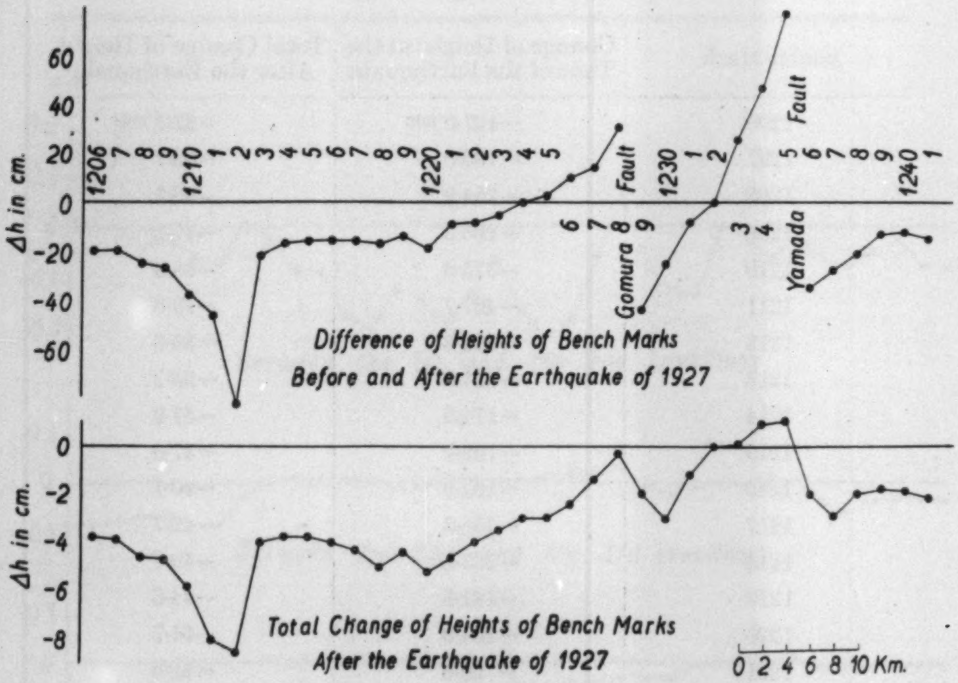

Fig. 3.

one, as is the case in Fig. 3, the two curves are seen very much similar in their forms. This implies that the vertical deformation after the earthquake has been of the same sense and proprotion with what was produced at the time of the earthquake. In the neighbourhood of the Gômura and Yamada seismic faults both of which were produced at the time of the earthquake, the vertical deformtion of the ground is sensibly different for the two curves. B.M. 1229 and B.M. 1236 in the immediate neighbourhood of the faults have been sensibly drag up from the positions which they would have respectively occupied otherwise. This would seem to indicate that the two land blocks on the opposite side of the faults have been healed up with each other and the relative vertical movements along these seismic fault planes have become somewhat ill-difined. The difference of heights of the bench-marks that lay on the opposite side of and nearest to the Gômura fault increased rapidly after the earthquake but soon approached to an asymptotic value. The case for the Yamada fault is somewhat different, the decrease in the velocity of the change of the difference of the heights of the bench-marks on its opposite sides being small with a little sign of tending to its asymptotic value. These circumstances may be seen in Table 4 and Fig. 4.

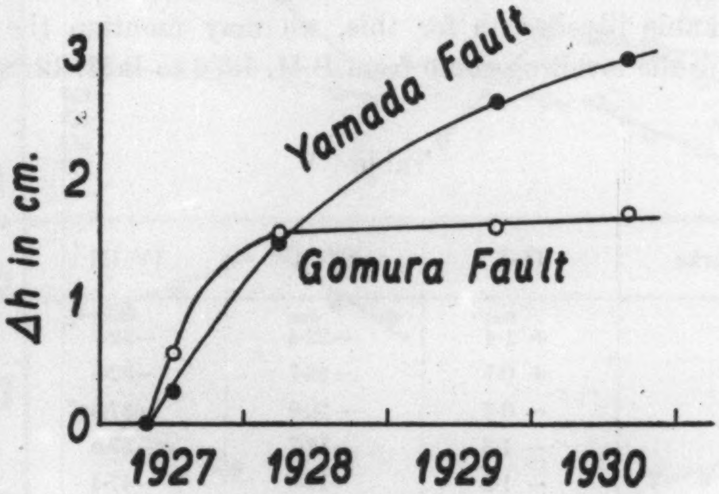

Fig. 4. Relative Vertical Movements along the Gomura and Yamada Seismic Faults.

Table IV.

Gômura Fault (B. M. 1228—1229)

		mm
April 24,	1927	0
June 5,	1927	5·6
March 9,	1928	15·6
Sept. 2,	1929	15·8
Aug. 8,	1930	17·1

Yamada Fault (B. M. 1235—1236)

		mm
April 23,	1927	0
June 5,	1927	2·7
March 13,	1928	15·0
Sept. 11,	1929	26·3
July 30,	1930	29·9

The witer pointed out in previous papers that the evidence of block movements is pronounced in the results of the repated precise levellings in the Tango District. By the results of the fifth precise levellings, we find that the block movement is still predominant in this district, with the boundaries of the land blocks remaining at the same positions as before As a remarkable illustration for this, we may mention the change of heights along the levelling route from B.M. 1206 to B.M. 1218.

Table V.

Bench-Marks	II-I	III-II	IV-III	V-IV
	mm	mm	mm	mm
1206	+ 1·4	−22·4	−32·0	+15·3
1207	+ 0·1	−22·7	−32·5	+16·0
1208	− 0·2	−20·9	−37·6	+12·7
1209	− 1·8	−17·7	−37·5	+ 9·8
1210	− 1·2	−16·9	−47·4	+ 7·2
1211	− 2·4	−22·2	−54·4	− 0·6
1212	− 3·0	−23·5	−57·8	− 0·6
1213	+ 0·4	− 7·3	−43·0	+10·2
1214	− 1·1	− 0·4	−44·5	+ 8·1
1215	− 3·5	+ 2·4	−47·7	+11·0
1216	− 3·6	+ 2·6	−42·0	+ 2·9
1217	− 7·1	+ 1·9	−38·9	+ 1·4
1218	− 8·5	+ 0·2	−39·3	− 2·1

The values given in this table are graphically shown in Fig. 5, in which the points were connected by broken straight lines, each of them corresponding to land blocks. The boundaries of these land blocks agree in position with minor tectonic lines in the district which were traced by means of geological surveys. What a characterictic structure the earth's crust was found to have which has mostly been assumed to be homogeneous and isotropic in geophysical especially in seismometrical research only for the sake of simplicity for the application of mathematics. It seems hardly necessary to say that most of the conceipts in seismology, such as epicentre, uniform propagation of elastic waves through the homogeneous earth's crust without hysterisie, etc., must be rewritten under the new light as to the structure of the earth's crust which revealed itself as a natural *fact* by means of geodetic surveys.

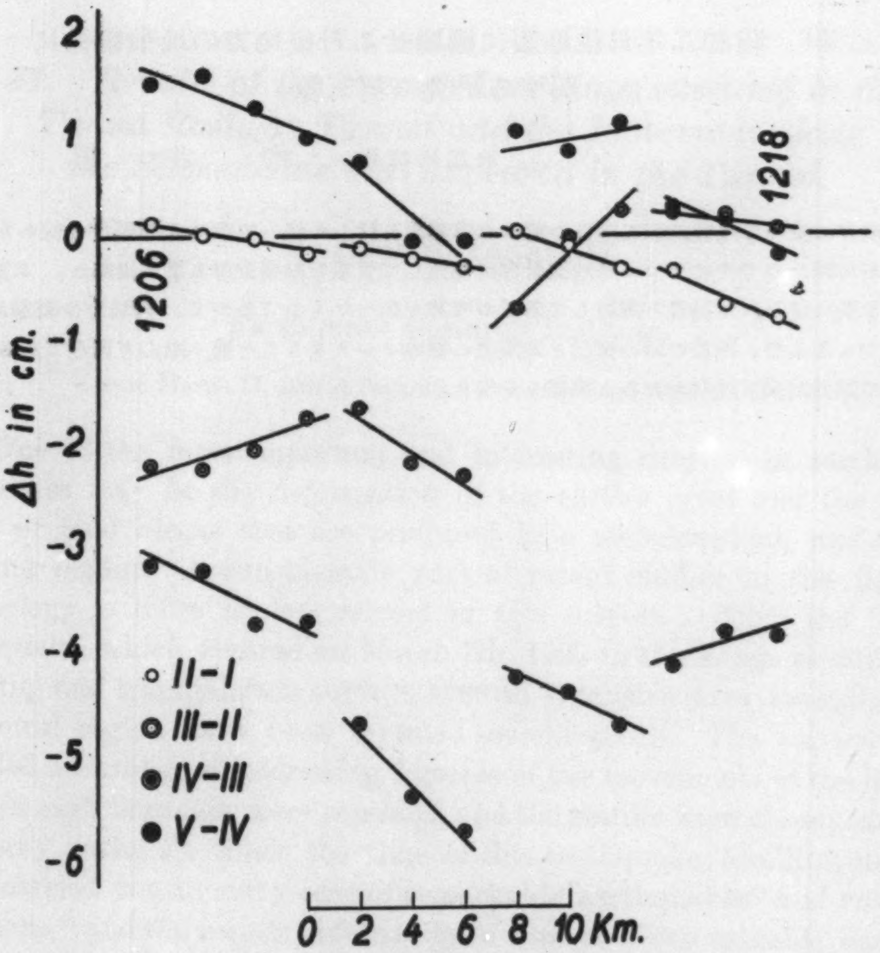

Fig. 5.

Block Movements as Revealed by Means of Precise Levellings.

In conclusion the writer expresses his sincere thanks to the Imperial Academy for the grant which enabled the writer to make this investigation. Thanks are also due to Professors K. Suyehiro and T. Terada for their interests in this work and also for their kindness in recommending us to the Academy for the grant. Last, but not least, thanks must be expressed to the Land Survey Department for the execution of the laborious work of the levelling surveys at our request.

30. 昭和二年丹後地震に關聯せる丹後地方の地殼變動に關する研究（第三報）

地震研究所　坪　井　忠　二

丹後地方に於いて地震後第五回目の精密水準測量を行ふに就いて幸にも帝國學士院から補助を仰ぐ事が出來たので夫によつて陸地測量部に委託して貴重な結果を得る事が出來た。本論文は其の結果を前に得られた結果と對照して若干の考案を加へたものであつて、同地方の變動が次第に納まりつゝある事、地震の時の變動と地震後の變動とが大きさこそ違へ殆んど同形である事、地塊運動の證據が未だに明かである事等を示した。

31. *Results of the Precise Levellings executed in the Tanna Railway Tunnel and the Movement along the Slicken-side that appeared in the Tunnel.*

By **Ryûtarô TAKAHASI**,

Earthquake Research Institute.

(Read March 17, 1931 & Sept. 15, 1931.—Received Sept. 20, 1931.)

One of the most important and interesting subjects in earthquake researches may be the deformation of the earth's crust and the movement of land blocks that are produced in a meizo-seismal, and neighbouring regions. A considerable part of recent studies in the field of seismology is more or less related to this subject. After the Tango earthquake, which occured on March 7th. 1927 in the Tango penninsula, levelling and triangulation surveys over an extensive area including the epicentral region have been repeated several times. The surveys have revealed a number of interesting features of the movements of the earth's crust in each time they were repeated, and the results were closely studied by many authors[1]. Since the time of this earthquake, levelling surveys were carried out in every case of remarkable earthquakes[2] and volcanic eruptions,[3] and the results obtained have always given valuable data for the investigation of the deformation of the earth's crust. Tiltmeter observation may be another method of power to investigate the motion of land blocks. Such observations were already enforced with many interesting results in several reseaches[4].

In the case of the recent earthquake of North Idu, which occured on Nov. 26 th. 1930, various surveys were also performed in order to find out the deformation of the earth's crust, i. e. levelling surveys arround the Idu penninsula and across the epicentral region of the earthquake, triangulation over an area of about 1400 km. squares, including 4 first order triangulation points and 17 second order triangulation points. Beside these surveys carried out by the hand of the Land Survey Department of the Imperial Army, levellings and triangulations were executed several times by Mr. Tsuboi in the Tanna Basin, where the largest fault appeared in the case of the earthquake.

---

[1] C. Tsuboi, *Bull. Earthq. Res. Inst.*, 8 (1930), 153; T. Terada & N. Miyabe, 8 (1930), 338.

[2] Land Survey Department, *Bull. Earthq. Res. Inst.*, 9 (1931), 109; 8 (1930), 375.

[3] C. Tsuboi, *Bull. Earthq. Res. Inst.*, 8 (1930), 237.

[4] M. Ishimoto & R. Takahasi, *Bull. Earthq. Res. Inst.*, 8 (1930), 427; M. Ishimoto, *Bull. Earthq. Res. Inst.*, 4 (1928), 203; 8 (1930), 222.

In the present communication are described the results of the precise levellings effected in the Tanna tunnel. The tunnel is being excavated in nearly E-W direction through the epicentral region of the recent earthquake for the purpose to connect Atami to Misima, and the excavation had been proceeding from the two ends of the tunnel. At the time of the earthquake, the heading of the pioneer drift of the west part of the tunnel was being driven right under the Tanna Basin. The heading of the east side of the tunnel was under Mt. Takiziyama, leaving the central 1300 m. unexcavated. The presence of the tunnel has offered a special opportunity for the parallel observation, on the ground and in the earth, not only of the nature of seismic waves of after-shocks, but also of the deformation of the earth's crust produced at the time of and after the earthquake.

In Fig. 1 is shown the size and form of the bench-marks used for the present levellings in the tunnel. It is made of gun-metal to prevent it from rusting by the enormously damped air in the tunnel. Its working surface *a* was covered with vaseline when it is not in use. The bench-marks as a whole is ring-shaped with a handle *b* at its one side. To the handle *b* is screwed an iron bolt of 2 cm. in diameter and 30 cm. long. The bolt was buried horizontally into the side-wall of the tunnel, to such a depth as to make the centre of *a* 9 cm. apart from the wall. The plantation of the bench-marks was carried on under great care to minimize the effect

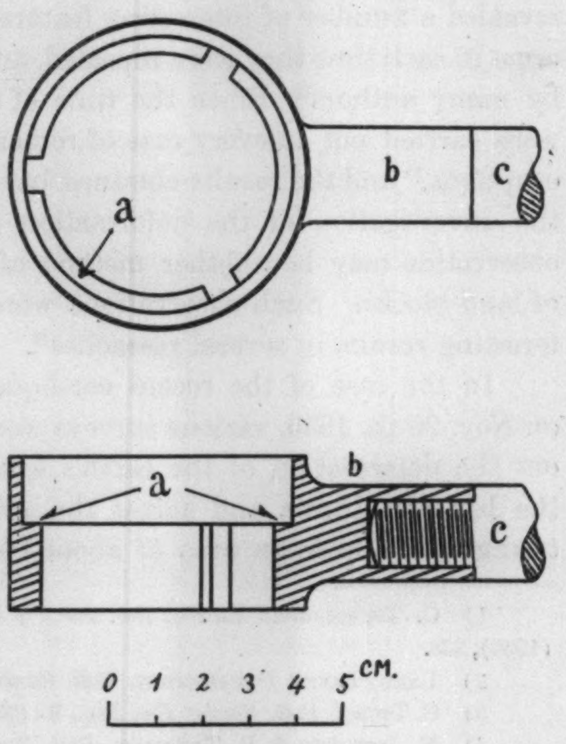

Fig. 1. Bench-mark.

of shrinkage of the mortar used, and to make the plane of the working surface *a* horizontal as accurately as possible.

It would have been the best way for the original purpose of the survey to plant these bench-marks to the natural wall of the tunnel not lined with other materials. In the present case, however, almost all the strata penetrated by the tunnel are of soft materials, such as sand, volcanic scolia, agglomerate and clay. It could not therefore be expected that the bench-marks planted in such materials are held rigidly enough to permit such precise measurement as is required in this case. Moreover, because the main tunnel is lined with concrete, the natural rock wall is to be met with only in drain drifts which lie parallelly to and on both side of the main tunnel. Dangers and difficulties may accompany the works in the drain drifts, as the water flowing in them is of considerable amount even in usual time. Under these circumstances, we have decided to plant the bench-marks in the side-wall of the main tunnel, and to deduce the movement of the earth's crust from the deformation of the tunnel wall. This concession may perhaps be permitted to some extent, as the lining of the tunnel is parted every 10 meters by construction joints and can

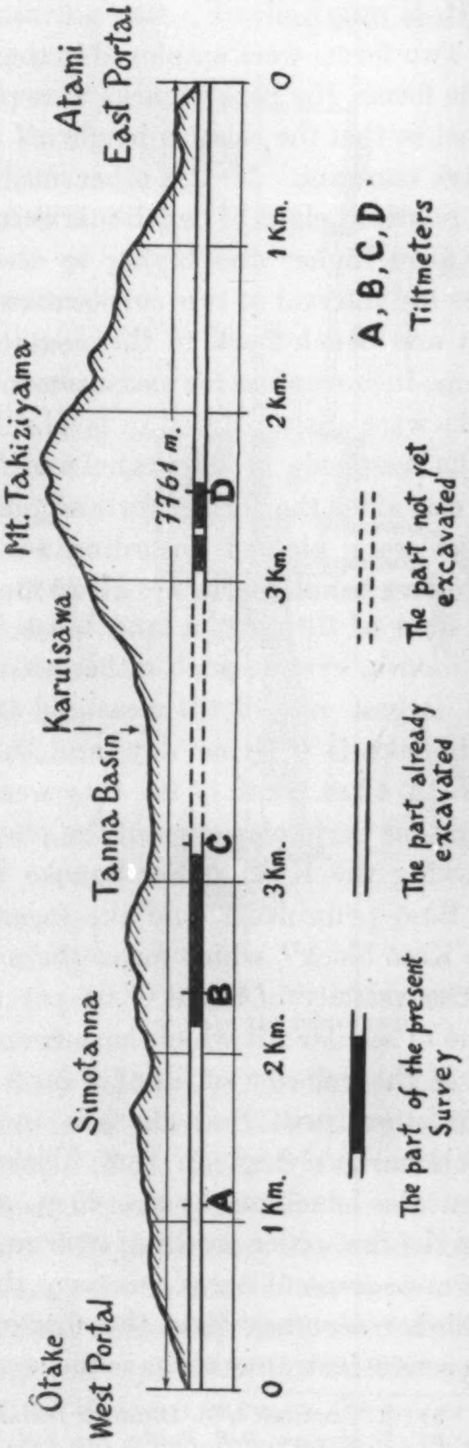
Ôtake
West Portal
Simotanna
Tanna Basin
Karuisawa
Mt. Takiziyama
Atami
East Portal
7761 m.
A
B
C
D
0
1 Km.
2 Km.
3 Km.
3 Km.
2 Km.
1 Km.
0
The part of the present Survey
The part already excavated
The part not yet excavated
A, B, C, D Tiltmeters

Fig. 2. Profile of the Tanna Tunnel.

move freely at these joints. It is to be regretted that the surveys were not executed along the entire length of the tunnel, but were restricted to the part of the tunnel indicated in Fig. 2 by thick lines, whose total length is 1500 m.

Two forms were employed in the plantation of bench-marks. In one of the forms, the bench-marks were planted along the gradient line of the tunnel so that the relative height of the bench-marks to the observer is always constant. In the other form, bench-marks are planted in level. The relative height of bench-marks to the observer becomes therefore in this form higher and higher by the amount, the gradient of the tunnel times the interval of two consecutive bench-marks, as the observer goes from one bench-mark to the next. When the height of bench-marks became inconvenient for measurements, the level is lowered and the bench-marks were again planted in level. From No.-3 bench-mark to No. 15 in the west side of the tunnel and from No. 30 bench-mark to No. 42 in the east side, the former form of plantation was adopted. Other bench-marks were planted according to the latter form. Intervals of two successive bench-marks are all 20 m.

Rate of tilting of a land block is generally less than a second of arc per month, even in such rather active period as after a great earthquake. The largest rate of tilt measured at Itô by a tiltmeter during the Itô earthquake is $0''.7$ per day, and the largest monthly rate was $4''.5$. At Kawana, 4 km. south of Itô, they were $0''.7$ and $6''.0$ respectively.[5] These are rather particular cases of the phenomena. The largest tilting motion following the Kwantô Earthquake was observed at Kamogawa block, in the Bôsô penninsula, and the mean rate of tilt was $0''.01$ per month.[6]. The Kôtô block[7], which forms the south-west end of Tôkyô, tilts secularly by the velocity of about $0''.04$ per month. This is probably the largest value of secular tilt which have ever found by levelling surveys.

If the velocity of tilt of a land block be $0''.1$ per month, monthly observations will find changes in height difference of two successive bench-marks lying on that block of the amount of only 0·05 mm., when the bench-marks are 20 m. apart. This amount is so small that even the first order levelling instrument can hardly detect it In the present measurement it was necessary, therefore, to use a measuring intrument of higher accuracy than the first order levelling instrument. In this aim a new instrument was made as described in the following.

---

[5] R. Takahasi & M. Ishimoto, *Bull. Earthq.Res. Inst.*, 8 (1930), 427.
[6] N. Miyabe, *Bull. Earthq. Res. Inst.*, 9 (1931), 263.
[7] A. Imamura, *Disin*, 3 (1931), 141; *Proc. Imp. Acad.*, 7 (1931), 1.

The instrument consists essentially of a flexible metal pipe 25 m. long, 1 cm. thick in internal diametre connecting two measuring parts of identical construction. The instrument as a whole forms therefore a U-tube. In Fig. 3 is shown the measuring part. In the figure H_1,H_2 are steel nails with which the measuring part hangs on the working surface of a bench-mark. There are three H_1's and three H_2's on the outer surface of the cylinder L. When the instrument is filled with a suitable quantity of water, when it is hanged on bench-marks, water surfaces appear at the window C which is covered with a sheet of plate glass. The water surface reflects the image of a needle N, when viewed obliquely from beneath. The position of the needle, when brought in contact with its image by means of the micrometer screw S, can be read off by the indices F, G. The micrometer screw is made of stainless steel and its pitch is 0.5 mm. The index G is graduated into 50 divisions so that the smallest division correponds to 0·01 mm. When two successive bench-marks to be measured are planted nearly in level, H_1 nails are used in both measuring parts. If the bench-marks to be measured were planted along the slope of the tunnel, H_1 is used at one measuring part and H_2 at the other to bring the water surfaces to the windows C, C′ in both measuring parts. Other part of the instrument is of brass, except the packing P, which is of caoutchouc. The calibration of the screw S was carried out using a dividing engine made by Société Genèvoise, and the error of the screw proved not to exceed 0·01 mm. By laboratory tests this instrument proved to be capable of determining the position of the water surface so accurately as to 0·001 mm. but in field works the fractions of divisions was not read for the sake of simplicity and rapidity of the measurements.

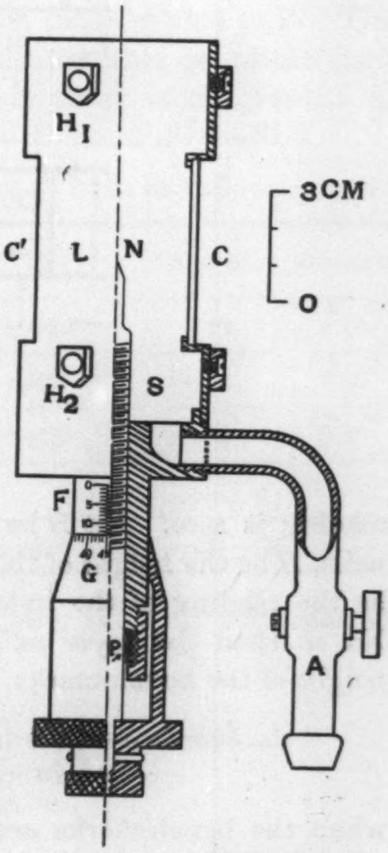

Fig. 3. Measuring part of the instrument.

Now in Fig. 4 let *C* be the vertical distance between the upper nail H_1 of the instrument and the position of the needle when the index

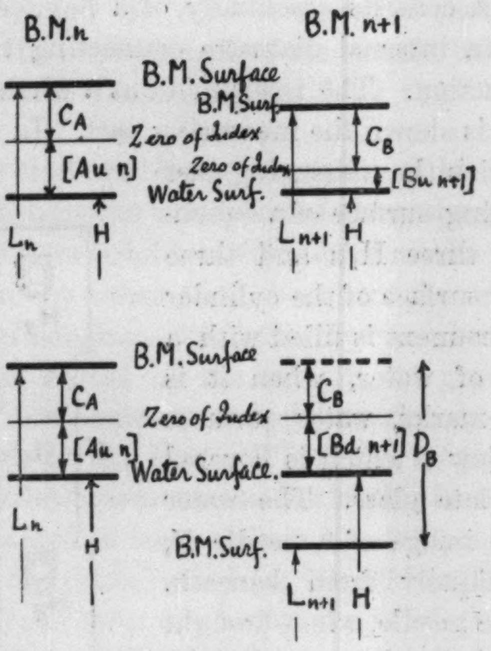
B.M.n
B.M. n+1
B.M. Surface
B.M. Surf.
C_A
Zero of Index
C_B
[Au n]
Zero of Index
[Bu n+1]
Water Surf.
L_n
H
L_{n+1}
H
B.M. Surface
C_A
C_B
Zero of Index
[Au n]
[Bd n+1]
D_B
Water Surface.
L_n
H
B.M. Surf.
L_{n+1}
H

Fig 4.

reading is zero. Let D be the distance between the upper and the lower nails, H be the height of the water surface in the instrument, and $[Au\ n]$ be the reading of the index of the measuring part A at the bench-mark No. n when the *upper* nail is used. Then the difference $L_n - L_{n-1}$ in height of the bench-marks No. n and No. $n+1$ is given by

$$\begin{aligned} L_n - L_{n+1} &= \{H + [Au\ n] + C_A\} - \{H + [Bu\ n+1] + C_B\} \\ &= [Au\ n] - [Bu\ n+1] + (C_A - C_B), \end{aligned}$$

when the bench-marks are planted nearly in level. Interchanging the measuring parts, we have similarly

$$L_n - L_{n+1} = [Bu\ n] - [Au\ n+1] - (C_A - C_B).$$

Therefore by addition we get

$$2L \equiv 2(L_n - L_{n+1}) = \{[Au\ n] - [Bu\ n+1]\} + \{[Bu\ n] - [Au\ n+1]\} \quad (1)$$

and by substraction

$$\varDelta \equiv -2(C_A - C_B) = \{[Au\ n] - [Bu\ n+1]\} - \{[Bu\ n] - [Au\ n+1]\}. \quad (2)$$

When the bench-marks to be measured are planted along the slope of the tunnel, we have instead of (1) and (2),

$$\begin{aligned} 2L &\equiv 2(L_n - L_{n+1}) \\ &= \{[Au\ n] - [Bd\ n+1]\} + \{[Bu\ n] - [Ad\ n+1]\} + (D_A + D_B) \quad (3) \end{aligned}$$

and

$$\begin{aligned}\Delta' &\equiv -2\,(C_A - C_B) + (D_A - D_B)\\ &= \{[Au\;n] - [Bd\;n+1]\} - \{[Bu\;n] - [Ad\;n+1]\}.\end{aligned} \tag{4}$$

In the above equations the suffixes A, B are used to distinguish the quantities related to the measuring part A from those related to B. The quantities expressed in (2) and (4) do not involve other quantities than instrumental constants and serve for the direct check of the results of observation. In the present instrument $\Delta = -60{\cdot}3$ and $\Delta' = -81{\cdot}2$.

The observed quantities are recorded in such form as follows.

B. M.	D Pos.		R Pos.		Diff.	2L	Δ or Δ′	Remark
30	Au	2758	Bu	2350	+0484	+1028	−60	$8^{h}\,35^{m}$
31	Bu	2274	Au	1806	+0544			
31	Au	0927	Bu	0712	−1694	−3307	−81	$9^{h}\,05^{m}$
32	Bd	2621	Ad	2325	−1613			
32	Au	1978	Bu	2072	+0296	+0673	−81	$9^{h}\,20^{m}$
33	Bd	1682	Ad	1695	+0377			
n	(1)		(4)		(3) = (1) − (2)	(7) = (3) + (6)	(8) = (3) − (6)	
n+1	(2)		(5)		(6) = (4) − (5)			

Observations were executed several times in such schedule as follows:

I levelling	Dec.	29-30,	1930	D only		
II „	Jan.	7—9,	1931	„	10 days	West side only
III „	Feb.	5-12,	„	D and R	32 „	
IV „	Mar.	3—9,	„	„	28 „	
V „	Apr.	13-18,	„	„	40 „	
VI „	July	18-24,	„	„	90 „	

In the above table "D and R" shows that the observation was carried out in direct and reversed positions of the instrument and "D only" shows that the observation was carried out only in the direct position. The height difference between two consecutive bench-marks is able to be obtained by the "D only" observations as well as the "D and R" ones, when the instrumental constants are known. In this view the "D only" observation was carried on in the first and second surveys to save time and labour, but the results were not satisfactory, being of unexpected low accuracies resulting from some causes which cannot be elliminated in the missing condition of the check method.

Results of each levelling are given in the following table.

Table I. Height differences between successive bench-marks. (Unit = 0·005 mm.)
(*……Renewed bench-marks.)

B. M.	I	II	III	IV	V	VI
East side						
10						
11		−2794	2797	2782	2765	2726
12		−2654	2657	2642	2634	2626
13		+4950	−4905	4919	4915	4918
14		−1848	1887	1864	1893	1906
15		—	4158	4164	4161	4166
16		−0494	0514	0516	0514	0511
17		−0144	0174	0140	0142	0119
18		+4552	4547	4538	4551	4552
19		−2644	2660	2686	2735	2828
20		+1558	1508	1515	1500	1466
30		+1080	1028	1033	1012	0949
31		−3268	3307	3300	3296	3285
32		+0698	0673	0682	0679	0693
33		−0928	0961	0960	0963	0970
34		+0610	0613	0600	0602	0603
35		−0270	0283	0285	0276	0251
36		+0412	0378	0381	0378	0368
37		−3440	3499	3484	3494	3512
38		+3190	3155	3127	3088	2995
39		+0230	0269	0285	0330	0400
40		+4792	4841	4857	4870	4917
41		+6140	6138	6133	6128	6126
42						
West side						
− 3						
− 2	—	3554	—	—	—	1296*
− 1	−3652	3700	—	—	—	3872
0	—	+5542	5519	5487	5463	5420
1	+2566	2580	2468	2447	2422	2384
2	−0970	0996	1081	1149	1202	1300
3	−0612	0618	0688	0699	0751	0799
4	+6280	6286	6291	6280	—	4463*
5	−5372	5393	5455	5475	—	3783*
6	+4468	4416	4413	4401	4381	4364
7	−0088	0128	0145	0153	0157	0087

(*to be continued.*)

Table I. (*continued.*)

B. M.	I	II	III	IV	V	VI
West side						
8	−5276	5298	5328	5339	5340	5451
9	+0724	0662	0659	0646	0642	0639
10	−4660	4694	4686	4689	4694	4723
11	+3574	3568	3565	3561	3564	3557
12	−3024	3044	3068	3074	3059	3069
13	−2000	2030	2030	2027	2056	2046
14	+0696	0638	0646	0649	0645	0639
15	—	−5633	5640	5650	5645	5642
16	—	—	6678	6679	6674	6742
17	−2742	2744	2753	2744	2737	2722*
18	−0294	0304	0317	0311	0319	0314
19	+3770	3836	3841	3843	3840	3844
20	−1968	—	1965	1948	1932	1898
21	+3758	3782	3762	3778	3788	3808
22	—	−3244	3283	3275	3277	3254
23	+5606	5610	5655	5659	5662	5700
24	−0886	0866	0924	0930	0908	0913
25	−2660	2642	2673	2661	2659	2647
26	+2046	2030	2035	2059	2049	2058
27	+2536	2530	2542	2545	2549	2556
28	−0700	0716	0695	0695	0698	0702
29	−2266	2294	2290	2288	2286	2292
30	+2398	2334	2332	2341	2347	2349
31	+1594	1574	1545	1530	1533	1514
32	−2578	2574	2553	2540	2514	2483
33	+0392	0402	0387	0405	0420	0437
34	−3652	3672	3682	3681	3671	3680
35	−4616	4674	4769	4767	4786	4809
36	−1442	1446	1424	1407	1389	1254
37	+2040	2108	2160	2210	2282	2398
38	+1314	1360	1386	1422	1484	1557
39	+0346	0360	0265	0237	0202	0139
40	+0414	0342	0173	0108	0013	−0132
41			−5083	5061	5043	5005
42			—	—	—	—
43			+5781	5796	5794	5831
44			−2929	2945	2961	2992
45			−4329	4321	4313	4272
46			+3365	3373	3380	3359
47			−1732	1730	1727	1763
48			−1260	1273	1273	1299
49			−0743	0735	0722	0728
50			−2593	—	1237*	1233

Table II. Variation of height differences between successive bench-marks. (Unit=0·005 mm.)

B. M.	II–I	III–II	IV–III	V–IV	VI–V
East side					
10		− 3	+ 15	+ 17	+ 39
11		− 3	+ 15	+ 8	+ 8
12		− 45	+ 14	− 4	+ 3
13		− 41	+ 23	− 29	− 13
14		—	− 6	+ 3	− 5
15					
		− 20	− 2	+ 2	+ 3
16		− 30	+ 34	− 2	+ 23
17		− 5	− 19	+ 13	+ 1
18		− 16	− 26	− 49	− 93
19		− 50	+ 7	− 1	− 34
20					
		− 52	+ 5	− 21	− 63
30		− 39	+ 7	4	+ 11
31		− 25	+ 9	− 4	+ 14
32		− 33	+ 1	− 3	− 7
33		+ 3	− 13	+ 2	+ 1
34					
		− 13	− 2	+ 9	+ 25
35		− 34	+ 3	− 3	− 10
36		− 59	+ 15	− 10	− 18
37		− 35	− 28	− 39	− 93
38		+ 39	+ 16	+ 45	+ 70
39					
		+ 49	+ 16	+ 13	+ 47
40		− 2	− 5	− 5	− 2
41					
42					
West side					
− 3					
− 2	—	—	—	—	—
− 1	—	—	—	—	—
0	—	− 23	− 32	− 24	− 43
1	+ 14	−112	− 21	− 25	− 38
2	− 26	− 85	− 68	− 53	− 98
3	− 6	− 70	− 11	− 52	− 48
4	+ 6	+ 5	− 11	—	—
5	− 21	− 62	− 20	—	—
6	− 52	− 3	− 12	− 20	− 17
7	− 40	− 17	− 8	− 4	+ 70

(*to be continued.*)

Table II. (*continued.*)

B. M.	II-I	III-II	IV-III	V-IV	VI-V
West side					
8	− 22	− 30	− 11	− 1	−112
9	− 62	− 3	− 13	+ 6	− 3
10	− 34	+ 8	− 3	− 5	− 29
11	− 6	− 3	− 4	− 2	− 6
12	− 20	− 24	− 6	+ 15	− 10
13	− 30	0	+ 3	− 24	+ 5
14	− 58	+ 8	+ 3	− 4	− 6
15	—	− 7	− 10	+ 5	+ 3
16	—	—	− 1	+ 5	—
17	− 2	− 9	+ 9	+ 7	+ 15
18	− 10	− 13	+ 6	− 8	+ 5
19	+ 66	+ 5	+ 2	− 3	+ 4
20	—	—	+ 17	+ 6	+ 44
21	+ 24	− 20	+ 16	+ 10	+ 20
22	—	− 39	+ 8	− 2	+ 23
23	+ 4	+ 45	+ 4	+ 3	+ 38
24	+ 20	− 58	− 6	+ 20	− 03
25	+ 18	− 31	+ 12	+ 2	+ 12
26	− 16	+ 5	+ 24	− 10	+ 09
27	− 6	+ 12	+ 3	+ 4	+ 7
28	− 16	− 26	− 5	− 3	− 4
29	− 28	+ 4	+ 2	+ 2	− 6
30	− 64	− 2	+ 9	+ 6	+ 2
31	− 20	− 29	− 15	+ 3	− 19
32	+ 4	+ 21	+ 13	+ 26	+ 29
33	+ 10	− 15	+ 18	+ 15	+ 17
34	− 20	− 10	+ 1	+ 10	− 9
35	− 58	− 95	+ 2	− 19	− 23
36	− 4	+ 22	+ 17	+ 18	+ 35
37	+ 68	+ 52 + 26	+ 50	+ 72	+116
38	+ 46		+ 36	+ 62	− 73
39	+ 14	− 95	− 28	− 35	− 58
40	− 72	−169	− 65	− 95	−145
41			+ 22	+ 20	+ 36
42			—	—	—
43			+ 15	− 05	+ 40
44			− 16	− 16	− 31
45			+ 08	+ 08	+ 41
46			+ 08	+ 7	− 16
47			+ 2	+ 3	− 36
48			− 13	0	− 26
49			+ 8	+ 13	− 6
50			—	—	− 4

By these results, height differences between two consecutive bench-marks were plotted against time taken in abscissa. The origin of height difference is taken arbitrary. In Fig. 5, thus constructed, the inclination of curves indicates therefore the velocity of variation of height difference of the corresponding bench-marks. Generally speaking, the variation of height difference is more rapid in the west side of the tunnel than in the east side. The velocity of tilting is showing clearly an exponential-like decrease in the west side while in the east side it is rather linear and constant.

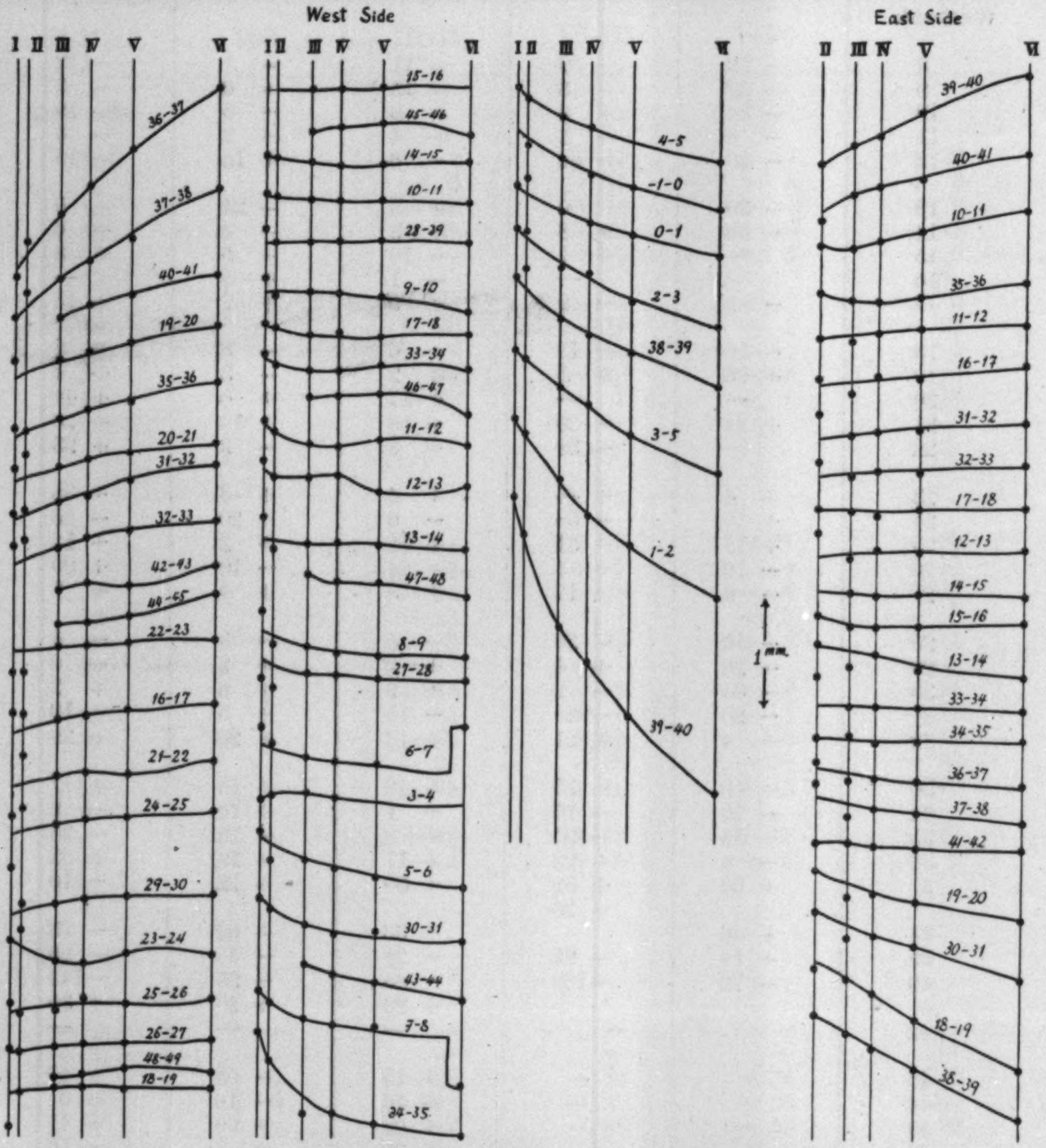

Fig. 5. Time-variation of height difference between two successive bench-marks.

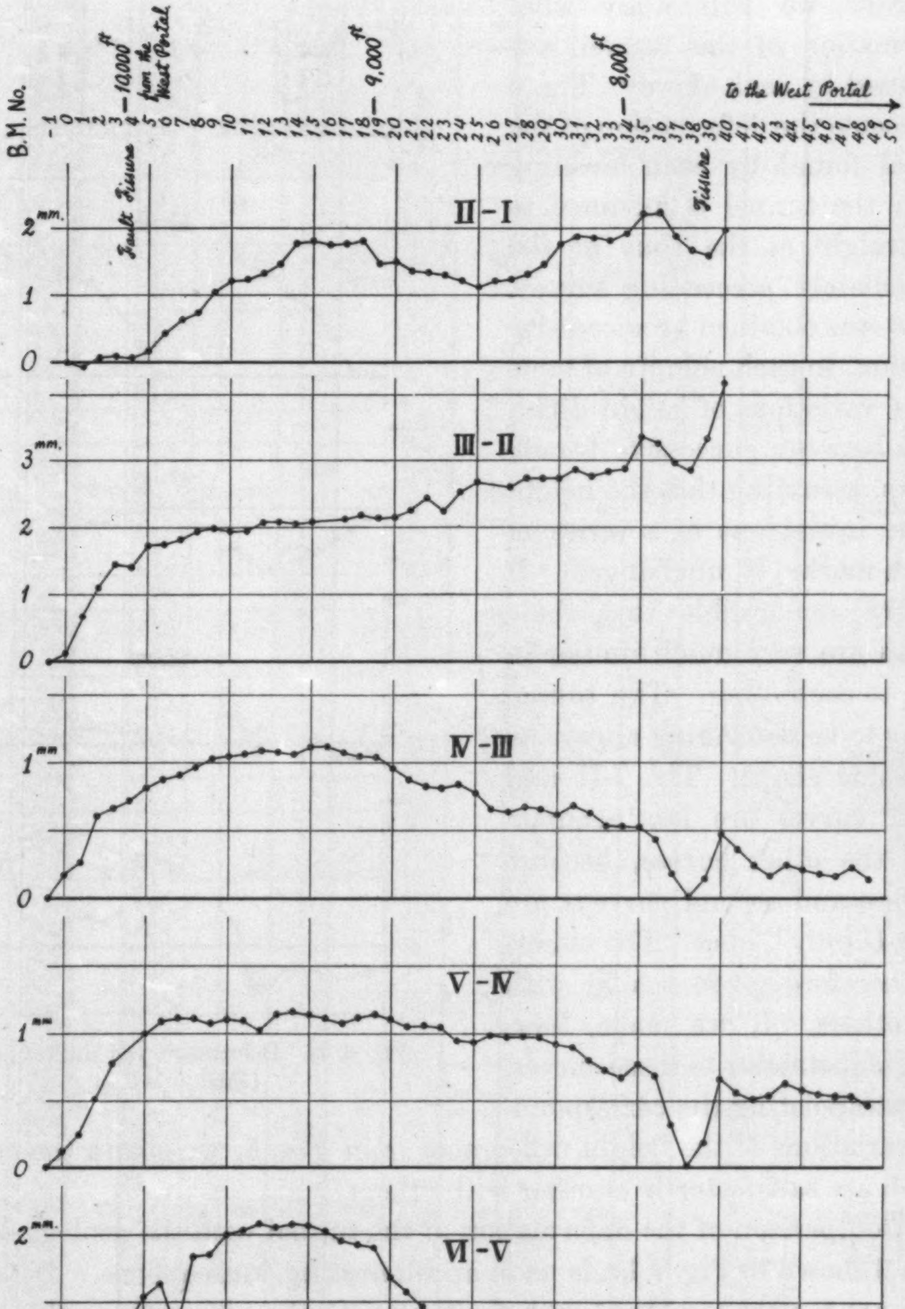

Fig. 6. a. Deformation of the tunnel.
(West side).

Now we will study what deformation of the tunnel was disclosed by each survey. Fig. 6 represents the deformation of the tunnel found by each levelling when the tunnel is assumed to be straight at the time of the immediately preceeding survey. Fig. 6 was obtained by successive addition, in each column of table II, of variations of height differences between successive bench-marks, assuming that the height of the initial one of a series of bench-marks is unchanged. It is very remarkable that these curves are very much similar in form to each other. The tunnel seems to be deforming always to the same shape. The I-II and II-III curves are less accurate than the other curves, because the first and second surveys are the "D only" ones. The curves are therefore not so similar with the others. If we make, however, adjustments to these curves, by extrapolating the corresponding variations of the height differences from Fig. 5, we obtain the curves which are satisfactorily simillar with others.

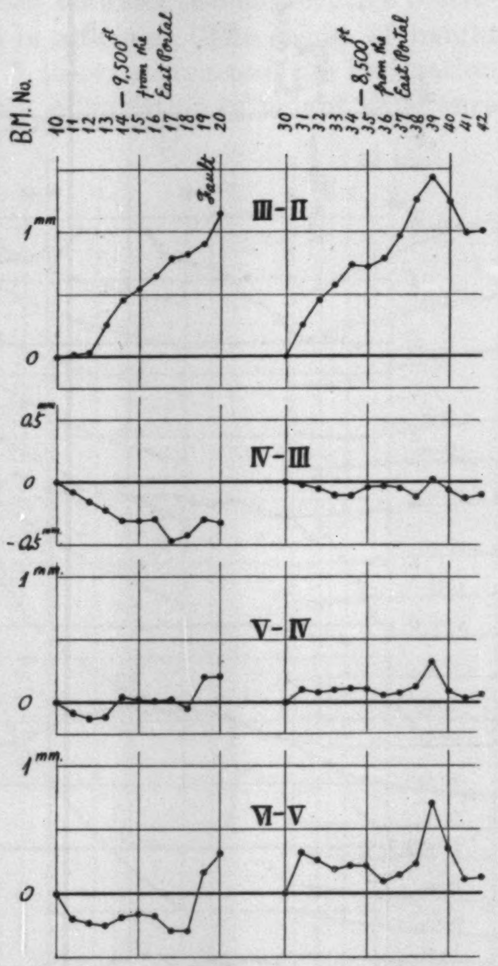

Fig. 6. b. Deformation of the tunnel. (East side).

Comparison of the deformation of the tunnel with the geology of the tunnel shown in Fig. 7 leads us to an interesting consequence. Deformations are mostly combined with faults or with the place where the strata make sudden change in strength, and the remaining part of the tunnel is generally less active. This fact leads us to the consideration that the the yielding of the earth's crust occurs for the most part at some particular weak lines, though slight bending deformations may be seen in the remaining part. These weak lines form therefore the boundaries of so-called land blocks. This consideration harmonizes very beautifully with

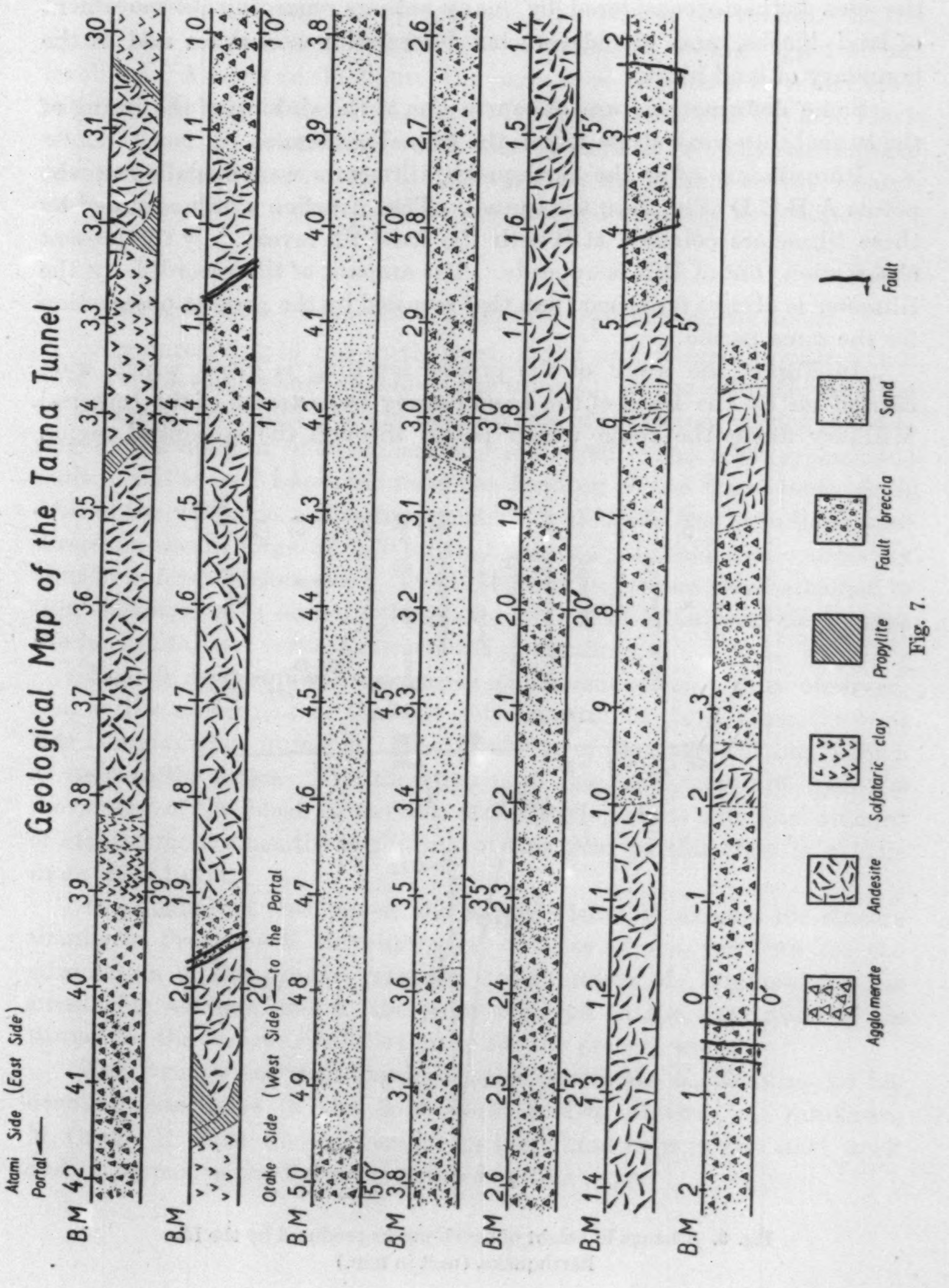
Geological Map of the Tanna Tunnel
Atami Side (East Side)
Portal
B.M 42 41 40 39 38 37 36 35 34 33 32 31 30
B.M 2.0 1.9 1.8 1.7 1.6 1.5 1.4 1.3 1.2 1.1 1.0
39'
34'
20'
14'
10'
Otake Side (West Side)—to the Portal
B.M 5.0 4.9 4.8 4.7 4.6 4.5 4.4 4.3 4.2 4.1 4.0 3.9 3.8
15.0'
B.M 3.8 3.7 3.6 3.5 3.4 3.3 3.2 3.1 3.0 2.9 2.8 2.7 2.6
45'
40'
B.M 2.6 2.5 2.4 2.3 2.2 2.1 2.0 1.9 1.8 1.7 1.6 1.5 1.4
35'
30'
25'
20'
15'
B.M 1.4 1.3 1.2 1.1 1.0 9 8 7 6 5 4 3 2
5'
B.M 2 1 0 -1 -2 -3
0'
Agglomerate
Andesite
Solfataric clay
Propylite
Fault breccia
Sand
Fault

Fig. 7.

the idea hetherto considered by many authors regarding the movement of land blocks, and elucidates what deformation occurs in and at the boundary of land block.

Some deformations are of course due to the sinking of the lining of the tunnel into weak strata which the tunnel penetrates.

Immediately after the earthquake, tiltmeters were installed at the points **A B C D** (Fig. 2) in the tunnel. The direction of tilt recorded by these tiltmeters coincide at **B** with the local tilt revealed by the present observation, but at **D** it is opposite. The amount of tilt recorded by the tiltmeter is always far larger than that revealed by the present observation for the same period.

In Fig. 8, the result of the precise levelling is given which were carried on by the hand of the Land Survey Department of the Imperial Millitary along the route which passes through the epicentral region

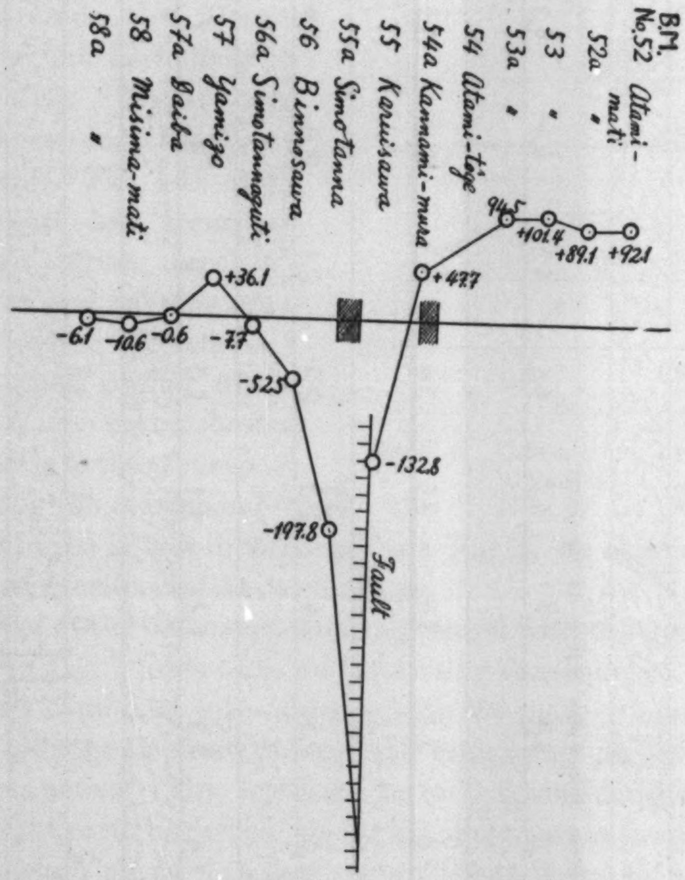

Fig. 8. Change in height of bench-marks produced by the Idu Earthquake. (unit in mm.)

of the earthquake and is approximately parallel to the tunnel. In the figure the shaded parts of the route correspond to the region of our levelling. As seen in the figure, the parts were subjected to remarkable tilting in the case of the earthquake. It is to be noted that the land block which tilted so remarkably with the occurrence of the earthquake becomes inmobile so quickly as discovered by the present survey, though there is remaining a slow movement which is decreasing with time.

Movement of the slicken-side of a fault that appeared in the tunnel.

Accompanying to the earthquake, faults and fissures appeared not only on the earth's surface, but in the tunnel. At the point between the bench-mark No. 3 and No. 4 in the west side of the tunnel vertical dislocation of the amount of 40 cm. ca. was measured. The most remarkable fault in the tunnel appeared near the heading of the third south drain drift of the west side. The displacement, which was nearly in horizontal direction, was as large as 2·70 m. that the drain tunnel was completely shut by a fresh slicken-side. Two dial-guage indicators were attached to this slicken-side as seen in the photograph, (Fig. 9) in order to measure the horizontal and vertical movements of the fault.

Fig. 10 represent the movement of the slicken-side thus observed, that is the movement of the east side block of the fault, when the west side is regarded as immoble. The direction of the motion is north-down as seen in the figure. The direction is in the same quadrant with the movement of the block in the case of the earthquake. The total amount of displacement since the beginning of this year to this time is a little more than 1 mm.

In concluding this paper, the writer wishes to express his sincere thanks to Professor K. Suyehiro, the director of our Institute for the stimulation of the present research, to Professor M. Ishimoto for his invaluable advices, and to the party engaged in the excavation of the tunnel for the various facillities given for the present works.

The writer's heartfull thanks are also due to Mr. K. Kakuma for his devoting assistance in the field work, and to Messrs. A. Zitukawa, M. Otuka, R. Takei and M. Iwasita for their kind help in the field work and in preparing the figures contained in this paper.

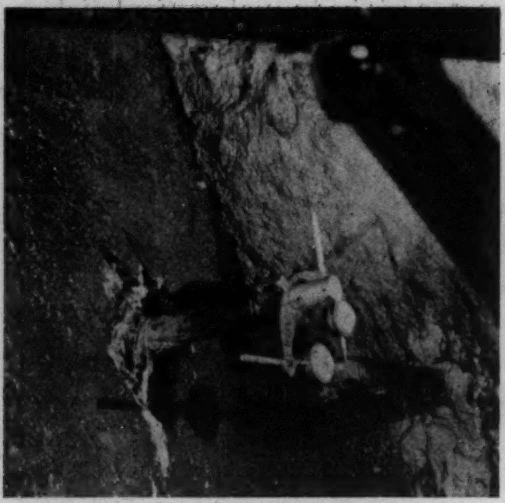

Fig. 9.

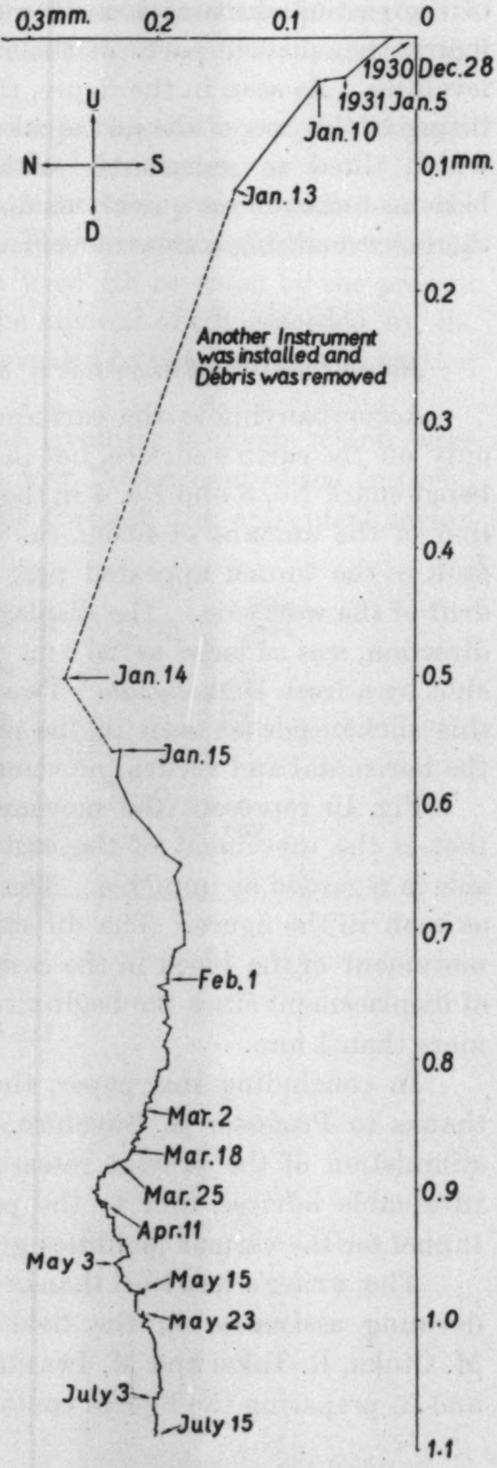

Fig. 10. Movement of the slicken-side that appeared in the tunnel.

31. 丹那隧道内に於ける精密水準測量の結果、及び同隧道内に現れた斷層鏡面の運動

地震研究所 高橋龍太郎

昭和五年十一月廿六日北伊豆地方に起つた激震後の地殼の運動を調査する目的を以て、十二月以來次の如く合計六回に亘つて、丹那隧道内に於て水準測量を爲した。其の時日を擧げれば

第一回　昭和五年十二月廿九日一卅日
第二回　昭和六年一月七日一九日
第三回　　同　二月五日一十二日
第四回　　同　三月三日一九日
第五回　　同　四月十三日一十八日
第六回　　同　七月十八月一廿四日

である。測量爲された範圍は本文第二圖中黑線を以て示してある。地塊の運動を精查するには一等水準以上の精度を必要とする爲、此の測量に於ては第三圖に示す如き特別の器械を製作使用した。測量の結果は第六圖に示された如くである。此圖は前回の測量の時、隧道が直線であつたと假定した時の隧道の變形を示すものである。此等の結果を第七圖に示す處の隧道内の地質圖と比較する事に依つて地殼の運動に依る變形は特殊の弱線のみが其の大部分を受持つて、他の部分は殆んど變形に與からない事が判明する。此等の弱線は卽ち地塊の境界を爲すものであらう。

北伊豆地震に伴つて、地表にも亦隧道内にも斷層が現れた。隧道内に現れた斷層の中、最も著しきものは大竹口南側水拔導孔最奥に現れたものである。此處では導孔は新しい斷層鏡面の出現によつて完全に閉塞されて終つた。此の斷層鏡面の上下及び垂直の運動を測定する爲にダイアル、ゲーヂ二個を取付けた。第十圖に示すものは其に依つて測定された斷層鏡面の運動で、西側が不動と考へた時の斷層東側の地塊の運動を示してゐる。本年一月中旬以來の運動の總量は一粍餘に上つてゐる。

32. *Comparative Studies of Earthquake Motions Above-ground and in a Tunnel.* (*Part I*)

By Nobuji **NASU**,

Earthquake Research Institute.

(Read Feb. 17 and June 16, 1931.—Received Sept. 20, 1931.)

Introduction. The observation of subsurface earthquake motion is an important problems not only of practical seismology, but also of mining and civil engineering. It was found in the great Kwantô earthquake of 1923, and also in the recent Idu earthquake of last year that the interiors of some of the tunnels in the seismic districts showed less of the effects of the earthquake than the surface ground just above them. This fact may be attributed either to the aseismatic construction of the tunnel or to the highly probable fact that earthquake motion at depths are less intense than on the surface of the earth. So far the only investigation of the earthquake motion at depths is that made by Prof. Saemontaro Nakamura.[1] In his investigations, two Omori seismographs of the same type were employed; one being installed at the mouth of the tunnel and the other in a side adit 89·2 m. below the surface and 451 m. distant from the entrance of the tunnel. The results showed that the amplitude of the earthquake motion inside of the tunnel was in general less than that at the portals. The ratio of the earthquakes motion inside to that outside of the tunnel was 0·43—0·80 in the component parallel to the direction of the tunnel and was 0·60—1·12 in the component perpendicular to the direction just mentioned. The ratio, however, is not constant but varies with the period of the earthquake. As the earthquake motion is greatly influenced by the nature of the soil and the depth of the point of observation from the earth's surface, the diminution of the under ground earthquake motion will, of course, differ according to the conditions governing the observations.

The recent successive outbreaks of the Idu earthquake after-shocks provided us with opportunities for comparing the earthquake intensity at the surface with that underground. In this comparative study, the surface station was in the Tanna Basin and the underground station in the Tanna Tunnel, right underneath the surface station. These two stations are equipped with seismographs of the same type. The observations are still being continued.

---

[1] Saemontaro NAKAMURA, *Proc. Physico-Mathem. Soc.*, Japan, 7 (1925), 127, "Preliminary report of the observation in railway tunnel."

Tanna Tunnel. For the purpose of shortening the main Tôkaidô line which connects Tôkyô and Kôbe, the Department of Railways is now driving a tunnel, the Tanna tunnel through the meridional mountain range in the Idu peninsula. The total length of this tunnel is 7807 m.

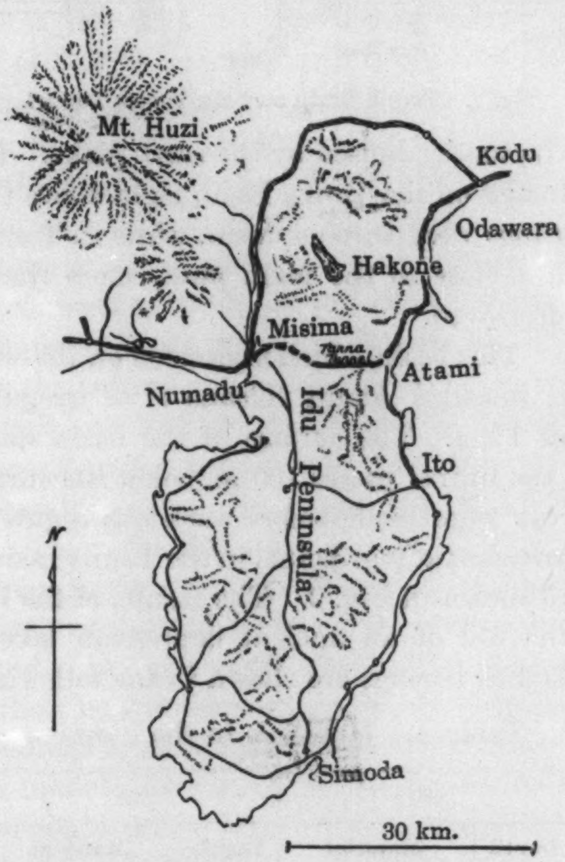

Fig. 1. Map of the Idu Peninsula.

Work was commenced in July, 1918, from both ends, simultaneously. At the time of the recent destructive Idu earthquake the heading on the eastern side had advanced about 3350 m. from the entrance and that on the western side to about 3650 m., leaving more than 800 m. in the middle yet to be bored.

On Nov. 26, 1930, a fault of which the earthquake of that date was an accompaniment, dislocated the tunnel laterally to the extent of 2·4 m.

at a point about 0·5 m. westward of the heading that was being driven from the western portal. Beyond a few cracks in the walls this was the only damage to the tunnel caused by the earthquake. But in the village of Karuizawa, situated on the Tanna Basin right above the tunnel, 55 per cent. of the dwellings were thrown down, while in Tanna and Hata, two villages that are also close to the main fault, more than 40 per cent. of the houses were destroyed.

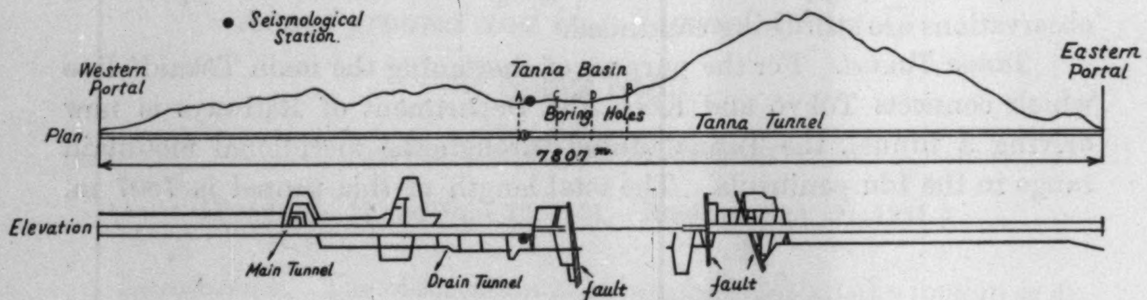

Fig. 2. Tanna Basin and the Tanna Tunnel.

Tanna Basin. This basin which is situated on the western side of the crater wall of the so-called Atami volcano is of irregular shape with a diameter of about 1 km. The surface of the basin stands 240 m. above the sea-level and the tunnel passes 160 m. below the surface of this basin.

Boring surveys were made before work was begun on the tunnel by the Railway Department at four points in the Tanna basin. The positions of these points are shown in Fig. 2. The results of the borings show that this basin was the bed of an ancient depression lake. The materials brought up in the four borings are shown in the following table:

Table I. Materials in the borings.

A		B		C		D	
Depth	Material	Depth	Material	Depth	Material	Depth	Material
0–30m.	Lake deposit (Sandy clay and Boulders)	0–20m.	Talus	0–40m.	Lake deposit (Sandy clay)	0–50m.	Lake deposit (Sandy clay and Boulders)
		20-40	Lake deposit (Sandy clay and Boulders)	45-50	Blocks of andesite		
				50–60	Agglomerate	50 55	Large blocks of andesite and Boulders
30–40	(Lava bed Double pyroxene andesite)	>40	Agglomerate	60–70	Olivine pyroxene andesite		
40-140	Agglomerate			>70	Agglomerate	55 99	Agglomerate
140–160	Olivine pyroxene andesite.					99-118	Olivine pyroxene andesite
						>118	Agglomerate.

Seismic observation. For the purpose of studying the aftershocks of the Idu earthquake two seismographs were installed at Tanna and Hiyekawa, in addition to those already working, at Itô and Aziro since the 1930 Itô earthquake, thus forming a network of stations. At Tanna a set of horizontal portable seismographs which was specially designed by Mr. F. Kishinouye was first installed. But for comparative observations of the earthquake, it became necessary to use two seismographs of the same type. The surface station on the Tanna basin stands on agglomerate which is developed along the western mergin of the basin but not on the soft lake-deposit. These comparative observations began on January 15 of this year, and is still being continued. The positions of the surface and the underground stations are shown in Fig. 2.

Earthquakes studied. Seismograms for the period between January 15 to June 30 of this year were examined. In this period many aftershocks of the Idu earthquake were recorded, the total number of which exceeded 100. Earthquakes in other districts are also included in this study. But the records are confined to moderate and strong earthquake. In the case of distant earthquakes, only waves of periods less than 6 seconds were considered. As the natural oscillation period of the seismographs were nearly 6·0 seconds, we had great difficulty in computing the real amplitude of the earthquake motion whenever the period of the earth's vibration was nearly equal to the proper period of the seismograph, and particularly so, when the damping of the seismograph was not very effective. Further, in the case of slight shocks, considerable error might creep into the ratio of the amplitudes of the earth motion upground and that underground. In such slight shocks the maximum amplitude is generally less than one millimeter on the seismogram, so that personal errors in the readings of amplitudes may considerably effect the ratio of the earthquake motions for the two positions just stated. In the present study, records of slight earthquakes were not considered, only the stronger ones being studied.

Instruments. During the period covered by this study there were in service two mechanically registered seismographs that had been built on the designs of Profs. A. Imamura and K. Suyehiro. The instrument consists of two horizontal and one vertical pendulum. The steady mass of each component pendulum weighs 7 kg. and the static magnification ranges between 25 and 50. The bobs of the horizontal pendulum are so pivoted to a durable brass frame that the mass rotates about a vertical line which passes through its centre of gravity. The upper and lower ends of this frame are suported by steel points so that the system can rotate about the line joining these two points. Detailed descriptions of the horizontal pendulum have already been published by Prof. Imamura.[2]

The main improvement in the seismographs used in this study was the adoption of stainless steel for the construction of the registering apparatus and the clock-work that drives the recording drum, since the interior of a tunnel or mine adit is always damp and rust in the instruments would vitiate the records obtained by them. But stainless steel being softer than ordinary hard steel, it cannot be used for the points of support of the brass frame of the horizontal pendulum. These points in our seismographs were consequently made of tempered steel and greased to prevent corrosion.

Instrumental constants. It is highly important for the comparative observation of earthquakes that all the instrumental constants shall be nearly equal in the two seismographs. Experience shows, however, that it is very difficult to set a pair of mechanically registering seismographs to operate in the same way. This difficulty is mainly due to the effects of friction that are inseparable from such instruments. Friction in a seismograph being a matter of great complexity it is perhaps impossible to cause their effects in two seismographs to be exactly alike. But in practice, a slight difference in the instrumental constants, is not an insuperable objection.

The measurement of the instrumental constants is therefore an important method by which we can decide the degree of sensitiveness of the seismograph. Thus in the course of our studies the constants were determined at every opportunity. The instrumental constants were determined in the following manner:

Period. The period is calculated from the curves of the free oscillation of the pendulum and the following values were obtained with six component pendulums. As will be seen from the following table, every trial determination differs slightly from the other. Thus in the numerical computations of the magnification of each component pendulum the mean values of the periods were taken.

---

[2] A. IMAMURA, *Bul. Earthq. Res. Inst.*, 1 (1926), "Note on our Seismometrial Improvements."

Table II. Observed periods of the seismographs.

Basin				Tunnel			
Date	NS	EW	V	Date	NS	EW	V
	sec.	sec.	sec.		sec.	sec.	sec.
Feb. 3	5·9	5·9	2·7	Feb. 8	5·9	5·4	—
7	6·2	6·0	3·0	19	5·9	5·6	4·8
15	6·2	5·6	2·8	25	5·7	5·6	4·9
24	6·4	6·1	2·7	28	6·2	5·3	—
25	5·9	5·9	2·8	16	5·7	5·5	—
Mar. 4	5·5	5·5	3·0	21	5·6	5·7	4·7
19	5·7	5·8	3·4	Mar. 3	5·7	5·6	4·9
24	6·2	5·6	3·5	11	5·9	5·6	—
Ap. 6	5·6	5·7	3·7	Ap. 11	5·7	—	5·3
10			3·6	9	5·7	5·4	4·8
				17	5·9	5·3	4·9
Mean	5·96	5·79	3·12		5·81	5·50	4·90

Damping ratio and friction. For the sake of convenience let us begin with the equation for the free oscillation of a pendulum with fluid and solid dampings, that is

$$\ddot{y}+2\varepsilon\dot{y}+n^2(y+\rho)=0, \quad \cdots\cdots\cdots\cdots\cdots\cdots(1)$$

where ε is the constant relating to the fluid damping and ρ to the solid damping (friction), in other words, ρ represents the amount of deviation of the index end from its equilibrium position, assuming there is no friction between the writing index and the smoked paper. Here ρ is assumed to be constant, but in practice it is difficult to obtain this as a constant. Perhaps, it depends on the amplitude and velocity of the motion of the writing index, as has been discussed by Galitzin.[3] But, our trial determination of the friction failed to yield any conclusive results. The equation above given is only sufficient for a first approximation but it is in general use because of its simplicity.

For the general solution of this equation we get the following expression ;

$$y+\rho=e^{-\varepsilon t}[C_1\cos\lambda t+C_2\sin\lambda t]. \cdots\cdots\cdots\cdots\cdots\cdots(2)$$

---

[3] Galitzin, „Vorlösungen über Seismometrie."

Now, let the free vibration curve be like that shown in Fig. 3. In the case of no friction, the writing point rests on a horizontal dotted line. Let y_1 be the deviation of the first turning point A of the curve from this line. The two arbitrary constants C_1 and C_2 can be determined with the initial conditions, $y = y_1 \cdot \dot{y} = 0$, when we get the following:

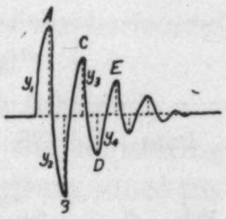

Fig. 3.

$$C_1 = y_1 - \rho, \qquad C_2 = \frac{\varepsilon}{\lambda}(y_1 - \rho). \qquad \cdots\cdots\cdots\cdots\cdots\cdots(3)$$

Putting these values in the general solution, we have

$$y - \rho = (y_1 - \rho)\, e^{-\varepsilon t}\left[\cos \lambda t + \frac{\varepsilon}{\lambda} \sin \lambda t\right]. \qquad \cdots\cdots\cdots\cdots\cdots(4)$$

The ordinate of the second turning point B can be determined from the condition $\frac{dy}{dt} = 0$. The complete calculation has been shown by Galitzin so that they are omitted here. y_2 is given by the following expression:

$$-(y_2 - \rho) = (y_1 - \rho)\frac{1}{v}, \qquad \cdots\cdots\cdots\cdots\cdots\cdots\cdots(5)$$

where v denotes the damping ratio, that is the ratio of the two consecutive ordinates. In this expression the negative sign before y_2 means that this ordinate is measured downwards. Between B and C in the curve where $\dot{y}$ and ρ are both positive, we get the following expression:

$$(y_3 + \rho) = -(y_2 + \rho)\frac{1}{v}. \qquad \cdots\cdots\cdots\cdots\cdots\cdots\cdots(6)$$

For the sake of convenience let us remove the signs and let the absolute magnitudes of the successive amplitudes be represented by $y_1, y_2, y_3 \cdots y_{k+2}$ etc. Then we have the following series of expressions

$$\left.\begin{aligned} y_1 - \rho &= (y_2 + \rho)\, v, \\ y_2 - \rho &= (y_3 + \rho)\, v, \\ &\vdots \qquad \vdots \\ y_k - \rho &= (y_{k+1} + \rho)\, v, \\ y_{k+1} - \rho &= (y_{k+2} + \rho)\, v. \end{aligned}\right\} \qquad \cdots\cdots\cdots\cdots\cdots\cdots\cdots(7)$$

In calculating the damping ratio, double amplitudes are always taken, because of the indeterminateness of the position of the zero-line.

Thus the formula

$$(y_k+y_{k+1})-2\rho = \{(y_{k+1}+y_{k+2})+2\rho\}\, v \quad \cdots\cdots\cdots\cdots\cdots(8)$$

is in general use for determining the damping ratio and the friction. As a special example,if v is nearly equal to unity, as in the case of weak damping, the formula becomes much simpler and the friction can be easily determined. In such a case the following expression is applicable.

$$\rho = \frac{1}{4}(y_\kappa - y_{\kappa+2}). \quad \cdots\cdots\cdots\cdots\cdots\cdots\cdots(9)$$

The damping ratio and the friction can simultaneously be determined if three successive double amplitudes of the free vibration are known. Let these three double amplitudes be Y_1, Y_2 and Y_3. In Fig. 3, Y_1 is equal to AB, Y_2 to BC and Y_3 to CD. Between A-B and C-D in the curve, the velocity takes the negative sign, whlie in B-C it takes the positive. Assuming that the damping ratio is the same throughout a free oscillation curve, then the following simultaneous equations are obtained ;

$$\left.\begin{aligned} \frac{Y_1-2\rho}{Y_2+2\rho} &= v, \\ \frac{Y_2+2\rho}{Y_3-2\rho} &= v. \end{aligned}\right\} \quad \cdots\cdots\cdots\cdots\cdots\cdots\cdots(9)$$

From these equations we have the following expression for the friction :

$$2\rho = \frac{Y_1\,Y_3-Y_2^2}{Y_1+2Y_2+Y_3}. \quad \cdots\cdots\cdots\cdots\cdots\cdots(10)$$

If, for example, the first double amplitude Y_1 be taken as B-C, then the right-hand side of the above expression must take the negative sign. The methods so far described have been used throughout this work for determining the damping ratio and the friction. Their values are listed as below. In this list the (-) sign is attached to the amplitude when the initial turning point of the curve lies on the upper side of the zero line, and *vice versa*. To make this clear, let us take an example from Fig. 3. If the amplitude is taken in the part of the curve between A and B, the amplitude in this case is expressed with a negative sign, while in the part of the curve between B and C the amplitude is expressed with a positive sign, but in this case the sign is of course dispensed with. We must here call attention to the fact that these signs are used for specifying the sense in which the amplitude is measured.

Table III.

(A) Instrument at Tanna Basin.

NS-Comp.

Date of Measurement	Y_1	Y_2	Y_3	Damping ratio v	Friction 2ρ
	mm.	mm.	mm.		mm.
Feb. 3	18·6	−10·0	5·0	1·90	0·16
5	39·0	−24·5	13·0	1·69	0·97
6	−73·5	48·0	−33·0	1·50	0·60
7	31·0	−19·0	10·0	1·72	0·65
15	18·3	−11·5	5·0	1·80	0·88
17	45·5	−31·2	17·5	1·57	1·42
19	67·8	−45·0	29·0	1·53	0·31
20	−62·5	38·0	−24·0	1·52	0·38
23	35·5	−24·3	12·5	1·62	1·52
24	−82·0	55·0	−39·0	1·46	0·74
25	58·5	−42·0	28·0	1·44	0·70
Mar. 4	32·3	−23·0	14·0	1·50	0·83
5	26·0	−24·0	22·0	1·09	0·04
19	55·5	−42·5	31·5	1·32	0·34
21	41·5	−29·0	18·5	1·49	0·62
24	19·0	−11·5	5·0	1·84	0·78
26	18·0	−10·0	3·0	2·15	1·12
Ap. 6	47·5	−34·0	23·0	1·43	0·45
		Mean		1·58	mm. 0·66

EW-Comp.

Date of Measurement	Y_1	Y_2	Y_3	Damping ratio v	Friction 2ρ
	mm.	mm.	mm.		mm.
Feb. 3	61·0	− 47·0	35·0	1·31	0·39
5	53·0	− 40·0	29·5	1·34	0·22
6	14·5	− 7·0	2·0	2·40	0·66
7	66·5	− 53·5	41·5	1·26	0·48
15	23·0	− 15·3	8·5	1·61	0·61
17	105·0	− 84·0	67·0	1·25	0·00
19	51·5	− 40·0	29·5	1·32	0·50
20	65·2	− 52·0	38·5	1·30	0·93
23	58·0	− 46·0	36·0	1·27	0·17
24	140·0	−114·0	92·5	1·23	0·10
25	117·5	− 95·0	76·5	1·24	0·09
Mar. 4	24·0	− 12·0	4·6	2·17	0·64
5	46·0	− 31·5	20·0	1·50	0·56
19	55·5	− 42·5	31·5	1·32	0·34
21	41·5	− 29·0	18·5	1·49	0·62
24	−36·0	29·0	−24·0	1·22	0·20
26	16·0	− 11·0	5·5	1·63	0·76
Ap. 6	31·5	− 24·5	18·0	1·32	0·33
		Mean		1·45	mm. 0·42

(B) Seismograph in the Tanna Tunnel.

NS-Comp.

Date of Measurement	Y_1	Y_2	Y_3	Damping ratio v	Friction 2ρ
	mm.	mm.	mm.		mm.
Feb. 8	37·5	−26·8	17·5	1·45	0·57
19	52·7	−37·0	24·6	1·46	0·48
21	35·0	−23·0	13·0	1·61	0·79
25	51·2	−34·5	20·5	1·56	1·00
28	30·0	−15·0	5·0	2·25	1·15
Mar. 3	49·0	−32·1	19·5	1·57	0·56
4	24·5	−15·0	7·0	1·80	0·87
10	35·0	−21·0	9·7	1·82	1·17
16	32·5	−21·0	12·0	1·62	0·59
19	21·0	−10·5	3·0	2·30	1·05
21	41·5	−30·5	21·5	1·38	0·31
23	−76·8	−55·5	—41·0	1·37	0·30
26	39·5	−28·0	17·0	1·50	1·00
28	34·0	−24·0	16·0	1·44	0·33
		Mean		1·66	mm. 0·73

EW-Comp.

Date of Measurement	Y_1	Y_2	Y_3	Damping ratio v	Friction 2ρ
	mm.	mm.	mm.		mm.
Feb. 8	30·5	−17·5	9·0	1·82	0·43
21	−75·2	48·2	−32·5	1·52	0·59
25	40·0	−20·2	6·5	2·28	1·70
Mar. 16	41·0	−29·5	16·2	1·54	1·77
19	78·5	−48·0	22·0	1·81	2·93
21	60·0	−38·0	21·5	1·65	0·97
23	66·5	−37·0	14·5	2·01	2·61
26	32·5	−17·5	5·0	2·23	1·98
28	40·5	−24·0	10·2	1·88	1·65
		Mean		1·86	mm. 1·63

The friction, R, in dynes is given as $R = \dfrac{4\pi^2 \rho M}{T_1^2 V^2}$,

where ρ is the half-width in centimeters of the zone within which the writing pen has been arrested by friction, T_1 is the undamped oscillation period, M the mass of the pendulum in grams, V is the static magnification. For each component pendulum, M and V take the following values, respectively.

$$M = 7000 \text{ g}, \qquad V = 50.$$

The friction in dynes works out as shown in the following table. In this table the values of the periods used in this calculation are also given.

Seismograph	Basin		Tunnel	
	N. S.	E. W.	N. S.	E. W.
Period of natural Oscillation (in sec.)	5·90	5·75	5·74	5·39
Friction in dynes	0·11	0·07	0·12	0·31

The frictions thus calculated are considerably low in value for such mechanically recording seismographs. In the recent Publication of the Dominion Observatory, Ottawa, L. Don Leet[4] determined the friction of the Wiechert vertical seismograph installed there as 0·13 dynes from a decay curve whose maximum amplitude was 45 mm. He advocates, as does Mohorovičić, that the best instruments, when properly handled should have a friction of less than one-half of a dyne. Our experience confirms the opinions of these two investigators. In the case of friction greater than this maximum value the instrument failed to register the slow pulsatory oscillations. In such cases the instruments were promptly remedied.

We must add here a few words about the friction itself. It is doubtful whether friction thus defined and calculated can be applied in the reduction of the true earthquake motion. We have first to bear in mind that the friction so far calculated is the value for the case of a slow earthquake motion, since our calculation of the friction is based on the decay curves, the periods of which are comparatively slow, being about 6 seconds. In such a slow vibration the writing pen may register the earthquake motion without running off the smoked paper. But in the case of sudden sharp shocks the writing pen jumps off the recording paper with the result that the earthquake motion are often registered as broken curves. In this case the effective friction will be very small perhaps negligible so that no correction for friction need be made. Another difficulty in this matter of correction lies in the following fact. We are often puzzled in deciding whether the correctional term should be 2 ρ or simply ρ, owing to the positions of the two consecutive turing points relative to the zero line which is indeterminate in most cases. If the two turning points lie one on each of the zero line, the correction for friction must be 2 ρ, whereas if these two points lie on the same side of the zero line, the value of the correction must be ρ.

---

[4] L. Don Leet, *Pub. Dominion Obs.*, Ottawa, June 1931, "Empirical investigation of the Surface Waves."

Thus the corrections for friction beginning with equation (1) are unsatisfactory in general practice.

Theoretical values of the period of natural oscillation. The theoretical natural oscillation period is that of the pendulum oscillating without any damping force. This value may be reduced from the following expression:

$$T_1 = \frac{T_1'}{\sqrt{1+0{\cdot}53720\Delta^2}}.$$

In this, T_1 is the theoretical period, T_1' is the observed period and Δ the logarithmic decrement, that is, the common logarithum of the ratio of the two successive amplitudes. In the case of weak damping, the theoretical period is nearly equal to the observed period. The theoretical value of the period is necessary in calculating the dynamical magnification of the seismograph.

For our seismographs the theoretical periods are worked out as follows:

Instrument	Basin		Tunnel	
	N. S.	E. W.	N. S.	E. W.
Period (in sec.)	5·91	5·75	5·74	5·39

Determination of the damping ratio. As is shown in the previous table, the damping ratio is not constant but varies considerably with every trial determination. The results of these determinations showed that this ratio depends on the maximum amplitude of the decay curve.

In the E.W. component of the seismograph that is installed in the tunnel, the mean damping ratio was a little greater than that of the other component seismographs. In this component we could not find any relation between the damping ratio and the amplitude. Excluding the values obtained with this component, let us plot the damping ratio as ordinates and the maximum amplitudes as abscissae.

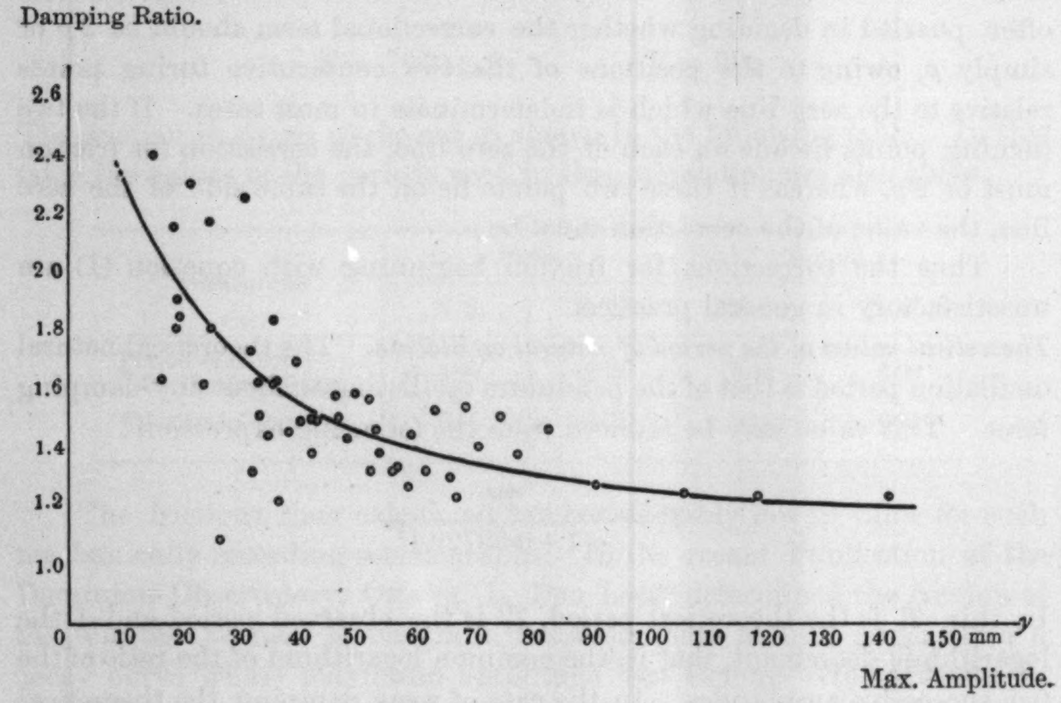

Fig. 4.

The amplitudes in this case range between 14·5 mm. and 140·0 mm. Against these values the damping ratio takes a value between 2·40 and 1·09. When the amplitude becomes larger than 100 mm. the damping ratio approaches 1·20, while when the amplitude becomes as small as 20 mm. it takes a value of nearly 2·00. By means of the method of least squares, the curve was obtained, which shows the relation between the above two quantities. It follows that our first assumption as made in equations (9) is not satisfactory. In these equations the damping ratio is assumed to be constant throughout the decay curve, but the observations showed contrary results. It is probable that there are superior methods of determining the damping ratio and the friction to what has been described so far. However, we shall not carry the discussion further, but merely report the results of our studies.

Magnification of the seismograph. Assuming that the earth's motion is simple harmoic, the dynamical magnification of the seismograph can be calculated by the following formula:

$$\mathfrak{B} = \frac{V}{(1+u^2)\sqrt{1-\mu^2 f(u)}},$$

where V is the static magnification, u is the ratio of the periods of the earth's motion and the undamped period of the seismograph, and u and $f(u)$ represent respectively the following quantities

$$\mu^2 = 1-\left(\frac{\varepsilon}{n}\right)^2,$$

$$f(u) = \left(\frac{2u}{1+u^2}\right)^2,$$

in which ε and n are the two constants in the differential equation of the motion of a pendulum under the action of seismic waves, that

$$\ddot{y}+2\varepsilon\dot{y}+n^2y+V\ddot{x} = 0,$$

where $\ddot{y}$, $\dot{y}$ and y are, respectively, the acceleration, velocity and displacement of the index end, and $\ddot{x}$ is the acceleration of the earth's motion. Magnification curves have been constructed for each component pendulum as shown in Figs. 5 and 6. For ease of comparison all the magnifications of one component are show in the first figure and the same for the other component in the second figure. In the calculation of the magnification, the observed period and the damping ratio are used in their respective mean values as shown in Table III.

On comparing the magnification curves of the two N.S. component pendulums installed, one in the tunnel and the other on the ground surface outside and right above the tunnel, we see that the magnifications of these component seismogrphs are practically identical for earthquake periods less than 4 sec., so that there is no need for correction for difference in the magnifications. The same applies to the E.W. components, of these instruments.

Testing of the seismographs. Before the seismographs were installed in the Tanna district, they were thoroughly tested at the laboratory of the Earthq. Res. Inst. The two instruments were made to function in an underground room of the Institute. In all the earthquakes recorded the two seismographs showed identical results. These seismograms are shown in Figs. 7 and 8.

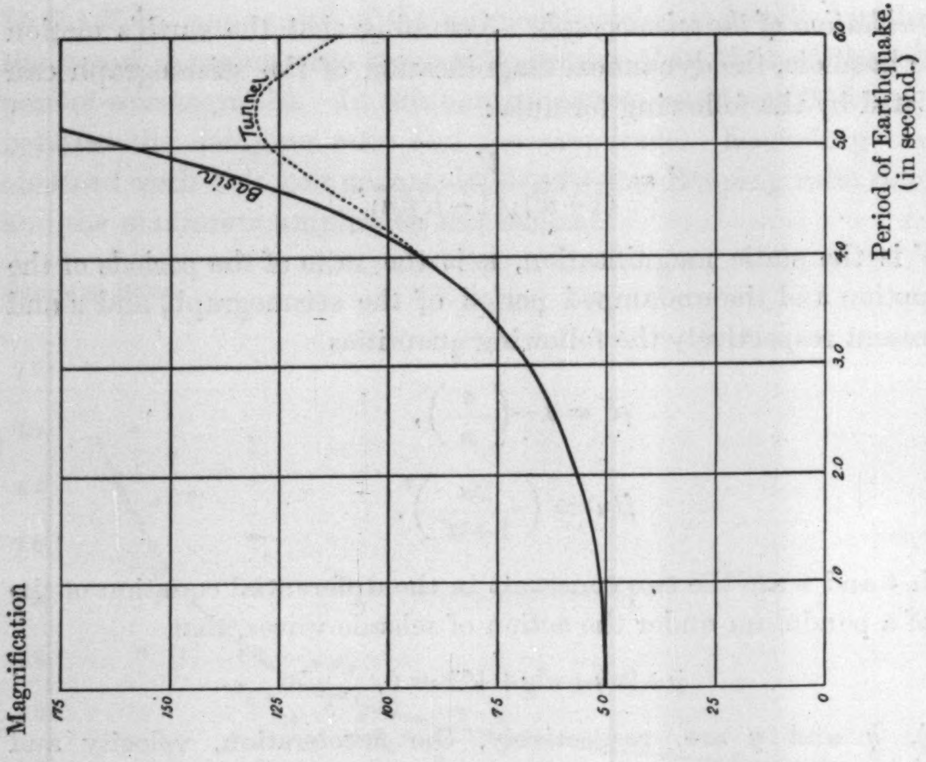

Fig. 6. Magnification Curves (E.W. Comp.)

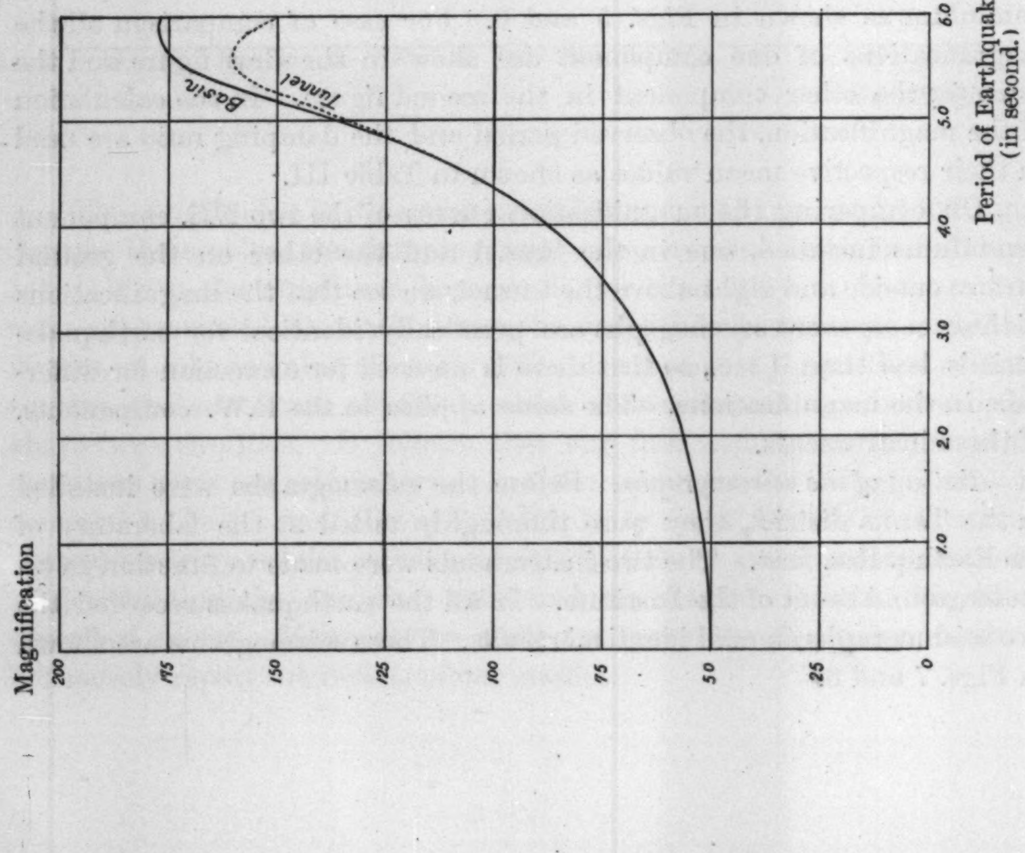

Fig. 5. Magnification Curves (N.S. Comp.)

Comparison of the earthquake effects. These studies made it clear that the movements of the ground surface is genarally greater than that under ground. In the case of quick vibrations, the difference in the magnitude of the earthquake motions above and below ground are much larger than in the case of slow vibrations. When the period of the earthquake is less than 1 sec. the ratio of the amplitude above ground to that below ground is always greater than 2 : 1, while if the period should be as large as 4 sec. this ratio tends to unity.

The results obtained for the earthquakes studied are shown in the following table.

Table IV.

Date	Reading of the Range (2A) of Motion				Period	Ratio of Motions	Mean Ratio of Motions	Remarks
	Upground		In the Tunnel					
	N. S.	E. W.	N. S.	E. W.				
	mm.	mm.	mm.	mm.	sec.			
Jan. 23	1·5 1·3		1·0 0·9		3·0	1·5 1·5	1·50	Distant eqk.
	1·2 1·0		0·8 1·0		2·8	1·5 1·0	1·25	
Jan. 29	1·4 2·7		1·0 3·0		3·4	1·4 0·9	1·15	
	7·3 8·5		6·2 9·2		3·6	1·2 0·9	1·05	
Jan. 30 (No. 1)	6·4 5·8		1·8 1·8		0·5	3·6 3·4	3·50	
		10·0 —		2·9 —	0·5	3·5 —	3·50	
Jan. 30 (No. 2)	5·2 4·8		1·7 1·0		0·3	3·1 4·8	4·14	Eqk. in Idu
	3·3 5·6		0·7 1·4		0·3	4·7 4·0		
Feb. 7	1·8 2·7		0·5 0·8		0·4	3·6 3·6	3·23	Eqk. in Idu
	1·0 —		0·4 —		0·4	2·5 —		
Feb. 20	5·9 7·0		3·7 6·4		3·2	1·6 1·1	1·35	
	8·4 5·1		6·1 5·2		2·2	1·4 1·0	1·20	
		5·0 5·9		3·6 5·4	1·8	1·4 1·1	1·25	
		8·1 5·8		4·2 2·6	1·1	1·9 2·2	2·05	
		4·0 3·5		2·0 1·8	1·0	2·0 1·8	1.90	

(*to be continued.*)

Table IV. (*continued.*)

Date	Reading of the Range (2A) of Motion				Period	Ratio of Motions	Mean Ratio of Motions	Remarks
	Upground		In the Tunnel					
	N.S.	E.W.	N.S.	E.W.				
	mm.	mm.	mm.	mm.	sec.			
Mar. 7	21·2 —		5·1 —		0·3	4·1	4·10	Strong eqk. in Idu.
	43·5 —		20·7 —		0·9	2·1	2·10	
	38·5 62·0		23·7 50·0		2·2	1·6 1·2	1·40	
Mar. 8		12·8 16·6		5·3 4·4	0·5	2·4 3·8	3·10	Eqk. in Idu
	16·0 22·5		5·3 6·6		0·5	3·9 3·4	3·65	
Mar. 9 (No. 1)	5·6 3·9		2·1 1·4		0·6	2·7 2·8	2·75	
	1·0 4·8		0·4? 2·2		0·6	2·5? 2·2	2·35?	Eqk. in Idu
Mar. 9 (No. 2)		7·8 7·8		2·8 3·1	0·5	2·8 2·5	2·65	Eqk. in Idu
		1·6? 7·2		2·0? 3·4	0·5	0·8? 2·1	1·45?	
Mar. 9 (No. 3)	63·0 95·5 86·0 —		66·0 86·0 83·0 —		4·4	1·0 1·1 1·0 —	1·03	
Mar. 29	3·0 2·2		2·9 2·4		4·5	1·0 0·9	0·95	
	1·2 1·8		1·2 1·8		3·7	1·0 1·0	1·00	
June 2	18·5 51·5		14·0 58·5		4·0	1·3 0·9	1·11	
	55·5		56·7 —		5·0	1·0 —	1·00	
		53·5 76·5 64·5 —		39·0 60·5 55·5 —	4·5 4·5	1·4 1·3 1·2 —	1·30	Corrected mean ratio=1·19
June 11	10·7 23·6 18·0 —		8·6 17·0 16·0 —		4·5 4·5 —	1·24 1·39 1·12 —	1·25	
		10·6 16·0		5·4 10·6	1·8	1·74	1·74	

In Fig. 9 the relation between the ratio of the amplitude of the motion above ground to that below ground and the [period of the earthquake motion is shown.

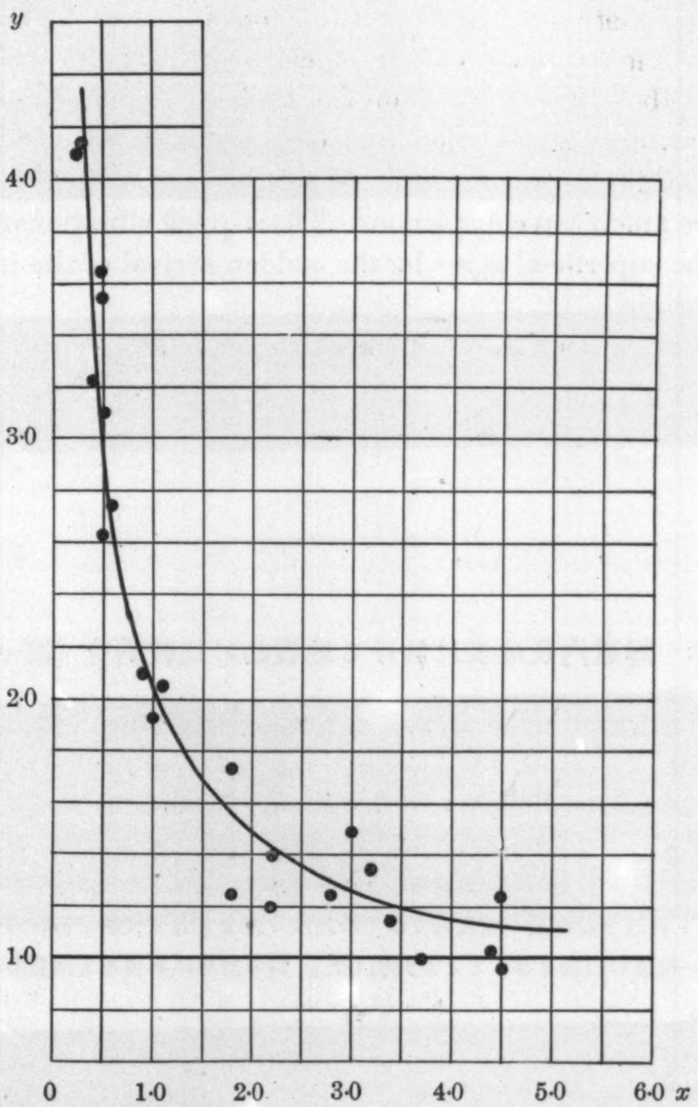

Fig. 9. shows the relation between the ratio of earthquake motions above-ground to that in the tunnel and the period of earthquake.

y = Ratio of earthquake otionsm. (Amplitude in the tunnel is taken to be unity.)

x = Period of earthquake (in second).

Remarks. Earthquake motion consisting of quick vibrations such as with period less than 1 sec. is much influenced by the nature of the soil. As already found from observations at 33 stations in Tôkyô after the great 1923 earthquake, the motion in soil of weak formation is in general greater than that in harder formation. But in our present study there is no difference in the nature of the soils above and below ground since both are agglomerate rock. Thus the difference in the intensity of the earthquake motion in the tunnel and outside must be accounted for by the dinimution of earthquake intensity with depth. In some of the seismographs that were obtained on the surface ground, quick vibrations superposed on a slow vibration and of period less that 1 sec. are very conspicuous while in seismographs obtained in the tunnel these quick vibrations are much less conspicuous. These quick vibrations are probably caused in the superficial layer by the sudden arrival of the impulse from the seismic origin.

Further studies of these quick earthquake motion being desirable we are now contemplating more refined observations with instruments that have recently been designed.

---

32. 隧道內及地表に於ける地震動の比較研究（第一）

地震研究所 那須信治

丹那隧道內とその直上なる丹那盆地とに目下不銹鋼製の同型の地震計を据付けて地震動の比較研究を繼續してゐる。その結果隧道內の地震動は地表のそれに比較して一般に小さいことが判つた。隧道內の地震動を單位として地表の地震との比を求めて見るとそれは地震動の週期に支配されること、及び1秒以下の週期の地震動ではその比は3以上となり又約5秒位の地震動では地下地表共にほゞ同一程度の震動をなすことが判明した。尙ほ計算に必要なる地震計の常數をも合せて記しておいた。

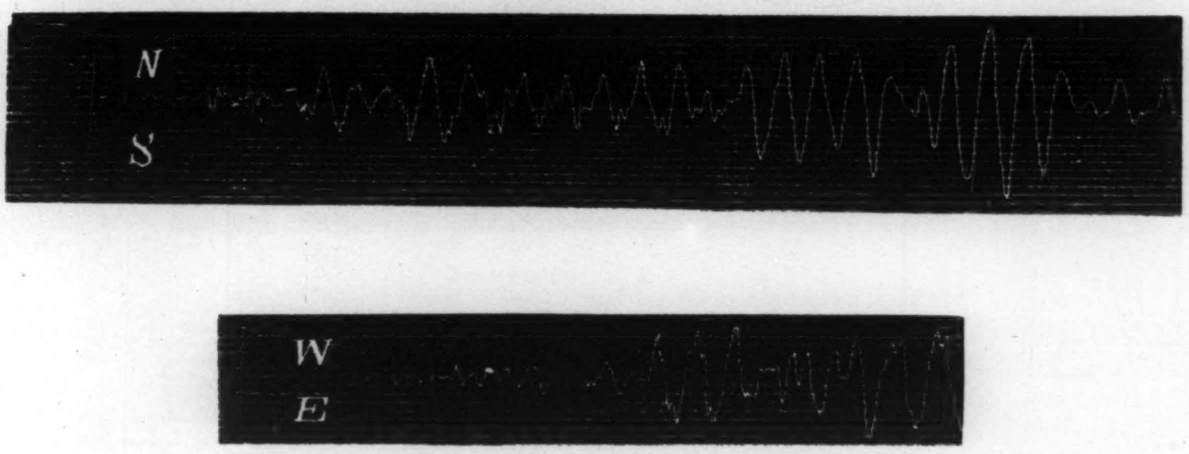

Instrument No. 1

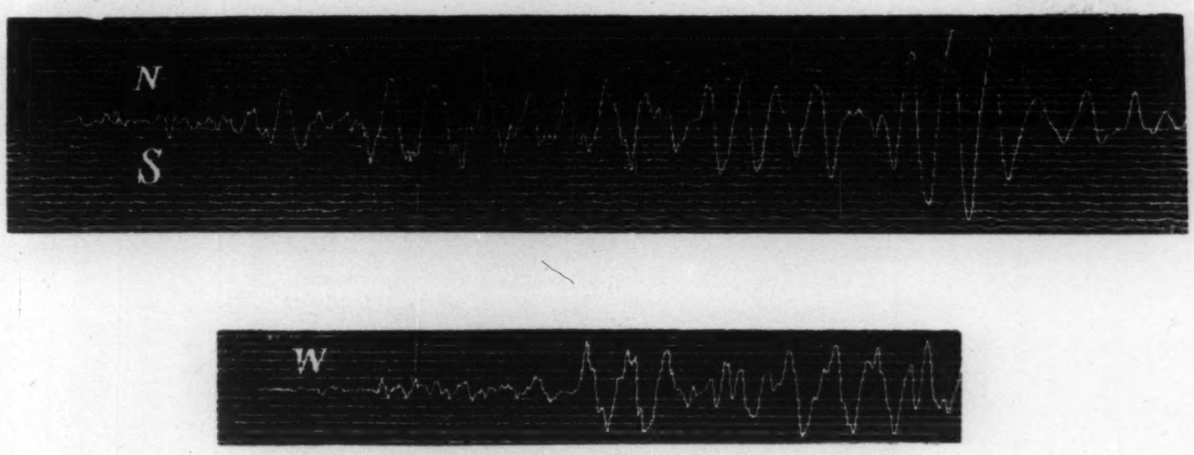

Instrument No. 2.

Fig. 7. Diagrams of the earthquake of March 13, 1930, recorded by the seismographs inatalled at the Earth. Res. Inst.

（震研彙報、第九號、圖版、那須）

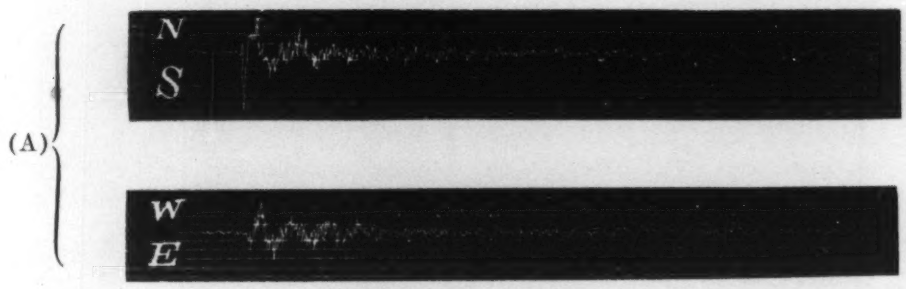

Instrument No. 1.

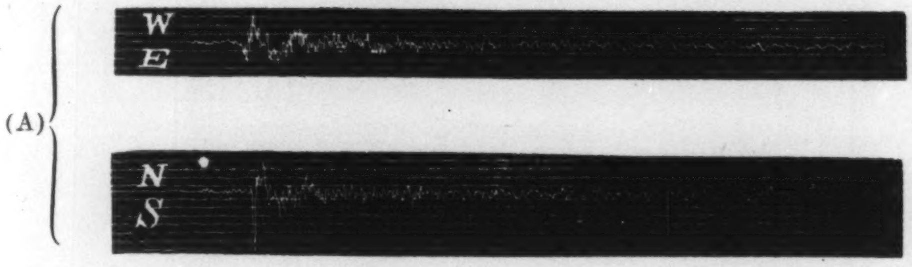

Instrument No. 2.

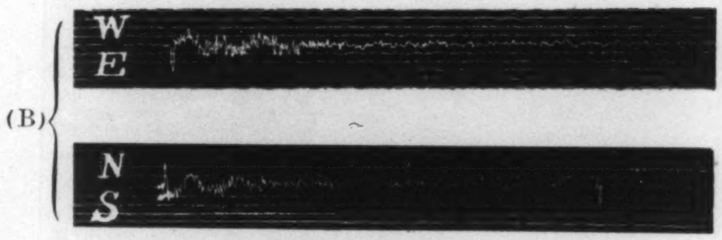

Instrument No. 1.

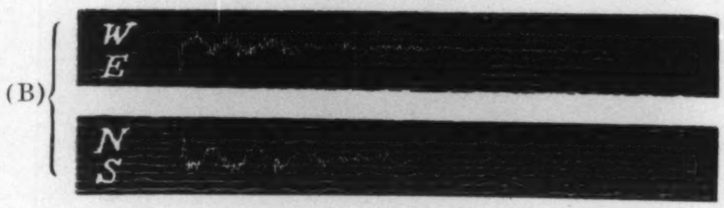

Instrument No. 2.

Fig. 8. Diagrams of the earthquakes recorded by the seismographs installed at the Earth. Res. Inst. (A) Earthquake of March 2, 1930. (B) Earthquake of December 27, 1929.

（震研彙報、第九號、圖版、那須）

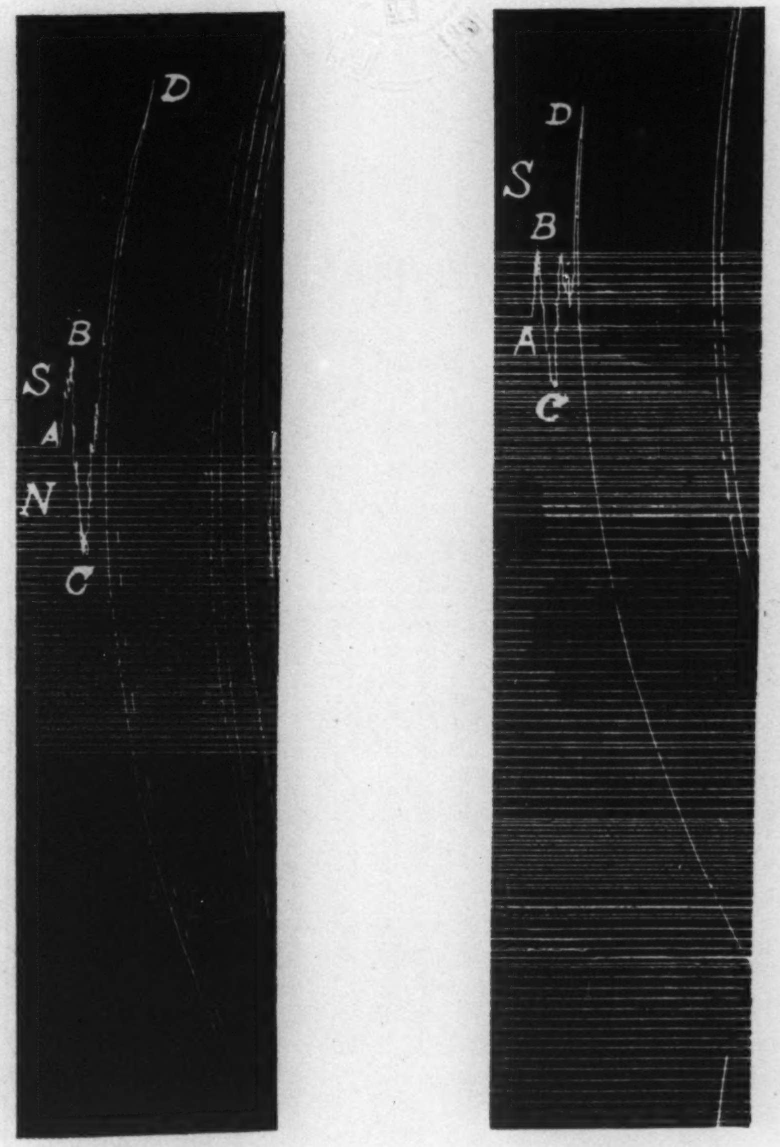

Basin

Tunnel

Fig. 10. Seismograms of the earthquake of June 11, 1931.
(N.S. Component.)

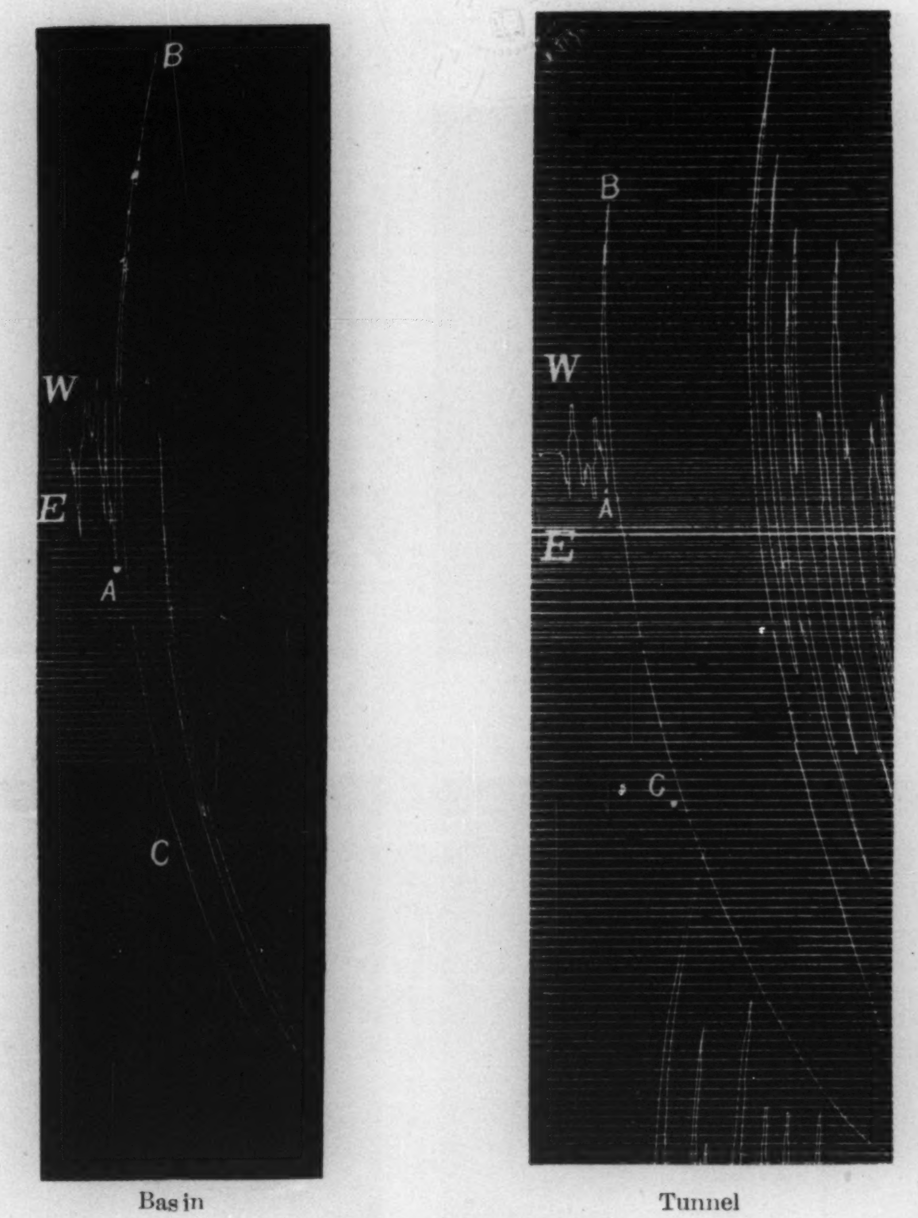

Basin Tunnel

Fig. 11. Seismograms of the earthquake of June 11, 1931.
(E.W. Component.)

（震研彙報、第九號、圖版、那須）

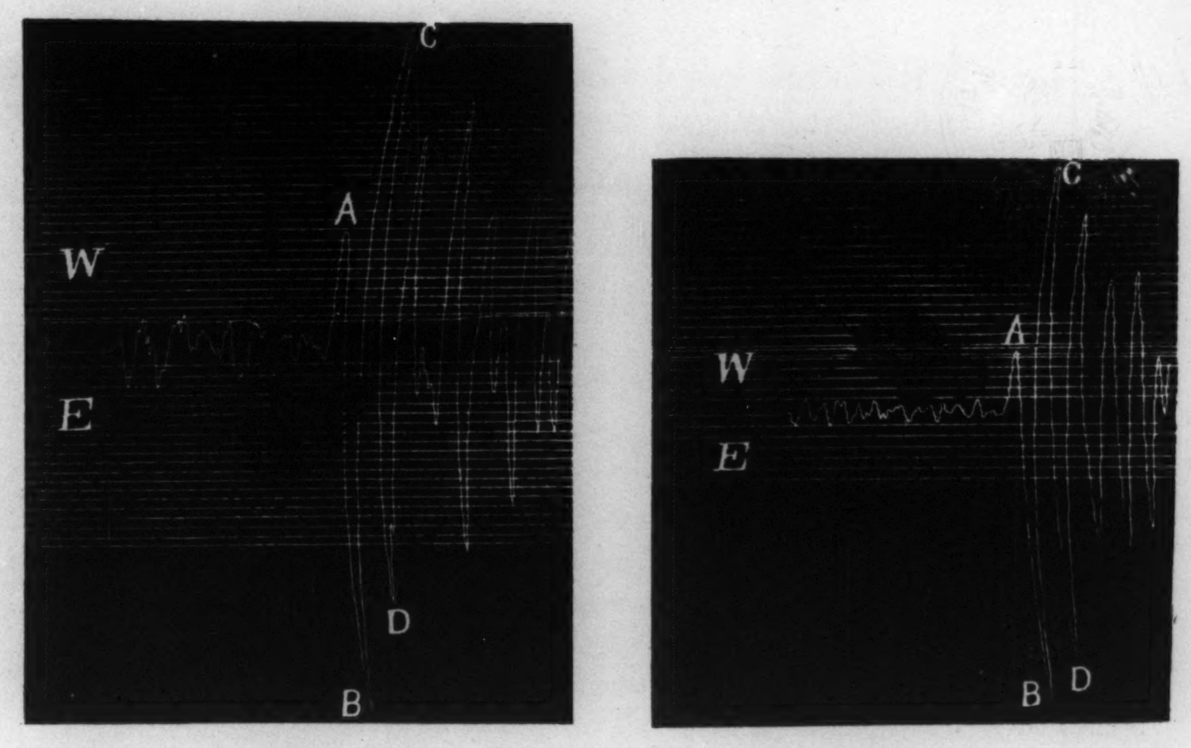

Basin Tunnel

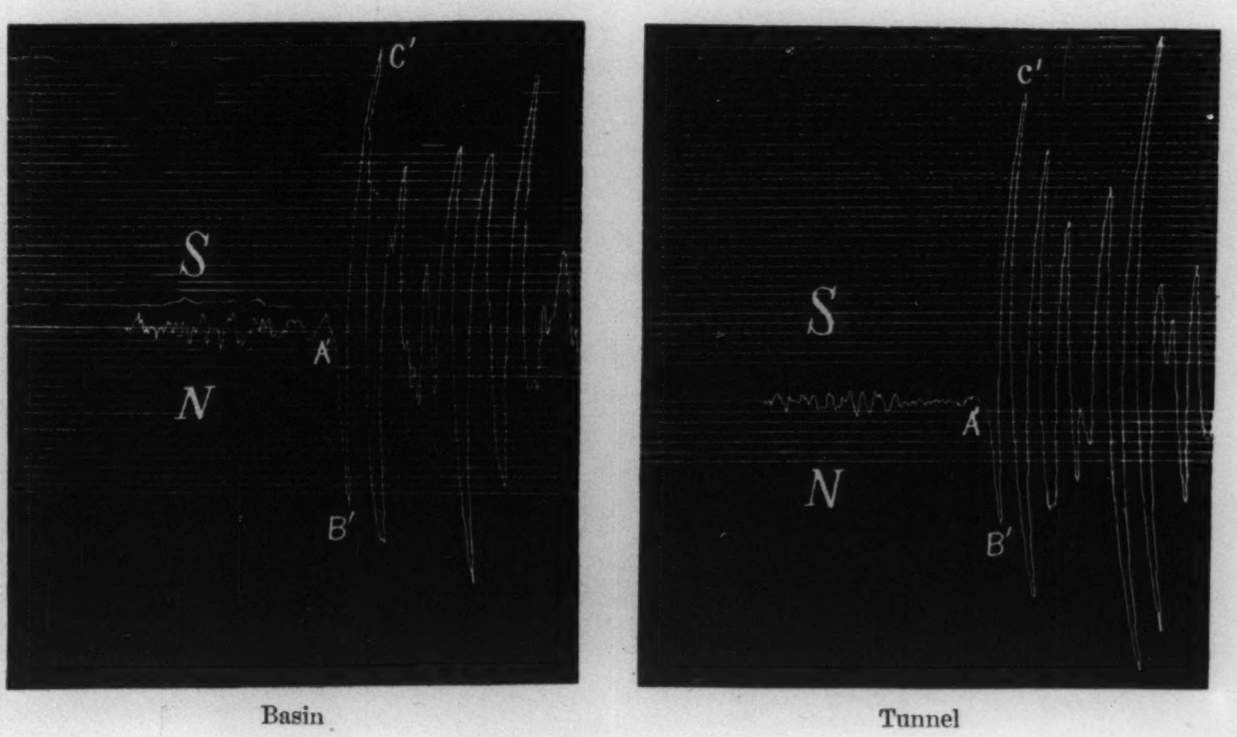

Basin Tunnel

Fig. 12. Seismograms of the earthquake of June 2, 1931.

33. Caractéristiques des ondes séismiques d'après les enregistrements accélérométriques

par **Mishio Ishimoto,**

Institut de Recherches sur les Tremblements de terre.

(Lu le 7 juillet 1931.—Reçu le 20 septembre 1931.)

1. Introduction.

Quand on veut déterminer la position épicentrale d'un séisme, ou étudier la constitution de la croûte terrestre, on porte son attention sur le temps d'occurence ou sur les changements brusques de phases dans les enregistrements sismiques : mais, généralement on a très peu discuté la nature des secousses inscrites, surtout dans la portion principale. Or, nous pouvons distinguer deux sortes de secousses prédominant dans les séismes. Le séismographe enregistre habituellement des secousses de grande période dans le cas d'un fort séisme, tandis qu'il n'enregistre que des ondes de petite période dans le cas d'un faible séisme. Nous distinguons, dans les secousses du grand tremblement de terre d'Idu (le 26 novembre 1930), enregistrées à Tôkyô, la période de 7·5 secondes comme période prédominante[1], tandis qu'on ne voit que des secousses de petite période dans les séismes apparus le jour précédent dans la même région. Ce fait sera expliqué, d'une part comme conséquence d'une différence de mécanisme de production des ondes au foyer, d'autre part en remarquant que, dans l'inscription sismographique, les secousses de grande amplitude, quand elles existent, masquent toujours les secoussses dont la période et l'amplitude sont inférieures[2].

Considérons quelle est l'origine de ces grandes ondes. Il y a deux explications possibles : I) les grandes secousses sont produites au foyer même. 2) Elles se produisent à la surface du sol quand les ondes originelles y arrivent. Nous discutons souvent ce sujet, mais il reste toujours un problème irrésolu parce qu'il n'y a presque pas de témoignages pour décider. Naturellement, puisqu'on installe le seismographe sur le sol, il enregistre en même temps les ondes originelles envoyées du foyer, et les secousses produites secondairement à la surface.

---

1) A. Imamura, *Bull. Earthq. Res. Inst.*, 9 (1931), 36.
2) M. Ishimoto, *ibid.*, 9 (1931), 316.

Dans les enregistrements de séismes lointains, cependant, on constate l'existence d'ondes superficielles, ondes qui se trouvent surtout dans la dernière portion des secousses. On croit, en effet, que la plupart d'entre elles sont des ondes produites dans la région épicentrale, et se propagent jusqu'à la station d'observation. Maintenant nous limiterons notre attention seulement aux séismes voisins ayant une intensité médiocre, qui manquent toujours de coda, portion dernière des secousses, et par suite nous exécuterons notre discussion surtout sur des ondes prédominant dans les parties préliminaire et principale des secousses.

Comme nous l'avons déjà signalé dans le mémoire précédent[3], les secousses de grande amplitude n'ont pas une grande accélération. Naturellement les amplitudes inscrites sur le sismogramme sont celles des déplacements du sol, et il est possible que les ondes de grande amplitude ne soient pas celles qui donnent les accélérations les plus grandes. Certes il y a beaucoup de raisons pour croire que les secousses de grande période ne sont pas celles qui sont envoyées directement du foyer sismique.

Considérons alors deux sortes d'ondes : des ondes primaires et des ondes secondaires. Les primaries sont celles qui sont envoyées du foyer jusqu'à la surface, où elles provoqueront les secondaires. Par suite il est certain qu'il y a en général deux sortes d'ondes enregistrées dans les inscriptions sismographiques.

Nous avons déjà parlé de la différence d'inscriptions obtenues[4] par le sismographe accélérométriques et par le sismographe de type ordinaire. Nous constatons que la plupart des ondes de grande amplitude ont une grande période dans les secondes, tandis que cette sorte d'onde disparaît dans les premières où nous voyons seulement une série d'ondes dont la période est toujours comparativement petite.

Considérons l'énergie cinétique des ondes sismiques que nous supposerons constituées par des ondes sinusoïdales : l'énergie de cette sorte d'ondes rapportée à l'unité de temps est donnée par :

$$E=\pi^2 V^2 \rho \Sigma \frac{a^2}{T^2}$$

où V est la vitesse de l'onde, ρ la densité du sol, a son amplitude, et T sa période. On comprend tout de suite que les ondes de petite période peuvent transporter beaucoup d'énergie bien qu'elles n'aient pas grande amplitude. Cependant, l'existence du frottement intérieur de la croûte terrestre empêche le transport de l'énergie avec des ondes de courte période, et pour une certaine valeur de sa période, l'onde pourra transporter une énergie maxima.

---

[3] M. ISHIMOTO, *loc. cit.*

[4] M. ISHIMOTO, *loc. cit.*

Dans les inscriptions accélérométriques, on a : $A = \frac{4\pi^2 a}{T^2}$ comme amplitude de secousses pour des ondes sinusoïdales. Nous pouvons donc écrire : $E \propto A.a$ qui nous apprend que les amplitudes d'accélération seront exagérées suivant la fréquence, si la distribution d'énergie demeure constante pour toutes les ondes de différentes fréquences : autrement dit le sismographe accélérométrique convient mieux pour inscrire les secousses de petite période. Mais comme le sismographe accélérométrique a sa période propre d'oscillation, sa sensibilité diminue brusquement quand la période approche de zéro, et la proportion d'exagération ne s'appliquera pas aux valeurs inférieures à sa période propre d'oscillation. Nous allons maintenant examiner les inscriptions accélérométriques des séismes apparus au voisinage de Tôkyô.

2. Caractéristiques générales des inscriptions.

Les fig. 1, 2, 3, 4, 5, etc..., sont les inscriptions accélérométriques de secousses sismiques obtenues dans la cave de notre Institut.

Le tableau I indique les données de ces séismes. On comprendra d'un coup d'oeil leurs caractéristiques génerales. Nous allons les donner les unes après les autres.

Tableau I.5)

No.	Temps d'occurence					Epicentres	
		j	h	m	s		
25	mai	4	23	48	29	E 139°·8	N 36°·2
26		12	03	27	08	141·2	37·3
27		25	15	49	37	141·4	37·9
28		25	19	27	52	139·1	35·2
29		26	18	12	25	141·8	37·2
30	juin	2	11	38	35	—	—
31		9	14	08	09	140·5	36·5
32		11	15	16	20	138·9	35·6
34 6)		17	21	09	50	139·6	35·7
37		23	15	15	26	141·4	36·2

---

5) Les détails des données se trouvent dans *Bull. Earthq. Res, Inst.*, 9 (1931), 509.

6) Son inscription a été déjà montrée dans ce Bulletin, 9 (1931), 374, Pl. XLIII.

1. Le début des secousses demeure assez petit.

2. Il y a plusieurs types de secousses préliminaires : a) les amplitudes restent toujours uniformes, comme c'est le cas dans les séismes apparus au large d'Iwaki ; b) les amplitudes varient brusquement ; c) il y a deux ou trois étages d'amplitudes.

3. Il y a un changement très net d'amplitude entre les secousses préliminaires et les secousses principales : cette distinction correspondra certainement à la distinction des ondes *P* et *S* définies par l'inscription sismographique.

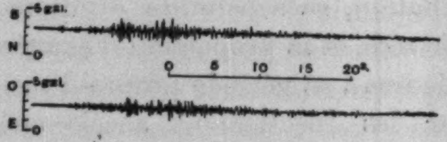

Fig. 1. (No. 25).

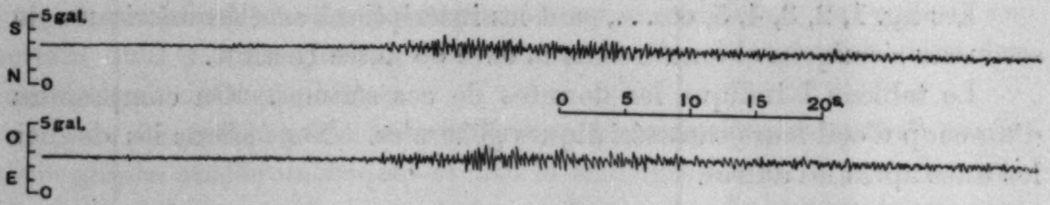

Fig. 2. (No. 26).

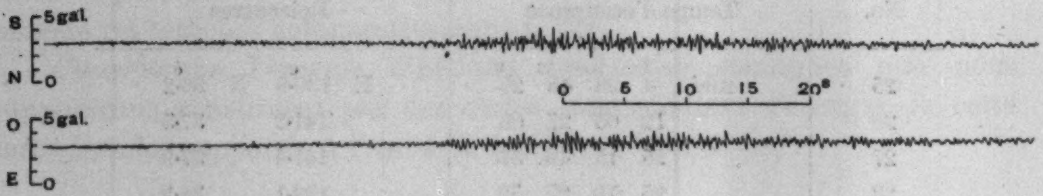

Fig. 3. (No 27).

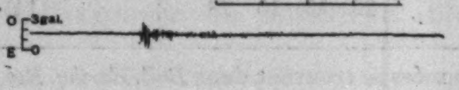

Fig. 4. (No. 28).

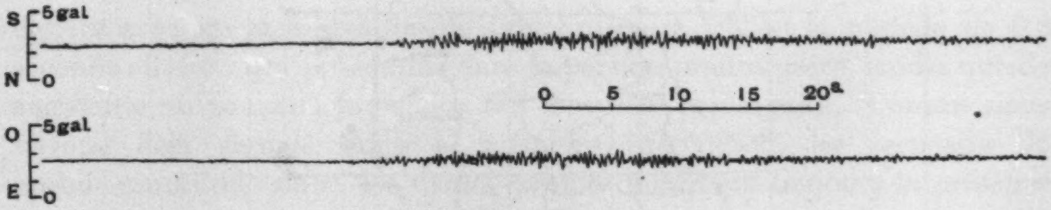

Fig. 5. (No. 29).

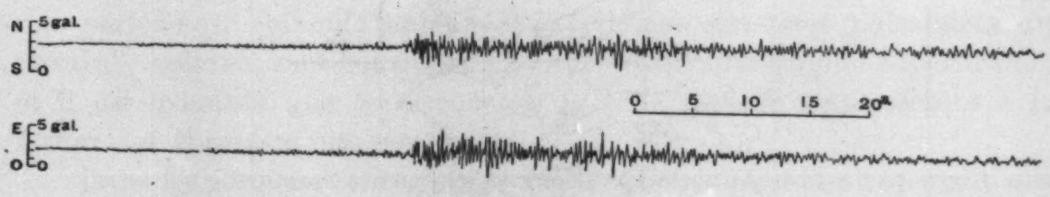

Fig. 6. (No. 30).

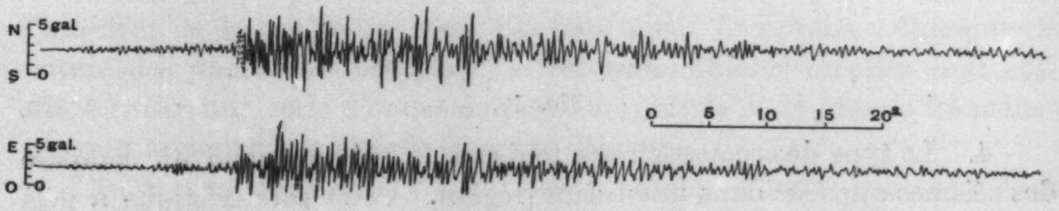

Fig. 7. (No. 31).

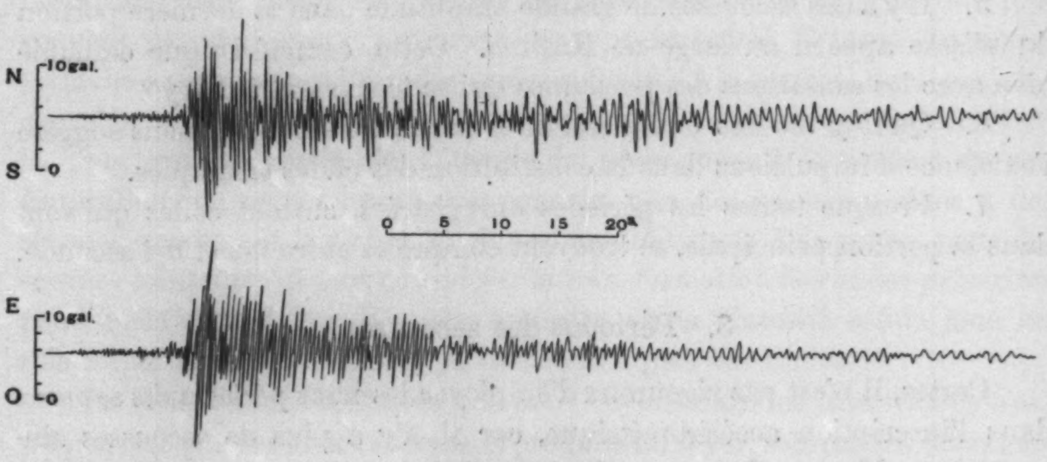

Fig. 8. (No. 32).

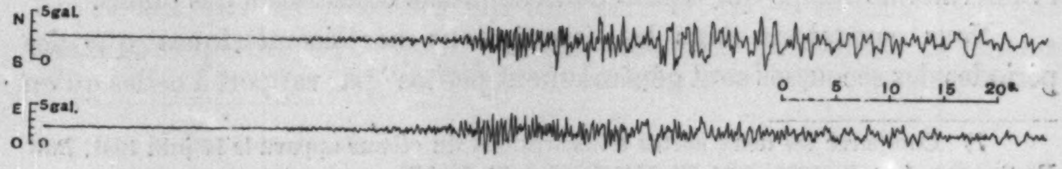

Fig. 9. (No. 37).

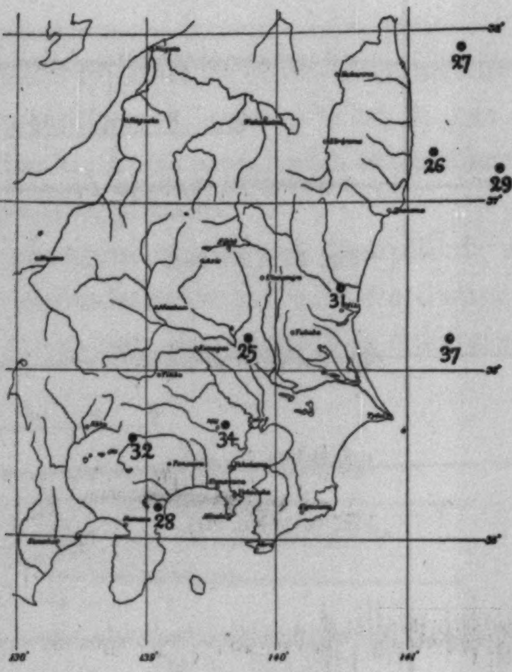

Fig. 10.

4. Le type de secousses reste toujours le même quand on compare des séismes apparus dans une même région. Cette caratéristique a déjà été indiquée par le Prof. Omori d'après l'inscription sismographique.

5. Il y a des secousses de grande amplitude dans la dernière portion du séisme apparu au large de Kasima. Cette caractéristique coïncide bien avec les sensations des personnes qui se trouvaient à Tôkyô.

6. Qu'il y ait des ondes solitaires parmi les secousses nous suggère l'existence d'impulsions dans la constitution des ondes sismiques.

7. Presque toutes les périodes enregistrées, surtout celles qui sont dans la portion principale, se trouvent comprises entre 0·2 et 0·4 seconde.

3. Périodes des secousses.

Certes, il n'est pas rigoureux d'employer les mots *périodes des secousses* dans l'inscription accélérométrique, car il n'y a plus de secousses sinusoïdales. Nous voulons cependant élargir le sens de ce mot qui signifiera l'intervalle de temps qui sépara deux sommets consécutifs des ondes.

Nous constatons dans les inscriptions accélérométriques que les périodes des secousses sont généralement petites[7] par rapport à celles qu'on obtient avec un sismographe de type ordinaire. C'est la période de 0·2 seconde environ qui prédomine dans la portion préliminaire, tandis qu'elle augmente un peu dans la portion des secousses principales. Comme nous l'avons déja signalé dans le mémoire précédent[8], les secousses de grande amplitude dans les sismogrammes masquent toujours la présence des secousses dont la période et l'amplitude sont petites. Les secousses de grande amplitude energistrées par le sismographe de type ordinaire ont une période qui coïncide toujours avec celle des secousses pulsatoires du terrain[9]; celles-ci sont considérées comme ayant une origine superficielle, et il est possible que les secousses de telle période apparaissent à la faveur des ébranlements sismiques.

---

[7] Comparer les deux sortes d'inscirptions du séisme apparu le 17 juin 1931. *Bull Earthq. Res. Inst.*, 9 (1931), 374, Pl. XXXVII et Pl. XLIII.

Dans les secousses enregistrées accélérométriquement on aperçoit des secousses ayant un rapport étroit avec les ondes primaires envoyées directement du foyer. Mais ces ondes primaires se modifient en traversant l'intérieur de la croûte qui n'est pas tout à fait homogène. Quoique la nature des ondes soit complexe, il est vraisemblable qu'elles sont constituées par une série d'ondes de petite amplitude et de grande fréquence pouvant apporter une grande quantité d'énergie.

Nous constatons qu'il y a un certain nombre d'ondes solitaires dans les inscriptions accélérométriques : elles sont relativement visibles quand l'intensité reste médiocre. Certes les secousses de ce type seront provoquées par des ondes primaires de type impulsif. Comme les ondes primaires peuvent produire des ondes solitaires à la surface, nous pouvons considérer les ondes primaires comme une série de chocs qui transmettent la plus grande partie de l'énergie du foyer jusqu'à la surface du sol. Naturellement, nous ne nous occupons ici que des secousses dues à des séismes voisins, et il y aura quelques modifications à apporter pour les séismes lointains : il faut considérer la transformation des ondes primaires pendant le voyage dans la croûte terrestre, où la viscosité solide joue un rôle important pour modifier les caractéristiques des ondes.

La série d'ondes solitaires que nous voyons dans les inscriptions s'explique, soit par des chocs successifs produits au foyer, soit par les réflexions d'un seul choc dans la croûte hétérogène.

Le fait que les secousses ont une période de 0·3 seconde sera une même conséquence de ce qu'il y a des secousses pulsatoires de même période qui prédominent surtout dans la partie haute de la ville de Tôkyô. Cette période d'oscillation est due à l'oscillation propre de cet endroit, et il est possible qu'elle soit provoquée par l'arrivée des chocs. Une explication semblable a déjà été donnée par M. le Prof. K. SUYEHIRO(10), Directeur de notre Institut, en employant un appareil analysateur de secousses sismiques. Nous savons de plus que, même dans le cas de la chute d'un corps lourd sur le sol, il y a production d'ondes(11) dont la période est à peu près de 0.2 seconde.

---

[8] M. Ishimoto, *loc. cit.*

[9] On constate qu'il y a plusieurs valeurs de périodes prédominantes dans les secousses pulsatoires; leurs valeurs prédominantes sont 4·0 et 8·0 secondes environ

Parmi les secousses sismiques on peut donner comme exemple d'oscillations dont les amplitudes vont en augmentant celles qui sont obtenues sous l'action d'un excitateur(12). En tout cas, nous venons de constater certaines caractéristiques des secousses qui ont un rapport étroit avec la constitution régionale du terrain.

La Fig. 11 montre l'analyse des secousses d'un fort tremblement de terre(13) dont l'épicentre a été fixé aux environs de Tôkyô. On constate que les secousses sont constituées par des ondes dont la période va de 0.2 à 0.4 sec. : la période des secousses principales est plus grande que celle des secousses préliminaires. Il n'y a presque plus d'ondes inférieures à 0.2 seconde : cela dépend en partie du fait que la sensibilité de l'appareil diminue brusquement quand la période approche de zéro.

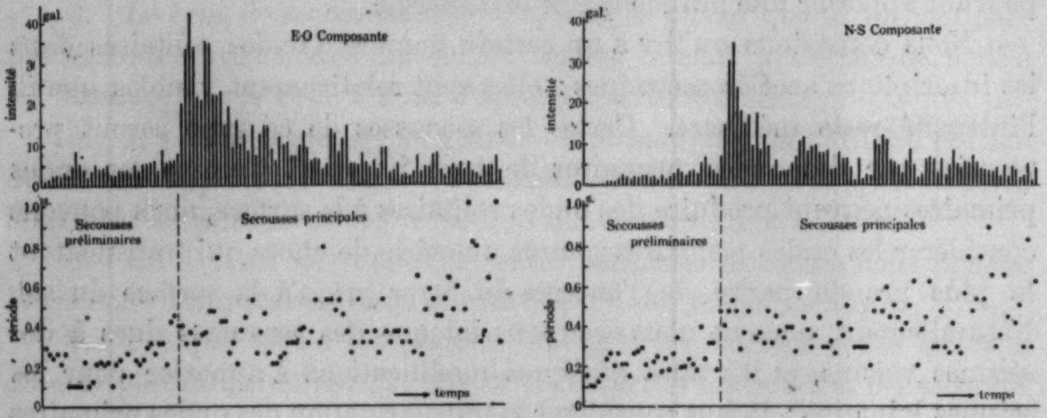

Fig. 11.

---

(10) K. SUYEHIRO, *Bull. Earthq. Res. Inst.*, 1 (1926), 59: *Proc. Imp. Acad.*, Japan, 2 (1926), 268.

(11) N. NASU, *Disin*, 1 (1929), 355.

(12) Voir la Fig. 1 où nous voyons les amplitudes aller en augmentant dans la partie préliminaire de secousses.

(13) Les inscriptions accélérométriques de ces séismes se trouvent dans ce Bulletin 9 (1931), 374, Pl. XLIII.

4. Structure des secousses.

Les amplitudes des secousses enregistrées accélérométriquement sont toujours inférieures dans la portion préliminaire à celles des secousses principales : cette relation existe aussi dans les enregistrements des sismographes de type ordinaire.

L'apparence de l'inscription dépend de l'intensité des secousses : quand elle est médiocre on peut constater facilement l'apparition des ondes solitaires dans la portion principale, et quelquefois même dans la portion préliminaire, des secousses ; leurs apparitions dépendent d'ailleurs de la position épicentrale. Quand les secousses sont assez fortes, il y a des cas où la prédominance des fortes secousses nous empêche de distinguer les ondes solitaires.

Le tableau II montre les intervalles des ondes solitaires dans les secousses ; ils ne sont pas constants ni pour tous les épicentres, ni pour la durée des secousses préliminaires. L'origine de tels intervalles s'explique par un seul choc passant par un certain nombre de sections verticales dont les paramètres d'élasticité sont différents. Le Prof. K. SEZAWA[14] a déjà considéré une telle constitution de la croûte et expliqué les secousses observées à la surface, par une étude théorique.

Tableau II.

No.	Dates		Intervalles des ondes solitaires consécutives
25	mai	4	4.7 5.6 seconde
26		12	5.2 6.6 9.3
27		25	4.5 8.4
28		25	6.8 7.4
29		26	6.9 7.3
30	juin	2	3.5 4.2 5.5 6.6
31		9	4.1 6.1
32		11	3.4 5.2
34		17	6.9 14.4
37		23	5.2 6.5

D'après nos observations cependant il nous semble qu'il est difficile d'avoir une solution complète avec les résultats obtenus à une station unique. Nous avions essayé de trouver quelque correspondance entre le changement de phase et l'apparition des ondes solitaires, mais il n'y a presque pas de coincidence entre eux. En tout cas nous pouvons considérer les secousses sismiques observées à la surface comme le résultat d'une série de chocs qui font réagir la couche superficielle, laquelle posséde une oscillation propre. Il y aura, en effet, des discontinuités des paramètres élastiques du sol, dans les directions horizontales et verticales, pour réaliser l'oscillation propre.

---

[14] K. SEZAWA, et G. NISHIMURA, *Bull. Earthq. Res. Inst.*, 8 (1930), 321.

Par suite, les secousses sismiques observées à la surface du sol sont d'une part, le résultat d'une série de chocs qui bombardent la surface, et d'autre part, des secousses provoquées secondairement à la surface[15], et nous sommes obligée de refléchir aux discussions faites jusqu'à maintenant. Certes, nous ne pouvons pas observer à Tôkyô les ondes primaires envoyées du foyer ; c'est parce qu'il y a une grande épaisseur de couches sédimentaires nouvelles dans cette région, qui les empêchent d'arriver jusqu'à la surface. Cependant, il nous semble qu'à Tukuba[16] région granitique, on peut constater que les secousses peuvent arriver à la surface sans être affectées par l'existence de couches superficielles : car nous entendons toujours des bruits qui accompagnent les secousses sismiques. Il est donc vraisemblable que les ondes originelles sont une sorte de bruit, en ce sens qu'elles sont une succession d'impulsions tant qu'elles restent dans la croûte. D'après l'étude de M. W. INOUE[17], nous pouvons constater qu'il a une même conception des secousses sismiques : il a montré que les secousses sismiques enregistrées à Tukuba semblent comporter les oscillations propres de cette région. Cela nous donne une preuve de l'hypothèse dont on a déjà parlé plus haut.

Quand on considère les ondes primaires comme une série de chocs il y a lieu de rappeler une expérience[18], exécutée par le Prof. T. TERADA. Il a pris un pendule dont la masse était bombardée par une chute de mitraille. Son résultat nous montre que le déplacement enregistré de la masse s'accorde très bien avec des inscriptions séismiques. Cette expérience nous suggère un modèle expliquant les phénomènes sismiques. Comparons les impulsions des mitrailles aux ondes primaires, et le pendule au terrain. On pourra aisèment imaginer un rapport entre les ondes primaires et les secousses secondaires produites à la surface.

---

[15] Quand l'intensité des ondes primaires est assez grande, il est vraisemblable que celles-ci provoquent des secousses de grande amplitude à la surface, et le sismographe de type ordinaire enregistre principalement ces secousses.

[16] montré dans Fig. 10.

[17] pas encore publié.

[18] T. TERADA, et U. NAKAYA, *Bull. Earthq. Res. Inst.*, 5 (1928), 93.

Nous pouvons encore remarquer un autre fait confirmant notre opinion. Monsieur N. NASU[19] a réussi à enregistrer un certain nombre de séismes en employant deux sismographes installés séparément, l'un dans le tunnel de Tanna, l'autre au-dessus. Son résultat nous montre que les ondes enregistrées sont toutes du type des ondes superficielles, c'est-à-dire que toutes les ondes sont des ondes secondaires conduites à la surface. Ce fait nous affirme que les secousses observées à la surface sont autre chose que ce qui est rayonné originellement du foyer.

Nous ne considérons jamais les ondes enregistrées par le sismographe accélérométrique, comme des ondes primaires; mais il est certain que quand on veut obtenir des ondes primaires, les enregistrements accélérométriques servent mieux. Nous avons en effet l'intention d'exécuter nos observations accélérométriques dans un endroit où il n'y aura pas de couches sédimentaires nouvelles.

En tout cas, pour les observations des secousses sismiques on ne peut pas se contenter des sismographes de type ordinaire. Nous croyons qu'il est rigoureusement nécessaire d'employer les sismographes accélérométriques quand on veut exécuter des observations sismiques pour savoir, d'une part, le degré d'intensité des secousses, d'autre part, la vraie nature du phénomène sismique. Bien que le sismographe du type ordinaire soit un appareil bien convenable pour observer des séismes éloignés, le sismographe accélérométrique sera un appareil très utile pour observer les secousses dont l'intensité est de l'ordre de celles ressenties par les hommes.

---

[19] N. NASU, *Bull. Earthq. Res. Inst.*, 9 (1931) 454.

33. 加速度地震計記象より考察せる地震の性質

地震研究所　石本巳四雄

地震觀測においては發震時或ひは位相の變化が專ら注意されるに拘らず震動其のものに對する議論は餘り行はれて居ない。大地震の場合一般地震計に記錄された震動の中には常に大なる振幅を有する數秒の周期が見受けられるが、此の波動は震源において發せられたものであるとは信じ難い。

加速度地震計を以て地震動を記錄する場合、以上の大なる振幅、周期を有する震動は消滅し0·2秒より0·4秒に至る周期の震動が常に卓越して居る事が確められた。地震觀測はすべて地表で爲される關係上、吾々の觀測結果中には震源において發せられた波動に加へて地表において二次的に誘發された震動をも同時に記錄され居る事は勿論であり、此の二種類の波を區別して考へて見る必要がある。

加速度地震計によつて記錄された地震動の中主要動附近には特に獨立波が存在し突發的に加速度の大なる運動が見出される。此の事實から吾々は地震の本體が斯樣な加速度を生ぜしむべきものである事、即ち不均質の地殼中を通過する間に多少の變化は受け乍らも震源において發せられたものは衝擊的のものである事を信ずる事が出來る。

0.3秒附近の周期は東京山手に常に存在する微動であり、此れが土地固有の震動周期である事から、震源において發せられた一次波が地表に達する場合此の固有震動が增長されると考へられる。此の事實は且て末廣所長によつて地震動分解器觀測結果から指摘されたものである。

一般地震計によつて記錄される大なる振幅、周期を有する震動も同樣に東京地方に存在する脈動に比較さるべきものであり、地震發生に伴つて誘發されるものと見られる。地震の本體が一次的に衝擊であり、地殼中においては恰も噪音に比較すべきものであると信ぜられる事から、表面層を缺除する地方においては地震に伴つて地鳴の出現する現象も容易に解釋されるものとなる。

最近那須理學士が丹那隧道中及び隧道上において同時觀測を行つた結果によれば記錄された地震動がすべて表面波的性質を具へて居ると云ふ事が確められた。此の事實は正に上記の考察を證明する上に充分力あるものと云はなければならない。又寺田博士によつて行はれた振子の實驗（振子の兩側に散彈の亂衝擊を加へて其の變位を記錄せしめたもの）は地表において觀測する地震動の機巧を理解するに最も適切な模型として考へる事が出來る。

34. 武田ビルデング振動驗測結果報告

福　富　孝　治

(昭和六年七月七日發表—昭和六年九月十七日受理)

獨逸工學博士久米權九郎氏の御依賴に依つて、昭和六年四月二十五日より五月二十六日まで一ヶ月間日本橋通一丁目の武田ビルデングの振動驗測を行ひました。此の結果に就きまして概略ではありますが報告申し上げます。

武田ビルデングは渡邊久米建築事務所設計、昭和土木株式會社施工の鐵筋コンクリート造の建築物でありまして、器械据付の當時は既に九分通り竣功して居りまして只上塗が殘つて居る程度でありました。建築物の大きさは第一圖に示します樣に建坪 271 平方米 (82·1 坪)、地面上の高さ約 30·2 米(約百尺)の比較的棒狀の建築物であります。敷地の地質は二回のボーリングの結果明らかでありまして、復興局建築部の調査[1]に依りますと地面より約6米の深さに於いては既に比較的堅硬な第三紀層が表れて居る事が知られて居ます。建築物は地下 5·45 米に基底がありましてその下には長さ 10·9 米の松の杭が 560 本打ちこんであります。建築物は地下一階、地上は一階、中二階、二階から九階まで十階であります。四月二十五日器械を先づ地階、四階、九階の◉印の場所に建築物の壁の方向に平行に据付けました。卽ち第一圖に示される樣に地震計の東西、南北を取りました。地震計の北の方向は實際の北から時計の針の進む方向に 26·5° 偏よつて居ます。驗測に用ひました器械は大正十四年式簡單微動計三臺でありまして、一分毎の time mark は同時に入れ又地震計の drum の廻轉速度は一分時につき 5 粍から 7 粍位でありました。五月十六日以後は四階の器械を六階に移轉して觀測致しました。各地震計の常數を示せば次の樣であります。

---

1) 復興局建築部　東京、橫濱地質調査報告

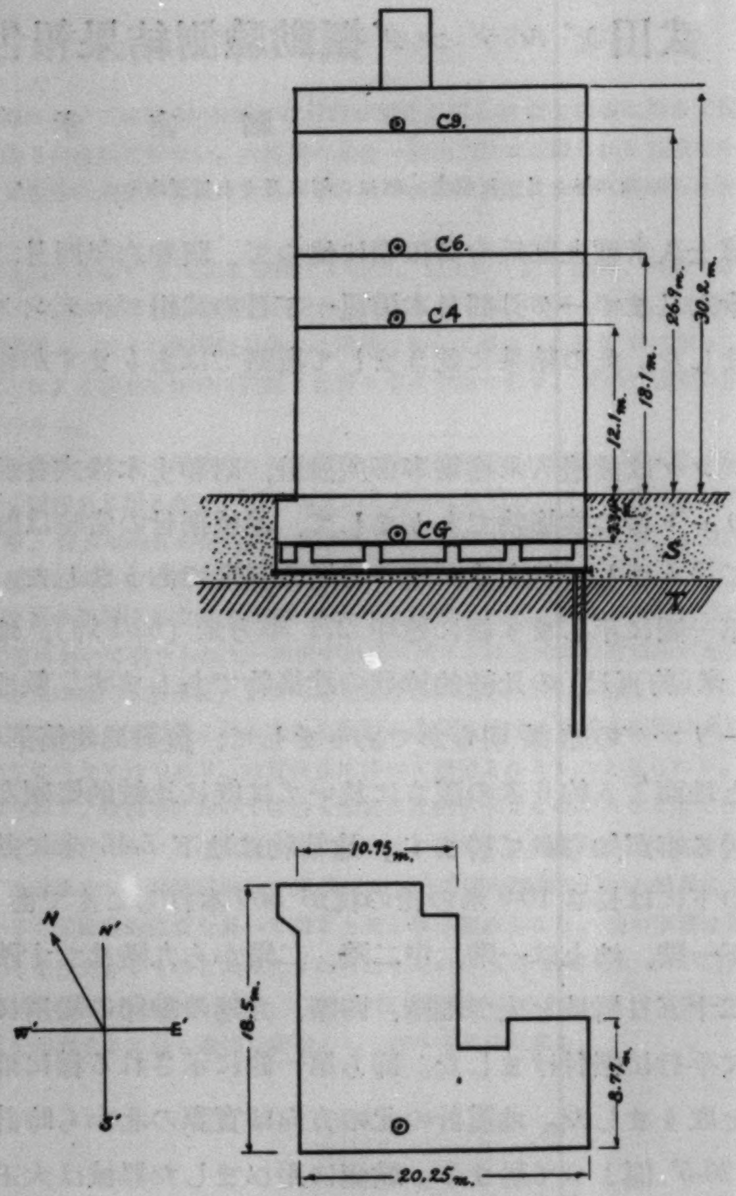
C9.
C6.
C4
CG
30.2 m.
26.7 m.
18.1 m.
12.1 m.
L
S
T
10.95 m.
18.5 m.
8.77 m.
20.25 m.
N
N'
W'
E'
S'

第一圖 武田ビルデング畧圖

Fig. 1. Sketch of the Takeda Building.

Small circle indicates the place where Tromometer was installed.

S indicates Filled-in soil.

T „ Tertiary layer.

第一表

微動計の常數
CG: 地階
C 4: 四階
C 6: 六階
C 9: 九階

Table I.

Constants of Tromometers
Underground of the structure
Fouth floor of " "
Sixth floor of " "
Ninth floor of " "

1. April 27th.

位置 Place	器械 Instrument	成分 Component	倍率 Mechanical Magnification	T_0*sec.*	ε	r mm.
CG	1925-type Portable Tromometer	EW	50	5·32	0·10	0·73
		NS	"	5·43	0·13	1·67
C4	"	EW	"	5·48	0·17	1·41
		NS	"	5·46	0·13	2·61
C9	"	EW	"	5·52	0·13	1·66
		NS	"	5·48	0·10	0·36

2. May 16th–18th.

CG	1925-type Portable Tromometer	EW	50	4·84	0·10	2·67
		NS	"	5·31	0·16	0·62
C6	"	EW	"	5·45	0·09	2·09
		NS	"	5·56	0·13	2·62
C9	"	EW	"	4·98	0·15	1·98
		NS	"	4·74	0·12	1·59

I. 建築物日常の振動

九階、六階、四階に据えられた器械では日常0·2秒から0·5秒位の週期の微動が見られましたが地階の器械では全く見えないか、痕跡的に見得る程度でありました。この微動に就いて針の吸上げ直前の振動を各階について比較しますと非常によく位相 (phase) が一致致しました。是れは建築物が部分的な振動をする事なく、全體としての振動をして居る爲め

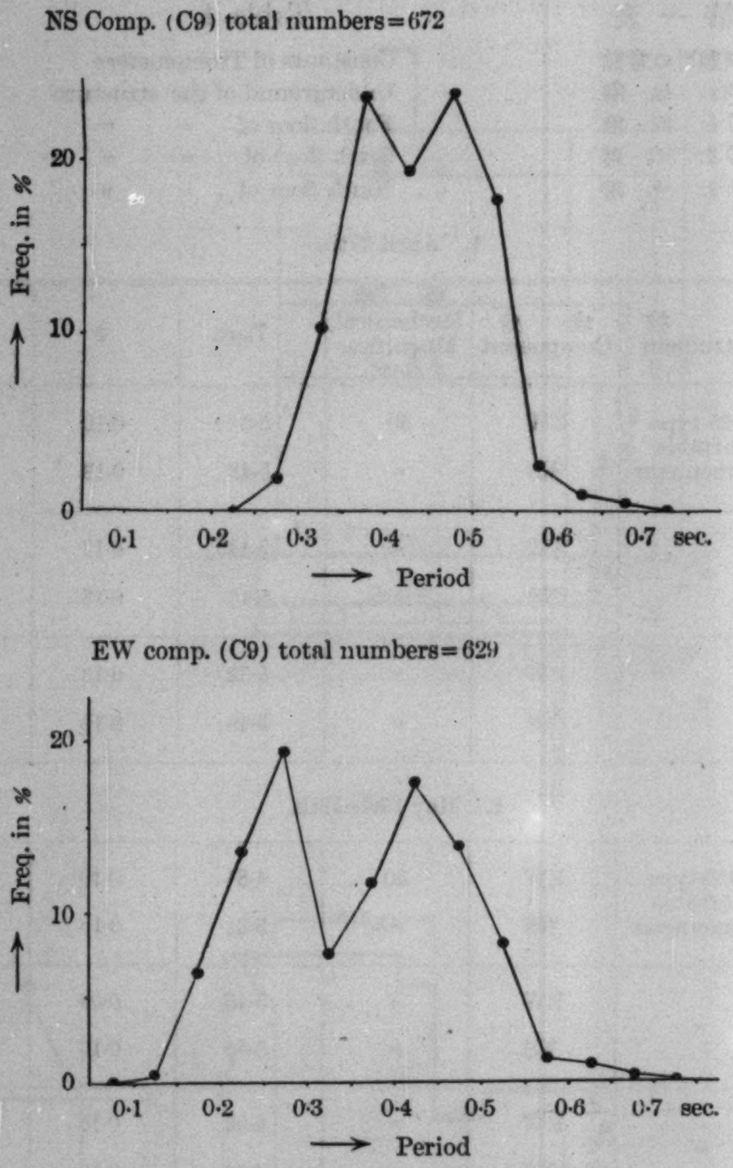

NS Comp. (C9) total numbers=672

EW comp. (C9) total numbers=629

第二圖　建築物の自己振動週期の頻度分布

Fig. 2. Frequency distribution of the self-vibration periods of the structure.

であると考へられます。それで九階の東西、南北の兩成分につきまして、その一つ一つの振動の週期を測つてその頻度曲線 (frequency curve) を作つて見ますと、第二圖の樣に東西動では 0·27 秒、0·43 秒で頻度が大となつて居ますし、南北動でも 0·37 秒、0·49 秒位で頻度が大となつて居ます。即ちこの建築物は大約 0·4 秒位の振動週期を有する事が知られます。

次ぎに一振動毎に、各階の振幅と9階の振幅との比を作り、これを多くの振動について調べてその頻度曲線を作りますと第三圖を得ます。即ち東西動では 9 階の振幅を 1 にとつた場合、6 階では 0·84、4 階では 0·72 位の振幅の振動が多く、南北動では 9 階の振幅を 1 に取つた場合、

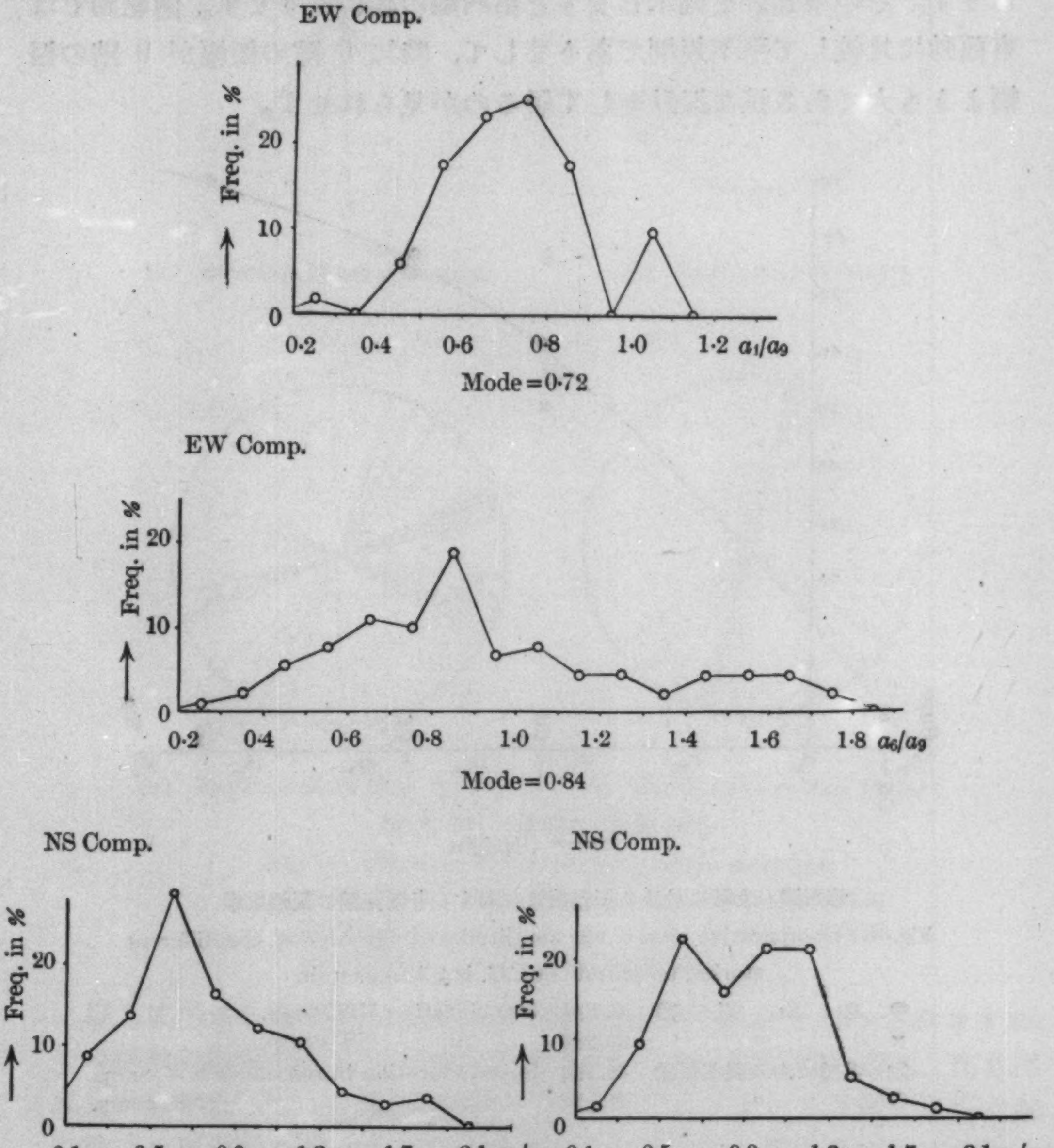

第三圖　自由振動振幅の各階と九階との比の頻度

Fig. 3. Frequency distribution of the ratios of amplitudes a^4/a_9 and a_6/a_9.

6 階は 0·62 及 1·09 卽平均 0·85、4 階では 0·61 位の振幅の振動が多くあります。地階に於ては東西、南北兩成分共に全く振動が見えないか痕跡的に見える程度でありましたが、9 階の振幅を 1 とすれば地階の振幅は平均 0·06 位であります。卽ち概して上層にゆく程、振動の振幅は增します。その增し方を圖示しますと第四圖の樣になります。南北動では東西動に比較して稍不規則でありまして、時に 6 階の振幅が 9 階の振幅よりも大である樣な振動をして居るのが見られます。

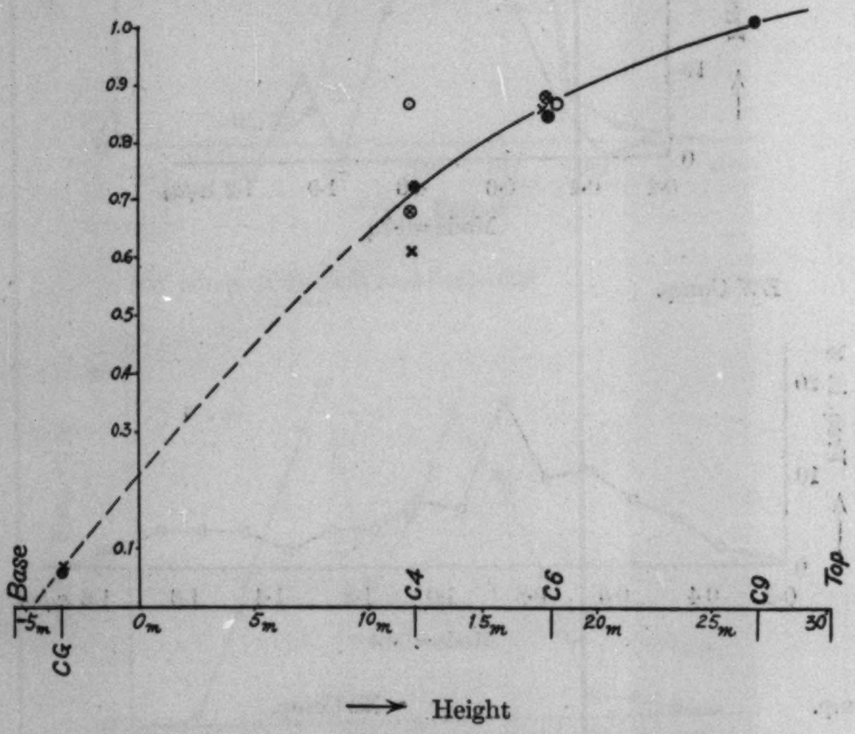

第四圖　九階に於ける振動振幅に對する各階振動の振幅比率

Fig. 4. Comparative view of the amplitudes of vibration at the different stories, amplitude at C.G. is taken as unit.

●	自由振動	東西動	free vibration EW comp.
×	”	南北動	” NS comp.
⊗	共鳴にある强制振動	東西動	forced vibration in resonance EW comp.
○	”	南北動	” NS comp.

次ぎに一振動每に 9 階の東西、南北兩成分を組合してその振動方向を求めて、その頻度を圖示しますと第五圖 (a) の樣になります。卽ち北東の方向の振動が最も多い事が知られます。

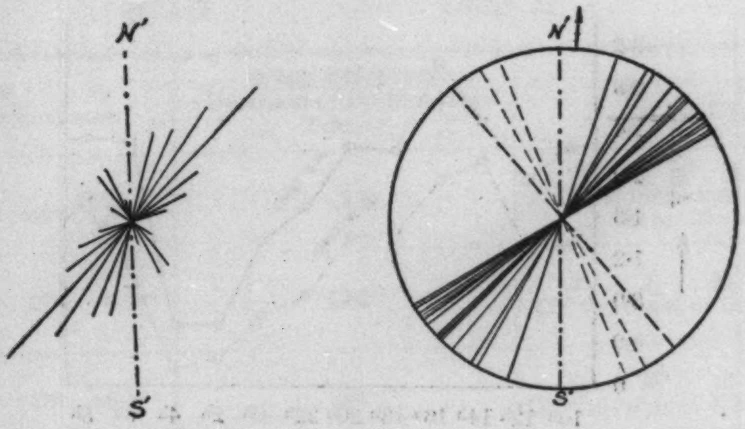

(a) direction of free-vibration. (b) Earthquake of May 4.

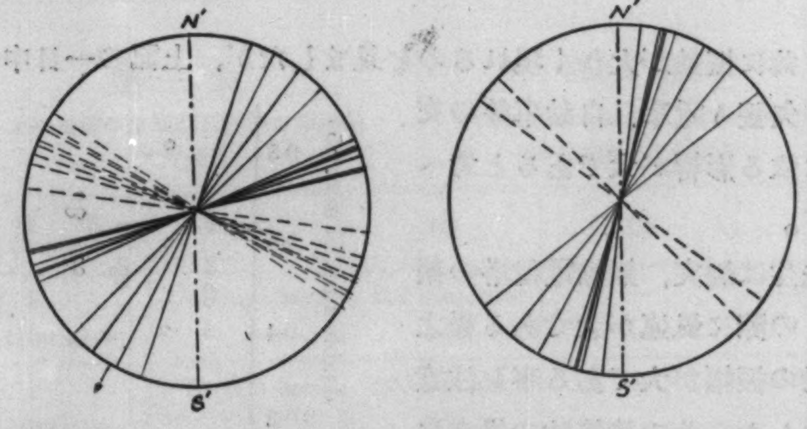

(c) Earthquake of May 5, 19^{h}. (d) Earthquake of May 25, 15^{h}.

第五圖、建築物の振動方向、

Fig. 5. Direction of the vibration of the structure.
Full line: direction of principal vibration at C9.
Broken line: " " " at C.G.
Arrow head: " " epicentre.

以上述べました振動は建築物に固有な振動であると考へられますが、この振動の振幅の一日中の消長を調べますと第六圖の様に東西、南北兩成分共に午後三時、午後四時頃振幅が最大となりまして9階では南北動で約 3μ 東西動で約 2μ となります。又午前二時、四時頃振幅は最小となりまして南北動で $0{\cdot}6\mu$、東西動で $0{\cdot}2\mu$ となります。南北、東西の兩成分を比較しますと南北動は東西動の約 1·8 倍位常に大であります。觀測の際、屢々電車が日本橋交叉點を通過する時に、がたん、がたんと云

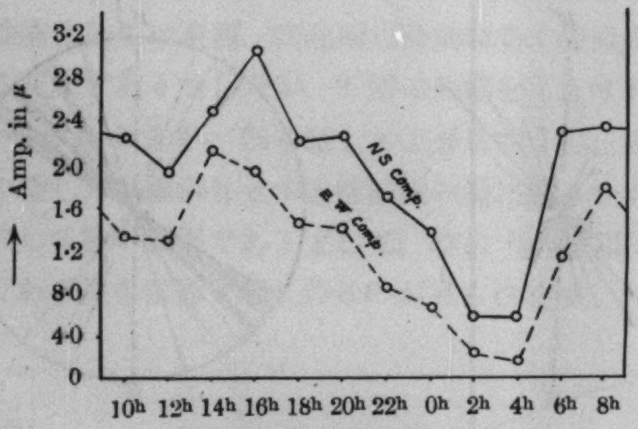

第六圖　建築物固有振動振幅の一日中の變化

Fig. 6. Diurnal variation of the amplitude of free vibration.

ふ音響と共に振動が大きく現れるのを見ましたが、上記の一日中の振動の消長も矢張り電車、自動車等の交通機關に依る影響が大であると考へられます。

大森先生は煙突、無線電信塔の振動驗測[2] の際に風速が大である程之等の振動の振幅が大である事を注意せられました。此の建築物の場合に於いては、毎日午前六時頃の平均振幅と天氣圖から讀み取つた午前六時の風速とを比較して見ましたが第七圖の樣にあまり明瞭な關係は見出せませんでした。

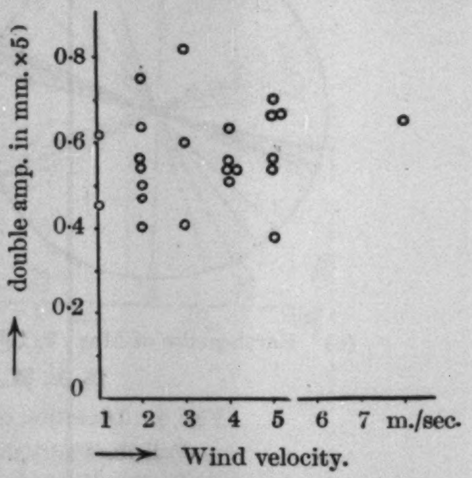

第七圖　固有振動振幅と風速との關係

Fig. 7. Correlation between the vibration of the structure and wind velocity.

II. 地震の際の建築物の振動

振動驗測中、有感地震四回、無感覺地震三十五回、遠震五回が觀測されました。有感地震の發震時、震央等を擧げれば第二表の樣であります。

---

[2] 大森房吉　構造物振動驗測調査報告前編（震災豫防調査會報告 97 號）.

第二表 Table II.

發震時 Time of Occurrence	初期微動繼續時間 Duration of Preliminary Tremor	震央 Epicentre
(1931) May 4 23^{h} 48^{m} $28{\cdot}6^{s}$	$8{\cdot}1^{s}$	利根川流域 Drainage basin of River Tone.
May 12 3^{h} 27^{m} $8{\cdot}3^{s}$	23·2	小名濱沖 Off the coast of Onahama.
May 25 15^{h} 50^{m} $36{\cdot}9^{s}$	29·9	金華山沖 Off the coast of Kinkwazan.
May 25 19^{h} 27^{m} $51{\cdot}5^{s}$	9·8	相模西南部 South-western part of Sagami province.

第三表 Table III.

上記地震の主要動五秒間の平均最大加速度

5-minute means of max. acc. of principal motions.

發震時 Time of Occurrence	CG	C4	C6	C9
May 4	4·9 mm./sec.^{2}	12·5 mm./sec.^{2}	—	17·4 mm./sec.^{2}
(Ratio)→	1	2·55		3·55
May 12	5·5 mm./sec.^{2}	12·0 mm./sec.^{2}	—	22·0 mm./sec.^{2}
(Ratio)→	1	2·18		4·00
May 25 (15^{h})	11·1 mm./sec.^{2}	—	43·5 mm./sec.^{2}	56·7 mm./sec.^{2}
(Ratio)→	1		3·92	5·10
May 25 (19^{h})	5·2 mm./sec.^{2}	—	19·4 mm./sec.^{2}	20·5 mm./sec.^{2}
(Ratio)→	1		3·73	3·94
Mean ratios of max. accelerations.	1	2·36	3·82	4·15

第三表は四有感地震の主要動五秒間の平均最大加速度であります。(地震動が正弦運動をするものと假定して計算しました)。表の様に上層程地震の際の最大加速度は大で、九階では地階の約四倍に達して居ます。

地震の際の各階の振動の位相 (phase) を見ますと、地階と其他の各階とを比較致しますと、初動及主要動の初め、地震の後尾部には差は認められませんが其の他の部ではあまりよく一致はして居りません。然し乍

ら四階、六階、九階の振動の位相は東西成分では非常によく一致して居ります。南北成分でも大體一致して居ります。これは此の建築物が全體として振動して居る事を益々強く證據立てる事であります。（第十圖、第十一圖の寫眞參照）

第四表

四有感地震の各階に於ける振幅週期の五秒間毎の平均値

數字は微動計に記錄された値の全振幅

Table IV.

5-minute means of amplitudes and periods of 4 sensible earthquakes observed at underground, 4th, 6th and 9th floors.

Figures indicate the double amplitude in mm. × 50.

(1) 五月四日の地震 (Earthquake of May 4.)

	EW comp.				NS comp.			
	Mean period in CG sec.	Mean double amp. in CG	Mean double amp. in C4	Mean double amp. in C9	Mean period in CG sec.	Mean double amp. in CG	Mean double amp. in C4	Mean double amp. in C9
1	0·37	0·29	1·52	1·83	0·42	0·65	1·62	1·58
2	0·39	1·36	3·64	5·69	0·39	1·22	2·90	3·11
3	0·39	0·99	2·95	4·93	0·39	1·19	4·09	6·14
4	0·42	1·34	4·74	6·19	0·46	1·51	5·16	6·54
5	0·42	0·71	2·23	4·81	0·39	1·09	2·83	3·01
6	0·39	0·68	2·85	4·55	0·46	1·53	4·77	4·18
7	0·31	0·53	1·29	2·98	0·39	0·50	1·39	3·15
8	0·39	0·54	1·70	2·27	0·46	0·56	1·00	1·83
9	0·42	0·57	0·94	1·47	0·50	0·64	1·46	1·85
10	0·42	0·47	0·76	1·66	0·56	0·47	1·68	2·09
11	0·56	0·41	0·91	1·00	0·72	0·64	1·05	1·56
12	0·63	0·49	1·21	1·61	0·46	0·42	0·99	1·48
13	0·50	0·39	0·88	1·32	0·50	0·30	1·36	1·35
14	0·50	0·35	0·63	0·81	0·56	0·40	1·14	1·04
15	0·50	0·32	0·86	1·01	0·63	0·30	1·26	0·94
16	0·72	0·29	0·41	0·62	0·63	0·32	1·00	0·75
17	0·72	0·29	0·38	0·56	0·63	0·26	0·53	0·46
18	0·72	0·30	0·35	0·49	0·63	0·21	0·77	0·65
19	0·84	0·28	—	—	1·00	0·46	0·55	0·55
20	1·00	0·45	—	—	0·72	0·13	0·27	0·37
21	0·84	0·17	—	—	0·84	0·23	0·28	0·27
22	0·84	0·22	—	—	1·25	0·28	0·29	0·31
23	2·50	0·23	—	—	1·25	0·20	0·26	0·24
24	1·00	0·15	—	—	2·00	1·57	0·20	0·17
25	0·72	0·15	—	—	1·00	0·17	0·22	0·17
26	1·25	0·18	—	—	1·25	0·18	0·24	0·16
27	1·67	0·28	—	—	1·67	0·33	—	0·33
28	1·67	0·33	—	—	1·67	0·36	—	0·35

(2) 五月十二日の地震 (Earthquake of May 12).

	EW comp.				NS comp.			
	Mean period in CG sec.	Mean double amp. in CG	Mean double amp. in C4	Mean double amp. in C9	Mean period in CG sec.	Mean double amp. in CG	Mean double amp. in C4	Mean double amp. in C9
1	0·31	0·14	0·34	0·43	0·45	0·25	0·77	0·72
2	0·50	0·22	0·55	0.94	0·50	0.35	1·59	1·37
3	0·46	0·37	1·27	1·52	0·39	0·38	1·36	1·30
4	0·50	0·59	0·93	1·38	0·39	0·45	0·93	1·25
5	0·39	1·50	4·40	7·44	0·50	2·28	6·18	11·75
6	0·33	1·36	4·78	8·20	0·50	2·88	9·65	7·74
7	0·39	1·87	7·63	8·14	0·39	1·99	8·23	10·82
8	0·33	1·01	4·17	6·11	0·50	3·25	9·90	10·32
9	0·50	1·63	2·91	5·37	0·50	2·17	5·60	7·65
10	0·46	2·01	4·57	4·32	0·46	1·86	5·68	7·89
11	0·50	1·35	3·67	4·81	0·46	2·07	3·60	4·04
12	0·46	1·67	3·25	4·14	0·42	1·03	3·09	2·77
13	0·46	0·94	1·97	2·97	0·56	1·19	1·39	3·98
14	0·72	1·59	1·97	1·91	0·63	1·22	2·69	1·90
15	0·72	1·47	1·59	3·31	0·63	1·33	2·00	3·37
16	1·00	2·37	1·44	1·62	0·56	1·55	2·29	3·16
17	0·56	0·67	2·40	2·59	0·63	0·96	2·05	2·75
18	0·56	0·84	1·68	2·51	0·56	1·31	2·35	2·62
19	0·63	1·13	1·23	1·98	0·63	1·19	1·91	2·08
20	1·00	1·28	1·50	1·40	0·72	1·53	1·48	2·90
21	1·67	1·85	1·70	1·72	0·84	1·72	1·97	1·88
22	0·72	1·11	0·68	1·42	1·67	2·70	1·31	1·83
23	1·25	1·66	0·75	1·25	2·00	5·30	2·27	4·09
24	1·00	0·70	0·74	1·17	1·65	2·16	0·89	1·37
25	1·67	1·45	1·08	0·82	2·00	1·87	1·28	1·73

(3) 五月二十五日十五時の地震 (Earthquake of May 25, 15^h)

	EW comp.				NS comp.			
	Mean period in CG sec.	Mean double amp. in CG	Mean double amp. in C6	Mean double amp. in C9	Mean period in CG sec.	Mean double amp. in CG	Mean double amp. in C6	Mean double amp. in C9
1	0·42	0·36	0·97	1·05	0·56	0·41	1·21	1·18
2	0·46	0·70	1·44	2·08	0·56	0·79	1·94	2·00
3	0·36	0·48	1·63	2·62	0·50	0·54	1·92	2·08
4	0·33	0·41	1·39	2·18	0·46	0·79	1·85	2·11
5	0·63	1·62	2·38	2·46	0·50	1·36	5·27	4·18
6	0·42	1·06	6·76	9·41	0·50	5·56	24·40	24·80
7	0·56	4·96	15·66	18·22	0·50	4·42	17·10	19·73
8	0·33	1·79	10·91	10·69	0·56	4·21	14·58	16·15
9	0·39	1·95	7·91	8·56	0·56	3·81	10·62	8·25
10	0·42	1·95	5·82	6·74	0·46	2·11	9·55	10·95
11	0·56	1·67	3·74	6·16	0·50	2·20	6·14	7·18
12	0·50	1·08	3·07	4·40	0·46	2 36	8·55	8·34
13	0·72	2·27	4·28	4·59	0·56	1·57	3·78	2·11
14	0·72	2·57	3·90	4·15	0·72	3·55	5·33	6·44
15	0·83	2·28	3·13	3·39	0·56	2·00	4·05	4·38
16	0·72	2·07	2·79	2·99	1·00	2·74	4·17	3·38
17	1·25	3·83	2·75	2·82	1·00	1·90	2·72	1·75
18	0·72	1·37	1·75	2·36	1·00	2·41	2·73	2·33
19	1·25	3·07	1·92	2·09	0·72	1·65	2·19	2·18
20	0·83	0·86	1·13	1·38	0·84	1 62	2·00	1·95
21	1·00	1·50	1·28	1·45	1·25	1·60	1·22	1·71
22	1·25	1·41	1·14	1·23	1·67	3·42	1·64	1·77
23	1·00	0·71	0·84	0·89	1·67	3·44	6·13	3·62
24	1·67	1·64	0·74	0·95	1·67	2·18	3·25	1·98

(4) 五月二十五日十九時の地震 (Earthquake of May 25, 19^h)

	EW comp.				NS comp.			
	Mean period in CG sec.	Mean double amp. in CG	Mean double amp. in C6	Mean double amp. in C9	Mean period in CG sec.	Mean double amp. in CG	Mean double amp. in C6	Mean double amp. in C9
1	0·29	0·21	0·67	0·73	0·36	0·22	0·66	1·03
2	0·29	0·19	0·49	0·53	0·29	0·16	1·02	0·65
3	0·31	1·33	6·67	6·50	0·46	1·46	4·23	4·14
4	0·26	0·38	2·62	2·22	0·36	0·59	1·47	3·07
5	0·36	0·47	2·71	2·13	0·50	0·64	2·11	3·26
6	0·33	0·23	1·51	1·22	0·42	0·41	1·72	1·89
7	0·42	0·26	1·21	1·02	0·50	0·32	1·08	1·29
8	0·50	0·40	0·93	0·81	0·39	0·32	0·94	1·23
9	0·50	0·37	0·75	0·95	0·50	0·34	0·70	0·87
10	0·56	0·24	0·56	0·69	0·63	0·32	0·86	0·73
11	0·63	0·30	0·53	0·67	0·56	0·31	0·83	0·92
12	0·56	0·17	0·53	0·65	0·72	0·25	0·52	0·60
13	0·84	0·30	0·34	0·51	0·56	0·18	0·49	0·40
14	1·00	0·27	0·30	0·31	0·72	0·20	0·52	0·38

振動の振幅は概して上層程大でありましたが建築物の振動の振幅がある特定の週期の地震動に對して大となると云ふ現象卽共鳴 (Resonance) の様な現象の存在の有無を確めますために上述の有感地震に就きまして、地震動を五秒間毎に區分して各區分毎に平均の週期、平均の振幅を測定しまして(第四表)、第八圖の様に横軸に地階で測定された地動の五秒間毎の平均週期をとり、縱軸に 9 階、6 階又は 4 階の地震動の五秒間毎の平均振幅と地階の平均振幅との比を取つて見ますと地階の震動の五秒間毎の平均週期が 0·3 秒から 0·5 秒の間では、卽ち建築物の固有振動週期に近い所では上層の振動の振幅は著しく大となりますが、地階の振動週期が一秒以上になりますと、上層の振動の振幅は地階の振幅とほとんど等しくなると云ふ著しい現象が見られます。卽ち共鳴の現象が地階の平均週期が 0·3 秒から 0·5 秒の場合に起つて居ると考へられます。

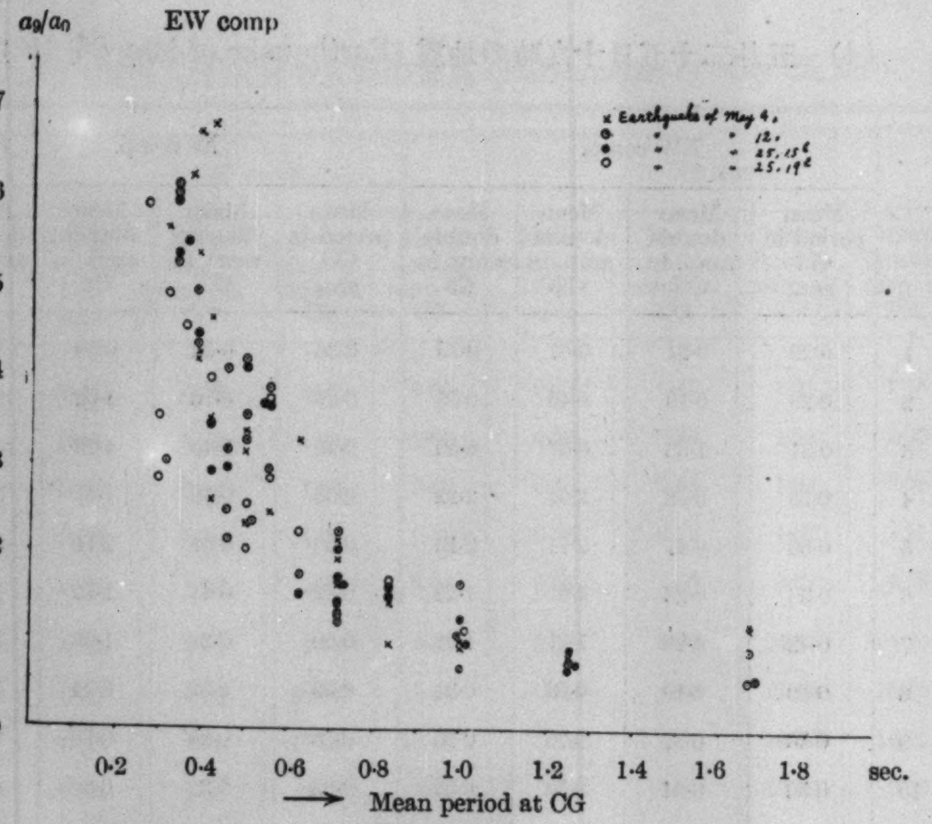
a_g/a_0
EW comp
7
6
5
4
3
2
1
0
0·2
0·4
0·6
0·8
1·0
1·2
1·4
1·6
1·8
sec.
→ Mean period at CG
× Earthquake of May 4.
◐ " " 12.
● " " 25. 15h
○ " " 25. 19h

Fig. 8 (a).

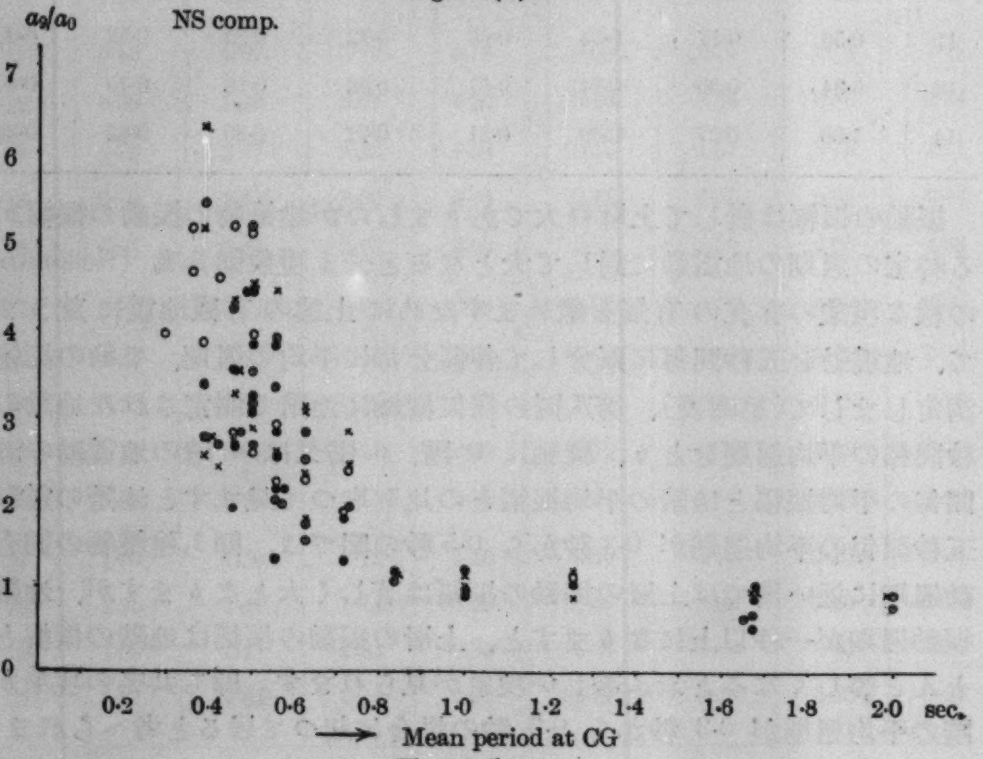
a_g/a_0
NS comp.
7
6
5
4
3
2
1
0
0·2
0·4
0·6
0·8
1·0
1·2
1·4
1·6
1·8
2·0
sec.
→ Mean period at CG

Fig. 8 (b).

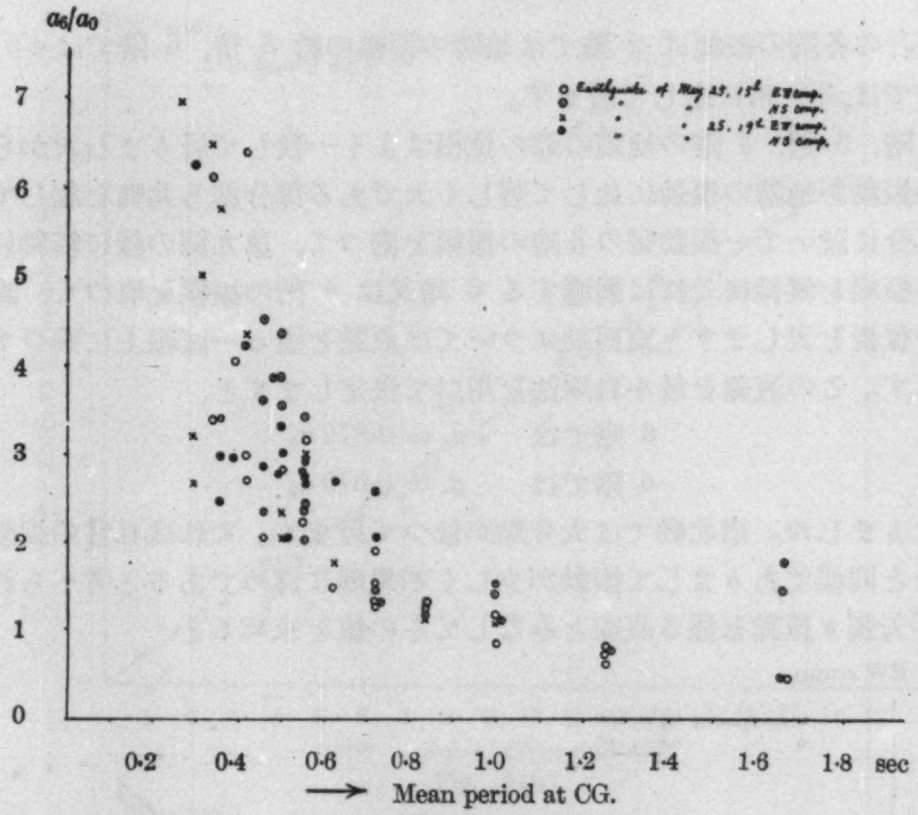

Fig. 8 (c).

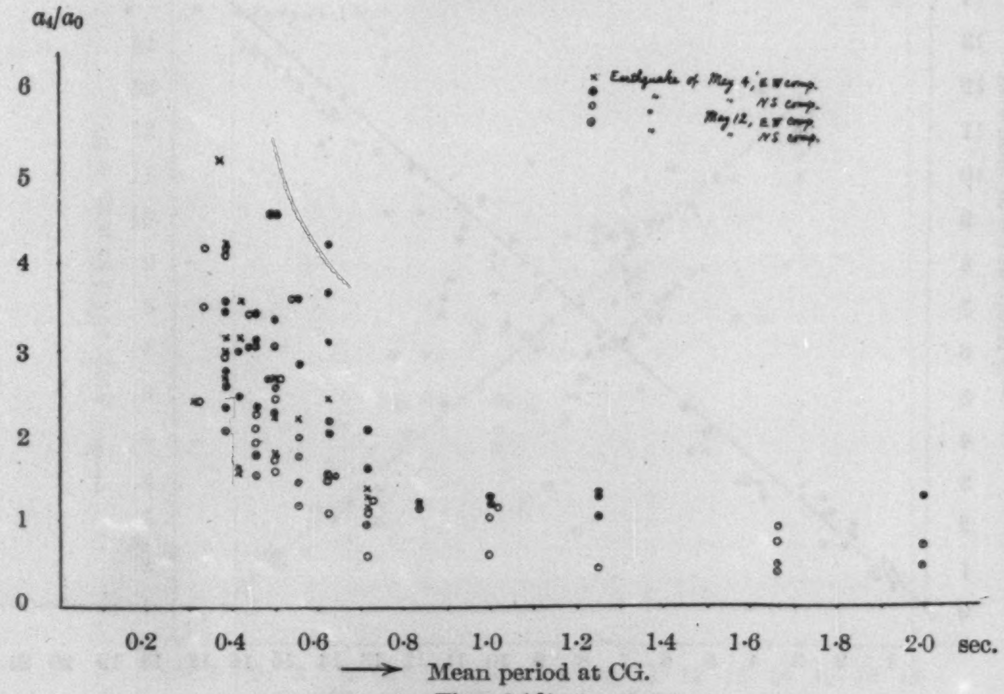

Fig. 8 (d).

第八圖 a_9/a_0, a_6/a_0, a_4/a_0 と地階の平均週期との關係

Fig. 8. Relation between the ratios of amplitude a_9/a_0, a_6/a_0, a_4/a_0 and the mean period of vibration at the underground floor.

此場合の各階の振幅は 9 階では地階の振幅の約 5 倍、6 階では 4·5 倍、4 階では 3·5 倍に達して居ます。

9 階、6 階、4 階の地震の際の位相はよく一致して居りましたから上層の振動が地階の振動に比して著しく大である部分卽ち共鳴を起して居る部分に就いて一振動每の各階の振幅を測つて、第九圖の樣に橫軸に 9 階の振幅を縱軸にこれに對應する 6 階又は 4 階の振幅を取つて、點でその位置を表しますと東西動についでは原點を通る一直線上に乘つて居ります。この直線を最小自乘法を用ひて決定しますと、

6 階では $a_6 = 0{\cdot}872\, a_9$

4 階では $a_4 = 0{\cdot}679\, a_9$

となりました。南北動では大分點が散つて居ます。これは日常の振動の場合と同樣でありまして振動が少しく不規則な爲めであると考へられますが矢張り原點を通る直線とみなしてその値を求めると

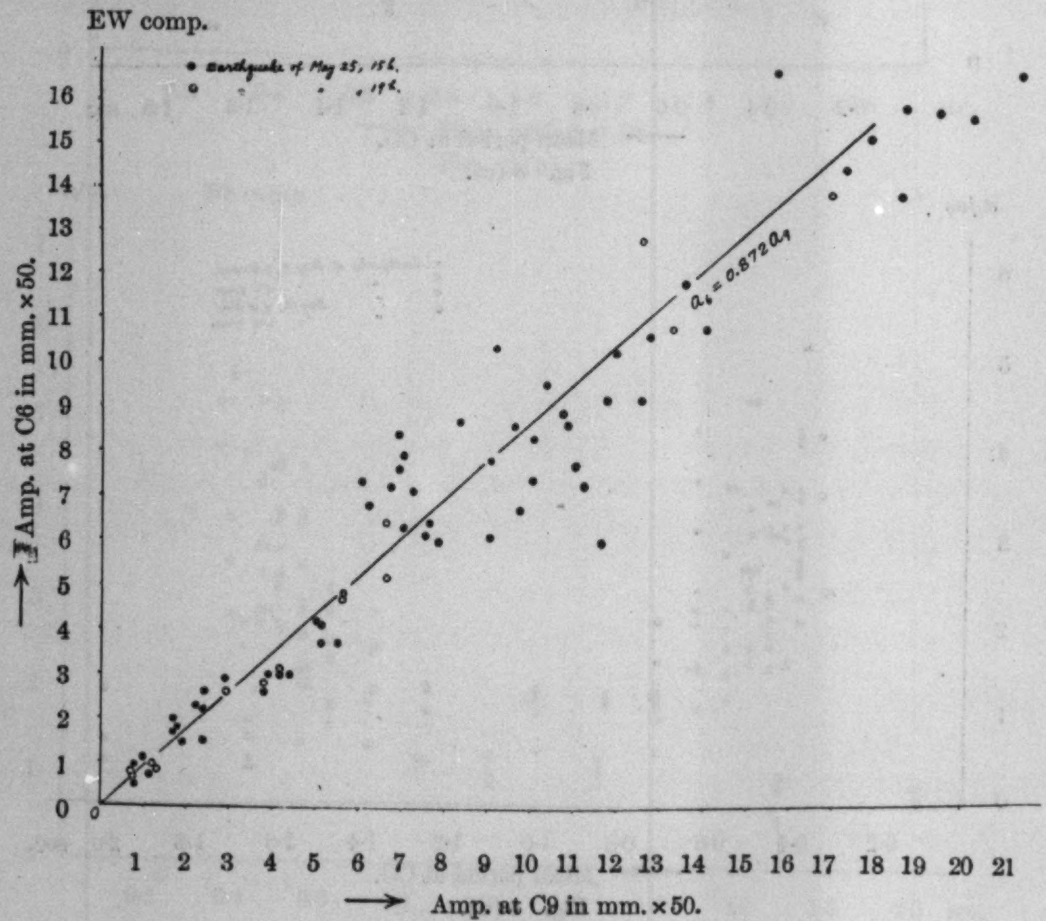

Fig. 9 (a).

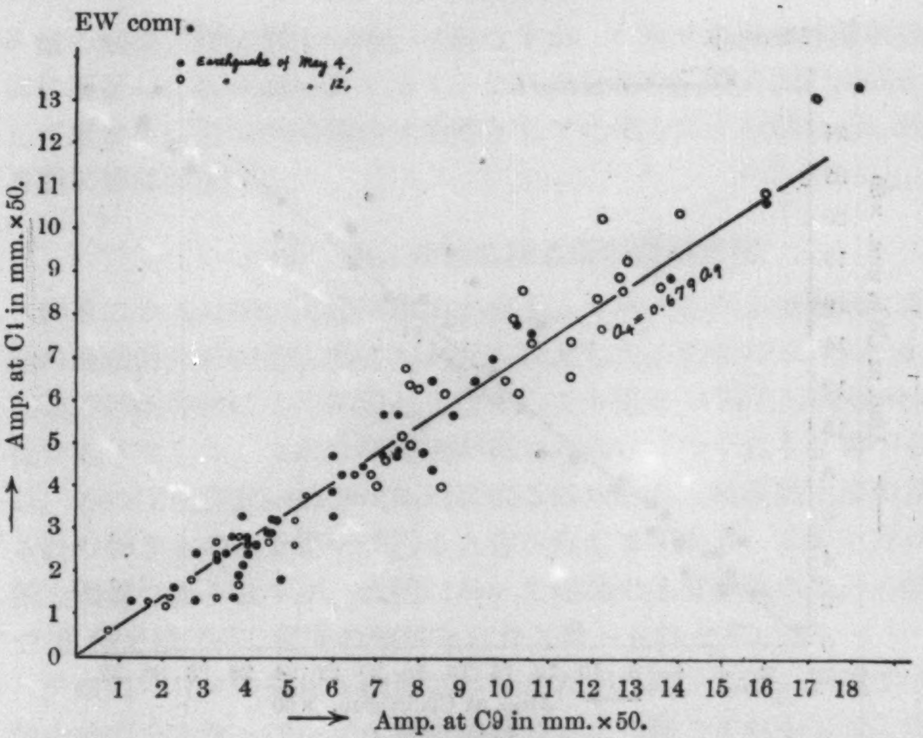
EW comp.
● Earthquake of May 4,
○ " " " 12,
$a_4 = 0.679\,a_9$
0
1
2
3
4
5
6
7
8
9
10
11
12
13
14
15
16
17
18
→ Amp. at C4 in mm. ×50.
→ Amp. at C9 in mm. ×50.

Fig. 9 (b).

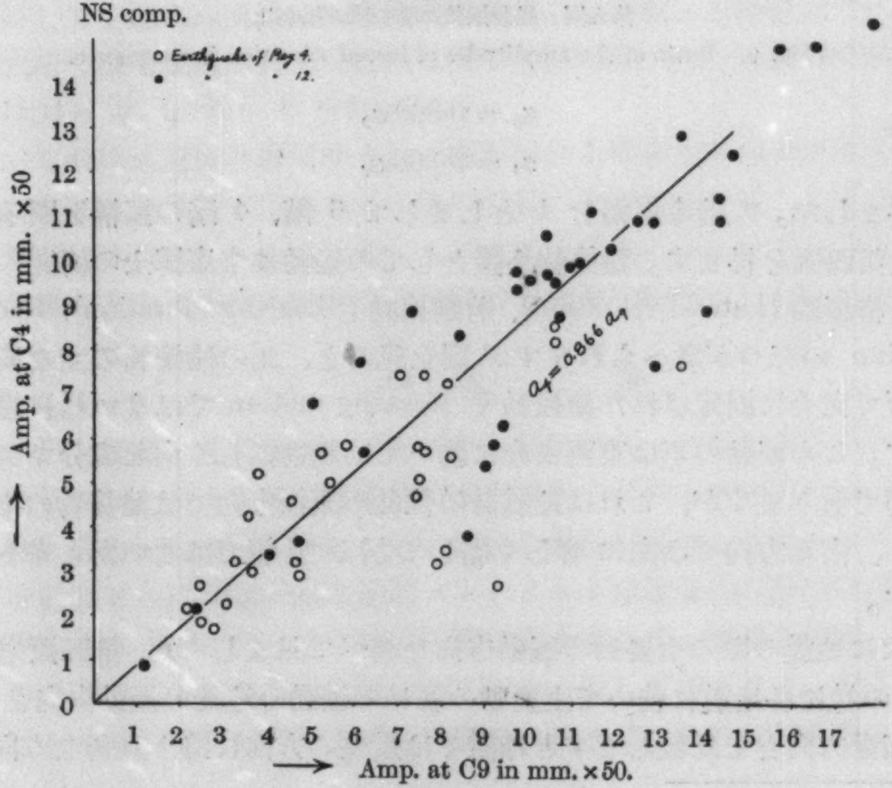
NS comp.
○ Earthquake of May 4.
● " " " 12.
$a_4 = 0.866\,a_9$
0
1
2
3
4
5
6
7
8
9
10
11
12
13
14
15
16
17
→ Amp. at C4 in mm. ×50
→ Amp. at C9 in mm. ×50.

Fig. 9 (c).

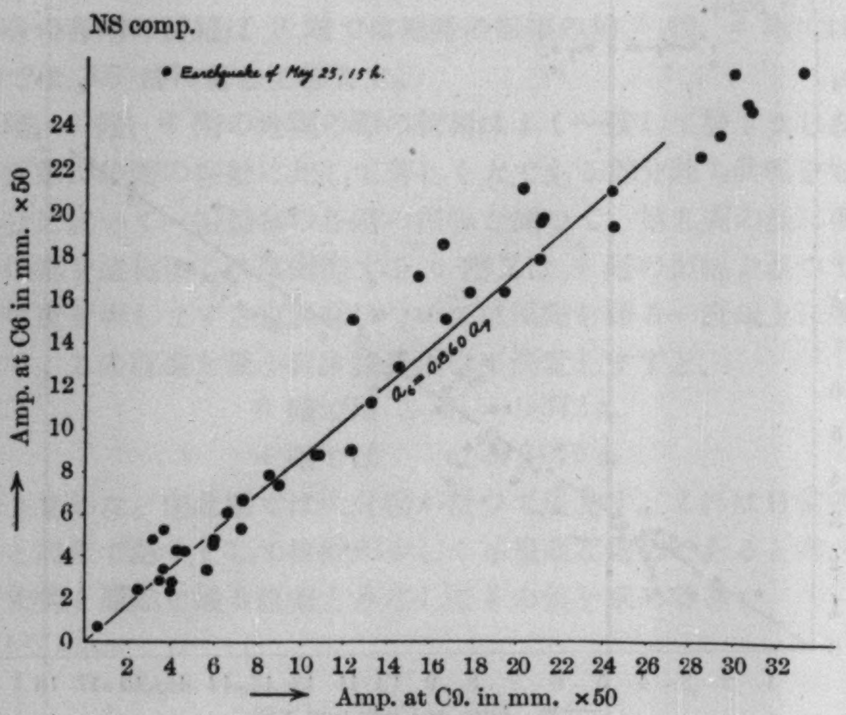

Fig. 9 (d).

第九圖 强制振動共鳴の際の振幅比

Fig. 9. Ratio of the amplitudes of forced vibration in resonance.

$$a_6 = 0{\cdot}860\, a_9$$

$$a_4 = 0{\cdot}866\, a_9$$

を得ました。9 階の振幅を 1 としまして 6 階、4 階の振幅を圖示しますと第四圖を得ます。建築物全體としての振動は末廣博士の研究[3] に依れば横振動 (Lateral vibration)、剪斷振動 (Shearing vibration)、Rocking motion の三つが考へられますが圖を見ると、此の建築物の主な振動は地面で完全に固定された横振動や Rocking motion ではない樣に思はれます。この振動の形は東西成分に就いては規則正しく南北成分では稍不規則でありますが、これは地震計の位置が東西方向では建築物の中部に近く、南北方向では南に著しく偏して居る影響ではないかと考へられます。

次に地震の際の主要動の振動方向を調べて見ましたが、第五圖 (b) (c) (d) の樣に各地震に就いて主要動の初めの振動の地階の振動方向と 9 階の振動方向とを比較しますと地階では震央の方向に略〻直角な方向卽ち

---

3) 末廣恭二 構造物振動の理論及其測定法（建築雜誌、大正十五年七月）

S 波の振動方向に略〻一致して居ますが、9 階では常に建築物の北東方向に振動して居る様であります。これは日常の振動の振動方向とも一致して居ます。即ち此建築物は全體として北東方向に振動し易い性質がある様に思はれます。

III. 風、日射に依る床の傾斜變化

四月二十八日朝は非常に南風が強く、ヒューと云ふ音と共に九階、四階の地震計の針が南に動くのが見られました。此時の 9 階と 4 階との記象の形は非常によく類似して居まして 9 階と 4 階との振幅の比は 2:1 位でありました。これは建築物が風でたわむだのであると考へられますが、この際地震計の描針は傾斜に依る針の動きと建築物上層の移動に依る針の動きとの差を書いて居ると考へられますから、之等を分ける事は稍〻困難でありますが、大體に於いて建築の上層程風のための傾斜が大で 9 階では 6·5″ 程度の傾斜をしたと考へられます。

又傾斜の日々の變化が觀測されましたが九階、六階、四階では毎日午前十時頃から北へ傾いて午後六時頃最も北へ傾きそれから逆に南方に傾斜して午前九時頃最も南に傾斜します。その量は上層程大でありまして九階では全振幅が約 6 秒(五日間平均)に達します。(各階の傾斜量の比は大約 $I_9 : I_6 : I_4 = 1 : 0{\cdot}4 : 0{\cdot}3$)

これは地震計を据付けました室が何れも建築物の南側の壁に接して居たために、日射の爲めのこの壁の膨脹、收縮に依つて、上記の傾斜變化が惹起されたのであると考へられます。地階に於いては上層と異なり東北東の方向に平均一秒位の全振幅の日々傾斜變化が見られました。

VI. 結　論

以上に於いて武田ビルデングの日常の振動、地震の際の振動に就いて論じたのでありますが建築物の固有振動の週期は東西方向 0·27 秒、0·43 秒、南北方向で 0·37 秒と 0·49 秒位の振動が優越して居ります。今日まで驗測せられた略同高の鐵筋コンクリート造建築物の振動週期4) は第五表の様に 0·4 秒から 0·7 秒位の間にありまして、何れも微震、弱震程度の地震の主要動の振動週期(第六表)と一致して居ります。即ち主要動の部と共鳴の現象を起して居る様に思はれます。これは建築學上注意すべ

---

4) 2) に同じ。

第五表 Table V.

鐵筋コンクリート造建築物の固有振動週期

Free vibration periods of reenforced concrete buildings.

建築物の名稱 Name of building	建築物の高さ Height of building	驗測年月日 Date of measurement	東西動週期 Period in EW comp.	南北動週期 Period in NS comp.
明海ビルヂング Meikai Building	30·3 m (100 尺)	April, 1923	—	0·5 sec.
日本銀行北別館 A house of Nippon bank	30·3 m (100 尺)	May, 1923	0·50 sec.	0·48 sec.
東京日々新聞社 Tôkyô-niti-niti newspaper office	24·3 m (80 尺)	June, 1922	0·52 sec.	0·52 sec.
内外ビルヂング Naigai Building	30·3 m (100 尺)	August, 1923	0·65 sec.	0·65 sec.

第六表 Table VI.

地震主要動初五秒間の平均週期

（東京本郷觀測）

5-Minute means of periods of principal earthquake motions.

(observation at Tôkyô)

發震時 Time of Occurrence	震央 Epicentre	震度 Intensity	平均週期 Mean period	平均最大加速度 Mean max. acc.
July 17, $19^{h}\,49^{m}\,33^{s}$ (1929)	Drainage basin of River Tone.	III	0·24 sec.	230 mm./sec.^{2}
May 24, $1^{h}\,38^{m}\,38.4^{s}$ (1930)	Far off the coast of Mera.	III	0·50 sec.	90 mm./sec.^{2}
May 1, $10^{h}\,16^{m}\,5^{s}$ (1930)	Off the coast of Tyôsi.	II	0·50 sec.	65 mm./sec.^{2}
June 1, $2^{h}\,58^{m}\,43^{s}$ (1930)	Vicinity of city of Mito.	IV	0·50 sec.	330 mm./sec.^{2}
June 17, $21^{h}\,09^{m}\,50^{s}$ (1931)	Central part of Musasi province	IV	0·46 sec.	600 mm./sec.^{2}
May 4, $23^{h}\,48^{m}\,28{\cdot}6^{s}$ (1931)	Drainage basin of River Tone.	I	0·25 sec.	10 mm./sec.^{2}

き問題であると思はれますが建築物の破壊を惹起す様な强震、烈震程度の地震の主要動では、今村先生の研究[5] に依りますと非常に振幅の大きな比較的長い週期の振動（1 秒から 1·5 秒位）の上に小振幅の上記の様な週期の振動が重つて居る事が知られて居ます。この様な複雜な振動が建築物に如何なる影響を與へるかは尙今後の研究に俟たねばなりませぬ。又建築物の振動減衰率 (damping ratio) も振動週期と同樣に建築物の振動に重要な影響を及ぼすものと考へられますから、これも決して等閑に附す事の出來ない事であります。

永田氏の關東大地震の際の鐵筋コンクリート造建築物の破壊狀況の研究[6] に依りますと、建築物の固有振動週期が大なるに從つてその被害の程度が大でありまして、その週期の數值が略建築物の耐震强度に逆比例すると云ふ事卽ち帳壁式鐵筋コンクリート造建物の固有振動週期は 0·3 秒及至 0·65 秒でありまして 0·65 秒の內外ビルデングは全潰しました事を注意せられて居ます。此見地よりしますと、武田ビルデングは高層鐵筋コンクリート造建築物としては比較的耐震强度の大なる建築物であると考へられます。

終りに臨み、終始色々と指導を賜つた今村先生に厚く御禮申し上げます。又大正十四年式簡單微動計一臺を期間中使用する事をお許し下されました建築學敎室の武藤先生に厚く御禮申し上げます。

---

34. *On the Vibration of the Takeda Building.*

By Takaharu FUKUTOMI.

At the request of Dr. G. Kume, the writer measured with three 1925-type tromometers the vibrations of the Takeda Building which is situated at Nihon-basi street in Tôkyô during a period from April 25th to May 25th.

The Takeda Building which is made of reenforced concrete, was almost in completion at the time. It is comparatively long prismatic and has, besides the underground floor, nine floors with a total height of about 30.2 m. and an area of about 271 square metres (Fig. I). On April 25th the tromometers (see Table 1) were installed on the underground, on the 4th and on the 9th floors, and on May 16th the instrument which had been installed on the 4th floor, was removed into the 6th, 4 sensible, 35 non-sensible and 5 distant earthquakes having been observed with them during the above-mentioned period.

The results of observations may be summerized as follows:—

---

5) 今村明恒 關東大地震調査報告（震災豫防調査會報告百號（甲））

6) 永田忞郞 鐵筋「コンクリート」造被害調査報告（震災豫防調査會報告百號（丙））

I. Free vibrations of the structure.

1) The whole structure vibrates with a period of about 0·4 sec. in the direction about N 70°E and with amplitudes in the ratios of 1:0·84:0·67: 0·06, on the 9th, on the 6th, on the 4th and the underground floors. This seems to suggest that the structure vibrates in the type of fundamental vibration with the upper end free and the other end fixed—perhaps fixed at the level of the base of structure.

2) As seen in Fig. 6, the vibration of the structure has a diurnal variation of amplitude, showing the max. of about 3 μ at 3 or 4 p.m. and the min. of about 0·6 μ at 2 or 4 a.m. in NS component on the 9th floor. The ratio of amplitude of NS comp. to that of EW comp. is approximately 1·8:1.

The writer tried to find out possible correlation between the vibrations of the structure and wind velocity, but could not find any distinct one.

During the observations, however, the writer frequently noticed the vibrations becoming larger whenever tram-car passes through the Nihonbasi junction with rattling noise. The diurnal variation of amplitude of vibration above mentioned may thus be attributed to the effect of traffic.

II. Vibrations due to earthquake.

1) The 5-minute means of max. accelerations of the principal motion in 4 sensible earthquakes have been calculated; the ratios of accelerations on the underground, the 4th, the 6th and the 9th floors came out as 1:2·36:3·82:4·15.

2) When the period of vibrations of the underground floor due to earthquake approaches 0·4 sec., the structure shows a phenomenon of resonance. (See Fig. 8). The ratios of amplitudes in this case are as follows.

$a_9:a_6:a_4=1:0{\cdot}872:0{\cdot}679$ in EW comp.

$a_9:a_6:a_4=1:0{\cdot}860:0{\cdot}866$ in NS comp.

As for the motion of whole structure, there may be three cases, namely, the lateral vibration, the shearing vibration and a rocking motion.

According to the results above mentioned, it seems that the principal vibration of the Takeda Building may be neither the lateral vibration fixed perfectly at the earth's surface, nor the rocking motion on the ground on which the structure stands.

3) On the underground floor, the direction of vibration of the structure due to the principal motion of earthquake is nearly perpendicular to that of the epicentre, whereas, on the 9th floor, it is nearly coinsident with the direction of the free vibration, suggesting that the structure vibrates at the foot in the direction of forced vibration, but at the top in the direction of free vibration

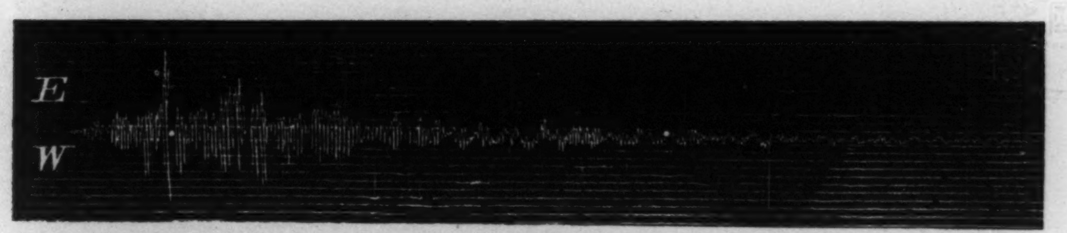

C9

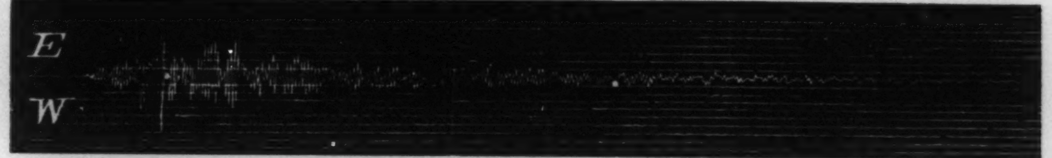

C4

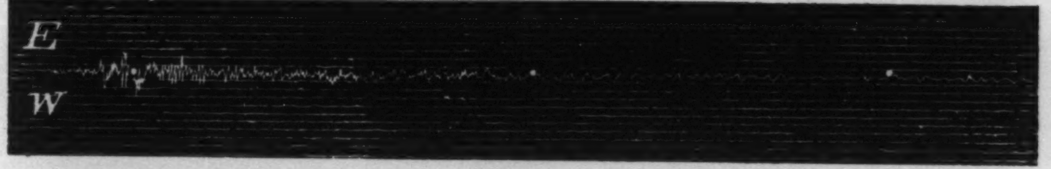

CG

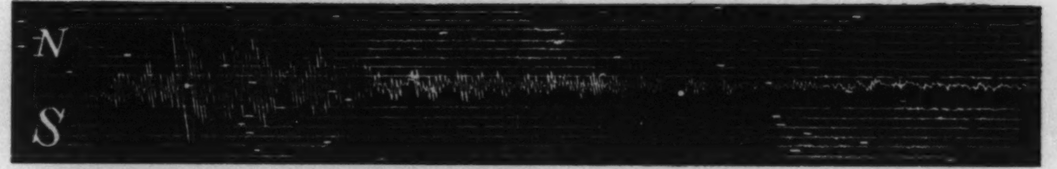

C9

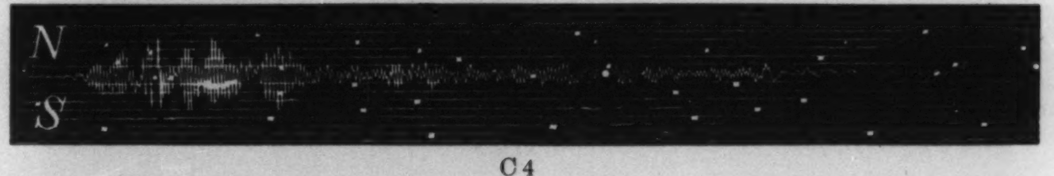

C4

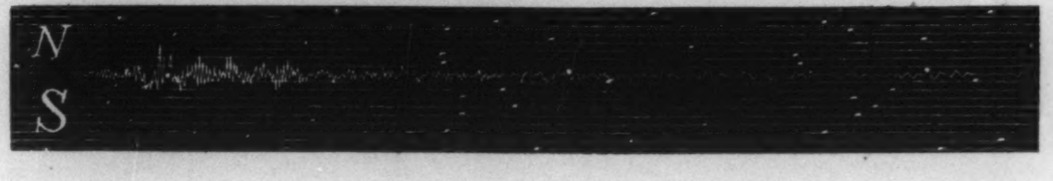

CG

第十圖　昭和六年五月四日二十三時四十八分二十九秒の微震の記象（五十倍）

Fig. 10. Seismograms due to the earthquake of May 4, 1931, at 23^h 48^m 29^s.
(Dot indicates minute mark) Magnification = 50

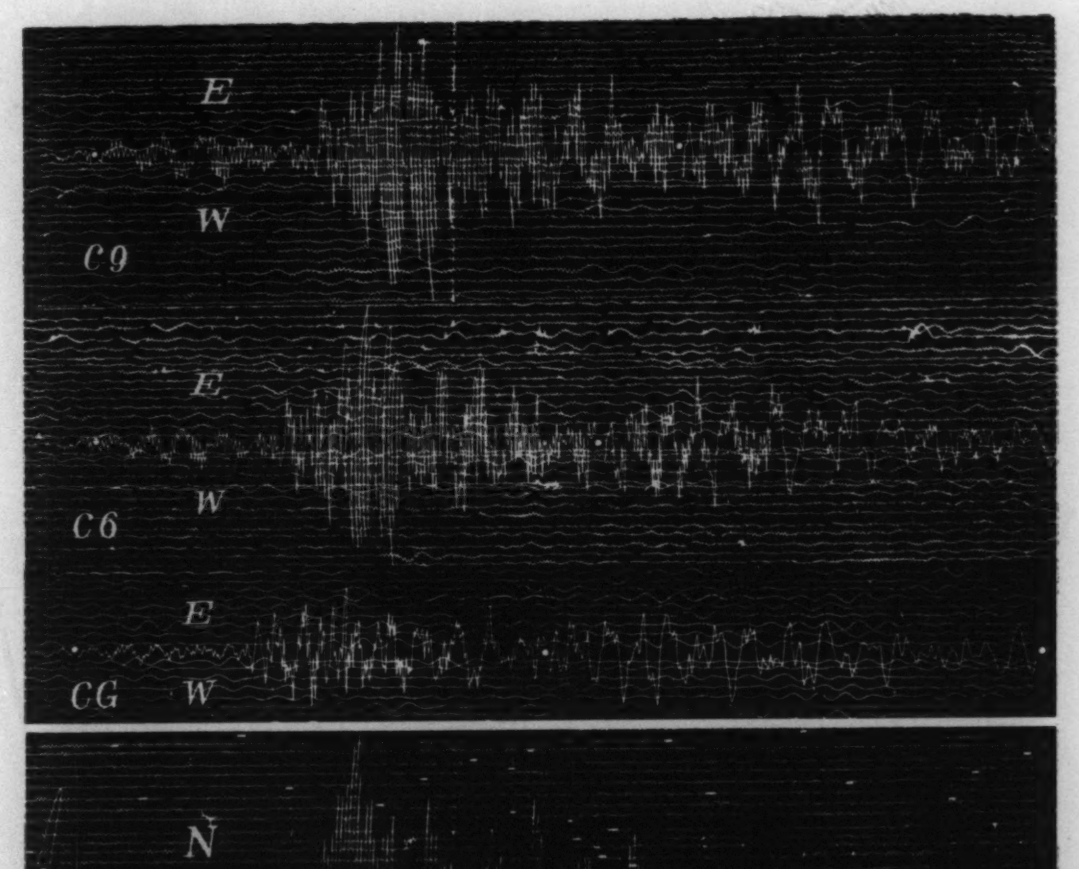

第十一圖　昭和六年五月二十五日十五時五十分三十七秒の微震の記象（五十倍）

Fig. 11. Seismograms due to the earthquake of May 25, 1931, at 15^h 50^m 37^s
(Dot indicates minute mark.) Magnification = 50.

III. Tilting of floors due to wind and sun-shine.

1) On the morning of April 28th, bendings of the structure due to strong winds were observed, the amount of inclination at the 9th floor having been in an order of 6·5 seconds. The daily change of inclination of the floor, which may be attributed to the expansion of the south wall of the structure due to sun-shine, was also noticed.

In conclusion, the writer wishes to express his hearty thanks to Professor A. Imamura for his kind guidance and revision of this paper and also to Professor K. Mutô for his kind permission to use one of the 1925-type tromometers.

35. 東京市內及近郊に於ける一等水準測量成果

當所に於ける研究上の必要により曩に陸軍陸地測量部に依賴し東京市內及其北方近郊に於て附圖に示す水準線路に沿て一等水準測量を行へり。

其成果を最近檢測のものと比較して求め得たる土地高低變化は測量の期日と共に附圖に掲げて參考に供す。

（昭和六年九月二十一日　所　長）

35. The Results of Precise Levellings in Tôkyô and the Environs.

A precise levelling in Tôkyô and the environs was done lately by the Land Survey Department at our request.

The result of comparison of the data of the present survey with those of previous survey, and the routes and the dates of the present and previous surveys are shown in the accompanying plate.

(Sept. 21st., 1931. The Director)

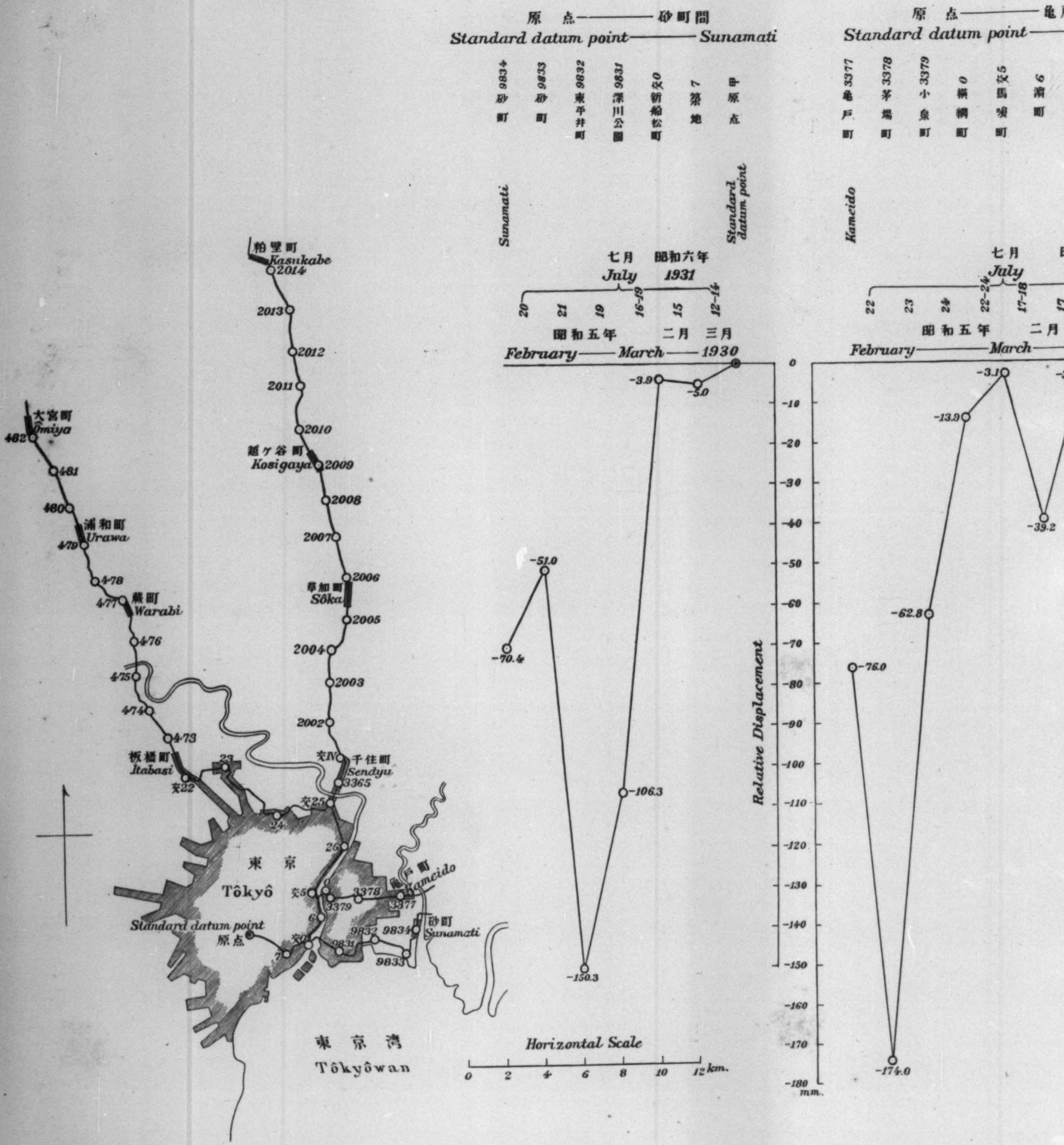
原　点——砂町間
Standard datum point——Sunamati
砂町 9834
砂町 9833
東平井町 9832
深川公園 9831
新船松町 交0
築地 7
原点 甲
Sunamati
Standard datum point
七月 昭和六年
July 1931
20
21
19
16-19
15
12-14
昭和五年 二月 三月
February——March——1930
0
-3.9
-5.0
-51.0
-70.4
-106.3
-150.3
Relative Displacement
-10
-20
-30
-40
-50
-60
-70
-80
-90
-100
-110
-120
-130
-140
-150
-160
-170
-180 mm.
Horizontal Scale
0
2
4
6
8
10
12 km.
原　点——亀
Standard datum point——
亀戸町 3377
茅場町 3378
小泉町 3379
横網町 0
馬喰町 交5
濱町 6
Kameido
七月
July
22
23
24
22-24
17-18
17
昭和五年 二月
February——March——
-3.1
-13.9
-39.2
-62.8
-76.0
-174.0
粕壁町
Kasukabe
2014
2013
2012
2011
2010
越ヶ谷町
Kosigaya
2009
2008
2007
2006
草加町
Sōka
2005
2004
2003
2002
交N
千住町
Sendyu
3365
交25
26
大宮町
Ōmiya
482
481
480
浦和町
Urawa
479
478
477
蕨町
Warabi
476
475
474
473
板橋町
Itabasi
交22
23
24
東京
Tôkyô
交5
3378
3379
亀戸町
Kameido
3377
砂町
Sunamati
9834
9832
9831
9833
6
交0
7
Standard datum point
原点
東京湾
Tôkyôwan

(震研彙報、第九號、圖版、地震研究所)

亀戸間

Kameido

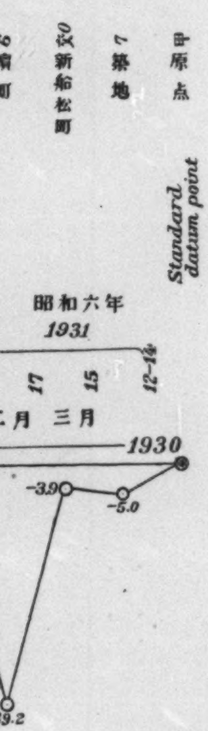

原点——粕壁間

Standard datum point——Kasukabe

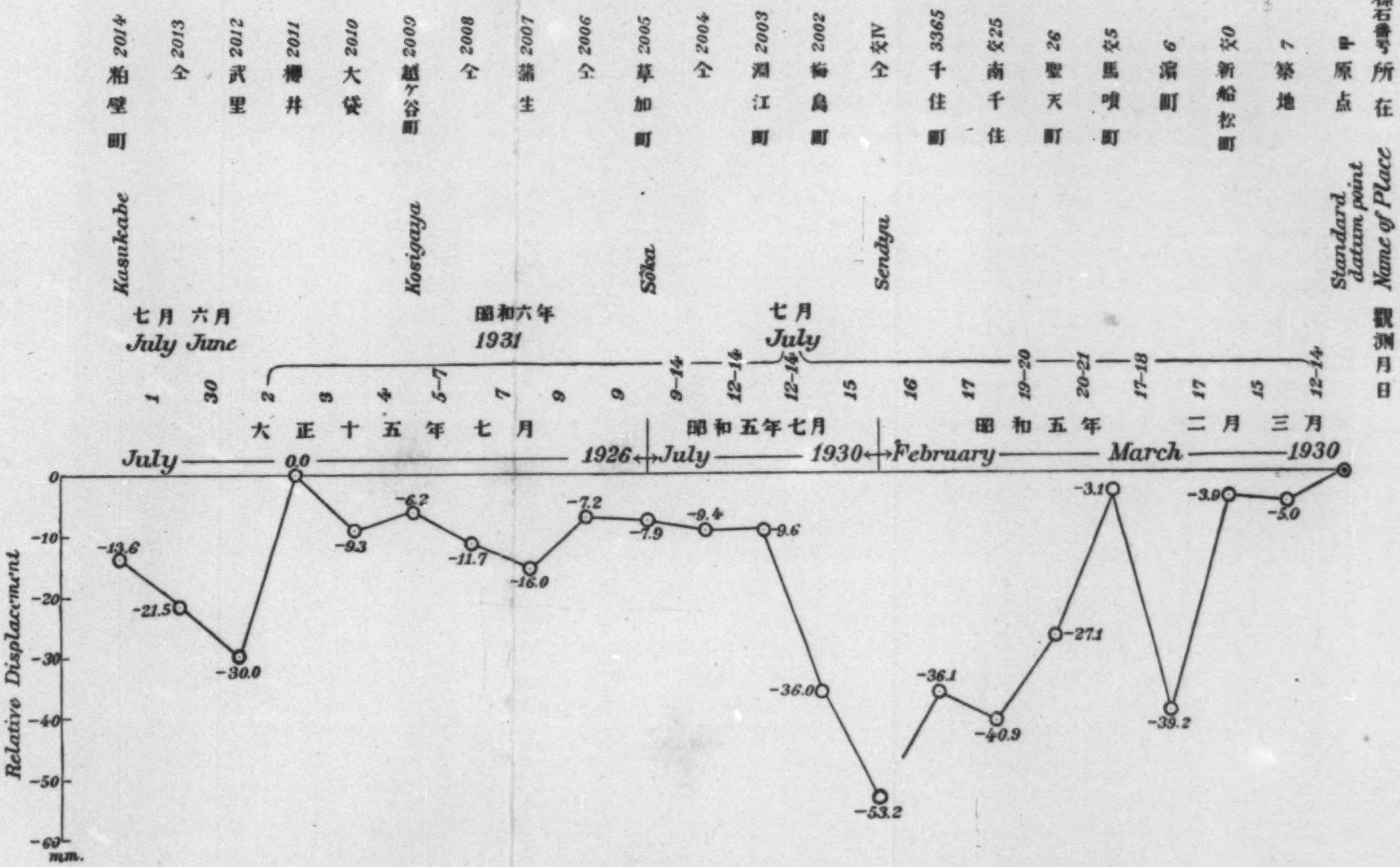

原点——大宮間

Standard datum point——Ômiya

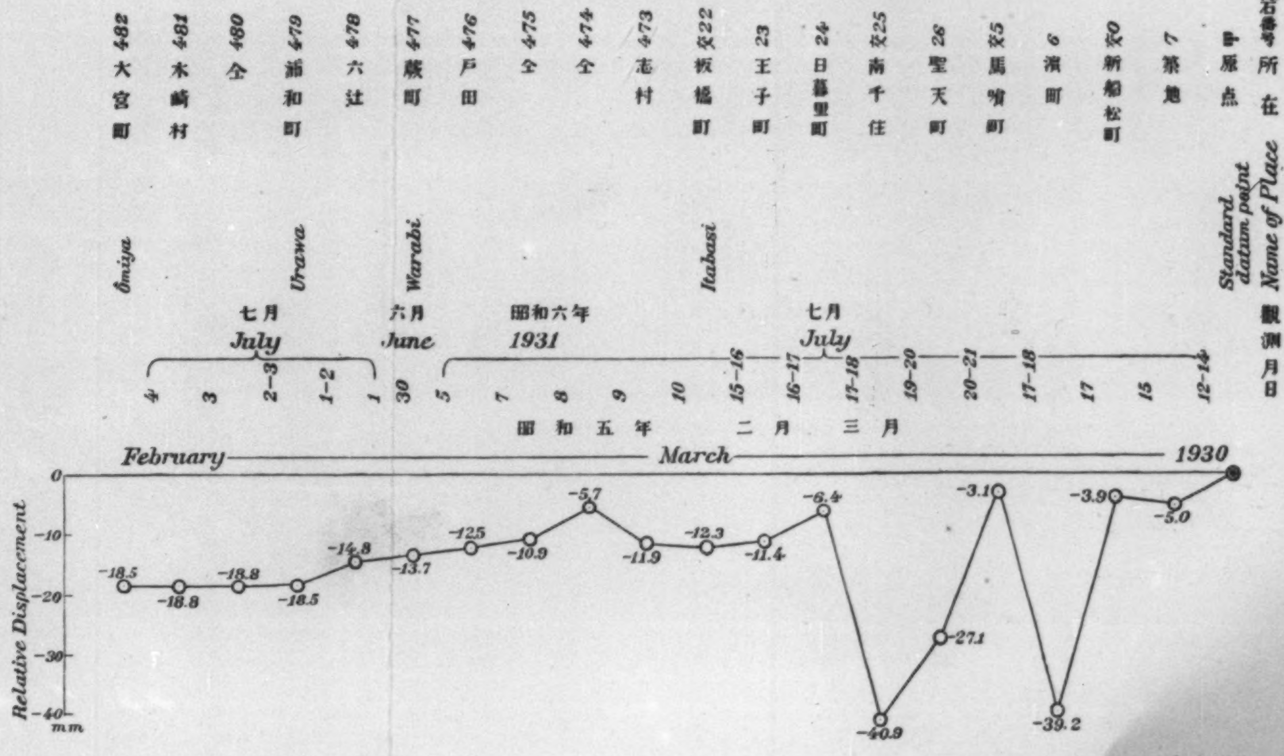

Instrument: NS Component = No. 15, EW Component = No. 14,
Vert. Component = No. 21.

Instrumental constants:

Component	Natural period	Magnification	Damping ratio
N.S.	sec. 60	20	2·0
E.W.	60	15	3·2
Vert.	15	20	1·7

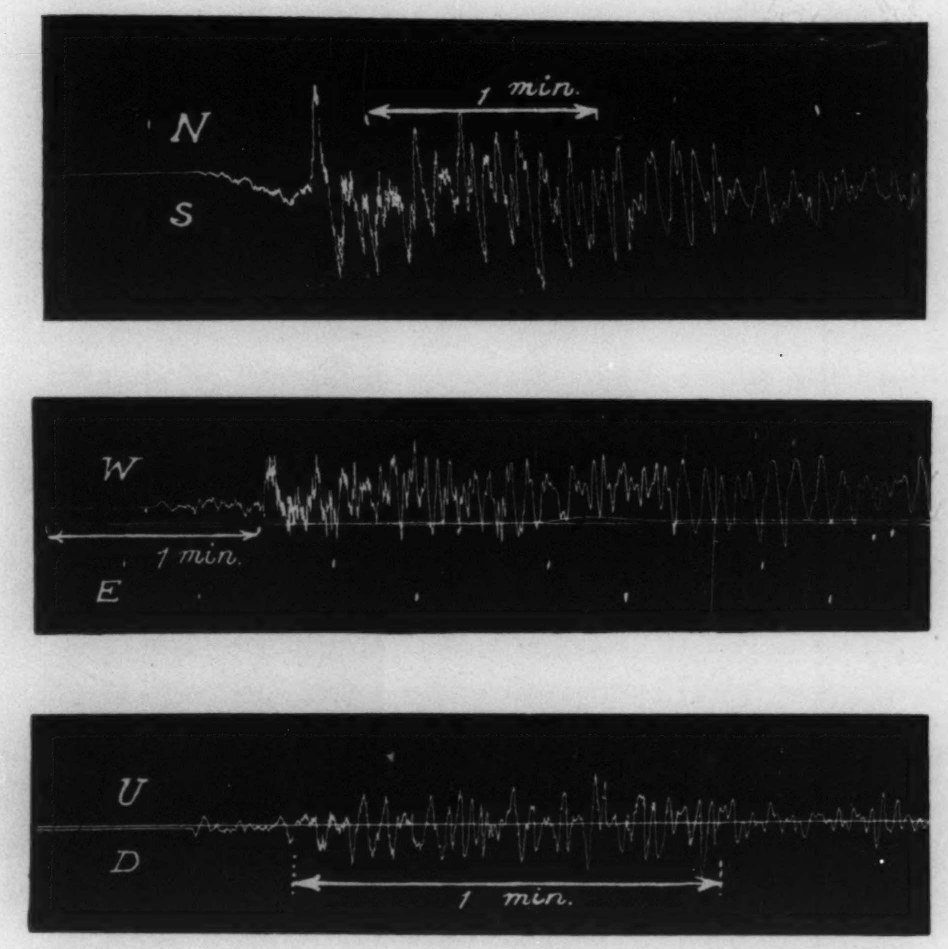

(*Natural size of the original diagrams.*)

Fig. 2. Tôkyô Observation of the Earthquake of June 2, 1931.

（震研彙報、第九號、圖版、震報）

Instrument: No. 4.

Instrumental constants:

Component	Natural period	Magnification	Damping ratio
E.W.	7 sec.	50	1·30
N.S.	7	50	1·30

N′ = N 13° W, S′ = S 13° E.
E′ = N 77° E, W′ = S 77° W.

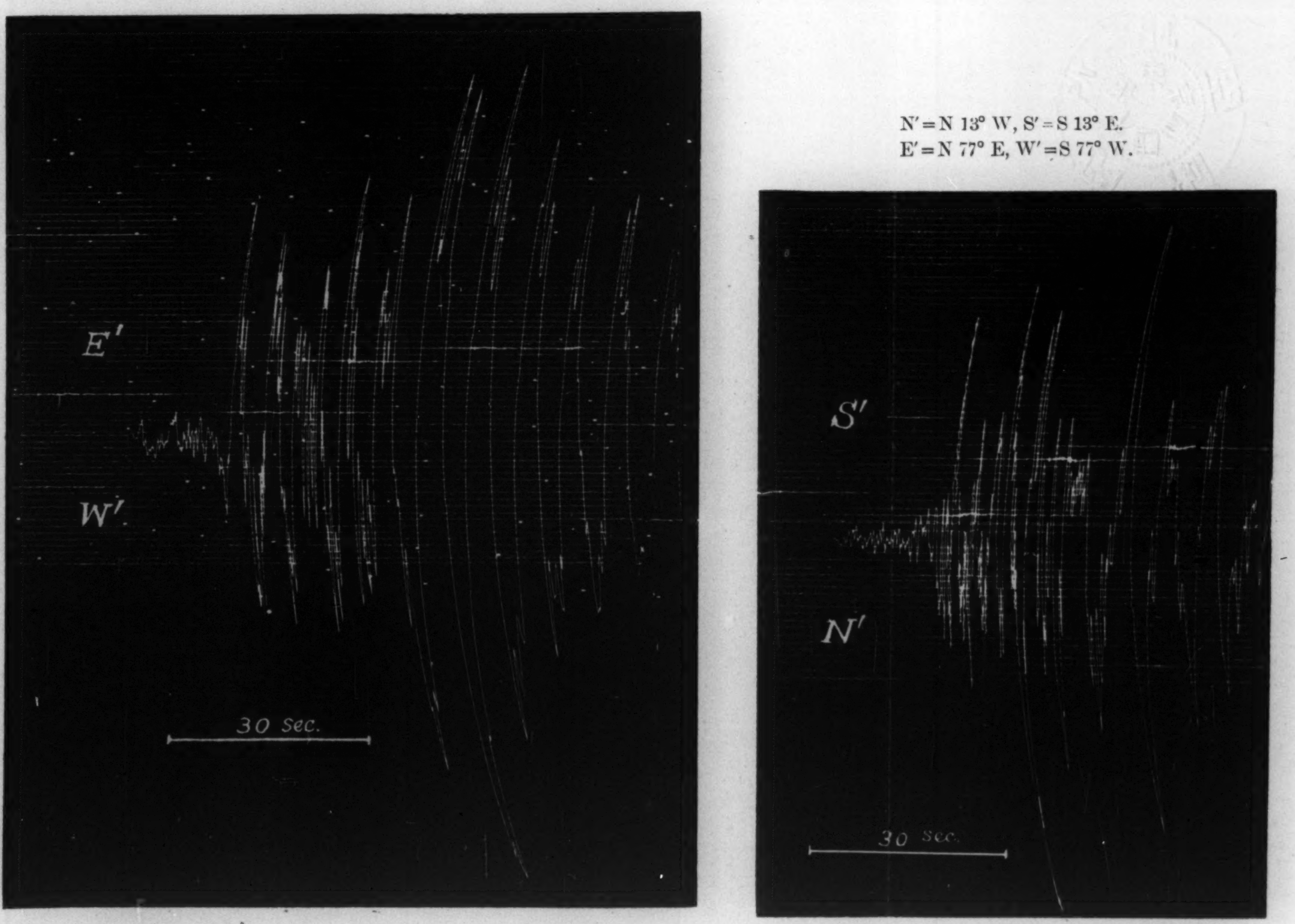

E.W. Component.

N.S. Component. (*Natural size of the original Diagrams.*)

Fig. 3. Tôkyô Observation of the Earthquake of June 9, 1931.

（震研彙報、第九號、圖版、震報）

Instrument: No. 7.

Instrumental constants: Magnification = 50. Natural oscillation period = 7 sec.
Damping ratio = 1·50.

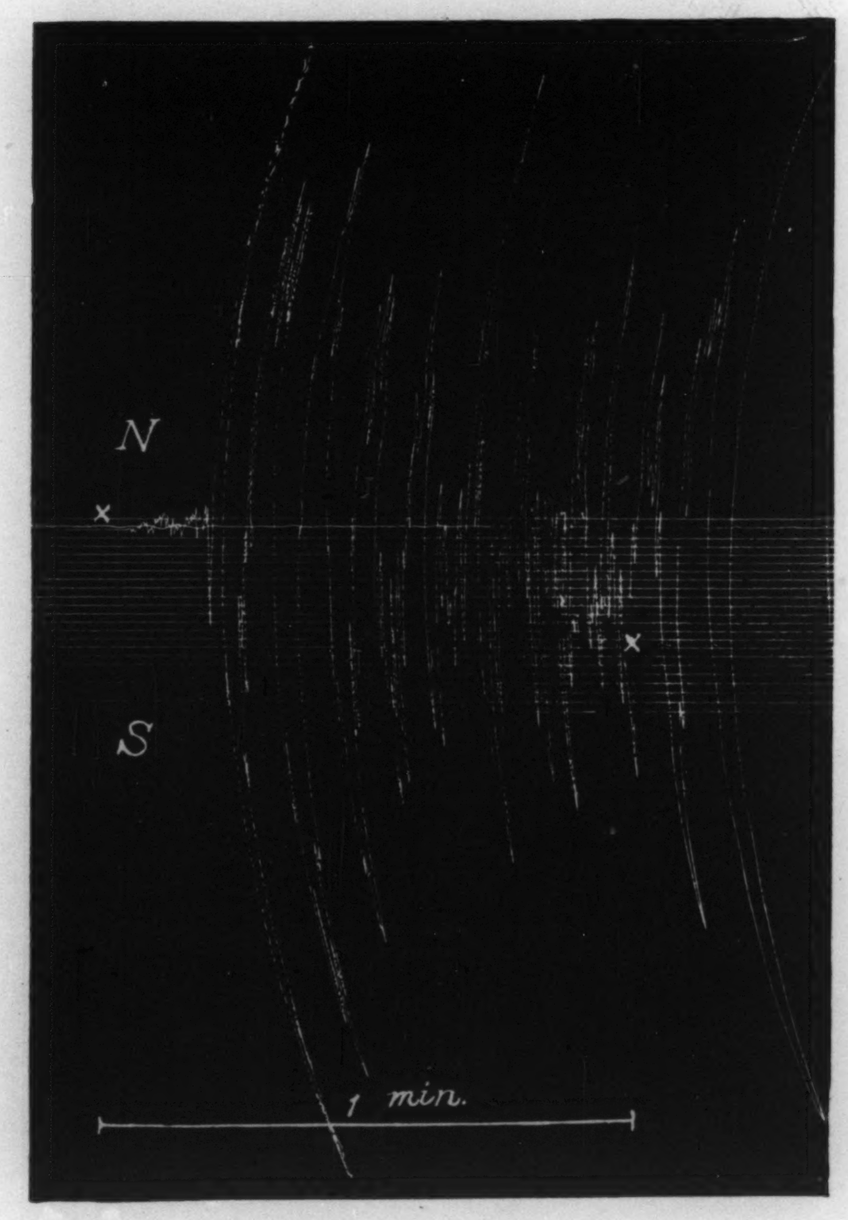

N.S. Component. (*Natural size of the original diagram.*)

Fig. 4. Tôkyô Observation of the Earthquake of June 11, 1931.

Instrument: No. 7.

Instrumental constants:

Component	Magnification	Natural period	Damping ratio
E.W.	50	7 sec.	1·50
Vert.	28	7	1·50

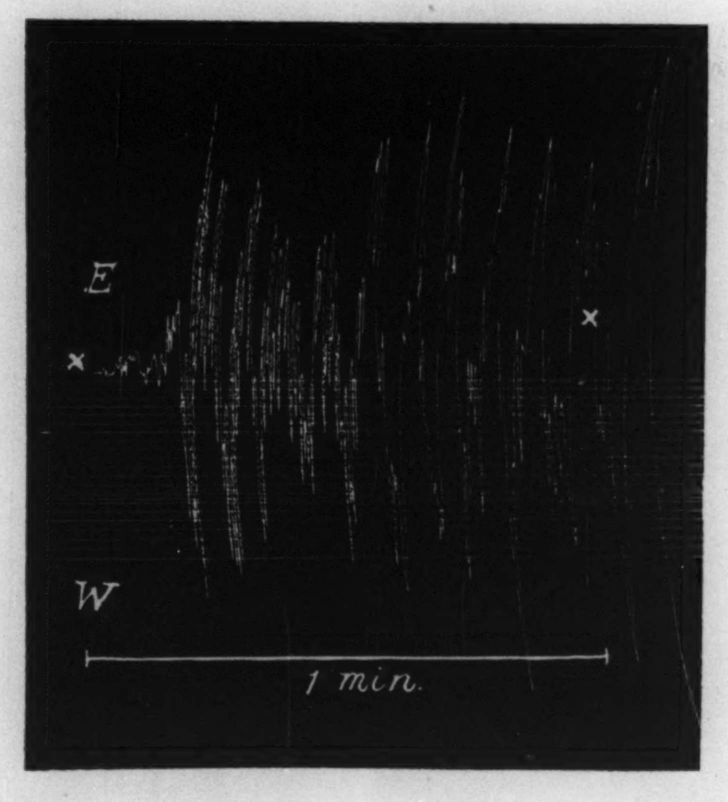

E.W. Component.

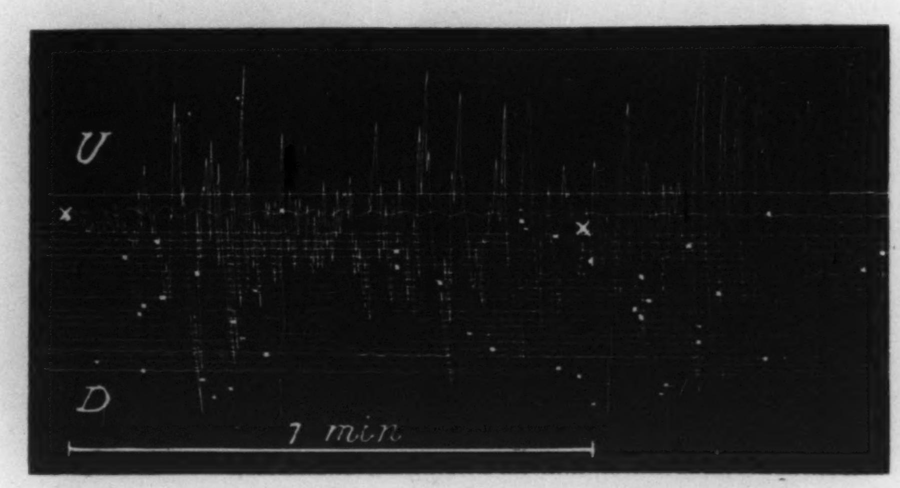

Vertical Component. (*Natural size of the original diagrams.*)

Fig. 5 Tôkyô Observation of the Earthquake of June 11, 1931

（震研彙報、第九號、圖版、震報）

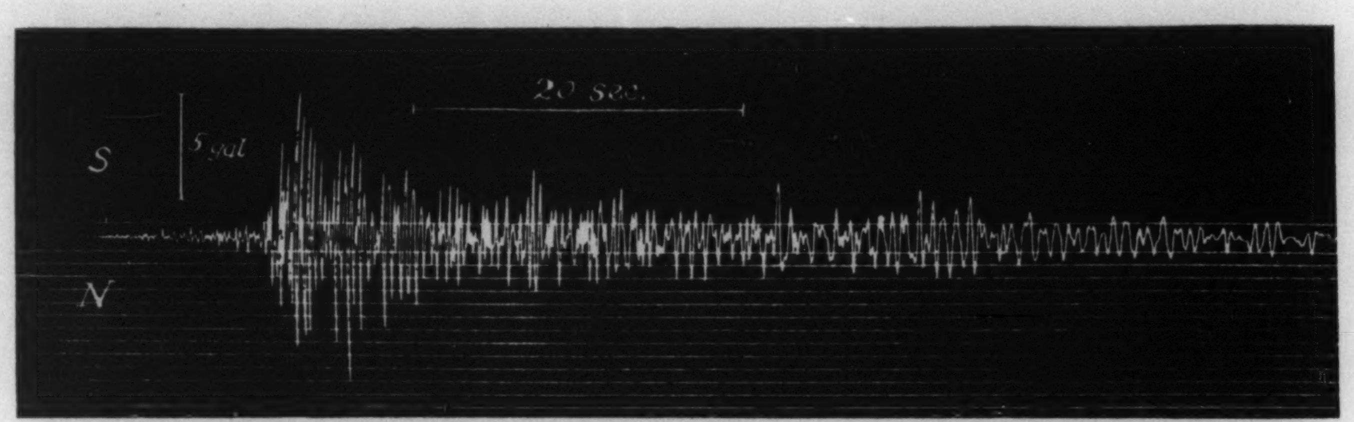

N.S. Component.

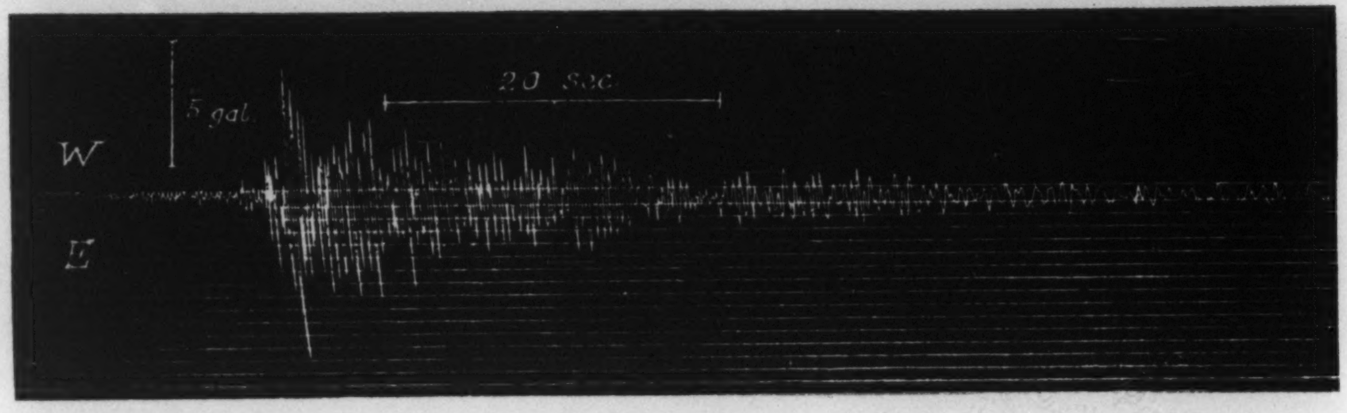

E.W. Component. (*Two times magnified the original diagram.*)

Fig. 6. Tôkyô Observation of the Earthquake of June 11, 1931.
Ishimoto Acceleration Seismograph Diagram.

——所　報——

○　談話會記事

第五十五回談話會　（昭和五年十二月十六日）

1.　伊豆地震直前に於ける伊東地方水準檢測成果報告	末廣恭二
1.　伊豆地震に於ける復舊水準及三角測量實施に關する件	鈴木三角科長
1.　伊豆地震と模型實驗との機巧の比較	藤原咲平 高山威雄
1.　伊豆地震後丹那隧道內に於ける傾斜變化觀測	石本巳四雄 高橋龍太郎
1.　地震後に於ける丹那斷層運動の逐時的測計　（豫報）	坪井忠二
1.　家屋の移動と筋違の效果	囑託　齊田時太郎
1.　土木工作物の被害	松村孫治
1.　伊豆地震調査概報	坪井誠太郎 津屋弘逵 大塚彌之助
1.　地震に伴ふ光の現象	寺田寅彦
1.　伊豆地震の振動計測結果に就いて	今村明恒
1.　伊豆地震と關東大地震との關係	長岡半太郎 白井俊明

第五十六回談話會　（昭和六年一月廿日）

1.　東京市內及臺灣に於ける水準測量の結果に就いて	鈴木三角科長
1.　關東に於ける地殼の垂直變動に就いて	宮部直巳
1.　關東に於ける地殼の水平移動と垂直變動との關係	宮部直巳
1.　衝上斷層の地形的特性と丹那浮橋線	大塚彌之助
1.　昭和三年五月廿一日東京强震當時竝に其以前に起りたる地塊運動に就いて	今村明恒
1.　伊豆地震調査報告　（補遺）	津屋弘逵
1.　箱根、熱海諸火山の基底地層と大磯附近に發達せる地層との構成物質に就いて	津屋弘逵
1.　箱根附近の地變に就いて	長岡半太郎 白井俊明

第五十七回談話會　（昭和六年二月十七日）

1.　日本に於ける地震傳播の研究（概報） *S* 波の速度に就いて *P* 波の走時の計算及其應用	囑託　河角廣

1. 伊豆地方水準測量の結果に就いて		鈴木三角科長
1. 伊豆半島の地形と地質		田山利三郎
1. 丹那隧道内及丹那盆地の地震動の比較研究　（豫報）		那須信治
1. 昭和五年十一月廿六日伊豆地震に伴つた音響異常傳播に就いて		井上宇胤 杉山友紀
1. 地震回數の統計的研究		井上宇胤
1. 廣島縣北部の强震に就いて		小平孝雄
1. 昭和五年十二月八日廿二日臺灣臺南州下の地震被害調査報告	囑託	齊田時太郎
1. 關東震災地方に於ける地殼の變形　（第二報）		坪井忠二
1. 伊豆地震後に於ける丹那斷層運動の逐次的計測　（第二報）		坪井忠二
1. 丹那隧道内傾斜變化觀測　（第二報）		石本巳四雄
1. 大地震と噴火の關係		長岡半太郎 白井俊明

第五十八回談話會　（昭和六年三月十七日）

1. 伊豆地震に伴ひたる光の現象に就て	囑託	武者金吉
1. 地震による建築物の移動に就て		末廣恭二
1. 洋底に傳はる地震波に就て		妹澤克惟
1. 島弧の曲率に就て　（第二報）		寺田寅彦
1. 三島町の被害に就て		寺田寅彦 宮部克巳
1. 地塊運動に就て　（序報）		宮部直巳
1. 丹那隧道内に於ける精密水準測量		高橋龍太郎
1. 伊豆半島の水準變化		坪井忠二
1. 伊豆地震調査報告第三報　（八幡――浮橋間）		津屋弘逵 大塚彌之助
1. 地軸の地質時代に於ける變動より推定したる世界の地震系		長岡半太郎 白井俊明

○　出張

昭和五和十二月十一日地震調査の爲め靜岡縣下へ出張	囑託	齊田時太郎
昭和五年十二月十三日地震調査の爲め靜岡縣下へ出張		高橋龍太郎
昭和五年十二月十七日地震調査の爲め靜岡縣下へ出張		坪井忠二
昭和五年十二月十九日地震調査の爲め靜岡縣下へ出張		石本巳四雄
昭和五年十二月二十二日地震調査の爲め靜岡縣下へ出張		高橋龍太郎
昭和五年十二月二十二日地形變動調査の爲め靜岡縣下へ出張		大塚彌之助
昭和五年十二月二十五日地變地質調査の爲め靜岡、神奈川兩縣下へ出張		津屋弘逵
昭和五年十二月二十六日地形地質調査の爲め靜岡、神奈川兩縣下へ出張		坪井誠太郎
昭和五年十二月二十六日地震事項調査の爲め靜岡、神奈川兩縣下へ出張		那須信治
昭和五年十二月二十七日地殼變動調査の爲め靜岡縣下へ出張		石本巳四雄

昭和五年十二月二十七日地震事項調査の爲め廣島縣下へ出張	囑託	小平孝雄
昭和五年十二月二十八日地震事項調査の爲め靜岡縣下へ出張		高橋龍太郎
昭和六年一月二日地震事項調査の爲め臺灣へ出張	囑託	齊田時太郎
昭和六年一月四日地震事項調査の爲め靜岡縣下へ出張		高橋龍太郎
昭和六年一月六日地震事項調査の爲め神奈川、靜岡兩縣下へ出張	囑託	武者金吉
昭和六年一月十一日地震事項調査の爲め靜岡縣下へ出張		那須信治
昭和六年一月十四日地震事項調査の爲め靜岡縣下へ出張		高橋龍太郎
昭和六年一月十四日地震事項調査補助の爲め靜岡縣下へ出張		鹿熊金太郎
昭和六年一月二十一日地震事項調査の爲め靜岡縣下へ出張		井上宇胤
昭和六年一月二十一日地震事項調査補助の爲め靜岡縣下へ出張		鹿熊金太郎
昭和六年一月二十二日地殼變動計測の爲め靜岡縣下へ出張		坪井忠二
昭和六年二月一日地質調査の爲め靜岡縣下へ出張		津屋弘逵
昭和六年二月五日地震事項調査の爲め靜岡縣下へ出張		高橋龍太郎
昭和六年二月六日地形地質調査の爲め靜岡、神奈川兩縣下へ出張		大塚彌之助
昭和六年二月七日地震事項調査補助の爲め靜岡縣下へ出張		鹿熊金太郎
昭和六年二月十八日地震事項調査補助の爲め靜岡縣下へ出張		鹿熊金太郎
昭和六年二月二十三日震災地寫眞に關する用務の爲め千葉縣下へ出張		石本巳四雄
昭和六年三月二日地震事項調査の爲め靜岡縣下へ出張		高橋龍太郎
昭和六年三月二日地震事項調査補助の爲め靜岡縣下へ出張		鹿熊金太郎
昭和六年三月十二日地震事項調査の爲め靜岡縣下へ出張	囑託	小平孝雄
昭和六年三月十六日地震事項調査の爲め北海道及宮城、岩手、青森三縣下へ出張		那須信治
昭和六年三月十八日地震事項調査補助の爲め靜岡縣下へ出張		鹿熊金太郎
昭和六年三月十八日地質調査の爲め靜岡縣下へ出張	理學部學生	久野久
昭和六年三月二十二日地殼變動計測の爲め靜岡縣下へ出張		坪井忠二
昭和六年三月二十三日土地變動測量の爲め和歌山縣下へ出張		岸上冬彦

——所　報——

○　談話會記事

第五十九回談話會　（昭和六年四月廿一日）

1.　房總半島水準測量結果に就て 1.　伊豆二等三角測量の概算結果に就て	鈴木元長
1.　加速度地震計及び其の記象	石本巳四雄
1.　三月九日東北地方强震に就て	那須信治
1.　伊豆地震の前震並に餘震の活動に就て　（第二報）	那須信治 岸上冬彦 小平孝雄
1.　地震と雷雨との關係	寺田寅彦
1.　彈性が深さに從て變る半無限體の表面波の研究　（第二報）	妹澤克惟
1.　海面大氣壓の擾亂によつて起る脈動に就て	妹澤克惟 西村源六郎
1.　船舶用振動計	末廣恭二
1.　地球廻轉軸の變化より推定したる世界火山の分布 1.　大嶋富士諏訪を通過する假定斷層線と富士山の起源に就て	長岡半太郎 白井俊明

第六十回談話會　（昭和六年五月十九日）

1.　地震發生火山噴火と潮汐との關係	福富孝治 川瀬二郎
1.　地軸變化と大地震との關係	越川善明 仁科伸彦
1.　再びＰ波の速度に就て	河角廣
1.　丹後地方に於ける地殼の變形　（第五報）	坪井忠二
1.　房總半島東北部に於ける谷の配列	矢部長克
1.　北伊豆地震と丹那隧道	川口愛太郎

○　出張

1.　昭和六年四月九日地質調査の爲靜岡縣下へ出張	津屋弘逵
1.　昭和六年四月九日地質調査の爲靜岡縣下へ出張	久野久
1.　昭和六年四月九日地震事項調査の爲神奈川縣下へ出張	武者金吉
1.　昭和六年五月一日地震事項調査の爲靜岡縣下へ出張	小平孝雄
1.　昭和六年五月六日地形變動及地質調査の爲靜岡縣下へ出張	大塚彌之助

——所　報——

○ 談話會記事

第六十一回談話會　（昭和六年六月十六日）

1.	日本の鮮新期初期の地殻運動に就て(一)	大塚彌之助
1.	丹那墜道内及丹那盆地の地震動比較(第二報)	那須信治
1.	本邦火山岩の特性に就て	坪井誠太郎
1.	ワレメに就て	寺田寅彦
1.	地震による家屋の振動に就て	末廣恭二

第六十二回談話會　（昭和六年七月七日）

1.	三鷹村東京文天臺に於ける地表傾斜變化觀測	辻光之助
1.	伊豆半島に於ける地殼變動(第二報)	坪井忠二
1.	地震と脈動	井上宇胤
1.	地震加速度の觀測	石本巳四雄
1.	地震群に就て	寺田寅彦
1.	地震動各位相の振副、振動周期、初動に就て	妹澤克惟
1.	內部歪核を有する半無限プラスチコ彈性體の變形	妹澤克惟
1.	地塊運動（第二報）	宮部直巳
1.	武田ビルデング振動驗測結果に就て	福富孝治
1.	大正十五年八月三日羽田强震當時並に其以前に現はれたる地形變動に就て	今村明恒
1.	地震の初動に就て(豫報)	河角廣

○ 出　　張

1.	昭和六年六月三日地震事項調査の爲靜岡縣下へ出張	宮部直巳
1.	昭和六年六月八日地震調査の爲千葉縣下へ出張を囑託	田山利三郎
1.	昭和六年六月廿二日地質調査の爲神奈川、靜岡縣下へ出張	津屋弘逵
1.	昭和六年六月廿二日傾斜計記錄調査の爲東京府下三鷹村へ出張	石本巳四雄
1.	昭和六年六月廿八日電車々輛振動測定の爲東京府下へ出張	那須信治 佐藤小太郎
1.	昭和六年七月二日地質調査の爲靜岡、神奈川兩縣下へ出張	久野久
1.	昭和六年七月十日地質調査の爲靜岡、神奈川兩縣下へ出張	津屋弘逵
1.	昭和六年七月十四日重力測定に關する調査の爲神奈川縣へ出張	坪井忠二

——所　報——

○　談話會記事

第六十三回談話會　（昭和六年九月十五日）

1.　本邦地震と世界地震との關係	山口生知
1.　伊豆半島北部地質調査概報	久野久
1.　表面層を有し垂直荷重を受ける彈性體の變形	西村源六郎
1.　深川に於けるメタン瓦斯湧出地	寺田寅彦 宮部直巳
1.　三角測量より得たる土地の水平移動の吟味	武藤勝彦
1.　地動に因りて誘起せられたる芦の湖のセイシュに就て	今村明恒 小平孝雄
1.　北伊豆地震に伴へる地塊運動の北方延長に就て	今村明恒
1.　丹那隧道內に於ける精密水準測量(續報)	高橋龍太郎

第六十四回談話會　（昭和六年十月廿日）

1.　筑波山に於ける傾斜觀測報告(其三)	井上宇胤
1.　震源の深さに依る我が國の地震分布	和達清夫
1.　西埼玉强震に就て	國富信一
1.　丸ノ內、本鄕に於ける地震加速度比較	石本巳四雄
1.　北武藏强震による震害に就て	齊田時太郎
1.　家屋震害と地盤と地震動の性質との關係	齊田時太郎
1.　埼玉地震の被害竝に餘震調査概要	那須信治 小平孝雄
1.　所謂北條地溝帶に就て	矢部長克
1.　狩野川冲積地地形と北伊豆地震の地變と水準點檢測の結果	大塚彌之助

第六十五回談話會　（昭和六年十一月十七日）

1.　四國東南部の海岸地形	渡邊光
1.　關東方面に於ける震源の移動方向に就て	山口生知
1.　三鷹菱形基線の面積變化に就て(第二報)	坪井忠二
1.　三鷹菱形基線の變化と地震頻度	寺田寅彦
1.　丹那隧道內に於ける傾斜變化觀測(第三報)	石本巳四雄
1.　日本鮮新期初期の地殼運動に就て	大塚彌之助
1.　南日向强震の震害に就て	齊田時太郎
1.　南日向强震に伴へる海水の一時的變化	那須信治

1. 硝子板のワレメに就て	西村源六郎 高山威雄

○出張

1. 昭和六年九月廿二日地震事項調査の爲め神奈川、埼玉、群馬の三縣下へ出張	那須信治
1. 昭和六平九月廿二日地震事項調査の爲め神奈川、埼玉、群馬の三縣下へ出張	小平孝雄
1. 昭和六年九月廿三日地震事項調査の爲め埼玉縣下へ出張	齊田時太郎
1. 昭和六年九月廿三日地震事項調査の爲め埼玉縣下へ出張	大塚彌之助
1. 昭和六年九月廿五日地震事項調査の爲め東京府下及埼玉縣下へ出張	那須信治
1. 昭和六年九月廿五日地震事項調査の爲め東京府下及埼玉縣下へ出張	小平孝雄
1. 昭和六年九月廿九日地震事項調査の爲め山梨縣下へ出張	齊田時太郎
1. 昭和六年九月卅日基線觀測に關する用務の爲め東京府下へ出張	坪井忠二
1. 昭和六年十月十日地震事項調査の爲め埼玉縣下へ出張	小平孝雄
1. 昭和六年十月十六日傾斜計觀測の爲め神奈川縣下へ出張	高橋龍太郎
1. 昭和六年十月十六日地震事項調査の爲め埼玉縣下出張	齊田時太郎
1. 昭和六年十一月六日地震事項調査の爲め宮崎、鹿兒島二縣下へ出張	齊田時太郎
1. 昭和六年十一月六日地震事項調査の爲め宮崎、鹿兒島二縣下へ出張	那須信治
1. 昭和六年十一月廿四日地震事項調査の爲め東京府下へ出張	宮部直巳
1. 昭和六年十一月廿四日地震事項調査の爲め東京府下へ出張	大塚彌之助
1. 昭和六年十一月廿四日地震事項調査の爲め東京府下へ出張	高山威雄
1. 昭和六年十二月一日地質調査の爲め靜岡縣下へ出張	大塚彌之助
1. 昭和六年十二月一日地質調査の爲め靜岡縣下へ出張	久野久
